INTERNATIONAL COUNCIL FOR RESEARCH AND INNOVATION
IN BUILDING AND CONSTRUCTION

WORKING COMMISSION W18 - TIMBER STRUCTURES

CIB - W18

MEETING FORTY-ONE

ST. ANDREWS

CANADA

AUGUST 2008

Lehrstuhl für Ingenieurholzbau und Baukonstruktionen
Universität Karlsruhe
Germany
Compiled by Rainer Görlacher
2008

ISSN 1864-1784

CONTENTS

0 List of Participants

INTERNATIONAL COUNCIL FOR RESEARCH AND INNOVATION IN BUILDING AND CONSTRUCTION
WORKING COMMISSION W18 - TIMBER STRUCTURES

MEETING FORTY-ONE
St. Andrews, Canada, 24 - 28 August 2009

LIST OF PARTICIPANTS

AUSTRIA	
R Brandner	Kompetenzzentum holz.bau.forschungs.gmbh
A Jöbstl	TU Graz
U Hübner	Kompetenzzentum holz.bau.forschungs.gmbh
CANADA	
A Asiz	University of New Brunswick, Fredericton
M Bartlett	University of Western Ontario
Ying H. Chui	University of New Brunswick, Fredericton
M Gong	University of New Brunswick, Fredericton
G Gupta	University of New Brunswick, Fredericton
F Lam	University of British Columbia
W Munoz	FPInnovations – Forintek Division, Ottawa
M Noory	University of New Brunswick, Fredericton
A Salenikovich	Université Laval
I Smith	University of New Brunswick, Fredericton
CROATIA	
V Rajcic	University of Zagreb
DENMARK	
H J Larsen	Copenhagen
J Munch-Andersen	Danish Timber Information Council, Lyngby
FINLAND	
A Kevarinmäki	VTT Technical Research Centre of Finland, Espoo
A Ranta-Maunus	VTT Technical Research Centre of Finland, Espoo
FRANCE	
C Faye	FCBA-CTBA, Bordeaux
GERMANY	
S Aicher	MPA University Stuttgart
H J Blaß	Universität Karlsruhe
J Denzler	Planungsgesellschaft Dittrich GmbH
M Frese	Universität Karlsruhe
R Görlacher	Universität Karlsruhe
U Kuhlmann	Universität Stuttgart
P Schädle	Universität Karlsruhe
K U Schober	Bauhaus University, Weimar
P Stapel	Holzforschung München
S Winter	TU München

ITALY

A Ceccotti	IVALSA-CNR
M Fragiacomo	University of Sassari, Alghero
A Polastri	University of Trento

JAPAN

K Komatsu	Kyoto University

NEW ZEALAND

A Buchanan	University of Canterbury
J Jensen	Auckland University

SLOVENIA

B Dujic	University of Ljubljana

SWEDEN

C Bengtsson	SP, Boras
J König	SP Trätek, Stockholm
B Källsner	SP Trätek, Stockholm
H Danielsson	Lund University

SWITZERLAND

M Sandomeer	ETH Zürich
J Köhler	ETH Zürich
R Steiger	EMPA Wood Laboratory, Dübendorf

THE NETHERLANDS

A Jorissen	TU Eindhoven
A J M Leijten	TU Eindhoven

USA

M Snow	Wentworth Institute of Technology, Boston
T Williamson	American Plywood Association, Tacoma
B Yeh	American Plywood Association, Tacoma

1. Chairman's Introduction

2. General Topics

3. Structural Design Codes

4. Test Methods

5. Fire

6. Structural Stability

7. Laminated Members

8. Timber Beams

9. Timber Joints and Fasteners

10. Stresses for Solid Timber

11. Stress Grading

12. Limit State Design

13. Any Other Business

14. Venue and Program for Next Meeting

15. Close

16. Peer Review of Papers for the CIB-W18 Proceedings

INTERNATIONAL COUNCIL FOR RESEARCH AND INNOVATION
IN BUILDING AND CONSTRUCTION

WORKING COMMISSION W18 - TIMBER STRUCTURES

MEETING FORTY-ONE

ST. ANDREWS, CANADA 25 TO 28 AUGUST 2008

MINUTES
(F Lam)

1 CHAIRMAN'S INTRODUCTION

Prof. Hans Blass welcomed the delegates to the 41st CIB W18 Meeting in St. Andrews Canada. He thanked Ian Smith for hosting the meeting. Ian Smith also previously hosted the 1990 IUFRO S5.02 meeting in New Brunswick. Twenty eight papers will be presented during the meeting. The presentations are limited to 20 minutes each, allowing time for meaningful discussions after each paper. The papers will be presented in reversed order compared to previous years as agreed during the last CIB W18 meeting. The Chair asked the presenters to conclude the presentation with a general proposal or statements concerning impact of the research results on existing or future potential application and development in codes and standards. R. Görlacher will deal with questions regarding the meeting proceedings.

Papers brought directly to the meeting would not be accepted for presentation, discussions, or publication. Papers presented by non-authors or non-co-authors are not recommended except in exceptional situations because the discussion process might be compromised.

There are 11 topics covered in this meeting with a new topic on sustainability: Structural Design Codes (2), Sustainability (1), Test Methods (1), Fire (1), Structural Stability (5), laminated members (4), Timber beams (3), Timber joints and fasteners (5), Stresses for solid timber (4 papers), stress grading (1 paper), and Limit State design (1).

I. smith discussed organizational matters for the meeting.

2 GENERAL TOPICS

H.J. Larsen questioned why has the scope changed to include sustainability. H. Blass stated that this topic will have an influence on design decisions. A. Buchanan said that when he submitted the paper he was not sure that it would fit to the CIB W18 meeting but the sustainability concept may end up in codes. S. Winter stated that there are signs that sustainability will influence European codes. H.J. Larsen stated that if this is the case the scope should be changed formally to include sustainability as the expertise of current participants is not in this area. There are many other groups including CIB that focus in this area. A. Leijten agrees with H.J. Larsen that we should not change our current scope to include sustainability. Based on comments from the senior participants, H. Blass agreed that CIB W18 for the time being will not accept future papers in this topic. A. Buchanan's paper will be presented and included in the proceedings under a different topic as it is already accepted. The CIB W18 position can still be modified in future.

3 STRUCTUAL DESIGN CODES

41 - 102- 1 Consequences of EC 5 for Danish Best Practice - **J Munch-Andersen**

Presented by J. Munch-Andersen

I. Smith commented that in Canada design methods are given in the design code and not in a supporting standard. The influence of grade on density is treated differently in Canada. J. Munch-Andersen agreed that two committees are involved but this is not a problem as both are working towards the same safety level/concept. H.J. Larsen stated screw design has had a strange history in EC5 development as it started as very strict and then evolved. He questioned about the scientific basis behind screw design and whether the material was discussed in CIB W18. H. Blass disagreed and stated that there is a wide scientific basis behind the EC5 screw design provisions with discussion in CIB W18 meetings. H. Blass stated that head pull through should be the same for both screws and nails if the shapes of the head are the same; therefore, the values in EC5 are set conservatively. He agreed that restrictions to smooth shank nails are questionable. H. Blass and J. Munch-Andersen clarified the spacing requirement for laterally loaded and axially loaded cases. H. Blass commented that applying group effect to rope effect is incorrect and in 1994 CIB W 18 meeting R. Görlacher presented results showing that the failure modes belonging to thick steel plates were observed with 2 mm thick steel plates and 4 mm diameter nails. A. Leijten asked why these results were not presented earlier. J. Munch-Andersen responded that the work was just completed. J. König commented that EC5 was developed with few comments received outside the committee. It is a general problem that as EC5 is examined more closely inconsistencies are uncovered. He suggests comments should be forwarded to the EC5 secretariat so that the issues can be addressed in the next code cycle as this errors are on the side of too conservative. J. Munch-Andersen mentioned that being too conservative also requires immediate attention as it prevents some connectors from being used. H. Blass commented that EC5 and supporting standard TC124 need to coordinate. I. Smith discussed the issue of safety and the differences with current practice.

41 -102 - 2 Development of New Swiss Standards for the Assessment of Existing Load Bearing Structures - **R Steiger, J Köhler**

Presented by R. Steiger

T. Williamson mentioned that this is also a problem in the US and complimented the approach. He asked how to deal with the cases of altered members such as drilled holes and decay. He commented that seismic code has also changed in US recently and ASCE has a 400 page document on the issue. R. Steiger agreed with the 1st issue and there are additional standards under development in Switzerland to address them. The 2nd issue is also important in Switzerland as recent changes to seismic load also made it very difficult. There are standards developed to address this issue also. A. Ranta Maunus asked about the setting of target beta values. R. Steiger responded that the type of building is important as well as the cost or consequence of failure. A. Ceccotti stated that this work is especially important to historic structures where it is important to create a design solution not to significantly interfere with the original historic structure. Y.H. Chui received clarification from R. Steiger that ultrasonics and proof loading can be used to update information on stiffness and use the information in the new procedures. R. Steiger also stated that one needs to rely on prior research results in linking scientific work to code. H. Blass asked when measuring the deflection of structure to assess stiffness, how the influence of composite action and non-load bearing support is taken into consideration. R. Steiger stated that the example given is not a real problem but it was posed to illustrate the process.

Realistic static calculation is needed as a first step and should take into consideration of such issues. J. König stated that the target beta set in EC5 is based on assumptions of normal distrbution. In the paper the action is not taken as normal so a different set of beta should be used. R. Steiger stated that this issue is discussed in the paper and EC should start another standard on assessing existing buildings. M. Bartlett received clarification that C_W is the cost of restoring the functionality of the building. He also commented that serviceability is difficult to check. F. Lam received clarification that the building upgrade based on changes in loads are only required when the intended building usage is changed. U. Kuhlmann commented that how to use measurement values in assessing resistance is an important step. I. Smith commented that his work on restoration of historical bridges where knowledge of material properties was lacking; as such, very detailed procedure may represent precision misfit.

41 -102 - 3 Measuring the CO2 Footprint of Timber Buildings - **A Buchanan, S John**

Presented by A. Buchanan

T. Williamson stated that in US this is an important issue because LEEDS is unfriendly to wood. Two ANSI standards are available. LCA makes sense but concrete and steel are negative towards LCA as the results are favourable to wood. J. König stated that in EC stability and fire have been the key issues. The commission is now interested to develop Eurocodes for all essential requirements. Requirement #7 is sustainability of material and will be the future. The exercise is highly relevant and this committee should be involved. S. Winter agreed with J. König and added that health and environmental protection are also important issues. Leeds standard is driven by the concrete industry and tries to hide in the process with strong participation. Lifetime of the building is also important. We need scientific base information to help lobbying. The paper seems to be too favourable to wood as there seems to be some double accounting of CO2. J. Munch-Andersen states that it is very difficult to calculate CO2 footprint. For example the use of nuclear power or hydro power to make Aluminium will make a large difference. In N. America it is very apparent that there is a strong need to reduce energy consumption on heating and cooling of buildings.

4 TEST METHOD

41 - 21 - 1 Determination of Shear Modulus by Means of Standardized Four-Point Bending Tests - **R Brandner, B Freytag, G Schickhofer**

Presented by R. Brandner

H. Blass stated that the last slide shows low COV for G in the test. He asked why 20% was used in the proposal for characteristic values. R. Brandner explained that 20% COV is for single solid members when n (the number timber elements) increased, COV decreased which explained the COV values in the last slide. Since the test data was measured at a distance of h from the support, is there an influence from compression. R. Brandner answered that this was recognized in FEM analysis and already considered this in the study.

5 FIRE

41 - 16 - 1 Effect of Adhesives on Finger Joint Performance in Fire - **J König, J Norén, M Sterley**

Presented by J. König

S. Aicher stated that punishing melamine adhesive which is commonly used in glulam with a penalty factor is too harsh. In I joist finger joints in tensile flange melamine adhesive is dangerous. In glulam the random occurrence of finger joints and occurrence of other defects play a role and the influence also depends on timber quality. J. König agrees the reduction may be less and we need information to back it up. The results show that some adhesives are not equivalent to PRF. Only two PUR adhesives and one MUF adhesive were tested as they were originally regarded as equivalent to PRF but the results were surprising. S. Winter asked whether the glue for glulam or glue for finger joints were tested. J. König answered that in some test cases the same glue for both face and finger joint was used. S. Winter asked whether bending moment under code conditions were estimated. Here from test one can see the charring depth so moment resistance of the residual section can be estimated. In real fire situation of larger member size the influence may be less severe compared to the small cross section tested. B.J. Yeh commented that use of PRF as a benchmark was debated in the US since not all PRF are the same. In the US approach comparison with wood was used as a benchmark. J. Köhler received clarification that the mean values were used as comparison.

6 STRUCTURAL STABLITY

41 - 15 - 1 Need for a Harmonized Approach for Calculations of Ductility of Timber Assemblies - **W Muñoz, M Mohammad, A Salenikovich, P Quenneville**

Presented by W. Muñoz

B.J. Yeh received clarification as shown in Figure 4 that glued connections with screws have the highest ductility. He stated in the US adhesive in connection is not considered as ductility. F. Lam stated that it may be dangerous to use bolted connection test results loaded parallel to grain to quantify the ductility behaviour of assembly or system where there is no guarantee that moments may not be introduced which could cause different failure mode. W. Muñoz agreed that more work is needed. B. Dujic stated that this paper intends to discuss the meaning of ductility for seismic design, however the cyclic test protocol information is missing. This information can be used by looking at the load /capacity drop from cycle to cycle based on the work at UC Berkeley. A. Salenikovich stated that this was tried before. U. Kuhlmann stated that redistribution with a system is also important. System ductility should be examined as well where information on absolute deformation rather than ratios of deformation is needed. A. Ceccotti stated that timber structures copied from steel structures in the approach to consider ductility. It is a concept important in standard for comparison purposes. We should overpass this. In EC8 Q factor takes into account the system behaviour. I. Smith commented that he had forgotten why we had such a task group in Canada. He agreed that behaviour of connection does not map into the behaviour of system. F. Lam agreed that absolute displacement is important but the definition of limit state is also important for different building system. A. Ceccotti said that here engineering judgment is needed.

41 - 15 - 2 Plastic Design of Wood Frame Wall Diaphragms in Low and Medium Rise Buildings - **B Källsner, U A Girhammar**

Presented by B. Källsner

Tom Williamson asked if there is any information on the details of transfer connections. B. Källsner responded that this information is available. A Salenikovich asked whether experimental work is available. B. Källsner answered yes much data is available and more than one story wall tests will also be available. B. Dujic asked if this model can be used to calculate the performance of the 3 story CLT building tested in Japan. B. Källsner responded that he is not sure but thinks it is possible. A. Ceccotti received confirmation from B. Källsner that the book will be published in English.

41 - 15 - 3 Failure Analysis of Light Wood Frame Structures - **A Asiz, M Noory, Y H Chui, I Smith**

Presented by A. Asiz

Tom Williamson said that high wind area requires hurricane anchors. He received clarification of the details of the connections for concrete slab end with raised floor foundation (toe nailed first and anchors will be tied at University of Western Ontario tests). As such this also depends on the detailing of the raised wall. A. Buchanan asked about the contribution of gypsum and interior lining which is important. A. Asiz answered that this is not considered in the model and will look into this as part of the model. A. Asiz said that the contribution from gypsum is approximately 25% to the system of the system but older gypsum boards may not be very durable. A. Buchanan said this in such case better quality gypsum board would be needed. A Salenikovich questioned and Y.H. Chiu confirmed that system factor will depend on geometry and energy absorption mechanism.

41 - 15 - 4 Combined Shear and Wind Uplift Resistance of Wood Structural Panel Shearwalls - **B Yeh, T G Williamson**

Presented by B. Yeh

Y.H. Chiu received confirmation about the one of the failure modes as cross grain bending. A. Asiz asked about combined uplift and shear in 3 dimensions. T. Williamson said that this is not considered as the test is one of the most complicated set up at APA already. I. Smith said that the out of plane motion does not have interaction with the in plane motion. S. Winter asked why through anchor from top was not used. B.J. Yeh responded that a lot of cases this is not used in practice as it is too expensive. F. Lam asked about the dead load and its possible influence with the shear. B.J. Yeh answered that this is not yet done but will consider it in the future.

41 - 15 - 5 Behaviour of Prefabricated Timber Wall Elements under Static and Cyclic Loading - **P Schädle, H J Blass**

Presented by P. Schädle

B Dujic discussed contact issue related to shear wall resistance. A. Buchanan asked about the geometry of the system and why bigger sections were not used. P. Schädle said the size was designed so that it can be easily handled by few workers and can be built with few friends. A. Buchanan received clarification that downward load goes through the stud in compression and no glue is used. I. Smith asked about the detail of the intercept with floor. P. Schädle said that the floor would be installed be on top of the plates. F. Lam

commented that this is an interesting system. He suggested that dynamic behaviour be considered as the damping increase comes from increased vertical dead load. Here the vertical dead load will have an influence on the natural frequency of the system. Also the damping generated by the stones is very interesting. T. Williamson asked about the openings and the analysis of the walls with openings. Y.H. Chiu received confirmation that the system is approved for 3 storey buildings in Germany. He asked whether it is approved as bricks or system. P. Schädle said that it is approved for both as bricks and as system. J. M. Andersen stated that the gravels will move after shaking. P. Schädle said that after cyclic test the gravels may come out of the blocks. B.J. Yeh asked about fire protection and insulation. H. Blass said that in 160 mm wall thickness additional insulation may be needed. 240 – 300 mm wall thicknesses are also available. For fire protection gypsum boards will handle it and mineral rock fibre can also be used.

7 LAMINATED MEMBERS

41 - 12 - 1 Moment-Resisting Performance of Glulam Corner Joints Composed of Large Joints (LFJ)- **K Komatsu**

Presented by K. Komatsu

I. Smith asked if this information is used in the design of a structure, what kind of deformation can be predicted. K. Komatsu answered that in case of large span small rotations can cause large deformation. Time dependent issue may come into play. Engineers currently ignore rotation and consider LFJ as rigid joint which is not correct. A. Jorissen referred to Figure 2 and asked if the deformation is in the bending in the short element in the LFJ rather than the bending of the member. K. Komatsu offered explanation that bending deformation is observed. H.J. Larsen agreed with A. Jorissen that what happened in the glulam is more like the bending of a cantilever beam. K. Komatsu said that from practical point of view the use of rotational springs is easy to understand.

41 - 12 - 2 Bending Strength of Spruce Glulam - New Models for the Characteristic Bending Strength - **M Frese, H J Blass**

Presented by M. Frese

Y.H. Chiu asked whether the strength model for the higher glulam strength depended on the grading method. H. Blass stated no and the model covers a whole range of grading including knot size and density and dynamic MOE. The tensile strength limit was used where visually graded material would fall to the lower case hence the model is grading method independent. A. Ranta-Maunus stated that new data from Scandinavia is available where mechanical graded beam results agree with the model but visually graded beams have higher value compared to model. Also correlation between bending and tension strength of the finger joint is poor. Since QC tests uses bending strength, this is an issue. H. Blass added that there are in addition 40 bending tests in Karlsruhe. Currently Karlsruhe is waiting for the laminae and finger joint tests. J. Köhler said that it would be interesting to see the entire distribution rather than just the 5^{th} percentile values. M. Frese said that simulated mean and 5^{th} percentile values are available in the final report. T. Williamson said that QC of bending strength of finger joint was eliminated in US for some 10 years. The use of 21 MPa as limit may not be applicable to some visually graded material in the US. H. Blass said that this is not the case with European spruce where visually graded material rarely exceeds 21 MPa. T. Williamson commented that he is pleased to see glulam size factor finally recognized in Europe and the trend seems to agree

with US provisions. I. Smith asked how grading errors were captured in this work. H. Blass said that this was not done. I. Smith asked whether it means that the tensile strength is higher than 60% of the bending strength as normally assumed for timber. H. Blass said that they do not make statements about timber but with glulam this is the case. B.J. Yeh asked whether EN standard proposal is intended for spruce and fir or other species also. H. Blass said that the research was based on Spruce and fir in Europe. In practice Douglas fir, pine and others species will be used. S. Winter asked if it is true that the glulam strength in Europe was overestimated for a long time as in general a 10% over estimation of strength adding depth factor would come up to 50%. H. Blass stated that data has been presented to industry and reaction from industry is pure denial. S. Winter said that may be the information should also be presented to the engineering community. H.J. Larsen stated that reduction of claim factor of safety is also a possibility. J. Köhler said that safety factor also depends on COV. With glulam the COV may be less severe and additional work can be done. Y.H. Chiu said that this could be due to changing of resource characteristics so existing beams may not necessarily be unsafe. H. Blass stated that large database from the past was used in the analysis so changing resource characteristics is not the issue.

41 - 12 - 3 In-Plane Shear Strength of Cross Laminated Timber - **R A Joebstl, T Bogensperger, G Schickhofer**

Presented by R. A. Joebstl

H. Blass asked if the 10 MPa value is proposed for the code. R.A. Joebstl said that it is too early as only 20 specimens with uncommon sizes were studied. A. Salenikovich asked if this is a real shear failure mode and not perpendicular to grain failure. R.A. Joebstl responded that this is really a shear failure mode as observed in the specimen and drop of load in the load deformation curve. H. Blass asked if the test was stopped or the load reduced at 4 mm deformation. R.A. Joebstl responded that the test was stopped at this point so the specimen did not completely fail. A. Asiz asked if data of 7 or 9 layer material were available. R.A. Joebstl said no the 7 or 9 layer material was not tested.

41 - 12 - 4 Strength of Glulam Beams with Holes - Tests of Quadratic Holes and Literature Test Results Compilation - **H Danielsson, P J Gustafsson**

Presented by H. Danielsson

H. Blass received confirmation that the definition of failure was the occurrence of crack propagation. He asked why maximum load out of the test was not used. H Danielsson said that when crack propagation occurred in general the load was close to maximum and later on bending failure occurred. T. Williamson said that this is a common problem in N. America. Test just completed in APA with circular hole put in high shear area near end of the beam. H Danielsson explained that test set up No.2 took this into consideration although the crack propagation stopped as the hole was further from the end. R. Steiger asked what was the characteristic value of shear strength used in the analysis. H Danielsson said it was 3.8 MPa according to 1990 reference. R. Steiger stated that the 3.8 MPa has been reduced in recent code change and revise the paper to clarify the information. J. Köhler said that code results come from model and comparison with the model in the paper may not be totally appropriate. A. Buchanan received further clarification about whether load increase was observed when crack propagation stopped. H. Danielsson said that a small increase of 5 to 20% in general was observed. A. Buchanan and H. Danielsson further discussed the geometry of the hole with rounded corner and comparison with circular hole and relative comparison in terms of radius of the hole and the rounded corner. F. Lam commented the drying during service can cause

cracks in beams in service which can further influence results. B.J. Yeh stated that the location of hole has a strong influence on the results and asked whether this aspect has been studied. H. Danielsson said that this has not been studied in detail. S. Aicher stated that when moving the hole to the end, compression stress may be introduced which could reinforce the beam in shear mode thus increasing capacity. B.J. Yeh stated that this is different from US observations.

8 TIMBER BEAMS

41 - 10 - 1 Composite Action of I-Joist Floor Systems - **T G Williamson, B Yeh**

Presented by T.G. Williamson

H. Blass stated composite action is strongly dependent on the span. This study only deals with one span. T. Williamson and B.J. Yeh responded that this span was chosen to be the most critical case. F. Lam stated composite action also depends on depth and I. In this paper one factor was proposed for all cases. Would one look into additional depths? T. Williamson and B.J. Yeh responded that yes more depths will need to be considered but the most critical depth has been evaluated. A. Buchanan asked about multiple span applications where positive and negative moments exist. B.J. Yeh responded that from analytical studies this was considered but the results showed this was not critical that compared to single span. T. Williamson further clarified that there is no difference between long term and short term tests. Y.H. Chui asked whether mechanics based approach will be considered. B.J. Yeh responded that yes it would be good but engineers need a simple solution at the end rather than computer programs. S. Winter received clarification that elastomeric based glue, construction type silicon 98 was used. I. Smith stated why simple design in timber was discussed as if we were 2nd class. T. Williamson stated that in US most designs with wood are carried out by 2nd class engineers so we need more tools to help them. J. Munch-Andersen asked about vibration of these floors. T. Williamson said that US does not have explicit vibration provisions in floor design. V. Rajcic asked why EA perpendicular values declined. T. Williamson explained that in panel production E parallel is critical. Through qualification and Quality assurance process, OSB has been optimized for this property while EA perpendicular declined.

41 - 10 - 2 Evaluation of the Prestressing Losses in Timber Members Prestressed with Unbonded Tendons - **M Fragiacomo, M Davies**

Presented by M. Fragiacomo

H. Blass stated the graphs in paper with arrows with the time extended to 50 years. There is a need to clarify that this is extrapolation. A. Asiz asked why the tendons were placed in middle axis. M. Fragiacomo replied that the work was originally intended to provide righting forces. There was discussion on the issue of short term versus long term tests and the monitoring of pre-stress losses in tendon. U. Kuhlmann commented that the safety consideration and system behaviour should be considered and how to control the pre-stress in system. M. Fragiacomo replied that it would be difficult to test many specimens. This is preliminary work and more work is needed. M. Bartlett commented that FRP tendon has lower MOE than steel should be used. M. Fragiacomo agreed that his is a good idea. J. König stated that carbon fibre has been used in bridge deck pre-stressing to reduce pre-stress losses through time. I. Smith asked what happen when the building starts to collapse in terms of damage propagation and disproportional collapse.

M. Fragiacomo replied that one should not rely on pre-stressing for everything and one can

use shear key to take the gravity forces.

41 - 10 - 3 Relationship Between Global und Local MOE - **J K Denzler, P Stapel, P Glos**

Presented by P. Stapel

H. Blass stated that the findings confirmed EN 384 equations. J. Köhler asked which value is better. P Stapel replied that the global MOE is better. H.J. Larsen asked what is the intent of the research work. P Stapel stated that the work intended to check EN384 equations. A. Buchanan stated the reason for MOE measurement is to compute deformation. He asked why shear deflection is not mentioned or discussed in the paper. P Stapel agreed the shear deflection is important. A. Ranta-Maunus stated that a 4 to 5% difference between E local and E global is generally assumed for accepted G Values. As local MOE is measured in the weakest section, the importance of measuring local or global MOE is in question. Dynamic MOE is the method that can be used with less trouble. H. Blass commented that the relation between dynamic and static MOE on edge is then needed. B. Källsner stated that measurement of local MOE is difficult because measurements are taken off the neutral axis. In MOE measurement in his laboratory local MOE is measured off the tension side. Analysis has shown that the difference between the measurement off neutral axis and tension side is minor. I. Smith stated that MOE is just an artefact of theory. He asked and received clarification that in Germany the term scantling ranges from light framing to large beams. S. Aicher MOE and G are need for calculation of deformation. It is worth to look into vibration testing but states beam bending should be studied because not every laboratory has dynamic MOE testing equipment. J. Köhler stated that the placement of weakest point of the beam within the maximum stresses zone is an unfortunate situation.

9 TIMBER JOINTS AND FASTENERS

41 - 7 - 1 Applicability of Existing Design Approaches to Mechanical Joints in Structural Composite Lumber - **M Snow, I Smith, A Asiz, M Ballerini**

Presented by M. Snow

F. Lam asked how many specimens were tested in each cell. M. Snow replied 6 in some cases and 10 in other cases. F. Lam received confirmation that the 5th percentile values were based on normality assumption and cell COV. He commented that since there are large non-conservative differences between results and proposed provisions in Canadian code, one needs to carefully consider the information in code committee. I. Smith stated that this information was presented to the subcommittee on fastener design in Canada. The approach is to consider the LVL material to be equivalent to sawn DF timber which would be conservative. H.J. Larsen stated that the paper presented in CIB with low number of specimens should not use 5th percentile. The only way is to compare model with mean values and COV should be based on global values and not individual test cells. He commented that the results are confusing because material properties were not reported. He asked whether the yield moment, embedment strength, and withdrawal with rope effect were studied. A. Leijten asked about fracture energy values in EC5 and whether this would be appropriate for this type of material. He commented that referencing literature should mention the author. He asked whether embedment strength of single fastener was tested and expressed dissatisfaction with Table 4. H. Blass recommended that the paper be revised to provide missing information on material properties.

41 - 7 - 2 Validation of Proposed Bolted Connection Design Proposal - **P Quenneville, J Jensen**

Presented by J. Jensen

I. Smith commented that all models are inaccurate as the connections are complicated. More exact model will need computer. H. Blass commented that there is an easy solution to use full threaded screws to reinforce the connection to avoid brittle failure mode. A. Jorissen commented that in group tear out mode either shear or tension will have to collapse first therefore their strength should not be additive. A. Leijten discussed group tear out and other modes of failures and the simplified form of EYM. I. smith discussed the origin of the EYM current used in the Canadian code as a 1986 CIB W18 paper by Whale, Larsen and Smith. A. Salenikovich received confirmation that EYM only valid for ductile failure mode. H.J. Larsen commented that in EC the simplified EYM is not used. S. Winter received clarification of the treatment factor. H.J. Larsen stated that CIB W18 papers should not include these factors.

41 - 7 - 3 Ductility of Moment Resisting Dowelled Joints in Heavy Timber Structures - **A Polastri, R Tomasi, M Piazza, I Smith**

Presented by A. Polastri

H. Blass referred to slide 25 where EC 5 equation was presented. He commented that the 1.05 and 1.15 factors are not part of the Johansen formula and should be left out. He commented that stiffness with small connection test where values are comparable to EC5 while large specimens should have lower stiffness. He received confirmation that the specimens were made by hand which may have contributed to the lower stiffness values. With regard to the comment that there is no danger of splitting mentioned in the presentation, he stated that in reality dry climatic conditions can lead to splitting in the connection area. I. Smith answered that the specimens sat in the laboratory for a period of time. H. Blass received confirmation that they were not assembled specimens so his comments on splitting in dry climatic condition is still valid. A. Leijten asked if there was any literature survey as this was not the 1st work in this area. A Polastri responded yes and they wanted to do the comparisons later. A. Ceccotti asked what L/d is between the thickness of the specimens and the dowel diameter. A Polastri answered that thickness of the specimens was 110 mm and the dowel diameter was 20 mm. A. Ceccotti stated that the conclusion is that EC 8 is conservative. A Polastri answered that it depended on how many plastic hinges can develop and at what point of the cyclic loading scheme that this happened. They are working on a numerical model.

41 - 7 - 4 Mechanical Behaviour of Traditional Timber Connections: Proposals for Design, Based on Experimental and Numerical Investigations. Part I: Birdsmouth - **C Faye, P Garcia, L Le Magorou, F. Rouger**

Presented by C. Faye

H.J. Larsen commented that the detail was simple but load transfer was rather complicated. He asked how the influence of deformation on load transfer was considered. He expressed doubt about the validity of the model for example Kc90 must be bigger than 3 for this to work but a smaller Kc90 value was used. C. Faye explained that other variables were used in the calibration. H.J. Larsen commented that why stress concentration has to be introduced to account for the already high shear stress. W. Munoz asked about optimization of the geometry of the connection. C. Faye responded that this has not been

done yet. A. Leijten commented that if there was shrinkage, one can have different stress state. C. Faye agreed that if contact area was different then load transfer and stress state would be different.

41 - 7 - 5 Embedment Strength of European Hardwoods - **U Hübner, T. Bogensperger, G Schickhofer**

Presented by U. Hübner

H.J. Larsen commented that if you want to use the timber for standardized test, whole population could be used rather than limited to the density range because the test standard does not specify the condition of the specimens but specifies the method of testing. A. Leijten mentioned that EN 408 and 3838 specify the condition of the test specimens. A. Jorissen received clarification of where the 5 mm deformation specified in the test method occurred. J. Munch Andersen stated that the model depended on diameter and asked how much a difference it would make if the diameter was ignored. U. Hübner referred to Figure 4.1 in the paper which showed the differences. I. Smith explained the origin of 2.1 mm from a paper 25 years ago which is 1/12 of an inch. He commented that one should avoid setting embedment values too high as system behaviour may be compromised because of compatibility to structural system is important. He said the origin of the 5 mm comes from timber to timber connections. A. Leijten and U. Hübner discussed issue of moisture content and the oven dried specimens in term of hysteresis and dryness condition. U. Hübner mentioned also slow drying was used.

10 STRESSES FOR SOLID TIMBER

41 - 6 - 1 Design of Inclined Glulam Members with an End Notch on the Tension Face - **A Asiz, I Smith**

Presented by A. Asiz

H. Blass asked when the results were compared to design code was the local component perpendicular to member axis used. I. Smith answered that the calculations were done on this basis but the reaction forces were presented as the vertical component. H. Blass asked whey then would you need to test an inclined member rather than horizontal members. I. Smith stated that the horizontal beam tests have been done before and the inclined test concept originated from industry. He agreed that small specimen would be sufficient but precalculations indicated higher chances of notch failure rather than bending so the results were surprising. T. Williamson commented that the final graph seems to indicate CSA and EC approach yielded similar results and close to the test results. R. Steiger referred to Table 4 and asked how the shear strength design values based on EC5 model were established i.e. which gamma values were used and where did the 1.75 value come from and what is the strength of this grade of glulam. I. Smith clarified that it is a characteristic value back calculated from design value in code. A. Leijten asked how many tests were conducted. A. Asiz replied six. H.J. Larsen commented with 6 tests you can't get characteristics values. Actually only three test results were valid as the others did not have the same mode of failure. S. Aicher commented that the derivation was incorrect because the assumption of normal distribution would be incorrect as multiple mode of failure was present. J. Köhler commented as statistical uncertainties were ignored this could lead to wrong results. A. Asiz responded that they intend to develop numerical model based on the limited resources and available results. This will be the next step.

41 - 6 - 2 A New Design Approach for End-notched Beams - View on Code – **K Rautenstrauch, B Franke, S Franke, K U Schober**

Presented by K. U. Schober

I. Smith asked whether such steep notch is allowed. K.U. Schober answered yes. He questioned whether the same formula would apply to shallow notch say 0.2 because with deep notch one can force the total fracture energy to fit within LEFM but no so in shallow case. Modes 1 and 2 fractures and displacement versus load control issues were discussed. S. Aicher stated that this proposal was not accepted in Germany because the calibration base was too small. It was considered too extreme to come up with the conclusion that the present situation is not conservative. F. Lam commented that in service micro checks and large cracks can exists in timber due to environmental conditions. This could skew the results if such cracks did not develop in the test specimens. May be a practical solution is to use reinforcements to deal with the problem rather than refining the code. S. Aicher and K.U. Schober said that reinforcements are now commonly used. V. Rajcic and K.U. Schober discussed what fracture mechanics theory was used and its applicability to wood.

41 - 6 - 3 The Design Rules in Eurocode 5 for Compression Perpendicular to the Grain – Continuous Supported Beams - **H J Larsen, T A C M van der Put, A J M Leijten**

Presented by H.J. Larsen

I. Smith commented that there is a large Forintek database from Canada that covers this area. H. Blass commented that the equation with reference to EC5 A1 is incorrect and different from the proposal by Blass and Görlacher. H.J. Larsen stated that the equation is cited from the latest version of EC5 A1. H. Blass stated if so the quotation of Blass and Görlacher is incorrect and should be removed. He further explained the original proposal from Karlsruhe and requested the test results from Delft so that comparisons can be made.

41 - 6 - 4 Size Effects in Bending - **J K Denzler, P Glos**

Presented by J K Denzler

A. Buchanan asked if EN 384 is the standard to provide characteristic values and what about the design standard, should size effect not be included? J.K. Denzler replied that the size effect adjustments are not in the design code. I. Smith asked about commercially graded material and cited the effect of grading errors in Madsen's work. He mentioned that if Weibull was correct then one would expect more failures in buildings where one had 100 joists compared to one joist. J.K. Denzler stated that this work is based on laboratory grading. F. Lam commented that Weibull theory is based on series system and a building with many joists would be a parallel system. R. Steiger discussed width effect in Eqn. 2 of the paper and suggested clarification be added to paper. S. Aicher raised a practical question of whether it is possible to deal with the acceptance of new softwood species with ignoring size effect in standard. J.K. Denzler agreed as there may be a species effect also. A. Jorissen received clarification about the conclusions. J. Köhler agreed that this work should not be extrapolated to design situations and received clarification about the selection of weakest zone for testing. I. Smith stated that experience from testing softwood showed that defect features can "talk" to each other. He discussed the assumption of homogeneity and shear design issues in Canada and expressed further doubt about the Weibull theory. F. Lam commented the thickness effect is also a function of how the material is milled (centre versus side cut), the location within a tree, and the size of tree etc.

S. Aicher and J. Köhler debated the issue of whether Weibull effect in length is not appropriate. The appearance of knot is non continuous and Weibull is more on the empirical side.

11 STRESS GRADING

41 - 5 - 1 *Probabilistic Output Control for Structural Timber - Fundamental Model Approach* - **M K Sandomeer, J Köhler, M H Faber**

Presented by M. K. Sandomeer

H. Blass asked how many pieces of lumber needed to detect quality shift. M.K. Sandomeer responded in this study 1000. H. Blass questioned what to do with the 1000 pieces of out of control material. J. Köhler stated that fractile values related to population versus individual batch of lumber. It would be problematic to deal with the fractile of individual batch. M. Bartlett stated that the work is based on regression analysis which did not take into consideration of the error in the predictor or grading values. I. Smith added that the issue of grading error can come out. The issue of random versus bias was discussed. F. Lam commented that this is interesting work. In N. American output control system requires intensive testing of material if machine adjustments exceeded a certain small percentage. This is generally avoided by operator by setting machine conservatively. In the approach proposed would there be the same type of requirements. M.K. Sandomeer responded yes but not yet defined. A. Ranta-Maunus commented about shift in quality and the size of the shift. One should not only consider the 5^{th} percentile but also the lower tail in a package. S. Aicher asked whether this would be possible to apply this with a truncated function of the indicator variable and apply it to obtain the lower fractile. J. Köhler responded that this is already done.

12 LIMIT STATE DESIGN

41 - 1 - 1 *On the Role of Stiffness Properties for Ultimate Limit State Design of Slender Columns* - **J Köhler, A Frangi, R Steiger**

Presented by J. Köhler

H.J. Larsen received confirmation the "effective length method" is the correct wording. He commented that the relationship between strength and stiffness is sensitive to the fractile of interest. A. Jorissen received clarification about the design equation for column. He commented that γm seemed to have been taken into account twice. J. Köhler confirmed that the approach is correct. U. Kuhlmann commented that the existing variation should include imperfection and provided explanation about the steel column design approach as a possible comparison. J. Köhler responded that imperfection is already considered. In terms of long term performance the influence of creep on P-delta is important. R. Steiger commented that the stiffness of connection joints don't have 5^{th} percentile values and received clarification that the issue of isolated column and moment resistance where in the German code 5^{th} percentile / γm is considered.

13 ANY OTHER BUSINESS

B. Dujic suggested that a statement should be put into the proceedings that it is reviewer discussed and acceptance procedures of paper. H. Blass stated that this might require re-review of paper after the discussion process. I. Smith stated that the reviewers may not agree on the paper and one person may end up making the decision. J. Köhler commented that the delegate should conclude after the discussion whether a paper needs further reviewing and clarify the changes needed. J. Munch Andersen stated that this may create a better paper that can be provided to journal later. B. Dujic stated that may be we can't reach the Journal level but clear description of the acceptance process is important. J. König stated that discussion of paper guarantee that the authors are tested. Revised paper should include a short note about what was changed so that the information can be related to the minutes. Further presenters are expected to be able to defend the paper and should know all aspect of a co-authored work. H. Blass agreed that acceptance procedures of paper for CIB W18 will be put into proceeding.

M. Fragiacomo suggested an extension of STEP 1 and 2 in form of document or ppt presentation on design principles be produced. H.J. Larsen is working on a book on the background of EC5 and will be reviewing all CIB W18 proceedings. H. Blass stated that an updated STEP book in German will be produced. H. Blass said that it would be very time consuming at this stage to coordinate a multi-author effort for a STEP type document. T. Williamson suggested that ppt of presentation in pdf format be made available as part of the proceeding or in website. I. Smith commented that it is best to leave the technical program in the hands of the secretarial. H. Blass asked the delegate to send in their pdf file. As electronics copy is not a permanent record will consider the viability of providing a CD with the proceedings.

Master copy of the paper and pdf files with any corrections should be send to R Görlacher at the end of September 2008. Some of the papers will be renumbered. Changes to papers only needed if errors were identified.

14 VENUE AND PROGRAMME FOR NEXT MEETING

R. Steiger invited CIB W18 delegate to participate in next year's CIB W18 meeting Aug 24 – 28, 2008 in Dübendorf (near Zürich) Switzerland and provided information about the venue.

A. Buchanan invited the CIB W18 meeting to come to Christchurch New Zealand in end of August 2010.

B. Källsner invited CIB W18 meeting to come to Växjo Sweden in 2012 and there is also an invitation from Delft Netherlands for 2012.

The meeting venues for next few years are: Switzerland (2009), New Zealand (2010), Italy (2011), the Netherlands (2012) or Växjo (2012).

Photographs and participant list for 41st CIB W18 and their contact information will be available from the password protected area of the CIB W18 website.

15 CLOSE

The chair thanked the speakers for their presentations and the delegates for their participation. He also thanked I. Smith and the host team for their efforts to organize the meeting.

16. Peer Review of Papers for the CIB-W18 Proceedings

16. Peer review of papers for the CIB-W18 Proceedings

Experts involved:

Members of the CIB-W18 "Timber Structures" group are a community of experts in the field of timber engineering.

Procedure of peer review

- Submission of manuscripts: all members of the CIB-W18 group attending the meeting receive the manuscripts of the papers at least four weeks before the meeting. Everyone is invited to read and review the manuscripts especially in their respective fields of competence and interest.

- Presentation of the paper during the meeting by the author

- Comments and recommendations of the experts, discussion of the paper

- Comments, discussion and recommendations of the experts are documented in the minutes of the meeting and are printed on the front page of each paper.

- Final acceptance of the paper for the proceedings with
  no changes
  minor changes
  major changes
  or reject

- Revised papers are to be sent to the editor of the proceedings and the chairman of the CIB-W18 group

- Editor and chairman check, whether the requested changes have been carried out.

17. List of CIB-W18 Papers, St. Andrews, Canada 2008

List of CIB-W18 Papers, St. Andrews, Canada 2008

41 - 1 – 1 On the Role of Stiffness Properties for Ultimate Limit State Design of Slender Columns - **J Köhler, A Frangi, R Steiger**

41 - 5 - 1 Probabilistic Output Control for Structural Timber - Fundamental Model Approach - **M K Sandomeer, J Köhler, M H Faber**

41 - 6 - 1 Design of Inclined Glulam Members with an End Notch on the Tension Face - **A Asiz, I Smith**

41 - 6 - 2 A New Design Approach for End-notched Beams - View on Code – **K Rautenstrauch, B Franke, S Franke, K U Schober**

41 - 6 - 3 The Design Rules in Eurocode 5 for Compression Perpendicular to the Grain - Continuous Supported Beams - **H J Larsen, T A C M van der Put, A J M Leijten**

41 - 6 - 4 Size Effects in Bending – **J K Denzler, P Glos**

41 - 7 - 1 Applicability of Existing Design Approaches to Mechanical Joints in Structural Composite Lumber - **M Snow, I Smith, A Asiz, M Ballerini**

41 - 7 - 2 Validation of the Canadian Bolted Connection Design Proposal - **P Quenneville, J Jensen**

41 - 7 - 3 Ductility of Moment Resisting Dowelled Joints in Heavy Timber Structures - **A Polastri, R Tomasi, M Piazza, I Smith**

41 - 7 - 4 Mechanical Behaviour of Traditional Timber Connections: Proposals for Design, Based on Experimental and Numerical Investigations. Part I: Birdsmouth - **C Faye, P Garcia, L Le Magorou, F Rouger**

41 - 7 - 5 Embedding Strength of European Hardwoods - **U Hübner, T Bogensperger, G Schickhofer**

41 - 10 - 1 Composite Action of I-Joist Floor Systems - **T G Williamson, B Yeh**

41 - 10 - 2 Evaluation of the Prestressing Losses in Timber Members Prestressed with Unbonded Tendons - **M Fragiacomo, M Davies**

41 - 10 - 3 Relationship Between Global and Local MOE - **J K Denzler, P Stapel, P Glos**

41 - 12 - 1 Paper withdrawn by the author

41 - 12 - 2 Bending Strength of Spruce Glulam: New Models for the Characteristic Bending Strength - **M Frese, H J Blass,**

41 - 12 - 3 In-Plane Shear Strength of Cross Laminated Timber - **R A Joebstl, T Bogensperger, G Schickhofer**

41 - 12 - 4 Strength of Glulam Beams with Holes - Tests of Quadratic Holes and Literature Test Results Compilation - **H Danielsson, P J Gustafsson**

41 - 15 - 1 Need for a Harmonized Approach for Calculations of Ductility of Timber Assemblies - **W Muñoz, M Mohammad, A Salenikovich, P Quenneville**

41 - 15 - 2 Plastic Design of Wood Frame Wall Diaphragms in Low and Medium Rise Buildings - **B Källsner, U A Girhammar**

41 - 15 - 3 Failure Analysis of Light Wood Frame Structures under Wind Load - **A Asiz, Y H Chui, I Smith**

41 - 15 - 4 Combined Shear and Wind Uplift Resistance of Wood Structural Panel Shearwalls - **B Yeh, T G Williamson**

41 - 15 - 5 Behaviour of Prefabricated Timber Wall Elements under Static and Cyclic Loading - P **Schädle, H J Blass**

41 - 16 - 1 Effect of Adhesives on Finger Joint Performance in Fire - **J König, J Norén, M Sterley**

41 - 21 - 1 Determination of Shear Modulus by Means of Standardized Four-Point Bending Tests - **R Brandner, B Freytag, G Schickhofer**

41 - 102 - 1 Consequences of EC 5 for Danish Best Practise - **J Munch-Andersen**

41 - 102 - 2 Development of New Swiss standards for the Assessment of Existing Load Bearing Structures - **R Steiger, J Köhler**

41 – 102 - 3 Measuring the CO2 Footprint of Timber Buildings - **A Buchanan, S John**

18. Current List of CIB-W18(A) Papers

CURRENT LIST OF CIB-W18(A) PAPERS

Technical papers presented to CIB-W18(A) are identified by a code CIB-W18(A)/a-b-c, where:

a denotes the meeting at which the paper was presented. Meetings are classified in chronological order:

1 Princes Risborough, England; March 1973
2 Copenhagen, Denmark; October 1973
3 Delft, Netherlands; June 1974
4 Paris, France; February 1975
5 Karlsruhe, Federal Republic of Germany; October 1975
6 Aalborg, Denmark; June 1976
7 Stockholm, Sweden; February/March 1977
8 Brussels, Belgium; October 1977
9 Perth, Scotland; June 1978
10 Vancouver, Canada; August 1978
11 Vienna, Austria; March 1979
12 Bordeaux, France; October 1979
13 Otaniemi, Finland; June 1980
14 Warsaw, Poland; May 1981
15 Karlsruhe, Federal Republic of Germany; June 1982
16 Lillehammer, Norway; May/June 1983
17 Rapperswil, Switzerland; May 1984
18 Beit Oren, Israel; June 1985
19 Florence, Italy; September 1986
20 Dublin, Ireland; September 1987
21 Parksville, Canada; September 1988
22 Berlin, German Democratic Republic; September 1989
23 Lisbon, Portugal; September 1990
24 Oxford, United Kingdom; September 1991
25 Åhus, Sweden; August 1992
26 Athens, USA; August 1993
27 Sydney, Australia; July 1994
28 Copenhagen, Denmark; April 1995
29 Bordeaux, France; August 1996
30 Vancouver, Canada; August 1997
31 Savonlinna, Finland; August 1998
32 Graz, Austria, August 1999
33 Delft, The Netherlands; August 2000
34 Venice, Italy; August 2001
35 Kyoto, Japan; September 2002
36 Colorado, USA; August 2003
37 Edinburgh, Scotland, August 2004
38 Karlsruhe, Germany, August 2005
39 Florence, Italy, August 2006
40 Bled, Slovenia, August 2007
41 St. Andrews, Canada 2008

b denotes the subject:

1 Limit State Design
2 Timber Columns
3 Symbols
4 Plywood
5 Stress Grading
6 Stresses for Solid Timber
7 Timber Joints and Fasteners
8 Load Sharing
9 Duration of Load
10 Timber Beams
11 Environmental Conditions
12 Laminated Members
13 Particle and Fibre Building Boards
14 Trussed Rafters
15 Structural Stability
16 Fire
17 Statistics and Data Analysis
18 Glued Joints
19 Fracture Mechanics
20 Serviceability
21 Test Methods
100 CIB Timber Code
101 Loading Codes
102 Structural Design Codes
103 International Standards Organisation
104 Joint Committee on Structural Safety
105 CIB Programme, Policy and Meetings
106 International Union of Forestry Research Organisations

c is simply a number given to the papers in the order in which they appear:

Example: CIB-W18/4-102-5 refers to paper 5 on subject 102 presented at the fourth meeting of W18.

Listed below, by subjects, are all papers that have to date been presented to W18. When appropriate some papers are listed under more than one subject heading.

LIMIT STATE DESIGN

1-1-1	Limit State Design - H J Larsen
1-1-2	The Use of Partial Safety Factors in the New Norwegian Design Code for Timber Structures - O Brynildsen
1-1-3	Swedish Code Revision Concerning Timber Structures - B Noren
1-1-4	Working Stresses Report to British Standards Institution Committee BLCP/17/2
6-1-1	On the Application of the Uncertainty Theoretical Methods for the Definition of the Fundamental Concepts of Structural Safety - K Skov and O Ditlevsen
11-1-1	Safety Design of Timber Structures - H J Larsen
18-1-1	Notes on the Development of a UK Limit States Design Code for Timber - A R Fewell and C B Pierce
18-1-2	Eurocode 5, Timber Structures - H J Larsen
19-1-1	Duration of Load Effects and Reliability Based Design (Single Member) - R O Foschi and Z C Yao
21-102-1	Research Activities Towards a New GDR Timber Design Code Based on Limit States Design - W Rug and M Badstube
22-1-1	Reliability-Theoretical Investigation into Timber Components Proposal for a Supplement of the Design Concept - M Badstube, W Rug and R Plessow
23-1-1	Some Remarks about the Safety of Timber Structures - J Kuipers
23-1-2	Reliability of Wood Structural Elements: A Probabilistic Method to Eurocode 5 Calibration - F Rouger, N Lheritier, P Racher and M Fogli
31-1-1	A Limit States Design Approach to Timber Framed Walls - C J Mettem, R Bainbridge and J A Gordon
32 -1-1	Determination of Partial Coefficients and Modification Factors- H J Larsen, S Svensson and S Thelandersson
32 -1-2	Design by Testing of Structural Timber Components - V Enjily and L Whale
33-1-1	Aspects on Reliability Calibration of Safety Factors for Timber Structures – S Svensson and S Thelandersson
33-1-2	Sensitivity studies on the reliability of timber structures – A Ranta-Maunus, M Fonselius, J Kurkela and T Toratti
41-1–1	On the Role of Stiffness Properties for Ultimate Limit State Design of Slender Columns– J Köhler, A Frangi, R Steiger

TIMBER COLUMNS

2-2-1	The Design of Solid Timber Columns - H J Larsen
3-2-1	The Design of Built-Up Timber Columns - H J Larsen
4-2-1	Tests with Centrally Loaded Timber Columns - H J Larsen and S S Pedersen
4-2-2	Lateral-Torsional Buckling of Eccentrically Loaded Timber Columns- B Johansson
5-9-1	Strength of a Wood Column in Combined Compression and Bending with Respect to Creep - B Källsner and B Norén
5-100-1	Design of Solid Timber Columns (First Draft) - H J Larsen
6-100-1	Comments on Document 5-100-1, Design of Solid Timber Columns - H J Larsen and E Theilgaard
6-2-1	Lattice Columns - H J Larsen
6-2-2	A Mathematical Basis for Design Aids for Timber Columns - H J Burgess

6-2-3	Comparison of Larsen and Perry Formulas for Solid Timber Columns- H J Burgess
7-2-1	Lateral Bracing of Timber Struts - J A Simon
8-15-1	Laterally Loaded Timber Columns: Tests and Theory - H J Larsen
17-2-1	Model for Timber Strength under Axial Load and Moment - T Poutanen
18-2-1	Column Design Methods for Timber Engineering - A H Buchanan, K C Johns, B Madsen
19-2-1	Creep Buckling Strength of Timber Beams and Columns - R H Leicester
19-12-2	Strength Model for Glulam Columns - H J Blaß
20-2-1	Lateral Buckling Theory for Rectangular Section Deep Beam-Columns- H J Burgess
20-2-2	Design of Timber Columns - H J Blaß
21-2-1	Format for Buckling Strength - R H Leicester
21-2-2	Beam-Column Formulae for Design Codes - R H Leicester
21-15-1	Rectangular Section Deep Beam - Columns with Continuous Lateral Restraint - H J Burgess
21-15-2	Buckling Modes and Permissible Axial Loads for Continuously Braced Columns - H J Burgess
21-15-3	Simple Approaches for Column Bracing Calculations - H J Burgess
21-15-4	Calculations for Discrete Column Restraints - H J Burgess
22-2-1	Buckling and Reliability Checking of Timber Columns - S Huang, P M Yu and J Y Hong
22-2-2	Proposal for the Design of Compressed Timber Members by Adopting the Second-Order Stress Theory - P Kaiser
30-2-1	Beam-Column Formula for Specific Truss Applications - W Lau, F Lam and J D Barrett
31-2-1	Deformation and Stability of Columns of Viscoelastic Material Wood - P Becker and K Rautenstrauch
34-2-1	Long-Term Experiments with Columns: Results and Possible Consequences on Column Design – W Moorkamp, W Schelling, P Becker, K Rautenstrauch
34-2-2	Proposal for Compressive Member Design Based on Long-Term Simulation Studies – P Becker, K Rautenstrauch
35-2-1	Computer Simulations on the Reliability of Timber Columns Regarding Hygrothermal Effects- R Hartnack, K-U Schober, K Rautenstrauch
36-2-1	The Reliability of Timber Columns Based on Stochastical Principles - K Rautenstrauch, R Hartnack
38-2-1	Long-term Load Bearing of Wooden Columns Influenced by Climate – View on Code - R Hartnack, K Rautenstrauch

SYMBOLS

3-3-1	Symbols for Structural Timber Design - J Kuipers and B Norén
4-3-1	Symbols for Timber Structure Design - J Kuipers and B Norén
28-3-1	Symbols for Timber and Wood-Based Materials - J Kuipers and B Noren
1	Symbols for Use in Structural Timber Design

PLYWOOD

2-4-1	The Presentation of Structural Design Data for Plywood - L G Booth
3-4-1	Standard Methods of Testing for the Determination of Mechanical Properties of Plywood - J Kuipers
3-4-2	Bending Strength and Stiffness of Multiple Species Plywood - C K A Stieda
4-4-4	Standard Methods of Testing for the Determination of Mechanical Properties of Plywood - Council of Forest Industries, B.C.
5-4-1	The Determination of Design Stresses for Plywood in the Revision of CP 112 - L G Booth
5-4-2	Veneer Plywood for Construction - Quality Specifications - ISO/TC 139. Plywood, Working Group 6
6-4-1	The Determination of the Mechanical Properties of Plywood Containing Defects - L G Booth
6-4-2	Comparsion of the Size and Type of Specimen and Type of Test on Plywood Bending Strength and Stiffness - C R Wilson and P Eng
6-4-3	Buckling Strength of Plywood: Results of Tests and Recommendations for Calculations - J Kuipers and H Ploos van Amstel
7-4-1	Methods of Test for the Determination of Mechanical Properties of Plywood - L G Booth, J Kuipers, B Norén, C R Wilson
7-4-2	Comments Received on Paper 7-4-1
7-4-3	The Effect of Rate of Testing Speed on the Ultimate Tensile Stress of Plywood - C R Wilson and A V Parasin
7-4-4	Comparison of the Effect of Specimen Size on the Flexural Properties of Plywood Using the Pure Moment Test - C R Wilson and A V Parasin
8-4-1	Sampling Plywood and the Evaluation of Test Results - B Norén
9-4-1	Shear and Torsional Rigidity of Plywood - H J Larsen
9-4-2	The Evaluation of Test Data on the Strength Properties of Plywood - L G Booth
9-4-3	The Sampling of Plywood and the Derivation of Strength Values (Second Draft) - B Norén
9-4-4	On the Use of the CIB/RILEM Plywood Plate Twisting Test: a progress report - L G Booth
10-4-1	Buckling Strength of Plywood - J Dekker, J Kuipers and H Ploos van Amstel
11-4-1	Analysis of Plywood Stressed Skin Panels with Rigid or Semi-Rigid Connections- I Smith
11-4-2	A Comparison of Plywood Modulus of Rigidity Determined by the ASTM and RILEM CIB/3-TT Test Methods - C R Wilson and A V Parasin
11-4-3	Sampling of Plywood for Testing Strength - B Norén
12-4-1	Procedures for Analysis of Plywood Test Data and Determination of Characteristic Values Suitable for Code Presentation - C R Wilson
14-4-1	An Introduction to Performance Standards for Wood-base Panel Products - D H Brown
14-4-2	Proposal for Presenting Data on the Properties of Structural Panels - T Schmidt
16-4-1	Planar Shear Capacity of Plywood in Bending - C K A Stieda
17-4-1	Determination of Panel Shear Strength and Panel Shear Modulus of Beech-Plywood in Structural Sizes - J Ehlbeck and F Colling
17-4-2	Ultimate Strength of Plywood Webs - R H Leicester and L Pham

20-4-1 Considerations of Reliability - Based Design for Structural Composite Products - M R O'Halloran, J A Johnson, E G Elias and T P Cunningham

21-4-1 Modelling for Prediction of Strength of Veneer Having Knots - Y Hirashima

22-4-1 Scientific Research into Plywood and Plywood Building Constructions the Results and Findings of which are Incorporated into Construction Standard Specifications of the USSR - I M Guskov

22-4-2 Evaluation of Characteristic values for Wood-Based Sheet Materials - E G Elias

24-4-1 APA Structural-Use Design Values: An Update to Panel Design Capacities - A L Kuchar, E G Elias, B Yeh and M R O'Halloran

STRESS GRADING

1-5-1 Quality Specifications for Sawn Timber and Precision Timber - Norwegian Standard NS 3080

1-5-2 Specification for Timber Grades for Structural Use - British Standard BS 4978

4-5-1 Draft Proposal for an International Standard for Stress Grading Coniferous Sawn Softwood - ECE Timber Committee

16-5-1 Grading Errors in Practice - B Thunell

16-5-2 On the Effect of Measurement Errors when Grading Structural Timber- L Nordberg and B Thunell

19-5-1 Stress-Grading by ECE Standards of Italian-Grown Douglas-Fir Dimension Lumber from Young Thinnings - L Uzielli

19-5-2 Structural Softwood from Afforestation Regions in Western Norway - R Lackner

21-5-1 Non-Destructive Test by Frequency of Full Size Timber for Grading - T Nakai

22-5-1 Fundamental Vibration Frequency as a Parameter for Grading Sawn Timber - T Nakai, T Tanaka and H Nagao

24-5-1 Influence of Stress Grading System on Length Effect Factors for Lumber Loaded in Compression - A Campos and I Smith

26-5-1 Structural Properties of French Grown Timber According to Various Grading Methods - F Rouger, C De Lafond and A El Quadrani

28-5-1 Grading Methods for Structural Timber - Principles for Approval - S Ohlsson

28-5-2 Relationship of Moduli of Elasticity in Tension and in Bending of Solid Timber - N Burger and P Glos

29-5-1 The Effect of Edge Knots on the Strength of SPF MSR Lumber - T Courchene, F Lam and J D Barrett

29-5-2 Determination of Moment Configuration Factors using Grading Machine Readings - T D G Canisius and T Isaksson

31-5-1 Influence of Varying Growth Characteristics on Stiffness Grading of Structural Timber - S Ormarsson, H Petersson, O Dahlblom and K Persson

31-5-2 A Comparison of In-Grade Test Procedures - R H Leicester, H Breitinger and H Fordham

32-5-1 Actual Possibilities of the Machine Grading of Timber - K Frühwald and A Bernasconi

32-5-2 Detection of Severe Timber Defects by Machine Grading - A Bernasconi, L Boström and B Schacht

34-5-1 Influence of Proof Loading on the Reliability of Members – F Lam, S Abayakoon, S Svensson, C Gyamfi

36-5-1 Settings for Strength Grading Machines – Evaluation of the Procedure according to prEN 14081, part 2 - C Bengtsson, M Fonselius

36-5-2 A Probabilistic Approach to Cost Optimal Timber Grading - J Köhler, M H Faber

36-7-11 Reliability of Timber Structures, Theory and Dowel-Type Connection Failures - A Ranta-Maunus, A Kevarinmäki

38-5-1 Are Wind-Induced Compression Failures Grading Relevant - M Arnold, R Steiger

39-5-1 A Discussion on the Control of Grading Machine Settings – Current Approach, Potential and Outlook - J Köhler, R Steiger

39-5-2 Tensile Proof Loading to Assure Quality of Finger-Jointed Structural timber - R Katzengruber, G Jeitler, G Schickhofer

40-5-1 Development of Grading Rules for Re-Cycled Timber Used in Structural Applications - K Crews

40-5-2 The Efficient Control of Grading Machine Settings - M Sandomeer, J Köhler, P Linsenmann

41-5-1 Probabilistic Output Control for Structural Timber - Fundamental Model Approach – M K Sandomeer, J Köhler, M H Faber

STRESSES FOR SOLID TIMBER

4-6-1 Derivation of Grade Stresses for Timber in the UK - W T Curry

5-6-1 Standard Methods of Test for Determining some Physical and Mechanical Properties of Timber in Structural Sizes - W T Curry

5-6-2 The Description of Timber Strength Data - J R Tory

5-6-3 Stresses for EC1 and EC2 Stress Grades - J R Tory

6-6-1 Standard Methods of Test for the Determination of some Physical and Mechanical Properties of Timber in Structural Sizes (third draft) - W T Curry

7-6-1 Strength and Long-term Behaviour of Lumber and Glued Laminated Timber under Torsion Loads - K Möhler

9-6-1 Classification of Structural Timber - H J Larsen

9-6-2 Code Rules for Tension Perpendicular to Grain - H J Larsen

9-6-3 Tension at an Angle to the Grain - K Möhler

9-6-4 Consideration of Combined Stresses for Lumber and Glued Laminated Timber - K Möhler

11-6-1 Evaluation of Lumber Properties in the United States - W L Galligan and J H Haskell

11-6-2 Stresses Perpendicular to Grain - K Möhler

11-6-3 Consideration of Combined Stresses for Lumber and Glued Laminated Timber (addition to Paper CIB-W18/9-6-4) - K Möhler

12-6-1 Strength Classifications for Timber Engineering Codes - R H Leicester and W G Keating

12-6-2 Strength Classes for British Standard BS 5268 - J R Tory

13-6-1 Strength Classes for the CIB Code - J R Tory

13-6-2 Consideration of Size Effects and Longitudinal Shear Strength for Uncracked Beams - R O Foschi and J D Barrett

13-6-3 Consideration of Shear Strength on End-Cracked Beams - J D Barrett and R O Foschi

15-6-1 Characteristic Strength Values for the ECE Standard for Timber - J G Sunley

16-6-1 Size Factors for Timber Bending and Tension Stresses - A R Fewell

16-6-2	Strength Classes for International Codes - A R Fewell and J G Sunley
17-6-1	The Determination of Grade Stresses from Characteristic Stresses for BS 5268: Part 2 - A R Fewell
17-6-2	The Determination of Softwood Strength Properties for Grades, Strength Classes and Laminated Timber for BS 5268: Part 2 - A R Fewell
18-6-1	Comment on Papers: 18-6-2 and 18-6-3 - R H Leicester
18-6-2	Configuration Factors for the Bending Strength of Timber - R H Leicester
18-6-3	Notes on Sampling Factors for Characteristic Values - R H Leicester
18-6-4	Size Effects in Timber Explained by a Modified Weakest Link Theory- B Madsen and A H Buchanan
18-6-5	Placement and Selection of Growth Defects in Test Specimens - H Riberholt
18-6-6	Partial Safety-Coefficients for the Load-Carrying Capacity of Timber Structures - B Norén and J-0 Nylander
19-6-1	Effect of Age and/or Load on Timber Strength - J Kuipers
19-6-2	Confidence in Estimates of Characteristic Values - R H Leicester
19-6-3	Fracture Toughness of Wood - Mode I - K Wright and M Fonselius
19-6-4	Fracture Toughness of Pine - Mode II - K Wright
19-6-5	Drying Stresses in Round Timber - A Ranta-Maunus
19-6-6	A Dynamic Method for Determining Elastic Properties of Wood - R Görlacher
20-6-1	A Comparative Investigation of the Engineering Properties of "Whitewoods" Imported to Israel from Various Origins - U Korin
20-6-2	Effects of Yield Class, Tree Section, Forest and Size on Strength of Home Grown Sitka Spruce - V Picardo
20-6-3	Determination of Shear Strength and Strength Perpendicular to Grain - H J Larsen
21-6-1	Draft Australian Standard: Methods for Evaluation of Strength and Stiffness of Graded Timber - R H Leicester
21-6-2	The Determination of Characteristic Strength Values for Stress Grades of Structural Timber. Part 1 - A R Fewell and P Glos
21-6-3	Shear Strength in Bending of Timber - U Korin
22-6-1	Size Effects and Property Relationships for Canadian 2-inch Dimension Lumber - J D Barrett and H Griffin
22-6-2	Moisture Content Adjustements for In-Grade Data - J D Barrett and W Lau
22-6-3	A Discussion of Lumber Property Relationships in Eurocode 5 - D W Green and D E Kretschmann
22-6-4	Effect of Wood Preservatives on the Strength Properties of Wood - F Ronai
23-6-1	Timber in Compression Perpendicular to Grain - U Korin
24-6-1	Discussion of the Failure Criterion for Combined Bending and Compression - T A C M van der Put
24-6-3	Effect of Within Member Variability on Bending Strength of Structural Timber - I Czmoch, S Thelandersson and H J Larsen
24-6-4	Protection of Structural Timber Against Fungal Attack Requirements and Testing- K Jaworska, M Rylko and W Nozynski
24-6-5	Derivation of the Characteristic Bending Strength of Solid Timber According to CEN-Document prEN 384 - A J M Leijten
25-6-1	Moment Configuration Factors for Simple Beams- T D G Canisius

25-6-3	Bearing Capacity of Timber - U Korin
25-6-4	On Design Criteria for Tension Perpendicular to Grain - H Petersson
25-6-5	Size Effects in Visually Graded Softwood Structural Lumber - J D Barrett, F Lam and W Lau
26-6-1	Discussion and Proposal of a General Failure Criterion for Wood - T A C M van der Put
27-6-1	Development of the "Critical Bearing": Design Clause in CSA-086.1 - C Lum and E Karacabeyli
27-6-2	Size Effects in Timber: Novelty Never Ends - F Rouger and T Fewell
27-6-3	Comparison of Full-Size Sugi (Cryptomeria japonica D.Don) Structural Performance in Bending of Round Timber, Two Surfaces Sawn Timber and Square Sawn Timber - T Nakai, H Nagao and T Tanaka
28-6-1	Shear Strength of Canadian Softwood Structural Lumber - F Lam, H Yee and J D Barrett
28-6-2	Shear Strength of Douglas Fir Timbers - B Madsen
28-6-3	On the Influence of the Loading Head Profiles on Determined Bending Strength - L Muszyñsky and R Szukala
28-6-4	Effect of Test Standard, Length and Load Configuration on Bending Strength of Structural Timber- T Isaksson and S Thelandersson
28-6-5	Grading Machine Readings and their Use in the Calculation of Moment Configuration Factors - T Canisius, T Isaksson and S Thelandersson
28-6-6	End Conditions for Tension Testing of Solid Timber Perpendicular to Grain - T Canisius
29-6-1	Effect of Size on Tensile Strength of Timber - N Burger and P Glos
29-6-2	Equivalence of In-Grade Testing Standards - R H Leicester, H O Breitinger and H F Fordham
30-6-1	Strength Relationships in Structural Timber Subjected to Bending and Tension - N Burger and P Glos
30-6-2	Characteristic Design Stresses in Tension for Radiata Pine Grown in Canterbury - A Tsehaye, J C F Walker and A H Buchanan
30-6-3	Timber as a Natural Composite: Explanation of Some Peculiarities in the Mechanical Behaviour - E Gehri
31-6-1	Length and Moment Configuration Factors - T Isaksson
31-6-2	Tensile Strength Perpendicular to Grain According to EN 1193 - H J Blaß and M Schmid
31-6-3	Strength of Small Diameter Round Timber - A Ranta-Maunus, U Saarelainen and H Boren
31-6-4	Compression Strength Perpendicular to Grain of Structural Timber and Glulam - L Damkilde, P Hoffmeyer and T N Pedersen
31-6-5	Bearing Strength of Timber Beams - R H Leicester, H Fordham and H Breitinger
32-6-1	Development of High-Resistance Glued Robinia Products and an Attempt to Assign Such Products to the European System of Strength Classes - G Schickhofer and B Obermayr
32-6-2	Length and Load Configuration Effects in the Code Format - T Isaksson
32-6-3	Length Effect on the Tensile Strength of Truss Chord Members - F Lam
32-6-4	Tensile Strength Perpendicular to Grain of Glued Laminated Timber - H J Blaß and M Schmid

32-6-5 On the Reliability-based Strength Adjustment Factors for Timber Design - T D G Canisius

34-6-1 Material Strength Properties for Canadian Species Used in Japanese Post and Beam Construction - J D Barrett, F Lam, S Nakajima

35-6-1 Evaluation of Different Size Effect Models for Tension Perpendicular to Grain Design - S Aicher, G Dill-Langer

35-6-2 Tensile Strength of Glulam Perpendicular to Grain - Effects of Moisture Gradients - J Jönsson, S Thelandersson

36-6-1 Characteristic Shear Strength Values Based on Tests According to EN 1193 - P Glos, J Denzler

37-6-1 Tensile Strength of Nordic Birch - K H Solli

37-6-2 Effect of Test Piece Orientation on Characteristic Bending Strength of Structural Timber - P Glos, J K Denzler

37-6-3 Strength and Stiffness Behaviour of Beech Laminations for High Strength Glulam - P Glos, J K Denzler, P W Linsenmann

37-6-4 A Review of Existing Standards Related to Calculation of Characteristic Values of Timber - F Rouger

37-6-5 Influence of the Rolling-Shear Modulus on the Strength and Stiffness of Structural Bonded Timber Elements - P Fellmoser, H J Blass

38-6-1 Design Specifications for Notched Beams in AS:1720 - R H Leicester

38-6-2 Characteristic Bending Strength of Beech Glulam - H J Blaß, M Frese

38-6-3 Shear Strength of Glued Laminated Timber - H Klapp, H Brüninghoff

39-6-1 Allocation of Central European hardwoods into EN 1912 - P Glos, J K Denzler

39-6-2 Revisiting EN 338 and EN 384 Basics and Procedures - R Steiger, M Arnold, M Fontana

40-6-1 Bearing Strength Perpendicular to the Grain of Locally Loaded Timber Blocks - A J M Leijten, J C M Schoenmakers

40-6-2 Experimental Study of Compression and Shear Strength of Spruce Timber - M Poussa, P Tukiainen, A Ranta-Maunus

40-6-3 Analysis of Tension and Bending strength of Graded Spruce Timber - A Hanhijärvi, A Ranta-Maunus, H Sarkama, M Kohsaku, M Poussa, J Puttonen

41-6-1 Design of Inclined Glulam Members with an End Notch on the Tension Face - A Asiz, I Smith

41-6-2 A New Design Approach for End-notched Beams - View on Code - K Rautenstrauch, B Franke, S Franke, K U Schober

41-6-3 The Design Rules in Eurocode 5 for Compression Perpendicular to the Grain - Continuous Supported Beams - H J Larsen, T A C M van der Put, A J M Leijten

41-6-4 Size Effects in Bending – J K Denzler, P Glos

TIMBER JOINTS AND FASTENERS

1-7-1 Mechanical Fasteners and Fastenings in Timber Structures - E G Stern

4-7-1 Proposal for a Basic Test Method for the Evaluation of Structural Timber Joints with Mechanical Fasteners and Connectors - RILEM 3TT Committee

4-7-2 Test Methods for Wood Fasteners - K Möhler

5-7-1 Influence of Loading Procedure on Strength and Slip-Behaviour in Testing Timber Joints - K Möhler

5-7-2	Recommendations for Testing Methods for Joints with Mechanical Fasteners and Connectors in Load-Bearing Timber Structures - RILEM 3 TT Committee
5-7-3	CIB-Recommendations for the Evaluation of Results of Tests on Joints with Mechanical Fasteners and Connectors used in Load-Bearing Timber Structures - J Kuipers
6-7-1	Recommendations for Testing Methods for Joints with Mechanical Fasteners and Connectors in Load-Bearing Timber Structures (seventh draft) - RILEM 3 TT Committee
6-7-2	Proposal for Testing Integral Nail Plates as Timber Joints - K Möhler
6-7-3	Rules for Evaluation of Values of Strength and Deformation from Test Results - Mechanical Timber Joints - M Johansen, J Kuipers, B Norén
6-7-4	Comments to Rules for Testing Timber Joints and Derivation of Characteristic Values for Rigidity and Strength - B Norén
7-7-1	Testing of Integral Nail Plates as Timber Joints - K Möhler
7-7-2	Long Duration Tests on Timber Joints - J Kuipers
7-7-3	Tests with Mechanically Jointed Beams with a Varying Spacing of Fasteners - K Möhler
7-100-1	CIB-Timber Code Chapter 5.3 Mechanical Fasteners;CIB-Timber Standard 06 and 07 - H J Larsen
9-7-1	Design of Truss Plate Joints - F J Keenan
9-7-2	Staples - K Möhler
11-7-1	A Draft Proposal for International Standard: ISO Document ISO/TC 165N 38E
12-7-1	Load-Carrying Capacity and Deformation Characteristics of Nailed Joints - J Ehlbeck
12-7-2	Design of Bolted Joints - H J Larsen
12-7-3	Design of Joints with Nail Plates - B Norén
13-7-1	Polish Standard BN-80/7159-04: Parts 00-01-02-03-04-05. "Structures from Wood and Wood-based Materials. Methods of Test and Strength Criteria for Joints with Mechanical Fasteners"
13-7-2	Investigation of the Effect of Number of Nails in a Joint on its Load Carrying Ability - W Nozynski
13-7-3	International Acceptance of Manufacture, Marking and Control of Finger-jointed Structural Timber - B Norén
13-7-4	Design of Joints with Nail Plates - Calculation of Slip - B Norén
13-7-5	Design of Joints with Nail Plates - The Heel Joint - B Källsner
13-7-6	Nail Deflection Data for Design - H J Burgess
13-7-7	Test on Bolted Joints - P Vermeyden
13-7-8	Comments to paper CIB-W18/12-7-3 "Design of Joints with Nail Plates"- B Norén
13-7-9	Strength of Finger Joints - H J Larsen
13-100-4	CIB Structural Timber Design Code. Proposal for Section 6.1.5 Nail Plates - N I Bovim
14-7-1	Design of Joints with Nail Plates (second edition) - B Norén
14-7-2	Method of Testing Nails in Wood (second draft, August 1980) - B Norén
14-7-3	Load-Slip Relationship of Nailed Joints - J Ehlbeck and H J Larsen
14-7-4	Wood Failure in Joints with Nail Plates - B Norén

14-7-5	The Effect of Support Eccentricity on the Design of W- and WW-Trussed with Nail Plate Connectors - B Källsner
14-7-6	Derivation of the Allowable Load in Case of Nail Plate Joints Perpendicular to Grain - K Möhler
14-7-7	Comments on CIB-W18/14-7-1 - T A C M van der Put
15-7-1	Final Recommendation TT-1A: Testing Methods for Joints with Mechanical Fasteners in Load-Bearing Timber Structures. Annex A Punched Metal Plate Fasteners - Joint Committee RILEM/CIB-3TT
16-7-1	Load Carrying Capacity of Dowels - E Gehri
16-7-2	Bolted Timber Joints: A Literature Survey - N Harding
16-7-3	Bolted Timber Joints: Practical Aspects of Construction and Design; a Survey - N Harding
16-7-4	Bolted Timber Joints: Draft Experimental Work Plan - Building Research Association of New Zealand
17-7-1	Mechanical Properties of Nails and their Influence on Mechanical Properties of Nailed Timber Joints Subjected to Lateral Loads - I Smith, L R J Whale, C Anderson and L Held
17-7-2	Notes on the Effective Number of Dowels and Nails in Timber Joints - G Steck
18-7-1	Model Specification for Driven Fasteners for Assembly of Pallets and Related Structures - E G Stern and W B Wallin
18-7-2	The Influence of the Orientation of Mechanical Joints on their Mechanical Properties - I Smith and L R J Whale
18-7-3	Influence of Number of Rows of Fasteners or Connectors upon the Ultimate Capacity of Axially Loaded Timber Joints - I Smith and G Steck
18-7-4	A Detailed Testing Method for Nailplate Joints - J Kangas
18-7-5	Principles for Design Values of Nailplates in Finland - J Kangas
18-7-6	The Strength of Nailplates - N I Bovim and E Aasheim
19-7-1	Behaviour of Nailed and Bolted Joints under Short-Term Lateral Load - Conclusions from Some Recent Research - L R J Whale, I Smith and B O Hilson
19-7-2	Glued Bolts in Glulam - H Riberholt
19-7-3	Effectiveness of Multiple Fastener Joints According to National Codes and Eurocode 5 (Draft) - G Steck
19-7-4	The Prediction of the Long-Term Load Carrying Capacity of Joints in Wood Structures - Y M Ivanov and Y Y Slavic
19-7-5	Slip in Joints under Long-Term Loading - T Feldborg and M Johansen
19-7-6	The Derivation of Design Clauses for Nailed and Bolted Joints in Eurocode 5 - L R J Whale and I Smith
19-7-7	Design of Joints with Nail Plates - Principles - B Norén
19-7-8	Shear Tests for Nail Plates - B Norén
19-7-9	Advances in Technology of Joints for Laminated Timber - Analyses of the Structural Behaviour - M Piazza and G Turrini
19-15-1	Connections Deformability in Timber Structures: A Theoretical Evaluation of its Influence on Seismic Effects - A Ceccotti and A Vignoli
20-7-1	Design of Nailed and Bolted Joints-Proposals for the Revision of Existing Formulae in Draft Eurocode 5 and the CIB Code - L R J Whale, I Smith and H J Larsen
20-7-2	Slip in Joints under Long Term Loading - T Feldborg and M Johansen

20-7-3	Ultimate Properties of Bolted Joints in Glued-Laminated Timber - M Yasumura, T Murota and H Sakai
20-7-4	Modelling the Load-Deformation Behaviour of Connections with Pin-Type Fasteners under Combined Moment, Thrust and Shear Forces - I Smith
21-7-1	Nails under Long-Term Withdrawal Loading - T Feldborg and M Johansen
21-7-2	Glued Bolts in Glulam-Proposals for CIB Code - H Riberholt
21-7-3	Nail Plate Joint Behaviour under Shear Loading - T Poutanen
21-7-4	Design of Joints with Laterally Loaded Dowels. Proposals for Improving the Design Rules in the CIB Code and the Draft Eurocode 5 - J Ehlbeck and H Werner
21-7-5	Axially Loaded Nails: Proposals for a Supplement to the CIB Code - J Ehlbeck and W Siebert
22-7-1	End Grain Connections with Laterally Loaded Steel Bolts A draft proposal for design rules in the CIB Code - J Ehlbeck and M Gerold
22-7-2	Determination of Perpendicular-to-Grain Tensile Stresses in Joints with Dowel-Type Fasteners - A draft proposal for design rules - J Ehlbeck, R Görlacher and H Werner
22-7-3	Design of Double-Shear Joints with Non-Metallic Dowels A proposal for a supplement of the design concept - J Ehlbeck and O Eberhart
22-7-4	The Effect of Load on Strength of Timber Joints at high Working Load Level - A J M Leijten
22-7-5	Plasticity Requirements for Portal Frame Corners - R Gunnewijk and A J M Leijten
22-7-6	Background Information on Design of Glulam Rivet Connections in CSA/CAN3-086.1-M89 - A proposal for a supplement of the design concept - E Karacabeyli and D P Janssens
22-7-7	Mechanical Properties of Joints in Glued-Laminated Beams under Reversed Cyclic Loading - M Yasumura
22-7-8	Strength of Glued Lap Timber Joints - P Glos and H Horstmann
22-7-9	Toothed Rings Type Bistyp 075 at the Joints of Fir Wood - J Kerste
22-7-10	Calculation of Joints and Fastenings as Compared with the International State - K Zimmer and K Lissner
22-7-11	Joints on Glued-in Steel Bars Present Relatively New and Progressive Solution in Terms of Timber Structure Design - G N Zubarev, F A Boitemirov and V M Golovina
22-7-12	The Development of Design Codes for Timber Structures made of Compositive Bars with Plate Joints based on Cyclindrical Nails - Y V Piskunov
22-7-13	Designing of Glued Wood Structures Joints on Glued-in Bars - S B Turkovsky
23-7-1	Proposal for a Design Code for Nail Plates - E Aasheim and K H Solli
23-7-2	Load Distribution in Nailed Joints - H J Blass
24-7-1	Theoretical and Experimental Tension and Shear Capacity of Nail Plate Connections - B Källsner and J Kangas
24-7-2	Testing Method and Determination of Basic Working Loads for Timber Joints with Mechanical Fasteners - Y Hirashima and F Kamiya
24-7-3	Anchorage Capacity of Nail Plate - J Kangas
25-7-2	Softwood and Hardwood Embedding Strength for Dowel type Fasteners - J Ehlbeck and H Werner

25-7-4	A Guide for Application of Quality Indexes for Driven Fasteners Used in Connections in Wood Structures - E G Stern
25-7-5	35 Years of Experience with Certain Types of Connectors and Connector Plates Used for the Assembly of Wood Structures and their Components- E G Stern
25-7-6	Characteristic Strength of Split-ring and Shear-plate Connections - H J Blass, J Ehlbeck and M Schlager
25-7-7	Characteristic Strength of Tooth-plate Connector Joints - H J Blass, J Ehlbeck and M Schlager
25-7-8	Extending Yield Theory to Screw Connections - T E McLain
25-7-9	Determination of k_{def} for Nailed Joints - J W G van de Kuilen
25-7-10	Characteristic Strength of UK Timber Connectors - A V Page and C J Mettem
25-7-11	Multiple-fastener Dowel-type Joints, a Selected Review of Research and Codes - C J Mettem and A V Page
25-7-12	Load Distributions in Multiple-fastener Bolted Joints in European Whitewood Glulam, with Steel Side Plates - C J Mettem and A V Page
26-7-1	Proposed Test Method for Dynamic Properties of Connections Assembled with Mechanical Fasteners - J D Dolan
26-7-2	Validatory Tests and Proposed Design Formulae for the Load-Carrying Capacity of Toothed-Plate Connectored Joints - C J Mettem, A V Page and G Davis
26-7-3	Definitions of Terms and Multi-Language Terminology Pertaining to Metal Connector Plates - E G Stern
26-7-4	Design of Joints Based on in V-Shape Glued-in Rods - J Kangas
26-7-5	Tests on Timber Concrete Composite Structural Elements (TCCs) - A U Meierhofer
27-7-1	Glulam Arch Bridge and Design of it's Moment-Resisting Joints - K Komatsu and S Usuku
27-7-2	Characteristic Load - Carrying Capacity of Joints with Dowel - type Fasteners in Regard to the System Properties - H Werner
27-7-3	Steel Failure Design in Truss Plate Joints - T Poutanen
28-7-1	Expanded Tube Joint in Locally DP Reinforced Timber - A J M Leijten, P Ragupathy and K S Virdi
28-7-2	A Strength and Stiffness Model for the Expanded Tube Joint - A J M Leijten
28-7-3	Load-carrying Capacity of Steel-to Timber Joints with Annular Ring Shanked Nails. A Comparison with the EC5 Design Method - R Görlacher
28-7-4	Dynamic Effects on Metal-Plate Connected Wood Truss Joints - S Kent, R Gupta and T Miller
28-7-5	Failure of the Timber Bolted Joints Subjected to Lateral Load Perpendicular to Grain - M Yasumura and L Daudeville
28-7-6	Design Procedure for Locally Reinforced Joints with Dowel-type Fasteners - H Werner
28-7-7	Variability and Effects of Moisture Content on the Withdrawal Characteristics for Lumber as Opposed to Clear Wood - J D Dolan and J W Stelmokas
28-7-8	Nail Plate Capacity in Joint Line - A Kevarinmäki and J Kangas
28-7-9	Axial Strength of Glued-In Bolts - Calculation Model Based on Non-Linear Fracture Mechanics - A Preliminary Study - C J Johansson, E Serrano, P J Gustafsson and B Enquist

28-7-10	Cyclic Lateral Dowel Connection Tests for seismic and Wind Evaluation - J D Dolan
29-7-1	A Simple Method for Lateral Load-Carrying Capacity of Dowel-Type Fasteners - J Kangas and J Kurkela
29-7-2	Nail Plate Joint Behaviour at Low Versus High Load Level - T Poutanen
29-7-3	The Moment Resistance of Tee and Butt - Joint Nail Plate Test Specimens - A Comparison with Current Design Methods - A Reffold, L R J Whale and B S Choo
29-7-4	A Critical Review of the Moment Rotation Test Method Proposed in prEN 1075 - M Bettison, B S Choo and L R J Whale
29-7-5	Explanation of the Translation and Rotation Behaviour of Prestressed Moment Timber Joints - A J M Leijten
29-7-6	Design of Joints and Frame Corners using Dowel-Type Fasteners - E Gehri
29-7-7	Quasi-Static Reversed-Cyclic Testing of Nailed Joints - E Karacabeyli and A Ceccotti
29-7-8	Failure of Bolted Joints Loaded Parallel to the Grain: Experiment and Simulation - L Davenne, L Daudeville and M Yasumura
30-7-1	Flexural Behaviour of GLT Beams End-Jointed by Glued-in Hardwood Dowels - K Komatsu, A Koizumi, J Jensen, T Sasaki and Y Iijima
30-7-2	Modelling of the Block Tearing Failure in Nailed Steel-to-Timber Joints - J Kangas, K Aalto and A Kevarinmäki
30-7-3	Cyclic Testing of Joints with Dowels and Slotted-in Steel Plates - E Aasheim
30-7-4	A Steel-to-Timber Dowelled Joint of High Performance in Combination with a High Strength Wood Composite (Parallam) - E Gehri
30-7-5	Multiple Fastener Timber Connections with Dowel Type Fasteners - A Jorissen
30-7-6	Influence of Ductility on Load-Carrying Capacity of Joints with Dowel-Type Fasteners - A Mischler
31-7-1	Mechanical Properties of Dowel Type Joints under Reversed Cyclic Lateral Loading - M Yasumura
31-7-2	Design of Joints with Laterally Loaded Dowels - A Mischler
31-7-3	Flexural Behaviour of Glulam Beams Edge-Jointed by Lagscrews with Steel Splice Plates - K Komatsu
31-7-4	Design on Timber Capacity in Nailed Steel-to-Timber Joints - J Kangas and J Vesa
31-7-5	Timber Contact in Chord Splices of Nail Plate Structures - A Kevarinmäki
31-7-6	The Fastener Yield Strength in Bending - A Jorissen and H J Blaß
31-7-7	A Proposal for Simplification of Johansen`s Formulae, Dealing With the Design of Dowelled-Type Fasteners - F Rouger
31-7-8	Simplified Design of Connections with Dowel-type fasteners - H J Blaß and J Ehlbeck
32-7-1	Behaviour of Wood-Steel-Wood Bolted Glulam Connections - M Mohammad and J H P Quenneville
32-7-2	A new set of experimental tests on beams loaded perpendicular-to-grain by dowel-type joints- M Ballerini
32-7-3	Design and Analysis of Bolted Timber Joints under Lateral Force Perpendicular to Grain - M Yasumura and L Daudeville
32-7-4	Predicting Capacities of Joints with Laterally Loaded Nails - I Smith and P Quenneville

32-7-5	Strength Reduction Rules for Multiple Fastener Joints - A Mischler and E Gehri
32-7-6	The Stiffness of Multiple Bolted Connections - A Jorissen
32-7-7	Concentric Loading Tests on Girder Truss Components - T N Reynolds, A Reffold, V Enjily and L Whale
32-7-8	Dowel Type Connections with Slotted-In Steel Plates - M U Pedersen, C O Clorius, L Damkilde, P Hoffmeyer and L Esklidsen
32-7-9	Creep of Nail Plate Reinforced Bolt Joints - J Vesa and A Kevarinmäki
32-7-10	The Behaviour of Timber Joints with Ring Connectors - E Gehri and A Mischler
32-7-11	Non-Metallic, Adhesiveless Joints for Timber Structures - R D Drake, M P Ansell, C J Mettem and R Bainbridge
32-7-12	Effect of Spacing and Edge Distance on the Axial Strength of Glued-in Rods - H J Blaß and B Laskewitz
32-7-13	Evaluation of Material Combinations for Bonded in Rods to Achieve Improved Timber Connections - C J Mettem, R J Bainbridge, K Harvey, M P Ansell, J G Broughton and A R Hutchinson
33-7-1	Determination of Yield Strength and Ultimate Strength of Dowel-Type Timber Joints – M Yasumura and K Sawata
33-7-2	Lateral Shear Capacity of Nailed Joints – U Korin
33-7-3	Height-Adjustable Connector for Composite Beams – Y V Piskunov and E G Stern
33-7-4	Engineering Ductility Assessment for a Nailed Slotted-In Steel Connection in Glulam– L Stehn and H Johansson
33-7-5	Effective Bending Capacity of Dowel-Type Fasteners - H J Blaß, A Bienhaus and V Krämer
33-7-6	Load-Carrying Capacity of Joints with Dowel-Type Fasteners and Interlayers - H J Blaß and B Laskewitz
33-7-7	Evaluation of Perpendicular to Grain Failure of Beams caused by Concentrated Loads of Joints – A J M Leijten and T A C M van der Put
33-7-8	Test Methods for Glued-In Rods for Timber Structures – C Bengtsson and C J Johansson
33-7-9	Stiffness Analysis of Nail Plates – P Ellegaard
33-7-10	Capacity, Fire Resistance and Gluing Pattern of the Rods in V-Connections – J Kangas
33-7-11	Bonded-In Pultrusions for Moment-Resisting Timber Connections – K Harvey, M P Ansell, C J Mettem, R J Bainbridge and N Alexandre
33-7-12	Fatigue Performance of Bonded-In Rods in Glulam, Using Three Adhesive Types - R J Bainbridge, K Harvey, C J Mettem and M P Ansell
34-7-1	Splitting Strength of Beams Loaded by Connections Perpendicular to Grain, Model Validation – A J M Leijten, A Jorissen
34-7-2	Numerical LEFM analyses for the evaluation of failure loads of beams loaded perpendicular-to-grain by single-dowel connections – M Ballerini, R Bezzi
34-7-3	Dowel joints loaded perpendicular to grain - H J Larsen, P J Gustafsson
34-7-4	Quality Control of Connections based on in V-shape glued-in Steel Rods – J Kangas, A Kevarinmäki
34-7-5	Testing Connector Types for Laminated-Timber-Concrete Composite Elements – M Grosse, S Lehmann, K Rautenstrauch
34-7-6	Behaviour of Axially Loaded Glued-in Rods - Requirements and Resistance, Especially for Spruce Timber Perpendicular to the Grain Direction – A Bernasconi
34-7-7	Embedding characteristics on fibre reinforcement and densified timber joints - P Haller, J Wehsener, T Birk

34-7-8	GIROD – Glued-in Rods for Timber Structures – C Bengtsson, C-J Johansson
34-7-9	Criteria for Damage and Failure of Dowel-Type Joints Subjected to Force Perpendicular to the Grain – M Yasumura
34-7-10	Interaction Between Splitting and Block Shear Failure of Joints – A J M Leijten, A Jorissen, J Kuipers
34-7-11	Limit states design of dowel-fastener joints – Placement of modification factors and partial factors, and calculation of variability in resistance – I Smith, G Foliente
34-7-12	Design and Modelling of Knee Joints - J Nielsen, P Ellegaard
34-7-13	Timber-Steel Shot Fired Nail Connections at Ultimate Limit States - R J Bainbridge, P Larsen, C J Mettem, P Alam, M P Ansell
35-7-1	New Estimating Method of Bolted Cross-lapped Joints with Timber Side Members - M Noguchi, K Komatsu
35-7-2	Analysis on Multiple Lag Screwed Timber Joints with Timber Side Members - K Komatsu, S Takino, M Nakatani, H Tateishi
35-7-3	Joints with Inclined Screws - A Kevarinmäki
35-7-4	Joints with Inclined Screws - I Bejtka, H J Blaß
35-7-5	Effect of distances, Spacing and Number of Dowels in a Row an the Load Carrying Capacity of Connections with Dowels failing by Splitting - M Schmid, R Frasson, H J Blaß
35-7 6	Effect of Row Spacing on the Capacity of Bolted Timber Connections Loaded Perpendicular-to-grain - P Quenneville, M Kasim
35-7-7	Splitting Strength of Beams Loaded by Connections, Model Comparison - A J M Leijten
35-7-8	Load-Carrying Capacity of Perpendicular to the Grain Loaded Timber Joints with Multiple Fasteners - O Borth, K U Schober, K Rautenstrauch
35-7-9	Determination of fracture parameter for dowel-type joints loaded perpendicular to wooden grain and its application - M Yasumura
35-7-10	Analysis and Design of Modified Attic Trusses with Punched Metal Plate Fasteners - P Ellegaard
35-7-11	Joint Properties of Plybamboo Sheets in Prefabricated Housing - G E Gonzalez
35-7-12	Fiber-Reinforced Beam-to-Column Connections for Seismic Applications - B Kasal, A Heiduschke, P Haller
36-7-1	Shear Tests in Timber-LWAC with Screw-Type Connections - L Jorge, H Cruz, S Lopes
36-7-2	Plug Shear Failure in Nailed Timber Connections: Experimental Studies - H Johnsson
36-7-3	Nail-Laminated Timber Elements in Natural Surface-Composite with Mineral Bound Layer - S Lehmann, K Rautenstrauch
36-7-4	Mechanical Properties of Timber-Concrete Joints Made With Steel Dowels - A Dias, J W G van de Kuilen, H Cruz
36-7-5	Comparison of Hysteresis Responses of Different Sheating to Framing Joints - B Dujič, R Zarnić
36-7- 6	Evaluation and Estimation of the Performance of the Nail Joints and Shear Walls under Dry/Humid Cyclic Climate - S Nakajima
36-7-7	Beams Transversally Loaded by Dowel-Type Joints: Influence on Splitting Strength of Beam Thickness and Dowel Size - M Ballerini, A Giovanella
36-7-8	Splitting Strength of Beams Loaded by Connections - J L Jensen
36-7-9	A Tensile Fracture Model for Joints with Rods or Dowels loaded Perpendicular-to-Grain - J L Jensen, P J Gustafsson, H J Larsen

36-7-10	A Numerical Model to Simulate the Load-Displacement Time-History of Mutiple-Bolt Connections Subjected to Various Loadings - C P Heine, J D Dolan
36-7-11	Reliability of Timber Structures, Theory and Dowel-Type Connection Failures - A Ranta-Maunus, A Kevarinmäki
37-7-1	Development of the "Displaced Volume Model" to Predict Failure for Multiple-Bolt Timber Joints - D M Carradine, J D Dolan, C P Heine
37-7-2	Mechanical Models of the Knee Joints with Cross-Lapped Glued Joints and Glued in Steel Rods - M Noguchi, K Komatsu
37-7-3	Simplification of the Neural Network Model for Predicting the Load-Carrying Capacity of Dowel-Type Connections - A Cointe, F Rouger
37-7-4	Bolted Wood Connections Loaded Perpendicular-to-Grain- A Proposed Design Approach - M C G Lehoux, J H P Quenneville
37-7-5	A New Prediction Formula for the Splitting Strength of Beams Loaded by Dowel Type Connections - M Ballerini
37-7-6	Plug Shear Failure: The Tensile Failure Mode and the Effect of Spacing - H Johnsson
37-7-7	Block Shear Failure Test with Dowel-Type Connection in Diagonal LVL Structure - M Kairi
37-7-8	Glued-in Steel Rods: A Design Approach for Axially Loaded Single Rods Set Parallel to the Grain - R Steiger, E Gehri, R Widmann
37-7-9	Glued in Rods in Load Bearing Timber Structures - Status regarding European Standards for Test Procedures - B Källander
37-7-10	French Data Concerning Glued-in Rods - C Faye, L Le Magorou, P Morlier, J Surleau
37-7-11	Enhancement of Dowel-Type Fasteners by Glued Connectors - C O Clorius, A Højman
37-7-12	Review of Probability Data for Timber Connections with Dowel-Type Fasteners - A J M Leijten, J Köhler, A Jorissen
37-7-13	Behaviour of Fasteners and Glued-in Rods Produced From Stainless Steel - A Kevarinmäki
37-7-14	Dowel joints in Engineered Wood Products: Assessment of Simple Fracture Mechanics Models - M Snow, I Smith, A Asiz
37-7-15	Numerical Modelling of Timber and Connection Elements Used in Timber-Concrete-Composite Constructions - M Grosse, K Rautenstrauch
38-7-1	A Numerical Investigation on the Splitting Strength of Beams Loaded Perpendicular-to-grain by Multiple-dowel Connections – M Ballerini, M Rizzi
38-7-2	A Probabilistic Framework for the Reliability Assessment of Connections with Dowel Type Fasteners - J Köhler
38-7-3	Load Carrying Capacity of Curved Glulam Beams Reinforced with self-tapping Screws - J Jönsson, S Thelandersson
38-7-4	Self-tapping Screws as Reinforcements in Connections with Dowel-Type Fasteners- I Bejtka, H J Blaß
38-7-5	The Yield Capacity of Dowel Type Fasteners - A Jorissen, A Leijten
38-7-6	Nails in Spruce - Splitting Sensitivity, End Grain Joints and Withdrawal Strength - A Kevarinmäki
38-7-7	Design of Timber Connections with Slotted-in Steel Plates and Small Diameter Steel Tube Fasteners - B Murty, I Smith, A Asiz
39-7-1	Effective in-row Capacity of Multiple-Fastener Connections - P Quenneville, M Bickerdike
39-7-2	Self-tapping Screws as Reinforcements in Beam Supports - I Bejtka, H J Blaß

39-7-3 Connectors for Timber-concrete Composite-Bridges - A Döhrer, K Rautenstrauch

39-7-4 Block Shear Failure at Dowelled Double Shear Steel-to-timber Connections - A Hanhijärvi, A Kevarinmäki, R Yli-Koski

39-7-5 Load Carrying Capacity of Joints with Dowel Type Fasteners in Solid Wood Panels - T Uibel, H J Blaß

39-7-6 Generalised Canadian Approach for Design of Connections with Dowel Fasteners - P Quenneville, I Smith, A Asiz, M Snow, Y H Chui

40-7-1 Predicting the Strength of Bolted Timber Connections Subjected to Fire - M Fragiacomo, A Buchanan, D Carshalton, P Moss, C Austruy

40-7-2 Edge Joints with Dowel Type Fasteners in Cross Laminated Timber - H J Blaß, T Uibel

40-7-3 Design Method against Timber Failure Mechanisms of Dowelled Steel-to-Timber Connections - A Hanhijärvi, A Kevarinmäki

40-7-4 A EYM Based Simplified Design Formula for the Load-carrying Capacity of Dowel-type Connections - M Ballerini

40-7-5 Evaluation of the Slip Modulus for Ultimate Limit State Verifications of Timber-Concrete Composite Structures - E Lukaszewska, M Fragiacomo, A Frangi

40-7-6 Models for the Predictions of the Ductile and Brittle Failure Modes (Parallel-to-Grain) of Timber Rivet Connections - M Marjerrison, P Quenneville

40-7-7 Creep of Timber and Timber-Concrete Joints. - J W G van de Kuilen, A M P G Dias

40-7-8 Lag Screwed Timber Joints with Timber Side Members- K Komatsu, S Takino, H Tateishi

41-7-1 Applicability of Existing Design Approaches to Mechanical Joints in Structural Composite Lumber - M Snow, I Smith, A Asiz, M Ballerini

41-7-2 Validation of the Canadian Bolted Connection Design Proposal - P Quenneville, J Jensen

41-7-3 Ductility of Moment Resisting Dowelled Joints in Heavy Timber Structures - A Polastri, R Tomasi, M Piazza, I Smith

41-7-4 Mechanical Behaviour of Traditional Timber Connections: Proposals for Design, Based on Experimental and Numerical Investigations. Part I: Birdsmouth - C Faye, P Garcia, L Le Magorou, F Rouger

41-7-5 Embedding Strength of European Hardwoods - U Hübner, T Bogensperger, G Schickhofer

LOAD SHARING

3-8-1 Load Sharing - An Investigation on the State of Research and Development of Design Criteria - E Levin

4-8-1 A Review of Load-Sharing in Theory and Practice - E Levin

4-8-2 Load Sharing - B Norén

19-8-1 Predicting the Natural Frequencies of Light-Weight Wooden Floors - I Smith and Y H Chui

20-8-1 Proposed Code Requirements for Vibrational Serviceability of Timber Floors - Y H Chui and I Smith

21-8-1 An Addendum to Paper 20-8-1 - Proposed Code Requirements for Vibrational Serviceability of Timber Floors - Y H Chui and I Smith

21-8-2 Floor Vibrational Serviceability and the CIB Model Code - S Ohlsson

22-8-1 Reliability Analysis of Viscoelastic Floors - F Rouger, J D Barrett and R O Foschi

24-8-1 On the Possibility of Applying Neutral Vibrational Serviceability Criteria to Joisted Wood Floors - I Smith and Y H Chui

25-8-1 Analysis of Glulam Semi-rigid Portal Frames under Long-term Load - K Komatsu and N Kawamoto

34-8-1 System Effect in Sheathed Parallel Timber Beam Structures – M Hansson, T Isaksson

35-8-1 System Effects in Sheathed Parallel Timber Beam Structures part II. - M Hansson, T Isaksson

39-8-1 Overview of a new Canadian Approach to Handling System Effects in Timber Structures - I Smith, Y H Chui, P Quenneville

DURATION OF LOAD

3-9-1 Definitions of Long Term Loading for the Code of Practice - B Norén

4-9-1 Long Term Loading of Trussed Rafters with Different Connection Systems - T Feldborg and M Johansen

5-9-1 Strength of a Wood Column in Combined Compression and Bending with Respect to Creep - B Källsner and B Norén

6-9-1 Long Term Loading for the Code of Practice (Part 2) - B Norén

6-9-2 Long Term Loading - K Möhler

6-9-3 Deflection of Trussed Rafters under Alternating Loading during a Year - T Feldborg and M Johansen

7-6-1 Strength and Long Term Behaviour of Lumber and Glued-Laminated Timber under Torsion Loads - K Möhler

7-9-1 Code Rules Concerning Strength and Loading Time - H J Larsen and E Theilgaard

17-9-1 On the Long-Term Carrying Capacity of Wood Structures - Y M Ivanov and Y Y Slavic

18-9-1 Prediction of Creep Deformations of Joints - J Kuipers

19-9-1 Another Look at Three Duration of Load Models - R O Foschi and Z C Yao

19-9-2 Duration of Load Effects for Spruce Timber with Special Reference to Moisture Influence - A Status Report - P Hoffmeyer

19-9-3 A Model of Deformation and Damage Processes Based on the Reaction Kinetics of Bond Exchange - T A C M van der Put

19-9-4 Non-Linear Creep Superposition - U Korin

19-9-5 Determination of Creep Data for the Component Parts of Stressed-Skin Panels - R Kliger

19-9-6 Creep an Lifetime of Timber Loaded in Tension and Compression - P Glos

19-1-1 Duration of Load Effects and Reliability Based Design (Single Member) - R O Foschi and Z C Yao

19-6-1 Effect of Age and/or Load on Timber Strength - J Kuipers

19-7-4 The Prediction of the Long-Term Load Carrying Capacity of Joints in Wood Structures - Y M Ivanov and Y Y Slavic

19-7-5 Slip in Joints under Long-Term Loading - T Feldborg and M Johansen

20-7-2 Slip in Joints under Long-Term Loading - T Feldborg and M Johansen

22-9-1 Long-Term Tests with Glued Laminated Timber Girders - M Badstube, W Rug and W Schöne

22-9-2 Strength of One-Layer solid and Lengthways Glued Elements of Wood Structures and its Alteration from Sustained Load - L M Kovaltchuk, I N Boitemirova and G B Uspenskaya

24-9-1 Long Term Bending Creep of Wood - T Toratti

24-9-2 Collection of Creep Data of Timber - A Ranta-Maunus

24-9-3 Deformation Modification Factors for Calculating Built-up Wood-Based Structures - I R Kliger

25-9-2 DVM Analysis of Wood. Lifetime, Residual Strength and Quality - L F Nielsen

26-9-1 Long Term Deformations in Wood Based Panels under Natural Climate Conditions. A Comparative Study - S Thelandersson, J Nordh, T Nordh and S Sandahl

28-9-1 Evaluation of Creep Behavior of Structural Lumber in Natural Environment - R Gupta and R Shen

30-9-1 DOL Effect in Tension Perpendicular to the Grain of Glulam Depending on Service Classes and Volume - S Aicher and G Dill-Langer

30-9-2 Damage Modelling of Glulam in Tension Perpendicular to Grain in Variable Climate - G Dill-Langer and S Aicher

31-9-1 Duration of Load Effect in Tension Perpendicular to Grain in Curved Glulam - A Ranta-Maunus

32-9-1 Bending-Stress-Redistribution Caused by Different Creep in Tension and Compression and Resulting DOL-Effect - P Becker and K Rautenstrauch

32-9-2 The Long Term Performance of Ply-Web Beams - R Grantham and V Enjily

36-9-1 Load Duration Factors for Instantaneous Loads - A J M Leijten, B Jansson

39-9-1 Simplified Approach for the Long-Term Behaviour of Timber-Concrete Composite Beams According to the Eurocode 5 Provisions - M Fragiacomo, A Ceccotti

TIMBER BEAMS

4-10-1 The Design of Simple Beams - H J Burgess

4-10-2 Calculation of Timber Beams Subjected to Bending and Normal Force - H J Larsen

5-10-1 The Design of Timber Beams - H J Larsen

9-10-1 The Distribution of Shear Stresses in Timber Beams - F J Keenan

9-10-2 Beams Notched at the Ends - K Möhler

11-10-1 Tapered Timber Beams - H Riberholt

13-6-2 Consideration of Size Effects in Longitudinal Shear Strength for Uncracked Beams - R O Foschi and J D Barrett

13-6-3 Consideration of Shear Strength on End-Cracked Beams - J D Barrett and R O Foschi

18-10-1 Submission to the CIB-W18 Committee on the Design of Ply Web Beams by Consideration of the Type of Stress in the Flanges - J A Baird

18-10-2 Longitudinal Shear Design of Glued Laminated Beams - R O Foschi

19-10-1 Possible Code Approaches to Lateral Buckling in Beams - H J Burgess

19-2-1 Creep Buckling Strength of Timber Beams and Columns - R H Leicester

20-2-1 Lateral Buckling Theory for Rectangular Section Deep Beam-Columns - H J Burgess

20-10-1 Draft Clause for CIB Code for Beams with Initial Imperfections - H J Burgess

20-10-2 Space Joists in Irish Timber - W J Robinson

20-10-3 Composite Structure of Timber Joists and Concrete Slab - T Poutanen

21-10-1	A Study of Strength of Notched Beams - P J Gustafsson
22-10-1	Design of Endnotched Beams - H J Larsen and P J Gustafsson
22-10-2	Dimensions of Wooden Flexural Members under Constant Loads - A Pozgai
22-10-3	Thin-Walled Wood-Based Flanges in Composite Beams - J König
22-10-4	The Calculation of Wooden Bars with flexible Joints in Accordance with the Polish Standart Code and Strict Theoretical Methods - Z Mielczarek
23-10-1	Tension Perpendicular to the Grain at Notches and Joints - T A C M van der Put
23-10-2	Dimensioning of Beams with Cracks, Notches and Holes. An Application of Fracture Mechanics - K Riipola
23-10-3	Size Factors for the Bending and Tension Strength of Structural Timber - J D Barret and A R Fewell
23-12-1	Bending Strength of Glulam Beams, a Design Proposal - J Ehlbeck and F Colling
23-12-3	Glulam Beams, Bending Strength in Relation to the Bending Strength of the Finger Joints - H Riberholt
24-10-1	Shear Strength of Continuous Beams - R H Leicester and F G Young
25-10-1	The Strength of Norwegian Glued Laminated Beams - K Solli, E Aasheim and R H Falk
25-10-2	The Influence of the Elastic Modulus on the Simulated Bending Strength of Hyperstatic Timber Beams - T D G Canisius
27-10-1	Determination of Shear Modulus - R Görlacher and J Kürth
29-10-1	Time Dependent Lateral Buckling of Timber Beams - F Rouger
29-10-2	Determination of Modulus of Elasticity in Bending According to EN 408 - K H Solli
29-10-3	On Determination of Modulus of Elasticity in Bending - L Boström, S Ormarsson and O Dahlblom
29-10-4	Relation of Moduli of Elasticity in Flatwise and Edgewise Bending of Solid Timber - C J Johansson, A Steffen and E W Wormuth
30-10-1	Nondestructive Evaluation of Wood-based Members and Structures with the Help of Modal Analysis - P Kuklik
30-10-2	Measurement of Modulus of Elasticity in Bending - L Boström
30-10-3	A Weak Zone Model for Timber in Bending - B Källsner, K Salmela and O Ditlevsen
30-10-4	Load Carrying Capacity of Timber Beams with Narrow Moment Peaks - T Isaksson and J Freysoldt
37-10-1	Design of Rim Boards for Use with I-Joists Framing Systems - B Yeh, T G Williamson
40-10- 1	Extension of EC5 Annex B Formulas for the Design of Timber-concrete Composite Structures - J Schänzlin, M Fragiacomo
40-10-2	Simplified Design Method for Mechanically Jointed Beams - U A Girhammar
41-10-1	Composite Action of I-Joist Floor Systems - T G Williamson, B Yeh
41-10-2	Evaluation of the Prestressing Losses in Timber Members Prestressed with Unbonded Tendons - M Fragiacomo, M Davies
41-10-3	Relationship Between Global and Local MOE – J K Denzler, P Stapel, P Glos

ENVIRONMENTAL CONDITIONS

5-11-1	Climate Grading for the Code of Practice - B Norén

6-11-1 Climate Grading (2) - B Norén

9-11-1 Climate Classes for Timber Design - F J Keenan

19-11-1 Experimental Analysis on Ancient Downgraded Timber Structures - B Leggeri and L Paolini

19-6-5 Drying Stresses in Round Timber - A Ranta-Maunus

22-11-1 Corrosion and Adaptation Factors for Chemically Aggressive Media with Timber Structures - K Erler

29-11-1 Load Duration Effect on Structural Beams under Varying Climate Influence of Size and Shape - P Galimard and P Morlier

30-11-1 Probabilistic Design Models for the Durability of Timber Constructions - R H Leicester

36-11-1 Structural Durability of Timber in Ground Contact – R H Leicester, C H Wang, M N Nguyen, G C Foliente, C McKenzie

38-11-1 Design Specifications for the Durability of Timber – R H Leicester, C-H Wang, M Nguyen, G C Foliente

38-11-2 Consideration of Moisture Exposure of Timber Structures as an Action - M Häglund, S Thelandersson

LAMINATED MEMBERS

6-12-1 Directives for the Fabrication of Load-Bearing Structures of Glued Timber - A van der Velden and J Kuipers

8-12-1 Testing of Big Glulam Timber Beams - H Kolb and P Frech

8-12-2 Instruction for the Reinforcement of Apertures in Glulam Beams - H Kolb and P Frech

8-12-3 Glulam Standard Part 1: Glued Timber Structures; Requirements for Timber (Second Draft)

9-12-1 Experiments to Provide for Elevated Forces at the Supports of Wooden Beams with Particular Regard to Shearing Stresses and Long-Term Loadings - F Wassipaul and R Lackner

9-12-2 Two Laminated Timber Arch Railway Bridges Built in Perth in 1849 - L G Booth

9-6-4 Consideration of Combined Stresses for Lumber and Glued Laminated Timber - K Möhler

11-6-3 Consideration of Combined Stresses for Lumber and Glued Laminated Timber (addition to Paper CIB-W18/9-6-4) - K Möhler

12-12-1 Glulam Standard Part 2: Glued Timber Structures; Rating (3rd draft)

12-12-2 Glulam Standard Part 3: Glued Timber Structures; Performance (3 rd draft)

13-12-1 Glulam Standard Part 3: Glued Timber Structures; Performance (4th draft)

14-12-1 Proposals for CEI-Bois/CIB-W18 Glulam Standards - H J Larsen

14-12-2 Guidelines for the Manufacturing of Glued Load-Bearing Timber Structures - Stevin Laboratory

14-12-3 Double Tapered Curved Glulam Beams - H Riberholt

14-12-4 Comment on CIB-W18/14-12-3 - E Gehri

18-12-1 Report on European Glulam Control and Production Standard - H Riberholt

18-10-2 Longitudinal Shear Design of Glued Laminated Beams - R O Foschi

19-12-1 Strength of Glued Laminated Timber - J Ehlbeck and F Colling

19-12-2	Strength Model for Glulam Columns - H J Blaß
19-12-3	Influence of Volume and Stress Distribution on the Shear Strength and Tensile Strength Perpendicular to Grain - F Colling
19-12-4	Time-Dependent Behaviour of Glued-Laminated Beams - F Zaupa
21-12-1	Modulus of Rupture of Glulam Beam Composed of Arbitrary Laminae - K Komatsu and N Kawamoto
21-12-2	An Appraisal of the Young's Modulus Values Specified for Glulam in Eurocode 5- L R J Whale, B O Hilson and P D Rodd
21-12-3	The Strength of Glued Laminated Timber (Glulam): Influence of Lamination Qualities and Strength of Finger Joints - J Ehlbeck and F Colling
21-12-4	Comparison of a Shear Strength Design Method in Eurocode 5 and a More Traditional One - H Riberholt
22-12-1	The Dependence of the Bending Strength on the Glued Laminated Timber Girder Depth - M Badstube, W Rug and W Schöne
22-12-2	Acid Deterioration of Glulam Beams in Buildings from the Early Half of the 1960s - Prelimination summary of the research project; Overhead pictures - B A Hedlund
22-12-3	Experimental Investigation of normal Stress Distribution in Glue Laminated Wooden Arches - Z Mielczarek and W Chanaj
22-12-4	Ultimate Strength of Wooden Beams with Tension Reinforcement as a Function of Random Material Properties - R Candowicz and T Dziuba
23-12-1	Bending Strength of Glulam Beams, a Design Proposal - J Ehlbeck and F Colling
23-12-2	Probability Based Design Method for Glued Laminated Timber - M F Stone
23-12-3	Glulam Beams, Bending Strength in Relation to the Bending Strength of the Finger Joints - H Riberholt
23-12-4	Glued Laminated Timber - Strength Classes and Determination of Characteristic Properties - H Riberholt, J Ehlbeck and A Fewell
24-12-1	Contribution to the Determination of the Bending Strength of Glulam Beams - F Colling, J Ehlbeck and R Görlacher
24-12-2	Influence of Perpendicular-to-Grain Stressed Volume on the Load-Carrying Capacity of Curved and Tapered Glulam Beams - J Ehlbeck and J Kürth
25-12-1	Determination of Characteristic Bending Values of Glued Laminated Timber. EN-Approach and Reality - E Gehri
26-12-1	Norwegian Bending Tests with Glued Laminated Beams-Comparative Calculations with the "Karlsruhe Calculation Model" - E Aasheim, K Solli, F Colling, R H Falk, J Ehlbeck and R Görlacher
26-12-2	Simulation Analysis of Norwegian Spruce Glued-Laminated Timber - R Hernandez and R H Falk
26-12-3	Investigation of Laminating Effects in Glued-Laminated Timber - F Colling and R H Falk
26-12-4	Comparing Design Results for Glulam Beams According to Eurocode 5 and to the French Working Stress Design Code (CB71) - F Rouger
27-12-1	State of the Art Report: Glulam Timber Bridge Design in the U.S. - M A Ritter and T G Williamson
27-12-2	Common Design Practice for Timber Bridges in the United Kingdom - C J Mettem, J P Marcroft and G Davis
27-12-3	Influence of Weak Zones on Stress Distribution in Glulam Beams - E Serrano and H J Larsen

28-12-1	Determination of Characteristic Bending Strength of Glued Laminated Timber - E Gehri
28-12-2	Size Factor of Norwegian Glued Laminated Beams - E Aasheim and K H Solli
28-12-3	Design of Glulam Beams with Holes - K Riipola
28-12-4	Compression Resistance of Glued Laminated Timber Short Columns- U Korin
29-12-1	Development of Efficient Glued Laminated Timber - G Schickhofer
30-12-1	Experimental Investigation and Analysis of Reinforced Glulam Beams - K Oiger
31-12-1	Depth Factor for Glued Laminated Timber-Discussion of the Eurocode 5 Approach - B Källsner, O Carling and C J Johansson
32-12-1	The bending stiffness of nail-laminated timber elements in transverse direction- T Wolf and O Schäfer
33-12-1	Internal Stresses in the Cross-Grain Direction of Wood Induced by Climate Variation – J Jönsson and S Svensson
34-12-1	High-Strength I-Joist Compatible Glulam Manufactured with LVL Tension Laminations – B Yeh, T G Williamson
34-12-2	Evaluation of Glulam Shear Strength Using A Full-Size Four-Point Test Method – B Yeh, T G Williamson
34-12-3	Design Model for FRP Reinforced Glulam Beams – M Romani, H J Blaß
34-12-4	Moisture induced stresses in glulam cross sections – J Jönsson
34-12-5	Load Carrying Capacity of Nail-Laminated Timber under Concentrated Loads – V Krämer, H J Blaß
34-12-6	Determination of Shear Strength Values for GLT Using Visual and Machine Graded Spruce Laminations – G Schickhofer
34-12-7	Mechanically Jointed Beams: Possibilities of Analysis and some special Problems – H Kreuzinger
35-12-1	Glulam Beams with Round Holes – a Comparison of Different Design Approaches vs. Test Data - S Aicher L Höfflin
36-12-1	Problems with Shear and Bearing Strength of LVL in Highly Loaded Structures - H Bier
36-12-2	Weibull Based Design of Round Holes in Glulam - L Höfflin, S Aicher
37-12-1	Development of Structural LVL from Tropical Wood and Evaluation of Their Performance for the Structural Components of Wooden Houses. Part-1. Application of Tropical LVL to a Roof Truss - K Komatsu, Y Idris, S Yuwasdiki, B Subiyakto, A Firmanti
37-12-2	Reinforcement of LVL Beams With Bonded-in Plates and Rods - Effect of Placement of Steel and FRP Reinforcements on Beam Strength and Stiffness - P Alam, M P Ansell, D Smedley
39-12-1	Recommended Procedures for Determination of Distribution Widths in the Design of Stress Laminated Timber Plate Decks - K Crews
39-12-2	In-situ Strengthening of Timber Structures with CFRP - K U Schober, S Franke, K Rautenstrauch
39-12-3	Effect of Checking and Non-Glued Edge Joints on the Shear Strength of Structural Glued Laminated Timber Beams - B Yeh, T G Williamson, Z A Martin
39-12-4	A Contribution to the Design and System Effect of Cross Laminated Timber (CLT) - R Jöbstl, T Moosbrugger, T Bogensperger, G Schickhofer
39-12-5	Behaviour of Glulam in Compression Perpendicular to Grain in Different Strength Grades and Load Configurations - M Augustin, A Ruli, R Brandner, G Schickhofer
40-12-1	Development of New Constructions of Glulam Beams in Canada - F Lam, N Mohadevan

40-12-2 Determination of Modulus of Shear and Elasticity of Glued Laminated Timber and Related Examination - R Brandner, E Gehri, T Bogensperger, G Schickhofer

40-12-3 Comparative Examination of Creep of GTL and CLT-Slabs in Bending - R A Jöbstl, G Schickhofer,

40-12-4 Standard Practice for the Derivation of Design Properties of Structural Glued Laminated Timber in the United States - T G Williamson, B Yeh

40-12-5 Creep and Creep-Rupture Behaviour of Structural Composite Lumber Evaluated in Accordance with ASTM D 6815 - B Yeh, T G Williamson.

40-12-6 Bending Strength of Combined Beech-Spruce Glulam - M Frese, H J Blaß

40-12-7 Quality Control of Glulam: Shear Tests of Glue Lines - R Steiger, E Gehri

41-12-1 Paper withdrawn by the author

41-12-2 Bending Strength of Spruce Glulam: New Models for the Characteristic Bending Strength - M Frese, H J Blass,

41-12-3 In-Plane Shear Strength of Cross Laminated Timber - R A Joebstl, T Bogensperger, G Schickhofer

41-12-4 Strength of Glulam Beams with Holes - Tests of Quadratic Holes and Literature Test Results Compilation - H Danielsson, P J Gustafsson

PARTICLE AND FIBRE BUILDING BOARDS

7-13-1 Fibre Building Boards for CIB Timber Code (First Draft)- O Brynildsen

9-13-1 Determination of the Bearing Strength and the Load-Deformation Characteristics of Particleboard - K Möhler, T Budianto and J Ehlbeck

9-13-2 The Structural Use of Tempered Hardboard - W W L Chan

11-13-1 Tests on Laminated Beams from Hardboard under Short- and Longterm Load - W Nozynski

11-13-2 Determination of Deformation of Special Densified Hardboard under Long-term Load and Varying Temperature and Humidity Conditions - W Halfar

11-13-3 Determination of Deformation of Hardboard under Long-term Load in Changing Climate - W Halfar

14-4-1 An Introduction to Performance Standards for Wood-Base Panel Products - D H Brown

14-4-2 Proposal for Presenting Data on the Properties of Structural Panels - T Schmidt

16-13-1 Effect of Test Piece Size on Panel Bending Properties - P W Post

20-4-1 Considerations of Reliability - Based Design for Structural Composite Products - M R O'Halloran, J A Johnson, E G Elias and T P Cunningham

20-13-1 Classification Systems for Structural Wood-Based Sheet Materials - V C Kearley and A R Abbott

21-13-1 Design Values for Nailed Chipboard - Timber Joints - A R Abbott

25-13-1 Bending Strength and Stiffness of Izopanel Plates - Z Mielczarek

28-13-1 Background Information for "Design Rated Oriented Strand Board (OSB)" in CSA Standards - Summary of Short-term Test Results - E Karacabeyli, P Lau, C R Henderson, F V Meakes and W Deacon

28-13-2 Torsional Stiffness of Wood-Hardboard Composed I-Beam - P Olejniczak

TRUSSED RAFTERS

4-9-1	Long-term Loading of Trussed Rafters with Different Connection Systems - T Feldborg and M Johansen
6-9-3	Deflection of Trussed Rafters under Alternating Loading During a Year - T Feldborg and M Johansen
7-2-1	Lateral Bracing of Timber Struts - J A Simon
9-14-1	Timber Trusses - Code Related Problems - T F Williams
9-7-1	Design of Truss Plate Joints - F J Keenan
10-14-1	Design of Roof Bracing - The State of the Art in South Africa - P A V Bryant and J A Simon
11-14-1	Design of Metal Plate Connected Wood Trusses - A R Egerup
12-14-1	A Simple Design Method for Standard Trusses - A R Egerup
13-14-1	Truss Design Method for CIB Timber Code - A R Egerup
13-14-2	Trussed Rafters, Static Models - H Riberholt
13-14-3	Comparison of 3 Truss Models Designed by Different Assumptions for Slip and E-Modulus - K Möhler
14-14-1	Wood Trussed Rafter Design - T Feldborg and M Johansen
14-14-2	Truss-Plate Modelling in the Analysis of Trusses - R O Foschi
14-14-3	Cantilevered Timber Trusses - A R Egerup
14-7-5	The Effect of Support Eccentricity on the Design of W- and WW-Trusses with Nail Plate Connectors - B Källsner
15-14-1	Guidelines for Static Models of Trussed Rafters - H Riberholt
15-14-2	The Influence of Various Factors on the Accuracy of the Structural Analysis of Timber Roof Trusses - F R P Pienaar
15-14-3	Bracing Calculations for Trussed Rafter Roofs - H J Burgess
15-14-4	The Design of Continuous Members in Timber Trussed Rafters with Punched Metal Connector Plates - P O Reece
15-14-5	A Rafter Design Method Matching U.K. Test Results for Trussed Rafters - H J Burgess
16-14-1	Full-Scale Tests on Timber Fink Trusses Made from Irish Grown Sitka Spruce - V Picardo
17-14-1	Data from Full Scale Tests on Prefabricated Trussed Rafters - V Picardo
17-14-2	Simplified Static Analysis and Dimensioning of Trussed Rafters - H Riberholt
17-14-3	Simplified Calculation Method for W-Trusses - B Källsner
18-14-1	Simplified Calculation Method for W-Trusses (Part 2) - B Källsner
18-14-2	Model for Trussed Rafter Design - T Poutanen
19-14-1	Annex on Simplified Design of W-Trusses - H J Larsen
19-14-2	Simplified Static Analysis and Dimensioning of Trussed Rafters - Part 2 - H Riberholt
19-14-3	Joint Eccentricity in Trussed Rafters - T Poutanen
20-14-1	Some Notes about Testing Nail Plates Subjected to Moment Load - T Poutanen
20-14-2	Moment Distribution in Trussed Rafters - T Poutanen
20-14-3	Practical Design Methods for Trussed Rafters - A R Egerup
22-14-1	Guidelines for Design of Timber Trussed Rafters - H Riberholt

23-14-1 Analyses of Timber Trussed Rafters of the W-Type - H Riberholt

23-14-2 Proposal for Eurocode 5 Text on Timber Trussed Rafters - H Riberholt

24-14-1 Capacity of Support Areas Reinforced with Nail Plates in Trussed Rafters - A Kevarinmäki

25-14-1 Moment Anchorage Capacity of Nail Plates in Shear Tests - A Kevarinmaki and J. Kangas

25-14-2 Design Values of Anchorage Strength of Nail Plate Joints by 2-curve Method and Interpolation - J Kangas and A Kevarinmaki

26-14-1 Test of Nail Plates Subjected to Moment - E Aasheim

26-14-2 Moment Anchorage Capacity of Nail Plates - A Kevarinmäki and J Kangas

26-14-3 Rotational Stiffness of Nail Plates in Moment Anchorage - A Kevarinmäki and J Kangas

26-14-4 Solution of Plastic Moment Anchorage Stress in Nail Plates - A Kevarinmäki

26-14-5 Testing of Metal-Plate-Connected Wood-Truss Joints - R Gupta

26-14-6 Simulated Accidental Events on a Trussed Rafter Roofed Building - C J Mettem and J P Marcroft

30-14-1 The Stability Behaviour of Timber Trussed Rafter Roofs - Studies Based on Eurocode 5 and Full Scale Testing - R J Bainbridge, C J Mettern, A Reffold and T Studer

32-14-1 Analysis of Timber Reinforced with Punched Metal Plate Fasteners- J Nielsen

33-14-1 Moment Capacity of Timber Beams Loaded in Four-Point Bending and Reinforced with Punched Metal Plate Fasteners – J Nielsen

36-14-1 Effect of Chord Splice Joints on Force Distribution in Trusses with Punched Metal Plate Fasteners - P Ellegaard

36-14-2 Monte Carlo Simulation and Reliability Analysis of Roof Trusses with Punched Metal Plate Fasteners - M Hansson, P Ellegaard

36-14-3 Truss Trouble – R H Leicester, J Goldfinch, P Paevere, G C Foliente

40-14-1 Timber Trusses with Punched Metal Plate Fasteners - Design for Transport and Erection - H J Blaß

STRUCTURAL STABILITY

8-15-1 Laterally Loaded Timber Columns: Tests and Theory - H J Larsen

13-15-1 Timber and Wood-Based Products Structures. Panels for Roof Coverings. Methods of Testing and Strength Assessment Criteria. Polish Standard BN-78/7159-03

16-15-1 Determination of Bracing Structures for Compression Members and Beams - H Brüninghoff

17-15-1 Proposal for Chapter 7.4 Bracing - H Brüninghoff

17-15-2 Seismic Design of Small Wood Framed Houses - K F Hansen

18-15-1 Full-Scale Structures in Glued Laminated Timber, Dynamic Tests: Theoretical and Experimental Studies - A Ceccotti and A Vignoli

18-15-2 Stabilizing Bracings - H Brüninghoff

19-15-1 Connections Deformability in Timber Structures: a Theoretical Evaluation of its Influence on Seismic Effects - A Ceccotti and A Vignoli

19-15-2 The Bracing of Trussed Beams - M H Kessel and J Natterer

19-15-3 Racking Resistance of Wooden Frame Walls with Various Openings - M Yasumura

19-15-4	Some Experiences of Restoration of Timber Structures for Country Buildings - G Cardinale and P Spinelli
19-15-5	Non-Destructive Vibration Tests on Existing Wooden Dwellings - Y Hirashima
20-15-1	Behaviour Factor of Timber Structures in Seismic Zones. - A Ceccotti and A Vignoli
21-15-1	Rectangular Section Deep Beam - Columns with Continuous Lateral Restraint - H J Burgess
21-15-2	Buckling Modes and Permissible Axial Loads for Continuously Braced Columns- H J Burgess
21-15-3	Simple Approaches for Column Bracing Calculations - H J Burgess
21-15-4	Calculations for Discrete Column Restraints - H J Burgess
21-15-5	Behaviour Factor of Timber Structures in Seismic Zones (Part Two) - A Ceccotti and A Vignoli
22-15-1	Suggested Changes in Code Bracing Recommendations for Beams and Columns - H J Burgess
22-15-2	Research and Development of Timber Frame Structures for Agriculture in Poland- S Kus and J Kerste
22-15-3	Ensuring of Three-Dimensional Stiffness of Buildings with Wood Structures - A K Shenghelia
22-15-5	Seismic Behavior of Arched Frames in Timber Construction - M Yasumura
22-15-6	The Robustness of Timber Structures - C J Mettem and J P Marcroft
22-15-7	Influence of Geometrical and Structural Imperfections on the Limit Load of Wood Columns - P Dutko
23-15-1	Calculation of a Wind Girder Loaded also by Discretely Spaced Braces for Roof Members - H J Burgess
23-15-2	Stability Design and Code Rules for Straight Timber Beams - T A C M van der Put
23-15-3	A Brief Description of Formula of Beam-Columns in China Code - S Y Huang
23-15-4	Seismic Behavior of Braced Frames in Timber Construction - M Yasumara
23-15-5	On a Better Evaluation of the Seismic Behavior Factor of Low-Dissipative Timber Structures - A Ceccotti and A Vignoli
23-15-6	Disproportionate Collapse of Timber Structures - C J Mettem and J P Marcroft
23-15-7	Performance of Timber Frame Structures During the Loma Prieta California Earthquake - M R O'Halloran and E G Elias
24-15-2	Discussion About the Description of Timber Beam-Column Formula - S Y Huang
24-15-3	Seismic Behavior of Wood-Framed Shear Walls - M Yasumura
25-15-1	Structural Assessment of Timber Framed Building Systems - U Korin
25-15-3	Mechanical Properties of Wood-framed Shear Walls Subjected to Reversed Cyclic Lateral Loading - M Yasumura
26-15-1	Bracing Requirements to Prevent Lateral Buckling in Trussed Rafters - C J Mettem and P J Moss
26-15-2	Eurocode 8 - Part 1.3 - Chapter 5 - Specific Rules for Timber Buildings in Seismic Regions - K Becker, A Ceccotti, H Charlier, E Katsaragakis, H J Larsen and H Zeitter
26-15-3	Hurricane Andrew - Structural Performance of Buildings in South Florida - M R O'Halloran, E L Keith, J D Rose and T P Cunningham

29-15-1	Lateral Resistance of Wood Based Shear Walls with Oversized Sheathing Panels - F Lam, H G L Prion and M He
29-15-2	Damage of Wooden Buildings Caused by the 1995 Hyogo-Ken Nanbu Earthquake - M Yasumura, N Kawai, N Yamaguchi and S Nakajima
29-15-3	The Racking Resistance of Timber Frame Walls: Design by Test and Calculation - D R Griffiths, C J Mettem, V Enjily, P J Steer
29-15-4	Current Developments in Medium-Rise Timber Frame Buildings in the UK - C J Mettem, G C Pitts, P J Steer, V Enjily
29-15-5	Natural Frequency Prediction for Timber Floors - R J Bainbridge, and C J Mettem
30-15-1	Cyclic Performance of Perforated Wood Shear Walls with Oversize Oriented Strand Board Panels - Ming He, H Magnusson, F Lam, and H G L Prion
30-15-2	A Numerical Analysis of Shear Walls Structural Performances - L Davenne, L Daudeville, N Kawai and M Yasumura
30-15-3	Seismic Force Modification Factors for the Design of Multi-Storey Wood-Frame Platform Construction - E Karacabeyli and A Ceccotti
30-15-4	Evaluation of Wood Framed Shear Walls Subjected to Lateral Load - M Yasumura and N Kawai
31-15-1	Seismic Performance Testing On Wood-Framed Shear Wall - N Kawai
31-15-2	Robustness Principles in the Design of Medium-Rise Timber-Framed Buildings - C J Mettem, M W Milner, R J Bainbridge and V. Enjily
31-15-3	Numerical Simulation of Pseudo-Dynamic Tests Performed to Shear Walls - L Daudeville, L Davenne, N Richard, N Kawai and M Yasumura
31-15-4	Force Modification Factors for Braced Timber Frames - H G L Prion, M Popovski and E Karacabeyli
32-15-1	Three-Dimensional Interaction in Stabilisation of Multi-Storey Timber Frame Buildings - S Andreasson
32-15-2	Application of Capacity Spectrum Method to Timber Houses - N Kawai
32-15-3	Design Methods for Shear Walls with Openings - C Ni, E Karacabeyli and A Ceccotti
32-15-4	Static Cyclic Lateral Loading Tests on Nailed Plywood Shear Walls - K Komatsu, K H Hwang and Y Itou
33-15-1	Lateral Load Capacities of Horizontally Sheathed Unblocked Shear Walls – C Ni, E Karacabeyli and A Ceccotti
33-15-2	Prediction of Earthquake Response of Timber Houses Considering Shear Deformation of Horizontal Frames – N Kawai
33-15-3	Eurocode 5 Rules for Bracing – H J Larsen
34-15-1	A simplified plastic model for design of partially anchored wood-framed shear walls – B Källsner, U A Girhammar, Liping Wu
34-15-2	The Effect of the Moisture Content on the Performance of the Shear Walls – S Nakajima
34-15-3	Evaluation of Damping Capacity of Timber Structures for Seismic Design – M Yasumura
35-15-1	On test methods for determining racking strength and stiffness of wood-framed shear walls - B Källsner, U A Girhammar, L Wu
35-15-2	A Plastic Design Model for Partially Anchored Wood-framed Shear Walls with Openings - U A Girhammar, L Wu, B Källsner
35-15-3	Evaluation and Estimation of the Performance of the Shear Walls in Humid Climate - S Nakajima

35-15-4	Influence of Vertical Load on Lateral Resistance of Timber Frame Walls - B Dujič, R Žarnić
35-15-5	Cyclic and Seismic Performances of a Timber-Concrete System - Local and Full Scale Experimental Results - E Fournely, P Racher
35-15-6	Design of timber-concrete composite structures according to EC5 - 2002 version - A Ceccotti, M Fragiacomo, R M Gutkowski
35-15-7	Design of timber structures in seismic zones according to EC8- 2002 version - A Ceccotti, T Toratti, B Dujič
35-15-8	Design Methods to Prevent Premature Failure of Joints at Shear Wall Corners - N Kawai, H Okiura
36-15-1	Monitoring Light-Frame Timber Buildings: Environmental Loads and Load Paths – I Smith et al.
36-15-2	Applicability of Design Methods to Prevent Premature Failure of Joints at Shear Wall Corners in Case of Post and Beam Construction - N Kawai, H Isoda
36-15-3	Effects of Screw Spacing and Edge Boards on the Cyclic Performance of Timber Frame and Structural Insulated Panel Roof Systems - D M Carradine, J D Dolan, F E Woeste
36-15-4	Pseudo-Dynamic Tests on Conventional Timber Structures with Shear Walls - M Yasumura
36-15-5	Experimental Investigation of Laminated Timber Frames with Fiber-reinforced Connections under Earthquake Loads - B Kasal, P Haller, S Pospisil, I Jirovsky, A Heiduschke, M Drdacky
36-15-6	Effect of Test Configurations and Protocols on the Performance of Shear Walls - F Lam, D Jossen, J Gu, N Yamaguchi, H G L Prion
36-15-7	Comparison of Monotonic and Cyclic Performance of Light-Frame Shear Walls - J D Dolan, A J Toothman
37-15-1	Estimating 3D Behavior of Conventional Timber Structures with Shear Walls by Pseudodynamic Tests - M Yasumura, M Uesugi, L Davenne
37-15-2	Testing of Racking Behavior of Massive Wooden Wall Panels - B Dujič, J Pucelj, R Žarnić
37-15-3	Influence of Framing Joints on Plastic Capacity of Partially Anchored Wood-Framed Shear Walls - B Källsner, U A Girhammar
37-15-4	Bracing of Timber Members in Compression - J Munch-Andersen
37-15-5	Acceptance Criteria for the Use of Structural Insulated Panels in High Risk Seismic Areas - B Yeh, T D Skaggs, T G Williamson Z A Martin
37-15-6	Predicting Load Paths in Shearwalls - Hongyong Mi, Ying-Hei Chui, I Smith, M Mohammad
38-15-1	Background Information on ISO STANDARD 16670 for Cyclic Testing of Connections - E Karacabeyli, M Yasumura, G C Foliente, A Ceccotti
38-15-2	Testing & Product Standards – a Comparison of EN to ASTM, AS/NZ and ISO Standards – A Ranta-Maunus, V Enjily
38-15-3	Framework for Lateral Load Design Provisions for Engineered Wood Structures in Canada - M Popovski, E Karacabeyli
38-15-4	Design of Shear Walls without Hold-Downs - Chun Ni, E Karacabeyli
38-15-5	Plastic design of partially anchored wood-framed wall diaphragms with and without openings - B Källsner, U A Girhammar
38-15-6	Racking of Wooden Walls Exposed to Different Boundary Conditions - B Dujič, S Aicher, R Žarnić

38-15-7	A Portal Frame Design for Raised Wood Floor Applications - T G Williamson, Z A Martin, B Yeh
38-15-8	Linear Elastic Design Method for Timber Framed Ceiling, Floor and Wall Diaphragms - Jarmo Leskelä
38-15-9	A Unified Design Method for the Racking Resistance of Timber Framed Walls for Inclusion in EUROCODE 5 - R Griffiths, B Källsner, H J Blass, V Enjily
39-15-1	Effect of Transverse Walls on Capacity of Wood-Framed Wall Diaphragms - U A Girhammar, B Källsner
39-15-2	Which Seismic Behaviour Factor for Multi-Storey Buildings made of Cross-Laminated Wooden Panels? - M Follesa, M P Lauriola, C Minowa, N Kawai, C Sandhaas, M Yasumura, A Ceccotti
39-15-3	Laminated Timber Frames under dynamic Loadings - A Heiduschke, B Kasal, P Haller
39-15-4	Code Provisions for Seismic Design of Multi-storey Post-tensioned Timber Buildings - S Pampanin, A Palermo, A Buchanan, M Fragiacomo, B Deam
40-15-1	Design of Safe Timber Structures – How Can we Learn from Structural Failures? - S Thelandersson, E Frühwald
40-15-2	Effect of Transverse Walls on Capacity of Wood-Framed Wall Diaphragms—Part 2 - U A Girhammar, B Källsner
40-15-3	Midply Wood Shear Wall System: Concept, Performance and Code Implementation - Chun Ni, M Popovski, E Karacabeyli, E Varoglu, S Stiemer
40-15-4	Seismic Behaviour of Tall Wood-Frame Walls - M Popovski, A Peterson, E Karacabeyli
40-15-5	International Standard Development of Lateral Load Test Method for Shear Walls - M Yasumura, E Karacabeyli
40-15-6	Influence of Openings on Shear Capacity of Wooden Walls - B Dujič, S Klobcar, R Žarnić
41-15-1	Need for a Harmonized Approach for Calculations of Ductility of Timber Assemblies - W Muñoz, M Mohammad, A Salenikovich, P Quenneville
41-15-2	Plastic Design of Wood Frame Wall Diaphragms in Low and Medium Rise Buildings - B Källsner, U A Girhammar
41 15-3	Failure Analysis of Light Wood Frame Structures under Wind Load - A Asiz, Y H Chui, I Smith
41-15-4	Combined Shear and Wind Uplift Resistance of Wood Structural Panel Shearwalls B Yeh, T G Williamson
41-15-5	Behaviour of Prefabricated Timber Wall Elements under Static and Cyclic Loading – P Schädle, H J Blass

FIRE

12-16-1	British Standard BS 5268 the Structural Use of Timber: Part 4 Fire Resistance of Timber Structures
13-100-2	CIB Structural Timber Design Code. Chapter 9. Performance in Fire
19-16-1	Simulation of Fire in Tests of Axially Loaded Wood Wall Studs - J König
24-16-1	Modelling the Effective Cross Section of Timber Frame Members Exposed to Fire - J König
25-16-1	The Effect of Density on Charring and Loss of Bending Strength in Fire - J König
25-16-2	Tests on Glued-Laminated Beams in Bending Exposed to Natural Fires - F Bolonius Olesen and J König
26-16-1	Structural Fire Design According to Eurocode 5, Part 1.2 - J König

31-16-1	Revision of ENV 1995-1-2: Charring and Degradation of Strength and Stiffness - J König
33-16-1	A Design Model for Load-carrying Timber Frame Members in Walls and Floors Exposed to Fire - J König
33-16-2	A Review of Component Additive Methods Used for the Determination of Fire Resistance of Separating Light Timber Frame Construction - J König, T Oksanen and K Towler
33-16-3	Thermal and Mechanical Properties of Timber and Some Other Materials Used in Light Timber Frame Construction - B Källsner and J König
34-16-1	Influence of the Strength Determining Factors on the Fire Resistance Capability of Timber Structural Members – I Totev, D Dakov
34-16-2	Cross section properties of fire exposed rectangular timber members - J König, B Källsner
34-16-3	Pull-Out Tests on Glued-in Rods at High Temperatures – A Mischler, A Frangi
35-16-1	Basic and Notional Charring Rates - J König
37 - 16 - 1	Effective Values of Thermal Properties of Timber and Thermal Actions During the Decay Phase of Natural Fires - J König
37 - 16 - 2	Fire Tests on Timber Connections with Dowel-type Fasteners - A Frangi, A Mischler
38-16-1	Fire Behaviour of Multiple Shear Steel-to-Timber Connections with Dowels - C Erchinger, A Frangi, A Mischler
38-16-2	Fire Tests on Light Timber Frame Wall Assemblies - V Schleifer, A Frangi
39-16-1	Fire Performance of FRP Reinforced Glulam - T G Williamson, B Yeh
39-16-2	An Easy-to-use Model for the Design of Wooden I-joists in Fire - J König, B Källsner
39-16-3	A Design Model for Timber Slabs Made of Hollow Core Elements in Fire - A Frangi, M Fontana
40-16-1	Bonded Timber Deck Plates in Fire - J König, J Schmid
40-16-2	Design of Timber Frame Floor Assemblies in Fire - A Frangi, C Erchinger
41-16-1	Effect of Adhesives on Finger Joint Performance in Fire - J König, J Norén, M Sterley

STATISTICS AND DATA ANALYSIS

13-17-1	On Testing Whether a Prescribed Exclusion Limit is Attained - W G Warren
16-17-1	Notes on Sampling and Strength Prediction of Stress Graded Structural Timber - P Glos
16-17-2	Sampling to Predict by Testing the Capacity of Joints, Components and Structures - B Norén
16-17-3	Discussion of Sampling and Analysis Procedures - P W Post
17-17-1	Sampling of Wood for Joint Tests on the Basis of Density - I Smith, L R J Whale
17-17-2	Sampling Strategy for Physical and Mechanical Properties of Irish Grown Sitka Spruce - V Picardo
18-17-1	Sampling of Timber in Structural Sizes - P Glos
18-6-3	Notes on Sampling Factors for Characteristic Values - R H Leicester
19-17-1	Load Factors for Proof and Prototype Testing - R H Leicester
19-6-2	Confidence in Estimates of Characteristic Values - R H Leicester
21-6-1	Draft Australian Standard: Methods for Evaluation of Strength and Stiffness of Graded Timber - R H Leicester

21-6-2 The Determination of Characteristic Strength Values for Stress Grades of Structural Timber. Part 1 - A R Fewell and P Glos

22-17-1 Comment on the Strength Classes in Eurocode 5 by an Analysis of a Stochastic Model of Grading - A proposal for a supplement of the design concept - M Kiesel

24-17-1 Use of Small Samples for In-Service Strength Measurement - R H Leicester and F G Young

24-17-2 Equivalence of Characteristic Values - R H Leicester and F G Young

24-17-3 Effect of Sampling Size on Accuracy of Characteristic Values of Machine Grades - Y H Chui, R Turner and I Smith

24-17-4 Harmonisation of LSD Codes - R H Leicester

25-17-2 A Body for Confirming the Declaration of Characteristic Values - J Sunley

25-17-3 Moisture Content Adjustment Procedures for Engineering Standards - D W Green and J W Evans

27-17-1 Statistical Control of Timber Strength - R H Leicester and H O Breitinger

30-17-1 A New Statistical Method for the Establishment of Machine Settings - F Rouger

35-17-1 Probabilistic Modelling of Duration of Load Effects in Timber Structures - J Köhler, S Svenson

38-17-1 Analysis of Censored Data - Examples in Timber Engineering Research - R Steiger, J Köhler

39-17-1 Possible Canadian / ISO Approach to Deriving Design Values from Test Data - I Smith, A Asiz, M Snow, Y H Chui

GLUED JOINTS

20-18-1 Wood Materials under Combined Mechanical and Hygral Loading - A Martensson and S Thelandersson

20-18-2 Analysis of Generalized Volkersen - Joints in Terms of Linear Fracture Mechanics - P J Gustafsson

20-18-3 The Complete Stress-Slip Curve of Wood-Adhesives in Pure Shear - H Wernersson and P J Gustafsson

22-18-1 Perspective Adhesives and Protective Coatings for Wood Structures - A S Freidin

34-18-1 Performance Based Classification of Adhesives for Structural Timber Applications - R J Bainbridge, C J Mettem, J G Broughton, A R Hutchinson

35-18-1 Creep Testing Wood Adhesives for Structural Use - C Bengtsson, B Källander

38-18-1 Adhesive Performance at Elevated Temperatures for Engineered Wood Products - B Yeh, B Herzog, T G Williamson

39-18-1 Comparison of the Pull–out Strength of Steel Bars Glued in Glulam Elements Obtained Experimentally and Numerically - V Rajčić, A Bjelanović, M Rak

39-18-2 The Influence of the Grading Method on the Finger Joint Bending Strength of Beech - M Frese, H J Blaß

FRACTURE MECHANICS

21-10-1 A Study of Strength of Notched Beams - P J Gustafsson

22-10-1 Design of Endnotched Beams - H J Larsen and P J Gustafsson

23-10-1 Tension Perpendicular to the Grain at Notches and Joints - T A C M van der Put

23-10-2 Dimensioning of Beams with Cracks, Notches and Holes. An Application of Fracture Mechanics - K Riipola

23-19-1 Determination of the Fracture Energie of Wood for Tension Perpendicular to the Grain - W Rug, M Badstube and W Schöne

23-19-2 The Fracture Energy of Wood in Tension Perpendicular to the Grain. Results from a Joint Testing Project - H J Larsen and P J Gustafsson

23-19-3 Application of Fracture Mechanics to Timber Structures - A Ranta-Maunus

24-19-1 The Fracture Energy of Wood in Tension Perpendicular to the Grain - H J Larsen and P J Gustafsson

28-19-1 Fracture of Wood in Tension Perpendicular to the Grain: Experiment and Numerical Simulation by Damage Mechanics - L Daudeville, M Yasumura and J D Lanvin

28-19-2 A New Method of Determining Fracture Energy in Forward Shear along the Grain - H D Mansfield-Williams

28-19-3 Fracture Design Analysis of Wooden Beams with Holes and Notches. Finite Element Analysis based on Energy Release Rate Approach - H Petersson

28-19-4 Design of Timber Beams with Holes by Means of Fracture Mechanics - S Aicher, J Schmidt and S Brunold

30-19-1 Failure Analysis of Single-Bolt Joints - L Daudeville, L Davenne and M Yasumura

37 - 19 - 1 Determination of Fracture Mechanics Parameters for Wood with the Help of Close Range Photogrammetry - S Franke, B Franke, K Rautenstrauch

39-19-1 First Evaluation Steps of Design Rules in the European and German codes of Transverse Tension Areas - S Franke, B Franke, K Rautenstrauch

SERVICEABILITY

27-20-1 Codification of Serviceability Criteria - R H Leicester

27-20-2 On the Experimental Determination of Factor k_{def} and Slip Modulus k_{ser} from Short- and Long-Term Tests on a Timber-Concrete Composite (TCC) Beam - S Capretti and A Ceccotti

27-20-3 Serviceability Limit States: A Proposal for Updating Eurocode 5 with Respect to Eurocode 1 - P Racher and F Rouger

27-20-4 Creep Behavior of Timber under External Conditions - C Le Govic, F Rouger, T Toratti and P Morlier

30-20-1 Design Principles for Timber in Compression Perpendicular to Grain - S Thelandersson and A Mårtensson

30-20-2 Serviceability Performance of Timber Floors - Eurocode 5 and Full Scale Testing - R J Bainbridge and C J Mettem

32-20-1 Floor Vibrations - B Mohr

37 - 20 - 1 A New Design Method to Control Vibrations Induced by Foot Steps in Timber Floors - Lin J Hu, Y H Chui

37 - 20 - 2 Serviceability Limit States of Wooden Footbridges. Vibrations Caused by Pedestrians - P Hamm

TEST METHODS

31-21-1 Development of an Optimised Test Configuration to Determine Shear Strength of Glued Laminated Timber - G Schickhofer and B Obermayr

31-21-2 An Impact Strength Test Method for Structural Timber. The Theory and a Preliminary Study - T D G Canisius

35-21-1 Full-Scale Edgewise Shear Tests for Laminated Veneer Lumber- B Yeh, T G Williamson

39-21-1 Timber Density Restrictions for Timber Connection Tests According to EN28970/ISO8970 - A Leijten, J Köhler, A Jorissen

39-21-2 The Mechanical Inconsistence in the Evaluation of the Modulus of Elasticity According to EN384 - T Bogensperger, H Unterwieser, G Schickhofer

40 - 21 - 1 ASTM D198 - Interlaboratory Study for Modulus of Elasticity of Lumber in Bending - A Salenikovich

40 - 21 - 2 New Test Configuration for CLT-Wall-Elements under Shear Load - T Bogensperger, T Moosbrugger, G Schickhofer

41-21-1 Determination of Shear Modulus by Means of Standardized Four-Point Bending Tests - R Brandner, B Freytag, G Schickhofer

CIB TIMBER CODE

2-100-1 A Framework for the Production of an International Code of Practice for the Structural Use of Timber - W T Curry

5-100-1 Design of Solid Timber Columns (First Draft) - H J Larsen

5-100-2 A Draft Outline of a Code for Timber Structures - L G Booth

6-100-1 Comments on Document 5-100-1; Design of Solid Timber Columns - H J Larsen and E Theilgaard

6-100-2 CIB Timber Code: CIB Timber Standards - H J Larsen and E Theilgaard

7-100-1 CIB Timber Code Chapter 5.3 Mechanical Fasteners; CIB Timber Standard 06 and 07 - H J Larsen

8-100-1 CIB Timber Code - List of Contents (Second Draft) - H J Larsen

9-100-1 The CIB Timber Code (Second Draft)

11-100-1 CIB Structural Timber Design Code (Third Draft)

11-100-2 Comments Received on the CIB Code - U Saarelainen; Y M Ivanov, R H Leicester, W Nozynski, W R A Meyer, P Beckmann; R Marsh

11-100-3 CIB Structural Timber Design Code; Chapter 3 - H J Larsen

12-100-1 Comment on the CIB Code - Sous-Commission Glulam

12-100-2 Comment on the CIB Code - R H Leicester

12-100-3 CIB Structural Timber Design Code (Fourth Draft)

13-100-1 Agreed Changes to CIB Structural Timber Design Code

13-100-2 CIB Structural Timber Design Code. Chapter 9: Performance in Fire

13-100-3a Comments on CIB Structural Timber Design Code

13-100-3b Comments on CIB Structural Timber Design Code - W R A Meyer

13-100-3c Comments on CIB Structural Timber Design Code - British Standards Institution

13-100-4 CIB Structural Timber Design Code. Proposal for Section 6.1.5 Nail Plates - N I Bovim

14-103-2 Comments on the CIB Structural Timber Design Code - R H Leicester

15-103-1 Resolutions of TC 165-meeting in Athens 1981-10-12/13

21-100-1 CIB Structural Timber Design Code. Proposed Changes of Sections on Lateral Instability, Columns and Nails - H J Larsen

22-100-1 Proposal for Including an Updated Design Method for Bearing Stresses in CIB W18 - Structural Timber Design Code - B Madsen

22-100-2 Proposal for Including Size Effects in CIB W18A Timber Design Code - B Madsen

22-100-3 CIB Structural Timber Design Code - Proposed Changes of Section on Thin-Flanged Beams - J König

22-100-4 Modification Factor for "Aggressive Media" - a Proposal for a Supplement to the CIB Model Code - K Erler and W Rug

22-100-5 Timber Design Code in Czechoslovakia and Comparison with CIB Model Code - P Dutko and B Kozelouh

LOADING CODES

4-101-1 Loading Regulations - Nordic Committee for Building Regulations

4-101-2 Comments on the Loading Regulations - Nordic Committee for Building Regulations

37-101-1 Action Combination Processing for the Eurocodes Basis of Software to Assist the Engineer - Y Robert, A V Page, R Thépaut, C J Mettem

STRUCTURAL DESIGN CODES

1-102-1 Survey of Status of Building Codes, Specifications etc., in USA - E G Stern

1-102-2 Australian Codes for Use of Timber in Structures - R H Leicester

1-102-3 Contemporary Concepts for Structural Timber Codes - R H Leicester

1-102-4 Revision of CP 112 - First Draft, July 1972 - British Standards Institution

4-102-1 Comparsion of Codes and Safety Requirements for Timber Structures in EEC Countries - Timber Research and Development Association

4-102-2 Nordic Proposals for Safety Code for Structures and Loading Code for Design of Structures - O A Brynildsen

4-102-3 Proposal for Safety Codes for Load-Carrying Structures - Nordic Committee for Building Regulations

4-102-4 Comments to Proposal for Safety Codes for Load-Carrying Structures - Nordic Committee for Building Regulations

4-102-5 Extract from Norwegian Standard NS 3470 "Timber Structures"

4-102-6 Draft for Revision of CP 112 "The Structural Use of Timber" - W T Curry

8-102-1 Polish Standard PN-73/B-03150: Timber Structures; Statistical Calculations and Designing

8-102-2 The Russian Timber Code: Summary of Contents

9-102-1 Svensk Byggnorm 1975 (2nd Edition); Chapter 27: Timber Construction

11-102-1 Eurocodes - H J Larsen

13-102-1 Program of Standardisation Work Involving Timber Structures and Wood-Based Products in Poland

17-102-1 Safety Principles - H J Larsen and H Riberholt

17-102-2 Partial Coefficients Limit States Design Codes for Structural Timberwork - I Smith

18-102-1 Antiseismic Rules for Timber Structures: an Italian Proposal - G Augusti and A Ceccotti

18-1-2 Eurocode 5, Timber Structures - H J Larsen

19-102-1 Eurocode 5 - Requirements to Timber - Drafting Panel Eurocode 5

19-102-2 Eurocode 5 and CIB Structural Timber Design Code - H J Larsen

19-102-3	Comments on the Format of Eurocode 5 - A R Fewell
19-102-4	New Developments of Limit States Design for the New GDR Timber Design Code - W Rug and M Badstube
19-7-3	Effectiveness of Multiple Fastener Joints According to National Codes and Eurocode 5 (Draft) - G Steck
19-7-6	The Derivation of Design Clauses for Nailed and Bolted Joints in Eurocode5 - L R J Whale and I Smith
19-14-1	Annex on Simplified Design of W-Trusses - H J Larsen
20-102-1	Development of a GDR Limit States Design Code for Timber Structures - W Rug and M Badstube
21-102-1	Research Activities Towards a New GDR Timber Design Code Based on Limit States Design - W Rug and M Badstube
22-102-1	New GDR Timber Design Code, State and Development - W Rug, M Badstube and W Kofent
22-102-2	Timber Strength Parameters for the New USSR Design Code and its Comparison with International Code - Y Y Slavik, N D Denesh and E B Ryumina
22-102-3	Norwegian Timber Design Code - Extract from a New Version - E Aasheim and K H Solli
23-7-1	Proposal for a Design Code for Nail Plates - E Aasheim and K H Solli
24-102-2	Timber Footbridges: A Comparison Between Static and Dynamic Design Criteria - A Ceccotti and N de Robertis
25-102-1	Latest Development of Eurocode 5 - H J Larsen
25-102-1A	Annex to Paper CIB-W18/25-102-1. Eurocode 5 - Design of Notched Beams - H J Larsen, H Riberholt and P J Gustafsson
25-102-2	Control of Deflections in Timber Structures with Reference to Eurocode 5 - A Martensson and S Thelandersson
28-102-1	Eurocode 5 - Design of Timber Structures - Part 2: Bridges - D Bajolet, E Gehri, J König, H Kreuzinger, H J Larsen, R Mäkipuro and C Mettem
28-102-2	Racking Strength of Wall Diaphragms - Discussion of the Eurocode 5 Approach - B Källsner
29-102-1	Model Code for the Probabilistic Design of Timber Structures - H J Larsen, T Isaksson and S Thelandersson
30-102-1	Concepts for Drafting International Codes and Standards for Timber Constructions - R H Leicester
33-102-1	International Standards for Bamboo – J J A Janssen
35-102-1	Design Characteristics and Results According to EUROCODE 5 and SNiP Procedures - L Ozola, T Keskküla
35-102-2	Model Code for the Reliability-Based Design of Timber Structures - H J Larsen
36-102-1	Predicted Reliability of Elements and Classification of Timber Structures - L Ozola, T Keskküla
36-102-2	Calibration of Reliability-Based Timber Design Codes: Choosing a Fatigue Model - I Smith
38-102-1	A New Generation of Timber Design Practices and Code Provisions Linking System and Connection Design - A Asiz, I Smith
38-102-2	Uncertainties Involved in Structural Timber Design by Different Code Formats - L Ozola, T Keskküla

38-102-3 Comparison of the Eurocode 5 and Actual Croatian Codes for Wood Classification and Design With the Proposal for More Objective Way of Classification - V Rajcic A Bjelanovic

39-102-1 Calibration of Partial Factors in the Danish Timber Code - H Riberholt

41 - 102 - 1 Consequences of EC 5 for Danish Best Practise - J Munch-Andersen

41 - 102 - 2 Development of New Swiss standards for the Assessment of Existing Load Bearing Structures – R Steiger, J Köhler

41 – 102 - 3 Measuring the CO2 Footprint of Timber Buildings – A Buchanan, S John

INTERNATIONAL STANDARDS ORGANISATION

3-103-1 Method for the Preparation of Standards Concerning the Safety of Structures (ISO/DIS 3250) - International Standards Organisation ISO/TC98

4-103-1 A Proposal for Undertaking the Preparation of an International Standard on Timber Structures - International Standards Organisation

5-103-1 Comments on the Report of the Consultion with Member Bodies Concerning ISO/TC/P129 - Timber Structures - Dansk Ingeniorforening

7-103-1 ISO Technical Committees and Membership of ISO/TC 165

8-103-1 Draft Resolutions of ISO/TC 165

12-103-1 ISO/TC 165 Ottawa, September 1979

13-103-1 Report from ISO/TC 165 - A Sorensen

14-103-1 Comments on ISO/TC 165 N52 "Timber Structures; Solid Timber in Structural Sizes; Determination of Some Physical and Mechanical Properties"

14-103-2 Comments on the CIB Structural Timber Design Code - R H Leicester

21-103-1 Concept of a Complete Set of Standards - R H Leicester

JOINT COMMITTEE ON STRUCTURAL SAFETY

3-104-1 International System on Unified Standard Codes of Practice for Structures - Comité Européen du Béton (CEB)

7-104-1 Volume 1: Common Unified Rules for Different Types of Construction and Material - CEB

37-104-1 Proposal for a Probabilistic Model Code for Design of Timber Structures - J Köhler, H Faber

CIB PROGRAMME, POLICY AND MEETINGS

1-105-1 A Note on International Organisations Active in the Field of Utilisation of Timber - P Sonnemans

5-105-1 The Work and Objectives of CIB-W18-Timber Structures - J G Sunley

10-105-1 The Work of CIB-W18 Timber Structures - J G Sunley

15-105-1 Terms of Reference for Timber - Framed Housing Sub-Group of CIB-W18

19-105-1 Tropical and Hardwood Timbers Structures - R H Leicester

21-105-1 First Conference of CIB-W18B, Tropical and Hardwood Timber Structures Singapore, 26 - 28 October 1987 - R H Leicester

INTERNATIONAL UNION OF FORESTRY RESEARCH ORGANISATIONS

7-106-1 Time and Moisture Effects - CIB W18/IUFRO 55.02-03 Working Party

INTERNATIONAL COUNCIL FOR RESEARCH AND INNOVATION IN BUILDING AND CONSTRUCTION

WORKING COMMISSION W18 - TIMBER STRUCTURES

ON THE ROLE OF STIFFNESS PROPERTIES FOR ULTIMATE LIMIT STATE DESIGN OF SLENDER COLUMNS

J Köhler

A Frangi

Institute of Structural Engineering, ETH Zurich

R Steiger

Empa, Swiss Federal Laboratories for Materials Testing and Research, Dübendorf

SWITZERLAND

Presented by J. Köhler

H.J. Larsen received confirmation the "effective length method" is the correct wording. He commented that the relationship between strength and stiffness is sensitive to the fractile of interest. A. Jorissen received clarification about the design equation for column. He commented that γm seemed to have been taken into account twice. J. Köhler confirmed that the approach is correct. U. Kuhlmann commented that the existing variation should include imperfection and provided explanation about the steel column design approach as a possible comparison. J. Köhler responded that imperfection is already considered. In terms of long term performance the influence of creep on P-delta is important. R. Steiger commented that the stiffness of connection joints don't have 5^{th} percentile values and received clarification that the issue of isolated column and moment resistance where in the German code 5^{th} percentile / γm is considered.

On the role of stiffness properties for ultimate limit state design of slender columns

Jochen Köhler & Andrea Frangi
Institute of Structural Engineering, ETH Zurich, Switzerland
René Steiger
Empa, Swiss Federal Laboratories for Materials Testing and Research
Dübendorf, Switzerland

Keywords: LRFD; 1st order linear elastic analysis; 2nd order non-linear analysis; stiffness properties; ultimate limit state design; probability of failure.

1 Introduction

In the daily practice the engineering codes and regulations form the premises for the use of timber as a structural material. Code regulations in North America, Australia and Europe are based on the limit states design (LSD) approach which is put into practice as load and resistance factor design (LRFD) formats. Initially, LRFD methods where converted as so called "soft conversions" of allowable stress design (ASD), the design method which was commonly used in code regulations before LRFD was introduced and which is usually based to a major part on experience, tradition and judgment. In the last decades this situation has changed; structural reliability concepts have been developed and provide a rational basis for the reliability based calibration of LRFD formats.

Typically, reliability based code calibration takes basis in the assessment of rather simplified design situations, i.e. bending-, tension- or compression components sustaining some typical load combinations. The herewith calibrated partial safety factors are, strictly, only valid for these simple design situations. For the well known reasons of applicability and clarity - beside reliability two major objectives of codes and standards - the application of the same partial safety factors for different design situations is common in present structural design formats.

Strength related timber material properties are generally considered for ultimate limit states, whereas stiffness related timber material properties are of interest when serviceability limit states are considered. Both, strength and stiffness related timber material properties have to be considered for ultimate limit states where the stresses, i.e. the load bearing capacity of the structure, are directly dependent on the deformation of the structure. An example for this is the design of slender columns against axial loading. Within the present paper two European code formats, EN 1995-1-1 and DIN 1052, for the design of slender columns is considered and the role of the timber stiffness property is analysed.

2 LRFD formats and example design solutions

2.1 Timber stiffness in ultimate limit state design

Usually, ultimate limit states and serviceability limit states are considered for structural analysis. Stiffness related timber material properties (i.e. modulus of elasticity and shear modulus) and connection properties (i.e. slip modulus) are typically used for verifications of serviceability limit states, for example for the calculation of deformations. The influence of load duration (creep) is usually taken into account by reducing the modulus of elasticity.

For a linear (1st order) ultimate limit state analysis it is generally assumed that the internal force distribution is not influenced by the stiffness properties, unless if timber is combined with other materials in statically indeterminate structures. For a non-linear (2nd order) ultimate limit state analysis stiffness properties are taken into account to assess higher order effects caused by deformations. Deformations in timber structures are governed not only by the initial material (and joint) stiffness, but also by creep.

Stiffness properties and creep effects play an important role for assessing the stability of timber members (i.e. buckling and lateral-torsional buckling) and the overall stability of structures. Typical examples are columns subjected to compression, beams subjected to bending and beam-columns subjected to combined bending and compression. For the analysis of single members, standards generally give simplified calculation models that do not require a 2nd order ultimate limit state analysis. However, for the analysis of more complex systems like unbraced frame structures, a 2nd order structural analysis is more appropriate and accurate.

According to EN 1995-1-1 the analysis of structures for ultimate limit states shall be carried out using the following values for stiffness properties:

- Mean values shall be used for a 1st order structural analysis of a structure, where the distribution of internal forces is not affected by the stiffness distribution within the structure (e.g. all members have the same time-dependent properties);
- For a 1st order structural analysis of a structure, whose distribution of internal forces is affected by the stiffness distribution within the structure (e.g. composite members containing materials having different time-dependent properties), final mean values adjusted to the load component causing the largest stress in relation to strength shall be used; for example the final mean value of modulus of elasticity $E_{0,mean,fin}$ is defined as:

$$E_{0,mean,fin} = \frac{E_{0,mean}}{1+\psi_2 k_{def}} \tag{1}$$

  with $E_{0,mean}$, the mean value of the modulus of elasticity, $\psi_2\, k_{def}$ is a modification factor taking into account duration of load and moisture effect on the stiffness, and ψ_2 is a factor for quasi-permanent contribution of a variable action, according to EN 1990: 2002.

- For a 2nd order structural analysis of a structure, design values not adjusted for duration of load, shall be used; for example the design value of modulus of elasticity $E_{0,d}$ is defined as:

$$E_{0,d} = E_{0,mean} / \gamma_M \tag{2}$$

where γ_M is the partial safety factor on timber material resistance.

DIN 1052 also defines different design values for the stiffness properties for ultimate limit state design. For example the design modulus of elasticity $E_{0,d}$ is defined as:

- $E_{0,d} = E_{0,mean}/\gamma_M$ for a 1st order structural analysis.
- $E_{0,d} = E_{0,mean}/\gamma_M$ for a 2nd order analysis of structural systems.
- $E^*_{0,d} = E_{0,05}/\gamma_M$ for a 2nd order analysis of single structural members.

Table 1: A comparison of different design values for the modulus of elasticity (based on the strength class system of EN 338)

	γ_M [-]	$E_{0,mean}$ [N/mm²]	$E_{0,05} \approx 0.67E_{0,mean}$ [N/mm²]	$E_{0,d} = E_{0,mean}/\gamma_M$ [N/mm²]	$E^*_{0,d} = E_{0,05}/\gamma_M$ [N/mm²]
Solid timber C24	1.3	11'000	7'400	8'462	5'693

2.2 Design formats for columns subjected to axial compression

The structural behaviour of columns subjected to axial compression is characterised by the non-linear (2nd order) increase of the deformation due to the axial load (P-delta effects). P-delta effects are due to imperfections of the structural members and strongly depended on the column slenderness and stiffness. Since columns subjected to axial compression become more slender and less stiff to deformation, the influence of P-delta effects increases and the structural behaviour is governed by column stability (buckling). The stiffness properties (modulus of elasticity) of the structural members play therefore an important role for a 2nd order analysis, in particular for slender columns.

The influence of P-delta effects on the resistance of timber columns subjected to axial compression was first investigated in Tetmajer [1] followed by further investigations in Möhler [2], Buchanan [3] and Blaß [4].

2.2.1 Effective length method

For the analysis of columns subjected to axial compression most standards give simplified calculation models based on the Effective Length Method. The advantage of the Effective Length Method is that the design forces and moments resulting from loads acting on a structure can be calculated based on a simple 1st order ultimate limit state analysis. For example, according to EN 1995-1-1 and DIN 1052 the design buckling resistance of columns subjected to axial compression $N_{b,R,d}$ can be calculated as:

$$N_{b,R,d} = k_c \cdot N_{c,R,d} \text{ with } N_{c,R,d} = \frac{k_{\text{mod}} \cdot f_{c,0,k} \cdot A}{\gamma_M} \tag{3}$$

defined as the design compressive resistance without influence of buckling, i.e. $f_{c,0,k}$ is the 5%-fractile value of the compression capacity parallel to the grain, A is the cross-sectional area, k_{mod} is a modification factor taking into account moisture and duration of load effects on the compression capacity and γ_M is the partial safety factor on the material resistance.

The (non-linear) P-delta effects – which in this case is the non-linear bending moment caused by the axial compression due to initial imperfections of the structural members – is accounted for by the buckling factor k_c. In EN 1995-1-1 and DIN 1052 the calculation of k_c is based on tests and Monte Carlo simulations in Blaß [4]. There, a column model is

developed, where initial geometrical imperfections and material properties had been represented probabilistically. Further, the non-linearity of the stress-strain relationship in the compression zone was taken into account by applying a model developed in Glos [5].

Accordingly k_c is calculated as:

$$k_c = \frac{1}{k + \sqrt{k^2 - \lambda_{rel}^2}} \quad \text{with} \quad k = 0.5\left(1 + \beta_c\left(\lambda_{rel} - 0.3\right) + \lambda_{rel}^2\right) \tag{4}$$

where λ_{rel} is the relative slenderness, the factor β_c = 0.2 for solid timber and β_c = 0.1 for glulam, if the deviations from straightness do not exceed ℓ/300 for solid timber and ℓ/500 for glulam (ℓ is the length of the column).

The relative slenderness λ_{rel} takes into account the slenderness $\lambda = \ell_{eff}/i$ (with ℓ_{eff} the effective buckling length and i the radius of inertia), geometry and material properties (strength and stiffness) of the columns and is calculated as:

$$\lambda_{rel} = \frac{\lambda}{\pi} \cdot \sqrt{\frac{f_{c,0,k}}{E_{0,05}}} = \frac{\ell_{eff}}{i \cdot \pi} \cdot \sqrt{\frac{f_{c,0,k}}{E_{0,05}}} \tag{5}$$

2.2.2 2nd order ultimate limit state analysis

As alternative to the Effective Length Method the influence of P-delta effects can directly be considered with a 2nd order ultimate limit state analysis. In the case of columns subjected to axial compression the non-linear (second order) increase of the deformation due to the axial compression can be calculated considering the amplification factor α defined as (see e.g. [6]):

$$\alpha = \frac{1}{1 - \frac{N_d}{N_{crit}}} \tag{6}$$

With N_d the design value of the load effect, and $N_{crit} = \pi^2 \cdot EI/\ell^2$ the classic Euler's formula of buckling, i.e. with E the modulus of elasticity, I the moment of interia and ℓ the buckling length.

The resulting moment of 2nd order can be calculated as:

$$M_{d,II} = N_d \cdot \alpha \cdot e \tag{7}$$

The initial eccentricity e takes into account all geometric imperfections as well as material imperfections. For 2nd order ultimate limit state analysis in EN 1995-1-1 and DIN 1052 an eccentricity e = ℓ/400 is suggested for both, solid timber or glulam.

In the case of a 2nd order structural analysis the ultimate limit state of columns subjected to axial compression can be verified with common interaction equations for combined bending and axial compression. Investigations by Buchanan [3] showed that columns loaded by axial compression and bending tend to develop plastic deformations in the compression zone. Thus, a linear model for description of the interaction between bending and axial compression leads to conservative results. In EN 1995-1-1 and DIN 1052 this effect is taken into account by the following non-linear interaction curve for combined bending and axial compression:

$$\left(\frac{N_d}{N_{c,R,d}}\right)^2 + \frac{M_d}{M_{R,d}} \leq 1.0 \tag{8}$$

with N_d and M_d being the design load effects. $N_{c,R,d} = k_{\text{mod}} \cdot f_{c,k} \cdot A/\gamma_M$ and $M_{R,d} = k_{\text{mod}} \cdot f_{m,k} \cdot W/\gamma_M$ are the design resistances in compression and bending with $f_{c,k}$ and $f_{m,k}$ the 5%-fractile values of compression and bending capacity, A the cross sectional area and W the section modulus.

Equation (8) can be used for the verification of the ultimate limit state of columns subjected to axial compression assuming the resulting moment $M_{d,II}$ of 2nd order:

$$\left(\frac{N_d}{\frac{k_{\text{mod}} \cdot f_{c,k} \cdot A}{\gamma_M}}\right)^2 + \frac{1}{1 - \frac{N_d}{\frac{\pi^2 \cdot EI}{\ell^2}}} \cdot \frac{N_d \cdot e}{\frac{k_{\text{mod}} \cdot f_{m,k} \cdot W}{\gamma_M}} \leq 1.0 \tag{9}$$

The solution of Equation (9) gives the design solutions for columns subjected to design load effects N_d based on 2nd order ultimate limit state analysis.

2.3 Comparison of design formats

In section 2.2 two different design formats for axially loaded columns had been described. The formats are different in terms of their formal layout – a second order analysis compared with a simplified first order analysis with a buckling reduction factor, and they are different in regard to the perspective how stiffness and long-term effects are considered.

The differences of the methods and especially of the different consideration of the modulus of elasticity and k_{mod} has led to discussions in the engineering community, [7], [8]. The discussion takes in general basis in a direct comparison of the design solutions obtained by the following different approaches:

Figure 1 illustrates this comparison. The ratio between the design buckling resistance $N_{R,d}$ of columns subjected to axial compression and the design compressive resistance $N_{c,R,d}$ as a function of the column slenderness is illustrated. Three different cases had been investigated. The 2nd order analysis solutions with $E_{0,d} = E_{0,mean}/\gamma_M$ and $E_{0,d} = E_{0,05}/\gamma_M$ are compared with the solution of the effective length method. No duration of load effects are implemented here, i.e. the corresponding modification factor k_{mod} has been set to unity.

Table 2: Different design values for the modulus of elasticity.

Effective Length Method	2nd order structural analysis	
ELM: $E_{0,d} = E_{0,05}$	$E_{0,d} = E_{0,mean}/\gamma_M$	$E_{0,d} = E_{0,05}/\gamma_M$
EN 1995-1-1 DIN 1052	EN 1995-1-1 DIN 1052[1)]	EN 1995-1-1 DIN 1052[2)]

[1)]for system analysis

[2)]for single member analysis

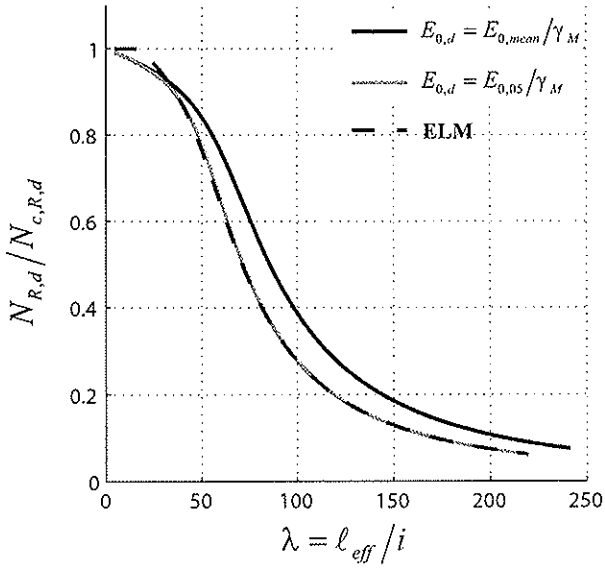

Figure 1: Ratio between the design buckling resistance $N_{R,d}$ of columns subjected to axial compression and the design compressive resistance $N_{c,R,d}$ as a function of the column slenderness ratio λ for different assumptions of the modulus of elasticity.

It is interesting to note that the design solutions according to the 2nd order analysis with a design value of the modulus of elasticity are rather similar with the design solutions following the effective length method.

2.4 Reliability considerations

2.4.1. Probabilistic Model

A probabilistic model for the column load bearing capacity is derived from Equation (9). The failure state is defined by

$$\mathbf{F} = \left\{ \mathbf{x} \middle| g_1(\mathbf{x}) \le 0 \cup g_2(\mathbf{x}) \le 0 \cup g_3(\mathbf{x}) \le 0 \right\} \tag{10}$$

with

$$g_1(\mathbf{X}) = 1 - X_1 \left(\frac{G+Q}{F_c h^2} \right)^2 - X_2 \frac{1}{1 - \dfrac{G+Q}{\dfrac{\pi^2 \cdot E h^4}{12\,\ell^2}}} \cdot \frac{(G+Q)e}{\dfrac{F_m \cdot h^3}{6}} \tag{11}$$

$$g_2(\mathbf{X}) = 1 - X_1 \frac{G+Q}{F_c h^2} \tag{12}$$

$$g_3(\mathbf{X}) = X_2 \frac{1}{1 - \dfrac{G+Q}{\dfrac{\pi^2 \cdot E h^4}{12\,\ell^2}}} - 1. \tag{13}$$

In Equations (11) - (13) h is the width of a square shaped column and ℓ is the length of the column. All other variables are explained in Table 3. Solid timber strength class C24 was assumed for the calculation.

Table 3: Variables of Equations (11) - (13), values for design and model input parameter for the Monte Carlo simulation.

Basic Variables	Char. value	Perc.	PDF	COV	Mean	Standard deviation
F_m : bending strength [N/mm^2]	24	5	Log-Normal	0.25	37.1	9.2
F_c : compression strength [N/mm^2]	21	5	Log-Normal	0.2	29.7	5.9
E : MOE [N/mm^2]	11000	-	Log-Normal	0.13	11000	1430
G : Dead Load [kN]	10.15	50	Normal	0.1	10.15	1.02
Q : Live Load [kN]	57.52	98	Gumbel	0.4	28.23	11.3
ξ : Initial Bow	$e = \ell/400$	-	Normal*	-	0	3
X_1, X_2 Model Uncertainty [-]	-	-	Log-Normal	0.1	1	0.1

Table 4: Correlation ρ of the basic variables.

BRV	F_c	E
F_m	0.8	0.8
F_c		0.6

Model for the initial bow.

The load bearing capacity of slender columns is sensitive against deviations from ideal axial loading, such as initial bow or eccentric loading. In the present analysis a model was derived, that represents both imperfections. In Ehlbeck and Blass [9] 140 insitu columns had been measured and probabilistic models for initial bow and out of plumpness had been derived based on that data. In the same citation initial bow was measured relatively as $\xi = \varepsilon/\lambda$ with $\varepsilon = Ae/W$. Resolving ξ one obtains $\xi = 1.73 \cdot 10^3 e/\ell$. Based on the results presented in [9] ξ is modelled here as a normal distributed variable with zero mean and an estimated standard deviation of 3.

2.4.2. Reliability estimation

The reliability of columns is estimated by crude Monte Carlo simulation. The length of the columns was varied from 0.1m to 20m. The width h of the square shaped columns was designed according to

I. EN 1995-1-1, 2nd order method (Equation (9)) with $E_{0,d} = E_{0,mean}/\gamma_M$.

II. DIN 1052, 2nd order method (Equation (9)) with $E_{0,d} = E_{0,05}/\gamma_M$.

III. EN 1995-1-1 / DIN 1052 according to the equivalent length approach (Equations (3) - (5).

For the design calculations, the characteristic values indicated in Table 3 are used.

The widths obtained for the different length are illustrated in Figure 2 a), the ratio between the column width design solutions of 2nd order design to effective length design over column length is illustrated in Figure 2 b).

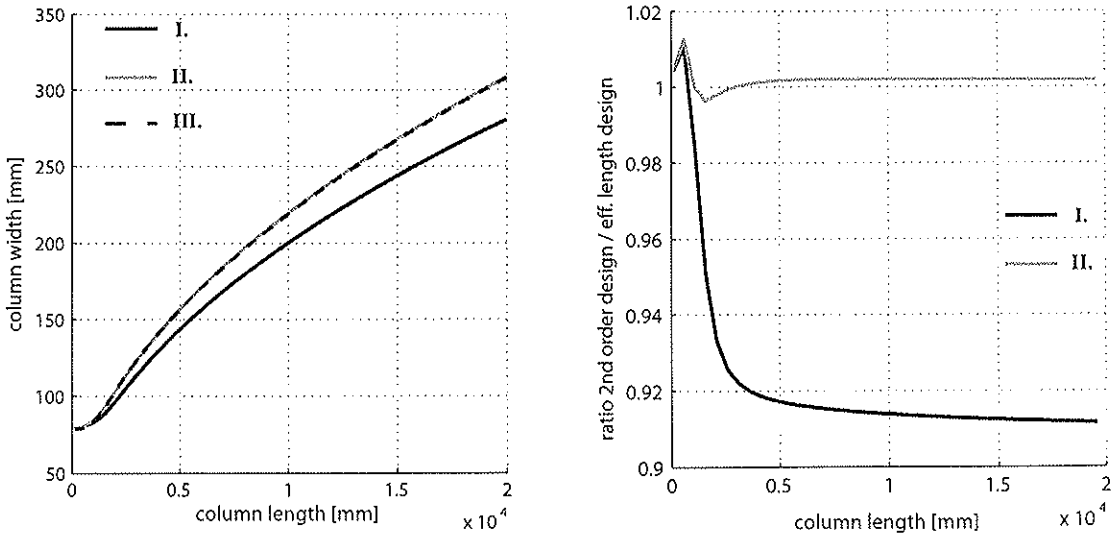

Figure 2: a) Design column width over column length, depending on the design formats I. – III. b) Ratio between the column width design solutions: 2nd order design / effective length design over column length.

The design solutions obtained above are now assessed in terms of their failure probability. Therefore, the models summarized in Table 3 and the corresponding correlation coefficients in Table 4 are used.

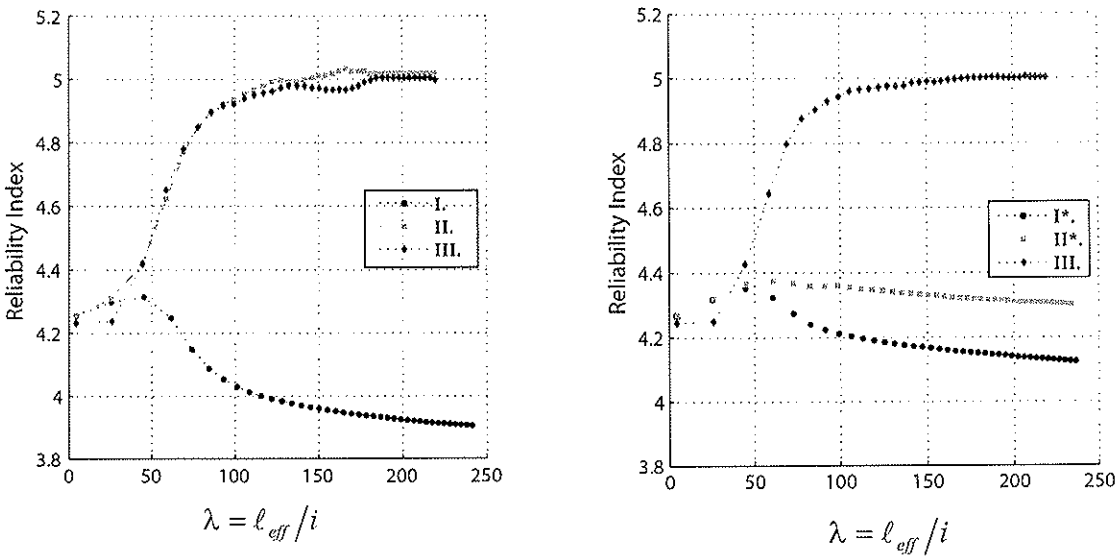

Figure 3: a) Reliability Index over slenderness for design solutions according to different design formats, b) modified factorisation of MOE. (The results are based on 10^8 simulations per dot.)

In Figure 3 a) the reliability index corresponding to the annual failure probability is illustrated for different slenderness and for columns designed according to methods I. – III. It can be seen that 2nd order design according to DIN 1052 delivers solutions with high

reliability indices for slender columns. 2nd order design according to EN 1995-1-1 delivers solutions with low reliability indices for increasing slenderness. As expected, the reliability indices for design solutions according to the effective length method are similar to those for 2nd order DIN 1052 - at least for slender columns.

Note that the suggested (annual) reliability index for normal structures is 4.2 [10], which corresponds to a annual probability of failure of 10^{-5}; a annual reliability index of 5 corresponds to a annual failure probability of $3 \cdot 10^{-7}$ and a annual reliability index of 4 corresponds to a annual failure probability of $3 \cdot 10^{-5}$.

The observations made in Figure 3 a) above underlines the importance of the representation of the stiffness term in Equation (9). The results of the reliability estimation are highly sensitive to the design value of the modulus of elasticity which is considered there.

For comparison the representation of the modulus of elasticity in Equation (9) is modified, as

I*. 2nd order method (Equation (9)) with $E_{0,d} = E_{0,mean}/1.4$

II*. 2nd order method (Equation (9)) with $E_{0,d} = E_{0,05}$

III. EN 1995-1-1 / DIN 1052 according to the equivalent length approach (Equations (3) - (5).

In Figure 2 b) it can be observed that with design values modified according to I*. and II*. more uniform reliability indices for different design solutions can be obtained.

3. Conclusions

Load and resistance factor design (LRFD) formats comprise simplified limit state design equations together with factored design values for loads and resistances. In general, the factorization takes in so-called characteristic values. Characteristic values correspond to fractile values of the underlying probability distributions of the load and resistance variables. For resistance variables the lower 5% fractile value is used in general, for load variables the 50% or the 98% fractile value is used, whereas variable loads are generally represented as the distribution of their annual extreme value.

Load and resistance factor design (LRFD) formats are also called semi-probabilistic because characteristic values are by definition understood as a simplified representation of the corresponding underlying random phenomena. Load and resistance factors could be understood as 'set screws' that are calibrated to facilitate for consistently safe and efficient design solutions over the wide range of different structural systems to be designed in our build environment.

In Europe the partial safety factor for solid timber resistance $\gamma_M = 1.3$ is such a 'set screw' factoring 5%-fractile values of timber strength related timber material properties. This factor has proven to be efficient for different simple design situations as bending or tension under different combination of loads [12], [13].

However, for more complex design situations or for different material properties involved in the limit state design equation, it has to be carefully assessed whether the factorisation by γ_M provides safe and efficient design solutions.

In the present paper it has been discussed how γ_M is used to factor the modulus of elasticity (MOE) in a 2nd order design formulation for slender axially loaded columns in

EN 1995-1-1 (mean value of MOE factored by $1/\gamma_M$) and in DIN 1052 (5% fractile value of MOE factored by $1/\gamma_M$). The reliability of different design solutions, according to EN 1995-1-1 and to DIN 1052 and for different slenderness, has been assessed. The reliability assessment indicated that design solutions are either too safe (DIN 1052) or show reliability indices which are on the limit of acceptance.

As a fast track solution an alternative factorisation of MOE has been assessed that showed consistent and acceptable reliability indices for both, compact and slender columns. However, this alternative factorisation should not be understood as a solution, but more as an indication for further research and proximate code review.

The significant sensitivity of reliability estimates to the representation of stiffness in the design equation suggests also that the creep effect caused by the load and climate history during the lifetime of a structure is a factor of utmost importance for column design. This aspect, entirely masked out in this study, should be taken into account in further investigations with greatest care.

4. References

[1] Tetmajer L. (1896): Methoden und Resultate der Prüfung der Schweizer Bauhölzer. Material Testing Laboratory (MPA) in Zurich.

[2] Möhler K. (1942): Tragkraft und Querkraft von ein- und mehrteiligen Holzdruckstaben nach Versuch und Rechnung. Dissertation Universität Karlsruhe und Bauplanung und Bautechnik 2 (1948) 41-47.

[3] Buchanan A.H., Johns K.C. and Madsen B. (1985): Column Design Methods for Timber Engineering. 18th Meeting, International Council for Research and Innovation in Building and Construction, Working Commission W18 – Timber Structures, CIB-W18, Paper No. 18-2-1, 2006.

[4] Blaß H.-J. (1987): Tragfähigkeit von Druckstäben aus Brettschichtholz unter Berücksichtigung streuender Einflussgrössen. Dissertation, Universität Fridericiana Karlsruhe (TH).

[5] Glos P. (1978): Zur Bestimmung des Festigkeitsverhaltens von Brettschichtholz bei Druckbeanspruchung aus Werkstoff- und Einwirkungsgrössen. Dissertation Technische Universität München 1978.

[6] Bolotin V. V. (1969): Statistical Methods in Structural Mechanics. Holden-Day Series in Mathematical Physics.

[7] Kessel M. H., Schönhoff T., Hörsting P. (2005): Zum Nachweis von druck-beanspruchten Bauteilen nach DIN 1052:2004-08, Teil 1, bauen mit holz 12/2005, S. 88–96.

[8] Möller G. (2007): Zur Traglastermittlung von Druckstäben im Holzbau. Bautechnik, DOI: 10.1002/bate.200710030.

[9] Ehlbeck J. and Blaß (1987): Zuverlässigkeit von Holzdruckstäben. Technical Report. Versuchsanstalt für Stahl, Holz und Steine, Abt. Holzbau; Universität Fridericiana Karlsruhe (TH).

[10] Joint Committee of Structural Safety (JCSS, 2008). Probabilistic Model Code, Internet Publication: www.jcss.ethz.ch.

[11] Melchers R. (1999). Structural Reliability: Analysis and Prediction. Ellis Horwood, Chichester, UK.

[12] Köhler J. (2005). Reliability of Timber Structures. Dissertation. Swiss Federal Institute of Technology.

[13] Sørensen J.D. and Hoffmeyer, P.. I (2000) Reliability Analysis of Structural Timber Systems. /: Proceedings of IFIP WG 7.5 Conference on Reliability and Optimization of Structural Systems, Ann Arbor, USA, 2000.

EN 1991-1-1, Eurocode 1: Actions on structures, Comité Européen de Normalisation, Brussels, Belgium, 2002.

EN 1995-1-1, Eurocode 5: Design of timber structures; part 1-1: general rules and rules for buildings. Comité Européen de Normalisation, Brussels, Belgium, 2004.

EN 338: Structural Timber – Strength Classes. Comité Européen de Normalisation, Brussels, Belgium, 2003.

DIN 1052 : 2004, Bemessungsregeln für Holzkonstruktionen.

INTERNATIONAL COUNCIL FOR RESEARCH AND INNOVATION
IN BUILDING AND CONSTRUCTION

WORKING COMMISSION W18 - TIMBER STRUCTURES

PROBABILISTIC OUTPUT CONTROL FOR STRUCTURAL TIMBER
- FUNDAMENTAL MODEL APPROACH -

M K Sandomeer
J Köhler
M H Faber

ETH Zürich
EMPA Dübendorf
SWITZERLAND

Presented by M. K. Sandomeer

H. Blass asked how many pieces of lumber needed to detect quality shift. M.K. Sandomeer responded in this study 1000. H. Blass questioned what to do with the 1000 pieces of out of control material. J. Köhler stated that fractile values related to population versus individual batch of lumber. It would be problematic to deal with the fractile of individual batch. M. Bartlett stated that the work is based on regression analysis which did not take into consideration of the error in the predictor or grading values. I. Smith added that the issue of grading error can come out. The issue of random versus bias was discussed. F. Lam commented that this is interesting work. In N. American output control system requires intensive testing of material if machine adjustments exceeded a certain small percentage. This is generally avoided by operator by setting machine conservatively. In the approach proposed would there be the same type of requirements. M.K. Sandomeer responded yes but not yet defined. A. Ranta-Maunus commented about shift in quality and the size of the shift. One should not only consider the 5^{th} percentile but also the lower tail in a package. S. Aicher asked whether this would be possible to apply this with a truncated function of the indicator variable and apply it to obtain the lower fractile. J. Köhler responded that this is already done.

Probabilistic Output Control for Structural Timber - Modelling Approach -

Markus K. Sandomeer[1, 2], Jochen Köhler[1], Michael H. Faber[1]

[1] Institute of Structural Engineering, ETH Zurich, Switzerland
[2] Swiss Federal Laboratories for Materials Testing and Research, EMPA Dübendorf, Switzerland

Abstract

Machine grading for quality control of structural timber in Europe presently takes basis in the so-called machine control method, rather than the output control method; the two alternative methods specified in the European Standard EN 14081 [14]. Despite its wide application it is, however, generally recognized that this method has potential for improvements. The issue is that the machine settings are fixed when the machine is taken into use and the present standard does not accommodate for adjustments of the machine settings based on the measured timber characteristics during the grading procedures. As a consequence in practice, the machine settings may be determined and fixed corresponding to a statistical population of timber material deviating from the populations subsequently being tested for quality control; as a result the quality control will be less efficient and/or even in extreme cases erroneous.

The present paper proposes an alternative approach for the control of grading machine settings by which systematic quality variations of the timber material may easily be identified during grading by means of monitoring of the non-destructive measurements of the grading machine (indicating properties) which have a certain relationship to the grade determining properties of the tested timber material (e.g. strength, stiffness and density). Systematic shifts (or deviations) in the values of the indicating properties may reveal that the tested timber material origins from a population of timber different from the population(s) on the basis of which the machine settings were calibrated. Thus a recalibration is required or might be optimal. The recalibration may then be achieved through "updating" of the grading model and a complete reassessment of the original grading machine settings based on destructive tests of specimens taken from the deviating population.

1 Introduction

Graded timber material can be utilized for structural purposes either directly as solid timber columns and beams or indirectly in the form of basic raw material for engineered timber products. In both cases, when timber products are utilized in high performance timber structures i.e. whenever the load bearing capacity or the stiffness determines the design, it is a requirement that the timber products are graded to ensure adequately performing mechanical properties. In modern production management, where speed, reliability and costs are prerequisites for competitiveness, machine grading is in reality the only viable option. As a consequence, advanced and modern methods for the calibration and running assessment of grading machines have to be developed and implemented into practice.

Different types of grading machines can be found in the market, measuring a different set of particular indicative properties during the grading process, e.g. bending deflection, ultrasound velocity, natural frequency, x-ray absorption, etc.. However, independent on the type of the grading machine and the number of measured properties, grading machines generate one compound variable as an output, which is a function of all particular indicative properties measured by the machine under stood as a prediction of the grade determining property (e.g. strength, stiffness, density). Disregarding the fact that this variable is an artifact composed from the machine measurements and the underlying function or algorithm the indicative variable is generally termed *indicating property* and this is the term also used in the remainder of the present paper.

For every grading machine grading acceptance criteria are formulated in form of intervals for the corresponding indicating property that have to be matched to qualify a piece of timber to a certain grade. These boundaries are termed *grading machine settings*. The performance, i.e. the statistical characteristics of the output of grading machines strongly depends on these settings, and in general very much attention is kept on how to control these machine settings.

The present European practice for machine based grading of structural timber is specified in the European Standard EN 14081. According to this standard the control of machine settings relies on two procedures, the so-called *machine control (cost matrix) method* and the *output control (CUSUM) method*, see e.g. [2], [6], [8] and [11].

Initial type testing of the machine control method is performed on large samples of the produced timber; indicative material characteristics which can be related to the grade determining material properties are measured and form the basis for the grading. In this process the settings of the grading machine are calibrated prior to commissioning based on a sample of timber material assumed representative for the timber the machine shall grade in the future. However, for various reasons there may be deviations between the characteristics of the timber used for the calibration and the timber subsequently graded by the machine. Depending on these deviations the effective quality of the graded timber may be higher or lower than those required by the grading criteria; the result being an effective quality loss.

According to present practice such deviations are only revealed through destructive testing procedures on few specimens taken out regularly of a relative large production, through the so-called *CUSUM* test method (EN 14081, part 3). In the aim of quality management and production optimization it is, however, desirable to be able to identify such systematic deviations as early as possible. In addition, it would be of high economic relevance only to perform destructive tests, if quality deviations are present.

At European level (e. g. COST Action E53 of the European Science Foundation) extensive discussions are ongoing concerning the existing grading standard EN 14081 and as a consequence revisions of this standard are presently being considered by the Technical Committee CEN TC124/WG2. The quality control procedures as specified in EN 14081 are broadly considered to be too complex; throughout Europe there are only a few experts who know how to deal with the required procedures addressed in the standard. Therefore, different projects have recently been directed on developing new approaches for quality control all aiming at substantial simplifications of the standard in its present form.

In the paper at hand, building on the probabilistic approach for machine grading quality control described in Faber et al. (2004) and Köhler and Steiger (2006), a methodology is outlined which facilitates the consistent and efficient control of grading machine settings for both, machine and output control strategies. Furthermore, a possible procedure for identification of systematic changes in the tested material quality directly based on the machine grading measurements, at the same phase as these are obtained, is outlined. The

proposed methodology thus could provide the basis for the developments of an alternative approach to the present methods specified in EN 14081. The methodical framework builds on Bayesian regression analysis to establish a regression model between the grading machines indicative property - *IP* and the material characteristics of concern for quality control (grade determining properties - *GDP*).

In the following first a general outline of the Bayesian regression analysis is given. Thereafter results are provided on the application of the Bayesian regression analysis framework for the control of grading machine settings. It is discussed how systematic changes in the tested material can be identified on the basis of continuous observations of the indicating property. Finally, it is described how recalibration and/or updating of the grading machine settings can be performed efficiently, i.e. based on a relatively small sample of destructive tests.

2 Methods and Model Approach

For the representation of the relationship between destructive test results on the grade determining material property and the indicating property Bayesian linear regression analysis forms a consistent and adequate methodical framework. In the following the general procedure of *simple linear Bayesian regression* analysis is described. The relationship between a response variable y and a set of explanatory variables, $\mathbf{x} = (x_1, x_2, ..., x_r)^T$ is modelled through:

$$y = \sum_{j=1}^{r} x_j \beta_j + \varepsilon \qquad (1)$$

where β_j , $j = 1,2,...,r$ are the regression coefficients, $x_1 = 1$ and ε is an error term representing random fluctuations, measurement errors and model uncertainty [1], [5]. The fundamental assumption for simple linear regression models is that y is random and follows a normal distribution. The error ε is also assumed to follow a normal distribution with zero mean and unknown variance σ_ε^2. σ_ε^2 is assumed to be constant over the entire domain of $\mathbf{x}$. The Bayesian regression analysis facilitates the development of a probabilistic model for y based on a series of e.g. n experiments at which simultaneous observations of the response y and the explanatory variables $\mathbf{x} = (x_1, x_2, ..., x_r)^T$ i.e. $\hat{y}_i$ and $\hat{\mathbf{x}}_i$, $i = 1,2,..,n$ have been made.

In the context of regression modelling for timber machine grading, the response variable represents the grade determining property and the (single) explanatory variable is represented by the indicating material property, the dimension of $\mathbf{x}$ therefore is $r = 2$. It is generally accepted that the statistical properties of the grade determining properties (e.g. the tension strength and modulus of elasticity) are best represented by a log-normal distribution [12]; the prediction of the grade determining properties based on the indicating material property should also be log-normal distributed. To facilitate the application of the simple regression model the random grade determining property and the explanatory variable is transformed logarithmically – i.e. the transformed variables are normal distributed and can be consistently assessed by the simple linear regression model.

In the following section it is shown how the regression coefficients β_j may be assessed depending on the available information at hand. The interested reader should refer to e.g. Gelman et al. (2004) and Raiffa and Schlaifer (1960) where the procedure is described in more detail.

2.1 Regression Analysis

To start with, it is assumed that n experiments have been performed at which simultaneous observations have been made, i.e. $\hat{\mathbf{y}} = (\hat{y}_1, ..., \hat{y}_n)^T$ and $\hat{\mathbf{X}} = [\hat{x}_{11} ... \hat{x}_{1r}; \hat{x}_{21} ... \hat{x}_{2r}; ... \; ... \; ...; \hat{x}_{n1} ... \hat{x}_{nr}]$.

Now, conditional on σ_ε^2, $\hat{\mathbf{X}}$ and $\hat{\mathbf{y}}$, the regression coefficients $\boldsymbol{\beta} = (\beta_1, ..., \beta_r)^T$ are estimated as normal distributed random variables [3], expressed by:

$$\boldsymbol{\beta} \left| \sigma_\varepsilon^2, \hat{\mathbf{X}}, \hat{\mathbf{y}} \sim \text{Normal}\left(\mathbf{E}_\beta, \mathbf{V}_\beta \sigma_\varepsilon^2\right) \right. . \tag{2}$$

The mean values of the regression coefficients ($\mathbf{E}_\beta$) are assessed by:

$$\mathbf{E}_\beta = (\hat{\mathbf{n}})^{-1} \hat{\mathbf{X}}^T \hat{\mathbf{y}} = \left(\hat{\mathbf{X}}^T \hat{\mathbf{X}}\right)^{-1} \hat{\mathbf{X}}^T \hat{\mathbf{y}} \tag{3}$$

and the variance of the regression coefficients by $\mathbf{V}_\beta \sigma_\varepsilon^2$ where:

$$\mathbf{V}_\beta = (\hat{\mathbf{n}})^{-1} = \left(\hat{\mathbf{X}}^T \hat{\mathbf{X}}\right)^{-1}. \tag{4}$$

The variance σ_ε^2 of the error term (describing the dispersion of the measurements around the regression line) is estimated by computing $\mathbf{E}_\beta$ according to Equation (3). Based on this, the sample variance s^2 is assessed by:

$$s^2 = \frac{1}{n-r} \left(\hat{\mathbf{y}} - \hat{\mathbf{X}} \mathbf{E}_\beta\right)^T \left(\hat{\mathbf{y}} - \hat{\mathbf{X}} \mathbf{E}_\beta\right) \tag{5}$$

where $n-r$ are the degrees of freedom. Note that $\hat{\mathbf{y}} - \hat{\mathbf{X}} \mathbf{E}_\beta$ is the vector of residuals.

The distribution of σ_ε^2 can be calculated with the assumption that it follows a scaled inverse χ^2 distribution, i.e.:

$$\sigma_\varepsilon^2 \left| \hat{\mathbf{y}}, \hat{\mathbf{X}} \sim Inv\chi^2\left(n-r, s^2\right) \right. \tag{6}$$

where the $Inv\chi^2$ distribution is fully defined by two parameters; the degrees of freedom and the scale factor s^2. Now, having derived the mean and variance of the regression coefficients, the multivariate distribution of $\boldsymbol{\beta}$ can be determined from Equation (2).

Note that n, $\boldsymbol{\beta}$ and σ_ε^2 together with Equation (1) constitute the regression model estimated based on n simultaneous observations of $\hat{\mathbf{y}} = (\hat{y}_1, ..., \hat{y}_n)^T$ and $\hat{\mathbf{X}} = [\hat{x}_{11} ... \hat{x}_{1r}; \hat{x}_{21} ... \hat{x}_{2r}; ... \; ... \; ...; \hat{x}_{n1} ... \hat{x}_{nr}]$.

2.2 Predictive distribution for the grade determining property

Based on the regression model the *predictive probability density function* of the response variable $\tilde{y}$, can be assessed given a set of m observations on the explanatory variables $\tilde{\mathbf{X}} = [\tilde{x}_{11} ... \tilde{x}_{1r}; \tilde{x}_{21} ... \tilde{x}_{2r}; ... \; ... \; ...; \tilde{x}_{m1} ... \tilde{x}_{mr}]$.

The predictive density functions, $f_{\tilde{y}}(\tilde{y})$, are t-distributed with mean values

$$\mathbf{E}_{\tilde{y}|\tilde{\mathbf{X}}} = \tilde{\mathbf{X}}\mathbf{E}_{\beta} \qquad (7)$$

, and Variances $$\mathbf{V}_{\tilde{y}|\tilde{\mathbf{X}}} = \left(\mathbf{I} + \tilde{\mathbf{X}}\mathbf{V}_{\beta}\tilde{\mathbf{X}}^{T}\right) s'^{2} \frac{\nu'}{\nu' - 2} \qquad (8)$$

with s'^2 the variance of the sample, with sample size n' on which basis the regression model is estimated and $\nu' = n' - r$ degrees of freedom.

Equations (7) and (8) may be utilized to assess the statistical characteristics of the grade determining property of a certain timber grade based on observations of the indicating property of a particular grading machine. A set of observations of the indicating property that fulfil the grading acceptance criteria for the certain grade can now be assigned to the corresponding set of predictive density functions of the grade determining property (Figure 1).

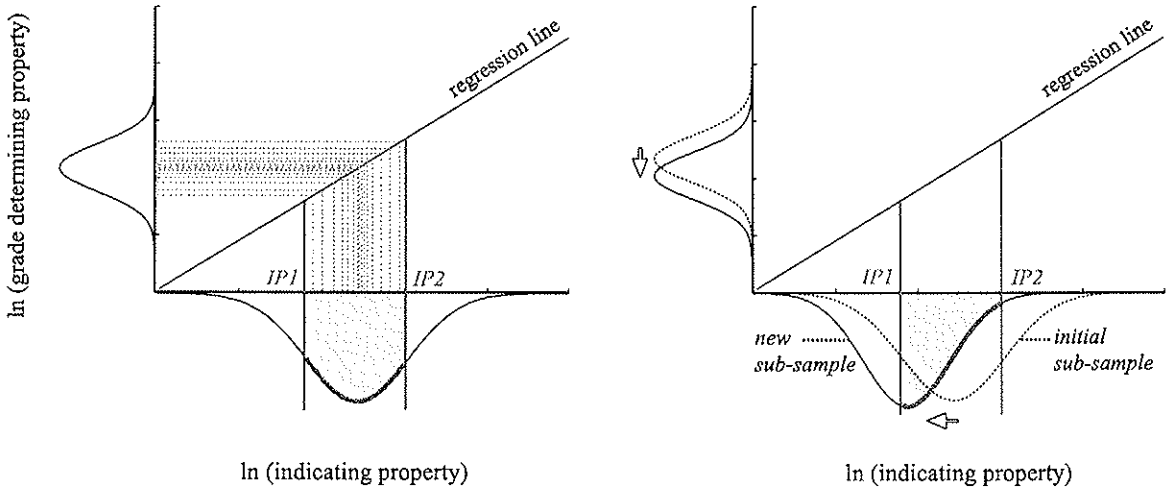

Figure 1: *Left: Observations of the indicating property in the interval between IP 1 and IP 2 are assigned to the predictive probability density function of the grade determining property which would be shifted downwards, if the multitude of the observations were made in the lower range between IP 1 and IP 2 (right).*

Given a sample of m new observations of the indicating property, $\tilde{\mathbf{X}} = \left[1 \;\; \tilde{x}_{12}; 1 \;\; \tilde{x}_{22}; \ldots \;\; \ldots; 1 \;\; \tilde{x}_{m2}\right]$ that fulfil the grading acceptance criteria for a certain grade, the individual predictive density functions are coupled to one envelope predictive probability distribution function of the grade determining property as

$$f\left(y \middle| \tilde{\mathbf{X}}, \mathbf{E}_{\tilde{y}|\tilde{\mathbf{X}}}, \mathbf{V}_{\tilde{y}|\tilde{\mathbf{X}}}\right) = \frac{1}{m}\sum_{i=1}^{m} f\left(y \middle| \tilde{X}_i, E_{\tilde{y}|\tilde{x}_i}, V_{\tilde{y}|\tilde{x}_i}\right). \qquad (9)$$

The cumulative probability distribution of the grade determining property can be assessed by integrating over its probability density function of the from equation (9) [3]. Based on this, the predictive characteristic value is easily calculated.

3 Experimental Results

3.1 Sample Preparation

Data of Nordic spruce specimens originating from $n = 1162$ simultaneous observations of the indicating property of the grading machine *GoldenEye 706* [4] and the timber tension strength are used in this study. The tension tests have been performed in accordance to EN 408 [15]. The specimens that have been tested are originating from different growth areas within Europe. The entire dataset is utilized for the representation of the average timber material quality. This sample is subsequently denoted as *initial sample*. Two additional sub-samples

are selected, *sub-sample 1* ($n = 50$) with lower strength related timber material properties than the initial sample and *sub-sample 2* ($n = 50$) with higher strength related properties.

The aim is to perform investigations based on three different samples which represent three different levels of timber material quality running through the grading device; the initial sample represents the timber quality for which the grading machine is calibrated, sub-sample 1 and sub-sample 2 represent qualities that deviate from the quality of the initial sample.

In Europe timber grading is verified on basis of three material properties, i.e. for a certain grade, requirements for the characteristic values of these properties have to be fulfilled, EN 338 [13]. In the context of this paper it is focused solely on the tension strength for the purpose of clarity. However, extensions of the model for the simultaneous control of all three material properties are straightforward..

3.2 Outcomes of regression analysis

In accordance to the approach outlined in Chapter 2 the parameters of the regression models for the different samples are identified and summarized in Table 1. Note that all the data are transformed logarithmically before the analysis.

Table 1: *Assessed model parameters for each of the investigated sub-samples.*

sample	n	E_{β_1}	V_{β_1}	E_{β_2}	V_{β_2}	ρ_{β_1,β_2}	s
initial	1162	0.2137	0.0044	0.9278	0.0004	-0.9942	0.0591
sub 1	50	-0.7047	0.2667	1.2065	0.0274	-0.9983	0.0448
sub 2	50	-0.2083	0.1595	1.0339	0.0138	-0.9955	0.0719

Figure 2 illustrates the regression model for the initial sample together with the corresponding data. The left part of the illustration shows the linear relationship when the indicating property and the grade determining property are transformed logarithmically. In Figure 2, right, re-transformed into normal scale, the relationship appears non-linear.

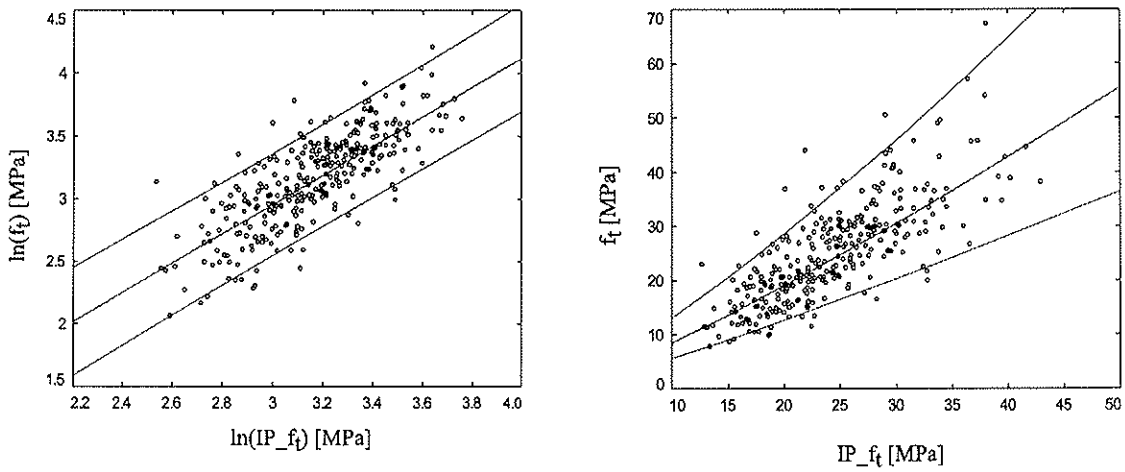

Figure 2: *Illustration of the established regression model based on observations of the indicating property of the tension strength and the tension strength. Left: logarithmic scale. Right:*

normal scale. The line in the centre represents the regression line, the additional lines above and below represent the 95%-and the 5%-fractile values, respectively.

3.3 Detection of Quality Shifts

Timber is a natural grown material and its material characteristics are depending among other factors on the region where the timber is grown. An operator of a machine grading device, e.g. a sawmill owner or a glulam manufacturer, might vary the source of the timber supply over time. Deviations between the characteristics of the timber used for the calibration and the timber subsequently graded by the machine might therefore be expected during the operation phase of the grading machine. Depending on these deviations the effective quality of the graded timber may be higher or lower than those required by the grading criteria; the result being an effective quality loss.

An important goal of the current investigations is to develop an efficient control tool which detects significant shifts in the input timber material quality of the grading machine. An obvious way of detecting quality shifts is by monitoring the continuous observations of the indicating property during the grading process. Since the indicating property is related to the grade determining property this method would provide first qualitative indication of changes in quality of the timber supply.

Figure 3 illustrates 3000 simulated values of the tension strength indicating property. The simulations take basis in the statistical properties of the sub-samples investigated above. The first 1000 simulations represent the 'initial sample', the second and third 1000 'sample 1' and sample 2', respectively. Remarkable fluctuations of the simulated values of the indicating property can be observed between and even within the particular samples in part a) of Figure 3. Changes in the timber material quality between the different sub-samples become more apparent, if mean values of the simulated indicating property are recorded. This is done for small sub sets of $n=5$ and $n=100$ simulated IP-values in Figure 3 b) and c), respectively.

According to Figure 3 the quality shift between the initial sample and sub-sample 2 seems to be more significant than the quality shift between the initial sample and sub-sample 1.

An interesting question now arises in regard to the formulation of criteria that divide acceptable quality shifts from non-acceptable ones. To answer that question, the influence of quality shifts on the accuracy of the grading machine with given settings has to be assessed.

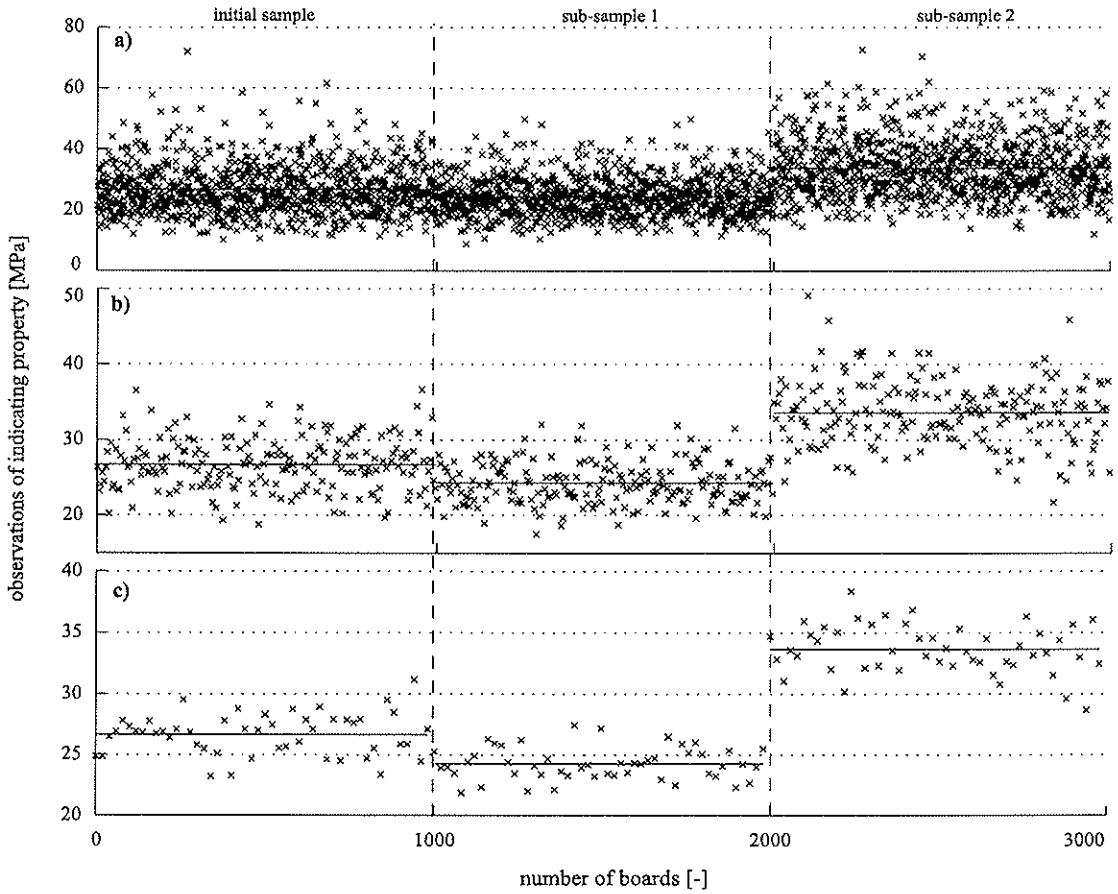

Figure 3: *Simulations of the tension strength indicating property of three samples representing three different quality levels of timber material properties due to different growth areas.* ***a)*** *individual simulations* ***b)*** *mean values, each assessed on n=5 simulated values and* ***c)*** *n=20 simulated values.*

3.4 Effect of Quality Shifts on Grading Results

In the following the effect of quality shifts on the grading performance is investigated. The different samples (the initial sample $n = 1167$, sub-sample 1 $n = 50$ and 2 $n = 50$) are graded into the strength grade combination L36 and L25. The requirements for the characteristic values for these grades are recorded in the tables of EN 14081, part 4. In case the tension strength is the grade determining property, the 5%-quantile values of 22.0 MPa (L36) and 14.5 MPa (L25) have to be fulfilled.

Table 2 provides the results of the comparison, segmented into two consecutive grading steps:

1. Grading machine settings for strength grades L36 and L25 are derived according to EN 14081, parts 2 and 4 on the initial sample containing $n = 1162$ observations of indicating property and tension strength (cp. Chapter 3.1). The characteristic tension strength value (5%-quantile value) is assessed first by means of ordered sample statistics. In column 5 in Table 2 the 5%-fractile values of the predictive distributions of the tension strength of the two grades are shown. This prediction is based on the regression model parameters estimated for the initial sample summarized in Table 1 and Equations (6) – (9). Sub-samples 1 and 2 with expected lower and higher material quality level are graded with fixed machine settings and fixed model parameters (coefficients of regression analysis) all assessed on the initial sample.

2. In step 2 the regression coefficients of the grading model are reassessed based on 50 new observations of the indicating property and the tension strength for each of the sub-samples, see Table 1. In addition, the grading machine settings are calibrated such, that the 5%-fractile values of the predictive distributions fulfil the requirements of the particular strength grades.

Table 2: *Results of the grading procedures for different samples.*

		1	2	3	4	5
step	sub-sample	grade *acc. EN 14081-4*	settings *fP_MOR [MPa]*	yield *[%]*	char. values *sample [MPa]*	char. values *probabil. model [MPa]*
1	initial sample *(average quality)*	L36 L25 reject	29.2 19.0 ---	32.2 52.6 15.2	22.0 14.5 ---	21.8 15.1 ---
	sub-sample 1 *(lower quality)*	L36 L25 reject	29.2 19.0 ---	19.1 62.7 18.2	20.4 13.2 ---	21.0 15.1 ---
	sub-sample 2 *(higher quality)*	L36 L25 reject	29.2 19.0 ---	69.9 25.2 4.9	21.7 14.1 ---	22.2 16.5 ---
2	sub-sample 1 *reassessed parameters & adjusted settings*	L36 L25 reject	28.4 18.6 ---	20.0 65.5 14.5	22.5 14.4 ---	22.0 14.5 ---
	sub-sample 2 *reassessed parameters & adjusted settings*	L36 L25 reject	33.2 14.0 ---	48.5 49.5 2.0	22.6 13.5 ---	22.0 14.5 ---

Since the grading machine settings are directly derived on 1162 observations of the indicating property and the corresponding tension strength, the sample characteristic values of the initial sample in step 1 exactly fulfil the requirements for the assigned strength grades according to EN 14081, part 4. Comparison of these sample characteristics to the predicted characteristic values of the probabilistic model indicates good consistency with the sample characteristics even though statistical and model uncertainties are incorporated into the grading model. When the fixed grading machine settings are applied to the sub-samples of deviant timber material quality it can be observed that the sample characteristics of the therewith sub-divided timber grades do not match with the corresponding grade requirements (column 4 of Table 2). It can be also noted that in this case the predictive 5%- values assessed with the probabilistic model which is calibrated to the initial sub-sample do not represent the sample characteristics of the graded sub-samples of deviant timber quality.

Assuming that a quality shift is detected and it is decided that the machine grading settings have to be reassessed a method is required that facilitates the recalibration of the grading device based on a number of destructive tests. In step 2 of the described procedure such a recalibration takes basis in 50 destructive tests on the timber with deviant quality. The regression model parameters are reassessed and the grading machine settings are adjusted based on the modelling approach described in Chapter 2. It can be seen in Table 2 that the reassessed regression model delivers quite accurate predictions of the sample characteristics of the graded timber.

For sub-sample 2 the large amount of timber graded to L36 should be noticed.

4 Conclusions

Bayesian regression analysis is the basis for the model of graded timber material properties described in this paper. A consistent grading model for the probabilistic control of grading machine settings can be established based on varying sample sizes. This provides the possibility to reassess grading procedures with relatively low cost when quality shifts have been detected.

The present paper describes possible approaches which might be further developed and considered for implementation into future practice of output control based timber grading. However, research has to be continued especially on the following topics:

- Definition of critical (significant) quality deviation. I. e. which extend of quality shift has to be considered as critical for the grading quality?
- Definition of adequate criteria for the indication of significant quality shifts in timber quality.
- Definition of an adequate number of additional destructive tests to facilitate the recalibration of the grading model and the adjustment of the grading.
- Implementation of the described procedures in the daily industrial production environment.

As an outlook for future investigations it is intended to implement the introduced approach into an overall hierarchical model, i.e. the regression line representing the entire timber population to be graded is treated on the highest level. At the same time it is known that there are sub-samples of different regression parameters and quality. Within daily quality control it might be possible to respect the different sub-samples with the sub-regression models accordingly.

Acknowledgements

Contributions by *MiCROTEC Brixen (Italy)* are acknowledged with gratitude for allowing us to publish the results of machine grading by the grading device *GoldenEye 706.*

References

[1] Benjamin J. R., Cornell C. A. (1970). *Probability, Statistics and Decisions for Civil Engineers*. Mc Graw – Hill Book Company.

[2] Boström L., Enjily V., Gaede G., Glos P., Holland C., Holmqvist C., Joyet P. (2000). *Control of Timber Strength Grading Machines*. SP REPORT 2000:11.

[3] Gelman A., Carlin J. B., Stern H. S., Rubin D. B. (2004). *Bayesian Data Analysis*. Second Edition. Chapman & Hall/CRC.

[4] Giudiceandrea F. (2005). *Stress grading lumber by a combination of vibration stress waves and X-ray scanning*. Proceedings of the 11th International Conference on Scanning Technology and Process Optimization in the Wood Industry (ScanTech 2005), July 24th-26th 2005, Las Vegas, Nevada U.S.A., pp. 99-108.

[5] Jordaan J. (2005). *Decisions under Uncertainty*. Cambridge University Press.

[6] Köhler J. (2006). *Reliability of Timber Structures*. Dissertation ETH no. 16378. Swiss Federal Institute of Technology, Zurich, Switzerland.

[7] Faber M.H., Köhler J., Sorensen, J.D. (2004)
Probabilistic Modeling of Graded Timber Material Properties
Journal of Structural Safety, Volume 26, Issue 3, Pages 295-309, July 2004.

[8] Köhler J., Steiger R. (2006). *A discussion on the control of grading machine settings – Current Approach, Potential and Outlook*. Proceedings of the 39th Meeting, International Council for Research and Innovation in Building and Construction, Working Commission W18 – Timber Structures, CIB-W18, Paper No.39-5-1, Florence, Italy, 2006.

[9] Raiffa H., Schlaifa R. (1960). *Applied statistical decision theory.* Chichester, UK: John Wiley and Sons Ltd.; 1960.

[10] Rencher A. C., Schaalje G. B. (2008). *Linear Models in Statistics*. New York: Wiley.

[11] Sandomeer M. K., Köhler J., Linsenmann P. (2007). *The efficient control of grading machine settings*. Proceedings of the 40th Meeting, International Council for Research and Innovation in Building and Construction, Working Commission W18 – Timber Structures, CIB-W18, Paper No.40-5-2, Bled, Slovenia, 2007.

[12] JCSS : *Joint Probabilistic Model Code. Part 3: Resistance Models. Timber.* Joint Committee on Structural Safety, 2006.

[13] EN 338: *Structural Timber – Strength Classes.*
Comité Européen de Normalisation, Brussels, Belgium, 2003.

[14] EN 14081 parts 1-4: *Timber Structures – Strength Graded Timber with rectangular Cross Section.* Comité Européen de Normalisation, Brussels, Belgium, 2005.

[15] EN 408: *Timber structures - Structural Timber - Determination of some physical and mechanical properties.* Comité Européen de Normalisation, Brussels, Belgium, 2004.

INTERNATIONAL COUNCIL FOR RESEARCH AND INNOVATION
IN BUILDING AND CONSTRUCTION

WORKING COMMISSION W18 - TIMBER STRUCTURES

DESIGN OF INCLINED GLULAM MEMBERS WITH AN END NOTCH ON THE TENSION FACE

A Asiz

I Smith

University of New Brunswick, Fredericton

CANADA

Presented by A. Asiz

H. Blass asked when the results were compared to design code was the local component perpendicular to member axis used. I. Smith answered that the calculations were done on this basis but the reaction forces were presented as the vertical component. H. Blass asked whey then would you need to test an inclined member rather than horizontal members. I. Smith stated that the horizontal beam tests have been done before and the inclined test concept originated from industry. He agreed that small specimen would be sufficient but precalculations indicated higher chances of notch failure rather than bending so the results were surprising. T. Williamson commented that the final graph seems to indicate CSA and EC approach yielded similar results and close to the test results. R. Steiger referred to Table 4 and asked how the shear strength design values based on EC5 model were established i.e. which gamma values were used and where did the 1.75 value come from and what is the strength of this grade of glulam. I. Smith clarified that it is a characteristic value back calculated from design value in code. A. Leijten asked how many tests were conducted. A. Asiz replied six. H.J. Larsen commented with 6 tests you can't get characteristics values. Actually only three test results were valid as the others did not have the same mode of failure. S. Aicher commented that the derivation was incorrect because the assumption of normal distribution would be incorrect as multiple mode of failure was present. J. Köhler commented as statistical uncertainties were ignored this could lead to wrong results. A. Asiz responded that they intend to develop numerical model based on the limited resources and available results. This will be the next step.

Design of Inclined Glulam Members With an End Notch on The Tension Face

Andi Asiz and Ian Smith
University of New Brunswick, Canada

1. Introduction

Notching glue laminated (glulam) timber beams at the tension side is a crucial decision that arguably should be avoided by design engineers because of the high stress concentrations that develop around such notches inducing high tension perpendicular to grain and high shear parallel to grain stresses. However, it is done in practice to facilitate construction and to reduce the total necessary depth of floors and roofs. Most current design code provisions permit design of notches at the tension side providing that they are located close to the ends of members and at a simple structural support point. The key design process is normally done through modification terms that are part of assessing the shear capacity of members. Traditional practices in this respect are empirical and of uncertain origin (AITC, 2005). Strictly the problem requires a rational fracture mechanics analysis and that is done in a few related instances. For example, the notch design equation in Canada for sawn timber members is based on a simple fracture mechanics theory (CSA, 2005). However, the same practices are not adopted in design of notched glulam members, because of concern that a simple fracture theory might be inaccurate when notches remove only a small proportion of a member's depth. Moreover contemporary notch design provisions in codes were developed mostly from empirical observations of how flat notched solid lumber beam behave. It is questionable that results apply to notching of large glulam members, particularly those with inclined configurations.

The objective of this study is to investigate the effects of small bird-mouth end-notches on failure behaviour and associated strength of inclined glulam members subjected to short-term static load. Test result is compared with current design codes taking into account various possible failure mechanisms for glulam member loaded under statically determinate four-point bending arrangement. Simple design rule is proposed regarding whether there is a need to consider notching effect for small bird-mouth end-notches.

2. Current design practice

In traditional design practice for a sharp-notched member such as shown in Figure 1(a), shear (reaction) force V_f (N) is commonly limited accounting for the notch geometry via the expression:

$$V_f = \frac{2bf_v(d-d_n)}{3}\left(\frac{d-d_n}{d}\right)^2 \qquad (1)$$

where f_v = shear parallel to grain (MPa), b = width of the member (mm), d = depth of the member (mm), and d_n = depth of the notch (mm). Equation (1) is actually

derived based on empirical equation, and is limited to notches that are less than 10% of the member depth or 76 mm (inches), which ever is less (AITC, 2005). It is recommended that this equation be applied to solid lumbers and not for glulam members.

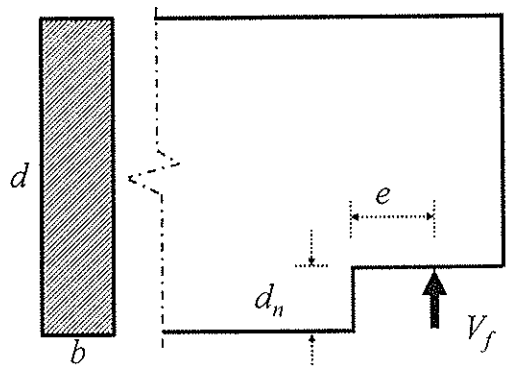

(a) sharp notch member

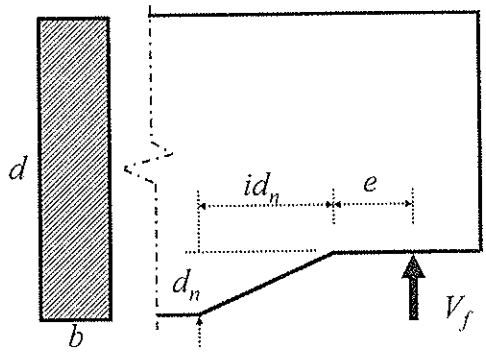

(b) tapered notched member

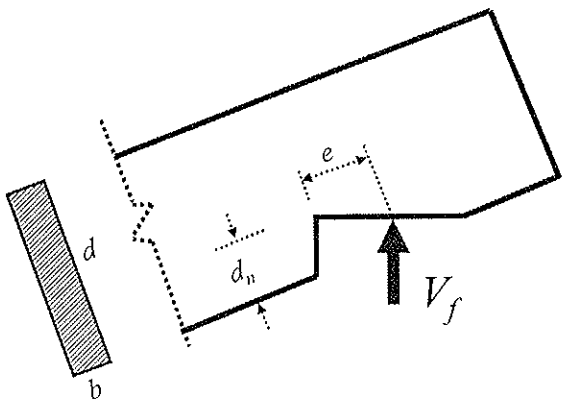

(c) inclined notched member

Figure 1: Notched geometry

In Canadian Standard CSA O86-01 (CSA, 2005), factored reaction force resistance for lumber joists is used as the basis of a design method for notches on the tension face and is expressed as:

$$F_r = \Phi F_f A K_N \qquad (2)$$

where Φ = resistance factor; $F_f = f_f K_D K_H K_{Sf} K_T$ is the modified reaction force strength, with f_f being the specified reaction force strength (0.5 MPa, for all lumbers), K_D the duration of load factor, K_H the system factor, K_{Sf} the service factor, and K_T the treatment factor; A is the gross cross-sectional area (mm^2); and K_N is the notch factor for rectangular cross-section members given by the following expression:

$$K_N = \left\{0.006d\left(1.6\left(\frac{1}{\alpha}-1\right)+\eta^2\left(\frac{1}{\alpha^3}-1\right)\right)\right\}^{-\frac{1}{2}} \qquad (3)$$

in which $\alpha = 1 - d_n/d$ (Figure 1a), d_n = depth notch measured normal to the member axis (mm), $\eta = e/d$, and e = length notch measured parallel to the member axis (mm, Figure 1a). Despite of this design rule, CSA O86-01 provides a note that notches or abrupt changes of cross section should be avoided because of high stress concentrations issue.

In Eurocode 5 (CEN, 2003), the critical reaction (shear) force for end notched beams is expressed as

$$V_f = \frac{2b(d-d_n)}{3} k_v f_{v,d} \qquad (4)$$

where b = width of the member (mm), d = depth of the member (mm), and d_n = depth of the notch (mm); $f_{v,d}$ = design shear strength (MPa); and k_v = reduction factor given by the minimum value between 1.0 and the following expression:

$$\frac{k_n\left(1+\frac{1.1i^{1.5}}{\sqrt{d}}\right)}{\sqrt{d}\left(\sqrt{\alpha(1-\alpha)}+0.8\frac{x}{d}\sqrt{\frac{1}{\alpha}-\alpha^2}\right)} \qquad (5)$$

in which i = notch inclination (Figure 1b); x = distance from line of action to the notch corner (mm, equal to e in CSAO86 code); $\alpha = 1 - d_n/d$; and k_n = 6.5 for glulam member.

The Engineered Wood Association recommended several options to reduce high stress concentration effect for end-notching glulam members including (APA, 2003):

- limiting notching height by 10% of the member depth or 3 inches (76mm), whichever is the smaller;
- providing gradual tapered notch configuration or rounding notch corners, instead of a sharp-square notches, Figure 1b;
- strengthening notch areas by inserting perpendicular-to-grain screws that extend to above the neutral axis of the member.

3. Test program

3.1 Test set up

Two sets of glulam members with 80 x 532 and 175 x 646 mm cross-sections were tested under a four-point bending arrangement as shown in Figures 2 and 3. The system had frictionless horizontal roller bearings placed under the two interior point loads and at the lower bearing support. The bird-mouth notch cut in the glulam wrapped around the upper bearing support with the member resting on a steel support shoe that could not rotate. This provided horizontal frictional restraint to the member against effects of any horizontal forces resulting from imperfections in the

arrangement or large deformation of the member. Only vertical external forces were applied and the system was symmetrical with respect to lines of action of external forces, and each vertical reaction force (i.e. outer external forces) was one half of the total applied force. Transverse support was provided to members near each end and at three interior span locations to prevent lateral instability, Figure 3. Teflon coated plates inserted between the member and transverse supports prevented friction and allowed free vertical deformation of the member. Based on expectations about what failure mechanisms might occur, six Linear Variable Displacement Transformers (LVDTs) were attached to specimens to record movements at locations shown in Figure 3. Those LVDTs measured bending deflections, crushing at the upper and lower supports, and crack opening displacement if a fracture plane developed from the corner of the notch towards the interior of the span and parallel to the laminations, Figure 4a.

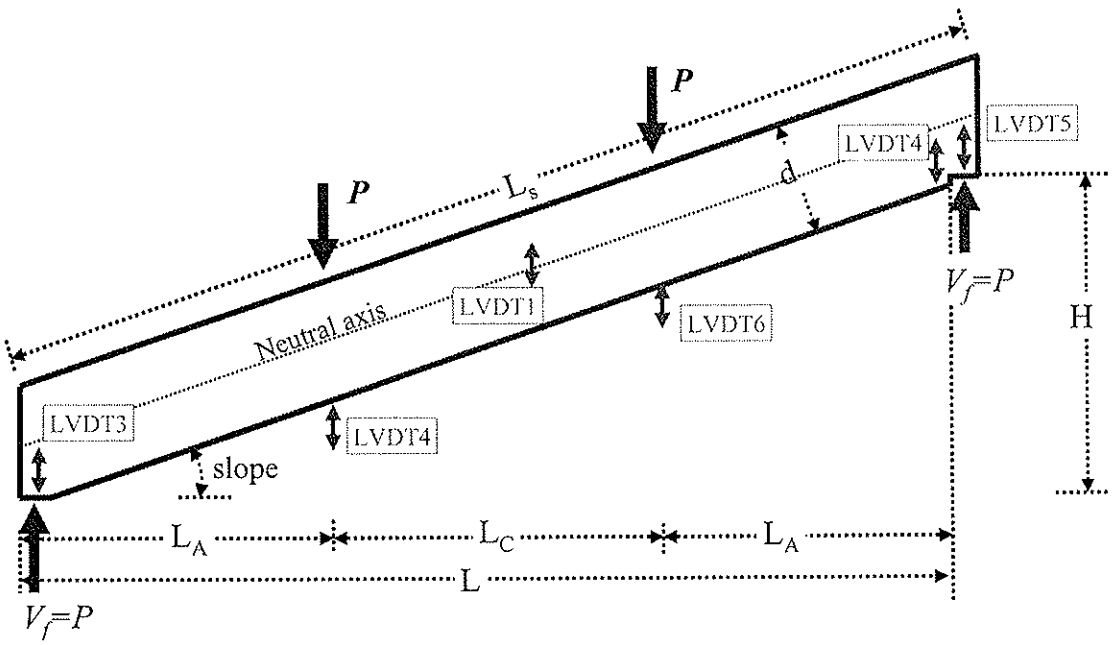

(a) Test configuration and LVDT locations

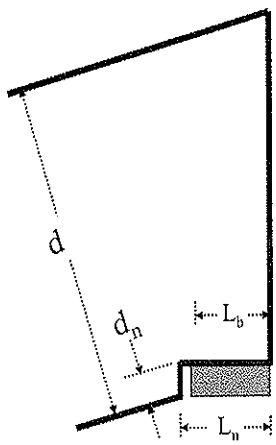

(b) Notch detail

Figure 2: Test arrangement and geometric notation

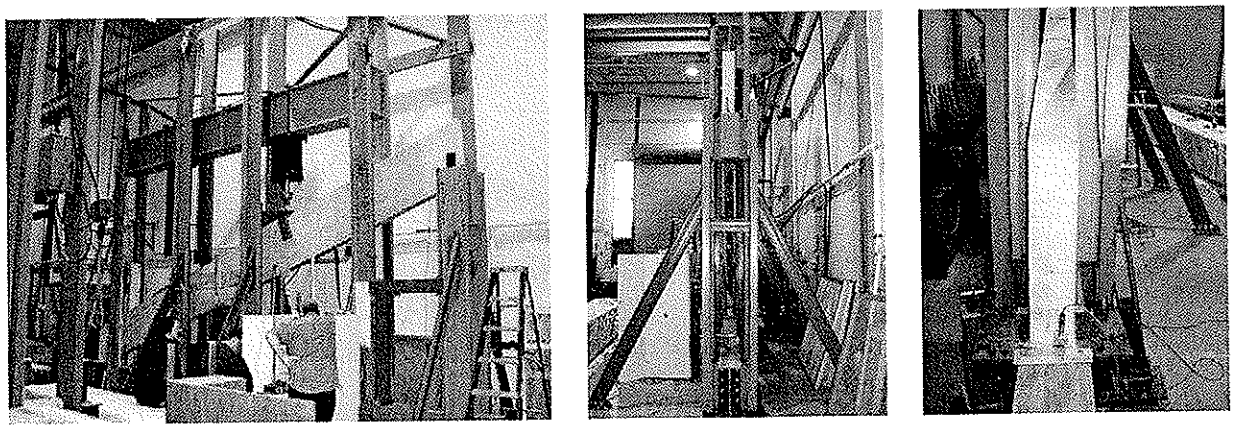

(a) loading frame (b) upper support (c) lower support

Figure 3: Test apparatus

3.2 Glulam materials

Test materials were Canadian manufactured Spruce-Pine glulam of 20f-E grade. Cross-sections of such material have an unbalanced arrangement of 'laminate quality' relative to the mid-depth layer. Specified bending strengths are 25.6 MPa and 19.2 MPa depending on which outer surface is loaded in tension (CSA, 2005). Two cross-section sizes (80 x 532 and 175 x 646 mm) were used to reflect the possibility that there may be size of member effects on mechanisms controlling how specimens failed. Also, for one set of specimens (80 x 532) the notch removed about 8% of the cross-section, while for the other (175 x 646) the notch removed 10% of the cross-section. Details of selected geometric variables for each cross-section size are given in Table 1. Loads were applied by monotonically advancing the loading actuators (interior loading points), at about 4mm per minute, until complete specimen failure. Complete failure occurring in about 15 to 30 minutes after the commencement of loading. Thus, observed behaviour is what is commonly referred to as the 'static loading response'. There were six specimens in each set.

Table 1: Geometric variables for tests (based on notation in Figure 3)

Variable	Cross-section size	
	80 x 532 mm	175 x 646 mm
L (mm)	5900	6682
H (mm)	1966	2366
L_s (mm)	6219	7295
Slope (degree)	18.4	19.5
L_A (mm)	1970	2200
L_C (mm)	1960	2282
d (mm)	532	646
d_n (mm)	42	65
d_n / d (%)	7.9	10
Span/depth=L/d	11.1	10.3
L_b (mm)	120	185
L_n (mm)	126	195

4. Test results

Figures 4 and 5 show images of typical failures observed during the two sets of glulam tests. Before the photographs were taken loading had been continued beyond the point of peak load resistance, under displacement control, until damage propagation was extensive, because that helped clarify the nature of the controlling mechanisms. Bending failures produced highly visible damage that typically was widespread in the tension zone of the cross-section at locations between the interior loading points (Figures 4a and 5a). As illustrated in Figure 4a, damage due to excessive bending moment did not always initiate in the outer lamination. Shear failures were located at about mid-depth of the cross-section at locations between a loading point and an end of a member. Associated fractures exited at an end(s) of members (Figures 4b and 5b). Localised cracking always occurred emanating from the stress concentration at the corner of the bird-mouth notch before the peak load point. However, such cracking did not always propagate into a catastrophic systemic failure. For 80 x 532 members, none of the specimens exhibited signs of incipient unstable fracturing at the notch prior to global instability (Figure 4c). For 175 x 646 members three of six specimens failed catastrophically due to propagation of cracking at the notch. Crack opening deformations recorded by LVDT-4 never exceeded 5 mm, before abrupt unstable crack extension occurred. Tables 2 and 3 summarise the test results for each specimen.

(a) bending failure *(b) shear failure* *(c) stable notch crack*

Figure 4: Typical failure mechanisms observed for 80 x 532 members

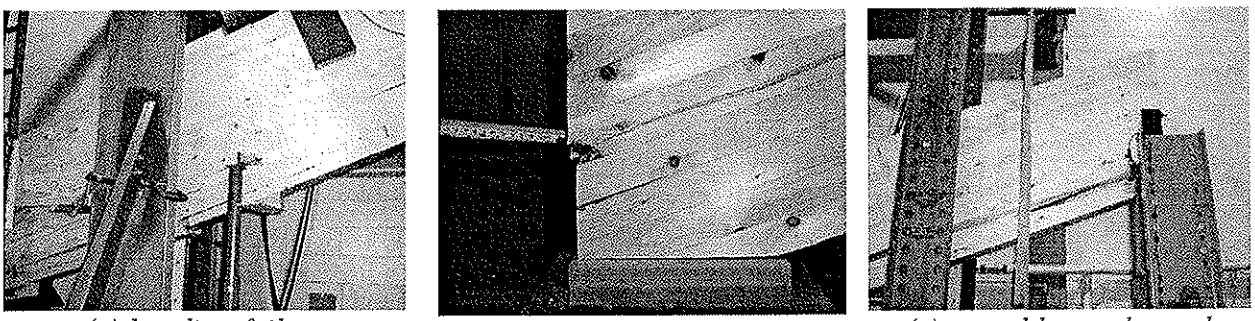

(a) bending failure *(b) shear failure* *(c) unstable notch crack*

Figure 5: Typical failure mechanisms observed for 175 x 646 members

Table 2: Test result (80 x 532)

Specimen No.	Time to failure (minute)	Deformation at failure (mm) *	Total load at failure (kN)	P_u ** (kN)	Ultimate failure mechanism
1	13.1	43.8	104.8	52.4	bending
2	15.0	54.5	126.0	63.0	bending
3	16.5	77.2	155.3	77.65	bending
4	14.8	68.7	144.4	72.2	bending
5	15.2	70.4	152.2	76.1	bending
6	29.7	68.2	147.0	73.5	shear
Average (CoV)	**17.4 (0.35)**	**63.8 (0.19)**	**138.3 (0.14)**	**69.14 (0.14)**	

* measured by LVDT-1 (mid-span); ** = ultimate reaction force at the upper support

Table 3: Test result for (175 x 646)

Specimen No.	Time to failure (minute)	Deformation at failure (mm) *	Total load at failure (kN)	P_u ** (kN)	Ultimate failure mechanism
1	31.6	71.6	281.3	140.7	shear
2	24.4	57.8	281.8	140.9	bending
3	15.9	37.9	173.4	86.7	notch fracture
4	26.1	61.1	270.8	135.4	bending
5	29.4	68.5	242.5	121.3	notch fracture
6	21.7	52.1	265.2	132.6	notch fracture
Average (CoV)	**24.9 (0.23)**	**58.2 (0.21)**	**252.5 (0.16)**	**126.3 (0.16)**	

Figure 6 shows plots of total load versus mid-span displacement for both sets of specimens. As is usual for timber members loaded in bending, the load-deformation curves exhibit initial linear elastic behaviour, followed by limited softening of the response prior to quite brittle systemic failure. There was always rapid reduction in resistive capability after the peak load was reached irrespective of the nature of the controlling mechanism.

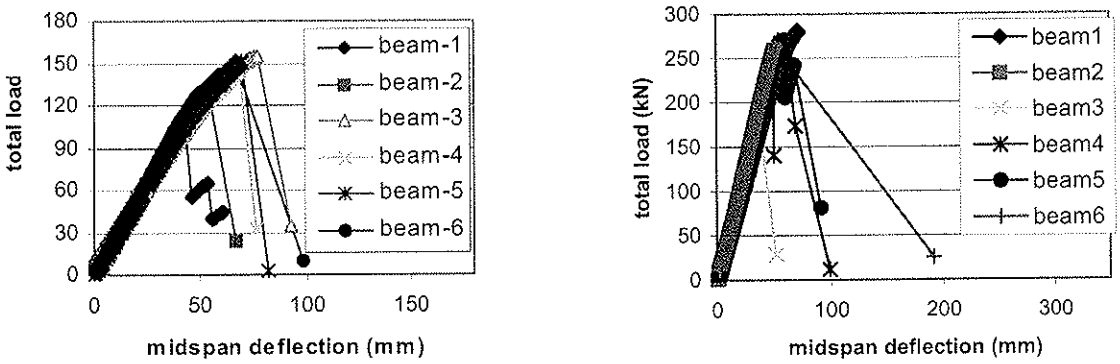

(a) 80 x 532 (b) 175 x 646

Figure 6: Total load versus mid-span deflection

5. Discussion

For 80 x 532 members, it can be concluded that cutting a quite shallow (42mm deep) notch that removes 7.9% of the member depth at an end support did not lead to a critical notch fracturing situation for an inclined member with a span to depth ratio (L/d) of about 11. However, for 175 x 646 members, a deeper (65 mm) notch removing 10% of the member depth did lead to a critical notch fracturing situation in 50 percent of tests for a span-to-depth ratio of about 10. This finding supports the idea that effects of end notches on tension faces of simply supported members are negligible if the ratio d_n / d is less than a certain value. However, the results also indicate that the recommendation of the APA-The Engineered Wood Association (APA, 2003) that stress concentrating effects of notches that do not exceed either 10% of the cross-section depth or 76mm (3 inches) is too liberal for inclined softwood glulam members with bird-mouth notches.

Existing design procedures for strength of notched glulam members involve checking four possible failure mechanisms, i.e. bending, shear with reduced cross-section, shear at the notch, and support bearing capacity. Using specified strengths applicable in Canada (CSA, 2005) for Spruce-Pine glulam of 20f-E grade, and applying equations (1), (2), and (4) to the calculation of the shear capacity at the notch, the expected characteristic reaction resistances for tested members are as summarised in Table 4. The values in the table are expected 5-percentile values applicable to what is termed Standard Term loading. Figure 7 compares 5-percentile test and expected code reaction resistances for various modes. For consistency what are termed test values were estimated from the data (assuming a normal distribution) multiplied by a factor of 0.8, which converts from test loading duration to Standard Term duration.

Comparing the predicted reaction forces and the test results (Figure 7), it can be seen that the design prediction is that shear at the notch (including the effects of stress concentration) should govern for both test situations. The predicted reaction capacity is fairly accurate for the smaller members (80 x 532), but non-conservative

for the larger members (175 x 64). Overall, it would seem that the principle of the APA design recommendation is correct (APA, 2003), but for inclined glulam members it is appropriate to limit those notches for which effects of stress concentrations can be ignored to ones that do not exceed 8% of member depth.

Table 4: Predicted 5-percentile reaction forces based on the current design codes

Failure mechanism	Related strength property (MPa)	Predicted reaction force equation	Predicted reaction force (kN)	
			80 x 532	175 x 646
Bending	$f_{b\text{-}d=646} = 25.6$	$f_b bd^2/(6L_A)$	49.0	141.6
Shear	$f_v = 1.75$	$2/3(f_v bd_n)$	45.7	95.4
Shear at notch	$f_v = 1.75$	Equation 1*	38.8	95.9
Shear at notch	$f_f = 0.5$	Equation 2**	31.7	66.5
Shear at notch	$f_{v,d} = 1.75$	Equation 4***	40.5	82.0
Support bearing	$f_{c\text{-}18.4} = 6.28$ $f_{c\text{-}19.5} = 6.34$	$f_c L_b b$	60.3	205.3

Notes: - f_b = bending strength on the bottom side of the member, $f_{c\alpha}$ = compression strength with reaction load oriented with angle (90^0-α) to the grain.
- Geometrical parameters are given in Table 1.
- *AITC (2005) &APA (2003), **CSAO86-1 (CSA, 2005); ***Eurocode 5 (CEN, 2003)

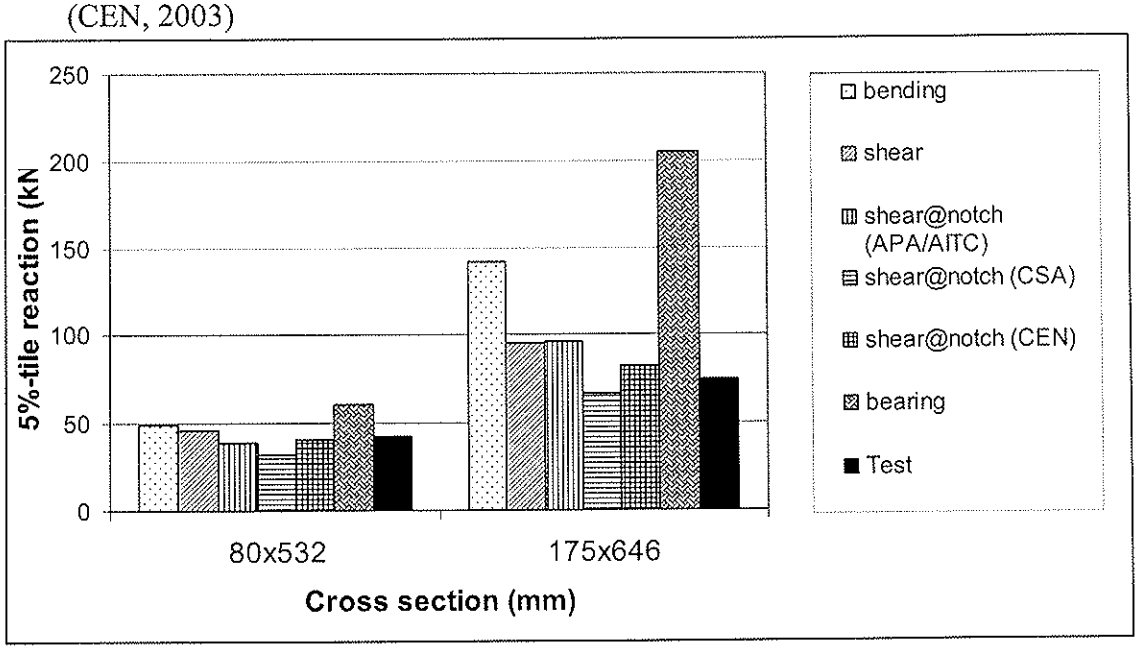

Figure 7: 5-percentile reaction forces, comparison of code expected and test values for 'standard term' load conditions

6. Design recommendation

The following recommendations are proposed to CSAO86-01 Committee in respect of end notches on tension faces of inclined glulam members:

- Stress concentrating effect for notches that remove not more than 8% of member depth are negligible and can be neglected in structural design.
- Stress concentrating effects of notches that remove more than 8% of member depth (up to 25%) should not be ignored in structural design, and fracture mechanic check as per solid lumber must be performed in addition to shear checking on the residual cross-section.

Continuing work by the authors is placing emphasis on creating numerical models that properly explain test findings, reinforcing members with screws in the area of end notches, and drafting appropriate design rules.

7. Acknowledgements

The authors gratefully acknowledged the contribution of glulam material by Canadian manufacturers. Thanks are also extended to Mr. Gary Williams, President of Timber Systems Limited, Markham, Ontario for technical advice and provision of metal loading and support hardware.

8. References

American Institute of Timber Construction (AITC). 2005. *Timber Construction Manual*, 5th edition, John Wiley & Sons, Hoboken, NJ, USA.

APA-The Engineered Wood Association. 2003. Field Notching and Drilling of Glued Laminated Timber Beams, *Technical Notes*, No. EWS S560E, APA, Tacoma, WA, USA.

Canadian Standard Association (CSA). 2005. Engineering Design in Wood, *CAN/CSA Standard 086-01 (consolidated edition)*, CSA, Toronto, ON, Canada.

CEN.2003. Eurocode 5 – Design of timber structures – Part 1-1: General rules and rules for buildings, prEN 1995-1-1, Brussels, Belgium.

Smith, I., Chui, Y.H., Hu, L.J. 1996. Reliability Analysis for Critical Reaction Forces of Lumber Members With an End Notch, *Canadian Journal of Civil Engineering*, 23(1): 202-210.

INTERNATIONAL COUNCIL FOR RESEARCH AND INNOVATION
IN BUILDING AND CONSTRUCTION

WORKING COMMISSION W18 - TIMBER STRUCTURES

A NEW DESIGN APPROACH FOR END NOTCHED BEAMS - VIEW ON CODE

K Rautenstrauch

B Franke

S Franke

K U Schober

Department of Timber and Masonry Engineering

Bauhaus-University of Weimar

GERMANY

Presented by K. U. Schober

I. Smith asked whether such steep notch is allowed. K.U. Schober answered yes. He questioned whether the same formula would apply to shallow notch say 0.2 because with deep notch one can force the total fracture energy to fit within LEFM but no so in shallow case. Modes 1 and 2 fractures and displacement versus load control issues were discussed. S. Aicher stated that this proposal was not accepted in Germany because the calibration base was too small. It was considered too extreme to come up with the conclusion that the present situation is not conservative. F. Lam commented that in service micro checks and large cracks can exists in timber due to environmental conditions. This could skew the results if such cracks did not develop in the test specimens. May be a practical solution is to use reinforcements to deal with the problem rather than refining the code. S. Aicher and K.U. Schober said that reinforcements are now commonly used. V. Rajcic and K.U. Schober discussed what fracture mechanics theory was used and its applicability to wood.

A new design approach for end-notched beams

View on code

K. Rautenstrauch, B. Franke, S. Franke, K.U. Schober

Department of Timber and Masonry Engineering

Bauhaus-University of Weimar, Germany

1 Introduction

The determination of the load-carrying capacity of timber structures can be done by means of the theory of elasticity in most cases. This excludes areas of high demanding loads and stress concentration, e.g. notches and holes. For these areas, different empirical approaches on the basis of the shear resistance and the theory of elasticity have been developed over the past years and included in design codes. In the European and German Standard for the design of timber structures similar energy balanced approaches can be found. The background for these design models was the proposal of GUSTAFSSON [1], who estimates the material resistance against crack initiation in dependence of the energy release rate and the resilience of the structure. In his model, he is simplifying the mixed mode ratio of the total fracture energy is approximately equal to the fracture energy for transversal tension when fracture occurs. Recent experimental and numerical investigations of the strain condition around notches and holes lead to an extension of this theoretical approach, considering also fracture mode I and fracture mode II [2], [3].

2 Experimental investigations

2.1 Test program

The experimental investigations of the strain situation on the groove of end-notched beams have been done by means of close-range photogrammetry on solid timber and glued laminated timber specimen with natural defects distribution and constant cross-section. Additionally, deflections in the mid-span of the beams and at the supports have been measured with inductive displacement transducers. All specimens were tested in displacement controlled 3-point bending tests to assure a constant crack development until fracture (tab. 1, fig. 1). Here, the beginning crack propagation could be measured non-destructive, directly and continuously in a special post process by photogrammetry sequence analysis [4], [5].

Table 1 - Test program

Series	Span	Quantity	Cross-section	Notch ratio $\alpha = h_e / h$	Density	M.C.
Solid	600 mm	42	40 / 80 mm	0.5 / 0.625 / 0.75 / 0.875	480 kg/m³	11%
Glulam	1,600 mm	12	80 / 160 mm	0.5 / 0.688 / 0.875	450 kg/m³	11%
		12	80 / 200 mm	0.5 / 0.688 / 0.875		
		7	100 / 200 mm	0.625 / 0.875		

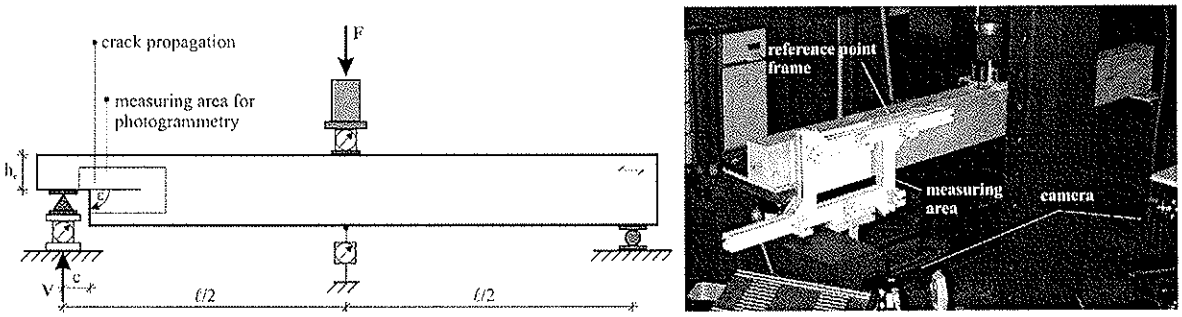

Figure 1 Principle sketch and realized test set-up of a glulam beam

2.2 Experimental results

The lab tests confirm the markedly brittle fracture of timber due to tension perpendicular to the grain. After a temporary stable crack development in the groove softening occurred by instable crack propagation until the mid-span of the specimens. This typical failure behavior could be observed without any visual notices and predeflections around the groove. The obtained loads are shown in fig. 2.

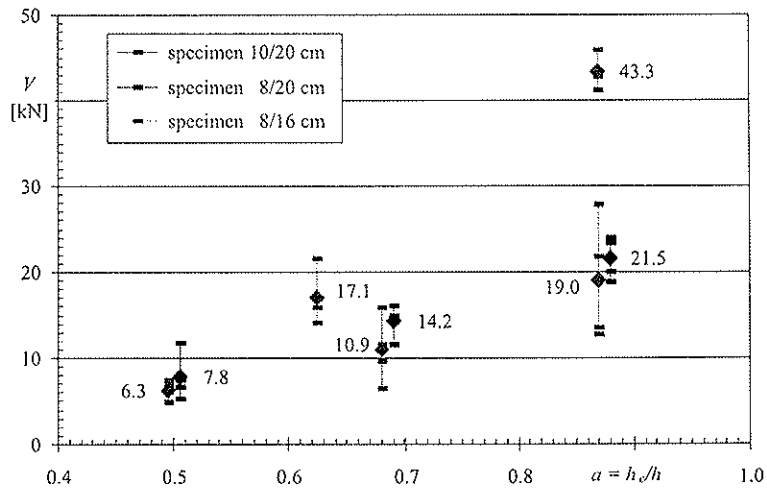

Figure 2 Ultimate loads over notch ratio for glulam series

To investigate the geometrical influence of the notch on the structural and fracture behavior of the specimens, fracture resistance curves have been derived by a numerical procedure from the photogrammetric determined data of the crack propagation. These curves describe the overall energetically balance of the structure during the observed softening. Fig. 3 shows the crack resistance curves on a glulam beam with a notch ratio of $\alpha = 0.875$ under combined tension and shear loading, separated for fracture mode I and II.

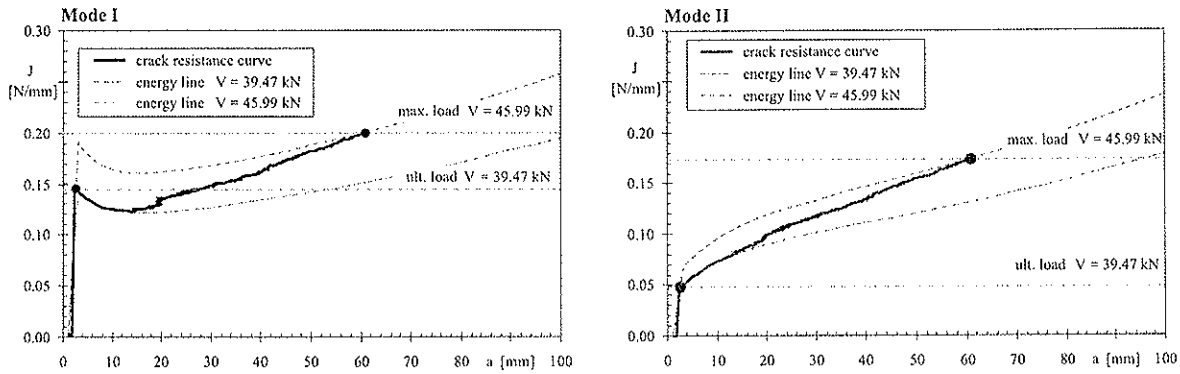

Figure 3 Crack resistance curves separated for tension perp. to the grain and shear

The separation into mode I and mode II has been done by the approach of ISHIKAWA et al. [6]. The energetically curve sketching shows clearly that after initial cracking the propagation becomes temporary instable followed by a stable crack development until the ultimate load is achieved. Furthermore, the critical fracture energies assimilate each other with a growing notch ratio (fig. 4).

$$\lim_{\alpha \to 1} \left(\mathcal{G}^{I}_{A,c} / \mathcal{G}^{II}_{A,c} \right) = 1 \tag{1}$$

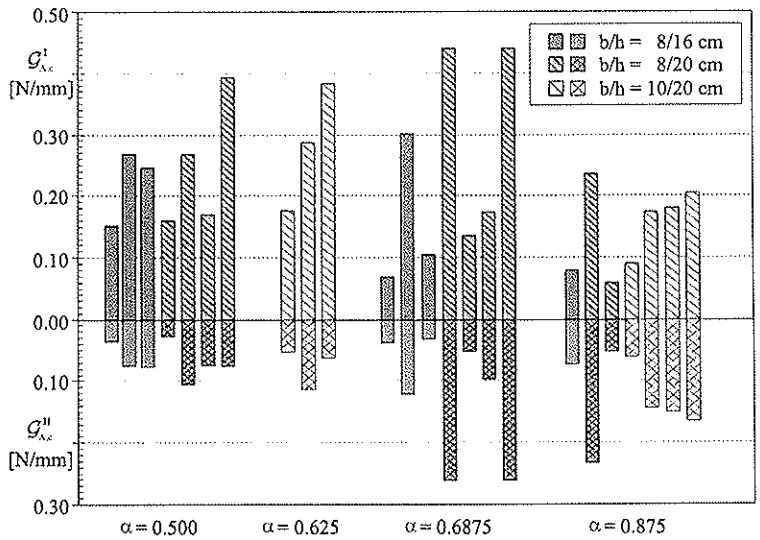

Figure 4 Fracture parameters depending on the notch ratio α (glulam test)

3 Numerical investigations

3.1 Numerical model

The numerical simulation has been done with a finite element model (ANSYS® Rev. 11 package) consisting of the bulk material formulation and cohesive contact elements to describe the crack propagation (fig. 5). After exceeding the maximum strength value the crack initiation occurs by complete energy dissipation and contact opening over the full element length. The crack initiation is characterized also by the geometry of the groove and propagates here parallel to the grain in longitudinal beam direction. Thus, the definition of the crack path for the contact elements is clearly specified. To account the combined loading of the structure a quadratic power law of mode I and mode II interaction

has been used for the contact material description [7]. Structural differences between the cross-sections of solid timber and the glued lamellae in glulam have been considered in the numerical model by a different elastic initial stiffness.

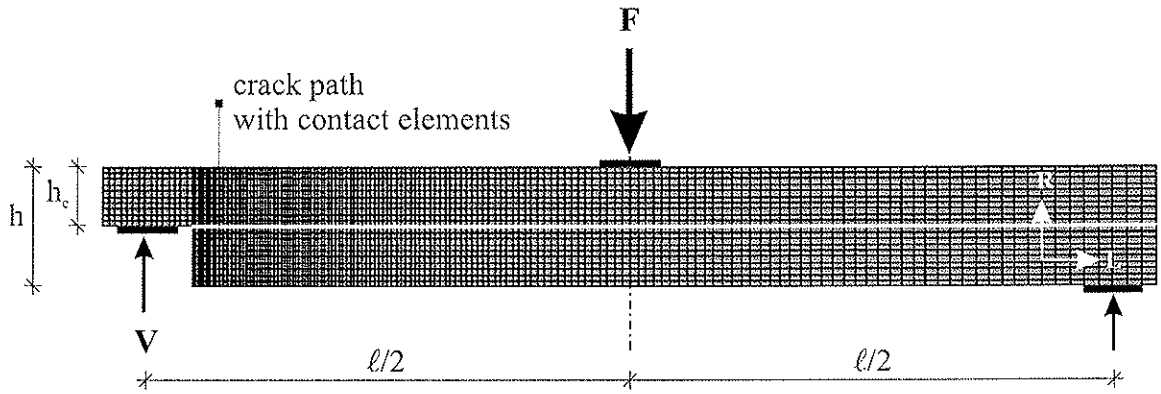

Figure 5 Numerical simulation model of end-notched beams

3.2 Numerical results

It was possible to simulate the linear-elastic initial stiffness, the mean values of the serial ultimate loads, as well as the brittle softening during the fracture process close to reality. Fig. 6 shows for the practice-related notch ration $\alpha = 0.5$ the comparison of numerical experimental results of this series with a close agreement of the obtained curves.

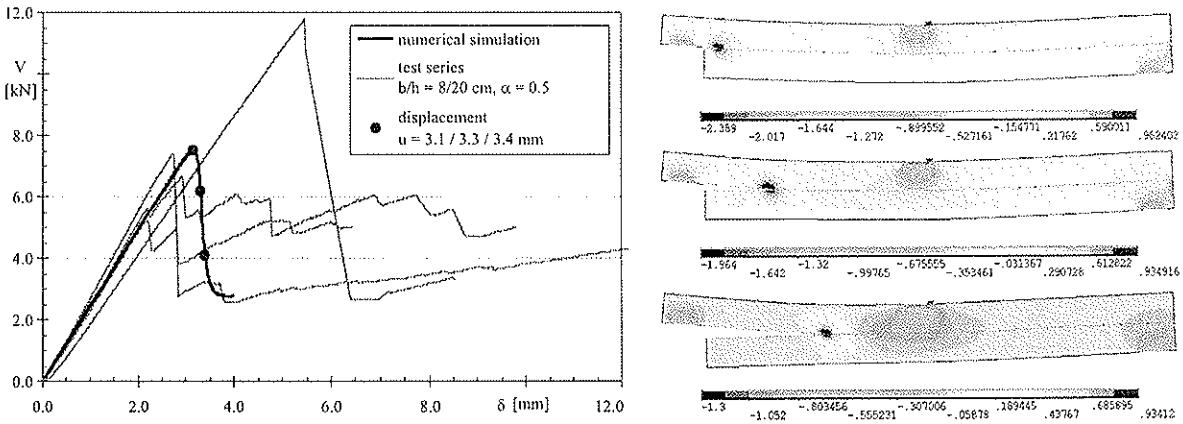

Figure 6 Simulation results vs. load-deformation curve (left) and tension stresses perp. to the grain of the marked load steps

The only numerical induced crack growth correlates with the real structural behavior, thus the used model, material and fitting parameters are suitable to obtain crack resistance curves for other constellations on the base of numerical simulations only. During the crack propagation process new surfaces will be generated by the release of fracture energy. Within the numerical simulation, it was now possible to calculate the corresponding energy release rate in fracture mode I and II and derive crack resistance curves and for other geometry based parameter studies (fig. 7, [8]).

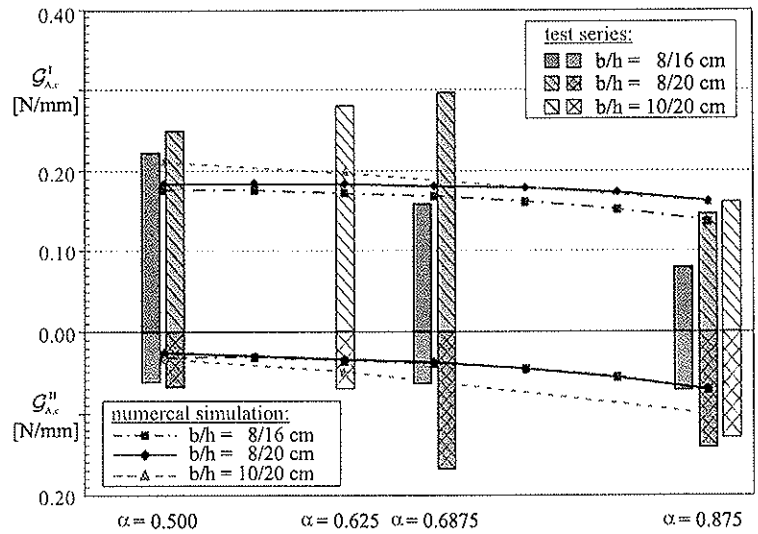

Figure 7 Comparison of experimental and only numerical calculated critical fracture parameters of end-notched beams in glulam

4 Design proposal for rectangular end-notched beams

4.1 Determination of the energy release rate

The experimental and numerical approach discussed here have shown the load-bearing capacity for end-notched beams according to the German Standard DIN 1052:2004 is slightly overestimated and the strain situation around notches and holes cannot be reduced to predominant tension perpendicular to the groove. Therefore, an extended design approach will be proposed, taking into account transverse tension and shear stresses together. The proposal is based on the calculation model of GUSTAFSSON [1] assuming the global critical energy release rate of the structure $\mathcal{G}_c$ is approximately equal to the critical fracture energy $\mathcal{G}_c^I$ in fracture mode I when fracture occures. The supporting load can be calculated from the energy balance between the applied loads and the potential energy at the structure (eq. 2):

$$V = \frac{b\,\alpha\,h\sqrt{\mathcal{G}_c/h}}{\sqrt{0.6\left(\alpha-\alpha^2\right)/G_{xy}}+\beta\sqrt{\frac{6}{E_x}\left(\frac{1}{\alpha}-\alpha^2\right)}} \tag{2}$$

In contrast to the investigations of GUSTAFSSON the critical fracture parameter derived from the different crack resistance curves show the presence of a combined loading situation of transverse tension and shear in end-notched beams depending on the notch ratio α. Therefore, the global critical energy release rate $\mathcal{G}_c$ in eq. (2) will be substituted by the summation of the identified fracture energies, $\mathcal{G}^{I}_{A,c}$ for fracture mode I and $\mathcal{G}^{II}_{A,c}$ for fracture mode II. Additionally, a calibration factor k will be introduced, calculated by comparison of the experimental obtained flexibility of the structure with the corresponding theoretical flexibility in GUSTAFSSON'S model [9].

$$V = \frac{b\,\alpha\,h \cdot k\sqrt{\left(\mathcal{G}_{A,c}^{I} + \mathcal{G}_{A,c}^{II}\right)/h}}{\sqrt{0.6\left(\alpha-\alpha^2\right)/G_{xy}} + \beta\sqrt{\frac{6}{E_x}\left(\frac{1}{\alpha}-\alpha^2\right)}} \tag{3}$$

The comparison of the load-bearing capacity calculated by eq. (3) with the experimental obtained results show a close agreement for all notch ratios (fig. 8). The calibration factor has be determined to $k = 0.8$ by comparison of the experimental obtained shear force capacity with the capacity calculated from eq. (3) using the specific energy release rate (fig. 4) derived from crack resistance curves. The results of the parameter study on specimen with varying span, height and notch ratio have shown the summation of separated specific fracture energies $\left(\mathcal{G}_{A,c}^{I} + \mathcal{G}_{A,c}^{II}\right)$, depending on the wood density, is nearly constant [9]. Thus, the following relationship to the known energy release rate for fracture mode I $\mathcal{G}_c^I$ [10] can be established:

$$\mathcal{G}_{c\,(\rho=460\,\mathrm{kg/m^3})}^{I} \approx 0.32\ \mathrm{N/mm} \tag{4}$$

$$\left(\mathcal{G}_{A,c}^{I} + \mathcal{G}_{A,c}^{II}\right)_{\rho=460\,\mathrm{kg/m^3}} = 0.21\ \mathrm{N/mm} \approx 0.65\,\mathcal{G}_{c\,(\rho=460\,\mathrm{kg/m^3})}^{I} \tag{5}$$

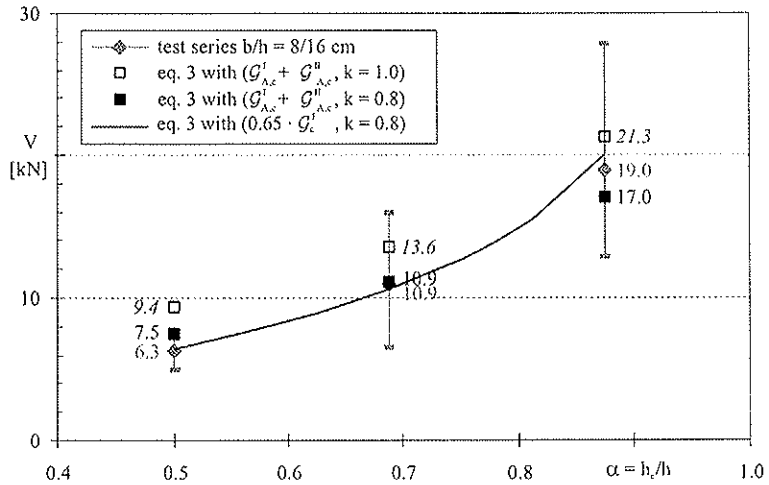

Figure 8 Experimental shear force capacities of the glulam series b/h = 8/16 cm in comparison to the calculated capacities according to eq. (3)

4.2 View on German design code

The following proposal for the German design code is set up, using the introduced relationship from LARSEN et al. [11] (without the global critical energy release rate $\mathcal{G}_c$) and equations' (2) and (3):

$$k_n = \frac{\sqrt{\mathcal{G}_c^I E_x}}{3 f_v} \tag{6}$$

$$k_n^{new} = \frac{\sqrt{0.65\,\mathcal{G}_c^I E_x}}{3 f_v} = \sqrt{0.65}\,k_n = 0.8\,k_n \tag{7}$$

$$k_{90}^{new} = \frac{k_n^{new}}{\sqrt{h}\left(\sqrt{(\alpha-\alpha^2)} + 0.8\,\frac{c}{h}\sqrt{\frac{1}{\alpha}-\alpha^2}\right)} \tag{8}$$

$$k_v = \min\begin{cases}1\\ k_{90}^{new}\,k_c\end{cases} \tag{9}$$

$$V = \frac{2}{3}\,b\,h\,\alpha\,k_v\,f_v \tag{10}$$

The calculation of the design load can be done using shear force capacity according to DIN 1052:2004 reduced by the new introduced parameter k_{90}^{new}, calculated from the specific critical fracture energies for transverse tension and shear. The new characteristic shear force capacities are shown for some test series in fig. 9, using a shear strength of $f_{v,k} = 2.0$ N/mm² for solid timber and $f_{v,k} = 2.5$ N/mm² for glulam. In comparison to the existing German design code the new proposal lead to a more comprehensive description of the structural behavior of end-notched beams and an improved safety level.

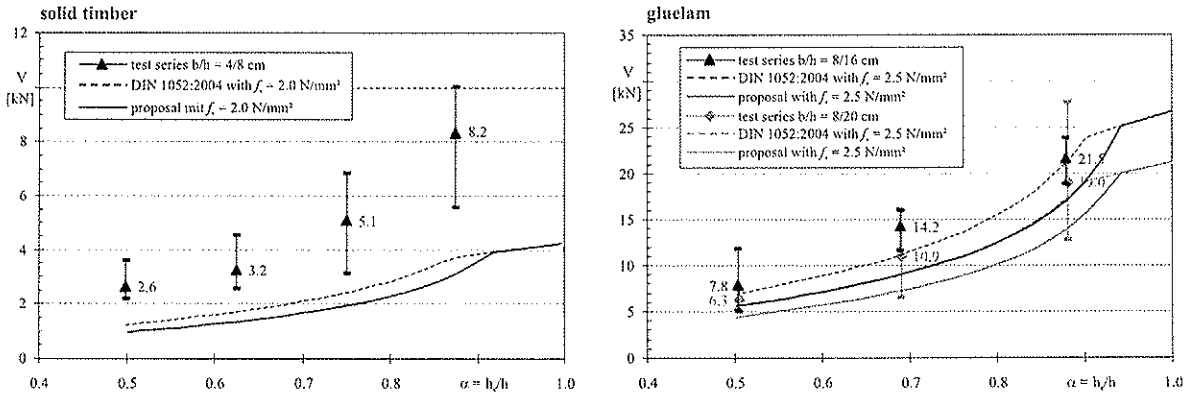

Figure 9 Experimental shear force capacities in comparison to the calculated capacities according to the design proposal and DIN 1052:2004

4 Conclusions

The overall loading situation in rectangular end-notched beams consisting of transverse tension and shear influence was considered for design issues by use of critical fracture parameters for mode I and II. The parameters derived from experimental and numerical data have been calculated independently from the numerical and test results of the same specimen. The measured strain fields correspond very well with the numerically obtained structural behavior. The presented results initialized a new revised and optimized design proposal to estimate the load-carrying capacity of end-notched beams. The introduced solution and methodology to determine the capacity of rectangular end-notched beams can be easily extended to similar problems with high stress singularities.

5 Acknowledgements

The presented work was funded by DFG and AiF [2], [3].
The support is grateful acknowledged.

6 References

[1] Gustafsson, P. J.: *A study of strength of notched beams.* International Council for Research and Innovation in Building and Construction, Working Commission W18 - Timber Structures, Proceedings of meeting 21, 1988, Parksville, Canada.

[2] Rautenstrauch, K. et al.: *Beanspruchungsanalyse von Bauteilen aus Voll- und Brettschichtholz durch Industriephotogrammetrie am Beispiel von Ausklinkungen und Durchbrüchen.* Forschungsbericht zum AiF-Vorhaben 14494 BR/1, Research Report, Bauhaus-University of Weimar, Weimar, 2008.

[3] Rautenstrauch, K. and Franke, B: *Anwendung eines optischen Einzelstellenmessverfahrens zur Untersuchung bruchmechanischer Kenngrößen und des dehnungsabhängigen Festigkeitsverhaltens von Holz.* DFG-Forschungsbericht Research Report, Bauhaus-University of Weimar, Weimar, 2007.

[4] Franke, S., Franke, B. and Rautenstrauch, K.: *Strain analysis of wood components by close range photogrammetry.* Materials and Structures 40 (2007):37-46.

[5] Franke, S., Franke, B., Schober, K.U. and Rautenstrauch, K.: *Experimental verification of FE-Simulations of wood using photogrammetry.* Proceedings of the 9th World Conference on Timber Engineering (WCTE 2006), Portland OR, USA, 2006.

[6] Ishikawa, H., Kitagawa, H. and Okamura, H.: *J-Integral of a mixed mode crack and its application.* Proceedings ICM3, Vol. 3, Cambridge, England, 1979.

[7] ANSYS®, Inc.: Documentation for Release 11.0. SAS IP, Inc. 2007

[8] Franke, S., Franke, B., Schober, K.U. and Rautenstrauch, K.: *The strength behavior of wood in experiment and simulations.* Proceedings of the 10th World Conference on Timber Engineering (WCTE 2008), Miyazaki, Japan, 2008.

[9] Franke, B.: *Zur Bewertung der Tragfähigkeit von Trägerausklinkungen in Nadelholz.* Dissertation, Bauhaus-Universität Weimar, Weimar, 2008.

[10] Larsen, H.J. and Gustafsson, P.J.: *The Fracture Energy of wood in tension perpendicular to the grain. Results from a joint testing project.* International Council for Research and Innovation in Building and Construction, Working Commission W18 - Timber Structures, Proceedings of meeting 23, 1990, Lisbon, Portugal.

[11] Larsen, H.J., Riberholt, H. and Gustafsson, P.J.: *Eurocode 5 – Design of Notched Beams.* International Council for Research and Innovation in Building and Construction, Working Commission W18 - Timber Structures, Proceedings of meeting 25, 1992, Åhus, Sweden.

INTERNATIONAL COUNCIL FOR RESEARCH AND INNOVATION
IN BUILDING AND CONSTRUCTION

WORKING COMMISSION W18 - TIMBER STRUCTURES

THE DESIGN RULES IN EUROCODE 5 FOR COMPRESSION PERPENDICULAR TO THE GRAIN - CONTINUOUS SUPPORTED BEAMS

H J Larsen
DENMARK

T A C M van der Put
TU-Delft

A J M Leijten
TU-Eindhoven

THE NETHERLANDS

Presented by H.J. Larsen

I. Smith commented that there is a large Forintek database from Canada that covers this area. H. Blass commented that the equation with reference to EC5 A1 is incorrect and different from the proposal by Blass and Görlacher. H.J. Larsen stated that the equation is cited from the latest version of EC5 A1. H. Blass stated if so the quotation of Blass and Görlacher is incorrect and should be removed. He further explained the original proposal from Karlsruhe and requested the test results from Delft so that comparisons can be made.

Paper revised based on discussions at the CIB-W18 meeting. The main changes concern correction of an incorrect description of the rules in Eurocode 5, amendment EC5/A1.

The Design Rules in Eurocode 5 for Compression Perpendicular to the Grain - Continuous and semi continuous supported beams

H. J. Larsen[1], A.J.M. Leijten[2], T. A. C. M. van der Put[3]
[1]Denmark, [2] TU-Eindhoven, [3] TU-Delft

1 Introduction

An important task for CEN TC 124 has been drafting standards for determination of the basic properties of timber. A point of discussion has been whether the standards should aim at getting well defined basic material properties or reflect typical uses. TC124 has opted for the former (the scientific) approach assuming that it would then be possible to calculate the behaviour in practical use situations, whilst US and Australia has chosen the other (the technological).

This is for example reflected in the European test method for shear (EN 408) where a test set-up as shown in Figure 1 has been chosen, while most countries use short test beams loaded in bending and shear (and compression perpendicular to the fibres).

For compression perpendicular to the grain the two options shown in Figure 2 were discussed. To the left is shown a test where a block of timber is loaded in uniform compression over the full surface. To the right is shown a situation where the test specimen (e.g. a sill) is loaded over part of the length corresponding to a rail on a sleeper. The latter method that is used in US and Australia gives higher strength values than the block test because the fibres adjacent to the loaded area contributes in

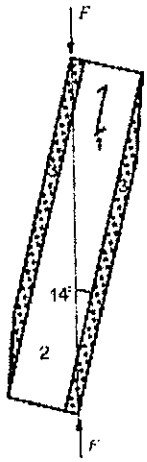

Figure 1. Shear test according to EN 408. The load is transferred through steel plates glued to the timber specimen that is loaded in shear at an angle to the grain.

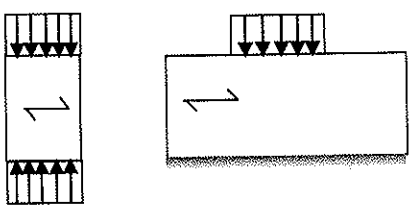

Figure 2. Pure block compression versus rail test.

taking the load, see Figure 3. The first method was chosen in Europe, an argument being that it reflected the situation in pre-stressed timber decks, and it was assumed that the rail test results could be derived from the block results.

Typical load-deformation curves are shown in Figure 3.

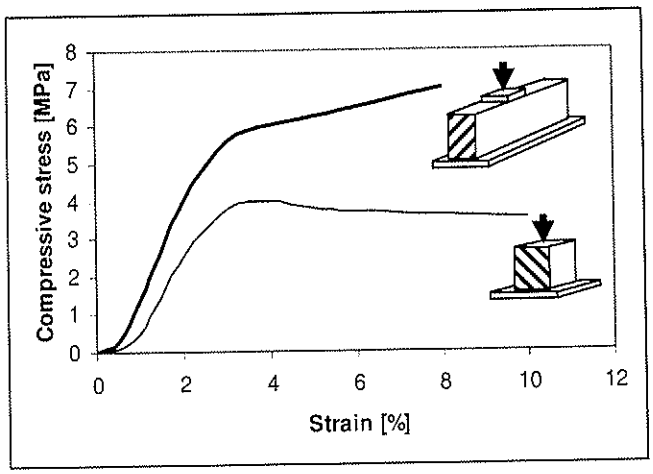

Figure 3. Load-deformation curves for uniform stress (lower curve) and for a rail situation (upper curve). From [9].

To be able to report and compare test results it is for a load-deformation curve that is not linear necessary to define a failure criterion. The definition according to EN 408 for block compression is shown in Figure 4. The compression strength is defined by the intersection between the test stress strain curve and a line parallel to the initial curve at a distance of $0{,}01h$ where h is the specimen height.

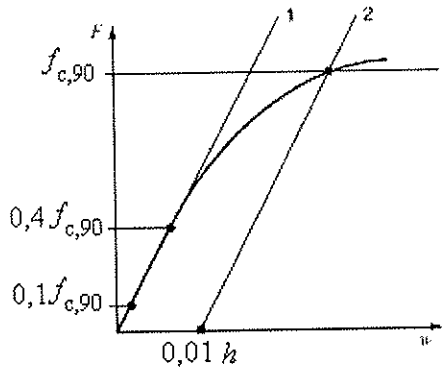

Figure 4. Load-deformation curve for compression perpendicular to the grain, definition of compression strength $f_{c,90}$ at 1% off set.

Since the result exceeding $f_{c,90}$ is not collapse but only large deformations, it has been proposed, e.g. by Thelandersson and Mårtensson [1] to regard this situation as violation of a Serviceability limit state. But even by taking advantage of the lower partial safety factors for Serviceability instead of those for Ultimate limit states, many details in traditional timber structures, e.g. timber frame houses will no longer be acceptable.

And it is difficult, to put it mildly, to understand why exceeding a marginal deformation in a block compression test should be taken as the governing criteria for structures where much larger deformations are normally acceptable and loaded in a completely different way.

2 Limit states

In the Eurocodes a distinction is made between Ultimate and Serviceability limit states. Ultimate limit states correspond to failure of the whole structure or part of it. Serviceability limit states correspond to the unacceptable behaviour at normal use. An example of exceeding serviceability limit are deflections that are visually or functionally unacceptable.

There are quite precise requirements regarding Ultimate limit states: Sufficient load-carrying capacity shall be verified according to Eurocode 5 (EN1995) [2] with actions and safety factors according to EN 1990 [3] and EN 1991 [4].

For Serviceability limit states on the contrary there are no precise requirements. It is to a large extent left to the designer in consultation with the client to decide on the limits. It is a matter of tradition and taste whether a deformation is acceptable or not. And put to the extremes it is not even required that there is a formal serviceability verification as long as it is possible to perform the ultimate state calculations.

For compression perpendicular to the grain, it seems in some cases relevant to define the limit state as the stress at a specified strain. But a compression of 1% or even 10% of a typical wall sill with depth 45mm will cause no harm to the sill or to a multi-storey timber framed house as long as the stress-strain curve is increasing for increasing strain i.e. that no brittle failure will occur in the bottom rail. In some cases a more relevant definition would be an absolute compression. But Riberholt [9] argues: "for thin timber members a compression of for example 5 mm would result in a complete destruction or collapse of the wood cells, which could result in uncontrolled deformations. For thicker timber members such a maximum of the absolute compression would result in compression strength values which are far below the real maximum stresses".

Fortunately, it is not necessary to have a common definition of the limit state: It is acceptable to have one definition for low sills and another for high beams.

Since the serviceability load is generally less than about 50% of the ultimate load, deformations perpendicular to the grain will normally be within reasonable limits and a rough estimate is sufficient.

3 Load-carrying capacity

Since the difference between the block test and the rail test is that the load is carried not only by the fibres directly under the loaded length l but also by the neighbouring lengths, see Figure 5, several researchers, e.g. Madsen [5], Blass and Görlacher [6], Van der Put et al. [7] and Bleron et al. [8] have proposed that the design is based on the assumption of an effective length l_{ef} loaded in uniform compression corresponding to the ultimate compression strength.

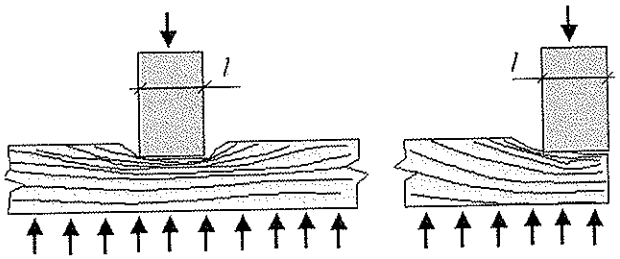

Figure 5. Deformation under a concentrated load.

Several proposals have been given for the effective length. In EN 1995-1-1:2004 some very complicated empirical rules were given based on Riberholt [9]. In amendment EC5/A1 [2007] simpler rules are given, but again they are purely empirical and not supported by theory which is a break of the traditions for cooperation between CEN TC 250/SC 5 and CIB W18 and the traditions within CIB W18.

EC5/A1 is based on a model set out in Blass & Görlacher [6]. The starting point for this model is the tests reported in Madsen [5] where an effective length of $l_{ef} = l + 2*30\text{mm}$ was found.

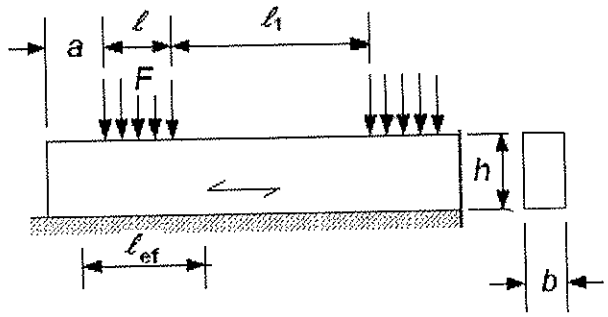

Figure 6 – Member on continuous support

According to this amendment the design load-carrying capacity F_d of a fully supported beam loaded perpendicular to the grain with $l_1 \geq 2h$, given in Figure 6 is:

$$\frac{F_d}{A_{ef}} = \frac{F_d}{b\, l_{ef}} = k_c f_{c,90,d} \quad \Rightarrow \quad \frac{F_d}{b\, l} = k_{c,90} f_{c,90,d} \frac{l_{ef}}{l} \tag{1}$$

where:

F_d is the design load perpendicular to grain

l is the actual contact length.

l_{ef} is the effective contact length parallel to the grain, where l at each side is increased by 30 mm, but no more than a, l or l_1, Figure 6.

$f_{c,90,d}$ is the design reference compressive strength

$k_{c,90}$ is a factor taking into account the load configuration, the possibility of splitting and the degree of compressive deformation.

Examples on $k_{c,90}$ are for beams on a continuous support:
$k_{c,90}$ = 1,25 for solid softwood timber
$k_{c,90}$ = 1,5 for glued laminated softwood timber
for other cases;
$k_{c,90}$ = 1,0
The background for the $k_{c,90}$ factors is obscure.

4 Theoretical load-carrying capacity

Van der Put [7] has developed a theoretical expression for the load-carrying capacity perpendicular to the grain.

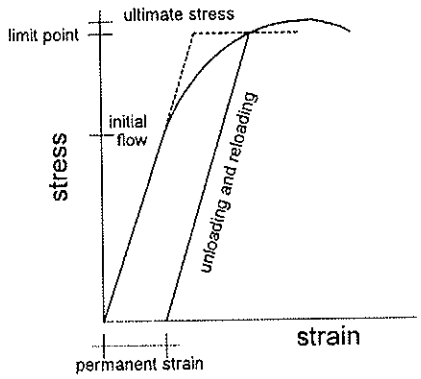

Figure 7. Assumed linear elastic-plastic relation.

The theory is based on an equilibrium method assuming linear elastic-plastic behaviour, Figure 7, to determine a stress field under a bearing plate, Figure 8b satisfying the boundary conditions while none of the stresses exceed the plastic failure criterion, i.e. an exact one.

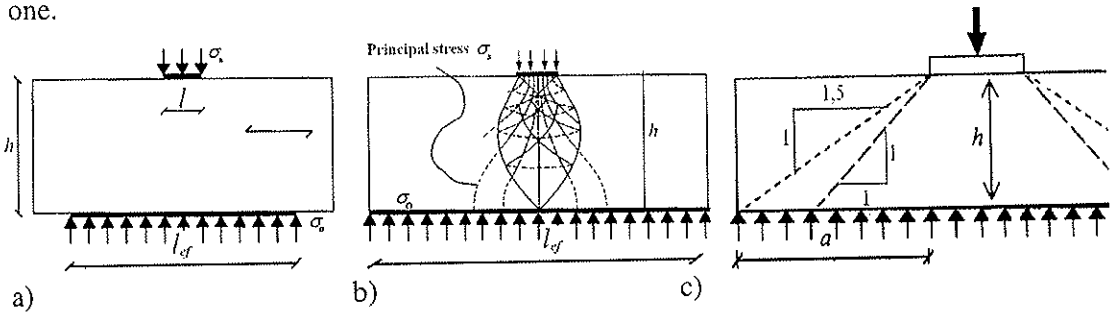

Figure 8. Compression test perpendicular to the grain.
a) Actual situation. b) Assumed stress field. c) Stress dispersion 1:1 and 1:1.5.

The result is that for small strains the effective length, l_{ef}, may as a good approximation be found assuming a 1: 1 slope of the stress dispersion and a 1:1,5 slope for larger strains where the strain hardening is fully developed, i.e

$$\frac{F_d}{b\,l} = k_{c,90} f_{c,90,d} \quad \text{with} \quad k_{c,90} = \sqrt{\frac{l_{ef}}{l}} = \sqrt{\frac{l+3h}{l}} \tag{2}$$

The latter result is experimentally confirmed by optical tests carried out by Schoenmakers [11] and FEM analyses by Schoenmakers [11] and Petersen [12], who showed that outside $l_{ef} = l + 3h$ the stresses can be neglected, Figure 9.

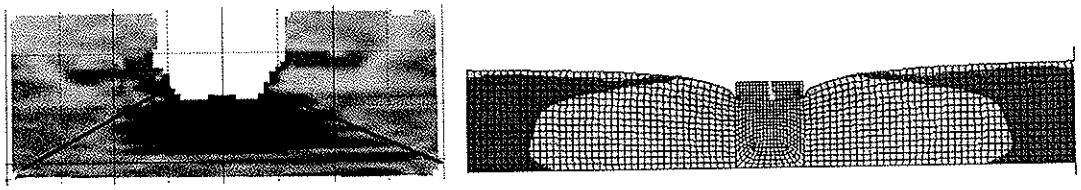

Figure 9. Results of optical test and FEM analyses by Schoenmakers[11], of perpendicular to the grain stresses.

The stress dispersion according to the theory is larger than found by Madsen. However, Madsen did not recognise the beam depth as a parameter that affects the compressive strength. Bleron at al [8] showed this to be important to explain the differences.

5 Evaluation of the models

During the last years several researchers have focused on perpendicular to the grain tests, which allow evaluating the models mentioned.

An overview of all the experiments used to evaluate the models is presented in Table 1. With an exception of the pre war tests where neither the wood species nor the moisture conditions were reported, the tests were carried out according to the standard test procedure of EN408. The reference compressive strength is determined using pure block compression specimens, see Figure 9A, at a standard climate of 20°C and 65% R.H. resulting in about12% moisture content for coniferous wood.

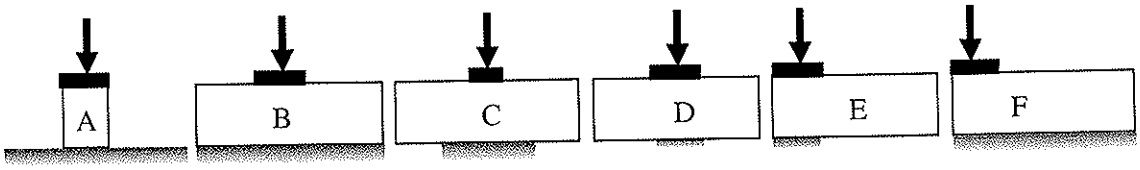

Figure 10. Loading configurations of tests evaluated.

Loading configurations as shown in Figure 10B to 10F were investigated. The reference compressive strength is defined as shown in Figure 4 using a 1% off-set strain (deformation) except for test by Suenson reported in [12] and Graf reported in [12]. In addition some report the compressive stress at 10% deformation or 10% off-set. Since differences are marginal the data are combined.

An overview of the dimensions of specimens, the number and reference compressive strength is presented in Table 1. A total of 582 test results from 52 samples were evaluated for the 1% off-set strength values and 105 results from 23 samples for the 10% deformation limit making a total of 687 results.

Table 1: Overview of the experiments evaluated.

Source	Specimen dimensions* for determination of reference strength only [mm]			Test type	Wood species	Ref. mean strength [N/mm^2]	Deformation [%]	Series and number of specimens per Series
	Depth	Width	Length					
Suenson in [12]	150	150	150	A,B	?	3.6	5 to 15	4/1
Graf in [12]	178	180	179	A,C	?	1.6	3	4/1
Korin [14]	90	40	180	A,B	American white wood	2.62	2.5	7/3
Korin [14]	90	40	180	A,F		2.54		7/3
Petersen [12]	40 80 145	40	160	A,B	Picea Abies (Spruce)	3.2 3.5 2.7	1% off-set & 10%	4/6 2/6 4/6
Augustin et al. [15]	200 480	160	160	A,B,F	Picea Abies	3.31 2.87	1% off-set	3/54 3/54
Poussa et al. [16]	90	45	70	A,D, E	Picea abies	2.8	1% off-set	2/27
Hansen in [9]	95 145 220	45	70	A,B	Picea abies	2.8 2.7 2.6	1% off-set & 10%	3/5 3/5 3/5
Bleron et al. [8]	300	78	100	A,B, D,E	GL 32h (Spruce)	3.01	1% off-set	4/10 1/9
			Total number of specimens			418		582

**) Test specimens type B to F have the same cross-section as type A*

6 Evaluation of test results

The evaluation results are split into two parts representing the test data for 1% off-set deformation and 10% deformation. Table 2 shows the $k_{c,90}$ values used in the evaluation of the EC5/A1 model, (1).

Table 2: Overview of $k_{c,90}$ values in accordance with the EC5/A1 amendment

Load configuration Figure 9	$k_{c,90}$				
	B	C	D	E	F
Solid wood	1.25	1.0	1.0	1.0	1.25
Glued laminated	1.5	1.0	1.0	1.0	1.5

In Figures 11 and 12 the data are plotted against the model predictions.
To assist further evaluation a model uncertainty analysis has been carried out. The uncertainty plots are based on the model versus data results according to the following:

$Y=RX \rightarrow \ln(Y/X)=\ln(R)$ ideally: $\ln(R)=0 \rightarrow R=1$

where X and Y are the test data and model prediction data, respectively.

Normal probability curves are fitted to the results of the model uncertainty analyses. The results are presented in Figures 13 and 14 and the statistical mean and standard deviation of the curves in Tables 3 and 4. Even if the most deviating data point in Figure 12 is ignored the difference in standard deviation between the models does not vanish.

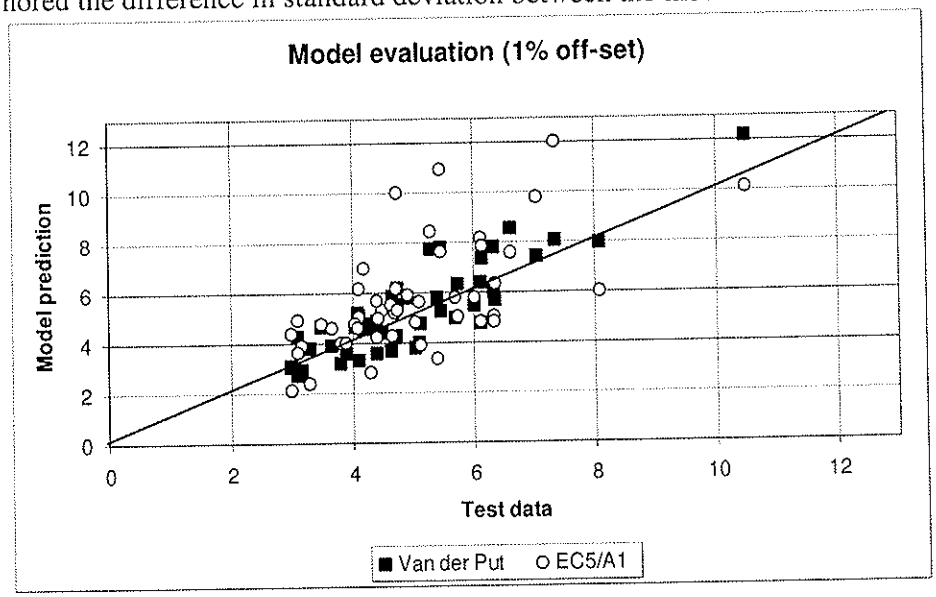

Figure 11. Model comparison for 1% off-set deformation.

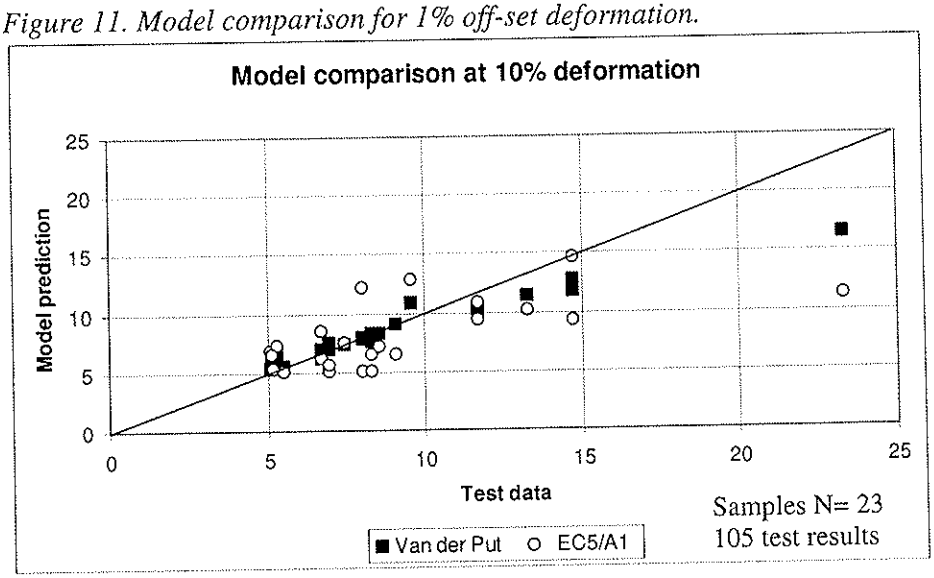

Figure 12. Model comparison at 10% deformation.

The analyses showed no bias with respect to the size of the specimen or the specimen depth to width ratio, Figure 15. It is recognised that for high depth to width ratios ($h/b > 5$) other failure mechanisms may occur. However, for the data analysed only perpendicular to the grain failures were observed.

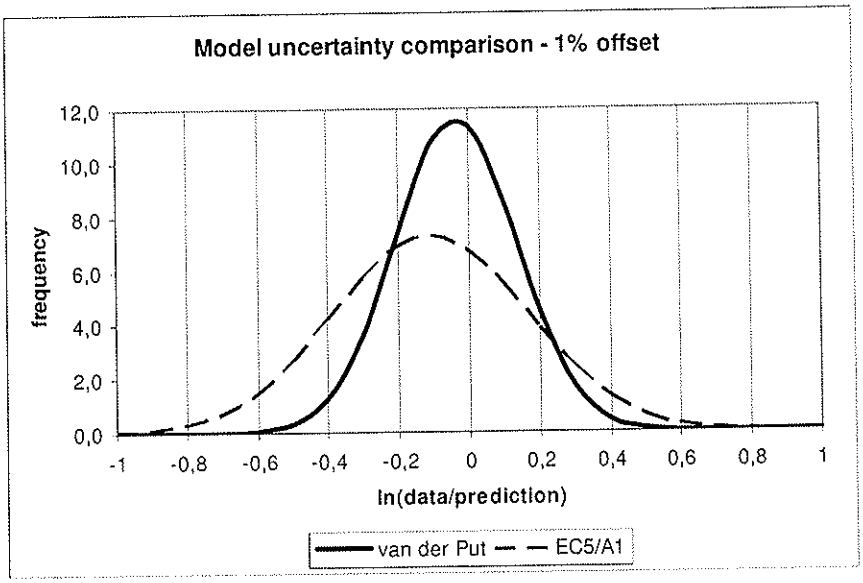

Figure 13. Model uncertainty evaluation - 1% off-set.

Table 3. Model uncertainty statistics for 1% off-set

n = 582	Van der Put	EC5/A1
Mean	-0.04	-0.11
Standard deviation	0.17	0.27

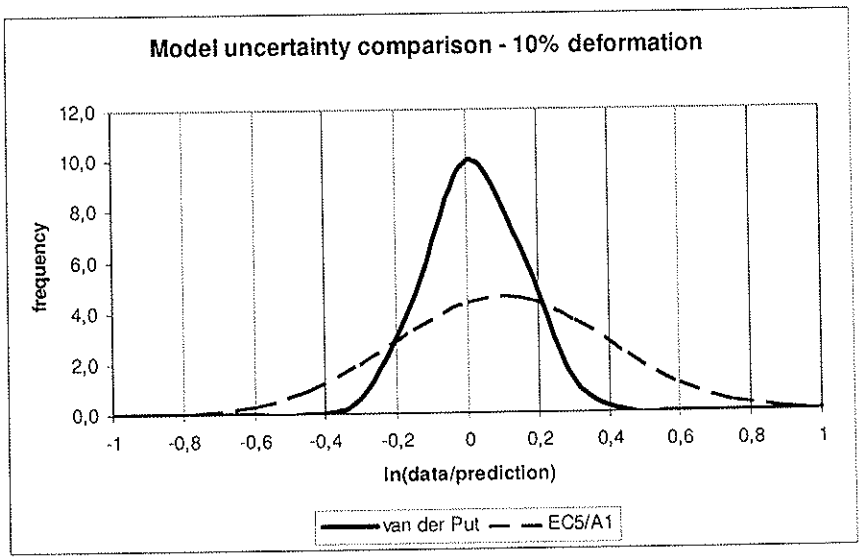

Figure 14: Model uncertainty evaluation - 10% off-set-

Table 4: Model uncertainty statistics for 10% off-set

n = 105	Van der Put	EC5/A1
Mean	0.02	0.10
Standard deviation	0.14	0.30

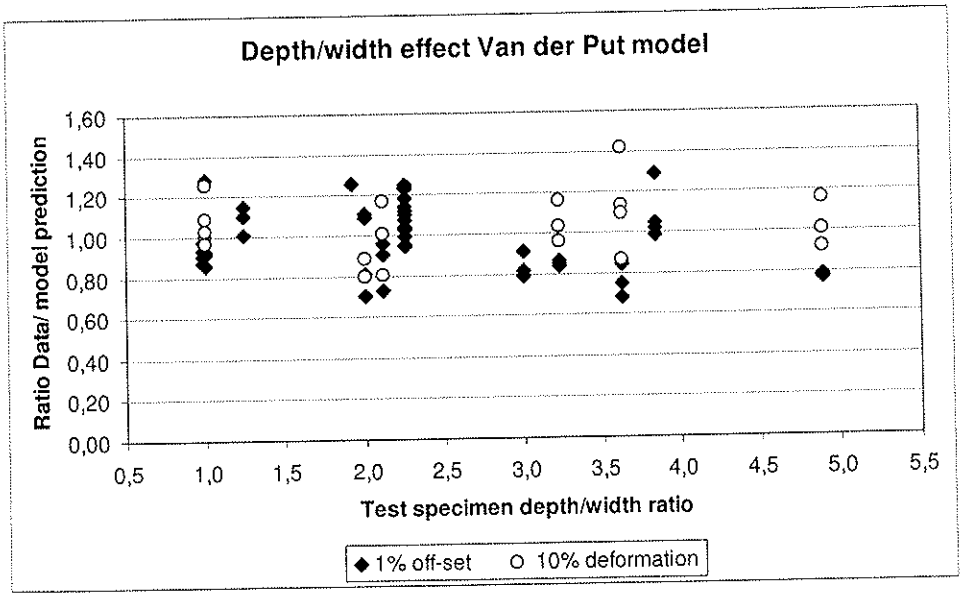

Figure 15: Effect of specimen depth and width ratio.

7 Conclusion

On the bases of the evaluation of the model presented in the amendment of Eurocode 5/A1 and the model by Van der Put the following conclusions can be drawn:

- Van der Put model is the more accurate and reliable in predicting the bearing strength perpendicular to the grain.
- The less reliable results of the Eurocode 5/A1 model is due to the inability to take account of differences in beam height, load configuration and deformation. This causes sometimes unsafe and sometimes conservative results.
- It is suggested to replace Eurocode 5/A1 model by the model according to Van der Put [7], as given below.

8. Eurocode 5 Code Proposal

Compression perpendicular to the grain

The following expression shall be satisfied:

$$\sigma_{c,90,d} \leq k_{c,90} f_{c,90,d} \qquad \text{(EC5.1)}$$

where:

$\sigma_{c,90,d}$ is the design compressive stress in the contact area with the applied load
$f_{c,90,d}$ is the design compressive strength perpendicular to the grain
$k_{c,90}$ is a factor taking into account the load configuration, the possibility of splitting and the degree of compressive deformation

For a member with a depth $h \leq 5b$, where the reaction results from an applied compressive force occurring directly over a continuous support, the factor $k_{c,90}$ should be calculated from:

$$k_{c,90} = \sqrt{\frac{A_{ef}}{A}} \leq 5 \qquad \text{(EC5.2)}$$

were:

A_{ef} is the effective contact area

A is the contact area with the compression load perpendicular to the grain

The effective contact area, A_{ef}, should be determined taking into account an effective contact length parallel to the grain, l_{ef}, and the width b.

The effective length l_{ef} is found as the actual contact length, l, increased at each side by $1.5h$ but not more than a or $0{,}5\,l_1$ or $3h$, see Figure EC5.1

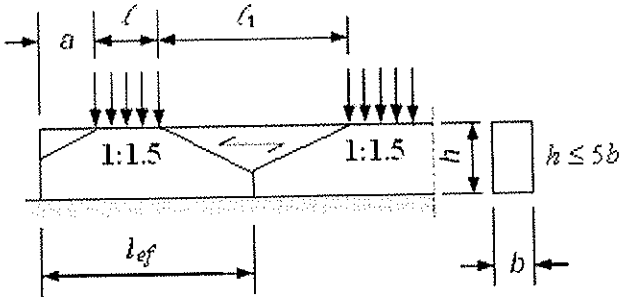

Figure EC5.1. Member on a continuous support

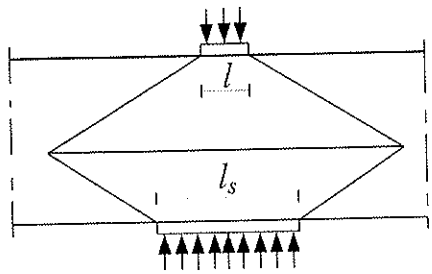

Figure EC5.2: Opposite loads

For opposite load situations, see Figure EC5.2, where the width b of both loaded areas is equal:

$$k_{c,90} = \sqrt{0{,}5 + \frac{3h + l_s}{2l}} \qquad \text{(EC5.3)}$$

NOTE: The resulting compressive deformation at the ultimate limit state will be approximately 10%. If the designer wants to limit the deformation, smaller slope of the stress dispersion should be used. A slope of 1:1 will result in a compressive deformation of about 3% at the ultimate state (and much less at serviceability stresses).

8 Acknowledgement

The authors wish to thank D. Schoenmakers, TU-Eindhoven, The Netherlands and dr. Staffan Svensson, DTU, Demark allowing to use some of their graphs.

References

[1] Thelandersson, S. and Mårtensson, A.: *Design Principles for Timber in Compression Perpendicular to Grain*. Proceedings of the CIB W18. Paper 30-2-1.

[2] EN 1995-1-2, Eurocode 5 - Part 1-1: Design of timber structures, General - Common rules and rules for Building, European Committee for Standardization, Brussels, Belgium, 2004.

[3] EN 1990: Eurocode. Basis of Structural Design, European Committee for Standardization, Brussels, Belgium, 2002.

[4] EN 1991-1, Eurocode 1- Part 1-1, Actions on structures., European Committee for Standardization, Brussels, Belgium, 2002.

[5] Madsen, B., Leijten, A.J.M., Gehri, E., Mischler, A., and Jorissen, A.: *Behaviour of Timber Connections*. Timber, Behavior of Timber Connections, ISBN 1-55056-738-1, Timber Engineering Ltd, 2000, p 139-162

[6] Blass, H.J. and Görlacher, R.: *Compression perpendicular to the grain.* World Conference Timber Engineering, Finland 2004, Vol 2, p. 435-440

[7] Van der Put, T.A.C.M.: *Derivation of the bearing strength perpendicular to the grain of locally loaded timber blocks*. Delft Wood Science Foundation, 2006.

[8] Bleron, L., Cabaton, L., Sauvignet, E.: *Compression perpendiculaire aux fibres, Essais mechaniques - Modelisation numerique*, in review Forest Product Journal.

[9] Riberholt, H.: *Compression perpendicular to the grain of wood.* COWI-report P-42239-1, 3-8-2000,

[10] Van der Put, T.A.C.M. and Leijten, A.J.M.: *Evaluation of perpendicular to grain failure of beams caused by concentrated loads of joints*. Proceedings of CIB-W18. Paper 33-7-7, 2000, Delft, The Netherlands.

[11] Schoenmakers, D.: *Bearing behaviour perpendicular to grain of dowel type fasteners*.÷ Short Scientific Mission, DTU, Lyngby, Demark. Report of COST E55, Eindhoven, The Netherlands , 2008.

[12] Petersen, T. J., *Trykpåvirket træs svind og krybning / Compressed wood - shrinkage and creep*. In Danish. Main report 137 pp, Enclosure report 153 pp. Institut for Bærende Konstruktioner og Materialer, Technical University Denmark, 1999.

[13] Kollmann, Coté: *Principles of Wood Science and Technology,* Vol.1, Springer-Verlag, 1984, p.339-341.

[14] Korin, U.: *Timber in compression perpendicular to grain*, Proceedings of CIB-W18. Paper 23-6-1, 1990, Lisbon, Portugal.

[15] Augustin, M., Schickhofer, G., Ruli, A., Brandner, R.: Behaviour of glulam in compression perpendicular to grain in different strength grades and load configurations, Proceedings of CIB-W18. Paper 39-12-5, 2006, Florence, Italy.

[16] Poussa, M., Tukiainen, P., Ranta-Manus, A.: Proceedings of CIB-W18. Paper 40-6-2, 2007, Bled, Slovenia.

INTERNATIONAL COUNCIL FOR RESEARCH AND INNOVATION
IN BUILDING AND CONSTRUCTION

WORKING COMMISSION W18 - TIMBER STRUCTURES

SIZE EFFECTS IN BENDING

J K Denzler
Planungsgesellschaft Dittrich GmbH

P Glos
Holzforschung München

GERMANY

Presented by J K Denzler

A. Buchanan asked if EN 384 is the standard to provide characteristic values and what about the design standard, should size effect not be included? J.K. Denzler replied that the size effect adjustments are not in the design code. I. Smith asked about commercially graded material and cited the effect of grading errors in Madsen's work. He mentioned that if Weibull was correct then one would expect more failures in buildings where one had 100 joists compared to one joist. J.K. Denzler stated that this work is based on laboratory grading. F. Lam commented that Weibull theory is based on series system and a building with many joists would be a parallel system. R. Steiger discussed width effect in Eqn. 2 of the paper and suggested clarification be added to paper. S. Aicher raised a practical question of whether it is possible to deal with the acceptance of new softwood species with ignoring size effect in standard. J.K. Denzler agreed as there may be a species effect also. A. Jorissen received clarification about the conclusions. J. Köhler agreed that this work should not be extrapolated to design situations and received clarification about the selection of weakest zone for testing. I. Smith stated that experience from testing softwood showed that defect features can "talk" to each other. He discussed the assumption of homogeneity and shear design issues in Canada and expressed further doubt about the Weibull theory. F. Lam commented the thickness effect is also a function of how the material is milled (centre versus side cut), the location within a tree, and the size of tree etc. S. Aicher and J. Köhler debated the issue of whether Weibull effect in length is not appropriate. The appearance of knot is non continuous and Weibull is more on the empirical side.

Size effects in bending

J.K. Denzler
Planungsgesellschaft Dittrich mbH, Munich, Germany

P. Glos
Holzforschung München, Germany

1 Introduction

In general, the size effect describes the influence of a single dimension or a whole volume on the strength of materials. So far, a lot of papers have dealt with the size effect of solid timber and a lot of different and somehow contrary results are included in them. Up to now, it is unclear to what extent the size effect is influenced by the timber quality or the test method and therefore, it can differ between various countries. This paper aims at clarifying these questions concerning the size effect of European spruce tested in bending. In Europe, the bending strength is investigated according to EN 408 by a four-point bending test with a span of 18 times the height of the specimen and the two loading heads placed in the third points of the span (Fig. 1). According to EN 384, the critical defect identified either by visual means or by a grading machine should be placed between the loading heads.

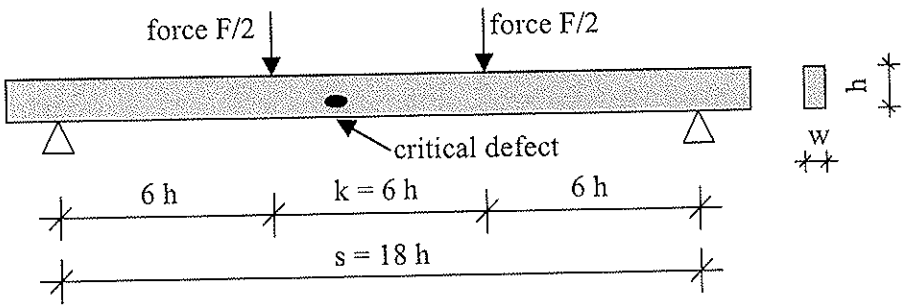

Fig. 1: 4-point-bending test acc. to EN 408.

To consider the influence of the size on the bending strength, the European Standards specify size factors. The characteristic bending strength given in EN 338 is valid for a height of h = 150 mm and a test set-up according to EN 408. For specimens with different heights, EN 384 specifies a factor to transform the characteristic bending strength of a height h into a characteristic bending strength of a height h = 150 mm:

$$k_h = (150/h)^{0.2} \quad (1)$$

This factor is called "height factor" and should consider the influence of the height on the characteristic bending strength of solid timber. An influence of width on the bending strength is not considered in EN 384. The span needs to be corrected by a length factor according to EN 384 if the bending strength is tested with a span different from 18 times the height of the specimen or if the loading heads are not placed in the third points of the span.

All size factors are based on the WEIBULL theory or the weakest link theory. For homogeneous materials, the probability of a weak element included in a specific volume increases with increasing volume. Due to this weak element the strength of the volume is limited. Therefore, the strength decreases with increasing volume. As the strength of timber usually decreases with increasing volume this theory was used to describe the size effect and to develop size factors for solid timber in many countries.

This paper deals with the modelling of size effects of spruce in bending with respect to European standards. Beside the direct influence of size on bending strength, which includes the relationship between timber dimensions and strength properties (WEIBULL theory), the indirect effect of size on bending strength is considered. The indirect effect is based on the relationship between timber dimensions and timber properties followed by the relationship between timber properties and strength properties.

2 Materials and Methods

A total of 6501 specimens were used in the investigation consisting of the data of 15 research projects from the database of Holzforschung München and additional tested material. 4156 specimens were tested in bending: 3899 specimens represent the timber quality in Europe, 257 specimens were totally free of knots to investigate the size effect of defect-free material in structural size. 2345 specimens were tested in tension and were used to complete the database for the relationship of timber dimensions and timber properties. Figure 2 shows the dimensions of all 6501 specimens separated by the type of testing (edgewise bending (edge), flatwise bending (flat), tension).

Beside bending or tension strength a lot of parameters were measured to provide a broad database: The dimensions (width, height, span, distance between loading heads, length) were measured with a measuring tape. Between the loading heads all knots with a diameter greater than 5 mm were determined and the correct size and position of each knot was documented in a computer program created to calculate different knot values. Dry density, moisture content, growth ring width, compression wood, distance to the pith and orientation of growth rings were determined on defect-free slides which were cut out of each specimen next to the failure after testing. To prevent an influence of moisture content on the results, the strength was corrected to a moisture content of u = 12 % by equation (2):

$$f_m(u = 12\ \%) = f_m(u) + f_m(u) \cdot (u - 12) \cdot (0.02 + (f_m(u) - 45) / 2000) \quad (2)$$

This equation was derived from GLOS 1981 (Table 2) and MADSEN ET AL. 1980 (Figure 3) (GLOS 1981). Among 11 different knot values (different knot values acc. to DIN 4074, ECE-method, KAR-method,...) the ones with the best direct correlation to the bending strength at u = 12% were identified and used for further analysis. Subsequently, tKAR and mKAR were selected and used to describe knottiness.

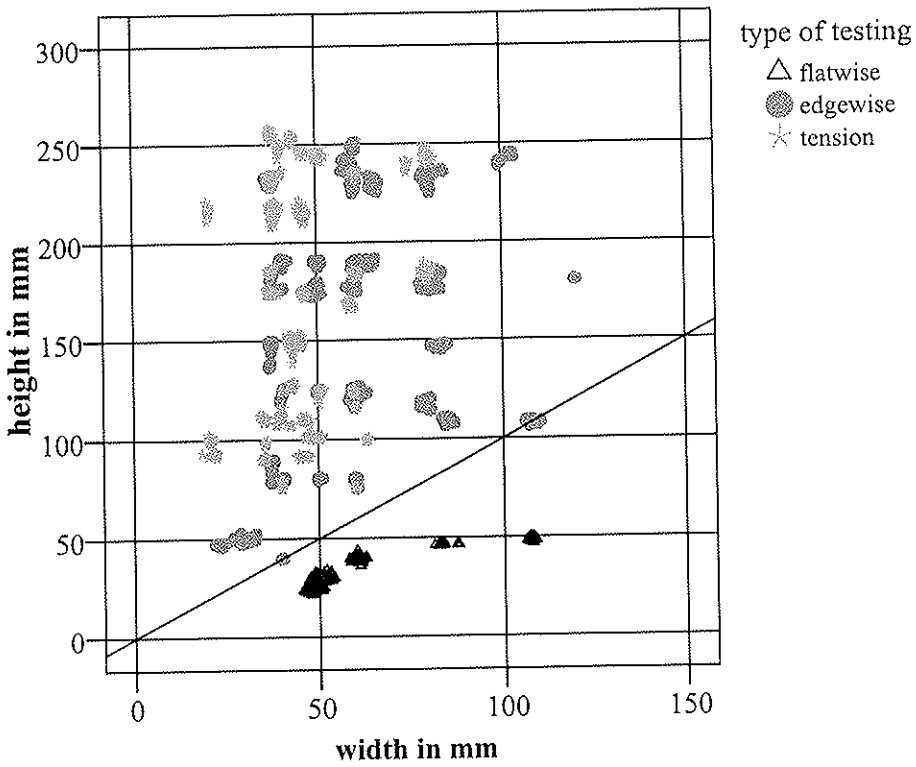

Fig. 2: Height versus width separated by the type of testing, n = 6501 specimens.

3 Relationship between timber dimensions, timber properties and timber bending strength

To investigate the relationship between timber dimensions and timber bending strength 3899 bending specimens were used. The different span-to-depth-ratios were not considered in this first step. Figures 3 and 4 show the relationship between bending strength and width or height, respectively. As all specimens were tested with a span to depth ratio between 12.5 and 20, the span is not shown separately. The influence of height is combined with the influence of length due to the ratio. On average, the bending strength decreases with increasing height and length being totally in line with the WEIBULL theory. The increase of strength with on average increasing width does not follow the WEIBULL theory (Fig. 3). Therefore, there must be some other influences overlapping the influence of volume on strength for solid timber.

Figures 5 and 6 show the relationship between bending strength and knot values tKAR and mKAR, respectively. On average, both knot values decrease with increasing bending strength. To find out, if there are relationships between volume and timber properties, Figures 7 and 8 were created. As the relationship between timber dimensions and knot values is independent of the type of testing all 6422 specimens with knots were used. On average, both knot values decrease with increasing dimension.

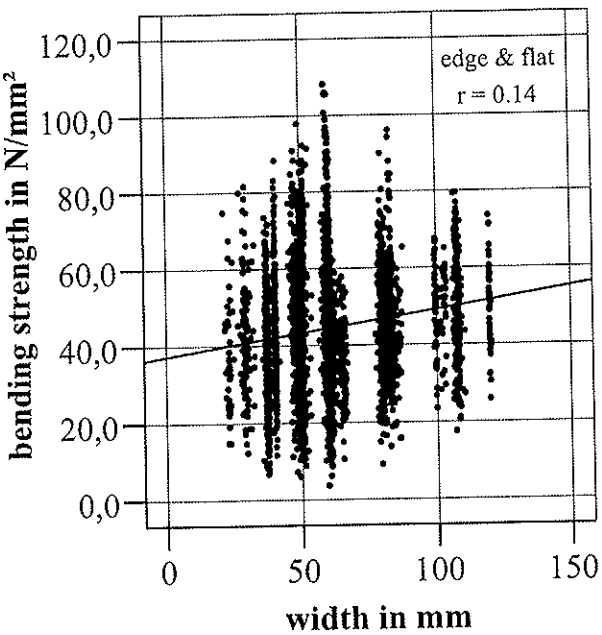

Fig. 3: Bending strength versus width, n = 3899 specimens.

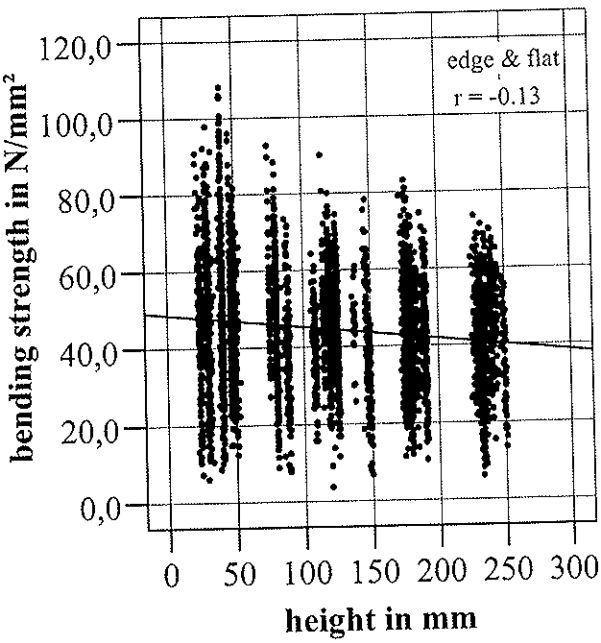

Fig. 4: Bending strength versus height, n = 3899 specimens.

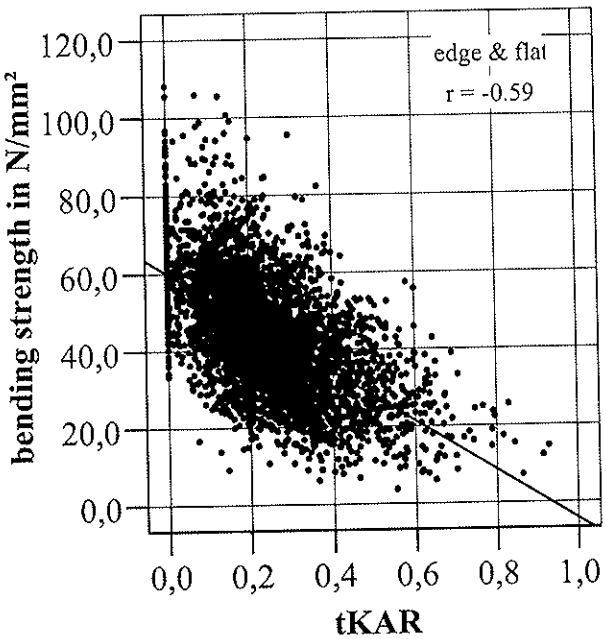

Fig. 5: Bending strength versus tKAR, n = 3899 specimens.

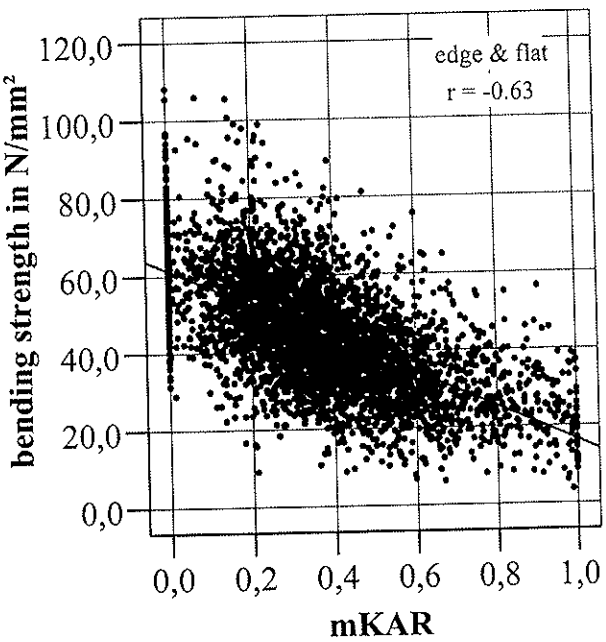

Fig. 6: Bending strength versus mKAR, n = 3899 specimens.

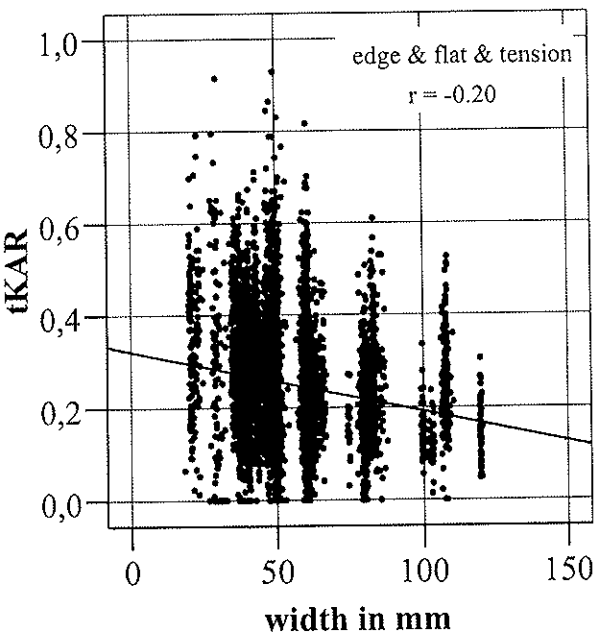

Fig. 7: tKAR versus width, n = 6244 spec.

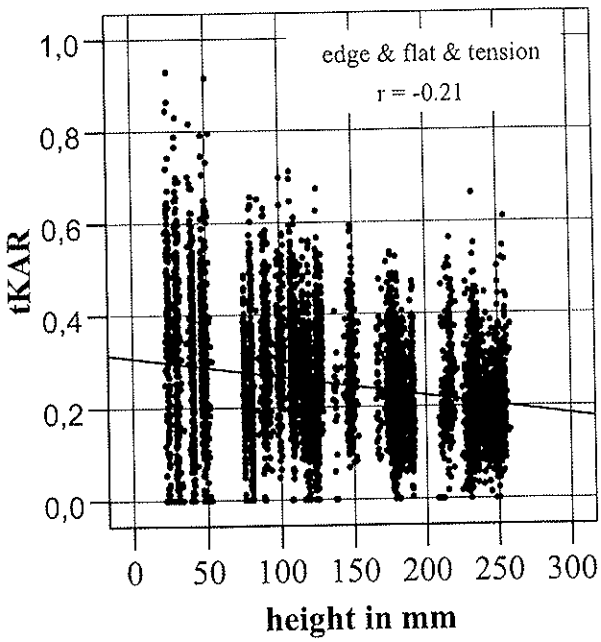

Fig. 8: tKAR versus height, n = 6244 spec.

These basic relationships lead to a model, which is summarized in Figure 9. There is a direct influence of the volume on the bending strength of timber. In the following, this influence is called "direct size effect" and is linked to the WEIBULL theory. Additionally, there is an "indirect size effect" based on the influence of the volume on timber properties and the influence of timber properties on the bending strength. All parameters (tKAR, mKAR, growth ring width, density, direction of the growth rings, compression wood) were tested for their contribution to the indirect size effect. The indirect size effect is mainly caused by knots: With increasing volume the knot values decrease and therefore, strength increases. Other parameters are also influenced by timber size but these effects are small compared to the ones on knots.

In real bending tests only a combination of direct and indirect size effect can be investigated. In the following, this effect is called "combined size effect" and can only be mathematically separated by its two components.

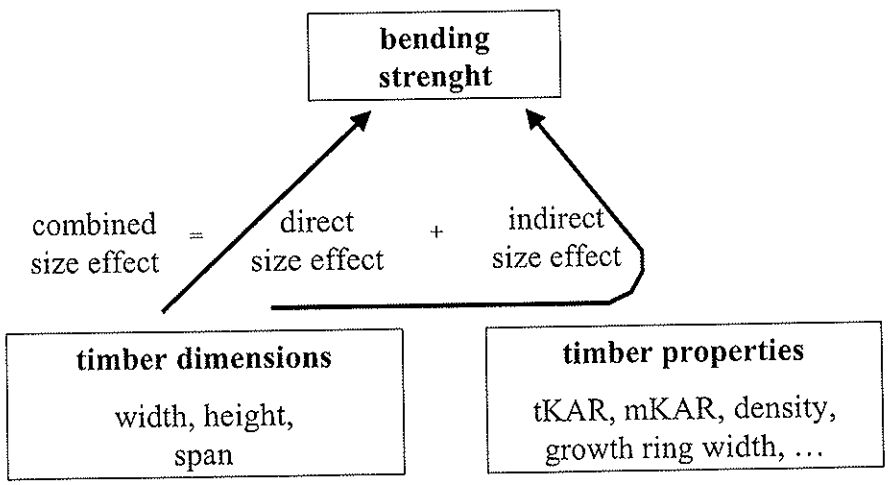

Fig. 9: Combined, direct and indirect size effect.

4 Modelling the size effect in bending

With the help of Figure 9, a mathematical model can be created to describe the combined size effect of timber in bending. The model was based on 2975 specimens tested with a span to depth ratio of 18 times the height and the worst defect placed between the loading heads on the tension side. This case was chosen as this applied for most data available. For a given span to depth ratio the influence of length and the influence of height on strength can not be separated. Therefore, both influences are combined in one factor referring to the height. The exponent is named "g_0" to show that it is a combined influence of length and height. Equation (2) summarizes the mathematical model in principal:

$$E(f_{m,u=12\%}) = \underbrace{f(\text{wood properties})}_{\text{indirect size effect}} \cdot \underbrace{\left(\frac{75}{w}\right)^{w_0} \cdot \left(\frac{150}{h}\right)^{g_0}}_{\text{direct size effect}} \quad (2)$$

In a first step, all parameters were examined due to their potential to improve the correlation with bending strength by multiple regressions. Only those parameters should be used, which improve the description of strength significantly. Within the multiple regressions all parameters were used solely, squared, combined and up to the third dimension in every combination possible. This regression analysis showed that only mKAR, density, growth ring width, height and tKAR significantly influence the bending strength. All other parameters like compression wood, distance to the pith, growth ring orientation and width did not contribute significantly, as their influence on bending strength is represented by other parameters included in the multiple regressions. Based on this knowledge equation (3) was used to develop the size effect in bending:

$$E(f_{m,u=12\%}) = f(\rho_0, \text{jrb}, \text{tKAR}, \text{mKAR}) \cdot \left(\frac{150}{h}\right)^{g_0} \quad (3)$$

Equation (3) was used for different sub-samples. First of all it was used for 304 specimens with a tKAR <= 0.05 to investigate the size effect of defect-free material. The exponent of height is $g_0 = 0.09$ in this case (Tab. 1). Then the equation was used for the remaining 2671 specimens with a tKAR > 0.05. In order to check the significance of the result these 2671 specimens were separated: 1778 were used to calculate the equation, 893 were used to control the result. Table 1 summarizes the different equations and correlation coefficients with bending strength at u = 12%. The correlation of the test sample is as high as the correlation of the basic sample. The exponent of height of these pieces slightly differs from the one of the defect free sample.

Tab. 1: Summary of results for a span of 18 times height.

sample	n	$E(f_{m,u=12\%}) =$		r
-	-	N/mm²		-
defect free, 18*h	304	$(30.2 + 0.0810 \cdot \rho_0 - 1.82 \cdot \text{jrb}) \cdot \left(\frac{150}{h}\right)^{0.09}$	(4)	0.55
basic 18*h	1778	$(29.4 + 0.0917 \cdot \rho_0 - 2.76 \cdot \text{jrb} - 21.8 \cdot \text{tKAR} - 31.6 \cdot \text{mKAR}) \cdot \left(\frac{150}{h}\right)^{0.10}$	(5)	0.79
test 18*h	893			0.79

To check the influence of the location of the worst defect (location in the tension or in the compression zone) on size effect 517 specimens tested without special orientation were analysed. Figure 10 shows that the effect of size on strength is not influenced by the location of the knots. Therefore, the given equations can be used in both cases.

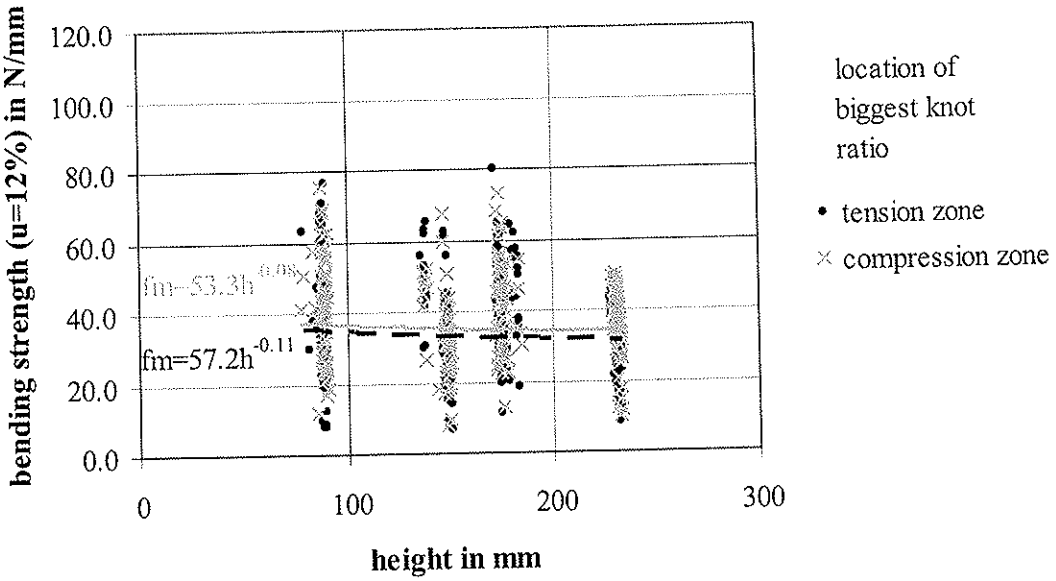

Fig. 10: Effect of orientation of worst defect on bending strength at u = 12 %, n = 517 specimens.

Table 1 leads to the following conclusions: The size effect is a combination of a direct and an indirect effect. The width does not influence the bending strength of solid timber directly. It influences the properties and therefore, it is an indirect one. With a constant span to depth ratio the influence of height and length can not be separated. The influence of height and length is a combination of a direct and an indirect effect.

The size effect of width and height according to equation (5) is shown in Figures 11 and 12 separated by percentiles. The exponent of the size effect of width varies between $w_0 = -0.02$ and $w_0 = +0.35$ depending on percentile. The exponent of the combined size effect of height varies between $w_0 = -0.09$ and $w_0 = +0.08$ also depending on percentile. The 95 percentile values represent the direct influence of volume on strength. They follow the WEIBULL theory for both width and height. For lower percentiles, the indirect size effect increases: As knot sizes increase with decreasing percentile, the indirect size effect increases with decreasing percentile. The direct size effect is overlapped by the influence of volume on wood properties which is contrary to the first one. With increasing volume, the knot value decreases and therefore, strength increases. On the level of 5 percentile values the combined effect leads to an increasing strength with increasing dimension.

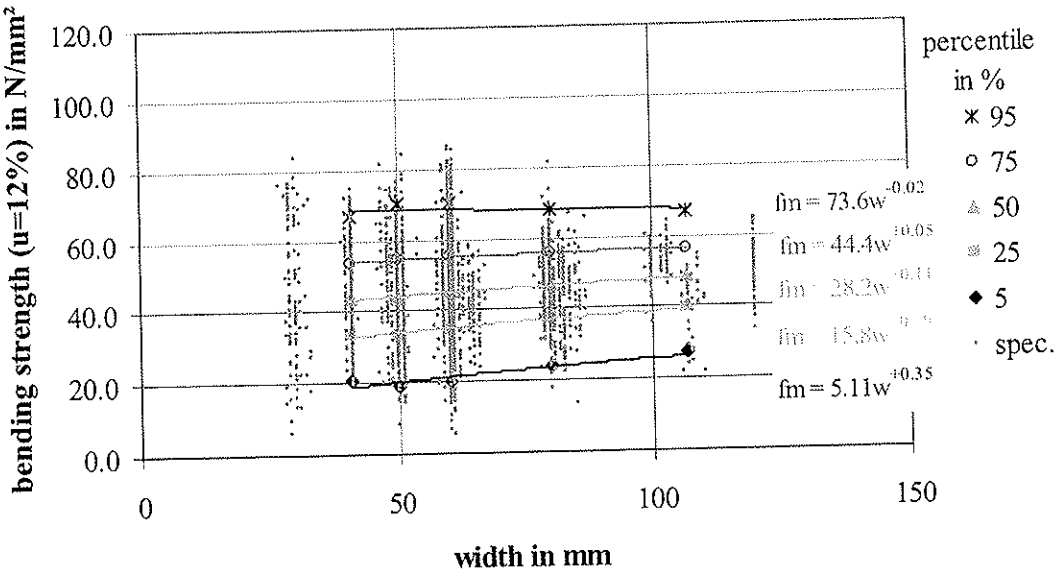

Fig. 11: Bending strength at u = 12 % versus width, n = 2889 specimens.

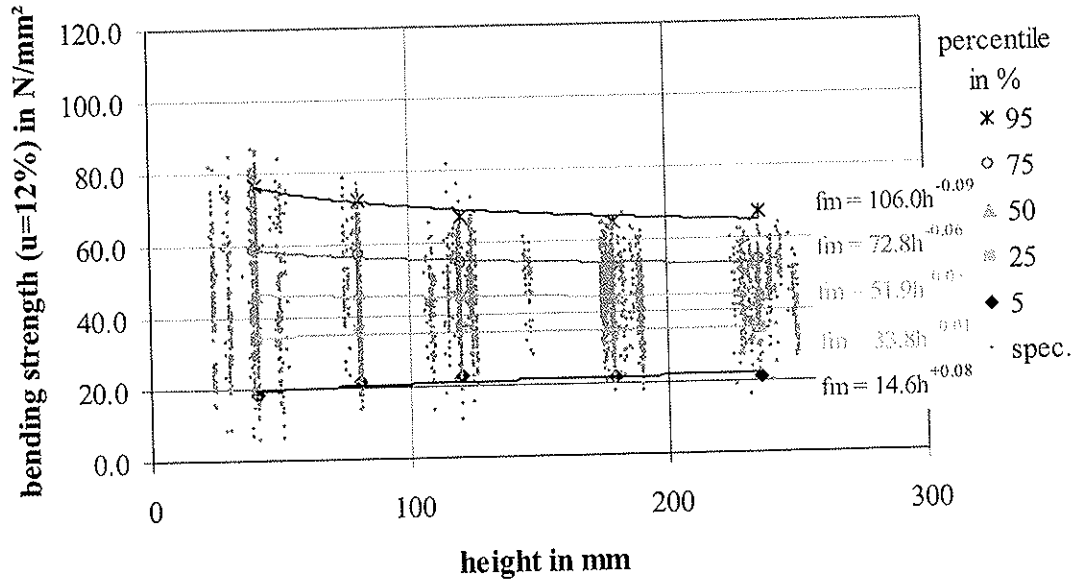

Fig. 12: Bending strength at u = 12 % versus height, n = 2889 specimens.

To especially check the great positive influence of the width on the characteristic strength literature has been studied. Figure 13 shows that other researchers too came to this result for 5 percentile values with a similar behaviour and with comparable exponents.

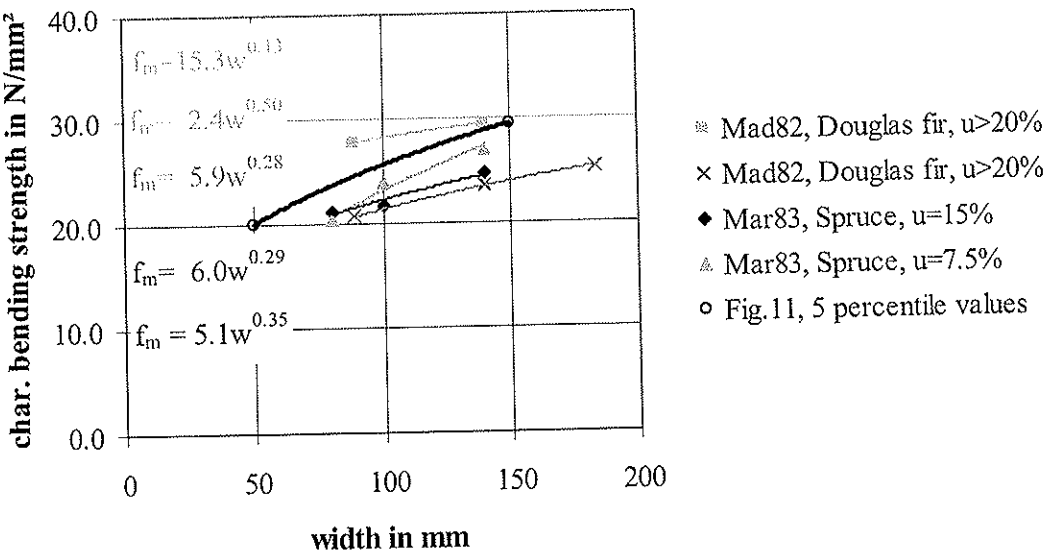

Fig. 13: Characteristic bending strength at u = 12 % versus width (literature results).

After having solved the equation for a constant span-to-depth-ratio of 18 times the height, the equation was extended to different span to depth ratios in a consistent manner: In a first step, the combined height and length factor was separated and calculated for defect-free specimens. As the equation of the influence of wood properties was not changed, all 2889 specimens with knots and 257 defect-free specimens were used to investigate the separated effect of height and length. The result was checked on 493 specimens of solid timber tested at span-to-depth-ratios different from 18 times the height. In this case too the correlation is the same for the basic and the test sample (Tab. 2).

Tab. 2: Summary of results for different span-to-depth-ratios.

sample	n	$E(f_{m,u=12\%}) =$	r
-	-	N/mm²	-
basic x*h	3146	$(29.4 + 0.0917 \cdot \rho_0 - 2.76 \cdot jrb - 21.8 \cdot tKAR - 31.6 \cdot mKAR) \cdot \left(\frac{150}{h}\right)^{0.04} \cdot \left(\frac{2700}{s}\right)^{0.06}$	0.80
test x*h	493		0.80

The results summarized in Table 2 were obtained with a limited number of specimens. Therefore, these results should be checked and verified by a bigger number of test results before they are used.

4 Influence of test method and grading rules

The size effect given in this paper was investigated for bending tests according to EN 408 meaning in particular that the worst defect is located between the loading heads. Boards from the database were mathematically analysed to investigate the influence of length on bending strength when the worst defect is not systematically placed between the loading

heads (Fig. 14). With increasing length tKAR increases on average and on 95 percentile values. The increase depends on the height of the specimen. Therefore, compared to the factor determined in chapter 3 a higher length effect factor will be detected when the worst defect is not systematically placed between the loading heads.

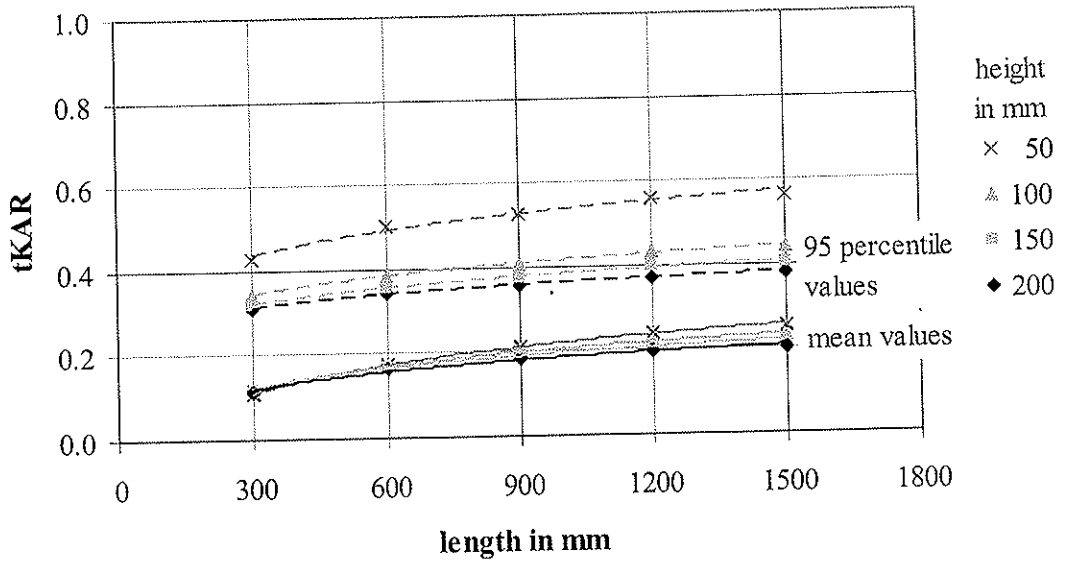

Fig. 14: Influence of length on maximum knot size between loading heads, if the test piece is placed randomly into the testing machine i.e. the worst defect is not placed systematically between the loading heads, n = 1496 specimens.

To answer the question if the grading rule can influence the size effect, 517 specimens were graded according to the German rule DIN 4074 and the American NGR. Figure 15 shows that the NGR leads to higher size effect factors than DIN 4074 on 5 percentile level especially for low grades. The indirect influence of volume on bending strength depends on the grading method. Grading influences the effect of volume on wood properties and therefore, influences the size effect.

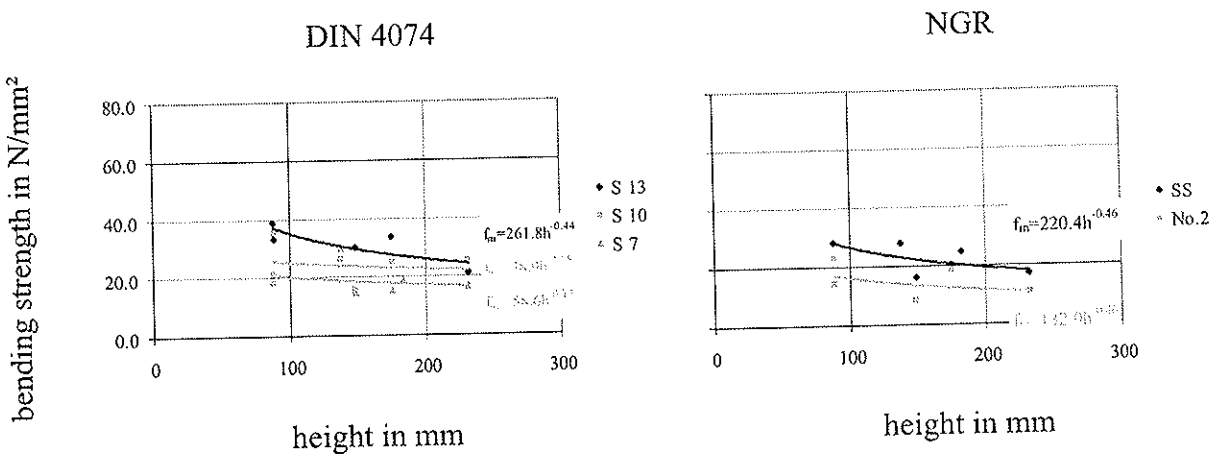

Fig. 15: Bending strength versus height for timber graded acc. to DIN 4074 and to NGR on the 5 percentile level, n = 517 specimens.

Due to the indirect influence of volume on strength the size effect can differ between various countries, for example due to the applied test method and the grading rules. It can be shown that the size effect factors in North America must exceed the ones in Europe due to different test standards and different grading methods.

4 Conclusion

This paper deals with the relationship between dimensions, properties and bending strength of spruce timber. The size effect on the basis of the WEIBULL theory has been extended by the effect of the properties on the bending strength, which has not been sufficiently taken into account so far. It is shown that the size effect consists of a direct as well as an indirect effect of timber dimensions on the bending strength. The indirect effect is based on the interaction between timber dimensions and timber properties and therefore, depends on the grading method. Beside this relationship, the size effect significantly depends on the test method and can therefore, due to different test standards, differ between countries. Based on the results, it is recommended not to include a size effect factor in the European Standards.

6 Literature

EN 338:2003-04
Structural timber - Strength classes. CEN European Committee for Standardization, Brussels. 9.

EN 384:2004-01
Structural timber - Determination of characteristic values of mechanical properties and density. CEN European Committee for Standardization, Brussels. 15.

EN 408:2003-08
Timber structures - Structural timber and glued laminated timber - Determination of some physical and mechanical properties. CEN European Committee for Standardization, Brussels. 32.

GLOS, P. (1981):
Zur Modellierung des Festigkeitsverhaltens von Bauholz bei Druck-, Zug- und Biegebeanspruchung. Berichte zur Zuverlässigkeitstheorie der Bauwerke, Heft 61, SFB 96, TUM. München, Germany. 54. (only available in German)

MADSEN, B.; JANZEN, W.; ZWAAGSTRA, J. (1980):
Moisture effects in lumber. Structural research Series Rep. No. 27. University of British Columbia. Vancouver, Canada. 94.

MADSEN, B.; STINSON, T. (1982):
In-grade testing of timber four or more inches in thickness. Structural Research Series Rep. No. 25, Department of Civil Engineering. University of British Columbia. Vancouver, Canada. 34.

MARCHAND, G.E.; FUX, W. (1983):
Statistisch gesicherte Untersuchungen von Festigkeitswerten biegebeanspruchter Bauteile aus Schweizer Holz. SAH Bulletin. Zürich, Schweiz. 3-26. (only available in German)

INTERNATIONAL COUNCIL FOR RESEARCH AND INNOVATION
IN BUILDING AND CONSTRUCTION

WORKING COMMISSION W18 - TIMBER STRUCTURES

APPLICABILITY OF EXISTING DESIGN APPROACHES TO MECHANICAL JOINTS IN STRUCTURAL COMPOSITE LUMBER

M Snow
Wentworth Institute of Technology & University of New Brunswick
Boston, USA & Fredericton
CANADA

I Smith
A Asiz
University of New Brunswick, Fredericton
CANADA

M Ballerini
Università degli Studi di Trento
ITALY

Presented by M. Snow

F. Lam asked how many specimens were tested in each cell. M. Snow replied 6 in some cases and 10 in other cases. F. Lam received confirmation that the 5th percentile values were based on normality assumption and cell COV. He commented that since there are large non-conservative differences between results and proposed provisions in Canadian code, one needs to carefully consider the information in code committee. I. Smith stated that this information was presented to the subcommittee on fastener design in Canada. The approach is to consider the LVL material to be equivalent to sawn DF timber which would be conservative. H.J. Larsen stated that the paper presented in CIB with low number of specimens should not use 5th percentile. The only way is to compare model with mean values and COV should be based on global values and not individual test cells. He commented that the results are confusing because material properties were not reported. He asked whether the yield moment, embedment strength, and withdrawal with rope effect were studied. A. Leijten asked about fracture energy values in EC5 and whether this would be appropriate for this type of material. He commented that referencing literature should mention the author. He asked whether embedment strength of single fastener was tested and expressed dissatisfaction with Table 4. H. Blass recommended that the paper be revised to provide missing information on material properties.

Applicability of Existing Design Approaches to Mechanical Joints in Structural Composite Lumber

Monica Snow*
Wentworth Institute of Technology & University of New Brunswick
Boston, USA & Fredericton, Canada
(*Corresponding author: msnow@unb.ca)

Ian Smith & Andi Asiz
University of New Brunswick
Fredericton, Canada

Marco Ballerini
Università degli Studi di Trento
Trento, Italy

1 Introduction

Despite recent increase of Structural Composite Lumber (SCL) consumption in construction, there is little knowledge about how to make efficient connections using such material. From a design perspective, it is essential that failure characteristics in SCL connections be recognized and understood. To date a very conservative approach based on an assumption of equivalency between performances of SCL and solid wood lumber connections has been adopted in day-to-day design practice in North America. The purpose of this paper is to investigate applicability of existing design approaches to mechanical joints in SCL based on comparison with test data collected at the University of New Brunswick [1, 2].

Experimental work investigated failure characteristics of mechanical joints constructed using the types of SCL known as Laminated Veneer Lumber (LVL), Parallel Strand Lumber (PSL) and Laminated Strand Lumber (LSL). These materials are manufactured as proprietary products in nominal sizes similar to those for dimensional lumber, and their mechanical responses are highly dependent on manufacturing process variables. LVL, PSL and LSL corresponded to the most diverse alternative commercially available SCL products at the time of the investigation. Thus tested joints were surrogates for establishing how mechanical responses of all mechanical joints in SCL might differ from mechanical responses of similar joints in sawn lumber. Joints were constructed using commonly available dowel-type metal fasteners like bolts, nails and screws. Centre members were either SCL or sawn lumber, with the lumber alternative being the benchmark situation. Side members were made from sawn softwood lumber, SCL, steel plates or a high strength transparent plastic. Single or multiple fasteners in single or double shear arrangements were loaded in joint configurations

that resulted in SCL or lumber members being loaded parallel or perpendicular to the strong axis of material symmetry. Test results including joint strengths and failure mechanisms that were compared with those assumed as the basis of existing design provisions applicable or proposed for use in Canada [3] and Europe [4].

2 Experimental program

2.1 Bolted joints

Three series of tests were performed on bolted SCL joints. One series evaluated the failure behaviour of single and multiple-bolt joints with a central LVL, PSL or LSL member loaded parallel to the strong axis and GE Lexan® (a high strength transparent polycarbonate) as side members. Another series of tests investigated similar joints with the SCL member loaded perpendicular to the strong axis. A third series examined simple tension joints in LVL with exterior steel splice plates. All tests were conducted under static load conditions. In all tests high strength SAE Grade-8 bolts [5] were used to minimize possibility of yielding of the bolts, and to ensure failure of the wood products rather than the fasteners. As a comparison, matched specimens with either Eastern white pine [*Pinus strobus* L.] or spruce [*Picea sp.*] sawn lumber substituted for SCL members. All specimens were conditioned in an environment of 20°C/65% RH for more than three weeks prior to preparation and testing. This corresponded to equilibrium moisture contents of between 6 and 9% for SCL and 12% for sawn lumber members.

2.1.1 SCL bolted joints with polycarbonate side members

LVL Microllam® Grade 2600Fb-1.9E Douglas fir [*Pseudotsuga menziesii* (Mirb.) Franco], PSL Parallam® Grade 2900Fb-2.0E Douglas fir, and LSL TimberStrand® Grade 2250Fb-1.5E Yellow poplar [*Liriodendron tulipifera* L.] were used as the centre members in parallel to the strong axis of SCL joint tests. Weldwood® LVL (currently West Fraser® LVL) Grade 3100Fb-2.0E Southern Yellow Pine [*Pinus sp.*], Parallam® PSL Grade 2900Fb-2.0E Douglas fir, and TimberStrand® LSL Grade 2250Fb-1.5E Yellow poplar were used in perpendicular to strong axis of SCL tests. North American design practice is that all SCL are assigned identical bolt capacities as for similar joints with sawn lumber members from the Douglas fir–Larch species group with a specific gravity of 0.5. Thus the present tests where Pine was used as the control species departed from that practice. All SCL and sawn lumber members were 44 mm thick by 89 mm deep in cross-section. There were six replications of each test series as was practice in similar past studies [6 9]. Test series followed the protocol outlined in ASTM D5652-95 R2000 [10]. For single bolt tests, 19mm diameter bolts were used. Either 19mm diameter or 9.5mm diameter bolts were used for the multiple bolt configurations, with sizing for specific bolt arrangements based on the principle of constant net cross-section. The intent was to minimize the reduction in shear capacity of the member due to removal of material to create bolt holes. For more complete details see Snow [11].

2.1.2 LVL bolted joints with steel side members

LVL and sawn lumber joints were tested in simple tension in a double shear arrangement. Temlam® Grade 3300Fb-2.0E birch [*Betula sp.*] and aspen [*Populus sp.*] LVL [12] was used as the centre member and 13mm thick Grade A36 [13] steel splice plates as side members. The joint had either one row of three 13mm bolts or 2 rows or three 13mm bolts, with a one-bolt arrangement tested for comparison. Wood members were 44mm thick by 164mm deep LVL, or 38mm thick by 164mm Select Structural grade Spruce or Pine sawn lumber. Effects of variations in spacing, edge and end distances were studied. There were ten replications of each test series. For more complete details see Smith et al [1].

2.2 Joints with nails and screws

Three-member LVL–LVL–LVL splice joints were tested using nails or various types of screws. Fastener types were slender nails, lag screws and proprietary self-tapping screws. Specifically, LVL was Temlam® Grade 3300Fb-2.0E birch and aspen. Prior to testing the LVL was conditioned at a temperature of 20°C/65% RH. Nails were driven manually from the sides towards the centre member without pre-drilled lead holes. Lag screws were inserted through 4.8mm pre-drilled lead holes. The self-tapping screws were installed without pre-drilled holes. Because general experience is that mechanical properties of wood joints with slender fasteners are similar under compressive and tensile static loading [14], all connections were statically tested in the compressive mode following general principle of ASTM Standard D1761-06 [15]. LVL specimen member cross-sections were 44mm by 146mm or 44mm by 95mm. Figures 1 and 2 and Tables 1 and 2 summarize fastener sizes and arrangements studied.

3 Design approaches

Standard practice in Canada and elsewhere [16] is to assume that validity of design code models for the capacities of isolated components like members and joints is proven if model predictions accurately agree with experimental observations of the 5-percentile strengths under static load conditions. Here, estimates of 5-percentile ultimate experimental strengths are compared to current and proposed code models. Bolted joint strength predictions are based on existing design provisions of CSA Standards O86-01 [3] and Eurocode 5 [4], as well as proposed models by Quenneville [17] and Ballerini [18] that address brittle failure mechanisms.

3.1 CSA Standard O86-01

Currently the Canadian timber design code requires assessment of laterally loaded bolts and lag screws to be based on solely what North Americans call the European Yield Model (EYM) failure capacity. EYM capacities are calculated according to clause 10.4.4.2 of CSA Standard O86-01 [3]. There is no explicit account of brittle failure mechanisms but the approach does contain empirically based adjustments to allow for the possibility of splitting failures if fasteners are not slender, or if fastener end, edge and spacing distances are small. It is also required that minimum requirements be met in respect of fastener end, edge and spacing distances. However, as Quenneville has demonstrated, the practices are inconsistent in their ability to discriminate between fastener arrangements that promote splitting and those that do not. Thus Quenneville has proposed a simplified set of design equations accounting effects of a range of potentially governing brittle mechanisms.

3.2 Eurocode 5

Eurocode 5 (EC5) specifies need for evaluation of bolted joints for both ductile and brittle failure mechanisms, and specifically addresses the use of LVL. EYM equations, of similar intent but differing in the details (relative to Canadian practice), are used to assess the ductile failure mechanisms and capacity of joints with dowel type fasteners. The possibility of brittle failure is addressed through specification of minimum spacing, edge, and end distance rules. When fasteners load members of sawn lumber, glulam or LVL perpendicular to grain, a semi-analytical calculation is made of member splitting capacity. That splitting capacity is compared with the total load applied to a group of fasteners to assess whether splitting is possible. The member splitting capacity formula is calculated based on a proposal by van der Put [19] that incorporates Linear Elastic Fracture Mechanics (LEFM) considerations.

Van der Put's work, and therefore the EC5 method, considers only the influence of some joint configuration variables on splitting strength of a member and is thus quite simple (Equation 1).

$$F_{R,90,k} = 2b \cdot k_k \cdot \sqrt{\frac{h_e}{1-\alpha}} \quad [\text{N}] \qquad \text{with} \quad k_k = \left(\sqrt{GG_c / 0.6}\right)_k = 14 \tag{1}$$

The joint specific design parameters are: b = member thickness, h = member depth, h_e = distance from the loaded edge to the furthest fastener (loaded edge distance), G = shear modulus of member, G_c = critical fracture energy release rate, $\alpha = h_e / h$.

3.3 Quenneville proposal

Embodied in the proposal from Quenneville [17] are design processes for assessment of brittle failure mechanisms in joints with bolts and dowels that load members of solid wood either parallel or perpendicular to grain.[1] A major component of the proposal is quantification of the resistances of wood members with laterally loaded fasteners for brittle failure mechanisms of 'shear failure in the row', 'group tear-out', and 'net tension', applicable when fasteners load wood parallel to grain. Similarly a proposal is made for calculation of the 'splitting resistance' applicable when fasteners load wood perpendicular to grain. The equations for performing such calculations are extensive and readers should refer to the paper by Quenneville for details.

3.4 Ballerini proposal

Ballerini has proposed a semi-empirical formula for prediction of splitting strength of wood members loaded perpendicular to grain by dowel-type fasteners. It is based on both theoretical analysis and extensive experimental research, and is a refinement of approach by van der Put's already incorporated into EC5. The proposed formula refines the consideration of joint geometry (i.e. arrangement of fasteners) so as to better address the complexity of multi-dowel joint failures. The generalized form of the Ballerini equation (Equation 2) as given here determines both the average strength and the 5-percentile characteristic strength for single and multiple-dowel joints loaded perpendicular to grain:

$$F_{R,90} = 2b \cdot k \cdot \sqrt{\frac{h_e}{1-\alpha^3}} \cdot f_w \cdot f_r \quad [\text{N}] \quad \text{where } k = \begin{cases} 14 & \textit{for the average strength} \\ 9 & \textit{for the characteristic strength} \end{cases} \tag{2}$$

$$\text{with} \quad f_w = 1 + 0.75\frac{l_r + l_l}{h} \le 2 \qquad \text{and} \qquad f_r = 1 + 1.75\frac{n \cdot h_m / 1000}{1 + n \cdot h_m / 1000}$$

The joint specific design parameters additional to those applicable to Equation 1 are:
n = number of rows of fasteners, h_m = height of fastener group, l_r = width of fastener group, l_l = distance between fastener groups.

3.5 Comparison of test results with design models

3.5.1 SCL joints with bolts and polycarbonate side members

Experimental results for joint where fasteners loaded SCL or sawn Pine lumber members perpendicular to their strong axis are compared with predictions by Ballerini and the EC5 splitting design equation. Table 3 summarizes the ratios of average (mean) ultimate test

[1] At the time this paper was written Quenneville's proposal was under consideration by the Canadian timber code committee,

strength to average and characteristic strengths predicted by models. Coefficient of variation (CoV) values within the table are rough indications of the variability in the test data.[2]

Comparisons in Table 3 suggest that the EC5 code model can be either conservative or non-conservative for design of joints where bolts load SCL or sawn lumber members perpendicular to their strong axis. The possibility of non-conservative predictions is greatest for sawn lumber members and least for LSL members. Predictions from the Ballerini model are always markedly conservative for SCL members, but can yield quite good agreement for joints with sawn lumber members. Predicted characteristic strengths according to the Ballerini model are about 2/3 of the associated predicted average strengths. Thus the Ballerini model is based on a CoV of joint strengths in the order of 20% [18], but CoV data in Table 3 suggests that variability in strength is much lower than that for joints in SCL. Overall the Ballerini model appears most reliable but neither that nor the EC5 model are accurate for joints in SCL.

3.5.2 LVL bolted joints with steel side members

Table -4 presents a comparison of the 5-percentile LVL bolted joint strengths predicted with two design approaches, the existing CSA Standard O86-01 (ductile failure mechanism based [3]) and the proposal submitted to the CSA code committee by Quenneville (ductile and brittle failure mode [17]). Both the existing Canadian design model and what Quenneville has proposed are both conservative predictions of the capacities of bolted joints in LVL.[3]

3.5.3 LVL joints with nails and screws

CSA Standard O86-01 uses the same design approach and model for joints made with either laterally loaded bolts or lag screws. Here assessment of lag screw joints is based on agreement between test 5-percentile resistances and code model predictions using the existing ductile response based EYM and the Quenneville proposal for ductile-brittle failure model (Tables -5). Tables 6 and 7 summarize results of comparisons of test data and design models for LVL joints made with nails and self-tapping screws.

For LVL joints with lag screws, it is clear that neither of the utilized design models is accurate in all cases. Both models tend to be conservative but there are exceptions. When the ductile failure mechanism governs, which is the case with few fasteners, the two models give the same result.

4 General discussion

Mechanical joints, especially those made using multiple dowel-type fasteners, are complex systems exhibiting a range of complex failure mechanisms. Therefore it is extremely difficult, and arguably impossible, to achieve robustly accurate predictions of which failure mechanisms will govern for particular joint designs. Similarly it is very difficult to predict strengths of joints accurately. Further, if it is desired to predict design capacities of joints using simple models, whether they are explicitly empirical or semi-analytical, it should not be surprising if they fail to make robust predictions of governing mechanisms or of failure loads. Introducing SCL as alternative types of structural members in lieu of products like sawn lumber will not in general alleviate the conundrum in general, but could in specific cases. For example, as discussed in detail by Snow [11], using a material like LSL instead of easily splitting wood products largely eliminates the need to consider brittle mechanisms and simple EYM type design models yield good results. More generally the message to be

---

[2] As the number of test replicates was small, it is only meaningful to calculate average test values from data.

[3] The Quenneville model was never explicitly intended or calibrated to apply to joints in LVL.

gleaned from this paper is that particular design models will only yield good predictions under well defined circumstances (i.e. for those of which they are intended and calibrated).

5 Conclusion

The existing Canadian and Eurocode5 design methods for joints in wood products made using dowel-type fasteners *did not perform consistently well* for joints with SCL members. The same is true for proposed alternative models that more explicitly address the possibility of brittle failure mechanisms governing the design of joints. It is imperative therefore that existing models and code rules be used with caution especially in an environment where the available range of structural wood products is evolving rapidly.

6 Acknowledgement

The authors gratefully acknowledge financial support from Natural Resources Canada under the projects UNB2 – Design Methods for Connections in Engineered Wood Structures (2003-2006) and UNB75 – Performance of Mechanical Fasteners Used with Engineered Wood Products (2007).

7 Literature

[1] Smith, I., Asiz, A. and Snow, M. 2006. Design methods for connections in engineered wood structures, Final Report UNB2, Value-to-Wood Program, Natural Resources Canada, Ottawa, ON, Canada.

[2] Smith, I., Asiz, A. and Snow, M. 2007. Performance of mechanical fasteners used with engineered wood products, Final Report UNB75, Value-to-Wood Program, Natural Resources Canada, Ottawa, ON, Canada.

[3]. Canadian Standards Association (CSA). 2005. Engineering design in wood, Standard O86-01 (consolidated issue), CSA, Toronto, ON, Canada.

[4] European Committee for Standardization (CEN). 2004. Design of timber structures - Part 1-1 General: Common rules for buildings, Eurocode 5 (Standard EN 1995-1-1), Brussels, Belgium.

[5] Society of Automotive Engineers. 1999. Mechanical and material requirements for externally threaded fasteners, Standard J429, SAE, Warrendale, PA, USA.

[6] Canadian Construction Materials Centre (CCMC). 2003. Microllam® LVL Evaluation Report, National Research Council (NRC), Ottawa, ON, Canada.

[7] CCMC. 2006. Parallam® PSL Evaluation Report, NRC, Ottawa, ON, Canada.

[8] CCMC. 2006. TimberStrand® LSL Evaluation Report, NRC, Ottawa, ON, Canada.

[9] CCMC. 2005. West Fraser® LVL Evaluation Report, NRC, Ottawa, ON, Canada.

[10] American Society for Testing and Materials (ASTM), Standard test methods for bolted connections in wood and wood base products, Standard D5652-95(2000), ASTM, West Conshohocken, PA, USA.

[11] Snow, M. 2006. Fracture development in engineered wood product bolted connections, PhD thesis, University of New Brunswick, Fredericton, NB, Canada.

[12] CCMC. 2006. Temlam® LVL Evaluation Report, NRC, Ottawa, ON, Canada.

[13] ASTM. 2005. Standard specification for carbon structural steel, Standard A36/A36 (2005), ASTM, West Conshohocken, PA, USA.

[14] Smith, I., Whale, L.R.J., Anderson, C., Hilson, B.O., and Rodd, P.H. 1988. Design properties of laterally loaded nailed or bolted wood joints, Canadian Journal of Civil Engineering, 15:633-643.

[15] ASTM. 2006. Standard test methods for mechanical fasteners in wood, Standard D1761 (2006), ASTM, West Conshohocken, PA, USA.
[16] Smith, I. and Foliente, G. 2002. LRFD of timber joints: International practice and future direction, ASCE Journal of Structural Engineering, 128(1):48-59.
[17] Quenneville, P. Draft of code change proposal for wood connections, Discussion paper (Meeting November 17-18, Montreal) CSAO86 Technical Committee, CSA, Toronto, ON, Canada.
[18] Ballerini, M. 2004. A new prediction formula for the splitting strength of beams loaded by dowel-type connections, CIB-W18 Conference Proceedings, Paper 37-7-5, Edinburgh, Scotland.
[19] van der Put T.A.C.M. 1990. Tension perpendicular to the grain at notches and joints, CIB-W18 Conference Proceedings, Paper 23-10-1, Lisbon, Portugal.

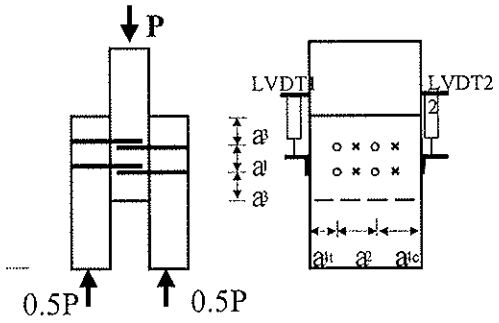

Figure 1: Layout of screws or nails in LVL loaded parallel to strong axis

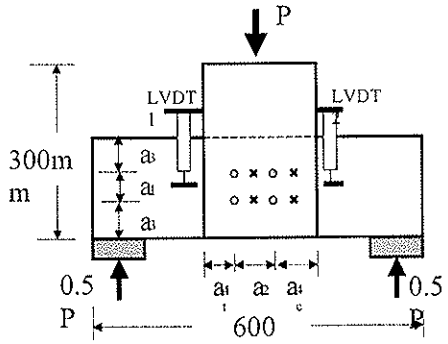

Figure 2: Layout of screws or nails in LVL loaded perpendicular to strong axis

Table 1: Placement of nails and screws in LVL joints loaded parallel to strong axis

Fastener type	Fasteners arrangement	Total no. of fasteners	a_1 (mm)	a_2 (mm)	a_3 (mm)	a_{4c} (mm)	a_{4t} (mm)
Common nail	76 mm, one each side	2	--	--	100	73	73
Spiral nail	76 mm, one each side	2	--	--	100	73	73
Lag screw	88 mm, one each side	2	--	--	100	73	73
Self-tapping screw	88 mm, one each side	2	--	--	100	73	73
Lag screw	88 mm, four each side	8	50	40	70	46	60
Self-tapping screw	88 mm, four each side	8	50	40	70	46	60
Common nail	76 mm, ten each side	20	70	70	50	35	41
Spiral nail	76 mm, ten each side	20	65	70	45	35	41
Lag screw	88 mm, ten each side	20	50	40	70	46	60
Self-tapping screw	88 mm, ten each side	20	50	40	70	46	60
Lag screw	127 mm, one in double-shear	1	--	--	100	73	73
Self-tapping screw	127 mm, one in double-shear	1	--	--	100	73	73
Lag screw	127 mm, four in double-shear	4	50	46	70	50	50
Self-tapping screw	127 mm, four in double-shear	4	50	46	70	50	50

Table 2: Placement of nails and screws in LVL joint loaded perpendicular to strong axis

Fastener type	Fastener arrangement	Total no. of fasteners	a_1 (mm)	a_2 (mm)	a_3 (mm)	a_{4c} (mm)	a_{4t} (mm)
Common nail	76 mm, one each side	2	--	--	73	73	73
Spiral nail	76 mm, one each side	2	--	--	73	73	73
Lag screw	88 mm, one each side	2	--	--	73	73	73
Self-tapping screw	88 mm, one each side	2	--	--	73	73	73
Common nail	76 mm, four each side	8	50	70	50	36	40
Spiral nail	76 mm, four each side	8	50	60	50	36	40
Lag screw	88 mm, four each side	8	50	40	50	36	40
Self-tapping screw	88 mm, four each side	8	50	40	50	36	40
Lag screw	127 mm, one in double-shear	1	--	--	73	73	73
Self-tapping screw	127 mm, one in double-shear	1	--	--	73	73	73
Lag screw	127 mm, four in double-shear	4	50	40	50	46	60
Self-tapping screw	127 mm, four in double-shear	4	50	40	50	46	60

Table 3: Comparison between experimental and predicted strength for SCL bolted joints: loaded perpendicular to strong axis
(F_u = average tests, $F_{m,pred}$ = average model, $F_{k,pred}$ = 5 percentile model)

Material	Fastener description	Total no. of fasteners	Ballerini proposal		EC5	COV test %
			$F_u / F_{m,pred}$	$F_u / F_{k,pred}$	$F_u / F_{k,pred}$	
Pine	Single bolt, 19mm	1	0.99	1.53	0.75	10.1
Pine	2 rows of 1 bolt, 19mm	2	0.87	1.36	0.96	32.1
Pine	1 row of 2 bolts, 9.5mm	2	1.00	1.56	0.76	6.8
Pine	2 row of 2 bolts, 9.5mm	4	0.74	1.16	0.79	4.2
LVL	Single bolt, 19mm	1	1.90	2.96	1.44	2.4
LVL	2 rows of 1, 19mm	2	0.94	1.47	1.03	6.7
LVL	1 row of 2 bolts, 9.5mm	2	1.46	2.27	1.10	9.7
LVL	2 row of 2 bolts, 9.5mm	4	0.90	1.40	0.95	7.1
PSL	Single bolt, 19mm	1	2.03	3.16	1.54	6.4
PSL	2 rows of 1, 19mm	2	1.07	1.66	1.17	8.8
PSL	1 row of 2 bolts, 9.5mm	2	1.64	2.55	1.24	7.1
PSL	2 row of 2 bolts, 9.5mm	4	1.18	1.83	1.25	9.3
LSL	Single bolt, 19mm	1	3.26	5.08	2.48	11.1
LSL	2 rows of 1, 19mm	2	2.92	4.54	3.20	9.8
LSL	1 row of 2 bolts, 9.5mm	2	2.31	3.59	1.75	16.4
LSL	2 row of 2 bolts, 9.5mm	4	1.99	3.09	2.11	13.3

Table 4: Comparison between experimental and predicted strength for LVL bolted joints: loaded parallel to strong axis
($P_{u,0.05}$ = 5 percentile test, All values adjusted to Standard Term Loading [3])

Joint description	Fastener spacing			Pu,0.05 (kN)	CSA O86-01 (kN)	Quenneville [minimum; ductile & brittle failure] (kN)
	End distance (mm)	Spacing of bolts within row (mm)	Spacing between rows (mm)			
LVL, 6 bolts (13mm), 2 rows of 3 bolts	89	51	63	44	22	22
	89	51	51	49	22	22
	127	51	63	50	29	29
	127	51	51	44	29	29
	89	76	63	42	24	24
	89	76	51	46	24	24
	127	76	63	62	32	32
	127	76	51	62	32	32

Table 5: Comparison between experimental and predicted strength for LVL lag screw joints
($P_{u,0.05}$ = 5 percentile test, All values adjusted to Standard Term Loading [3])

Direction of loading relative to strong axis	Description	Total no. of fasteners	$P_{u,0.05}$ (kN)	CSA O86-01 (kN)	Quenneville [minimum; ductile & brittle failure] (kN)
Parallel	3.5" Lag screw, one on each side	2	6.5	6.1	6.1
	3.5" Lag screw, 4 on each side	8	28	24	24
	3.5" Lag screw, ten on each side	20	48	48	61
	5.0" Lag screw, one double shear	1	7.2	6.1	6.1
	5.0" Lag screw, 4 double shear	4	23	24	24
Perpendicular	3.5" Lag screw, one on each side	2	7.0	4.7	4.7
	3.5" Lag screw, 4 on each side	8	22	18	12.4
	5.0" Lag screw, one double shear	1	9.0	4.7	4.7
	5.0" Lag screw, 4 double shear	4	25	19	12.4

Table 6: Comparison between experimental and predicted strengths for LVL nail and screw joints: loaded parallel to strong axis
($P_{u,0.05}$ = 5 percentile test, All values adjusted to Standard Term Loading [3])

Description	Total no. of fasteners	$P_{u,0.05}$ (kN)	CSA O86-01 (kN)	Quenneville [minimum; ductile & brittle failure] (kN)
Common nail, one on each side	2	6.0	2.3	2.3
Spiral nail, one on each side	2	4.3	1.7	1.7
3.5" self-tapping screw, one on each side	2	7.0	5.2	5.2
3.5" self-tapping screw, 4 on each side	8	25	21	21
Common nail, 10 on each side	20	25	23	23
Spiral nail, 10 on each side	20	22	17	17
3.5" self-tapping screw, 10 on each side	20	43	52	52
5.0" self-tapping screw, one double shear	1	6.0	5.2	5.2
5.0" self-tapping screw, 4 double shear	4	27	21	21

Table 7: Comparison between experimental and predicted strength for LVL nail and screw joints: loaded perpendicular to strong axis
($P_{u,0.05}$ = 5 percentile test, All values adjusted to Standard Term Loading [3])

Description	Total no. of fasteners	$P_{u,0.05}$ (kN)	CSA O86-01 (kN)	Quenneville [minimum; ductile & brittle failure] (kN)
Common nail, one on each side	2	7.1	1.8	1.8
Spiral nail, one on each side	2	6.2	1.3	1.3
3.5" self-tapping screw, one on each side	2	8.5	4.0	4.0
Common nail, 4 on each side	8	9.3	7.2	7.2
Spiral nail, 4 on each side	8	8.7	5.3	5.2
3.5" self-tapping screw, 4 on each side	8	23	16	12
5.0" self-tapping screw, one double shear	1	8.7	4.0	4.0
5.0" self-tapping screw, 4 double shear	4	26	16	12

INTERNATIONAL COUNCIL FOR RESEARCH AND INNOVATION
IN BUILDING AND CONSTRUCTION

WORKING COMMISSION W18 - TIMBER STRUCTURES

VALIDATION OF PROPOSED BOLTED CONNECTION DESIGN PROPOSAL

P Quenneville

J Jensen

The University of Auckland

NEW ZEALAND

Presented by J. Jensen

I. Smith commented that all models are inaccurate as the connections are complicated. More exact model will need computer. H. Blass commented that there is an easy solution to use full threaded screws to reinforce the connection to avoid brittle failure mode. A. Jorissen commented that in group tear out mode either shear or tension will have to collapse first therefore their strength should not be additive. A. Leijten discussed group tear out and other modes of failures and the simplified form of EYM. I. smith discussed the origin of the EYM current used in the Canadian code as a 1986 CIB W18 paper by Whale, Larsen and Smith. A. Salenikovich received confirmation that EYM only valid for ductile failure mode. H.J. Larsen commented that in EC the simplified EYM is not used. S. Winter received clarification of the treatment factor. H.J. Larsen stated that CIB W18 papers should not include these factors.

Validation of the Canadian Bolted Connection Design Proposal

Pierre Quenneville[1] and Jorgen Jensen[2]

[1] Professor of Timber Design, [2] Postdoctoral Research Fellow

The University of Auckland, New Zealand

1 Introduction

The Canadian wood design standard, O86 has recently adopted a design approach for the design of bolted connection based on the calculation of the resistances of the ductile and brittle failure modes. The engineering community realised that the approach to modify the European Yield Model (EYM) using in-row modification factors (or "row" or "end distance" factors) is not sufficient to account for all brittle failures. For instance, there are situations where the row spacing is not large enough to prevent group tear-out. Various sets of design equations have been proposed recently to account for the ductile and brittle failure modes for various types of bolted and dowelled connections. From work done during the last decade, a set of design equations is proposed to take into account the potential bolted connection failure modes, which are: yielding, row shear, group tear out (known as block shear in Europe), net tension and splitting perpendicular-to-grain. In this paper, the equations and their resistance equations are presented in their development and final design format and compared to past and recent experimental results. It is shown that these equations predict conservatively 99% of the specified resistance of individual available test data.

2 Design equations

In most design standards (CSA 2005, Eurocode 2005, NDS 2003), the approach for the design of multiple-bolted connections is solely based on the EYM, further modified in certain cases to attempt to account for potential brittle failure modes.

The failure modes which resistance needs to be verified are the ductile "yielding failures" and the brittle "fracturing failures" in the connection. The mode with the lowest estimated capacity will be the governing one. Some mode include a range of mechanisms; for example, the ductile modes will encompass the mechanisms associated with "Johansen type" dowel connection yield models, consisting of bearing of the wood in compression or in combination with yielding of the fastener. The brittle modes will include mechanisms associated with longitudinal shear or tension or tension perpendicular-to-grain.

As a result of the many recent studies on the brittle behaviour of connections in timber structures (Quenneville and Mohammad, 2000; Smith and Chui, 2006; Leijten and

Jorissen, 2001, Hanhijärvi and Kevarinmäki, 2008), failure modes have been identified and are as shown in Figure 1.

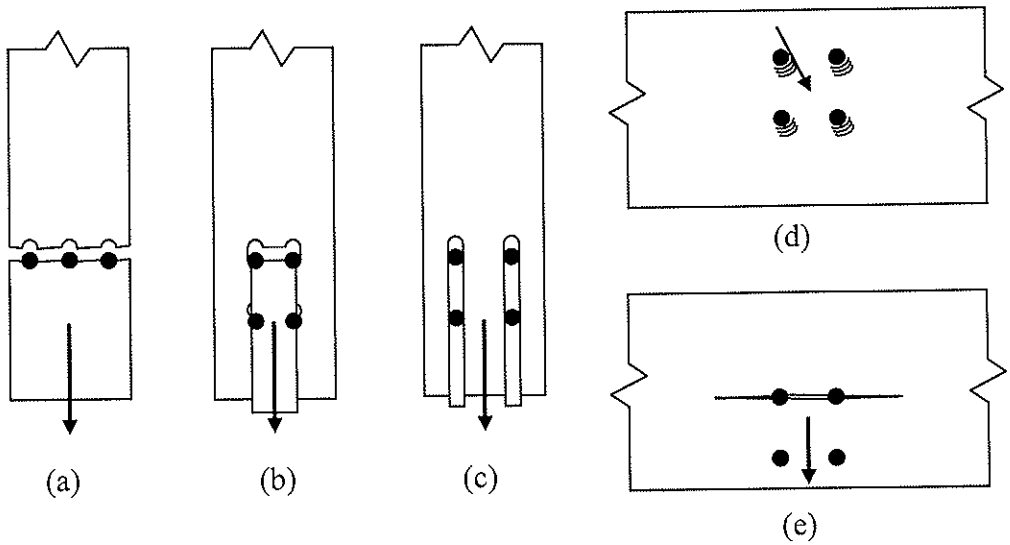

Figure 1 - Observed failure modes for timber bolted connections (a) net tension (b) group tear-out (c) row shear (d) bearing (e) splitting.

The design capacity of bolted connections will be the minimum value determined from the possible failures. Not all failure modes are possible in members loaded either parallel or perpendicular-to-grain and corresponding capacities will be compared to either the load applied or a function of its component parallel or perpendicular-to-grain. Basically, the designer will need to verify the following four equations:

$$N_f \leq R_{d\,b} \tag{1}$$

$$N_f \cos(\theta) \leq P_r = \text{Minimum}\,(R_{d\,rs}, R_{d\,gt}, R_{d\,nt}) \tag{2}$$

$$N_f \sin(\theta) \leq Q_r = \text{Minimum}\,(R_{d\,sp}, V_{d\,net}) \tag{3}$$

$$N_f \leq N_r = \frac{P_r\, Q_r}{P_r \sin^2(\theta) + Q_r \cos^2(\theta)} \tag{4}$$

Where N_f and N_r are the factored load and resistance at angle θ, $R_{d\,b}$ is the factored bearing resistance, $R_{d\,rs}$ is the factored row shear resistance, $R_{d\,gt}$ is the factored group tear-out resistance, $R_{d\,nt}$ is the factored net tension design capacity, $R_{d\,sp}$ is the factored splitting resistance and $V_{d\,net}$ is the reduced shear resistance.

2.1 Bearing capacity

For dowel type fasteners failing in one of the ductile modes, as shown in Figure 1(d), the bearing design capacity is given by:

$$R_{d\,b} = \phi\, B_u\, n_s\, n\, K_D\, K_{SF}\, K_T \tag{5}$$

ϕ = strength reduction factor = 0.8

B_u = minimum lateral ultimate bearing capacity (from the European Yield Model equations)
n = total number of fasteners in the joint
n_s = number of shear planes
K_D = duration of load factor
K_{SF} = service condition factor factor for the design of joints
K_T = treatment factor factor for the design of joints

where the lateral ultimate bearing capacity B_u, per shear plane is obtained from either equation 6 for one shear plane or equation 7, for two shear planes, whichever is applicable.

$$B_u = \text{Minimum} \begin{cases} f_1\, d\, t_1 \\ f_2\, d\, t_2 \\ f_1\, d^2 \frac{1}{5}\left[\frac{t_1}{d} + \frac{f_2}{f_1}\frac{t_2}{d}\right] \\ f_1\, d^2\left[\sqrt{\frac{1}{6}\frac{f_2}{(f_1+f_2)}\frac{f_y}{f_1}} + \frac{1}{5}\frac{t_2}{d}\right] \\ f_1\, d^2\left[\sqrt{\frac{1}{6}\frac{f_1}{(f_1+f_2)}\frac{f_y}{f_2}} + \frac{1}{5}\frac{t_1}{d}\right] \\ f_1\, d^2\sqrt{\frac{2}{3}\frac{f_2}{(f_1+f_2)}\frac{f_y}{f_1}} \end{cases} \quad (6)$$

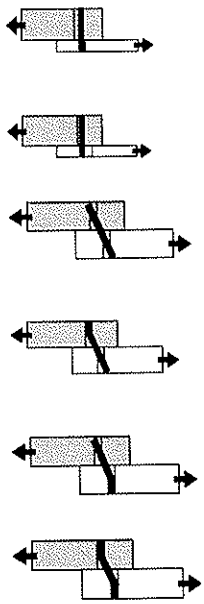

or

$$B_u = \text{Minimum} \begin{cases} 0.5\, f_2\, d\, t_2 \\ f_1\, d\, t_1 \\ f_1\, d^2\left[\sqrt{\frac{1}{6}\frac{f_2}{(f_1+f_2)}\frac{f_y}{f_1}} + \frac{1}{5}\frac{t_2}{d}\right] \\ f_1\, d^2\sqrt{\frac{2}{3}\frac{f_2}{(f_1+f_2)}\frac{f_y}{f_1}} \end{cases} \quad (7)$$

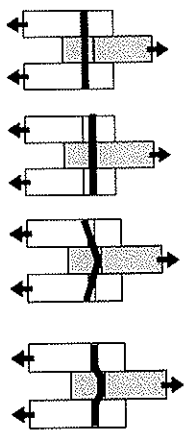

where f_1 = embedment strength of side member(s) calculated in accordance with equation 8, f_2 = embedment strength of middle member as per equation 8 as well, f_y = yield strength of the fastener of diameter d and t_1 and t_2 are the thickness of member 1 and 2 respectively. One will note that the Canadian equations for the ductile failures do not have second terms to take into account the potential rope effect. This is a potential impediment which, as it will be shown, makes most resistance predictions conservative.

For each wood member loaded at an angle θ, the embedment strength is obtained from:

$$f_{i\theta} = \frac{f_{i\,par}\, f_{i\,perp}}{f_{i\,par} \sin^2(\theta) + f_{i\,perp} \cos^2(\theta)} \qquad (8)$$

where:

$f_{i\theta}$ = embedment strength of member "i" for a fastener bearing at angle θ relative to grain (MPa).

$f_{i\,para}$ = design embedment strength for fastener bearing parallel to grain, (MPa)
= $f_{i\,para\,avg}$ 0.75/1.25 = 105 (0.8G) (1-0.01d) · 0.75 / 1.25
= 50 G (1-0.01d)

$f_{i\,perp}$ = design embedment strength for fastener bearing perpendicular to grain, (MPa)
= $f_{i\,perp\,avg}$ 0.75/1.25 = 46 (0.8G) (1-0.01d) · 0.75 / 1.25
= 22 G (1-0.01d)

G = mean relative density of the wood-based material, also known as specific gravity, for the oven dry condition. It is calculated as the density of the material for the oven dry condition normalized relative to the density of water, based on mass and volume after oven drying.

θ = angle of bearing relative to the strong material axis (parallel to grain of member)

The values of 0.75 and 1.25 are respectively to convert the average values to 5th percentiles (assuming a normal distribution and a CoV of 15%) and to convert from test to normal load durations. The 0.8 is a factor used to convert mean relative density to characteristic density values.

2.2 Row shear capacity

The row shear design capacity of bolted connections in a member under tension load is given by:

$$R_{d\,rs} = \phi\, RS_{i\,min}\, n_r\, K_D\, K_{SF}\, K_T \qquad (9)$$

ϕ = strength reduction factor = 0.7

$RS_{i\,min}$ = minimum row shear capacity of any row in the connection
= minimum (RS_1, RS_2, …, RS_{nr})

RS_i = design shear capacity along two shear planes of fastener row "i", in N
= 2 · 1.3 f_v K_{ls} t n_{fi} $a_{cr\,i}$ · 0.6 · 0.8 = 2 · 0.624 f_v K_{ls} t n_{fi} $a_{cr\,i}$
≈ 1.2 f_v K_{ls} t n_{fi} $a_{cr\,i}$

$a_{cr\,i}$ = minimum of e_t and s_b for row "i", mm

f_v = member specified shear strength, MPa

K_{ls} = factor for member loaded surfaces
= 0.65 for side member, 1 for internal member

n_{fi} = number of fasteners in row "i"

n_r = number of rows in the joint as per load component

t = member thickness, mm

The factor 1.3 is obtained from calibration. The values of 0.6 and 0.8 are respectively to convert the average values to 5th percentiles (assuming a normal distribution and a CoV of 25%) and to convert from test to normal load durations.

2.3 Group tear-out capacity

The group tear-out design capacity of dowel fasteners in a member under tension load is given by (refer to Figure 1(d)):

$$R_{d\,gt} = \phi\, GT\, K_D\, K_{SF}\, K_T \qquad (10)$$

where

ϕ = strength reduction factor = 0.7

GT $= 0.5\,(RS_1 + RS_{nr}) + (2 \cdot f_t\, A_{GT\text{-}net} \cdot 0.6 \cdot 0.8)$
$= 0.5\,(RS_1 + RS_{nr}) + 0.96\, f_t\, A_{GT\text{-}net}$
$\approx 0.5\,(RS_1 + RS_{nr}) + f_t\, A_{GT\text{-}net}$

RS_1 = shear capacity along row 1 bounding the fastener group
$= 1.2\, f_v\, K_{ls}\, t\, n_{f1}\, a_{cr\,1}$

RS_{nr} = shear capacity along row "n_r" bounding the fastener group
$= 1.2\, f_v\, K_{ls}\, t\, n_{f\,nr}\, a_{cr\,nr}$

f_t = member specified tension strength, MPa

$A_{GT\text{-}net}$ = critical area between the two rows 1 and n_r, mm^2

The factor 2 is obtained from calibration. The values of 0.6 and 0.8 are respectively to convert the average values to 5th percentiles (assuming a normal distribution and a CoV of 25%) and to convert from test to normal load durations.

2.4 Net tension capacity

The net tension design capacity of a member at a group of dowel fasteners is given by:

$$R_{d\,nt} = \phi\, T_n\, K_D\, K_{SF}\, K_T \qquad (11)$$

where

ϕ = strength reduction factor = 0.9

T_n $= f_t\, A_n$

A_n = member net area, mm^2

2.5 Splitting capacity

The splitting design capacity of a member loaded perpendicular-to-grain by bolts the one used in Eurocode 5, given by:

$$R_{d\,sp} = \phi\; 14\, t \sqrt{\frac{b_e}{1 - \frac{b_e}{b}}}\; K_D\, K_{SF}\, K_T \qquad (12)$$

where

ϕ = strength reduction factor = 0.7

b_e $= b - e_p$

b = depth of member

e_p = un-loaded edge distance

t = thickness of the member

3 Comparison with experimental data

The set of design equations for predicting the resistance of bolted connections loaded parallel-to-grain are based on a numerical model by Bickerdike (2006) and calibrated using experimental data obtained from studies reported in Massé et al. (1988), Mohammad et al. (1997), Jorissen (1998), Quenneville and Mohammad (2000), Mohammad and Quenneville (2001), Shin (2003), Reid (2005) and Bickerdike (2006). The results of this calibration is shown in Figure 2.

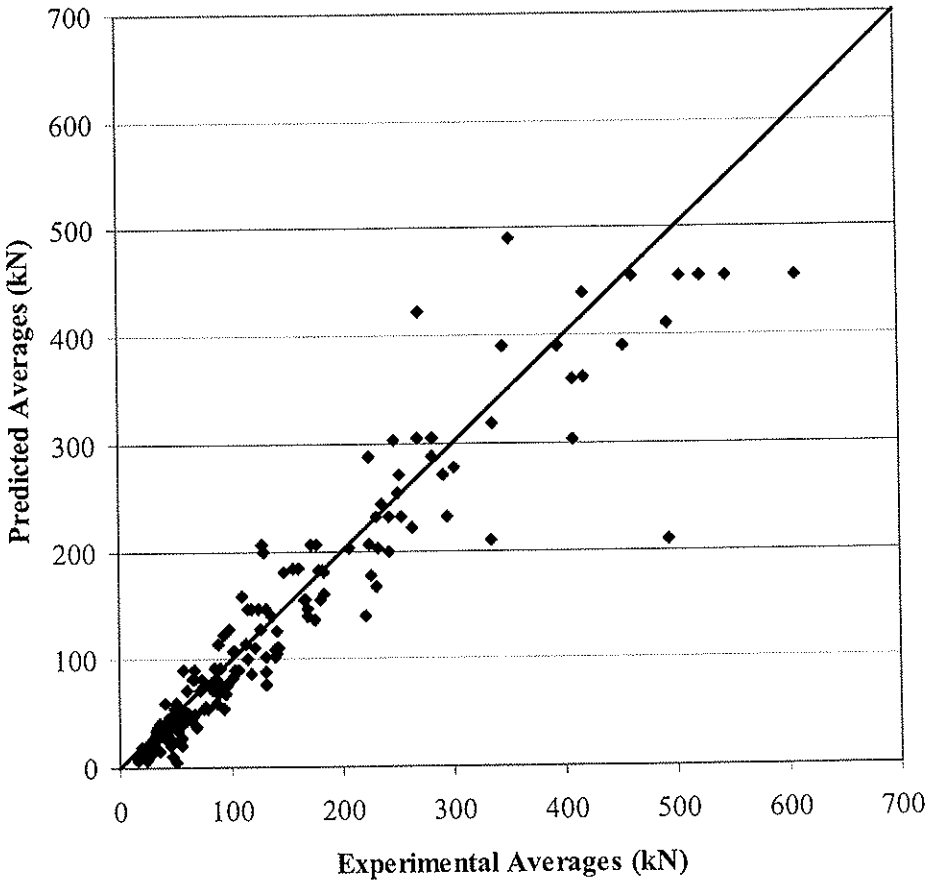

Figure 2 – Comparison of experimental and predicted averages for tested configurations by Massé et al. (1988), Mohammad et al. (1997), Jorissen (1998), Quenneville and Mohammad (2000), Mohammad and Quenneville (2001), Shin (2003), Reid (2005) and Bickerdike (2006).

One can see from Figure 2 that the set of design equation provide a reasonable fit of the average. The R^2 value for all the data points is 0.89. The most obvious outliers (2 above and two below the line) can be explained this way: the two points above the line are for 2 configurations tested by Massé et al. They are for two configurations for which the row spacing was 3d. This resulted in very weak group tear-out experimental values. They are the only two connection configurations tested which had a 3d row spacing. The two points below the line are for two configurations which failed by row shear but for which the bearing predictions governed the resistance. In the future, if the rope effect is included in the canadian EYM equations, the strength predictions for these points would be less conservative. A great portion of the points on the graph shown at Figure 2 is for configurations for which the bearing resistance governed the design. This does not mean that the main failure mode of these groups was necessarily by bearing. Since the Canadian

set of bearing equations does not have the capability to take into account the rope effect, bearing predictions will most likely be conservative and be the governing. It is thus desirable to add the capability of predicting the rope effect to the Canadian EYM equations.

The next figure shows the same graph but for which an new set of experimental data was added. Hanhijärvi and Kevarinmäki (2008) have conducted a study on the resistance of multi-dowelled connections using glulam and LVL. The data points are more scattered but lay reasonably along the line. One can thus say that the set of equations, developped from previous data points, can predict with reasonable accuracy, the trend of the average resistances.

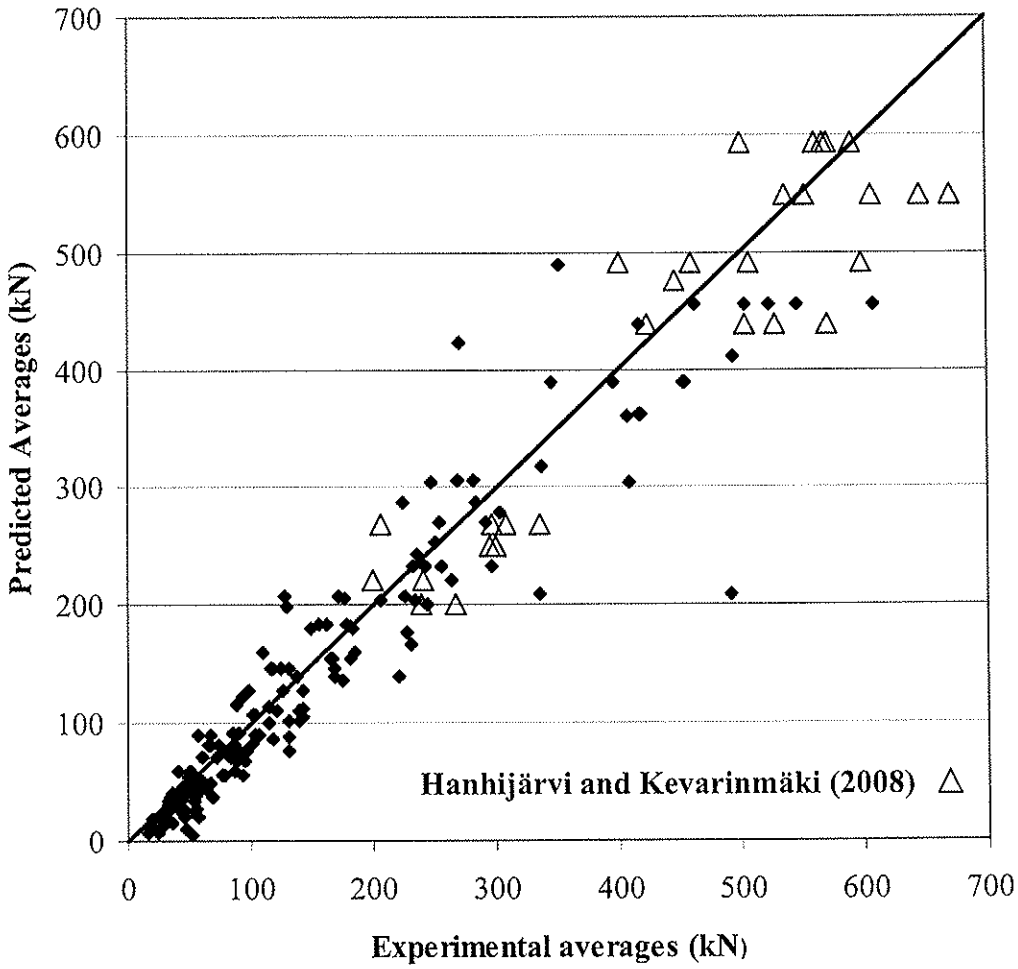

Figure 3 – Comparison of experimental and predicted averages for tested configurations by Massé et al. (1988), Mohammad et al. (1997), Jorissen (1998), Quenneville and Mohammad (2000), Mohammad and Quenneville (2001), Shin (2003), Reid (2005), Bickerdike (2006) and Hanhijärvi and Kevarinmäki (2008).

For the results reported in Hanhijärvi and Kevarinmäki (2008), the specified strength in shear and in tension for GL28h glulam and Kerto-S and Kerto-Q LVL were obtained for litterature. The specified strength values were then used in the various equations to predict the average resistances. The data points for the multiple layered specimens tested by Hanhijärvi and Kevarinmäki were not used.

The predictions shown on the graphs above can be shown in a different way. By calculating the ratio of the predicted averages over the experimental averages, one can show how often the predictions are on the safe side. The graph shown on Figure 4 shows a cumulative distribution relationship. All ratios have been sorted in ascending order. The graphs shows that for 70% of the connection configurations used in this analysis, the predictions are lower or equal to the experimental averages.

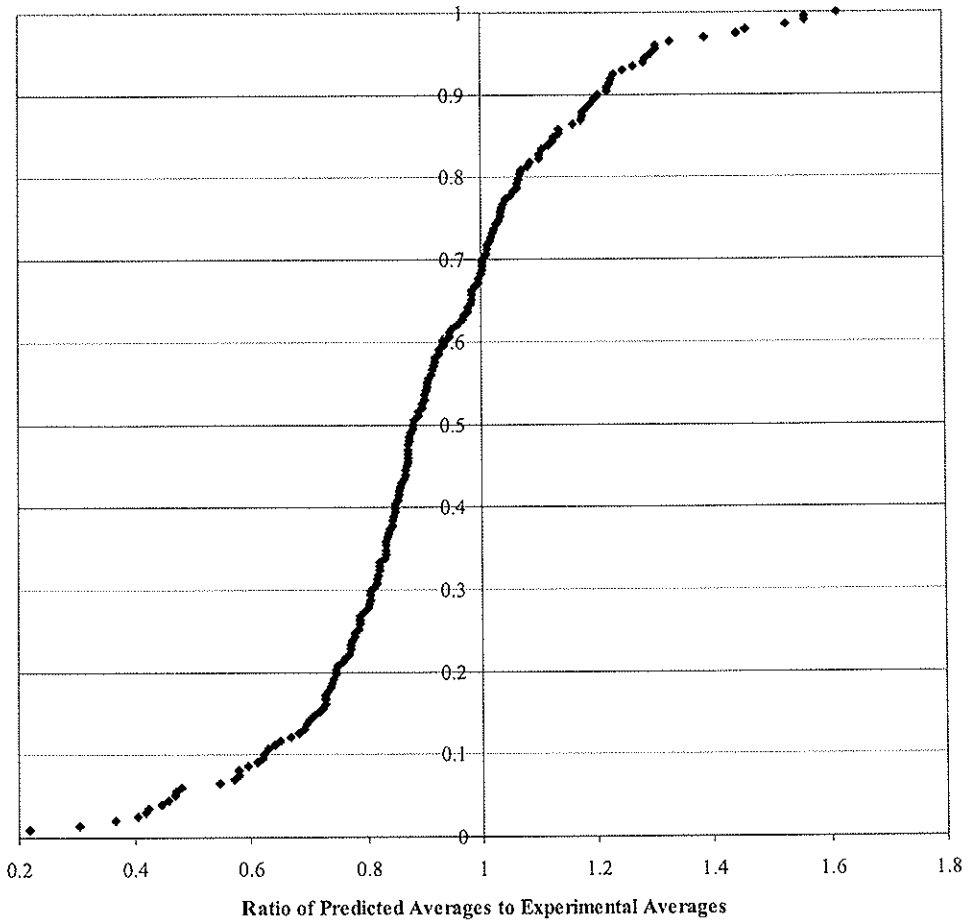

Figure 4 – Cumulative distribution relation for ratios of predicted averages over experimental averages (parallel-to-grain only).

However, the design of connections is not done with average resistances but with 5th percentile ones. To provide a measure of the practicality of these equations in predicting conservatively the resistance of connection configurations, the specified resistances were also calculated. For each of the different configurations tested and available in the database, the specified values were calculated for normal load duration (multiplying resistance by 0.8 and test results by 0.8) and the 5th % predicted resistances were obtained by multiplying the bearing average resistance prediction by 0.75 and the row shear and group tear-out by 0.6. These factors were obtained assuming a normal distribution and coefficient of variations of 0.15 and 0.25 for bearing and row shear and group tear-out respectively.

For each of the connection configurations, a ratio of the configuration specified resistance over the individual specimen results was calculated. The graph shown on figure 5 shows the cumulative distribution relationship for these ratios.

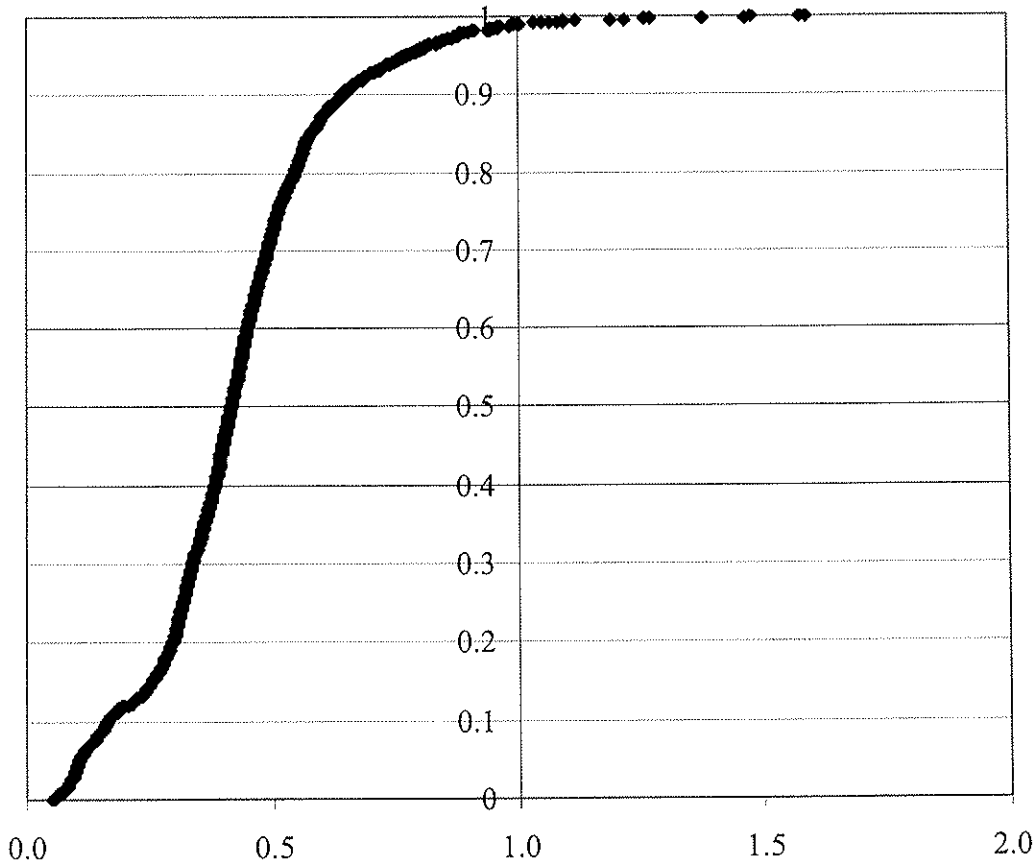

Figure 5 – Cumulative distribution relation for ratios of predicted specified resistances over experimental results (parallel-to-grain only).

The graph shown in figure 5 shows that the predicted specified resistances is higher than the individual test specimen resistances for 99% of the cases. One should remember that the use of the EYM equations without the contribution of the rope effect contributes to the shift of this curve towards the left of the graph.

This level of safety is more than acceptable and one could say that it is probably too high. The addition of the rope effect in the bearing resistance predictions would have the effect of shifting the major portion of the curve to the right but not necessarily altering the percentage of safe predictions significantly.

4 Conclusions

A set of design equations to determine the resistance of bolted connections failing in a ductile or brittle manner (bearing, row-shear, group tear-out, and net tension) for parallel-to-grain loading is proposed. These equations are based on a numerical model by Bickerdike (2006) and calibrated using experimental data from Massé et al. (1988), Mohammad et al. (1997), Jorissen (1998), Quenneville and Mohammad (2000), Mohammad and Quenneville (2001), Shin (2003), Reid (2005) and Bickerdike (2006).

These equations were used to predict the resistance of dowelled connections tested by Hanhijärvi and Kevarinmäki (2008). The predictions of the averages prooved to be adequate for this set of experimental data as well.

The set of equations were also used to predict specified resistances (parallel-to-grain) for the various connections configurations tested. These values were compared to individual test data of each configuration tested. The equations provide safe predictions in 99% of cases.

5 References

[1] Hanhijärvi, A. and Kevarinmäki, A. Timber failure mechanisms in high-capacity dowelled connections of timber to steel. Espoo 2008. VTT publication 677. 53 p.

[2] Bickerdike, M. 2006. Predicting the row shear failure mode and strength of bolted timber connections loaded parallel-to-grain. M.A.Sc. Thesis, Department of Civil Engineering, Royal Military College of Canada, Kingston, Canada. 231 p.

[3] CSA O86-01. 2001. Engineering design in wood. Canadian Standards Association, Toronto, Canada.

[4] EN 1995-1-1. 2004. Eurocode 5 – Design of timber structures. CEN, Brussels.

[5] Jorissen, A., Double Shear Timber Connections with Dowel Type Fasteners. Delft: Delft University Press, 264 p., 1998.

[6] Massé, D., Salinas, J., and Turnbull, J. 1988. Lateral strength and stiffness of single and multiple bolts in glue-laminated timber loaded parallel to grain. Engineering and Statistical Research Centre, Research Branch, Agriculture, Ottawa. 29 p.

[7] Mohammad, M., and Quenneville, J.H.P. 2001. Bolted wood-steel and wood-steel-wood connections: verification of a new design approach. Canadian Journal of Civil Engineering. Vol. 28, pp. 254-263.

[8] Mohammad, M., Quenneville, J.H.P., and Smith, I., Bolted timber connections: Investigations on failure mechanisms. International Conference of IUFRO S 5.02 Timber Engineering, pp. 211-226, Denmark, 1997.

[9] NDS-1997. 1997. National Design Specification (NDS) for wood construction. American Forest & Paper Association, Inc., United States of America.

[10] Quenneville, J.H.P., and Mohammad, M. 2000. On the failure modes and strength of steel-wood-steel bolted timber connections loaded parallel-to-grain. Canadian Journal of Civil Engineering. Vol. 27, pp. 761-773.

[11] Reid, M.S., Predictions of two-row multi-bolted timber connections resistance subjected to parallel-to-grain loading. MASc Thesis, Royal Military College of Canada, Kingston, ON., 146 p., 2004.

[12] Shin, J. 2003. A comparative study of single row multi-bolted connections in SP glulam subjected to parallel-to-grain loading using finite element methods and experimental data. MScE Thesis, Queen's University, Kingston, ON., 166 p., 2003.

INTERNATIONAL COUNCIL FOR RESEARCH AND INNOVATION IN BUILDING AND CONSTRUCTION

WORKING COMMISSION W18 - TIMBER STRUCTURES

DUCTILITY OF MOMENT RESISTING DOWELLED JOINTS IN HEAVY TIMBER STRUCTURES

A Polastri

R Tomasi

M Piazza

I Smith

Department of Structural and Mechanical Engineering

University of Trento, Italy

ITALY

Presented by A. Polastri

H. Blass referred to slide 25 where EC 5 equation was presented. He commented that the 1.05 and 1.15 factors are not part of the Johansen formula and should be left out. He commented that stiffness with small connection test where values are comparable to EC5 while large specimens should have lower stiffness. He received confirmation that the specimens were made by hand which may have contributed to the lower stiffness values. With regard to the comment that there is no danger of splitting mentioned in the presentation, he stated that in reality dry climatic conditions can lead to splitting in the connection area. I. Smith answered that the specimens sat in the laboratory for a period of time. H. Blass received confirmation that they were not assembled specimens so his comments on splitting in dry climatic condition is still valid. A. Leijten asked if there was any literature survey as this was not the 1st work in this area. A Polastri responded yes and they wanted to do the comparisons later. A. Ceccotti asked what L/d is between the thickness of the specimens and the dowel diameter. A Polastri answered that thickness of the specimens was 110 mm and the dowel diameter was 20 mm. A. Ceccotti stated that the conclusion is that EC 8 is conservative. A Polastri answered that it depended on how many plastic hinges can develop and at what point of the cyclic loading scheme that this happened. They are working on a numerical model.

Ductility of Moment Resisting Dowelled Connections in Heavy Timber Structures

Andrea Polastri, Roberto Tomasi, Maurizio Piazza and Ian Smith[1]
Department of Structural and Mechanical Engineering, University of Trento, Italy

1 Introduction

Despite the relative brittleness of large timber members loaded in bending, shear or tension structures built from such material are widely considered to perform well during seismic events. Good seismic behaviour is often attributed to the high ratio between strength and mass that timber components posses and the ability of completed structural systems to dampen and attenuate motions resulting from ground shaking [1]. However, this does not mean that timber structures per se are inherently resistant to seismic actions, which would for example be just as irrational as claiming them to be an inherent fire risk. Like those made primarily from other materials, particular timber construction systems owe any ability to resist damaging effects of external mechanical actions to many factors. Firstly it is important that constructed systems employ inherently stable geometric forms at systemic and substructure levels, and have ability to develop alternative load paths following one or more localised failure events. Secondly, and especially under seismic actions, it is important that systems and substructures be able to accommodate local deformations in components without failure of any embedded connections. That in turn depends on the geometry of components (i.e. individual members and connections) and how appropriately they combine materials. These requirements reflect that in many timber structures ability to absorb kinetic energy and attenuate effects of large amplitude ground motions is strongly dependent on energy dissipation (damping) associated with plastic deformation of metal parts in mechanical connections [1]. Apparent ductility / damping in connection responses results from actual ductility in metal parts, as does the apparent damping they impart to completed systems. This is why only structures that permit their connections to deform substantially prior to occurrence of systemic damage can be expected to perform well if overloaded during seismic events.

The classical structural form adopted in Italy for industrial buildings made of timber employs parallel arranged two-hinge or three-hinge portal-frames having moment resisting

[1] PhD student, Research Associate, Professor and Visiting Professor.

knee connections, Fig. 1. As the figure shows the frameworks separate the provision of robustness in the planes of portal-frames from provision of stability normal to their planes. Usually the knee connections are made using dowel fasteners arranged in one or two concentric rings, Fig. 2. The concern with such connections is that in order to resist moment forces some of the dowels have to load connected timber members with a considerable component of force perpendicular to grain, creating potential for splitting due to excessive tension perpendicular to the grain.

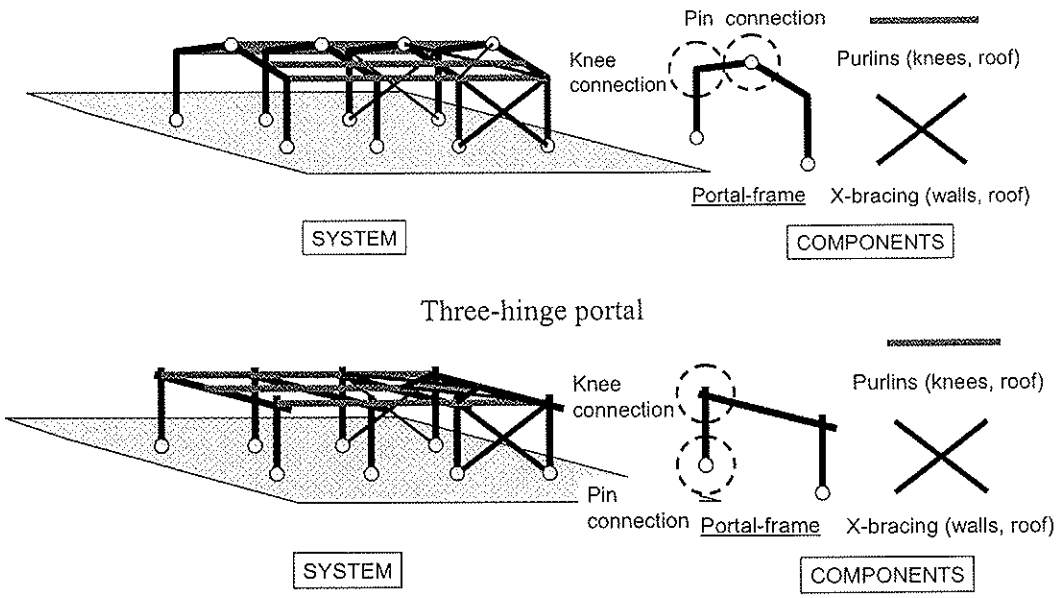

Fig. 1 Portal-frame systems typical in Italy (*schematic*)

Fig. 2 Typical knee connections made using dowel fasteners

Eurocode 8 [2] requires that connections be regarded as the only zones in timber portal-frames capable of dissipating energy during seismic events. Therefore in design analyses timber members are regarded as behaving elastically and to fail in a brittle manner. For statically determinate three-hinge portal-frames the design strategy can be that knee connections are designed to function in the elastic range, but for statically indeterminate two-hinge portal-frames the strategy must differ. For two-hinge portal-frames the requirements of EC8 dictate that after being overloaded knee connections must have ductile responses and their residual capacities must not degrade rapidly when repetitive cyclic forces are applied. Also it is necessary that the parent structural system must permit

substantial deformation at knee connections. However satisfying this last requirement is not problematic with systems like those illustrated in Fig. 1 [3].

The remainder of this paper presents an experimental study aimed at collecting information on the response of knee connections under high amplitude fully-reversed rotational deformations, and comparing findings with requirements of EC8. Attention is also directed at assessing whether the timber design provisions of Eurocode 5 [4] can be used to estimate moment capacities and rotational stiffness of such knee connections. The connections investigated attached twinned glulam column members to a glulam rafter using plain steel dowels. Those connections are types typically employed in Italy.

2 Experiments

The primary experiments were static and cyclic deformation tests on large moment connections. Supplementary experiments measured the density of the timber members, measure the ultimate strength of the steel dowels, and determined the response of small joints with laterally loaded dowels. The tests on small joints were conducted to improve confidence in ability of formulas in EC5 to predict capacities and stiffness of such components. This reflects that reliability of predictions for knee connections depends directly on reliability of the EC5 formulas. Only the primary experiments on large moment connections are described in detail here.

2.1 Tests on moment connections

Figs. 3 and 4 show how moment connections were tested. A lever-arm of 2.8 m was used to generate the moment force on the connection, meaning that the shear force on the twinned column members was 1/2.8 times the applied moment (based on units of kN and m). Materials used were spruce glulam of grade GL24h and mild steel dowels of 12, 14 and 16 mm diameter, with tests performed under dry (class 1 [4]) service conditions. Three dowel layout patterns were employed as illustrated in Fig. 5 representing a single ring of dowels (type 12 x 16mm) and two rings of dowels (types 26 x 12mm and 26 x 14mm) patterns. In static tests the loading was applied under actuator displacement control at a constant rate of 0.2mm/sec to cause failure in about 20 minutes from commencement of loading. The loading regime in cyclic deformation tests was that shown in Fig. 6 with the rate of loading approximately the same during the last cycle as in matched static tests. Tests were not replicated because the objective was not to characterise behaviour statistically.

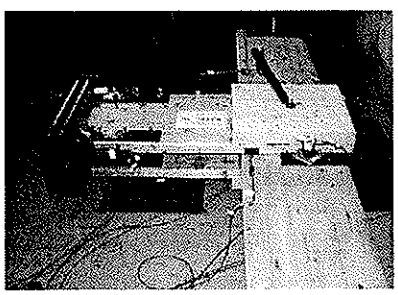

Fig. 3 Typical double shear moment connection specimen

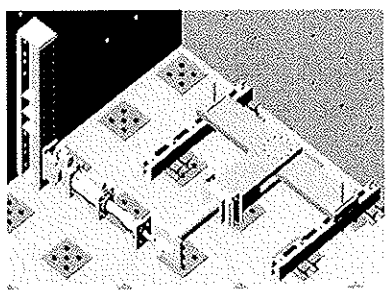

Fig. 4 Test arrangement

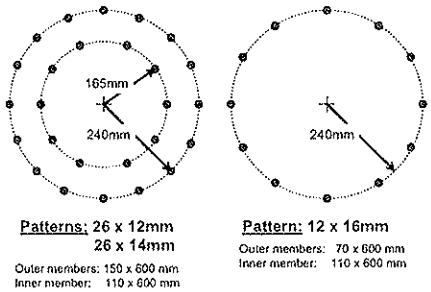

Fig. 5 Dowel layout patterns

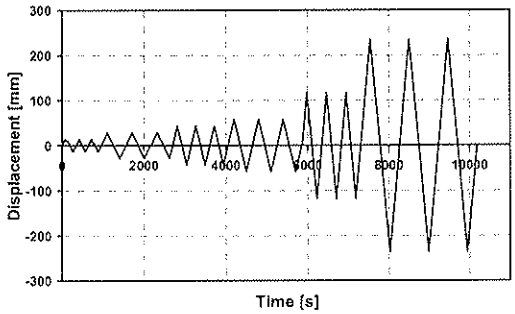

Fig. 6 Cyclic load sequence (actuator displacement)

2.2 Results

2.2.1 Small joints

Small joints tests produced ductile responses with failure mechanisms being consistent with assumptions embedded in EC5, i.e. plastic hinges formed in dowels accompanied by crushing failure in the timber. Typically there were two well developed plastic hinges in dowels located within centre members (one either side of each joint plane) and partially developed or no plastic hinges within side members. Fig. 7 shows a typical failed specimen. Average capacities were as summarised in Fig. 11 (Section 4.1).

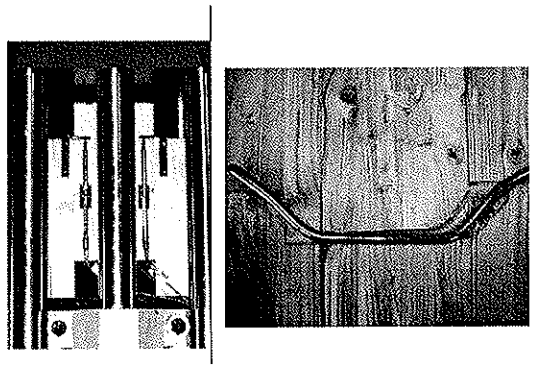

Fig. 7 Typical failed small joint specimen

2.2.2 Moment connections

Moment connections exhibited stable responses up to and beyond the point where it was obvious that localised fail had occurred at some dowels in either the side or centre members. With the exception of the 26 x 14mm dowel pattern (which was the stiffest and strongest type) damage to glulam members was not highly developed until rotational deformations greater than about 0.03 radians. When specimens were dismantled it was found that dowels had developed plastic hinges either side of each joint plane and that individually they had behaved similarly to dowels in small joint tests. There was well developed fracturing in members at the conclusion of tests, but that followed quite extreme deformations of about 0.07 radians. Fig. 8 shows failed specimens from cyclic load tests, and Fig. 9 shows the corresponding moment versus rotation relationships. In all cases the envelop curves mimicked the shape commonly associated with a ductile response and there were no dramatic losses in residual capacities up to the peak applied rotations. Also, there was only relatively modest degradation in residual capacities associated with three repetitions of each cyclic-deformation-amplitude. It is estimated that in practice deformations will be less than 0.05 radians for two-hinge portal frames and thus the degradation would not exceed that observed. As seen in Fig. 9, the responses for moment forces applied in positive and negative senses were similar and hysteresis loops were

pinched. These are further indications that the specimens exhibited high ductility in individual dowel behaviours. Although the results are not presented here, it was found that the envelope curves for matched static test specimens corresponded closely with those for cyclically loaded specimens.

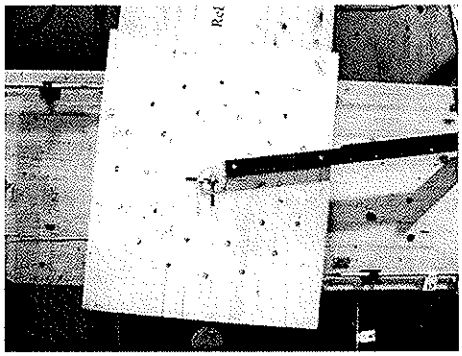

26x12mm

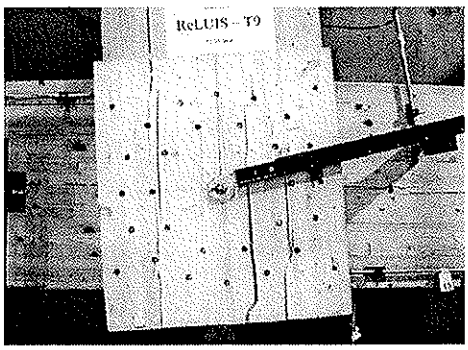

26x14mm

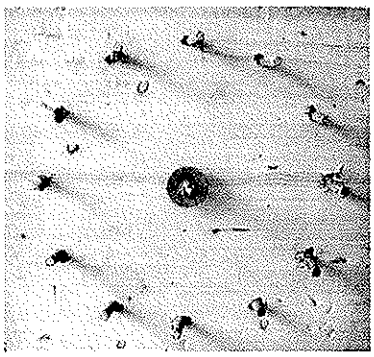

12x16mm

Fig. 8 Failed moment connection specimen after cyclic loading

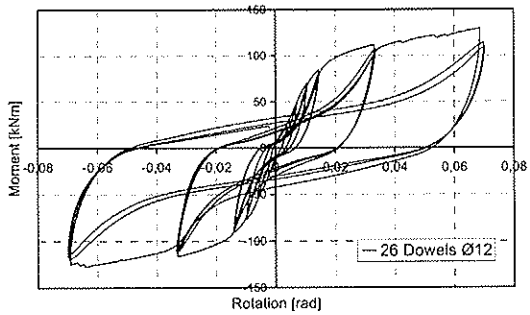

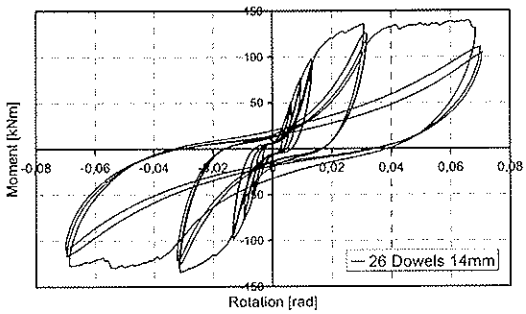

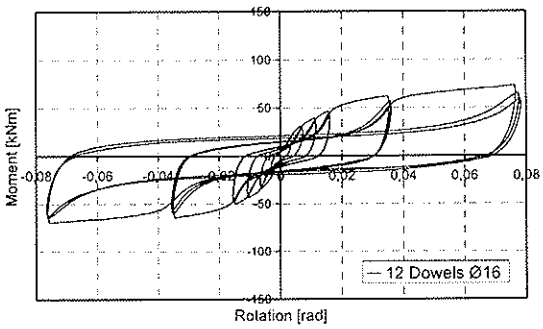

Fig. 9 Moment versus rotation responses for cyclic loading

2.2.3 Material properties

Density of glulam (ρ_m):

average 467 kg/m^3 (CoV = 4%)

Ultimate strength of dowels (f_u):

580 MPa for 12 and 14mm diameter

430 MPa for 16 mm diameter

3 Application of Eurocode 5 formulas

3.1 EC5 formulas for simple joints

EC5 [4] contains design equations for calculating the expected yield capacity and stiffness of joints with a single plain dowel fastener. The applicable equations for symmetric double shear joints are:

$$F_{V,R} = Min.\begin{bmatrix} f_{h,1}t_1 d \\ 0.5 f_{h,2}t_2 d \\ 1.05\dfrac{f_{h,1}t_1 d}{2+\beta}\left[\sqrt{2\beta(1+\beta)+\dfrac{4\beta(2+\beta)M_{Y,R}}{f_{h,1}dt_1^{\,2}}}-\beta\right] \\ 1.15\sqrt{\dfrac{2\beta}{1+\beta}}\sqrt{2M_{Y,R}f_{h,1}d} \end{bmatrix} \quad (1)$$

$$K_{Ser} = \rho_m^{1.5} d/23 \quad (2)$$

where $F_{V,R}$ and K_{Ser} are the yield capacity and stiffness per shear plane per dowel respectively. Input parameters are: d = dowel diameter, $f_{h,1}$ = embedment strength of member 1 (outer member), $M_{Y,R}$ = dowel yield moment, t_1 = thickness of member 1, β = ratio of embedment strength of member 2 (centre member) to the embedment strength of member 1, ρ_m = density of timber members. Subsidiary equations are:

$$f_{h,\alpha} = \frac{f_{h,0}}{k_{90}\sin^2\alpha + \cos^2\alpha} \quad (3)$$

$$f_{h,0} = 0.082(1-0.01d)\rho_m \quad (4)$$

$$f_{h,\alpha} = \frac{f_{h,0}}{k_{90}\sin^2\alpha + \cos^2\alpha} \quad (5)$$

$$k_{90} = f_{h,0}/f_{h,90} = 1.35 + 0.01d \quad (6)$$

$$M_{Y,R} = 0.3 f_u d^{2.6} \quad (7)$$

where: $f_{h,\alpha}$ = embedment strength at angle α relative to the grain (α = 0° corresponds to parallel to grain), f_u = ultimate tensile strength of dowel.

EC5 also provides a formula for calculating the splitting resistance of timber members that a group of dowels load perpendicular to grain:

$$F_{90,Rk} = 14b\sqrt{\frac{h_e}{1-h_e/h}} \quad (8)$$

where: b = member thickness, h = member depth, h_e = loaded edge distance.

3.2 Moment and shear yield capacities of knee connections

The yield moment resistance of a knee connection with concentric rings of dowels is predicted to equal the internal polar moment resistance:

$$M_Y = \left(\sum_{j=1}^{N_{rings}} r_j \sum_{i=1}^{N_{dowel\_j}} P_{j,i} \right) \quad (9)$$

where: r_j = the radius of the j^{th} ring of dowels, N_{rings} = the number of rings of dowels (1 or 2 in the present instance), N_{dowel_j} = the number of dowels in the j^{th} ring (10, 12 or 16 in the present instance), $P_{i,j}$ = the yield capacity of dowel i, j. For a double shear connection the capacity of any particular dowel is taken to be:

$$P_{i,j} = 2F_{V,R}\left(r_j / r_{j-\max}\right)^A \quad (10)$$

where: $r_{j-\max}$ = maximum r_j, A = constant accounting for the non-linearity in the load-deformation responses of isolated dowel joints (in this instance it is assumed A = 0.5). To predict moment capacities of test specimens equation (9) was used in conjunction with assuming linear interaction between effects of applied moment and shear forces on the moment capacity of a connection based on the interaction relationship $\left(M_a/M_Y + V_a/V_Y\right) = 1.0$ at failure, where M_a = applied moment, V_a = applied shear force and V_Y = shear yield capacity (equation 11). Alternative interaction equations could be utilized and include the effect of axial forces in members (in the tests performed no members transferred axial forces to connections).

The yield shear capacity of any member that transfers shear force to the connection is predicted to equal the sum of dowel yield capacities perpendicular to the axis of that member (based on $F_{V,R,i}$ for α = 90°):

$$V_Y = 2\sum_{j=1}^{N_{rings}} \sum_{i=1}^{N_{dowel\_j}} F_{V,R,i} \quad (11)$$

3.3 Rotational stiffness of knee connections

The rotational stiffness of a knee connection with one or more concentric rings of dowels is predicted to equal:

$$K_{Rot} = 2C_{Harmon}K_{Ser}\frac{\left(\sum_{j=1}^{N_{rings}}\sum_{i=1}^{N_{dowel\_j}} r_{j,i}\right)^2}{\sum_{j=1}^{N_{rings}} N_{dowel\_j}} \times 10^{-3} \qquad \text{(kNm/rad)}$$

(12)

where: C_{Harmon} = constant adjusting from the K_{Ser} value applicable to dowels loading timber parallel to grain to a harmonic average stiffness applicable to rotating connections.

3.4 Shear, splitting and bending capacities of members

The shear capacities of members were calculated to be:

$$V_S = \frac{Af_{v,d}}{1.5} \tag{13}$$

where: A = cross-section area, $f_{v,d}$ = design shear strength [in the present instance 2.5 MPa].

It is also assumed that the shear force flow from a member into a connection cannot exceed the splitting capacity of the member calculated according to equation (8). The splitting was therefore calculated assuming that when splitting initiated each dowel in a connection would carry an equal portion of the shear force in a member, and that the fracture plane would pass through the level in the connection that minimized the resistance per dowel. The logic of determining the critical location of the fracture plane is illustrated in Fig. 10 (in the tests performed only the outer members could split in this manner).

The bending capacities of members were calculated to be:

$$M_U = \frac{bd^2 f_{b,d}}{6} \tag{14}$$

where: b = member thickness, d = member depth, $f_{b,d}$ = design bending strength [in the present instance 24 MPa (grade GL24h)].

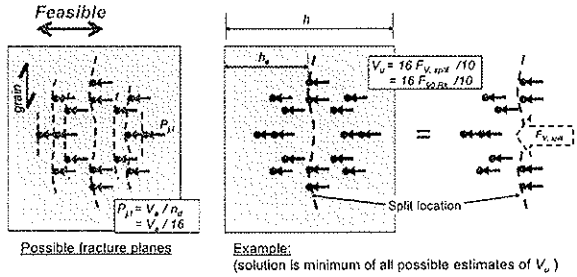

Fig. 10 Splitting resistance applying EC5 formula

4 Comparison of test data with predictions

4.1 Small joints

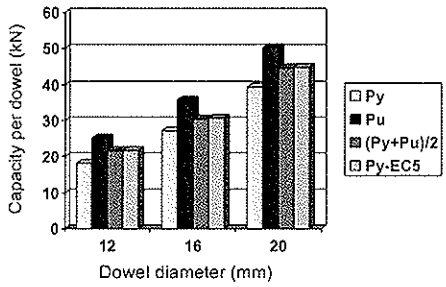

(a) Strength

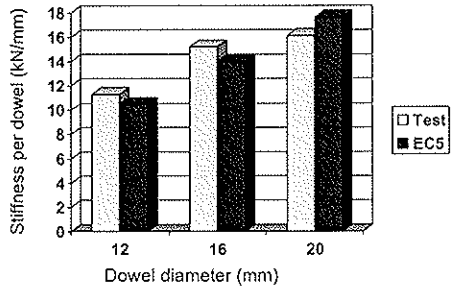

(b) Stiffness

Fig. 11 Comparison of experimental results and EC5 formulas: small joints

Fig. 11a shows experimental versus predicted yield capacities based on EC5 for small joints. Predictions are in excellent agreement with observed capacities. Fig. 11b compares experimental and predicted stiffness responses and again the agreement is good. The EC5 and actual stiffness corresponds to joints having all members loaded parallel to grain. Again test and predicted values are very similar.

4.2 Moment connections

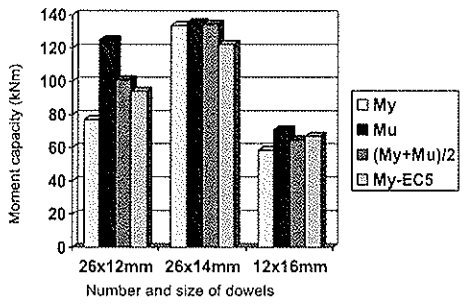

(a) Strength

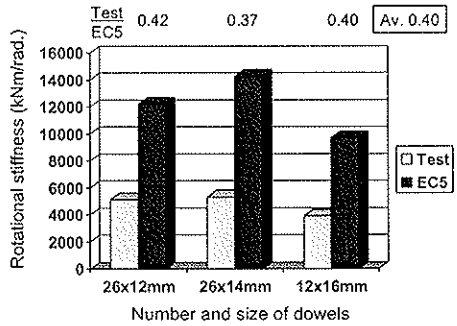

(b) Stiffness

Fig. 12 Comparison of experimental results and EC5 formulas: applied moment on connections (equation (9) plus effect of interaction between moment and shear forces)

Fig. 12a compares yield moment capacities obtained using equation (9) with observed moment capacities, while Fig. 12b compares rotational stiffness values from using equation (12) with observed rotational stiffness values. Predictions of stiffness shown correspond to C_{Harmon} = 1.0. Because predicted responses are based on joint properties obtained from approaches in EC5 the results are labeled EC5. In general it can be seen that the yield moment predictions are in good agreement with observed capacities for all three dowel patterns. This deduction is made assuming that the average of the experimentally obtained yield and ultimate moment capacities is a more appropriate basis for assigning design resistances than either yield or ultimate moment capacities alone. Reasoning for this is that yielding occurs at a lower deformation level than is applicable to failures in structural systems, while complete failure occurs at higher deformation than is applicable to structural systems. Reported ultimate test capacities are maximum values up to rotations of about 0.07 radians.

For specimen types 26x12mm and 26x14mm similar values of ultimate capacity were achieved, with the behaviour of the pattern with smaller dowels being more ductile.

Measured rotational stiffness values were in all instances about 0.4 times EC5 based predictions, which suggests that C_{Harmon} in equation (12) should be assigned the value 0.4. For the test specimens it was calculated that the bending, shear and splitting capacities of interconnected members were unlikely to be exceeded. However this outcome could differ were an alternative loading arrangement to be used.

The observed amount of degradation in the residual moment capacities for second and third deformation excursions was calculated based on the final cyclic deformation level (about 0.07 radians). For lower levels of repetitive deformation the extent of degradation in residual capacity was less. Results suggest that assuming the degraded capacity is about 15 percent less than the static capacity at any level of rotation would be reasonable. Assuming 20 percent degradation would probably be conservative.

5 General discussion

Moment carrying connections of types that are common in timber portal-frames in Italy meet the requirements of EC8 [2]. This statement is made primarily based on experimental proof that such connections have ductile responses and because there is evidence that individual dowels in such connections responded in a ductile manner for levels of deformation likely to occur within completed building systems. A second point of conformance with requirements of EC8 is that the degradation to be expected under repetitive deformations is not excessive.

The above said, it is important to emphasise that dowels employed in tested connections were relatively slender and therefore developed plastic deformation in bending. The implication is that assuming compliance with requirements of EC8 is contingent on connections having slender dowels. In practice that equates to requiring that connections fail by simultaneous plastic deformation of dowels and crushing of timber beneath them. Design must ensure that one of the lower two mechanism represented by equations (1), and preferably the last equation, will govern the capacity per dowel. Site quality control must ensure that the correct grade of steel is used because employing the wrong grade can change the governing failure mechanism to be brittle (i.e. using higher grade steel could prevent formation of necessary plastic hinges).

The formulae of EC5 for predicting capacities and stiffness of simple dowel joints forms a reliable basis from which to predict the behaviour of tested moment connections and it is therefore presumed those same provisions are reliable for design. Therefore it is recommended that equations presented in Sections 3.1 to 3.3 of this paper be used as the basis of designing dowelled moment connections.

For resisting the effects of loads other than those produced by seismic actions the yield moment resistance can be based directly on equation (9), but including usual adjustments for factors like the duration of the loading as specified in EC5.

6 Conclusions

Experiments have verified that it is possible to design satisfactory moment connections for two-hinge or three-hinge portal frame structures when effects of seismic actions must be resisted. In practical terms this means that the requirement of Eurocode 8 can be complied with. With only slight modification the connection design provisions of Eurocode 5 can be used to design such moment connections.

7 Acnowledgements

This research has been partially supported by the Italian Department of University and Research, under the research project 2006089730 (Years 2007/08) "Diagnosis techniques and totally removable low invasive strengthening methods for the structural rehabilitation and the seismic improvement of historical timber structures".

8 References

[1] Bouchair, A., Racher, P., Bocquet, J. F. (2007). "Analysis of dowelled timber to timber moment-resisting joints", Materials and Structures, 40(10), pp. 1127–1141.

[2] European Committee for Standardization (CEN), 2004. "Design of structures for earthquake resistance - Part 1 General rules seismic actions and rules for buildings", Eurocode 8, Standard EN 1998-1, Brussels, Belgium.

[3] Piazza, M., Tomasi, R., Modena, R. (2005). "Strutture in legno", Ulrico Hoepli Editore, Milano, Italia, pp. 627-680.

[4] European Committee for Standardization (CEN). 2004. "Design of timber structures - Part 1-1 General: Common rules for buildings", Eurocode 5, Standard EN 1995-1-1, Brussels, Belgium.

9 Related literature

[5] Chui, Y. H., Li, Y. (2005). "Modeling Timber Moment Connection under Reversed Cyclic Loading", J. Struct. Eng., ASCE, 131(11), pp. 1757–1763

[6] Karacabeyli, E., Popovski, M. (2003). "Design for earthquake resistance". *In* '*Timber Engineering*' (Ed. Thelandersson, S., Larsen, H.J.), John Wiley and Sons, Chichester, UK, pp. 267-299.

[7] Larsen, H. J., Jensen, J. L. (2000). "Influence of semirigidity of joints on the behaviour of timber structures." Prog. Struct. Eng. Mater., 2(3), pp. 267–277.

[8] Leijten, A. J. M. (1996). "Explanation of the translational and rotational behaviour of prestressed moment timber joints." Proc., International Council for Building Research Studies and Documentation, Working Commission W18-Timber Structures, Univ. of Karlsruhe, Karlsruhe, Germany, paper 29-7-5.

[9] Tomasi, R., Zandonini, R., Piazza, M., Andreolli, M. (2008). "Ductile End Connections for Glulam Beams", Structural Engineering International SEI, IABSE, 3/2008, pp. 290–296.

INTERNATIONAL COUNCIL FOR RESEARCH AND INNOVATION
IN BUILDING AND CONSTRUCTION

WORKING COMMISSION W18 - TIMBER STRUCTURES

MECHANICAL BEHAVIOUR OF TRADITIONAL TIMBER CONNECTIONS: PROPOSALS FOR DESIGN, BASED ON EXPERIMENTAL AND NUMERICAL INVESTIGATIONS. PART I: BIRDSMOUTH

C Faye

P Garcia

L Le Magorou

F Rouger

FCBA, French Institute of Technology for Forest Based and Furniture Sectors, Bordeaux

FRANCE

Presented by C. Faye

H.J. Larsen commented that the detail was simple but load transfer was rather complicated. He asked how the influence of deformation on load transfer was considered. He expressed doubt about the validity of the model for example Kc90 must be bigger than 3 for this to work but a smaller Kc90 value was used. C. Faye explained that other variables were used in the calibration. H.J. Larsen commented that why stress concentration has to be introduced to account for the already high shear stress. W. Munoz asked about optimization of the geometry of the connection. C. Faye responded that this has not been done yet. A. Leijten commented that if there was shrinkage, one can have different stress state. C. Faye agreed that if contact area was different then load transfer and stress state would be different.

Mechanical behaviour of Traditional Timber Connections: Proposals for design, based on experimental and numerical investigations. Part I: Birdsmouth

Carole Faye (carole.faye@fcba.fr)
Patrice Garcia
Laurent Le Magorou
Frédéric Rouger

FCBA, French Institut of Technology for Forest Based and Furniture Sectors,
Allée de Boutaut BP227, 33028 Bordeaux Cedex,
France

Introduction

Due to the development of CNC (Computer Numerically Controlled) machines, traditional timber connections become economically competitive. Consequently, the use of these wooden connections in construction is increasing.

In this context, it is necessary to provide appropriate design rules taking account of the specific geometry of these connections.
Indeed, failure of the birdsmouth connections occurs according to two phenomena:

- shear failure in the notch, for the low skew angles. In this case, criteria using the average shear stress is not adequate because of high peak stresses not taken into account;
- failure in compression with an angle to grain in contact zones for higher skew angles. In this case, non linear distribution of the compression stress has to be determined.

In order to solve these issues, an experimental and numerical study on the instantaneous mechanical behavior of birdsmouth connections was investigated.

Summary

This paper describes:
1/ an experimental study: birdsmouth connections were tested for glued laminated beams in eight geometric configurations varying the values of skew angle β, notch depth t and notch length l. The experimental and designed values were compared.
2/ a finite element modelling taking account of contact with friction between timber surfaces. The model allows the determination of shear and compression stresses with angle to grain profiles respectively in the notch and contact wooden zones.
3/ formulation of design proposals on the basis of experimental and numerical results.

1. Experimental results on instantaneous strength of birdsmouth connections:

1.1 Materials and test configurations

Configurations of experimental series of birdsmouth were determined according to these following conditions:

- Series tested have to be representative of birdsmouth connections produced in the industry and used in construction. For this purpose, six producers were interviewed to know their usual practice;

- Two failure modes (shear failure in the notch and compression failure with an angle to grain in the wooden contact zones) have to be obtained,
- The effect of the different geometric parameters has to be investigated.

In this context, eight experimental series of birdsmouth connections with glued laminated timber were performed with the following geometric parameters:

- 2 values of skew angle β : 25° and 55°;
- 2 values of notch depth t=30 and 45 mm,
- 3 values of notch length l=150mm, 200mm and 250 mm,
- 2 values of width b: 90 or 160 mm

The specimens height was taken equal to 225 mm.

The strength class of glulam delivered by the producer was GL 24. Specimens were fabricated by CNC machine in manufacture.

Each configuration contains a minimum of 5 specimens, which gives a grand total of 48 tests.

The detailed test configurations are reported in Table 1.

Series N°	nb	β	t	L	b_1	H_1	L_1	b_2	H_2	L_2	Strength class
1	8	25	30	200	90	225	2382	90	225	1500	GL24
2	6		45	200	90		2382	90			
3	5		45	200	160		2382	160			
4	6		45	250	90		2432	90			
5	5		30	150	90		2332	90			
6	5	55	30	150	90		2075	90			
7	8		45	200	90		2125	90			
8	5		45	200	130		2125	130			

Table 1 : geometrical parameters for series tested.

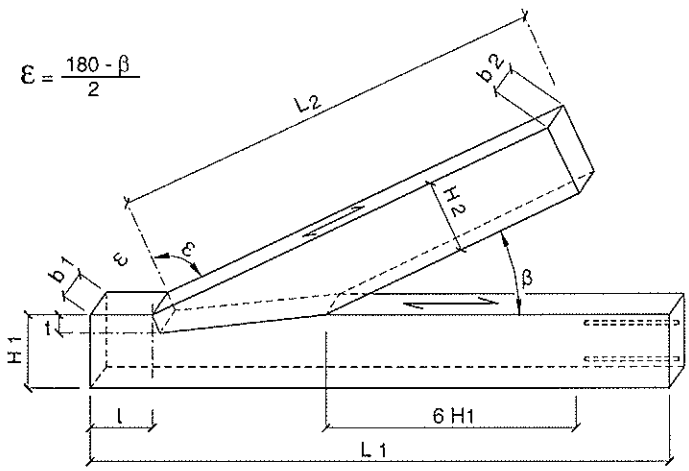

Figure 1 : definition of geometrical parameters.

1.2 Test Methods

Description of the mechanical tests is given in Figure 1.
Load F is applied to the element 2 by an hinged actuator.
Element 1 is simply supported, its horizontal location corresponding to the intersection of neutral axis of elements 1 and 2.
At the opposite end of the birsdmouth connection, element 1 is fixed by a hinged system.
Slip between elements 1 and 2 is registered for each test.
This test allows the determination of local strength values of the birdsmouth connections.
The loading mode corresponds to EN 26 891 standard.
The load carrying capacity is defined as the minimum value between:

- the load corresponding to the slip value of 15 mm ,
- the maximum value of the load.

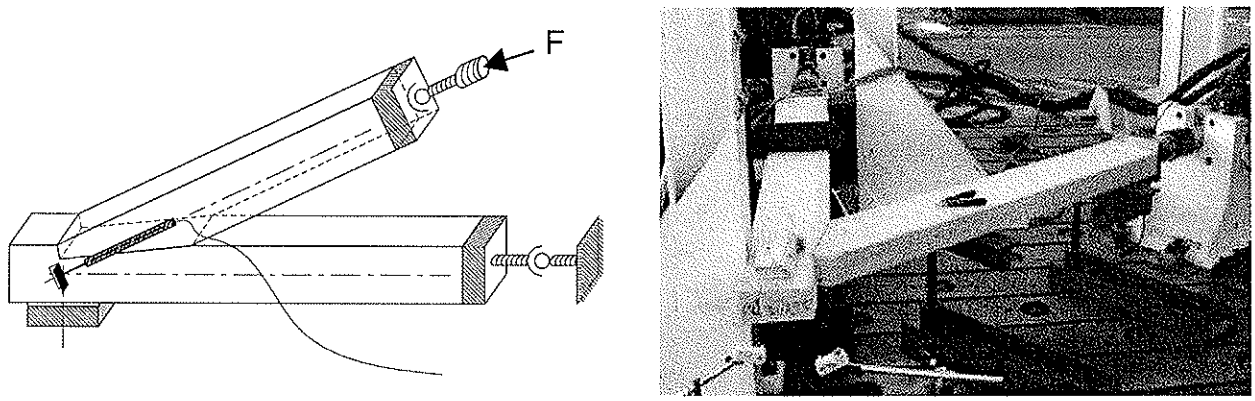

Figure 2 : test configuration.

1.3 Experimental results

Table 2 gives for each series test:

- the experimental average value of the load carrying capacity and the associated coefficient of variation,
- the characteristic value of the load carrying capacity calculated according to EN 14 358,
- the failure mode.

Series N°	**1**	**2**	**3**	**4**	**5**	**6**	**7**	**8**
$F_{average}$(kN)	74	76	123	92	62	153	170	230
Cov	8	18	19	7	20	10	16	5
F_k(kN)	60	49	76	76	38	116	116	197
failure mode	1	1	1	1	1	2 and 3	2 and 3	2 and 3

Table 2 : experimental results for each series test.

Failure mode 1: Shear failure in notch (see Figure 3)
Failure mode 2: Compression failure in contact zone of elements 1 and 2 (see Figure 4)
Failure mode 3: Mixed failure: compression in contact zone and shear in notch (see Figure 5)

Figure 3 : shear failure in the notch (series with β =25°) .

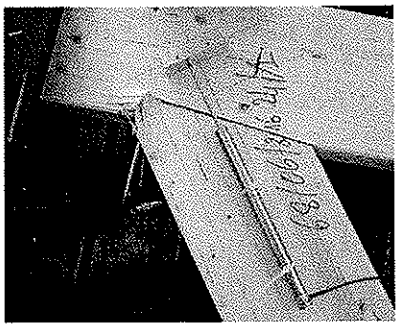

Figure 4 : Compression failure in contact zone of elements A and B (series with β=55°).

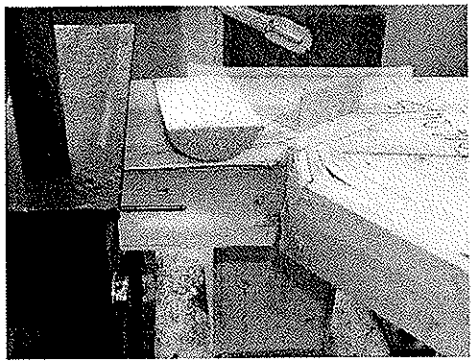

Figure 5 : Mixed failure:compression in contact zone and shear in notch (series with β=55°).

Load/displacement curves are presented in Figure 6 and Figure 7 respectively for a test with β=55°and β=25°.

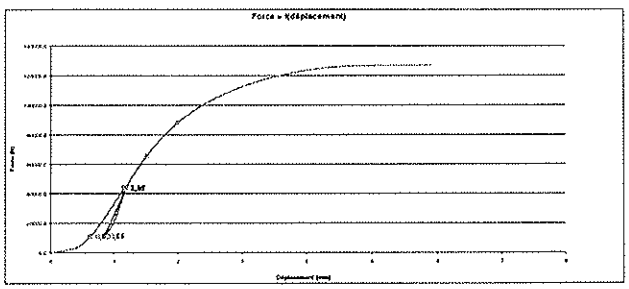

Figure 6 : Load/displacement curve for test with β=55° (specimen 1, series 6).

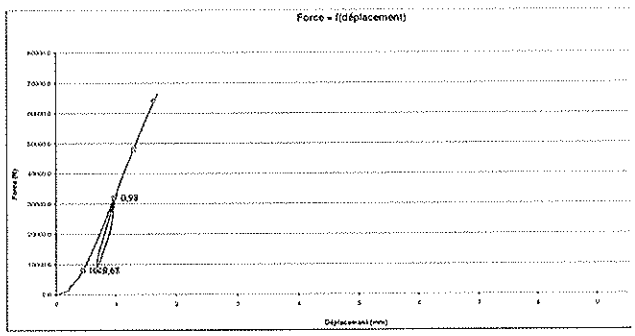

Figure 7 : Load/displacement curve for test with β=25° (specimen 2, Serie2).

The main observations are the following:

- the load carrying capacity for each specimen is always reached before the 15 mm slip,
- for all series with a skew angle β =25°, failures always occur in shear in notch and the mechanical behaviour is elastic (see figure 7).
- for all series with skew angle β =55°, two failure modes occur : in compression in contact zone of the two elements or in shear in notch after compression deformation in contact zone; the mechanical behaviour is plastic (see figure 6).

Additional tests to determine density (1) and compression strength perpendicular to grain (2) were performed.

(1) for each element 1 and 2 of each test, density was measured. Characteristic value was calculated according EN 384, and found equal to 420 kg/m^3 . This experimental value is close to the reference value of EN 1194 for the strength class GL28.

(2) For all specimens of series 6 and 7, compression strength perpendicular to grain was measured according to EN 408. The average and characteristic values were found respectively equal to 3.4 MPa and 2.8 MPa (characteristic value calculated according to EN 14 358). This value is close to the reference value of EN 1194 for the strength class GL24.

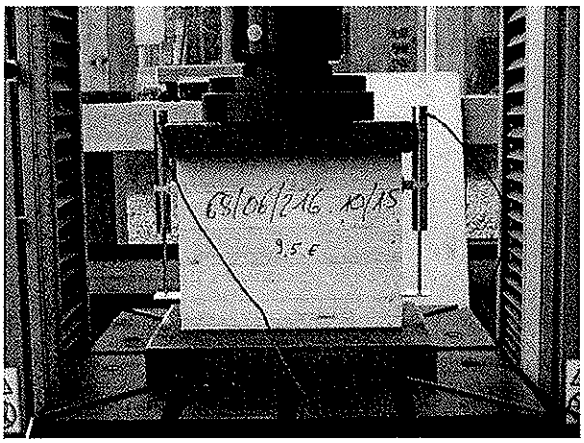

Figure 8 : perpendicular compressive test configuration

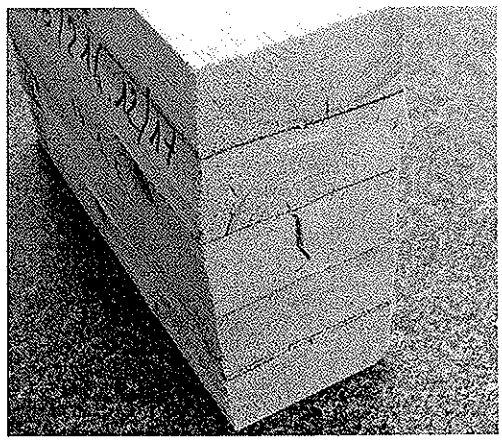

Figure 9 : specimen after failure (**280*225*90 mm^3.**)

1.4 Comparison between experimental and design values

1.4.1 Current design rules

Design rules define the following steps:

- Load transferred to the l_{c1} contact zone (F_3), as a function of the applied load F
- Stresses (τ_{XY}, $\sigma_{c,\alpha}$) are calculated from the applied load
- Shear and compression failure loads (F_{shear}, F_{comp}) are deduced from the previous step by equaling the stress to the strength,
- The load carrying capacity (F_{design}) of the birdsmouth connection is calculated as the minimum value between the shear failure load and the compression failure load.

Load transferred to the contact zone:

$$F_3 = F \cos(\beta / 2) \tag{1}$$

Where F is the applied load

Stresses

(a) Shear stress on l_{cis}

$$\tau = \frac{F \cos(\beta)}{b\, \ell_{cis}} \tag{2}$$

Where ℓ_{cis} is the shear length in the notch (see Figure 10)

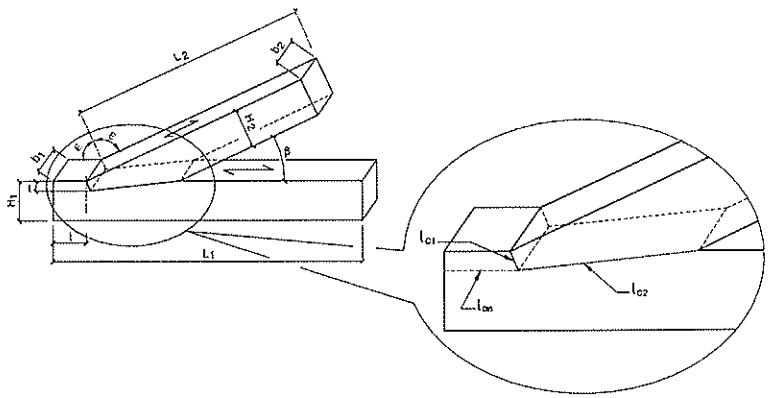

Figure 10 : Geometrical details of the contact zone

(b) Compression stress with an angle to grain on

$$\sigma_{c,\alpha} = \frac{F_3 \cos\left(\frac{\beta}{2}\right)}{bt} = \frac{F \cos^2\left(\frac{\beta}{2}\right)}{bt} \tag{3}$$

(c) Compression stress perpendicular to grain on l_{cis}

Note : This stress is not used in the current design rule, but is further used in this paper.

$$\sigma_{c,90} = \frac{F_3 \cos\left(\beta/2\right)\sin\left(\beta/2\right)}{bt} = \frac{F \cos^2\left(\beta/2\right)\sin\left(\beta/2\right)}{bt} \tag{4}$$

Shear failure load

$$\tau = f_v \Rightarrow F_{shear} = \frac{\ell_{cis}\ b\ f_v}{\cos(\beta)} \tag{5}$$

Compression failure load

$$\sigma_{c,\alpha} = f_{c,\alpha} \Rightarrow F_{comp} = \frac{f_{c,\alpha} bt}{\cos^2\left(\frac{\beta}{2}\right)} \tag{6}$$

Where

$$f_{c,\alpha} = \frac{f_{c,0}}{\frac{f_{c,0}}{k_{c,90}\ f_{c,90}} \sin^2\left(\frac{\beta}{2}\right) + \cos^2\left(\frac{\beta}{2}\right)} \tag{7}$$

Since $k_{c,90}$ is not defined for this geometrical configuration, it was taken equal to 1.

Load carrying capacity of the connection

$$F_{design} = \min\left(F_{shear}; F_{comp}\right) \tag{8}$$

1.4.2 Comparison between experimental and design load carrying capacities

The strength values, reported in Table 3, were evaluated from the following procedure:

- Compression perpendicular to grain as tested
- Compression parallel to grain and shear according to reference values of GL24 (new draft of EN 1194)

In order to evaluate the mean design load carrying capacities, to be compared with experimental values, mean strength values were used in equations (5) and (6). The mean strength values were calculated from the characteristic ones assuming a normal distribution. For compression perpendicular to grain, the coefficient of variation was take as tested. For the other strength properties, it was assumed equal to 20%.

	Characteristic value (MPa)	Mean Value (MPa)
Shear	3	4,5
Compression parallel to grain	24	36
Compression perpendicular to grain	2,8	3,4 [(a)]
(a) as tested		

Table 3 : Strength properties

The comparison between experimental and design mean load carrying capacities is reported in Table 4.

Series N°	β (°)	t	l	l_{cis}	b	$F_{exp,mean}$ (kN)	$F_{comp,mean}$ (kN)	$F_{shear,mean}$ (kN)	$F_{Design,mean}$ (kN)	F_{design}/F_{exp}
1	25	30	200	207	90	74	**70**	93	70	0.95
2		45	200	210	90	76	116	**94**	94	1.24
3		45	200	210	160	123	188	**167**	167	1.36
4		45	250	260	90	92	**106**	116	106	1.15
5		30	150	157	90	62	**70**	**70**	70	1.13
6	55	30	150	166	90	153	**46**	117	46	0.3
7		45	200	223	90	170	**68**	158	68	0.4
8		45	200	223	130	230	**99**	228	99	0.43

Table 4 : comparison between experimental and design load carrying capacities

Table 4 indicates that :

- for β=25°
  - failure modes are not correctly predicted, since 3 cases were predicted in compression, whereas all experimental failure modes were in shear
  - in most cases, the predicted load carrying capacity tends to be overestimated by 20%
- for β=55°
  - failure modes are not correctly predicted, since it was observed experimentally mixed modes of failure
  - the load carrying capacity tends to be underestimated by 60% in average

This discrepancy justifies the following sections dealing with numerical simulations and formulation of new design rules.

2. Finite element simulation

2.1 Mechanical model, geometric constraints and loading

The aim of the numerical approach is to determine:

- how the load is transmitted on wooden contact zones between elements 1 and 2,
- how shear and compression stresses distribute in the contact zone.

The geometry was taken identical to the experimental configuration (see Figure 10, previous section).

Glued laminated timber is considered as transverse isotropic material.

Despite mechanical behaviour of wood is elastic in shear and tension and plastic in compression, it was in this investigation as elastic. It is a simplified but safe approach because stresses are overestimated.

Values of elastic properties used in finite elements approach are given in Table 5.

Average values of stiffness, GL24 according EN 1194 (1999)
$E_{g,L}$= 11 600 MPa
$E_{g,R}$= $E_{g,T}$= 390 MPa
$G_{g,RL}$=$G_{g,TL}$=720 MPa
$\nu_{g,LR}$= $\nu_{g,LT}$= 0.4
$\nu_{g,RL}$= 0.3

Table 5 : Values of elastic properties for glued laminated elements.

In wooden contact zones (named l_{c1} and l_{c2} in Figure 10), friction is represented by Coulomb law according the following physical relations:

$$\begin{cases} \text{if } |\sigma_t| < \mu |\sigma_n| \ , \ \dot{u}_t = 0 \\ \text{if } |\sigma_t| = \mu |\sigma_n| \ , \ \dot{u}_t = \lambda r \\ \qquad\qquad \text{with } \lambda > 0 \text{ and } r = |\sigma_t| \end{cases} \tag{9}$$

Where

σ_t is the tangential stress in the contact zone

σ_n is the perpendicular stress in the contact zone.

$\dot{u}_t$ is the displacement rate

μ is the friction coefficient

λ and r are model parameters

The friction coefficient depends on grain direction, humidity, temperature and roughness of wooden contact zones. Therefore, it was varied between 0.3 and 0.6 in this study.

Simulations are performed with finite element Code Castem 2000.

2D elements and 1D contact elements are respectively used for wooden elements and wooden contact zones l_{c1} and l_{c2}.

The load F is uniformly distributed along the end of element 2. The resultant load used for the calculation was taken equal to 81 kN.

At the horizontal location corresponding to the intersection of neutral axis of elements 1 and 2, the 20 cm wide support is taken into account by forbidding vertical displacements. At the end of wooden element 1, horizontal displacements are forbidden.

2.2 Numerical Analysis

2.2.1 Loads

From the calculation, the load transferred to the contact zone F_3 can be directly evaluated.

2.2.2 Stress distributions

Shear stress τ_{crit}

In Figure 11, shear stress distribution along the length l_{cis} is represented. Since it is highly non linear, and that we need a local value of the stress that will generate the shear failure, an assumption was made to derive a critical stress.

- calculate the mean stress τ_{mean}
- evaluate the "critical shear length" l_{crit} as the portion of l_{cis} where the stress is higher than τ_{mean}
- calculate the critical stress τ_{crit} as the mean value of τ on this critical length.

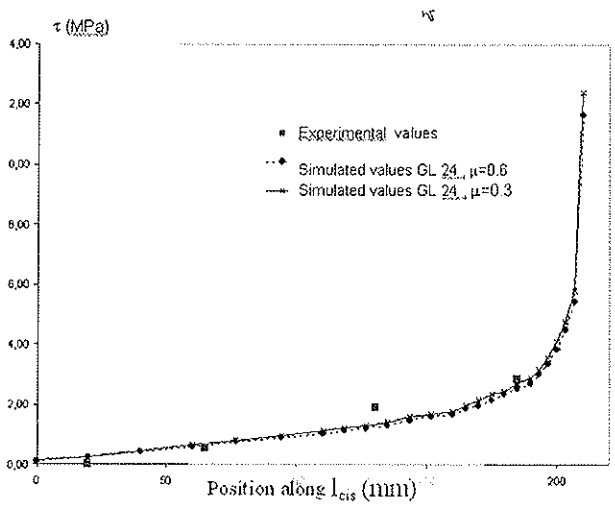

Figure 11 : An example of shear stress distribution along the shear zone

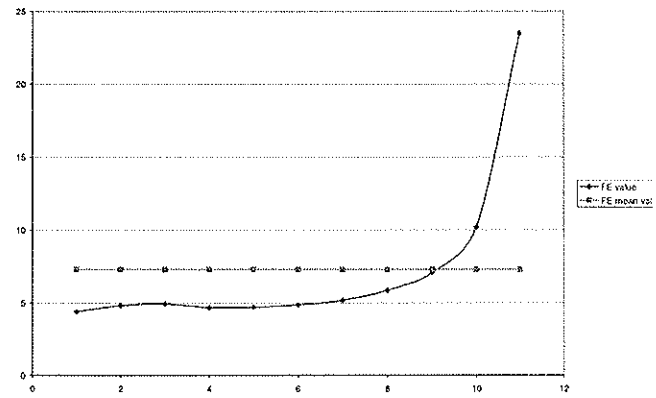

Figure 12 : compression stress distribution

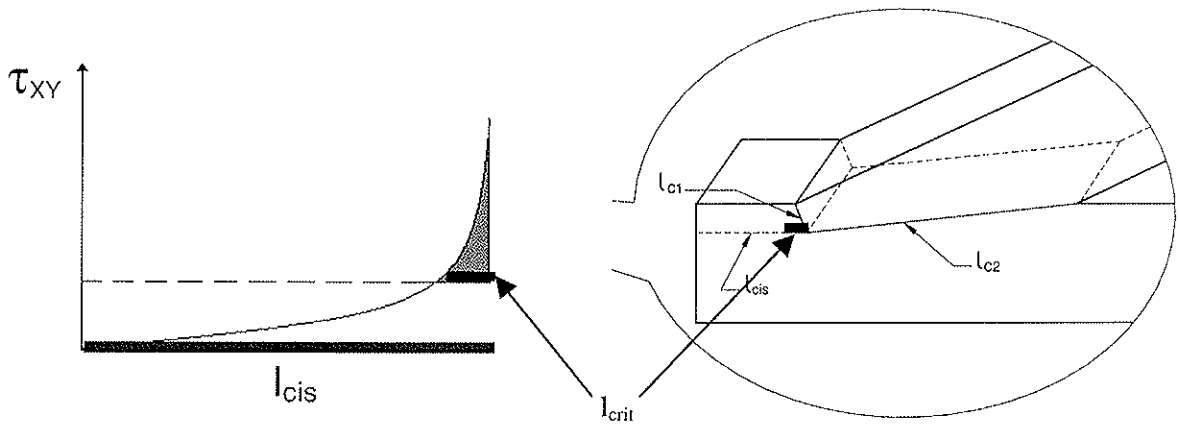

Figure 13 : Derivation of the critical shear stress

Compression stress perpendicular to grain in the shear zone $\sigma_{c,90,crit}$

Since this stress might influence the shear failure, it was also evaluated on the critical shear length l_{crit}.

Compression stress with an angle to grain in the contact zone $\sigma_{c,\alpha}$

In Figure 12, compression stress with an angle to grain distribution along the length l_{c1} is represented. Again, the distribution is non linear. Therefore, a mean value was derived, since the compression occurs on the total length l_{c1}.

2.3 Results

The calculations have been performed by varying the following parameters:

- β =25°, 55°
- μ =0.3, 0.6.

These calculations were used to evaluate the stresses.

For F_3, additional configurations were evaluated:

- β =40°
- μ =0.1, 0.9.

3. New design rules

3.1 Load transferred to the contact zone:

In order to take account of the friction coefficient and the angle between members, a modified equation was introduced:

$$F_{3,\text{new design}} = \frac{F_{3,\text{old design}}}{(1+\mu^a \beta^b)} = \frac{F\cos(\beta/2)}{(1+\mu^a \beta^b)} \qquad (10)$$

Parameters a and b were fitted by least square optimization, knowing that F = 81 kN, and varying μ and β.
The results are: a=0.5 and b = 1.

The comparison between the simulated load and the load given by the design equation (10) is reported in the following table. A comparison with the "old existing design rule" is also reported.

Series	β(°)	$\mu_{friction}$	$F_{3,finite\ elements}$ (kN)	$F_{3,old\ design}$ (kN)	$F_{3,new\ design}$ (kN)
2	25	0.01	76.6	79	75.8
		0.3	72.4		63.8
		0.6	67.5		59.1
		0.9	61.8		55.9
	40	0.01	69.7	76	71.1
		0.3	61.5		55.1
		0.6	52		49.4
		0.9	41.8		45.8
7	55	0.01	59.7	72	65.6
		0.3	47.5		47.1
		0.6	34.5		41.2

Table 6 : Comparisons for F_3

3.2 Stresses

Stresses given by the simulation were compared to the design values, given in equations (2), (3), (4). Adjustment factors were subsequently derived, resulting in the following design equations:

$$\tau = m_\tau \frac{F_{3,\text{new design}} \cos(\beta/2)}{b\, \ell_{cis}} \quad with\ m_\tau = 2 \tag{11}$$

$$\sigma_{c,\alpha} = m_{c,\alpha} \frac{F_{3,\text{new design}} \cos\left(\frac{\beta}{2}\right)}{bt} \quad with\ m_{c,\alpha} = 0.8 \tag{12}$$

$$\sigma_{c,90} = m_{c,90} \frac{F_{3,\text{new design}} \cos\left(\beta/2\right)\sin\left(\beta/2\right)}{bt} \quad with\ m_{c,90} = 0.5 \tag{13}$$

3.3 Limit state criteria

The purpose of this section is to propose a new criteria, taking into account the influence of compression perpendicular to grain in shear, and proposing a new value for $k_{c,90}$. These criteria were adjusted iteratively, by comparing simulated and experimental values.

(i) Since the compression perpendicular to grain influences the shear failure load, a combined stress criteria was formulated:

$$\frac{\tau}{f_v} + \alpha \frac{\sigma_{c,90}}{f_{c,90}} \le 1 \tag{14}$$

For each test configuration, the shear failure load F_{shear} is determined iteratively by converging the criteria given in equation (14). α was numerically determined on the basis of the experiments that failed in shear, i.e. for $\beta = 25°$, using a least square optimization between the shear failure loads and the experimental loads. α was found equal to -0.5.

(ii) The compression failure criteria is given by:

$$F_{comp} = \frac{f_{c,\alpha} bt}{m_{c,\alpha} \cos^2\left(\frac{\beta}{2}\right)} = \frac{bt}{m_{c,\alpha} \cos^2\left(\frac{\beta}{2}\right) \frac{f_{c,0}}{k_{c,90}\, f_{c,90}} \sin^2\left(\frac{\beta}{2}\right) + \cos^2\left(\frac{\beta}{2}\right)} \tag{15}$$

In order to adjust $k_{c,90}$, the experiments involving compression failures, i.e. for $\beta = 55°$, were used. Since mixed failure modes were observed, it was necessary to use a mixed criteria, the load carrying capacity being defined as the minimum value between the shear failure load and the compression failure load (see equation (8)). $k_{c,90}$ was found equal to 1.1, using least square optimization.

The failure load results are reported in Table 7.

It is demonstrated that the new approach is much closer to the experiments than with the "old rules".

Regarding code formulation, the failure criteria has to be written in the following manner:

"It should be verified that:

$$\max\left\{\frac{\tau_d}{f_{v,d}} + -0.5 \frac{\sigma_{c,90,d}}{f_{c,90,d}}; \frac{\sigma_{c,\alpha,d}}{f_{c,\alpha,d}}\right\} \le 1 \tag{16}$$

With

$$f_{c,\alpha,d} = \frac{f_{c,0,d}}{\frac{f_{c,0,d}}{1.1\, f_{c,90,d}} \sin^2\left(\frac{\beta}{2}\right) + \cos^2\left(\frac{\beta}{2}\right)} \qquad (17)$$

And

$\tau_d ; \sigma_{c,90,d} ; \sigma_{c,\alpha,d}$ *calculated according to equations* (11), (12), (13)"

Series N°	β (°)	t	l lcis	b	$F_{exp,mean}$ (kN)	$F_{comp,mean}$ (kN)	$F_{shear,m}$ (kN)	$F_{Design,mean}$ (kN)	F_{design}/F_{exp}
1	25	30	200 206.7	90	74	115	**78**	78	0.95
2		45	200 210	90	76	170	**71**	71	1.07
3		45	200 210	160	123	300	**125**	125	0.98
4		45	250 260	90	92	170	**93**	93	0.99
5		30	150 156.7	90	62	115	**55**	55	1.13
7	55	45	200 223.4	90	170	**147**	160	147	1.16
8		45	200 223.4	130	230	**213**	225	213	1.08

Table 7 : Newly designed load carrying capacities vs experimental failure loads.

Conclusion

By combining an extensive experimental investigation and finite element calculations, it has been possible to formulate new design rules that take into account the non linear effects (friction, stress peaks, etc) to evaluate the load carrying capacity of birdsmouth connections. These rules allow a proper design that will enable the use of these connections for modern type structures.
Further work will be dedicated to complementary experimental work, in order to confirm the proposal.

Aknowledments

The study was supported by 3 French professional syndicates (CAPEB, FFB and FIBC).

Bibliography

McKenzie W.M., Karpovic H., 1968,'The frictional behaviour of wood', Wood Sci. and Technologies' 2, 139-152.
EN 14358 Timber structures – Fasteners and wood-based products – Calculation of characteristic 5-percentile value and acceptance criteria for a sample
EN 1194 Timber structures. Glued laminated timber. Strength classes and determination of characteristic values
EN 1995-1-1 : Eurocode 5 – Design of timber structures
EN 408 Timber structures - Structural timber and glued laminated timber - Determination of some physical and mechanical properties
EN 384 Timber structures – Calculation of characteristic values
EN 26891:1991 Timber structures. Joints made with mechanical fasteners. General principles for the determination of strength and deformation characteristics.

INTERNATIONAL COUNCIL FOR RESEARCH AND INNOVATION
IN BUILDING AND CONSTRUCTION

WORKING COMMISSION W18 - TIMBER STRUCTURES

EMBEDDING STRENGTH OF EUROPEAN HARDWOODS

U Hübner
Competence Center holz.bau forschungs gmbh

T Bogensperger
G Schickhofer
Institute for Timber Engineering and Wood Technology
Graz University of Technology,

AUSTRIA

Presented by U. Hübner

H.J. Larsen commented that if you want to use the timber for standardized test, whole population could be used rather than limited to the density range because the test standard does not specify the condition of the specimens but specifies the method of testing. A. Leijten mentioned that EN 408 and 3838 specify the condition of the test specimens. A. Jorissen received clarification of where the 5 mm deformation specified in the test method occurred. J. Munch Andersen stated that the model depended on diameter and asked how much a difference it would make if the diameter was ignored. U. Hübner referred to Figure 4.1 in the paper which showed the differences. I. Smith explained the origin of 2.1 mm from a paper 25 years ago which is 1/12 of an inch. He commented that one should avoid setting embedment values too high as system behaviour may be compromised because of compatibility to structural system is important. He said the origin of the 5 mm comes from timber to timber connections. A. Leijten and U. Hübner discussed issue of moisture content and the oven dried specimens in term of hysteresis and dryness condition. U. Hübner mentioned also slow drying was used.

Embedding strength of European hardwoods

U. Hübner, Competence Center holz.bau forschungs gmbh
T. Bogensperger and G. Schickhofer, Institute for Timber Engineering and Wood Technology
Graz University of Technology, Austria

1 Introduction

The embedding strength tests presented in this paper were realised according to ON EN 383:2007 and with the species beech (*Fagus sylvatica* L.), ash (*Fraxinus excelsior* L.) and black locust (*Robinia pseudoacacia* L.). The test results will be used to dilate the existing base for the standardisation. Furthermore, the test results were analysed together with those of other authors. Whale, Smith and Hilson (1986) published the results of 1394 embedding strength tests with a deformation limit of 2.1 mm on four soft- and two tropical hardwoods (Keruing and Greenhart). The first European standard for the determination of embedding strength prEN 383:1990 with a deformation limit of 5 mm was used by Ehlbeck and Werner (1992) for 154 tests on six hardwood species, thereof 55 beech and 20 oak specimens. As the standardization at that time, DIN 1052-2:1988, only allowed the application of dowels from 8 mm and bigger. Ehlbeck and Werner (1992) did not provide tests with a dowel size of 6 mm as allowed today. Leijten (2004) published: "The embedment strength expressions in Eurocode 5 are based on a comprehensive study by Whale and Smith (1986b) and Ehlbeck and Werner (1992)". The calculation of embedding strength according to EN 1995-1-1:2004 is based on substantial and fundamental experiences with softwoods and tropical hardwoods but includes only 75 embedding strength tests with two European hardwood species.

2 Execution of the tests

Assuming a mean coefficient of variation of $COV_{fh} = 16\,\%$ for a mean embedding strength of $f_h = 60\,\mathrm{N/mm^2}$ and 20 specimen per sample, the mean embedding strength of the whole population can be estimated via Student's distribution to $f_h = 60 \pm 2.5\,\mathrm{N/mm^2}$ with a statistical reliability of 75 %. This means the mean embedding strength has an error of $\pm 4.2\,\%$ without any errors in measurement just for statistical reasons. More than 30 specimens were tested for each sample because the maximum of the coefficient of variation for all tested hardwood samples was 25 % and only a tolerance of $\pm 5\,\%$ with a statistical reliability of 75 % was accepted.
The ash timber came from "Bucklige Welt", a region between Vienna and Graz, and was sawn in such a way that neither the deformation nor the fracture behavior were influenced by any defects. The specimens were conditioned to a constant mass in an environment with a relative humidity of 65 % and a temperature of 20 °C. As the timber had had slightly less moisture content before the process, adsorption took place. Under such conditions, the equilibrium moisture content for ash wood is reached with 10.7 % (see Figure 3.2). This corresponds very well with the mean moisture content of 10.5 % for all ash specimens.
The ash specimens were tested with the dowel sizes 6 mm, 8 mm, 12 mm, 16 mm and 20 mm and load-to-grain angles of $0\,°, 30\,°, 60\,°$ and $90\,°$. Specimens of beech and black locust were analysed under the same load-to-grain angles to compare the load bearing bevaviour with

ash timber. Table 6.1 gives an overview of all own hardwood samples and softwood samples by Spörk (2007) from the Institute for Timber Engineering and Wood Technology. The specification of the samples is composed of a short cut for the wood species according to DIN 4076-1:1985, C for compression or T for tension test, the load-to-grain angle and optionally a 3-digit number for a special sample.
The sizes of the test pieces are given in ON EN 383:2007 for load-to-grain angles of $\alpha = 0\,°$ and $\alpha = 90\,°$ respectively. For the other angles in between the measures were linear interpolated. The hole for the dowel was realised after the climatisation by wood drill with a box column drill with the nominal diameter of the dowel.
The galvanized dowels were ordered in steel quality S235 JR. From tension tests resulted a yield strength of $f_{y,mean} = 553\,\mathrm{N/mm^2}$ and a tensile strength of $f_{u,mean} = 612\,\mathrm{N/mm^2}$. The values are much higher than recomended for this steel quality. As normal dowels were undeliverable, stainless-steel (material number 1.4301) was used only for the diameter of 6 mm.
The test configuration is shown in Figure 2.1. An adapter for the different load-to-grain angles was mounted between the spherical loadplate (fixed during the test) and the specimen. On contact surface of the specimen a Teflon stripe was aplicated to reduce the obstruction of lateral strain.

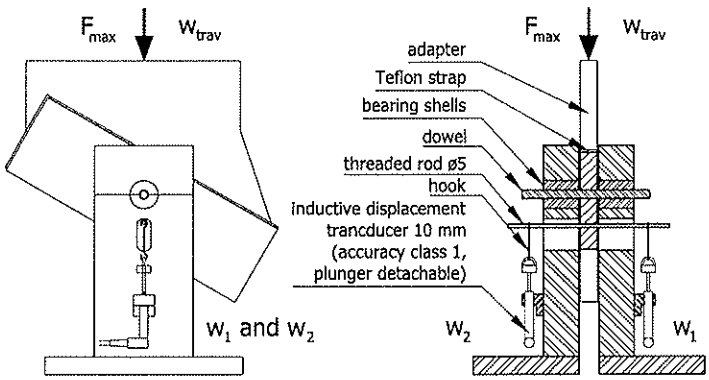

Figure 2.1: Test configuration

3 Dependencies of embedding strength

3.1 Moisture content for hardwoods

The embedding strength decreases between 5 % and 25 % of moisture content relative to the strength at 12 % with each percent raising moisture content 3 % according to Gehri (1982) (spruce) and 3.3 % according to Rammer and Winistorfer (2001) (Douglas Fir-Larch, Spruce-Pine-Fir, Southern Pine) respectively. Youngs (1957) forced clear wood specimens $0.5 \times 0.5 \times 2.0$ in. of Northern red oak (*Quercus rubra* L.) perpendicular to the grain until 2.5 % deformation. The strength perpendicular to the grain decreased 5.4 % with each percent raising moisture content. Ellwood (1954) observed 4.7 % with similar tests on rift of American beech (*Fagus grandifolia* Ehrh.). As no literature about the relationship between embedding strength and moisture content for European hardwoods had been published yet at the time of our research, samples of 40 ash specimens were conditioned to constant mass ander three different climates and tested with dowel size 12 mm and load-to-grain angles of 0 ° and 90 °. The mean moisture contents were 4.4 %, 16.3 % and 18.9 %.
Figure 3.1 shows the embedding strength $f_{h,\alpha}$ in function of moisture content u for the ash samples. The embedding strength parallel to the grain $f_{h,0}$ decreased between 4 % and 21 % moisture content relative to the strength at 12 % with each percent raising moisture content

4 % and 3 % perpendicular to the grain respectively. The regression lines are given in the equations (1) and (2). The difference between the mean moisture content of 10.41 % for hardwood samples under normal climate conditions and the reference moisture content of 12 % is low. Hence the relationship between embedding strength and the moisture content for ash wood was also applicated to Beech and black locust and esteemed precisely enough.

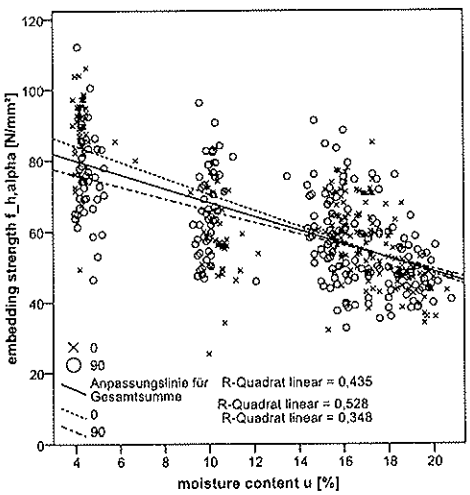

Figure 3.1: Moisture content versus embedding strength for ash

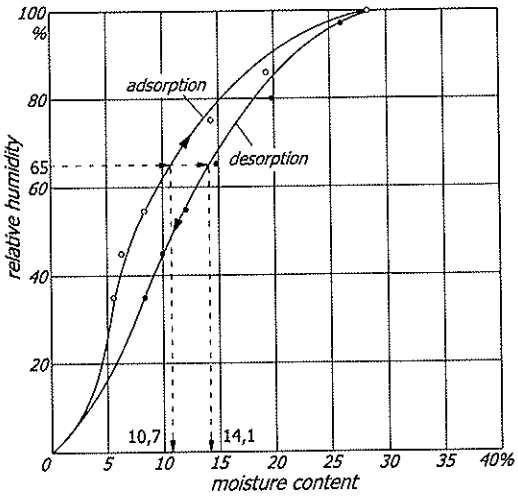

Figure 3.2: Hygroscopic equilibrium for ash wood at 20 °C according to Kollmann (1941)

$$f_{h,0} = 94.233 - 2.543 \cdot u \quad \text{with} \quad R^2 = 0.528 \tag{1}$$

$$f_{h,90} = 83.281 - 1.851 \cdot u \quad \text{with} \quad R^2 = 0.348 \tag{2}$$

The equations (3) were used to adapt the calculated embedding strength to the reference moisture content of 12 %:

$$f_{h,\alpha} = \frac{F_{max}}{d \cdot t_{test}} (1 - (12\,\% - u) \cdot \Delta_u) \quad \text{with} \quad \Delta_u = \Delta_{u0} + \frac{\Delta_{u90} - \Delta_{u0}}{90\,^\circ} \cdot \alpha \tag{3}$$

$f_{h,\alpha}$ embedding strength at 12 % moisture content [N/mm²]
F_{max} maximum load according to ON EN 383:2007 [N]
t_{test} thickness of specimen during test [mm]
u moisture content [%]
Δ_u diminishment of embedding strength with raising moisture content [%/%] for load-to-grain angle α, $\alpha = 0\,^\circ$ or $\alpha = 90\,^\circ$

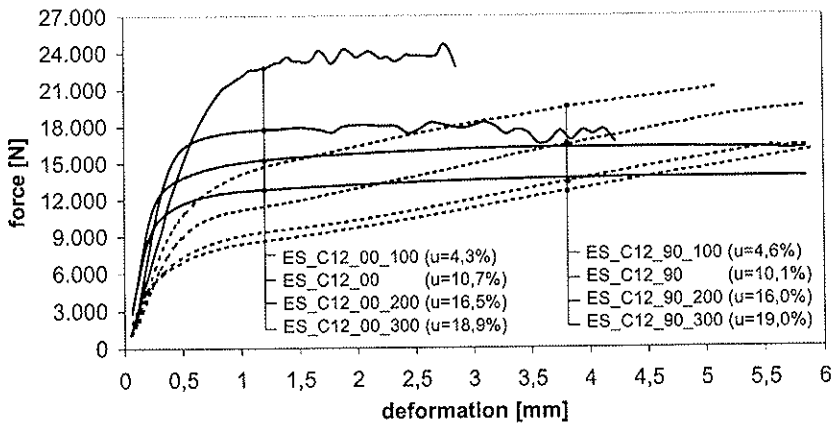

Figure 3.3: Mean curves of compressive force to deformation for ash samples with different moisture content levels (dowel size 12 mm, load-to-grain angle $\alpha = 0\,^\circ$ and $\alpha = 90\,^\circ$)

Figure 3.3 presents the mean curves of compressive force to deformation for eight ash samples. The solid and dashed curves describe the tests with force parallel and perpendicular to grain respectively for four different moisture content levels. Abstracting the curves with two lines interconnected with a circular arc, the slope of the initial linear portion differs but the lines for the plastic behavior are parallel for each load-to-grain angle. The radius of the circular arc and the level of the second lines for the plastic behavior rise, then the moisture content decreases. If the specimens are dry and the load-to-grain angle is 0 ° the specimen split before reaching the deformation limit of 5 mm. The discontinuous curves are caused by the decreasing number of specimens available for the calculation of the mean curve.

3.2 Density

The mean density has to be in the range of 1.05 to 1.25 times of the characteristic value according to method 2 of ON EN 28970:1991. The variation of the density of each specimen is limited to ±10 % to the mean value. The 5 %-percentile of the empirical distribution of the ash density is $\rho_{05} = 678\,\mathrm{kg/m^3}$ and the mean value is $\rho_{mean} = 761\,\mathrm{kg/m^3}$. 84 % of the 773 specimen fulfill the conditions required in method 2. The mean coefficient of determination for the relationship of density and to embedding strength is $R^2 = 0,54$ for all the ash samples with a mean moisture content of approximately 10.4 %. This means that the density is an important factor for embedding strength, but not the only one. Figure 3.4 supports the proposal of Leijten et al. (2006): "The density distribution of the test population and the whole population to which results apply should be identical". The specimen represented by black circles and dots in Figure 3.4 a) should be excluded according to ON EN 28970:1991 but they complement the gray dots in figure b) logically. Figure b) shows the relationship between experimental and calculated results according to equation (12). From the scientific point of view it is not reasonable to limit the density of the samples. The strength grading according to E DIN 4074-5:2008 requires no density limits and it would be uneconomic to reduce the yield.

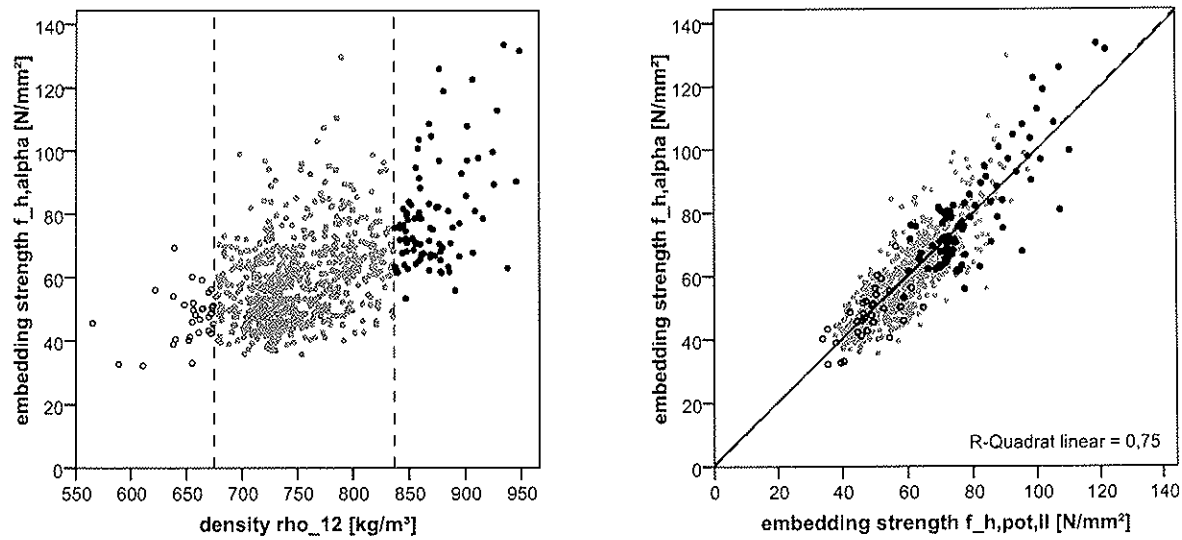

(a) Ash specimen (dowel diameter 6 mm to 20 mm)

(b) Experimental and calculated results according equation (12)

Figure 3.4: Influence of ON EN 28970:1991 on the selection of specimens

The mean densities of the ash wood samples vary from 737 kg/m³ to 804 kg/m³, i. e. between −3.1 % and 5.7 % of the mean density of all specimens. The minimum and maximum coefficient of variation for the density of one sample was $COV_{\rho,min} = 4.95\,\%$ and $COV_{\rho,max} = 10.33\,\%$ respectively and overall samples was $COV_{\rho} = 7.49\,\%$ calculated.

3.3 Friction between timber and dowel

Schmid (2002) described the influence of the friction between dowel and cladding timber by FE-modelling and stated its significant influence on the strength distribution.
The measurement system ARAMIS™ enabled Serrano and Sjödin (2007) to calibrate a linear-elastic FE-model with test results for smooth and rough dowels by variation of the friction coefficient $\mu_{smooth} = 0.1$ and $\mu_{rough} = 0.4$. Regarding the figure 7 of their article, the mean load at 5 mm deformation for smooth and rough dowels can be estimated to $F_{smooth} = 12.8\,\text{kN}$ and $F_{rough} = 18.0\,\text{kN}$. This means an increasing embedding strength from smooth to rough dowels to 141 %. The influence of the roughness of the dowel is very important and the roughness should be constant for all tests according to ON EN 383:2007 by using commercially available, electrogalvanise dowels.
The embedding strength tests of Spörk (2007) (spruce, load-to-grain angle $\alpha = 0\,°$, dowel size 20 mm) also showed significant differences between dowels with smooth and rough surfaces. The sample FI_C20_00_100 was tested with a dowel produces on a turning lathe and FI_C20_00_200 with a very smooth surface. The mean value for the embedding strength is 16 % higher for the rough dowel than a reference sample with electrogalvanised dowel and the smooth dowel caused a decrease of 6 %.

4 Calculation model for ash wood

4.1 Overview of experimental results

Figure 4.1 shows the experimental results of the embedding strength tests according to ON EN 383:2007. The box plots representing different diameters are grouped according to each load-to-grain angle. Regarding a single angle, the embedding strength decreases if the diameter increases. This trend becomes stronger if the load-to-grain angle increases. The embedding strength of dowels with diameter 6 mm increases then the load-to-grain angle becomes larger but for 8 mm and 12 mm no tendency is visible. The trend inverses to a declining embedding strength with raising load-to-grain angle for the larger diameters 16 mm and 20 mm.

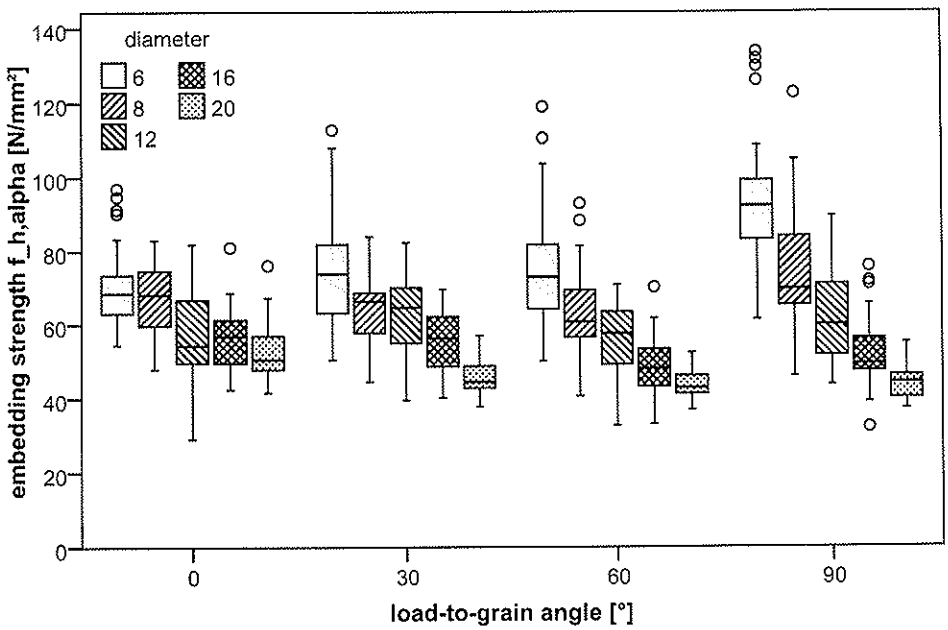

Figure 4.1: Boxplots of embedding strengths of different dowel sizes, grouped for each load-to-grain angle

4.2 EN 1995: 2004

The lognormal distribution of the embedding strength meets the empirical distribution very well. The quantile-quantile plot in Figure 4.2 for dowels with 12 mm diameter shows a good adaptation especially for low values.
The logarithmized embedding strength for 12 mm diameter dowels is plotted as a function of the density in Figure 4.3. If the density and the logarithmized embedding strength had the same coefficient of variation – but they differ significantly with 7.8 % and 4.3 % – the lines of the 5 %-percentile would intersect in on point one the regression line.

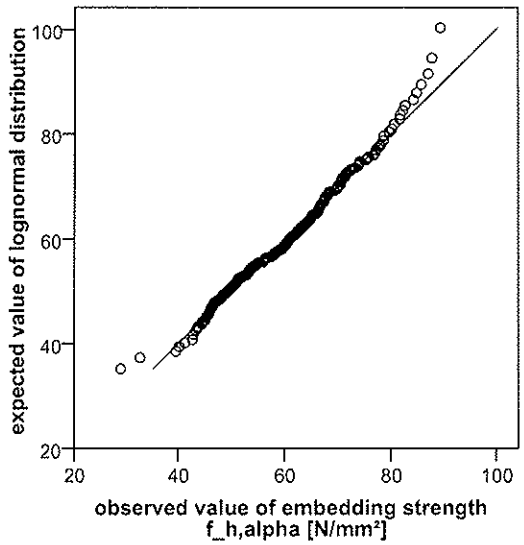

Figure 4.2: QQ-plot of logarithmized embedding strength for ash

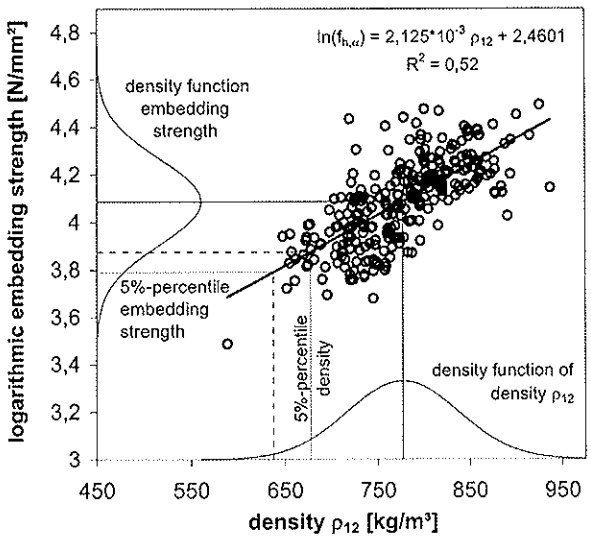

Figure 4.3: Density versus logarithmized embedding strength

Ehlbeck and Werner (1992) calculated the equations (4) and (5) with linear regression:

$$f_{h,0,m} = 0.102 \cdot (1 - 0.01\,d)\,\rho_m \tag{4}$$

$$f_{h,90,m} = 0.102 \cdot (1 - 0.016\,d)\,\rho_m \tag{5}$$

The regression line in Figure 6.1 a) is inclined with more than 45 ° assuming that the coefficients of variation are $COV_{f_h} = 15\,\%$ and $COV_\rho = 8\,\%$. The factor to adjust the inclination of the regression line results from $\mu = 1$ and equation (6):

$$\frac{X\left(P = 0.05|\mathcal{N}\left(\mu;\sigma^2_{f_h}\right)\right)}{X\left(P = 0.05|\mathcal{N}\left(\mu;\sigma^2_{\rho}\right)\right)} = \frac{X\left(P = 0.05|\mathcal{N}\left(1;0.15^2\right)\right)}{X\left(P = 0.05|\mathcal{N}\left(1;0.08^2\right)\right)} = 0.8674 \tag{6}$$

The characteristic embedding strength was determined by Ehlbeck and Werner (1992) introducing the characteristic value for the density and multiplication with the factor given in equation (6) as follows:

$$f_{h,0,k} = 0.8674 \cdot 0.102 \cdot (1 - 0.01\,d)\,\rho_k \approx 0.09 \cdot (1 - 0.01\,d)\,\rho_k \tag{7}$$

$$f_{h,0,k} = 0.8674 \cdot 0.102 \cdot (1 - 0.016\,d)\,\rho_k \approx 0.09 \cdot (1 - 0.016\,d)\,\rho_k \tag{8}$$

To calculate the embedding strength according to EN 1995-1-1:2004, in Figure 6.1 a) the density of each specimen instead of the characteristic density of ash was used without changing the factor as described before. Therefore, the inclination of the regression line is too steep but the coefficient of determination is $R^2 = 0.63$.

93 % of the experimental results are larger than the calculated results according to EN 1995-1-1:2004 if the characteristic density was determined to $\rho_k = 662\,\mathrm{kg/m^3}$ assuming a normal distribution and a coefficient of variation of 7.8 %. Consequently, the calculation model of EN 1995-1-1:2004 gives values that are marginally to uncertain for the real characteristic density. The embedding strength is a function of density, diameter and load-to-grain angle. The density and the angle are metric variables in the calculation model, the diameter values are only given diskret. The sum of all embedding strength values $\Sigma_{(eq.)}$ was calculated out of all combinations of density ($\rho_k = 500\,\mathrm{kg/m^3}, 550\,\mathrm{kg/m^3} \ldots 900\,\mathrm{kg/m^3}$), diameter (6 mm, 8 mm, 12 mm, 16 mm, 20 mm, 30 mm) and load-to-grain angle ($\alpha = 0\,°, 10\,° \ldots 90\,°$) to compare the performance of different following calculation models. The ratio of the analyzed model to the model in EN 1995-1-1:2004 $\Sigma_{(eq.)}/\Sigma_{EN1995}$ and the coefficient of determination should be used to evaluate the calculation models.

4.3 Modification of EN 1995: 2004

The following equations are the results of regression analyses:

$$f_{h,0} = \frac{0.0928 \cdot (1 - 0.00991\,d)\,\rho}{(0.580 + 0.0373 \cdot d)\,sin^2\alpha + cos^2\alpha} \quad \text{with } R^2 = 0.697 \tag{9}$$

$$f_{h,0,k} = \frac{0.0785 \cdot (1 - 0.00991\,d)\,\rho_k}{(0.580 + 0.0373 \cdot d)\,sin^2\alpha + cos^2\alpha} \quad \text{with } \Sigma_{(10)}/\Sigma_{EN1995} = 0.98 \tag{10}$$

The good correlation between the calculation model and the experimental results is shown in Figure 6.1 c) and expressed by the coefficient of determination $R^2 = 0.697$.
The characteristic density $\rho_k = 662\,\mathrm{kg/m^3}$ and an iteration of the prefactor were used to determine the equation for the characteristic embedding strength, that means only 5 % of the experimental are less than the calculated results.

4.4 Power function

In equation for the characteristic value of embedding strength of spruce loaded by the thread of a self-tapping woodscrew given by Blaß, Bejtka and Uibel (2006) the density and the diameter are considered as non-linear variables. The ratio $f_{h,0}$ to $f_{h,90}$ is independent of the screw diameter and taken into the equation as a constant $1/k_{90} = 2.5$.

Blaß and Uibel (2007) published the equation (11) with an exponent of 1.21 for the density to describe the results of embedding strength tests with spruce (16 mm and 24 mm dowels, slenderness $\lambda \approx 2$, load-to-grain angle $\alpha = 0\,°$ and $\alpha = 90\,°$):

$$f_{h,pred} = \frac{0.026(1 - 0.011 \cdot d) \cdot \rho^{1.21}}{(1.63 + 0.014 \cdot d)sin^2\alpha + cos^2\alpha} \tag{11}$$

$f_{h,pred}$	predicted value for embedding strength $[\mathrm{N/mm^2}]$
ρ	density $[\mathrm{kg/m^3}]$
d	diameter of the dowel [mm]
α	load-to-grain angle [°]

The calculation of embedding strength predicts the experimental results best, if an equation with exponents for the density and the diameter are used. The influence of the load-to-grain angle is considered with the formula of Hankinson (1921) and the dependence of the ratio $k_{90} = f_{h,0}/f_{h,90}$ from the diameter by a linear equation. A regression analyse determined the coefficients.

$$f_{h,\alpha} = \frac{2.43 \cdot 10^{-3} \cdot \rho_{12}^{1.61} \cdot d^{-0.240}}{(0.647 + 0.0273 \cdot d)\, sin^2\alpha + cos^2\alpha} \quad \text{with } R^2 = 0.747 \tag{12}$$

$$f_{h,\alpha,k} = \frac{2.29 \cdot 10^{-3} \cdot \rho_{k}^{1.61} \cdot d^{-0.240}}{(0.647 + 0.0273 \cdot d)\, sin^2\alpha + cos^2\alpha} \quad \text{with } \Sigma_{(13)}/\Sigma_{EN1995} = 0.98 \tag{13}$$

5 Interpretation together with other experimental data

5.1 Own data of ash, beech, black locust, spruce and pine

All available experimental data should be analyzed to determine a calculation method for the embedding strength of hardwoods. Therefore, the results of Ehlbeck and Werner (1992), Whale, Smith and Hilson (1986) and our own data for ash, beech and black locust were collected in one database.

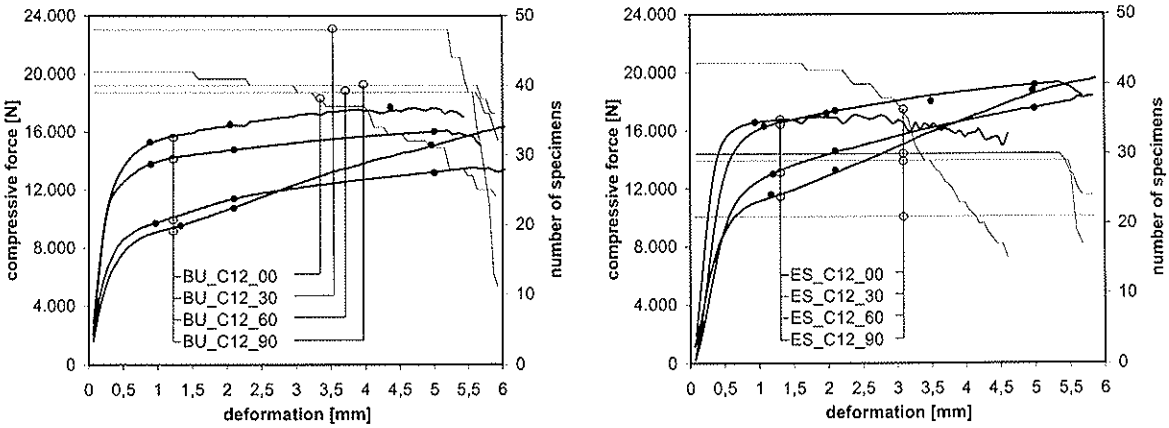

(a) beech (b) ash

Figure 5.1: Mean load-deformation curves and number of not splitted specimens

Figure 5.1 shows the mean load-deformation curves of some ash and beech samples (12 mm dowel, load-to-grain angle 0 °, 30 °, 60 ° and 90 °). The slope of the curve for the plastic behavior inclines with a rising load-to-grain angle. The number of specimen included in the calculation of the mean values decline with increasing deformation because splitting specimen fall out. This causes a non-continuous curve especially for $\alpha = 0\,°$. The black dots on the load-deformation curves mark the pair of variates per sample for the interpretation in the style of ASTM, at 2.1 mm deformation and according to ON EN 383:2007.
There are significant differences between the load-deformation curves of beech and ash. Beech splits later and the load increases at $\alpha = 0\,°$ even in the plastic part of the curve. Therefore, the beech is the only species with a ratio under one as indicated in Figure 5.2 at $\alpha = 0\,°$. The mean embedding strength at 0 ° according to ON EN 383:2007 is nearly the same but with an increasing load-to-grain angle beech falls to 80 % of the values for ash wood. The mean embedding strength of black locust was equal, i. e. up to 20 % better compared with ash.
The differences between the versions of interpretation are shown in Figure 5.2. The ratio of the value in the style of ASTM and the value of prEN 383 at 0 ° are less than one for all hardwoods (Figure 5.2 a). The changeover from elastic to plastic behavior is still running than yield load in the style of ASTM D5764-97a:2007 is reached. The softwoods spruce and pine split at very low deformations, therefore the different versions of interpretation give the same values at small load-to-grain angles and the ratio is always one. Large load-to-grain angles show substantial differences. The values for hardwood in the style of ASTM reach only 60 % of the values according to ON EN 383:2007 and at a deformation of 2.1 mm only 70 %.

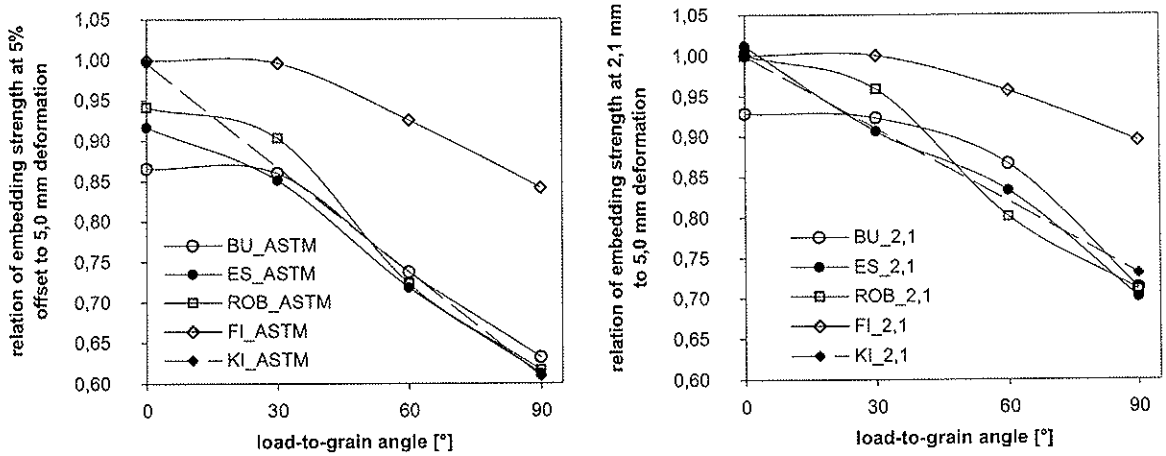

(a) In the style of ASTM D5764-97a:2007 to ON EN 383:2007

(b) Embedding strength at 2.1 mm deformation to ON EN 383:2007

Figure 5.2: Ratios of embedding strengths for different load-to-grain angles

5.2 Ehlbeck and Werner (1992)

The moisture content of the specimens is not documented in Ehlbeck and Werner (1992), but the specimens were conditioned in an environment with a relative humidity of $65 \pm 6\,\%$ and a temperature of $20 \pm 2\,°C$. At standard atmosphere according to DIN 50 014 – 20/65-1 with smaller tolerances $\Delta t = \pm 1\,K$ and $\Delta U = \pm 3\,\%$ most wood species have a moisture content of $(12 \pm 1.5)\,\%$ (see also Figure 3.2). For this reason, the presumed moisture content of $12\,\%$ is afflicted with uncertainties, which influences the reliability of the regression analysis negatively.

The relationship between density and embedding strength as seen in test results from Ehlbeck and Werner (1992) are presented in Figure 5.3 a). Azobé is not only exceptional because of its density but also because the embedding strength for dowels with 16 mm and 20 mm is not covered by the scatter plot of the other results (see Figure 5.3 b).

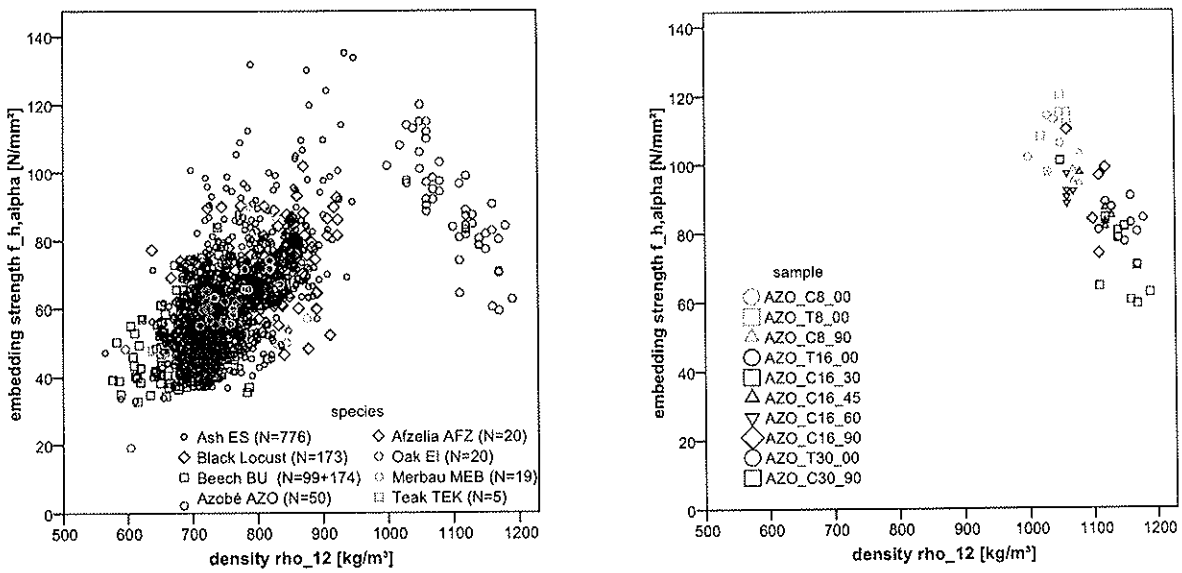

(a) All hardwoods, load-to-grain angles and diameters

(b) Azobé, all load-to-grain angles and diameters

Figure 5.3: scatterplots density versus embedding strength

The samples contain only five specimens and sometimes the variations of the density and the experimental results are very low, too low for a basic population on the background of our

own experiences. Hence the coefficients of variation for the density of teak and oak were fixed at $COV_\rho = 8\,\%$ to calculate the characteristic values with the normal distribution.

5.3 Whale and Smith (1986)

Foschi (1974) approximated the load-displacement curve of single lap joints with an equation (14) which was among others also used by Whale and Smith (1986) and Werner (1993).

$$p = (p_0 + p_1 w)\left[1 - exp\left(-\frac{k \cdot w}{p_0}\right)\right] \tag{14}$$

w	displacement
p_0	intersection of the tangent on the plastic part of the load-displacement curve and load axis
p_1	gradient of the tangent
k	initial modulus

The parameters of equation (14) were determined for a load-displacement curve up to 2.1 mm deformation for ash wood samples to estimate the variation between the extrapolated and the experimental value at 5 mm displacement. The extrapolation for dowels of 6 mm diameter is generally subject to errors. It differs unacceptably for single values of samples with a load-to-grain of $\alpha = 0\,°$ and 8 mm or larger. The mean values range between an underestimation of 5.1 % and an overestimation of 16.5 %. An acceptable accuracy is only given for $\alpha = 90\,°$ with -5.1 % to -0.30 %.
Only the extrapolated results of Whale, Smith and Hilson (1986) with a load-to-grain angle of $\alpha = 90\,°$ were used and the experimental data parallel to grain for 2.1 mm deformation were adopted without extrapolation based on Figure 5.2 b) and explanations of section 5.1.

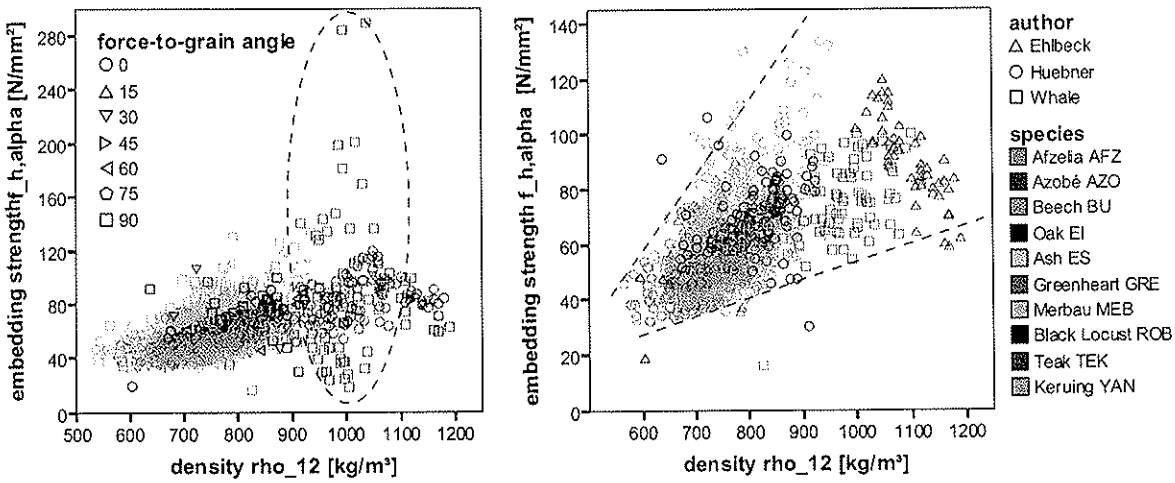

(a) All samples (b) Without Greenheart samples with load-to-grain angle $\alpha = 90\,°$

Figure 5.4: Embedding strength versus density for data from Ehlbeck and Werner (1992), Whale, Smith and Hilson (1986) and own samples

As the extrapolation for Greenheart perpendicular to the grain gives a wide range of unrealistic values (see Figure 5.4 a) the according samples were excluded (see Figure 5.4 b).
89 % of the experimental and extrapolated results are higher than the calculated results according to EN 1995-1-1:2004 if the characteristic density for each species is determined and assuming a normal distribution and a coefficient of variation of each species. Only the coefficients of variation of teak and oak were fixed at $COV_\rho = 8\,\%$ (see section 5.2). Consequently, the calculation model of EN 1995-1-1:2004 gives values that are not certain enough for the characteristic density of each specimen.

The algorithm that determined the equations for the data from Ehlbeck and Werner (1992), Whale, Smith and Hilson (1986), selected and extrapolated as described above, and our own hardwood samples was similar to the algorithm for ash.

$$f_{h,\alpha} = \frac{0.0920 \cdot (1 - 0.0104\, d)\, \rho}{(0.581 + 0.0400 \cdot d)\, sin^2\alpha + cos^2\alpha} \quad \text{with } R^2 = 0.590 \tag{15}$$

$$f_{h,\alpha,k} = \frac{0.0738 \cdot (1 - 0.0104 \cdot d) \cdot \rho_k}{(0.581 + 0.0400 \cdot d)\, sin^2\alpha + cos^2\alpha} \quad \text{with } \Sigma_{(16)}/\Sigma_{EN1995} = 0.92 \tag{16}$$

$$f_{h,\alpha} = \frac{0.0177 \cdot \rho_{12}^{1.29} \cdot d^{-0.179}}{(0.618 + 0.0351 \cdot d)\, sin^2\alpha + cos^2\alpha} \quad \text{with } R^2 = 0.616 \tag{17}$$

$$f_{h,\alpha,k} = \frac{0.0150 \cdot \rho_k^{1.29} \cdot d^{-0.179}}{(0.618 + 0.0351 \cdot d)\, sin^2\alpha + cos^2\alpha} \quad \text{with } \Sigma_{(18)}/\Sigma_{EN1995} = 0.95 \tag{18}$$

6 Conclusion and future prospects

The modification of the embedding strength calculation of hardwood according to present standards is proposed in equation (19):

$$f_{h,\alpha,k} = \frac{0.015 \cdot \rho_k^{1.3} \cdot d^{-0.2}}{(0.62 + 0.035 \cdot d)\, sin^2\alpha + cos^2\alpha} \quad \text{with } \Sigma_{(19)}/\Sigma_{EN1995} = 0.97 \tag{19}$$

Ideally, we would like to have embedding strength for all species used in load bearing constructions tests according to a unique standard for all diameters and load-to-grain angles 30 ° stepwise with 30 specimens in each sample. Only such database would allow a proper statistical interpretation. The scope given in ON EN 383:2007 should be restricted and a public data base should be completed step by step. It should be approved if the embedding strength under a load-to-grain angle of 90 ° at a deformation limit of 5 mm can be reached in a multi-dowel connection. Therefore, the data base should also contain the coefficients of equation (14).
The following propositions for the modification of ON EN 383:2007 are based on the experiences with 2187 tests according to this standard and a substantial literature research:

- It is common practice that the thickness of solid wood specimens is equal to two times the diameter. This should be fixed in the standard. The range of slenderness $\lambda = 1.5 \ldots 4$ is only necessary for commercially available thicknesses of wood products.
- The influence of the roughness of the dowel on load transmission, stress condition and modus of collapse is enormous. For this reason, only commercially available, electrogalvanised dowels should be used.
- The loading should be in compression only.
- The dimensions of the specimens for the force-to-grain angles between $\alpha = 0\,°$ and $\alpha = 90\,°$ should be fixed by linear interpolation.
- The moisture content of sitka spruce in an environment with a relative humidity of (65±5) % and a temperature of (20 ± 2) °C is in the range of 10.8 % to 13.0 %. The hysteresis of adsorption and desorption can cause an additional variation of ±1.7 %. The embedding strength of ash wood changes 3 % to 4 % if the moisture content moves only 1 %. So even if the restrictions of climate conditions are respected, a wide variation of ±7.9 % could be observed. The moisture content should be determined by oven dry method and the embedding strength should refer to 12 % moisture content to guarantee the reproducibility of results.
- It's practical to cut the specimens for the oven dry method from the undeformed part near the dowel and also to take the measurements to determine the density.

Table 6.1: Own hardwood samples and softwood samples from Spörk (2007)

sample	species	tensile or compr. test	nominal diameter d [mm]	force-to-grain angle α [°]	number of specimens N [Stück]	mean thickness t_{mean} [mm]	width b [mm]	length l [mm]	mean moisture content u_{mean} [%]	mean density $u = 12\,\%$ ρ_{mean} [kg/m^3]
ES_C6_00	ash	compr.	6	0	35	12.20	42	117	10.9	746
ES_C6_30				30	30	12.20	60	155	10.6	773
ES_C6_60				60	31	12.20	95	188	10.8	767
ES_C6_90				90	30	12.20	120	240	10.6	769
ES_C8_00	ash	compr.	8	0	34	16.10	54	158	10.4	763
ES_C8_30				30	30	16.00	90	182	10.2	737
ES_C8_60				60	30	16.00	110	250	10.0	745
ES_C8_90				90	30	16.10	110	320	9.9	744
ES_C12_00	ash	compr.	12	0	44	24.20	72	168	10.7	767
ES_C12_15				15	30	24.20	80	220	10.2	815
ES_C12_30				30	30	24.10	88	272	10.6	698
ES_C12_45				45	30	24.10	100	324	10.2	681
ES_C12_60				60	30	24.10	107	376	9.9	765
ES_C12_75				75	51	24.10	120	428	10.1	804
ES_C12_90				90	51	24.10	120	480	10.1	804
ES_C16_00	ash	compr.	16	0	30	30.20	96	224	10.6	746
ES_C16_30				30	30	30.30	118	362	10.3	750
ES_C16_60				60	30	30.20	138	502	10.2	749
ES_C16_90				90	30	30.20	150	640	10.6	740
ES_C20_00	ash	compr.	20	0	50	37.50	120	280	11.0	757
ES_C20_30				30	30	37.50	146	454	10.9	749
ES_C20_60				60	30	37.30	170	600	11.3	745
ES_C20_90				90	30	37.40	170	600	11.0	745
ES_C12_00_100	ash	compr.	12	0	44	23.44	72	168	4.3	768
ES_C12_90_100				90	42	23.64	120	480	4.6	818
ES_C12_00_200	ash	compr.	12	0	43	24.70	72	168	16.5	779
ES_C12_90_200				90	42	24.71	120	480	16.0	720
ES_C12_00_300	ash	compr.	12	0	42	24.77	72	168	18.9	765
ES_C12_90_300				90	42	25.05	120	480	19.0	686
BU_C12_00	beech	compr.	12	0	44	24.08	72	168	10.3	712
BU_C12_30				30	49	24.09	88	272	10.7	689
BU_C12_60				60	40	24.08	107	376	10.5	714
BU_C12_90				90	41	24.12	120	480	10.4	710
ROB_C12_00	black	compr.	12	0	47	24.14	72	168	9.8	804
ROB_C12_30	locust			30	42	24.13	88	272	10.4	790
ROB_C12_60				60	42	24.08	107	376	10.1	793
ROB_C12_90				90	42	24.16	120	480	10.0	804
FI_C8_00	spruce	compr.	8	0	56	15.99	50	115	9.3	391
FI_C8_90				90	56	16.01	80	320	9.1	399
FI_C12_00	spruce	compr.	12	0	64	24.91	72	168	10.4	397
FI_C12_10				10	14	23.9	77	203	10.6	403
FI_C12_20				20	14	24.03	83	237	10.7	407
FI_C12_25				25	51	23.99	85	255	9.8	401
FI_C12_30				30	14	24.06	88	272	10.7	404
FI_C12_40				40	14	24.04	93	307	10.8	407
FI_C12_50				50	65	24.01	99	341	10.1	399
FI_C12_60				60	14	24.04	104	376	10.7	412
FI_C12_70				70	14	24.05	109	411	10.8	405
FI_C12_80				80	14	24.05	115	445	10.7	405
FI_C12_90				90	65	24.02	120	480	10.1	400
FI_C20_00	spruce	compr.	20	0	41	39.98	120	280	9.9	400
FI_C20_00_100				0	55	41.2	120	280	10.3	396
FI_C20_00_200				0	14	41.13	120	280	10.0	383
FI_C20_90				90	51	34.08	200	800	10.6	401
KI_C12_00	pine	compr.	12	0	113	24.96	77	203	11.6	544
KI_C12_90				90	80	20.97	120	480	13.0	538

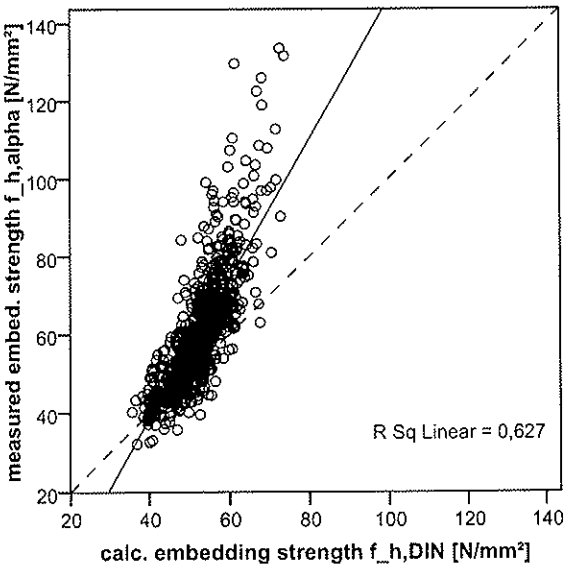

(a) values in the style of EN 1995-1-1:2004 vs. ($\rho_{specimen}$ in stet of ρ_k) vs. experimental data

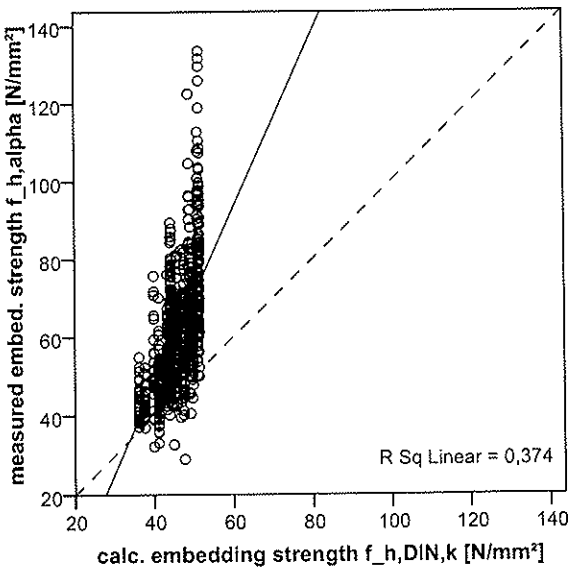

(b) char. values EN 1995-1-1:2004 vs. experimental results

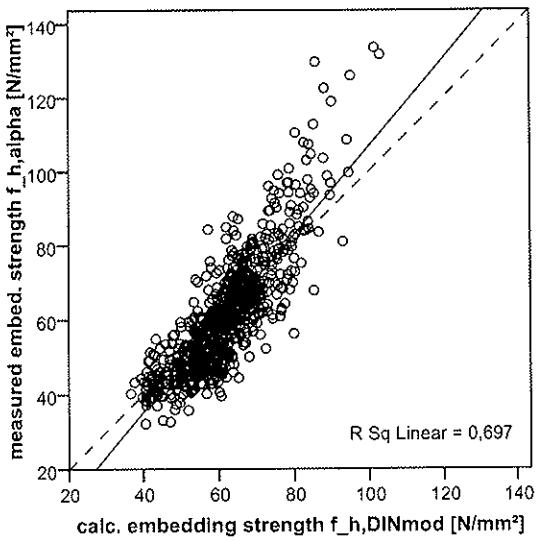

(c) equation (9) vs. experimental results

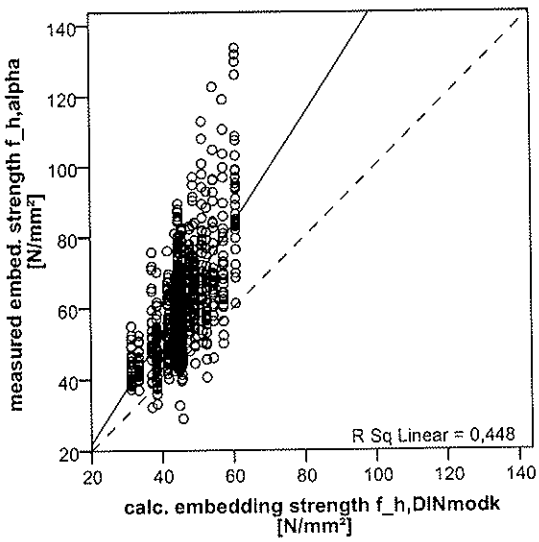

(d) equation (10) versus experimental results

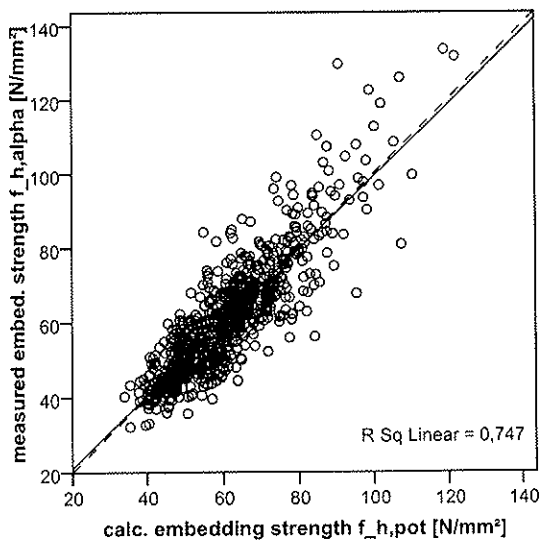

(e) equation (12) versus experimental results

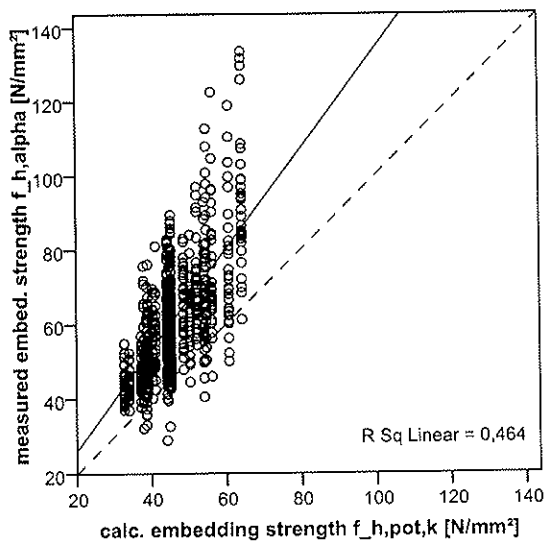

(f) equation (13) versus experimental results

Figure 6.1: Calculated vs. experimental results of embedding strength for ash

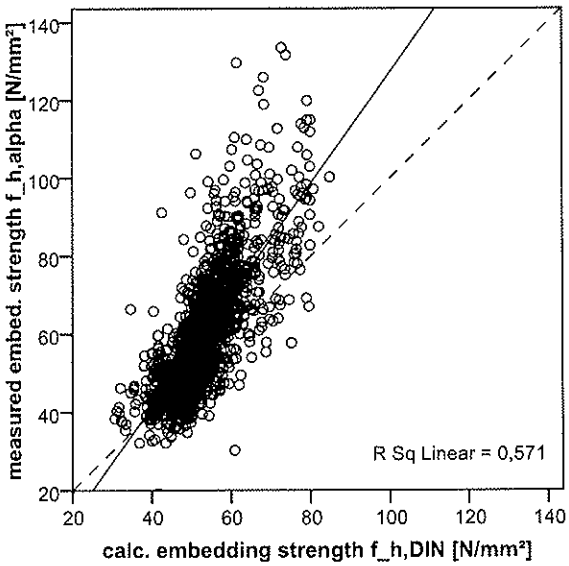

(a) values in the style of EN 1995-1-1:2004 vs. ($\rho_{specimen}$ in stet of ρ_k) vs. experimental data

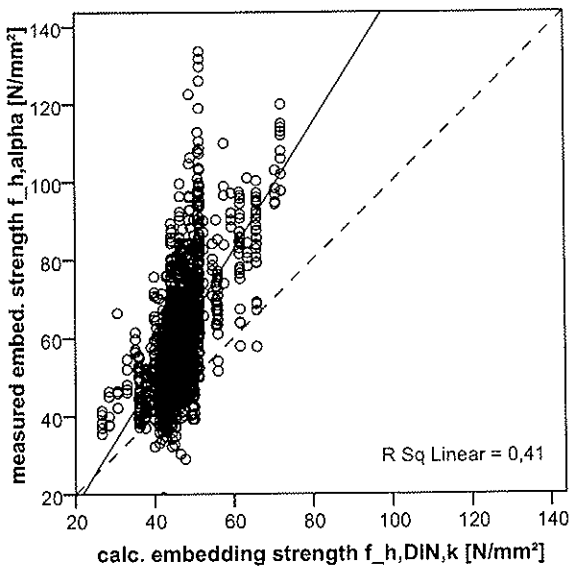

(b) char. values EN 1995-1-1:2004 vs. experimental results

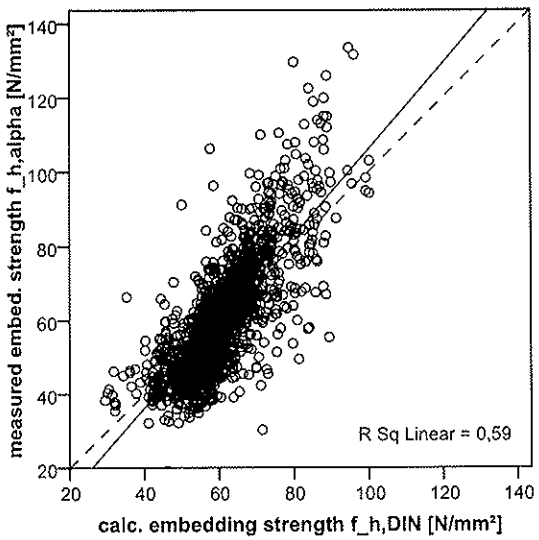

(c) equation (15) versus experimental results

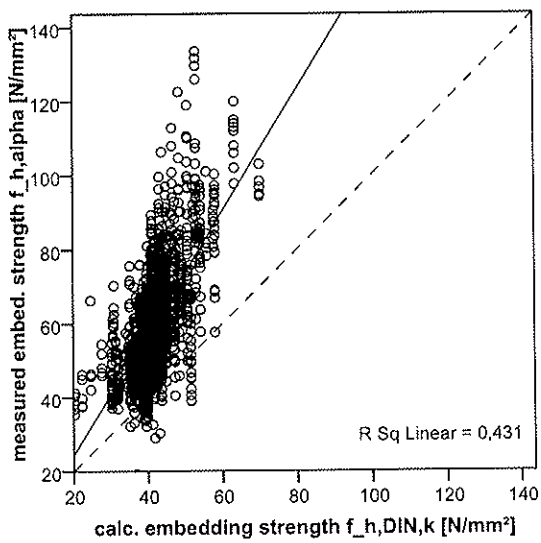

(d) equation (16) versus experimental results

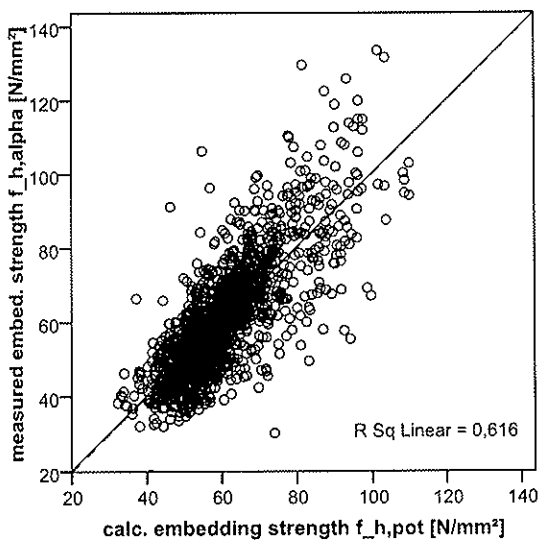

(e) equation (17) versus experimental results

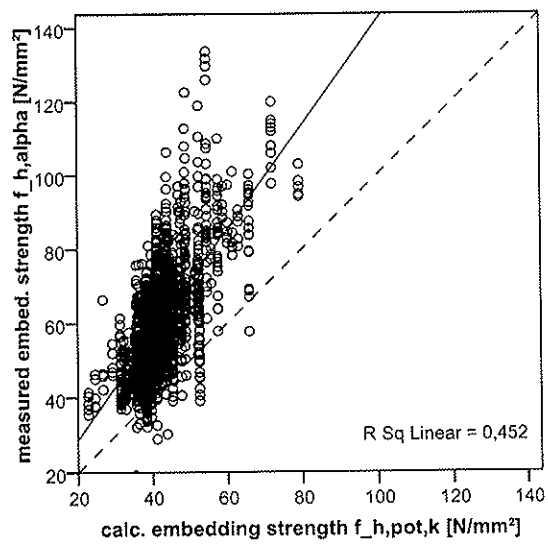

(f) equation (18) versus experimental results

Figure 6.2: Calculated vs. experimental results of embedding strength for beech, ash, black locust and values from Ehlbeck and Werner (1992) and Whale, Smith and Hilson (1986)

References

[ASTM D5764-97a: 2007] ASTM-D5764-97A: *Standard Test Method for Evaluating Dowel-Bearing Strength of Wood and Wood-Based Products.* 1. April 2007

[Blaß et al. 2006] BLASS, Hans Joachim ; BEJTKA, Ireneusz ; UIBEL, Thomas: Tragfähigkeit von Verbindungen mit selbstbohrenden Holzschrauben mit Vollgewinde / Universität Karlsruhe. Universitätsverlag Karlsruhe, 2006. – Band 4 der Reihe Karlsruher Berichte zum Ingenieurholzbau. – ISBN 978-3-86644-034-0

[Blaß and Uibel 2007] BLASS, Hans J. ; UIBEL, Thomas: Tragfähigkeit von stiftförmigen Verbindungsmitteln in Brettsperrholz / Universität Karlsruhe, Lehrstuhl für Ingenieurholzbau und Baukonstruktionen. 2007. – Band 8 der Reihe Karlsruher Berichte zum Ingenieurholzbau. – 204 S. – ISBN 978-3-86644-129-3

[DIN 1052-2: 1988] DIN 1052 TEIL 2: *Holzbauwerke – Mechanische Verbindungen.* April 1988

[DIN 4076-1: 1985] DIN 4076 TEIL 1: *Benennungen und Kurzzeichen auf dem Holzgebiet; Holzarten.* Oktober 1985

[E DIN 4074-5: 2008] ENTWURF DIN 4074-5: *Sortierung von Holz nach der Tragfähigkeit – Teil 5: Laubschnittholz.* Mai 2008

[Ehlbeck and Werner 1992] EHLBECK, Jürgen ; WERNER, Hartmut: Tragfähigkeit von Laubholzverbindungen mit stabförmigen Verbindungsmitteln / Versuchsanstalt für Stahl, Holz und Steine der Universität Karlsruhe, Abt. Ingenieurholzbau. Karlsruhe, 1992. – Tech. Report. – 196 S

[Ellwood 1954] ELLWOOD, Eric L.: Properties of American beech in tension and compression perpendicular to the grain and their relation to drying / Yale University, School of Forestry. 1954. – Bulletin 61. – 82 S

[EN 1995-1-1: 2004] EN 1995-1-1: *Eurocode 5: Bemessung und Konstruktion von Holzbauten – Teil 1-1: Allgemeines – Allgemeine Regeln und Regeln für den Hochbau.* November 2004

[Foschi 1974] FOSCHI, R. O.: Load-slip characteristics of nails. In: *Wood Science* 7 (1974), Nr. 1, S. 69–84

[Gehri 1982] GEHRI, Ernst: Fachwerkträger aus Buche und Fichte mit Stahlknotenplatten in eingeschlitzten Hölzern / Inst. für Baustatik und Stahlbau, ETH Zürich. Zürich, Juli 1982. – Int. Bericht 82-1

[Hankinson 1921] HANKINSON, R. L.: Investigation of Crushing Strength of Spruce at Various Angles to the Grain. In: *Air Service Information Circular* 3 (1921), Nr. 259. – Materials Section Paper No. 130

[Kollmann 1941] KOLLMANN, Franz: *Schriftenreihe Eigenschaften und Verwertung der deutschen Naturhölzer.* Vol. 1: *Die Esche und ihr Holz.* Berlin : Julius Springer, 1941

[Leijten 2004] LEIJTEN, Ad J. M.: Review of probability data for timber connections with dowel-type fasteners. In: *Proceedings of CIB-W18.* Edinburgh, UK, August 2004. – Paper 37-7-13

[Leijten et al. 2006] LEIJTEN, Ad J. M. ; KÖHLER, Jochen ; JORISSEN, Andre J. M.: Timber density restrictions for timber connection tests according to EN 28970/ISO 8970. In: *Proceedings of CIB W18.* Florence, Italy, August 2006. – Paper 39-21-1

[ON EN 28970: 1991] ONORM EN 28970: *Holzbauwerke – Prüfung von Verbindungen mit mechanischen Verbindungsmitteln – Anforderungen an die Rohdichte des Holzes (ISO 8970:1989).* 1. August 1991

[ON EN 383: 2007] ÖNORM EN 383: *Holzbauwerke – Prüfverfahren – Bestimmung der Lochleibungsfestigkeit und Bettungswerte für stiftförmige Verbindungsmittel.* 1. März 2007

[prEN 383: 1990] PREN 383: *Holzbauwerke – Bestimmung der Lochleibungsfestigkeit.* August 1990

[Rammer and Winistorfer 2001] RAMMER, Douglas R. ; WINISTORFER, Steve G.: Effect of Moisture Content on Dowel-Bearing Strength. In: *Wood and Fiber Science* 33 (2001), Nr. 1, S. 126–139

[Schmid 2002] SCHMID, Martin: *Anwendung der Bruchmechanik auf Verbindungen mit Holz.* Karlsruhe, Fakultät für Bauingenieur-, Geo- und Umweltwissenschaften, Promotionsarbeit, 2002. – 304 S

[Serrano and Sjödin 2007] SERRANO, Erik ; SJÖDIN, Johan: Dowel type joints — Influence of moisture changes and dowel surface smoothness. In: *Proceedings of COST Action E55 WG2.* Eindhoven, Netherlands, October 4-5 2007. – 2nd Workshop and 4th Management Committee Meeting

[Spörk 2007] SPÖRK, Anton: *Lochleibungsfestigkeit von Nadelhölzern – Einflußfaktoren und Modellvergleiche,* Technischen Universität Graz, Fakultät für Bauingenieurwissenschaften, Institut für Holzbau und Holztechnologie, Masterthesis, 2007

[Werner 1993] WERNER, Hartmut: *Tragfähigkeit von Holz-Verbindungen mit stiftförmigen Verbindungsmitteln unter Berücksichtigung streuender Einflußgrößen.* Karlsruhe, Technische Universität Karlsruhe, Phd-thesis, 1993

[Whale and Smith 1986] WHALE, Luke R. J. ; SMITH, Ian: Mechanical timber joints / CEC-project, Timber Reseach and Developement Association (TRADA). High Wycombe, UK, 1986. – Research Report RR18/86

[Whale et al. 1986] WHALE, Luke R. J. ; SMITH, Ian ; HILSON, Barry O.: Behaviour of Nailed and Bolted Joints under Short-Term Lateral Load – Conclusions from Some Recent Research. In: *Proceedings of CIB-W18.* Florence, Italy, 1986. – Paper 19-7-1

[Youngs 1957] YOUNGS, Robert Leland: The perpendicular-to-grain mechanical properties of red oak as related to temperature, moisture content, and time / U.S. Dept. of Agriculture, Forest Service, Forest Products Laboratory. URL `http://hdl.handle.net/1957/2526`, June 1957. – Report no. 2079

INTERNATIONAL COUNCIL FOR RESEARCH AND INNOVATION
IN BUILDING AND CONSTRUCTION

WORKING COMMISSION W18 - TIMBER STRUCTURES

COMPOSITE ACTION OF I-JOIST FLOOR SYSTEMS

T G Williamson

B Yeh

APA – The Engineered Wood Association

USA

Presented by T.G. Williamson

H. Blass stated composite action is strongly dependent on the span. This study only deals with one span. T. Williamson and B.J. Yeh responded that this span was chosen to be the most critical case. F. Lam stated composite action also depends on depth and I. In this paper one factor was proposed for all cases. Would one look into additional depths? T. Williamson and B.J. Yeh responded that yes more depths will need to be considered but the most critical depth has been evaluated. A. Buchanan asked about multiple span applications where positive and negative moments exist. B.J. Yeh responded that from analytical studies this was considered but the results showed this was not critical that compared to single span. T. Williamson further clarified that there is no difference between long term and short term tests. Y.H. Chui asked whether mechanics based approach will be considered. B.J. Yeh responded that yes it would be good but engineers need a simple solution at the end rather than computer programs. S. Winter received clarification that elastomeric based glue, construction type silicon 98 was used. I. Smith stated why simple design in timber was discussed as if we were 2nd class. T. Williamson stated that in US most designs with wood are carried out by 2nd class engineers so we need more tools to help them. J. Munch-Andersen asked about vibration of these floors. T. Williamson said that US does not have explicit vibration provisions in floor design. V. Rajcic asked why EA perpendicular values declined. T. Williamson explained that in panel production E parallel is critical. Through qualification and Quality assurance process, OSB has been optimized for this property while EA perpendicular declined.

Composite Action of I-Joist Floor Systems

Thomas G. Williamson, P.E. and Borjen Yeh, Ph.D., P.E.
APA – The Engineered Wood Association, U.S.A.

Abstract

In 1968, APA conducted field-glued plywood-joist floor system tests and established floor composite action factors based on the research results that have subsequently been in use in the United States for 40 years. Those composite action factors were based on the use of a single layer plywood floor (underlayment) glue-nailed to sawn lumber joist systems to improve the stiffness of the floor and to minimize the impact of nail pull-out and associated squeaks. Prefabricated wood I-joists, while having been used in the United States and Canada for over 30 years, are now gaining acceptance in Europe and other geographic regions such as Australasia for residential floor construction. In fact, approximately 45% of all raised wood floors constructed in North America now use I-joists which represent over 300 million lineal meters (984 x 10^6 lineal feet).

As a result, APA recently conducted a study to review the effect of glue-nailed assemblies on the stiffness capacity of I-joist floor systems with oriented strand board (OSB) floor sheathing since OSB is widely used in residential floor construction today. Bending tests on full scale-floor sections as well as T-beam sections with panels glue-nailed to the I-joist frame were conducted. Based on this research, a new composite action factor for glue-nailed I-joist floor systems was established.

APA also conducted an intensive testing program to assess the EA-perpendicular (axial stiffness) properties for OSB. An impact study was then conducted to investigate the effect of this new composite action factor on the allowable spans of I-joist floor systems when the axial stiffness of OSB floor sheathing in the direction perpendicular to the strength axis of the panel is reduced, as evidenced by these recent tests conducted by APA. This paper presents the results of these studies and provides recommendations for determining the spans of wood I-joists used in floor systems.

1. Introduction

Wood floors made of wood structural panel sheathing that is glue-nailed to wood joists are much stiffer than the stiffness of the wood joists alone. This phenomenon is attributed to the floor composite action and has been studied by several researchers, as summarized in the APA Laboratory Report LR-118 [1] and USDA Forest Products Laboratory Research Paper RP-289 [2]. As part of the APA LR-118, floor composite action factors for field-glued plywood-lumber joist floor systems were established. These same composite action factors have been adopted by the engineered products industry and the wood engineering community in the United States for 40 years.

According to the APA LR-118, the composite action factor, C, is defined in Equation 1. For floor systems with the floor sheathing glue-nailed to floor joists, C is equal to 0.90 if the tongue-and-groove (T&G) of the floor sheathing is also glued. Otherwise C is equal to 0.45 if the T&G of the floor sheathing is nailed only. For floor systems with the floor sheathing nailed to floor joists without gluing, it is assumed that there is no composite action, i.e., C is equal to 0.

$$C = \frac{\text{Actual \% increase in stiffness}}{\text{\% increase if fully composite}} = \frac{\frac{EI_{effective}}{EI_{joist}} - 1}{\frac{EI_{composite}}{EI_{joist}} - 1} \quad (1)$$

where $EI_{composite}$ = bending stiffness of the fully composite floor and
EI_{joist} = bending stiffness of the floor joists alone
C = composite action factor

The composite action factors established in APA LR-118 were based on the use of a single layer plywood floor (underlayment) glue-nailed to sawn lumber joist systems to improve the stiffness of the floor and to minimize the impact of nail pull-out and associated squeaks. Prefabricated wood I-joists, while having been used in the U.S. and Canada for over 30 years, are now gaining acceptance in Europe and other geographic regions such as Australasia for residential floor construction. In fact, approximately 45% of all raised wood floors constructed in North America now use I-joists which represent over 300 million lineal meters (984 x 10^6 lineal feet).

The wood I-joist industry has adopted the use of Equation 1 when calculating the allowable floor spans that are often governed by the live load deflection criterion of L/480, where L is the on-center floor span. This live load deflection criterion is more stringent than the code-specified L/360 and represents a voluntary standard adopted by the wood I-joist industry in the U.S. As a result, the composite action factor is an essential part of the allowable floor spans recommended by the wood I-joist manufacturers. As there have been no industry-wide data based on wood I-joist floor systems to confirm the composite action factors recommended in APA LR-118, APA recently conducted a study to review the effect of glue-nailed assemblies on the stiffness capacity of I-joist floor systems with oriented strand board (OSB) floor sheathing since OSB is widely used in residential floor construction today. This paper provides the test results and analyses.

2. Materials and Test Methods

2.1 Material Description

Table 1 provides the test matrix and materials used in this study. All materials were purchased locally in Tacoma, Washington, and were tested in the as-received conditions. The OSB floor sheathing contained T&G and had a nominal thickness of 15 mm (19/32 in.) meeting the requirements of a single floor 20 oc span rating in accordance with Voluntary Product Standard PS2 [3]. The wood I-joists were 241 mm (9-1/2 in.) in depth meeting the requirements of APA PRI-400, *Performance Standard for APA EWS I-Joists* [4]. To cover a range of manufacturing variables, two I-joist series were tested. The PRI-30 series I-joists used 33 x 38 mm (1-5/16 x 1-1/2 in.) laminated veneer (LVL) flanges and 9.5 mm (3/8 in.) OSB web oriented vertically (i.e., the strength axis is perpendicular to the length of the I-joist). The PRI-40 series I-joists used 38 x 64 mm (1-1/2 x 2-1/2 in.) spruce-pine-fir (SPF) lumber flanges and 9.5 mm (3/8 in.) OSB web oriented vertically. These I-joist series represent the smallest sizes of LVL and lumber flanges typically used in North America and it is expected that the floor composite action factors determined from this study can be conservatively applied to other I-joist floor systems with larger flange sizes and deeper I-joists.

Table 1. Numbers of specimens and test matrix

Floor Sheathing	I-joist	Floor Assembly			T-Beam	
		Individual I-joist EI	Bare I-joist Frame Assembly	Complete Assembly[(a)]	Individual I-joist EI	Complete T-beam[(a)]
15 mm (19/32 in.) OSB Floor Sheathing 20 oc, T&G	241 mm (9-1/2 in.) I-joists with 33 x 38 mm (1-5/16 x 1-1/2 in.) LVL Flange (PRI-30)	6	2	2	2	2
	241 mm (9-1/2 in.) I-joists with 38 x 64 mm (1-1/2 x 2-1/2 in.) SPF Lumber Flange (PRI-40)	6	2	2	2	2

[(a)] With the glue-nailed OSB floor sheathing installed.

The adhesive used to fabricate the T-beam and floor assembly was a commercially available elastomeric construction adhesive (Liquid Nails) meeting ASTM D 3498, *Standard Specification for Adhesives for Field-Gluing Plywood to Lumber Framing for Floor Systems* [5]. Details for the assembly preparation are provided in the following sections.

2.2 Test Methods

2.2.1 General

Prior to assembly tests, the EI and EA of the floor sheathing and the EI of individual I-joist were non-destructively tested. The sheathing and I-joists were sorted into different groups based on the material EI. The T-beams, I-joist frames, and floor assemblies were then fabricated by laboratory technicians according to the test matrix shown in Table 1.

2.2.2 Panel EI and EA Tests

OSB sheathing EI in the across-panel direction was non-destructively tested in accordance with Method C – Pure Moment of ASTM D 3043, *Standard Test Methods for Structural Panels in Flexure* [6]. OSB sheathing EA in the across-panel direction was non-destructively tested based on ASTM D 3501, *Standard Test Methods for Wood-Based Structural Panels in Compression* [7]. This loading direction matches the common construction practice of residential floors in North America where the floor sheathing is typically installed with the sheathing strength axis perpendicular to the supporting I-joists.

2.2.3 Individual I-Joist EI Tests

The third-point bending test method of ASTM D 198, *Standard Test Methods of Static Tests of Lumber in Structural Sizes* [8], was used for the non-destructive I-joist EI tests. The on-center test span was 4572 mm (180 in.) and the maximum load was limited to 6.7 kN (1,500 lbf) to avoid any damages to the I-joists.

2.2.4 I-Joist Frame Assembly Tests

I-joist frames without floor sheathing, as shown in Figure 1, were installed following the APA recommendation for I-joist floor installation as specified in *APA Performance Rated I-Joists* [9]. OSB rim boards meeting the requirements of APA PRR-401, *Performance Standard for APA EWS Rim Boards* [10], were nailed to the end of I-joists using one 8d common nail (3.3 x 64 mm or 0.131 x 2-1/2 in.) at the top and bottom flanges. Three I-joists that had the closest EI values were grouped to frame an I-joist assembly with a spacing of 406 mm (16 in.) on center. Each "bare frame assembly" was tested to obtain EI

values for the bare I-joist frame. For a given assembly, the bare I-joist frame EI was divided by 3 to represent EI_{joist} used in the composite action factor analysis.

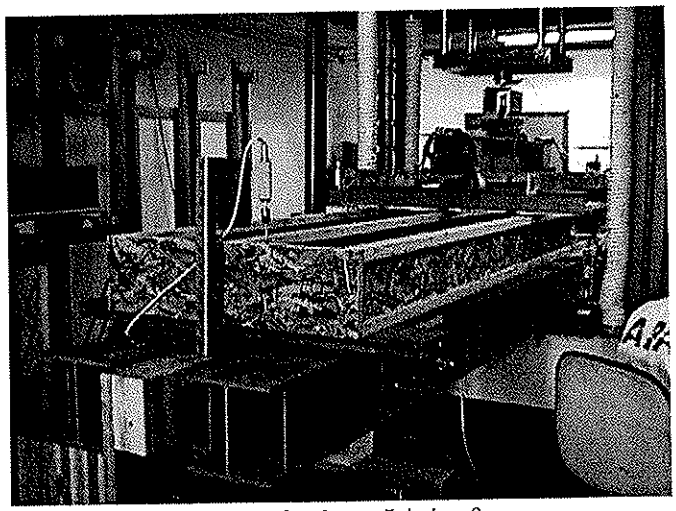

Figure 1. Test setup for bare I-joist frames

2.2.5 I-Joist Floor Assembly Tests

After the bare I-joist frame tests were completed, the 15-mm (19/32-in.) OSB floor sheathing that had been non-destructively tested was installed with the strength axis perpendicular to the supporting I-joists, as shown in Figure 2. A single 6.4-mm- (1/4-in.-) diameter bead of elastomeric construction adhesive meeting ASTM D 3498 was applied to the joists and rim boards. Two lines of adhesive were applied to I-joists where panel ends butt to assure proper gluing of each end. Eight-penny (8d) common nails (3.3 x 64 mm or 0.131 x 2-1/2 in.) were used to install the floor sheathing to the I-joists with a 152 mm (6 in.) spacing on the edges and 305 mm (12 in.) spacing in the field. A 3.2 mm (1/8 in.) gap was left between all panel edge joints in accordance with industry installation recommendations. Adhesive was not applied to the T&G of the floor sheathing. The floor assemblies were stored in the laboratory under an indoor environment (approximately 15-18°C or 60-65°F and 50% RH) for at least 10 days prior to testing. For a given floor assembly, the I-joist floor assembly EI was divided by 3 to represent $EI_{effective}$ used in the composite action factor analysis.

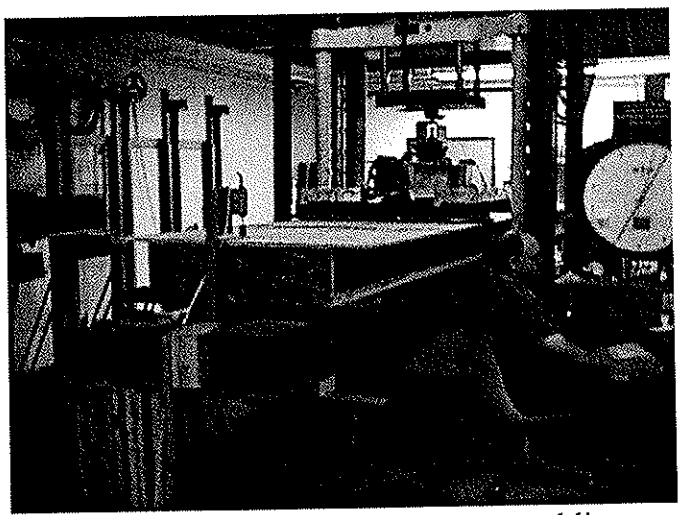

Figure 2. Test setup for I-joist floor assemblies

2.2.6 T-Beam Assembly Tests

T-beam assemblies were fabricated following the same installation details as specified for I-joist floor assemblies except that the width of the OSB was 406 mm (16 in.), as shown in Figure 3. The T-beams were stored in the laboratory under an indoor environment for at least 10 days prior to testing. For a given T-beam assembly, the assembly EI represents $EI_{effective}$ used in the composite action factor analysis.

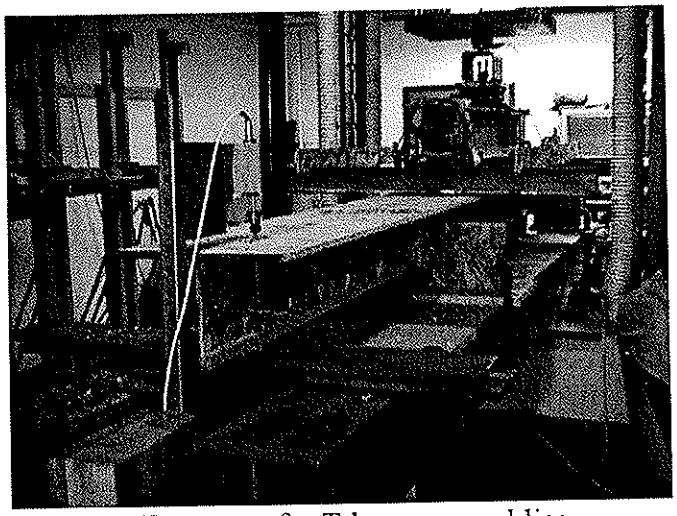

Figure 3. Test setup for T-beam assemblies

2.2.7 Assembly Tests Methods

The third-point bending test method of ASTM D 198 was used for non-destructive testing of (a) each bare I-joist frame (without the OSB floor sheathing installed), (b) the I-joist floor assembly (with the OSB floor sheathing installed), and (c) the T-beam assemblies. The on-center test span was 4572 mm (180 in.). Lateral supports were provided for the T-beam assemblies. The deflection at the mid-span of each I-joist at its neutral axis was measured. The deflection at the two ends of the center I-joist was also measured and subtracted from the measured mid-span deflection. For all assembly tests, a test load equivalent to the floor load of 2.4 kPa (50 lbf/ft^2) was applied at a loading rate of 12.7 mm/min (0.5 in./min). Three tests were repeated for each assembly with an approximate 3-min recovery interval between tests. The average of the three repeated tests was reported for each assembly.

3. Results and Discussions

Test results and the derived construction factors are summarized in Table 2. The $EI_{effective}$ values obtained from the floor assembly tests (F30 and F40) are in good agreement with the values measured directly from the T-beam tests (T-30 and T-40). With the EI_{joist} determined from individual I-joist EI tests (see Section 2.2.3) and sheathing $EI_{\perp}$ and $EA_{\perp}$ properties determined from panel tests (see Section 2.2.2), the $EI_{composite}$ can be calculated using the principle of engineering mechanics, as demonstrated in APA LR-118. Again, the calculated $EI_{composite}$ values are in good agreement between the floor assembly tests (F30 and F40) and the T-beam tests (T-30 and T-40).

Finally, the composite action factor, C, can be determined in accordance with Equation 1 using the values of EI_{joist}, $EI_{effective}$, and $EI_{composite}$. As can be seen from Table 2, the average floor composite factor determined from this study (based on floor assembly test results only) is equal to 0.57 for glue-nailed I-joist floor systems with unglued T&G.

Table 2. Summary of test results

Test[a]	I-Joist Properties			15 mm (19/32 in.) OSB Properties				$EI_{effective}$[d] (10^6 lbf-in.^{2})	$EI_{composite}$[e] (10^6 lbf-in.^{2})	C[f]
	A[a] (in.^{2})	I[b] (in.^{4})	EI_{joist}[c] (10^6 lbf-in^2)	Thickness (in.)	A (in.^{2}/ft)	$EA_{\perp}$ (10^6 lbf/ft)	$EI_{\perp}$ (10^3 lbf-in.^{2}/ft)			
F30-1	5.31	72.0	146	0.608	7.295	3.87	0.100	189	235	0.48
F30-2			140	0.610	7.324	3.95	0.103	188	229	0.53
F40-1	8.80	126.0	167	0.607	7.279	3.57	0.093	235	253	0.79
F40-2			184	0.607	7.287	3.81	0.095	227	277	0.46
T30-1	5.31	72.0	147	0.609	7.302	3.79	0.094	188	235	0.47
T30-2			153	0.610	7.326	3.47	0.081	197	237	0.52
T40-1	8.80	126.0	161	0.609	7.310	3,50	0.092	217	246	0.66
T40-2			159	0.607	7.283	4.00	0.099	224	251	0.71
									Average (All)	0.58
									Average (4 Floor Assemblies)	0.57
									Average (4 T-beams)	0.59

For SI: 1 lbf = 4.448 N; 1 in. = 25.4 mm; 1 ft = 304.8 mm

[a] F30 and F40 are the I-joist floor assemblies with PRI-30 PRI-40 I-joists (see Table 1), respectively. Two replicates were tested, which are denoted as 1 and 2 in the last digit of the test number. T30 and T40 are the T-beam assemblies with PRI-30 and PRI-40 I-joists, respectively.

[b] Nominal I-joist cross section (A) and moment of inertia (I) are based on a 0.20-in. (5 mm) transformed web thickness.

[c] For F30 and F40, I-joist EI is based on the average of 3 I-joists from the respective bare I-joist frame test without the OSB floor sheathing.

[d] For F30 and F40, effective floor EI is based on the average of 3 I-joists from the respective I-joist floor assembly test with the glue-nailed OSB floor sheathing installed.

[e] Composite floor EI is calculated based on the I-joist and sheathing properties tabulated in this table.

[f] The floor composite action factor (C) is determined based on Equation 1.

3.1 Discussion

While the data provided from this study is relatively limited, the increase in the composite action factor for I-joist floor systems is not unexpected due to consistent product quality for I-joists, as compared to sawn lumber joists. In addition, it is likely that the better adhesive technology available today, as compared to 40 years ago when APA LR-118 was studied, provides a more efficient mechanism for the development of the composite action for I-joist floor systems.

The effect of the increased composite action factor from the existing 0.45 to 0.55 (rounded down from 0.57) on the allowable I-joist spans is shown in Table 3 for simple-span applications and Table 4 for multiple-span applications using the I-joist properties published in the APA PRI-400 I-joist standard for residential floor construction. The effective EI of an I-joist floor system is calculated based on Equation 2, which is rearranged from Equation 1.

$$EI_{effective} = (C)\, EI_{composite} + (1 - C)\, EI_{joist} \qquad (2)$$

Table 3. Effect of increased composite action factor from 0.45 to 0.55 (simple-span)

I-Joist Series	Allowable Clear Span (mm) for Simple-Span Application[(a)]				Difference (mm)	
	C = 0.45		C = 0.55			
	On-Center Joist Spacing					
	406 mm (16 in.)	610 mm (24 in.)	406 mm (16 in.)	610 mm (24 in.)	406 mm (16 in.)	610 mm (24 in.)
9-1/2" PRI-20	4623	4089	4699	4166	76	76
9-1/2" PRI-30	4775	4216	4851	4293	76	76
9-1/2" PRI-40	5004	4420	5080	4470	76	51
9-1/2" PRI-50	4978	4394	5029	4470	51	76
9-1/2" PRI-60	5283	4648	5334	4724	51	76
11-7/8" PRI-20	5537	4877	5613	4877	76	0
11-7/8" PRI-30	5715	5029	5791	5131	76	102
11-7/8" PRI-40	5969	5080	6045	5080	76	0
11-7/8" PRI-50	5944	5232	6020	5309	76	76
11-7/8" PRI-60	6299	5537	6375	5613	76	76
11-7/8" PRI-70	6401	5639	6477	5715	76	76
11-7/8" PRI-80	6909	6045	6960	6121	51	76
11-7/8" PRI-90	7112	6223	7163	6299	51	76
14" PRI-40	6782	5588	6858	5588	76	0
14" PRI-50	6756	5969	6858	6045	102	76
14" PRI-60	7163	6299	7239	6375	76	76
14" PRI-70	7264	6375	7341	6477	76	102
14" PRI-80	7849	6883	7899	6960	51	76
14" PRI-90	8052	7061	8128	7137	76	76
16" PRI-40	7391	6020	7391	6020	0	0
16" PRI-50	7518	6147	7620	6147	102	0
16" PRI-60	7925	6960	8026	7061	102	102
16" PRI-70	8052	7036	8128	7036	76	0
16" PRI-80	8687	7620	8763	7696	76	76
16" PRI-90	8915	7798	8992	7899	76	102

[(a)] Based on the live load deflection criterion of L/480, where L is the on-center span

Table 4. Effect of increased composite action factor from 0.45 to 0.55 (multiple-span)

I-Joist Series	Allowable Clear Span (mm) for Multiple-Span Application[a]				Difference (mm)	
	C = 0.45		C = 0.55			
	On-Center Joist Spacing					
	406 mm (16 in.)	610 mm (24 in.)	406 mm (16 in.)	610 mm (24 in.)	406 mm (16 in.)	610 mm (24 in.)
9-1/2" PRI-20	5029	4089	5105	4089	76	0
9-1/2" PRI-30	5182	4572	5283	4572	102	0
9-1/2" PRI-40	5461	4445	5461	4445	0	0
9-1/2" PRI-50	5410	4750	5486	4851	76	102
9-1/2" PRI-60	5740	5029	5817	5131	76	102
11-7/8" PRI-20	5969	4089	5969	4089	0	0
11-7/8" PRI-30	6223	4572	6299	4572	76	0
11-7/8" PRI-40	6223	5055	6223	5055	0	0
11-7/8" PRI-50	6452	4902	6553	4902	102	0
11-7/8" PRI-60	6858	5969	6934	5969	76	0
11-7/8" PRI-70	6960	5639	7036	5639	76	0
11-7/8" PRI-80	7518	6579	7595	6655	76	76
11-7/8" PRI-90	7747	6756	7798	6833	51	76
14" PRI-40	6833	5563	6833	5563	0	0
14" PRI-50	7366	4902	7391	4902	25	0
14" PRI-60	7798	6020	7874	6020	76	0
14" PRI-70	7899	5639	7976	5639	76	0
14" PRI-80	8534	7290	8611	7290	76	0
14" PRI-90	8788	7671	8839	7747	51	76
16" PRI-40	7366	5994	7366	5994	0	0
16" PRI-50	7391	4902	7391	4902	0	0
16" PRI-60	8636	6020	8661	6020	25	0
16" PRI-70	8484	5639	8484	5639	0	0
16" PRI-80	9474	7290	9550	7290	76	0
16" PRI-90	9703	8103	9779	8103	76	0

[a] Based on the live load deflection criterion of L/480, where L is the on-center span

As seen from Tables 3 and 4, the increase in the composite action factor from 0.45 to 0.55 increases the allowable spans up to 102 mm (4 in.) in some cases. Those cases showing no increase in the allowable spans are those governed by moment, reaction, or shear capacities of the I-joist. The most significant increases are for simple span applications as would be expected as these are often controlled by deflection. While these relatively small increases in allowable spans may seem insignificant in most engineered applications, I-joists are very competitive with commodity products, such as sawn lumber or parallel chord trusses, in the North American marketplace and this increase is considered positive to the wood I-joist industry as a whole.

Note that the allowable spans shown in Tables 3 and 4 are affected by the properties of floor sheathing, especially $EA_{\perp}$. In recent years, the allowable $EA_{\perp}$ value for OSB sheathing has declined significantly due to a variety of reasons. For example, based on an extensive quarterly test program administered by APA, the design $EA_{\perp}$ value for 15-mm (19/32-in.) OSB floor sheathing that is typically used for the joist spacing of 488 mm (19.2 in.) or less has recently been reduced in the APA *Panel Design Specification* (PDS) [11] from 65660 kN/m (4.5×10^6 lbf/ft) to 42300 kN/m (2.9×10^6 lbf/ft), a 35% reduction. Similarly, the design $EA_{\perp}$ value for 18-mm (23/32-in.) OSB floor sheathing that is typically used for the joist spacing of 610 mm (24 in.) or less has also been reduced from 65660 kN/m (4.5×10^6 lbf/ft) to 48100 kN/m (3.3×10^6 lbf/ft), a 27% reduction.

These reduced $EA_{\perp}$ values for OSB floor sheathing have a negative effect on the allowable I-joist spans by as much as 127 mm (5 in.). Therefore, the combined effect between the increase in the composite action factor and the reduction in the OSB $EA_{\perp}$ values essentially offset each other. Considering the fact that the actual EI of I-joists manufactured in North America is usually 5 to 7% higher than the published EI values [12], it is believed that the I-joist floor systems designed to the existing allowable spans remain adequate for the intended purposes. This is consistent with filed experience in North America of I-joist floor systems since no obvious problems have been reported due to excessive I-joist floor deflection. Therefore, the wood I-joist industry has recommended no change to the existing allowable spans and the analytical procedures used to determine the composite floor stiffness.

4. Conclusions and Recommendations

Results obtained from this limited study confirm that the composite action factor currently used by the wood I-joist industry in the U.S. is conservative. A composite action factor of 0.55 seems justifiable for glue-nailed I-joist floor systems with unglued T&G. While these results are rational and as expected, additional floor assembly tests may be considered in the future to expand the database and gain more confidence in the results.

The increase in the composite action factor results in an increase of the I-joist floor spans in residential floor applications up to 102 mm (4 in.). However, this increase needs to be considered in conjunction with other factors contributing to the composite floor stiffness, such as the recent reduction in the $EA_{\perp}$ design value of OSB floor sheathing. The net effect supports the recommendation of the North American wood I-joist industry that no changes to the existing allowable spans are required. However, if other factors that contribute to the composite floor stiffness are changed in the future, the I-joist spans need to be re-evaluated, including the composite action factors.

5. References

1. Ross, J.R. 1968. Field-Glued Plywood Floor Tests. Laboratory Report 118. APA – The Engineered Wood Association (formally American Plywood Association), Tacoma, WA.
2. McCutcheon, W.J. 1977. Method for predicting the stiffness of wood-joist floor systems with partial composite action. Research Paper 289. USDA Forest Products Laboratory, Madison, WI.
3. National Institute of Standards and Technology. 2004. Voluntary Product Standard PS2-04, *Performance Standard for Wood-Based Structural-Use Panels*. Gaithersburg, MD.
4. APA – The Engineered Wood Association. 2004. *Performance Standard for APA EWS I-Joists*. PRI-400. Tacoma, WA.
5. ASTM International. 2007. *Standard Specification for Adhesives for Field-Gluing Plywood to Lumber Framing for Floor Systems*. ASTM D 3498-03. West Conshohocken, PA.
6. ASTM International. 2007. *Standard Test Methods for Structural Panels in Flexure*. ASTM D 3043-00 (2006). West Conshohocken, PA.
7. ASTM International. 2007. *Standard Test Methods for Wood-Based Structural Panels in Compression*. ASTM D 3501-05a. West Conshohocken, PA.

8. ASTM International. 2007. *Standard Test Methods of Static Tests of Lumber in Structural Sizes*. ASTM D 198-05a. West Conshohocken, PA.

9. APA – The Engineered Wood Association. 2004. *APA Performance Rated I-Joists*. EWS Z725. Tacoma, WA.

10. APA – The Engineered Wood Association. 2006. *Performance Standard for APA EWS Rim Boards*. PRR-401. Tacoma, WA.

11. APA – The Engineered Wood Association. 2008. *Panel Design Specification*. Tacoma, WA.

12. APA – The Engineered Wood Association. 2008. Unpublished data summary from I-joist qualification reports. Report provided to the APA Technical Advisory Committee. May 2008. Tacoma, WA.

INTERNATIONAL COUNCIL FOR RESEARCH AND INNOVATION
IN BUILDING AND CONSTRUCTION

WORKING COMMISSION W18 - TIMBER STRUCTURES

EVALUATION OF THE PRESTRESSING LOSSES IN TIMBER MEMBERS PRESTRESSED WITH UNBONDED TENDONS

M Fragiacomo
University of Sassari
ITALY

M Davies
Dunning Thornton Consultants
NEW ZEALAND

Presented by M. Fragiacomo

H. Blass stated the graphs in paper with arrows with the time extended to 50 years. There is a need to clarify that this is extrapolation. A. Asiz asked why the tendons were placed in middle axis. M. Fragiacomo replied that the work was originally intended to provide righting forces. There was discussion on the issue of short term versus long term tests and the monitoring of pre-stress losses in tendon. U. Kuhlmann commented that the safety consideration and system behaviour should be considered and how to control the pre-stress in system. M. Fragiacomo replied that it would be difficult to test many specimens. This is preliminary work and more work is needed. M. Bartlett commented that FRP tendon has lower MOE than steel should be used. M. Fragiacomo agreed that his is a good idea. J. König stated that carbon fibre has been used in bridge deck pre-stressing to reduce pre-stress losses through time. I. Smith asked what happen when the building starts to collapse in terms of damage propagation and disproportional collapse.
M. Fragiacomo replied that one should not rely on pre-stressing for everything and one can use shear key to take the gravity forces.

Evaluation of the prestressing losses in timber members prestressed with unbonded tendons

Massimo Fragiacomo* and Matthew Davies**

(*) Associate Professor of Structural Design, University of Sassari, Italy

(**) Design Engineer, Dunning Thornton Consultants, New Zealand

1 Introduction

Applying prestressing to timber structures has been done in a number of cases; however, unlike concrete structures, it is not common practice. Unbonded prestressing tendons have been used to reduce the deflections of sawn timber beams (Bond and Sidwell 1965), to laminate bridge decks from independent timber planks (Crews 2002), and to reduce creep-induced deformations and provide increased strength for timber-concrete composite floors (Deam et al. 2008). Recently, a new construction system for multi-storey timber buildings has been proposed at the University of Canterbury, New Zealand (Buchanan et al. 2008). This system consists of frames and walls made from LVL (laminated veneer lumber) prestressed with unbonded tendons for earthquake resistance. Prestressing is mostly used to achieve connections that accommodate the inelastic seismic demand through rigid rocking motion of one member on the other, minimizing the residual damage at the end of the earthquake (Pampanin et al. 2006).

There is some skepticism among the scientific community regarding the possibility of prestressing timber members. The main issue is the behavior of the system in the long-term. The tendon relaxation, together with the time-dependent phenomena of timber such as creep, mechano-sorption, and shrinkage/swelling may in fact significantly reduce the effect of the prestressing in the long-term, particularly if the structure was built in an environment characterized by high relative humidity. A further problem is that codes of practice for timber design do not usually include specific provisions for the evaluation of the prestress losses in the long-term. The Eurocode 5 Part 2 (CEN 2004b) only states that, for stress-laminated deck plates, the long-term residual prestressing stress may normally be assumed to be greater than 0.35 MPa, provided that the initial prestress is at least 1.0 MPa; the moisture content of the laminations at the time of prestressing is not more than 16%; and, the variation of the deck plate's in-service moisture content is limited by adequate protection. No formula such as that reported in the Eurocode 2 Part 1-1 (CEN 2003) for the loss of prestressing in post-tensioned concrete members is provided.

In order to address those issues, a research project was undertaken at the University of Canterbury, New Zealand (Davies 2007, Davies and Fragiacomo 2008). A number of LVL frames prestressed with unbonded tendons and subjected to different environmental conditions were monitored over time with the purpose of evaluating the prestressing

losses. Relaxation tests on prestressing tendons and creep tests on LVL loaded parallel and perpendicular to the grain were also performed with the purpose of evaluating the relaxation and creep coefficients of the materials used in the prestressed frame.

This paper reports the derivation of a closed-form solution for the prediction of prestressing losses over time. The solution is validated against the experimental results, then further simplified and rewritten in non-dimensional format.

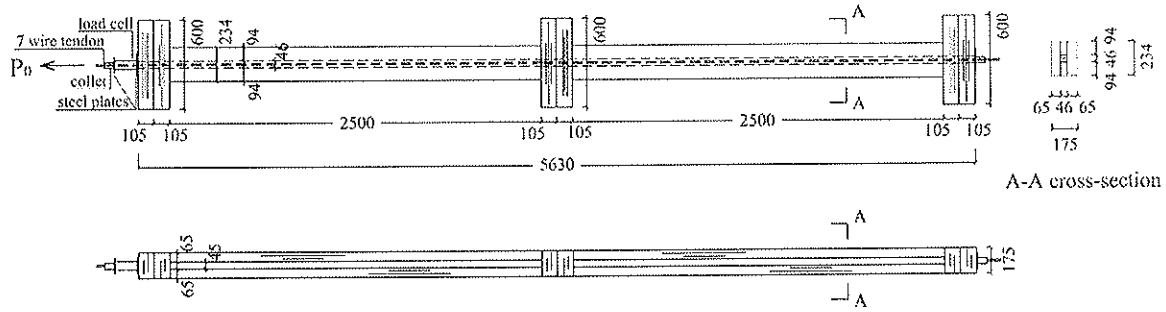

Fig. 1. Elevation (top), plan view (bottom), and cross-section (top right) of the LVL frame specimens prestressed with unbonded tendons tested at the University of Canterbury, New Zealand (dimensions in mm)

2 Derivation of a closed form solution

The purpose of this section is to derive formulas for evaluation of the prestress losses in a timber frame where the beams are prestressed with a straight tendon running in the centroid of the beams and anchored on the outer columns (see Fig. 1). All the beams are assumed to have the same geometrical (cross-sectional area A), physical (dilation coefficients α due to thermal T and moisture u variation), mechanical (Young's modulus E) and rheological (creep coefficient ϕ) properties. Also the columns are assumed to have all the same properties, but different from those of the beams. The only external load applied on the system is the prestress force P, which is assumed to be applied at the time t_0=0. Such a load induces a uniform distribution of stresses which are parallel to the grain in the beams and perpendicular to the grain in the columns. All properties of the beams and columns are therefore denoted with subscripts $\parallel$ and $\perp$, respectively.

2.1 Elastic solution

The uniformly distributed stresses σ_0 induced by the prestress load $P_0 = P(t_0)$ (assumed positive when in tension) applied at the time t_0=0 are given by:

$$\sigma_{\perp,0} = -\frac{P_0}{A_\perp} \qquad \sigma_{\parallel,0} = -\frac{P_0}{A_\parallel} \qquad \sigma_{p,0} = \frac{P_0}{A_p} \qquad (1)\ (2)\ (3)$$

where the subscript p refers to the tendon, and $A_\perp$ represents the cross-sectional area of the column perpendicular to the grain, i.e. the column area framed by the beam perimeter (usually, $A_\perp \approx A_\parallel$). The instantaneous axial displacements of the timber part and steel tendon, $\delta(t_0)$ and $\delta_p(t_0)$, assumed positive in the case of an elongation, are given by:

$$\delta(t_0) = \delta_\parallel(t_0) + \delta_\perp(t_0) = -\frac{P_0 l_\parallel}{E_\parallel A_\parallel} - \frac{P_0 l_\perp}{E_\perp A_\perp} \qquad \delta_p(t_0) = \frac{P_0 l}{E_s A_s} \qquad (4)\ (5)$$

where l, $l_{\parallel}$ and $l_{\perp}$ denotes the total length of frame, the total length of the beams and the total width of the columns within the frames, respectively ($l = l_{\parallel} + l_{\perp}$).

2.2 Time-dependent solution

After the prestressing load has been applied at the time t_0 and the tendon has been anchored at both ends of the frame, the system becomes a statically indeterminate structure. Any contraction or expansion of timber $\Delta\delta$ can no longer occur freely due to the restraint provided by the tendon, and will induce eigenstresses in all materials. The congruence equation for the prestressed system can then be written by imposing the same deflection for the wood and the prestressing steel at any time $t > t_0$:

$$\Delta\delta_{\parallel}(t) + \Delta\delta_{\perp}(t) = \Delta\delta_{p}(t) \quad \Rightarrow \quad \Delta\varepsilon_{\parallel}(t)l_{\parallel} + \Delta\varepsilon_{\perp}(t)l_{\perp} = \Delta\varepsilon_{p}(t)l \qquad (6)\ (7)$$

where $\Delta\varepsilon$ signifies the variation of total strain after the prestress force has been applied. In order to solve the equation, the constitutive laws of wood and tendon must be introduced.

2.2.1 Constitutive equations of timber and prestressing tendon

The time-dependent stress-strain relationships of timber loaded parallel and perpendicular to the grain subjected to uniaxial load can be described by advanced models (e.g. Toratti 1992, Hanhijärvi and Hunt 1998, Toratti and Svensson 2000, etc.). Those models are quite complex to manipulate as they are based on integral or differential equations.

With the intention of finding a closed form solution for the design of the prestressed timber frame in the long-term, reference to a simplified viscoelastic model of wood will be made:

$$\varepsilon(t) - \varepsilon_{in}(t) = \frac{\sigma_0}{E}\left[1 + \phi(t)\right] + \int_0^t \frac{1 + \phi(t-\tau)}{E} d\sigma(\tau) \qquad (8)$$

where $t_0 = 0$; $\sigma_0 = \sigma(t_0)$; ϕ is the creep coefficient, generally described by a power-type function (Eq. (9)), a and d being material parameters to be chosen depending on the type of wood-based material and species; and ε_{in} is the inelastic strain, given by Eq. (10), where u and T are the timber moisture content and temperature averaged over the section.

$$\phi(t-\tau) = a(t-\tau)^{d} \qquad \varepsilon_{in}(t) = \alpha_u\left[u(t) - u(t_0)\right] + \alpha_T\left[T(t) - T(t_0)\right] \qquad (9)\ (10)$$

This model has the advantage of simplicity when compared with the advanced rheological models. Even though the mechano-sorption phenomenon does not explicitly appear in Eq. (8), it can be implicitly taken into account by calibrating the material parameters a and d so as the creep coefficient ϕ includes an allowance for mechano-sorption. This is fairly common at the design level as many current codes of practice such as the Eurocode 5 (CEN 2004a), only provide the designer with a "total" creep coefficient accounting for all time-dependent phenomena (pure creep and mechano-sorption) depending on the type of conditions that the structure is exposed to. The simplified viscoelastic model (Eqs. (8) – (10)) will therefore be used for timber loaded parallel (beams) and perpendicular (columns) to grain, with all material parameters different in both directions.

The Eurocode 2 Part 1-1 (CEN 2003) suggests the following equation for the intrinsic relaxation of steel, $r_p(t,\tau)$:

$$r_p(t,\tau) = r_p(t-\tau) = -\frac{\Delta\sigma_p}{\sigma_p(\tau)} = 10^{-5} k_1 \rho_{1000} e^{k_2\left[\frac{\sigma_p(\tau)}{f_{pk}}\right]} \left(\frac{t-\tau}{1000}\right)^{0.75\left[1-\frac{\sigma_p(\tau)}{f_{pk}}\right]} \qquad (11)$$

where $\Delta\sigma_p = \sigma_p(t) - \sigma_p(\tau)$ is the change in tendon stress; $t - \tau$ is the time from the tensioning (in hours) ($\tau = t_0 = 0$); ρ_{1000} is the percentage of loss at 1000 hours after tensioning in a pure relaxation test; and k_1, k_2 are material parameters.

Unlike the pure creep coefficient of timber, the intrinsic relaxation of the tendon depends upon the stress level, making the time dependent behavior of the tendon a non-linear relaxation problem. A simplification is made in order to remove the non-linearity:

$$\sigma_p(\tau) = \sigma_p(t_0) = \sigma_{p,0} \tag{12}$$

for the bracketed terms in the exponents of Eq. (11). In this way it is possible to describe the time-dependent behavior of the prestressing tendon with the integral equation for linear viscoelastic materials:

$$\sigma_p(t) = \sigma_{p,0}\left[1 - r_p(t)\right] + \int_0^t E_p\left[1 - r_p(t-\tau)\right] d\left(\varepsilon_p(\tau) - \varepsilon_{p,in}(\tau)\right) \tag{13}$$

where E_p, ε_p and $\varepsilon_{p,in}$ signify the Young's modulus, total strain and inelastic strain of the prestressing steel, respectively, with the inelastic strain being given by:

$$\varepsilon_{p,in}(\tau) = \alpha_p\left[T(\tau) - T(t_0)\right] \tag{14}$$

α_p and T being the dilation coefficient and temperature of the prestressing steel.

2.2.2 Derivation of the final solution

In order to solve the congruence equation (Eq. (7)) and to calculate the variation in prestressing force ΔP over time, the time-dependent stress-strain relationships for timber (Eq. (8)) and prestressing steel (Eq. (13)) must be transformed into algebraic equations. The age-adjusted effective modulus method has been used in the following as it can lead to the best accuracy provided that a suitable aging coefficient χ is introduced (Trost 1967). Eqs. (15) and (16) show the algebraic equations that are equivalent to equations (8) and (13):

$$\varepsilon_i(t) - \varepsilon_{i,in}(t) = \frac{\sigma_{i,0}}{E_i}\left[1 + \phi_i(t)\right] + \frac{\Delta\sigma_i(t)}{E_i}\left[1 + \chi_i\phi_i(t)\right] \tag{15}$$

$$\sigma_p(t) = \sigma_{p,0}\left[1 - r_p(t)\right] + E_p\left[1 - \chi_p r_p(t)\right]\cdot\left[\Delta\varepsilon_p(t) - \Delta\varepsilon_{p,in}(t)\right] \tag{16}$$

where i=|| and $\perp$, $\Delta\sigma_i(t) = \sigma_i(t) - \sigma_{i,0}$, and $\Delta\varepsilon_i(t) = \varepsilon_i(t) - \varepsilon_i(t_0)$. Eqs. (15-16) can be manipulated further by noting that $\Delta\varepsilon_i(t) = \varepsilon_i(t) - \sigma_{i,0} / E_i$:

$$\Delta\varepsilon_i(t) - \Delta\varepsilon_{i,in}(t) = \frac{\sigma_{i,0}}{E_i}\phi_i(t) + \frac{\Delta\sigma_i(t)}{E_i}\left[1 + \chi_i\phi_i(t)\right] \tag{17}$$

$$\Delta\varepsilon_p(t) - \Delta\varepsilon_{p,in}(t) = \frac{\Delta\sigma_p(t) + \sigma_{p,0}r_p(t)}{E_p\left[1 - \chi_p r_p(t)\right]} \tag{18}$$

By using Eqs. (1)-(3) in conjunction with Eqs. (17)-(18) to calculate the variations of total strain over time and by substituting them into Eq. (7), the variation of prestress force $\Delta P(t)$ (positive if in tension) can finally be derived:

$$\Delta P(t) = \frac{-P_0\left\{\dfrac{l_{\parallel}\phi_{\parallel}(t)}{E_{\parallel}A_{\parallel}} + \dfrac{l_{\perp}\phi_{\perp}(t)}{E_{\perp}A_{\perp}} + \dfrac{l r_p(t)}{E_p A_p\left[1-\chi_p r_p(t)\right]}\right\} + \Delta\varepsilon_{\parallel,in}(t)l_{\parallel} + \Delta\varepsilon_{\perp,in}(t)l_{\perp} - \Delta\varepsilon_{p,in}(t)l}{\dfrac{l_{\parallel}\left[1+\chi_{\parallel}\phi_{\parallel}(t)\right]}{E_{\parallel}A_{\parallel}} + \dfrac{l_{\perp}\left[1+\chi_{\perp}\phi_{\perp}(t)\right]}{E_{\perp}A_{\perp}} + \dfrac{l}{E_p A_p\left[1-\chi_p r_p(t)\right]}} \quad (19)$$

where the inelastic strains can be calculated using Eqs. (10) and (14). Eq. (19) can be simplified in the case of a beam with no columns:

$$\Delta P(t) = A_p \frac{E_p\left[1-\chi_p r_p(t)\right]\cdot\left[\Delta\varepsilon_{\parallel,in}(t) - \Delta\varepsilon_{p,in}(t)\right] - \Delta\sigma_r(t) + \sigma_{\parallel,0}\dfrac{E_p}{E_{\parallel}}\phi_{\parallel}(t)\left[1-\chi_p r_p(t)\right]}{1+\dfrac{E_p A_p}{E_{\parallel}A_{\parallel}}\left[1+\chi_{\parallel}\phi_{\parallel}(t)\right]\cdot\left[1-\chi_p r_p(t)\right]} \quad (20)$$

where $\Delta\sigma_r(t) = \sigma_{p,0}r_p(t)$ is the stress reduction in the tendon due to pure relaxation, and $\sigma_{\parallel,0}$ is the stress in timber, positive if in tension. This formula is similar to that recommended by the Eurocode 2 Part 1-1 (CEN 2003) for post-tensioned precast concrete beams:

$$\Delta P(t) = A_p \frac{E_p\Delta\varepsilon_{cs}(t) - 0.8\Delta\sigma_r(t) + \sigma_c(t_0)\dfrac{E_p}{E_c}\phi_c(t,t_0)}{1+\dfrac{E_p A_p}{E_c A_c}\left[1+0.8\phi_c(t,t_0)\right]} \quad (21)$$

Eq. (21) can be derived from Eq. (20) by making the following assumptions: (i) the subscript $\parallel$ is replaced by c; (ii) concrete shrinkage (considered as negative) is the only inelastic strain, so $\Delta\varepsilon_{p,in}(t) = 0$ and $\Delta\varepsilon_{\parallel,in}(t) = \Delta\varepsilon_{cs}(t)$; (iii) the interaction between tendon relaxation, and shrinkage and creep of concrete is accounted for in a simplified manner by assuming $\chi_p = 0$, and by multiplying the stress reduction in the tendon due to pure relaxation $\Delta\sigma_r(t)$ by a 0.8 factor; and (iv) the creep of concrete can be modelled by assuming $\chi_{\parallel} = 0.8$.

Eqs. (19) and (20) are simple closed-form solutions that can be used in design to predict the prestress losses in a timber frame and beam prestressed with unbonded tendons. In order to use the formulas, however, some information on the aging coefficients $\chi_{\parallel}$, $\chi_{\perp}$ and χ_p must be provided. These coefficients have been be calibrated with the experimental results, as will be presented in the next section.

3 Validation and parametric study

The analytical solutions (Eqs. (19) and (20)) have been used to predict the prestress losses of a frame and a beam made from LVL subjected only to an initial prestress force P_0 of 107 kN and tested in the long-term in heated, unconditioned indoor condition. More information on the test outcomes is reported in previous papers (Davies 2007, Davies and Fragiacomo 2008). The frame is displayed in Fig. 1, with the geometrical, mechanical and rheological properties listed in Table 1. The beam had the same length as the frame, l, the same properties parallel to the grain, and no columns. Where a range of material properties was determined experimentally, the mean values were used in the analytical formulas. No inelastic strain was considered in the comparison. Since they are caused by environmental

temperature and humidity variations characterized by annual cycles, they would therefore cancel out at the end of 50 years of service life.

The experimental-analytical comparison is displayed in Fig. 2 for the prestressed beam. The experimental curve represents the projection over the service life of the prestress losses $-\Delta P(t)/P_0$ monitored during the 1-year test. It was found that varying the aging coefficients of both LVL, $\chi_{\parallel}$, and steel tendon, χ_p, had very little influence on the solution. To achieve the closest approximation, the aging coefficient for the prestressing steel, χ_p, was set to zero, as in the Eurocode 2 solution (Eq. (21)). The aging coefficient of LVL parallel to the grain was then varied and the result of this is presented in Fig. 2. The analytical solution underestimates the actual losses by about 2%, but it can be seen that the Eurocode equivalent (Eq. (21)) with no concrete shrinkage $\Delta\varepsilon_{cs}(t)$ is even less accurate.

Table 1. Geometrical, mechanical and rheological properties used in the experimental-analytical comparison

Quantity	Value	Quantity	No. Spec.	Min	Max	Mean
$A_{\parallel}$ [mm^2]	38925	$E_{\parallel}$ [GPa]	6	12.6	17.3	14.38
$A_{\perp}$ [mm^2]	38925	$E_{\perp}$ [GPa]	6	0.23	0.34	0.28
A_p [mm^2]	99	E_p [GPa]	-	-	-	200
$l_{\parallel}$ [mm]	5000	$\phi_{\parallel}$ (t = 50 y)	14	0.48	1.31	0.92
$l_{\perp}$ [mm]	630	$\phi_{\perp}$ (t = 50 y)	14	2.03	5.74	4.02
l [mm]	5630	r_p (t = 50 y)	1	0.035	0.035	0.035

The experimental-analytical comparison is displayed in Fig. 3 for the prestressed frame. The experimental curve represents the projection over the service life of the prestress losses $-\Delta P(t)/P_0$ monitored during the 1-year test and shows a loss of 33% at the end of the service life (50 years). It can be seen that the analytical solution provides an estimate of losses that is greater than the experimental one. Varying the aging coefficients reveals that the parallel to the grain LVL and prestressing steel aging coefficients, $\chi_{\parallel}$ and χ_p respectively, have a negligible influence on the estimate. However, varying the aging coefficient for perpendicular to the grain LVL, $\chi_{\perp}$, has a notable effect. This can be seen very clearly in Fig. 3 where a larger aging coefficient appears give more accurate estimates. The use of an aging coefficient for creep perpendicular to the grain LVL equal to one leads to an 8% overestimation of the losses with respect to the experimental value.

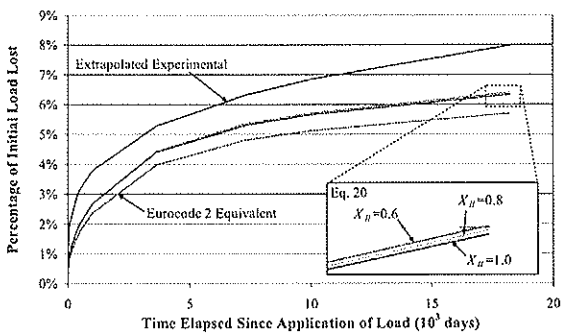

Fig. 2. Comparison between experimental results and analytical solutions for a prestressed beam specimen (no perpendicular to the grain LVL)

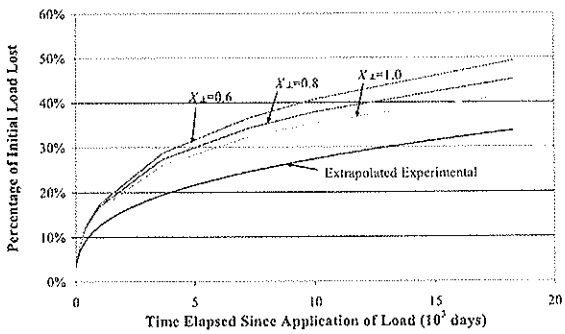

Fig. 3. Comparison between experimental results and analytical solutions for a prestressed frame specimen (11% of length is perpendicular to the grain LVL)

From the experimental results reported in previous papers (Davies 2007, Davies and Fragiacomo 2008), it was found that the proportion of length loaded perpendicular to the grain has a strong influence on the amount of prestress losses. The analytical formula (Eq. (19) with no inelastic strains, the parameters listed in Table 1, and the aging coefficients

$\chi_{\parallel} = 1$, $\chi_{\perp} = 1$, and $\chi_p = 0$) can then be used to evaluate the amount of prestress losses at different times t for varying proportions of column widths on the total frame length, $l_{\perp} / l$.

Fig. 4 displays the analytical solution for the complete range of member proportions, along with the points representing the experimental results and extrapolation over time for the prestressed beam ($l_{\perp} / l = 0\%$) and frame ($l_{\perp} / l = 11\%$) that were experimentally tested. It is evident that a significant increase in the loss occurs as perpendicular to the grain LVL is introduced into the system. As the proportion increases, the loss increases at an increasingly lower rate. In the limit case of only LVL loaded perpendicular to grain (100%) the loss raises to 72% at the end of the 50-year service life.

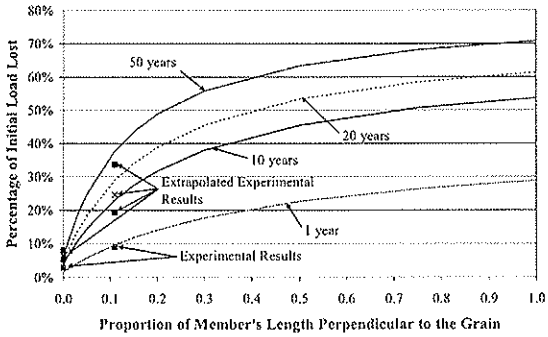

Fig. 4. Analytical solution for full spectrum of member proportions at different time from prestress loading

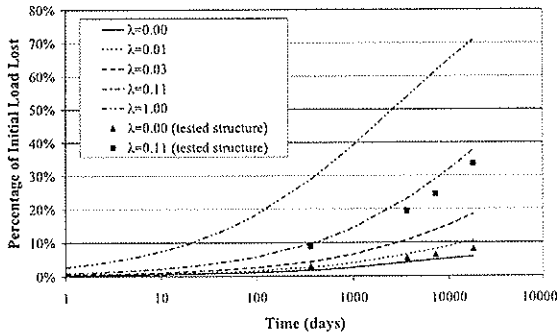

Fig. 5. Analytical trends of prestress losses over time for different member proportions

Fig. 5 displays the trend over time of the prestress losses for different member proportions $\lambda = l_{\perp} / l$. It can be noted that a significant proportion of the losses occur in the first year under load and that the rate of decrease in load decays over time. This is particularly evident for the case of all timber stressed perpendicular to the grain such as for a stress laminated deck plates, where the tendon should be restressed a few times during the service life to limit the prestress losses, as suggested by various authors (e.g. Quenneville and Van Dalen 1996). It should be noted that the actual losses in a stress laminated deck plate used for a bridge will generally be higher than the value predicted in this analysis because the timber is exposed to non-heated, uncontrolled outdoor conditions characterized by significantly higher creep coefficients with respect to a frame in heated, uncontrolled indoor conditions.

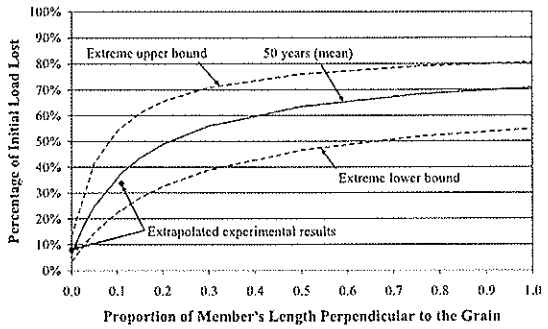

Fig. 6. The proposed solution evaluated using the "worst case" (extreme upper bound), mean and "best case" (extreme lower bound) material properties

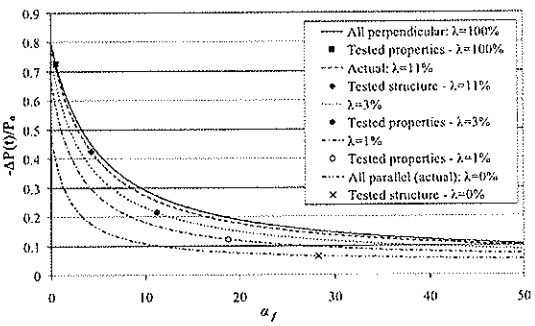

Fig. 7. Influence of the non-dimensional stiffness of the frame, α_f, on the prestress losses for different proportions of LVL loaded perpendicular to grain, λ

The analytical solution was found to represent the outcomes of the experimental tests, although with an underestimation and an overestimation of the prestress losses for the beam and the frame, respectively. A possible justification for these differences is the variability of LVL, particularly in terms of time-dependent properties like creep and

mechano-sorption (see Table 1). The analytical solution was evaluated using average experimental values for the Young's moduli, creep and relaxation coefficients. Fig. 6 shows the result of evaluating the analytical solution using the most-extreme, experimentally-determined material properties. To explain, the upper bound applies the smallest Young's moduli and largest creep coefficient values; whereas the lower bound applies the largest Young's moduli and smallest creep coefficient values (see Table 1). It may be concluded that the difference between experimental and analytical results as provided by the proposed formula is acceptable, and there is little point in searching for further refinement. Specifically, in terms of values of aging coefficients as their effect on the solution is far less significant than the actual scatter in material properties.

4 Simplification of analytical solution

At present, the complete analytical solution (Eq. (19)) is a rather complex equation. It may be of interest to simplify the formula by neglecting some relatively small terms in order to obtain a simpler solution similar to the Eurocode 2 equation (CEN 2003) for concrete structures (Eq. (21)). Firstly, during the experimental-analytical comparisons, the assumption that there is no change in inelastic strains was made: $\Delta\varepsilon_{\parallel,in}(t) = 0$, $\Delta\varepsilon_{\perp,in}(t) = 0$, and $\Delta\varepsilon_{p,in}(t) = 0$. This assumption can be justified by acknowledging that, if the solution is to be evaluated at multiples of whole years, these inelastic strains will return back to their initial value because of annual climate cycles. Secondly, it was shown (Fig. 2) that varying the parallel to the grain aging coefficient has an insignificant effect on the predicted losses. Therefore, it can be taken as unity and the term removed from the equation: $\chi_{\parallel} = 1$. Thirdly, the contribution made by relaxation of prestressing steel has also been found to be insignificant when compared to that made by LVL. Therefore, the aging coefficient of prestressing steel can be taken as zero and the corresponding relaxation terms are effectively removed from the equation: $\chi_p = 0$. Furthermore, comparison between experimental results and the analytical solution (Fig. 3) suggests that the most appropriate value for the aging coefficient of LVL perpendicular to the grain would be one: $\chi_{\perp} = 1$. The result of these simplifications is Eq. (22).

$$\Delta P(t) = \frac{-P(t_0)\left[\dfrac{l_{\parallel}\phi_{\parallel}(t)}{E_{\parallel}A_{\parallel}} + \dfrac{l_{\perp}\phi_{\perp}(t)}{E_{\perp}A_{\perp}} + \dfrac{lr_p(t)}{E_pA_p}\right]}{\dfrac{l_{\parallel}\left[1+\phi_{\parallel}(t)\right]}{E_{\parallel}A_{\parallel}} + \dfrac{l_{\perp}\left[1+\phi_{\perp}(t)\right]}{E_{\perp}A_{\perp}} + \dfrac{l}{E_pA_p}} \tag{22}$$

This simple equation was found to provide acceptable approximations for the prediction of the prestress losses, well within the range of the material variability. It may therefore be suggested for implementation in the new versions of the Eurocode 5 (CEN 2004b). The term in the numerator containing the relaxation coefficient was found to be very small, however it was not removed as in some other cases (different geometrical, mechanical and rheological properties of the system) it may not be negligible. Eq. (22) can be rewritten in another form to better recognize the parameters influencing the losses:

$$-\frac{\Delta P(t)}{P_0} = \frac{\dfrac{E_{\parallel}A_{\parallel}}{E_pA_p}r_p(t) + \dfrac{l_{\parallel}}{l}\phi_{\parallel}(t) + \dfrac{E_{\parallel}}{E_{\perp}}\cdot\dfrac{A_{\perp}}{A_{\parallel}}\cdot\dfrac{l_{\perp}}{l}\cdot\phi_{\perp}(t)}{\dfrac{E_{\parallel}A_{\parallel}}{E_pA_p} + \dfrac{l_{\parallel}}{l}\left[1+\phi_{\parallel}(t)\right] + \dfrac{E_{\parallel}}{E_{\perp}}\cdot\dfrac{A_{\perp}}{A_{\parallel}}\cdot\dfrac{l_{\perp}}{l}\cdot\left[1+\phi_{\perp}(t)\right]} \tag{23}$$

and

$$-\frac{\Delta P(t)}{P_0}=\frac{\alpha r(t)+(1-\lambda)\phi_{\parallel}(t)+n\mu\lambda\phi_{\perp}(t)}{\alpha+(1-\lambda)\left[1+\phi_{\parallel}(t)\right]+n\mu\lambda\left[1+\phi_{\perp}(t)\right]} \tag{24}$$

where $\alpha = E_{\parallel}A_{\parallel}/(E_pA_p)$, $\lambda = l_{\perp}/l$, $n = E_{\parallel}/E_{\perp}$, and $\mu = A_{\perp}/A_{\parallel}$. Eq. (24) has the advantage of being written in non-dimensional form, and shows the significant influence on the prestress losses of the α parameter. This parameter is the ratio between the axial stiffness of the timber member loaded parallel to the grain and the axial stiffness of the tendon. This result is consistent with what was found for stress-laminated bridge decks by Quenneville and Van Dalen (1996).

The α parameter incorporates the true axial stiffness of the system only when $\lambda = 0$, i.e. in the case of a beam prestressed parallel to the grain. In the case of a frame where, in general, $\lambda \neq 0$, the ratio α_f between the actual axial stiffness of the frame and that of the prestressing tendon is given by:

$$\alpha_f=\frac{\dfrac{1}{\dfrac{l_{\parallel}}{E_{\parallel}A_{\parallel}}+\dfrac{l_{\perp}}{E_{\perp}A_{\perp}}}}{\dfrac{E_pA_p}{l}}=\frac{\dfrac{E_{\parallel}A_{\parallel}}{E_pA_p}}{1+\dfrac{l_{\perp}}{l}\left(\dfrac{E_{\parallel}A_{\parallel}}{E_{\perp}A_{\perp}}-1\right)}=\frac{\alpha}{1+\lambda\left(\dfrac{n}{\mu}-1\right)} \tag{25}$$

Fig. 7 displays the influence of the non-dimensional stiffness of the frame, α_f, on prestress losses $-\Delta P(t)/P_0$ at the end of the service life (50 years) for different proportions of LVL loaded perpendicular to grain, λ. The points corresponding to the cross-sections of beams and frames experimentally tested are also displayed. It can be observed that the prestress losses reduce for frames characterized by high axial stiffness of the LVL relative to the axial stiffness of the prestress tendon, and vice versa. The curves of the frames lay between the case of all LVL loaded perpendicular to the grain (upper bound) and all LVL loaded parallel to the grain (lower bound). The difference between the curves is quite significant in the range of small λ ratios (0 to 10%), but almost negligible above 10-15%. However, the differences among the non-dimensional stiffnesses α_f and, therefore, the prestress losses (see the points in Fig. 7 representing the tested properties and structures) are significant over the whole spectrum of λ ratios.

5 Concluding remarks

The paper presents the derivation of a closed-form solution for the evaluation of the prestress losses of a timber frame in the long-term. The formulas are obtained by simplifying the integral equations describing the time-dependent behavior of the prestressing steel and timber loaded parallel and perpendicular to the grain. Allowance for relaxation, creep and inelastic strains was made. The age-adjusted effective modulus method was used to transform the integral equations into algebraic equations.

The closed-form solution was compared with the experimental results measured in a long-term test performed at the University of Canterbury, New Zealand. An acceptable approximation was found, bearing in mind the scatter of experimental values, particularly the Young's moduli and creep coefficients of LVL. The experimental-analytical comparison also allowed a calibration of some coefficients, the "aging coefficients", used

in the analytical solution. Based on the outcomes of the parametric study, the analytical solution was simplified further and rewritten in non-dimensional form. Such formula, easy and similar to that used for prestressed concrete structures, can be recommended for design of prestressed timber frames. The formula also allows an easy understanding of the main parameters affecting the prestress losses in the long-term, which are: (i) the ratio between the lengths of timber loaded perpendicular and parallel to the grain, and (ii) the ratio between the axial stiffness of the timber frame and the axial stiffness of the steel tendon.

References

Bond, D., and Sidwell, E.H. (1965). "Prestressed timber beams." *Civil Engineering (London)*, 60(705), 547-550.

Buchanan, A., Deam, B., Fragiacomo, M., Pampanin, S., and Palermo, A. (2008). "Multi-storey prestressed timber buildings in New Zealand." *Structural Engineering International, IABSE*, Special Edition on Tall Timber Buildings, 2/2008, 166-173.

Comité Européen de Normalisation (2003). "Eurocode 2: Design of Concrete Structures – Part 1-1: General Rules and Rules for Buildings." *prEN 1992-1-1*, Brussels, Belgium.

Comité Européen de Normalisation (2004a). "Eurocode 5 – Design of timber structures – Part 1-1: General rules and rules for buildings." *ENV 1995-1-1*, Brussels, Belgium.

Comité Européen de Normalisation (2004b). "Eurocode 5 – Design of Timber Structures – Part 2: Bridges." *EN 1995-2*, Brussels, Belgium.

Crews, K.I. (2002). *Behavior and critical limit states of transversely laminated timber cellular bridge decks*. Ph.D. Thesis, University of Technology, Sydney, Australia.

Davies, M. (2007). *Long term behaviour of laminated veneer lumber (LVL) members prestressed with unbonded tendons*. Research report, Dept. of Civil Engineering, University of Canterbury, Christchurch, New Zealand.

Davies, M., and Fragiacomo, M. (2008). "Long-term behaviour of laminated veneer lumber members prestressed with unbonded tendons." *Proc., The 10th World Conference on Timber Engineering WCTE 2008*, Miyazaki, Japan, June 2-5, 8 pp., CD.

Deam, B.L., Fragiacomo, M., and Gross, L.S. (2008). "Experimental behavior of prestressed LVL-concrete composite beams." *Journal of Structural Engineering*, 134(5), 801-809.

Hanhijärvi, A., and Hunt, D. (1998). "Experimental indication of interaction between viscoelastic and mechano-sorptive creep." *Wood Science and Technology*, 32, 57-70.

Pampanin, S., Palermo, A., Buchanan, A.H., Fragiacomo, M., and Deam, B.L. (2006). "Code provisions for seismic design of multi-storey post-tensioned timber buildings." *Proc., Meeting thirty-nine of the Working Commission W18-Timber Structures*, CIB, Florence (Italy), August 28-31, paper No. CIB-W18/39-15-6, 12 pp.

Quenneville, P., and Van Dalen, K. (1996). "Parameters affecting stress losses in stress-laminated timber bridge decks." *Proc., The International Wood Engineering Conference*, Portland, New Orleans, Lousiana, U.S.A., October 28-31, 2, 376-381.

Toratti, T. (1992). "Creep of timber beams in a variable environment." *Report No. 31*, Helsinki University of Technology, Helsinki, Finland.

Toratti, T., and Svensson, S. (2000). "Mechano-sorptive experiments perpendicular to grain under tensile and compressive loads." *Wood Science and Technology*, 34, 317-326.

Trost, H. (1967). "Implications of the superposition principle in creep and relaxation problems for concrete and prestressed concrete." *Beton- und Stahlbetonbau*, 62(10), 230-238; 62(11), 261-269 (in German).

INTERNATIONAL COUNCIL FOR RESEARCH AND INNOVATION IN BUILDING AND CONSTRUCTION

WORKING COMMISSION W18 - TIMBER STRUCTURES

RELATIONSHIP BETWEEN GLOBAL UND LOCAL MOE

J K Denzler

Planungsgesellschaft Dittrich mbH, München

P Stapel

P Glos

Holzforschung München

GERMANY

Presented by P. Stapel

H. Blass stated that the findings confirmed EN 384 equations. J. Köhler asked which value is better. P Stapel replied that the global MOE is better. H.J. Larsen asked what is the intent of the research work. P Stapel stated that the work intended to check EN384 equations. A. Buchanan stated the reason for MOE measurement is to compute deformation. He asked why shear deflection is not mentioned or discussed in the paper. P Stapel agreed the shear deflection is important. A. Ranta-Maunus stated that a 4 to 5% difference between E local and E global is generally assumed for accepted G Values. As local MOE is measured in the weakest section, the importance of measuring local or global MOE is in question. Dynamic MOE is the method that can be used with less trouble. H. Blass commented that the relation between dynamic and static MOE on edge is then needed. B. Källsner stated that measurement of local MOE is difficult because measurements are taken off the neutral axis. In MOE measurement in his laboratory local MOE is measured off the tension side. Analysis has shown that the difference between the measurement off neutral axis and tension side is minor. I. Smith stated that MOE is just an artefact of theory. He asked and received clarification that in Germany the term scantling ranges from light framing to large beams. S. Aicher MOE and G are need for calculation of deformation. It is worth to look into vibration testing but states beam bending should be studied because not every laboratory has dynamic MOE testing equipment. J. Köhler stated that the placement of weakest point of the beam within the maximum stresses zone is an unfortunate situation.

Relationship between global und local MOE

J.K. Denzler
Planungsgesellschaft Dittrich mbH, Munich, Germany

P. Stapel
Holzforschung München, Germany

P. Glos
Holzforschung München, Germany

1 Introduction

This paper discusses the determination of the modulus of elasticity in bending. According to the international standard EN 408, deflection can be measured between the loading points over a span consisting of five times the height. In the following the result of the measurement is called "local MOE", because it depends on the local performance of the specimen between the loading heads. The second method to evaluate the modulus of elasticity in bending according to EN 408 is to measure the whole deflection between the supports. The result of the measurement is called "global MOE" in the following, because it includes the information of the whole specimen. Figure 1 shows the two methods of determining the MOE according to EN 408.

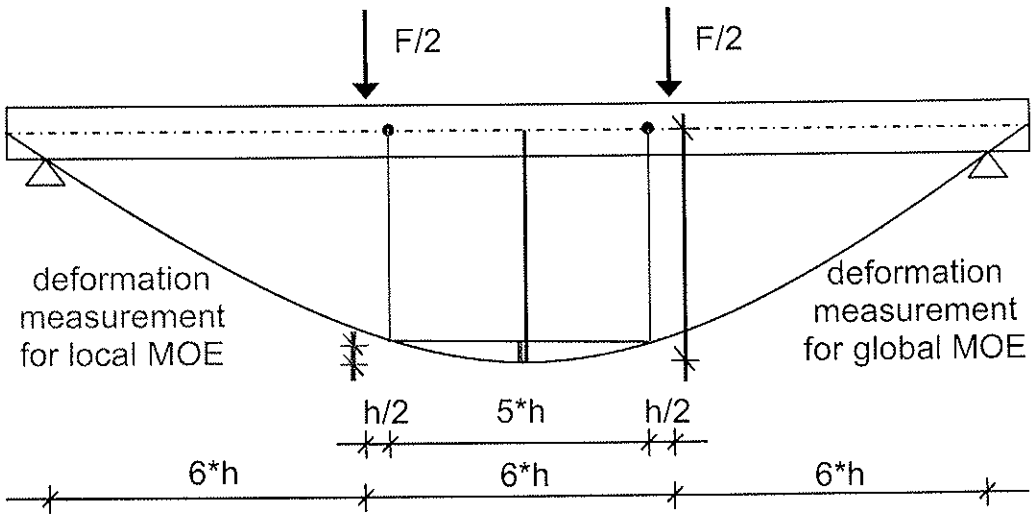

Fig. 1: Methods for the determination of local and global MOE according to EN 408.

Originally, the shear free local MOE was regarded as the most appropriate value. The characteristic MOE values in EN 338 and in Eurocode 5 are defined as local MOE. Meanwhile, existing experience has shown that the local MOE is more prone to measuring errors and is not necessarily relevant for the deformation behaviour of structures.

Therefore, it is discussed to use the global MOE instead of the local MOE. This is why an equation to convert the global MOE into the local MOE was included into EN 384:

$$MOE_{loc,EN384} = \left[\sum (MOE_{glob}) / n\right] \cdot 1.3 - 2690 \quad (1)$$

with

$MOE_{loc,EN384}$	local MOE calculated acc. to EN 384 in N/mm² (the local MOE is originally measured with a span of 5 times the height between the loading heads)
MOE_{glob}	global MOE in N/mm² (measured with a span of 18 times the height)
n	number of specimen

However, this equation is not yet generally accepted. Based on the results of over 4 000 bending tests of structural sawn timber (spruce, pine, Douglas fir, larch), where both local MOE and global MOE were measured, the relationship between the local MOE calculated according to EN 384 ($MOE_{loc,EN384}$) and the local MOE measured during bending tests (MOE_{loc}) is evaluated in the following, taking into account timber quality.

2 Materials and Methods

The modulus of elasticity describes the declination of the stress-strain diagram within the linear-elastic area. Normally, the declination is measured between 10% and 40% of the strength. The difference between the stress at 40% of the strength and the stress at 10% of the strength divided by the difference of the strain at 40% of the strength and the strain at 10% of the strength forms the basis of the MOE.

According to EN 408 the deflection can be measured in two ways. If the local MOE is measured the deflection is small. Therefore, the local MOE is sensitive with respect to measuring errors. If the global MOE is determined, the deflection is larger than the deflection for calculating the local MOE. Therefore, measuring errors do affect the global MOE to a lesser degree compared to the local MOE. However, the global MOE is affected by shear because there are shear stresses between the supports and the loading heads.

The database of Holzforschung München includes a lot of bending tests where both local and global MOE were determined. Based on these test results

- the influence of the test method (edgewise or flatwise bending),
- the influence of timber dimensions,
- the influence of visual grading according to DIN 4074 (S 13, S 10, S 7, reject) and
- the influence of the wood species

on equation (1) was investigated. Table 1 shows the test data divided by the wood species. 85% of the test data consists of spruce. Figure 2 shows the cross sections of spruce separated by timber dimensions.

Table 1: Total sample divided by the wood species.

species	number of specimens
spruce	3491
pine	202
Douglas fir	268
larch	152
Σ	4113

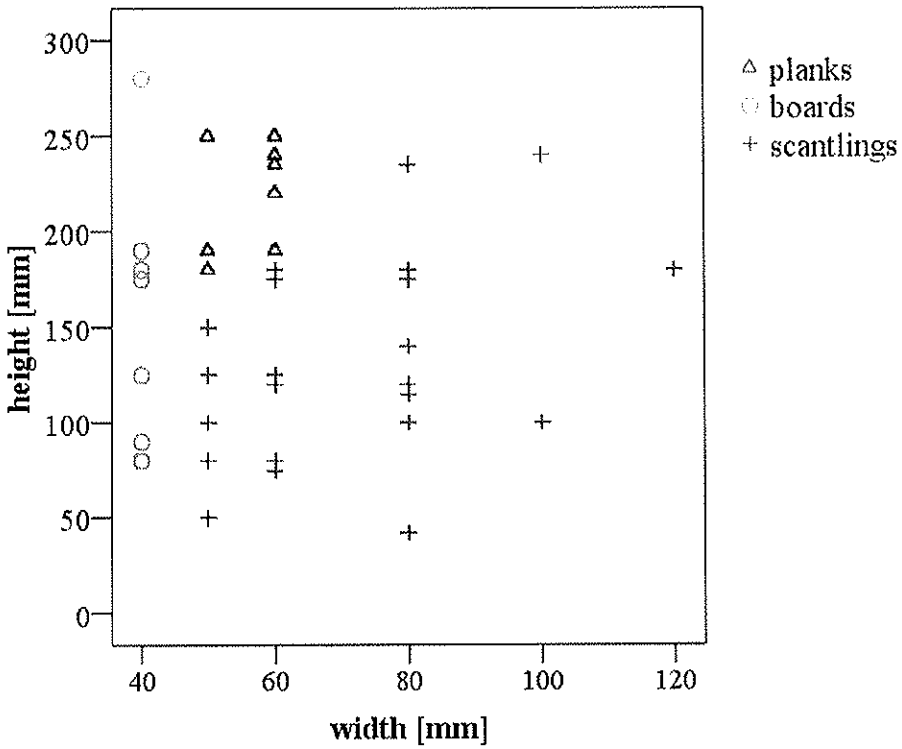

Fig. 2: Height versus width for spruce separated by timber dimensions, n = 3491 specimens.

Figure 3 compares the local and global MOE of 3491 spruce bending specimens. For a global MOE higher than MOE_{glob} = 9000 N/mm², the local MOE exceeds the global MOE. For values lower than MOE_{glob} = 9000 N/mm², the local MOE is smaller than the global MOE.

To evaluate the relationship between local and global MOE the database is divided into different sub-samples. For every sub-sample a linear regression for the local MOE is calculated ($MOE_{loc,reg}$) using the global MOE as independent variable. The result is compared with the formula in EN 384 ($MOE_{loc,EN384}$).

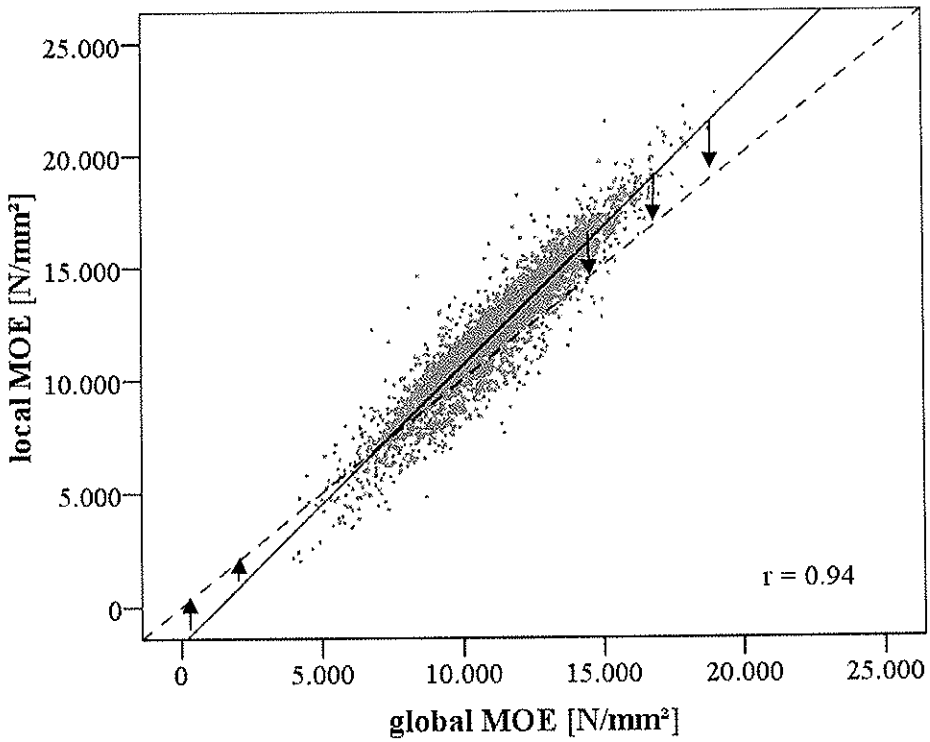

Fig. 3: Local MOE versus global MOE measured during bending tests, n = 3491 specimens.

The influence of the test method is based on 3491 specimens consisting of spruce and fir. The same sub-sample is used to investigate the influence of visual grading according to DIN 4074. To investigate the influence of timber dimensions on the relationship of local and global MOE of spruce and fir, only specimens tested in edgewise bending were used. To investigate the influence of the wood species, the total sample is used. Table 2 summarizes the different regression models for the different sub-samples.

3 Results*

For the total sample the mean global MOE measured during the bending tests is MOE_{glob} = 11436 N/mm², the mean local MOE is MOE_{loc} = 12377 N/mm². The local MOE exceeds the global MOE by approximately 8% on mean level. If the discrete global MOE values are converted with respect to equation (1) the converted $MOE_{loc,EN384}$ is $MOE_{loc,EN384}$ = 12177 N/mm² and therefore, 1.6 % lower than the local MOE on mean level measured during bending tests.

The regression model for the local MOE based on the global MOE and on the total sample of 4113 specimens is $MOE_{loc,reg} = MOE_{glob} \cdot 1.206 - 1421$ N/mm² which is similar to the equation given in EN 384 (Table 2). The gradient with a factor of 1.206 is slightly smaller than the gradient given in EN 384 with a factor of 1.3.

* Due to the inherent inaccuracies of MOE measurement MOE values should be restricted to three significant digits. In this chapter, the MOE values and the coefficients of the regression are given as calculated.

Table 2 shows the regression models $MOE_{loc,reg}$ for the local MOE based on the global MOE for different sub-samples. The regression models are calculated by comparing the global MOE value measured during the bending test with the equivalent local MOE value for every single specimen. In the following the influence of different parameters on this relationship of $MOE_{loc,reg}$ and the equation given in EN 384 is discussed. For all regression models the coefficients of correlation vary between 0.88 and 0.97. Due to these high coefficients of correlations the residuals are not given in Table 2.

Table 2: Summary of regression models for different sub-samples.

			n	regression model	r
EN 384				$MOE_{loc,EN384} = \sum[MOE_{glob}/n] \cdot 1.3 - 2690$	
all			4113	$MOE_{loc,reg} = MOE_{glob} \cdot 1.206 - 1421$	
spruce	test method	edgewise	3325	$MOE_{loc,reg} = MOE_{glob} \cdot 1.224 - 1584$	0.95
		flatwise	166	$MOE_{loc,reg} = MOE_{glob} \cdot 1.205 - 2025$	0.90
	visual grading acc. to DIN 4074	rejects	193	$MOE_{loc,reg} = MOE_{glob} \cdot 1.225 - 1630$	0.88
		S 7	690	$MOE_{loc,reg} = MOE_{glob} \cdot 1.173 - 1252$	0.89
		S 10	1580	$MOE_{loc,reg} = MOE_{glob} \cdot 1.219 - 1550$	0.90
		S 13	1028	$MOE_{loc,reg} = MOE_{glob} \cdot 1.217 - 1468$	0.95
	dimen-sions	scantlings	2018	$MOE_{loc,reg} = MOE_{glob} \cdot 1.232 - 1611$	0.95
		boards	535	$MOE_{loc,reg} = MOE_{glob} \cdot 1.204 - 1462$	0.94
		planks	772	$MOE_{loc,reg} = MOE_{glob} \cdot 1.205 - 1501$	0.94
spruce			3325	$MOE_{loc,reg} = MOE_{glob} \cdot 1.224 - 1584$	0.95
pine			202	$MOE_{loc,reg} = MOE_{glob} \cdot 1.197 - 1191$	0.97
larch			152	$MOE_{loc,reg} = MOE_{glob} \cdot 1.142 - 452$	0.96
Douglas fir			268	$MOE_{loc,reg} = MOE_{glob} \cdot 1.180 - 1245$	0.97

Figure 4 shows the influence of the test method on the difference between the $MOE_{loc,reg}$ calculated with the regression models given in Table 2 and the $MOE_{loc,EN384}$ calculated with equation (1) according to EN 384. For edgewise bending, the difference is always greater than zero which means that the $MOE_{loc,EN384}$ based on equation (1) is lower than the $MOE_{loc,reg}$ based on the regression model. For flatwise bending, the difference is always less than zero. Therefore, equation (1) overestimates the local MOE of flatwise bending specimens and underestimates the local MOE of edgewise bending specimens for spruce. Due to the small amount of specimens in flatwise bending (n = 166) this result is indicative only.

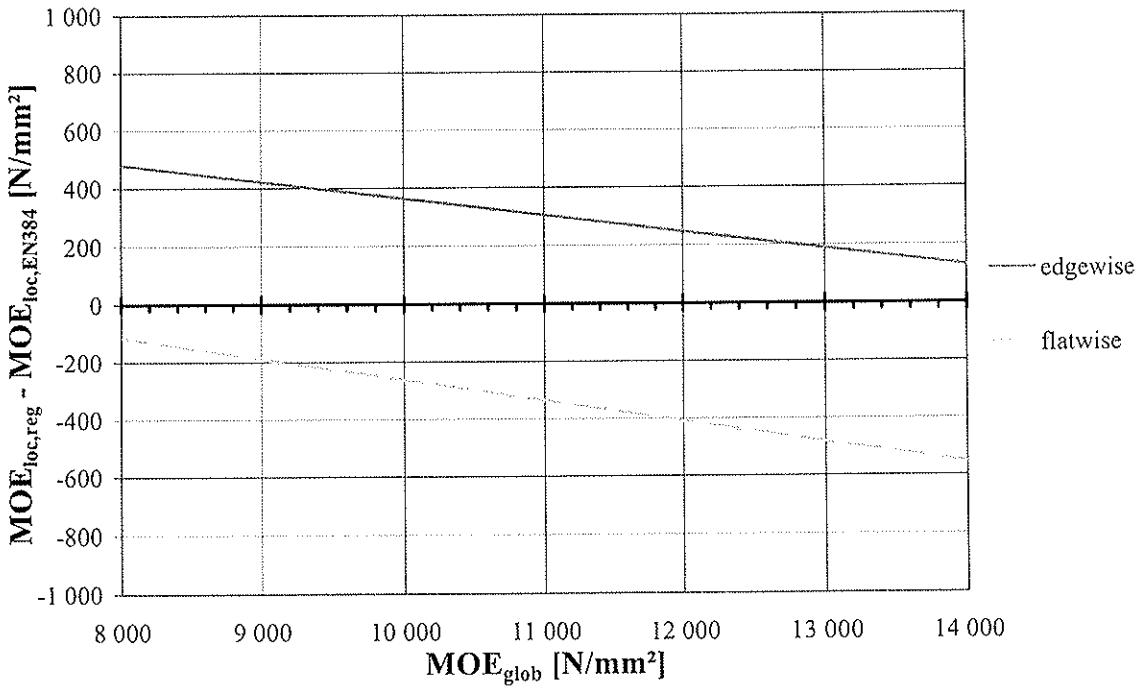

Fig. 4: Difference of $MOE_{loc,reg}$ and $MOE_{loc,EN384}$ separated by test method, n = 3491 specimens.

The same sample including 3491 specimens of spruce was visually graded according to DIN 4074 and used to investigate the influence of grading on the relationship between local and global MOE (Fig. 5). The difference between $MOE_{loc,reg}$ and $MOE_{loc,EN384}$ is similar for all three strength classes and rejects over the whole span of the global MOE. The tendency that $MOE_{loc,reg}$, calculated by the regression model in Table 2, exceeds the $MOE_{loc,EN384}$, calculated by equation (1), is comparable to the equation for specimens tested in edgewise bending. The smallest difference is achieved in strength class S7 (which is comparable to C18 according to EN 1912). For a global MOE value of MOE_{glob} = 11000 N/mm² the deviation varies between +0.4% for strength class S7 (C18) and up to +2.7% for strength class S13 (C30). In this case the equation given in EN 384 marginally underestimates the local MOE measured during the bending test.

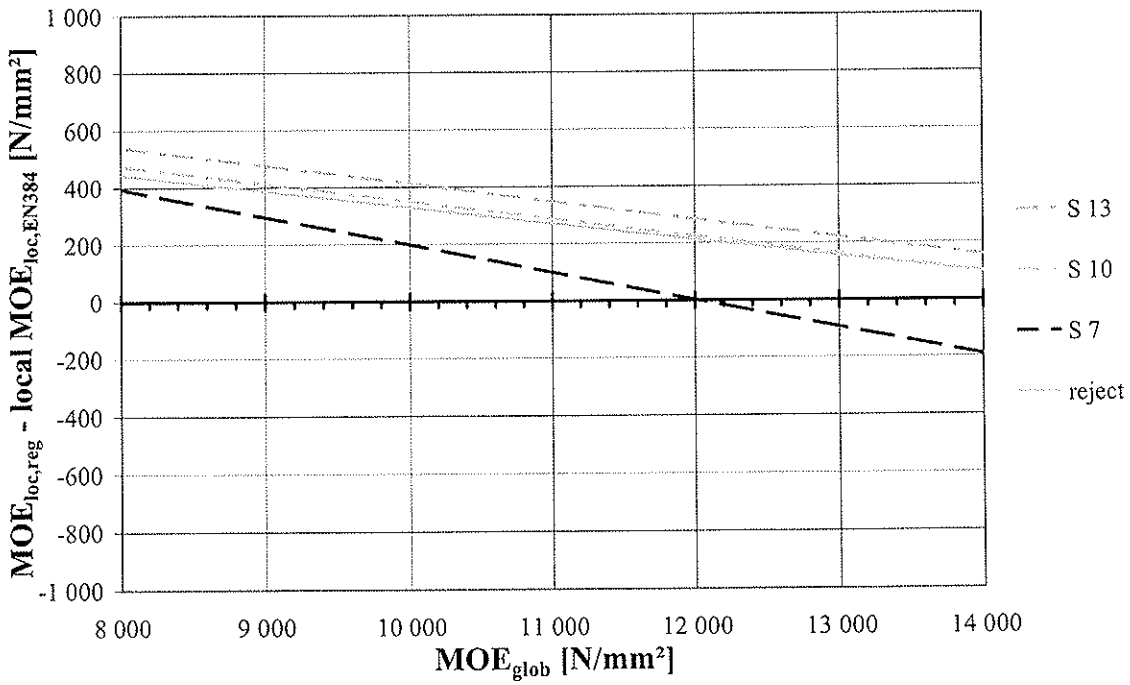

Fig. 5: Difference of $MOE_{loc,reg}$ and $MOE_{loc,EN384}$ separated by visual grading, n = 3491 specimens.

Due to the small amount of specimens tested in flatwise bending the influence of timber dimension on the relationship of local and global MOE is investigated by using only spruce specimens tested in edgewise bending (n = 3325 specimens). For all three different timber dimensions the $MOE_{loc,reg}$ exceeds the $MOE_{loc,EN384}$. If a global MOE of MOE_{glob} = 11000 N/mm² is considered, the local MOE_{EN384}, calculated by equation (1), gives a result of $MOE_{loc,EN384}$ = 11610 N/mm². The local MOE_{reg} of scantlings, calculated by a regression model based on test results, is $MOE_{loc,reg}$ = 11941 N/mm² (+2.9%), whereas the local MOE_{reg} of boards is $MOE_{loc,reg}$ = 11782 N/mm² (+1.5%) and the local MOE_{reg} of planks is $MOE_{loc,reg}$ = 11754 N/mm² (+1.2%) (Fig. 6). Therefore, the timber dimensions do not considerably influence the equation given in EN 384. The local MOE test values marginally exceed the $MOE_{loc,EN384}$ values.

Figure 7 shows the influence of the wood species on the relationship between local and global MOE. Also in this case the $MOE_{loc,EN384}$ underestimates the local MOE measured during bending tests. Assuming a global MOE of MOE_{glob} = 11000 N/mm² the deviation varies between +1.1% and +4.3%. Comparing the relationship between local and global MOE for four different wood species, the regression model for larch is the one with the biggest deviation.

In Table 2 the regression equations are based on comparing the local and global MOE-values of the specimens. The equation in EN 384 compares mean values of the whole sample. To find out whether this method gives different results, mean values were calculated from the global MOE measured during the bending test, converted by equation (1) and compared to the mean values calculated from the local MOE measured during the bending test. Figure 8 shows the results of eleven sub-samples, totalling 3947 specimens tested in edgewise bending. It shows that the equation in EN 384 predicts the results of our tests very well.

It can be concluded, that the equation given in EN 384 to convert the global MOE into a local MOE is not influenced by the wood species or by visual grading or by timber dimensions.

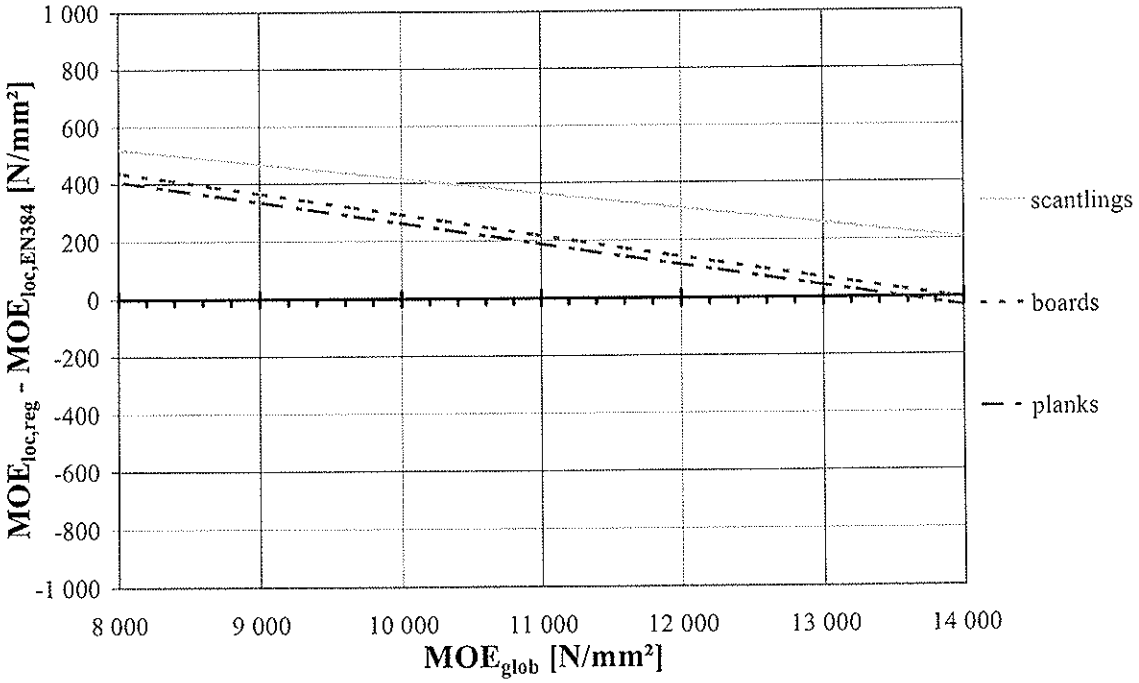

Fig. 6: Difference of $MOE_{loc,reg}$ and $MOE_{loc,EN384}$ separated by timber dimensions, n = 3491 specimens.

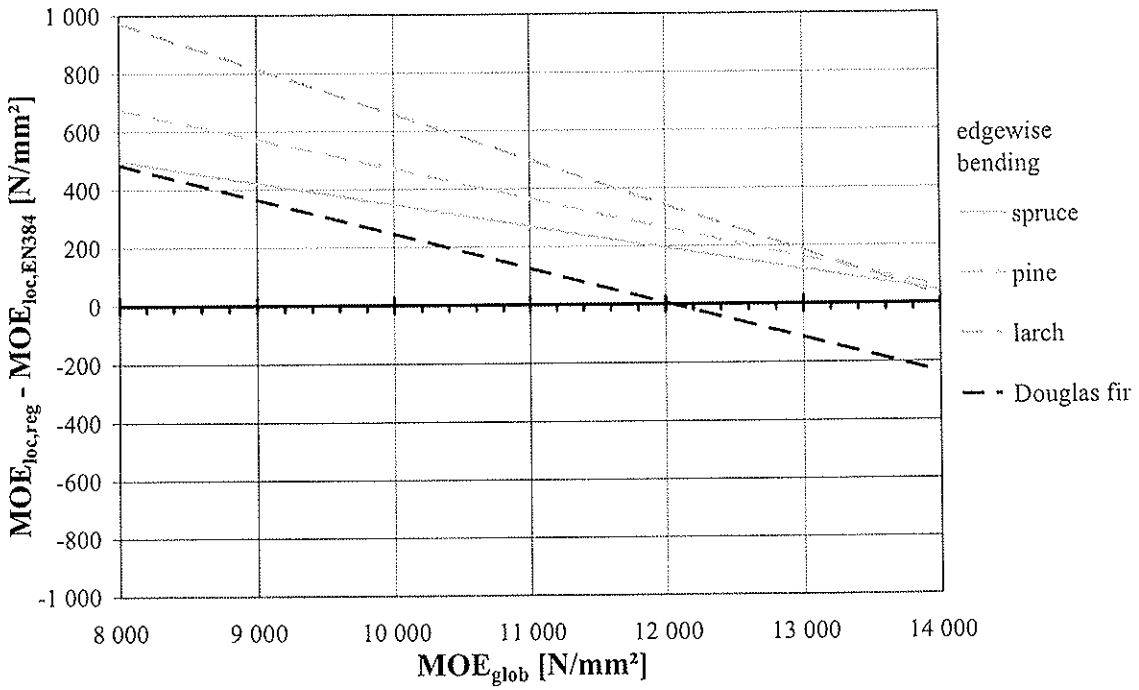

Fig. 7: Difference of $MOE_{loc,reg}$ and $MOE_{loc,EN384}$ separated by wood species for edgewise bending tests, n = 3847 specimens.

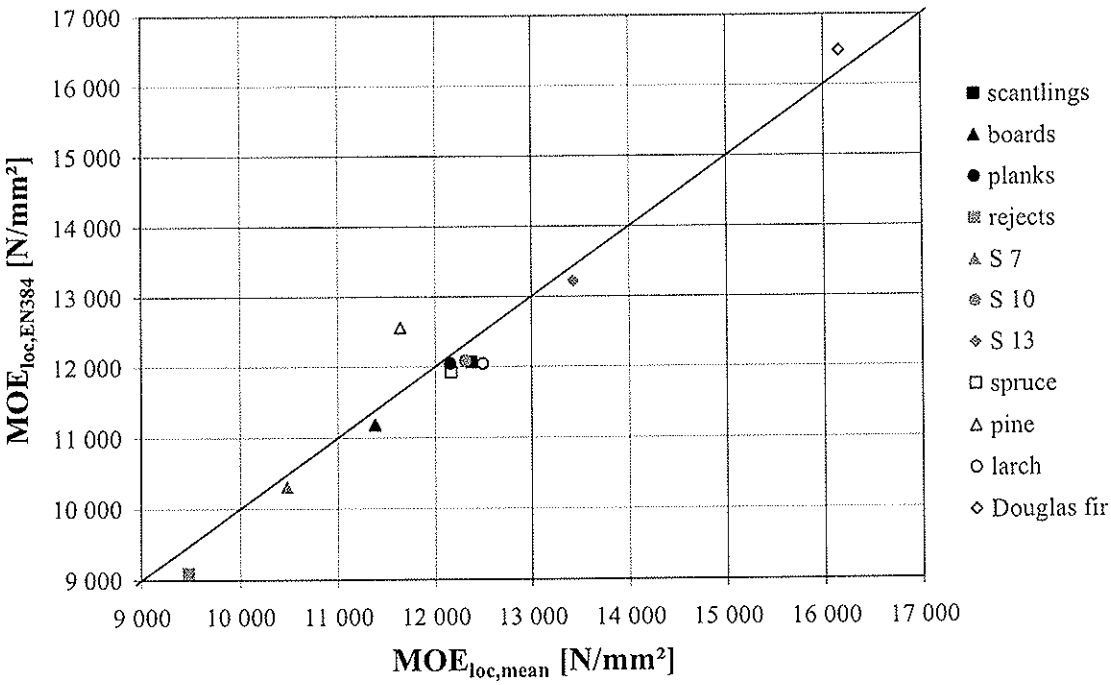

Fig. 8: $MOE_{loc,EN384}$ over $MOE_{loc,mean}$, n = 3947 specimens.

4 Conclusions

This paper deals with the equation given in EN 384 to convert a global MOE into a local MOE. The influences of test method, timber dimension, of timber quality and wood species were examined. The results show that the equation given in EN 384 tends to underestimate the local MOE at 11000 N/mm². The tendency decreases with increasing global MOE. At 14 000 N/mm², the local MOE calculated with the equation given in EN 384 is up to 1.5% higher than the local MOE measured during the bending test.

An equation $MOE_{loc} = MOE_{glob} \cdot 1.2 - 1400$ would fit the German data better than the equation in EN 384. However, keeping in mind the variation between different samples, the difference is marginal. Therefore it is recommended not to change the equation in EN 384.

5 Literature

EN 384:2004-01 Structural timber - Determination of characteristic values of mechanical properties and density. CEN European Committee for Standardization, Brussels. 15.

EN 408:2003-08 Timber structures - Structural timber and glued laminated timber - Determination of some physical and mechanical properties. CEN European Committee for Standardization, Brussels. 32.

EN 1912:2005-03 Structural timber. Strength classes. Assignment of visual grades and species. CEN European Committee for Standardization, Brussels. 15.

INTERNATIONAL COUNCIL FOR RESEARCH AND INNOVATION IN BUILDING AND CONSTRUCTION

WORKING COMMISSION W18 - TIMBER STRUCTURES

BENDING STRENGTH OF SPRUCE GLULAM
NEW MODELS FOR THE CHARACTERISTIC BENDING STRENGTH

M Frese

H J Blass

Universität Karlsruhe

GERMANY

Presented by M. Frese

Y.H. Chiu asked whether the strength model for the higher glulam strength depended on the grading method. H. Blass stated no and the model covers a whole range of grading including knot size and density and dynamic MOE. The tensile strength limit was used where visually graded material would fall to the lower case hence the model is grading method independent. A. Ranta-Maunus stated that new data from Scandinavia is available where mechanical graded beam results agree with the model but visually graded beams have higher value compared to model. Also correlation between bending and tension strength of the finger joint is poor. Since QC tests uses bending strength, this is an issue. H. Blass added that there are in addition 40 bending tests in Karlsruhe. Currently Karlsruhe is waiting for the laminae and finger joint tests. J. Köhler said that it would be interesting to see the entire distribution rather than just the 5^{th} percentile values. M. Frese said that simulated mean and 5^{th} percentile values are available in the final report. T. Williamson said that QC of bending strength of finger joint was eliminated in US for some 10 years. The use of 21 MPa as limit may not be applicable to some visually graded material in the US. H. Blass said that this is not the case with European spruce where visually graded material rarely exceeds 21 MPa. T. Williamson commented that he is pleased to see glulam size factor finally recognized in Europe and the trend seems to agree with US provisions. I. Smith asked how grading errors were captured in this work. H. Blass said that this was not done. I. Smith asked whether it means that the tensile strength is higher than 60% of the bending strength as normally assumed for timber. H. Blass said that they do not make statements about timber but with glulam this is the case. B.J. Yeh asked whether EN standard proposal is intended for spruce and fir or other species also. H. Blass said that the research was based on Spruce and fir in Europe. In practice Douglas fir, pine and others species will be used. S. Winter asked if it is true that the glulam strength in Europe was overestimated for a long time as in general a 10% over estimation of strength adding depth factor would come up to 50%. H. Blass stated that data has been presented to industry and reaction from industry is pure denial. S. Winter said that may be the information should also be presented to the engineering community. H.J. Larsen stated that reduction of claim factor of safety is also a possibility. J. Köhler said that safety factor also depends on COV. With glulam the COV may be less severe and additional work can be done. Y.H. Chiu said that this could be due to changing of resource characteristics so existing beams may not necessarily be unsafe. H. Blass stated that large database from the past was used in the analysis so changing resource characteristics is not the issue.

Bending strength of spruce glulam
New models for the characteristic bending strength

M. Frese and H.J. Blaß
Lehrstuhl für Ingenieurholzbau und Baukonstruktionen
Universität Karlsruhe (TH)

Abstract

A comprehensive research project regarding the bending strength of the beech glulam [1] showed: Combined visual and mechanical strength grading of boards is very competitive and a strength model, in which the glulam bending strength depends both, on the board tensile strength and the finger joint tensile strength, is a completely transparent model being particularly suitable to determine requirements for the board and for the finger joint tensile strength.
This paper describes the application of these principles to an alternative and new strength model for spruce glulam. For that the effect of the board and finger joint strength on the glulam bending strength is numerically determined by means of simulated glulam beams. According to the findings, described in this paper, current requirements for boards and finger joints are insufficient to ensure the nominal strength values of GL24 to GL36 according to EN 1194.

1 Introduction

1.1 Initial situation – impetus to research

38 bending tests on full size spruce glulam beams were performed at Universität Karlsruhe during the last two years [2]. Half the beams were produced according to strength class GL32c and GL36c, respectively. The boards from spruce were mechanically strength graded according to the grading principle bending and X-ray radiation. One single glulam manufacturer produced the beams at two different dates. The beams were 600 mm in depth and 100 mm in width. The tests were performed according to EN 408 with a span of 15 times the depth and an area between the single forces of six times the depth.
The probability plots in Fig. 1 show the bending strength distribution: According to the fitted normal distributions the 5^{th} percentile of the bending strength is 27.1 N/mm² for GL32c test beams. The 95% confidence limits are [23.8, 29.1]. Nearly the same results were found for the GL36c beams: 5^{th} percentile 27.6 N/mm² and 95% confidence limits [22.7, 30.7]. Hence the characteristic strength values were not sufficient to confirm the required characteristic bending strength of 32 N/mm² and 36 N/mm², respectively. In addition to that Fig. 1 exemplifies that 37% of the bending strength values fall below 32 N/mm² in case of GL32c and 42% in case of GL36c. Fig. 2 shows the bending strength values depending on the MOE.
The following observations verify that the quality of the test beams was not out of the ordinary and that the mechanical strength grading process during the manufacture was effective:

1. The MOE of the GL36c test beams is very high. The values (=star symbols) exceed 14400 N/mm².
2. The MOE values of the GL32c test beams on the one hand and the GL36c ones on the other hand are obviously separated from each other.

3. The characteristic finger joint bending strength meets the required values in DIN 1052. Therefore, the test results strongly questioned the reliability of spruce glulam and triggered further research towards the bending strength of spruce glulam.

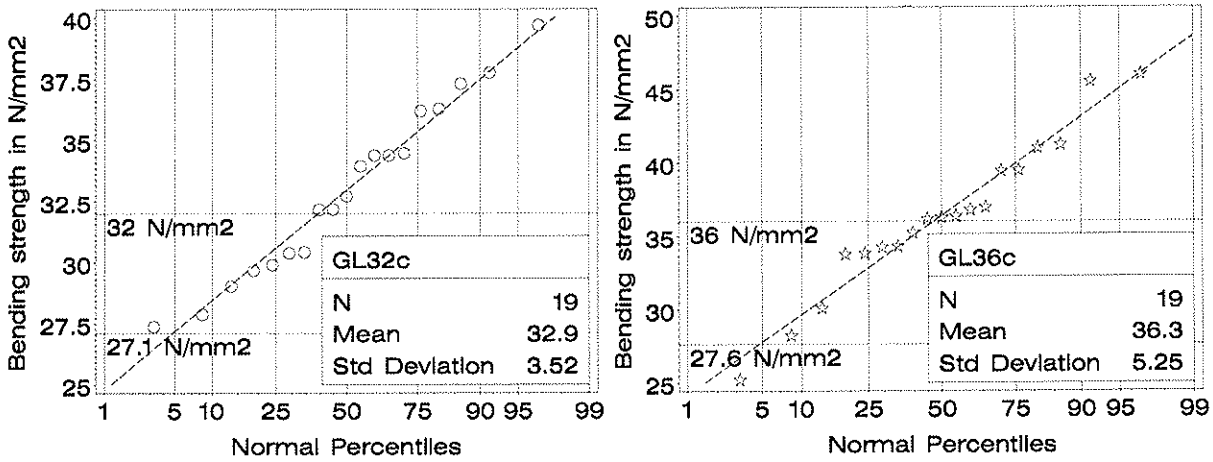

Fig. 1 Test results: empirical and fitted normal distribution of the bending strength; GL32c test beams (left-hand side) and GL36c ones (right-hand side). Values below the horizontal reference lines stand for theoretical 5th percentile values and strength targets.

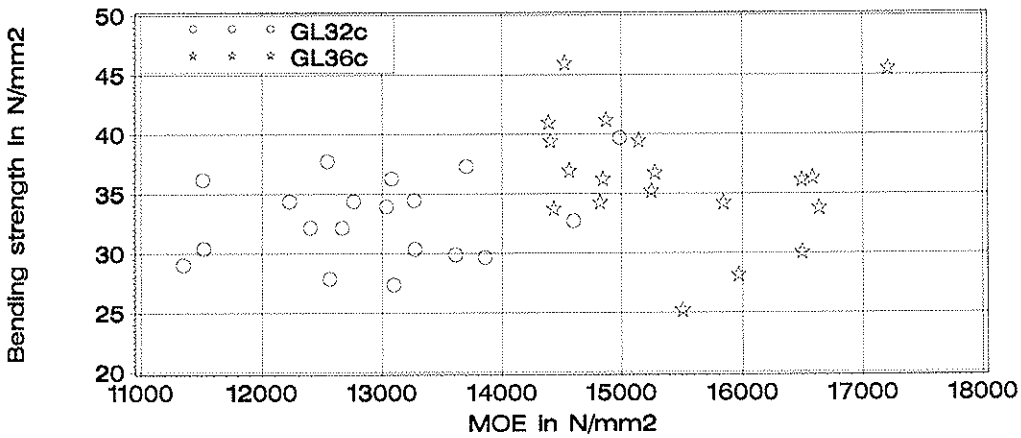

Fig. 2 Test results: bending strength in dependency on MOE

1.2 Review – Colling's strength model

Colling [3] published a relation between the characteristic glulam bending strength ($f_{m,g,k}$), the characteristic board tensile strength ($f_{t,\ell,k}$) and the characteristic finger joint bending strength ($f_{m,j,k}$) by means of a set of curves. With these curves and with the requirements in EN 1194 for boards and in DIN 1052 for finger joints characteristic bending strength values were calculated. These values are summarized in Table 1.

Table 1 Evaluation of Colling's model

Glulam strength class	Board strength class	$f_{t,\ell,k}$ EN 1194 N/mm²	$f_{m,j,k}$ DIN 1052 N/mm²	$f_{m,g,k}$ Colling's curves N/mm²
GL24	C24	14,5	30	21,8
GL28	C30	18	35	25,7
GL32	C35	22	40	29,3
GL36	C40	26	45	32,9

It is evident that they do not fulfil the targets of the strength classes GL24 to GL36. That may indicate insufficient requirements for boards and finger joints and strengthens the necessity to check their correctness.

1.3 Approach

A strength model, given in general terms by equation (1), in which the glulam bending strength depends both on the board and the finger joint tensile strength, is a completely transparent model. It is particularly suitable to determine requirements for the board tensile strength and for the finger joint tensile strength, see also [1].

$$f_{m,g,k} = f(f_{t,\ell,k}, f_{t,j,k}) \qquad (1)$$

To specify a strength model in detail, a large number of correlated triples of the parameters present in equation (1) are necessary. To determine those triples, the effect of the board strength and of the finger joint strength on the glulam bending strength was numerically determined by means of simulated glulam beams. For that a consisting finite element based computer model, which was originally developed for beech glulam, was applied to spruce glulam. For this purpose the knowledge and the fundamental input data of the Karlsruhe Rechenmodell (KAREMO) was used [4], [5] and [6]. Since KAREMO was developed during the 1980s no experience and no extensive data of mechanically strength graded boards was available. Holzforschung München provided a comprehensive data base of real boards describing the knot and density distribution of strength graded material. These distributions and the board strength values serve as input data. By means of empirical representation of this strength graded material within the computer model, which enables the simulation of a realistic strength grading process, it was possible to artificially generate glulam beams from differently strength graded boards. Different strength grading methods have a different effect on the board strength and stiffness distribution and finally on the glulam strength. That is the precondition to numerically describe the effect of the board tensile strength and of the finger joint tensile strength, stepwise increased during the simulations, on the glulam bending strength. Simulation results obtained in this way form a database in which the characteristic glulam bending strength depends on the examined grading methods and the variable characteristic finger joint tensile strength. The relation in equation (1) is derived by means of a multiple nonlinear regression analysis in which the glulam bending strength is the response variable and the board and the finger joint tensile strength are the explanatory variables. A detailed research report, also available in English, about the investigation will be published by Blaß et al [2].

2 Simulating the glulam bending strength

Up to 5400 bending tests were simulated by considering the grading methods in Table 2 at a time. The beams were 600 mm in depth and the simulated testing procedure complied with EN 408. Consequently, the reference depth for the bending strength is 600 mm. Fig. 6 in annex A 1 exemplarily shows the individual results for a part of the grading methods, VIS II, DENS I and EDYN I providing the highest yield. The simulated glulam bending strength over variable characteristic finger joint tensile strength is plotted on the left-hand side. It was required to perform up to five studies for each of the grading methods to stabilize the course connecting the means of the single dots or triangles. Each of the dots or triangles represents a statistical value, mean or 5^{th} percentile, based on up to 200 simulated tests. The number of dots or triangles equals the number of studies performed for each of the grading methods. The studies differ from each other through different random number sequences used to generate board properties. As a result, different random number sequences have a different effect on the simulated glulam bending strength. On the right-hand side of Fig. 6 the simulated portion

of finger joint failure is plotted: These diagrams by implication show the relation between board and finger joint strength. A balanced relation is indicated by a portion of 50%. Strongly different ones indicate poor matching between these strength values.

Table 2 Grading methods developed by Holzforschung München [2] and criteria knots, density, dynamic MOE, characteristic board tensile strength acc. to EN 408 and yield

Name	Method	Max KAR -	Min ρ_0 kg/m³	Min E_{dyn} in N/mm²	$f_{t,\ell,k}$ in N/mm²	Yield %
VIS I	Visual in S10[1]	-	-	-	13.3	52.8
VIS II	Visual in S10[1]+ S13[1]	-	-	-	14.4	78.6
VIS III	Visual in S13[1]	-	-	-	21.3	25.8
DENS I	Density + knots	0.35	450	-	23.4	22.7
DENS II		0.35	475	-	24.6	12.8
EDYN I	Dynamic MOE + knots	0.50	-	14000	26.7	24.2
EDYN II		0.50	-	15000	29.0	16.4
EDYN III		0.50	-	16000	33.0	9.8
EDYN IV		0.20	-	16000	34.6	5.0

[1] Visual grades according to DIN 4074-1

3 Strength models

3.1 Determination

Finally, the numerical base for the strength models consists of the strength values below:

1. Characteristic glulam bending strength determined by means of the simulated bending tests (exemplarily represented by the dots in Fig. 6 for three out of the nine grading methods).
2. Characteristic board tensile strength determined according to EN 408 (Table 2) as a result of the different grading methods. This value is assigned to each of the grading methods.
3. Characteristic finger joint tensile strength, increased from 20 to 40 N/mm² in steps of 2.5 N/mm² during the simulations (compare Fig. 6). This value refers to a board section 150 mm in length.

In order to additionally specify the strength models, depending on the characteristic finger joint bending strength, the empirical relation (2) is used to replace the characteristic finger joint tensile strength, referring to a section 150 mm in length (= $f_{t,j,k,\ell=150mm}$), by the characteristic finger joint bending strength [7] and [8].

$$f_{m,j,k} \approx 1,40 \cdot f_{t,j,k,\ell=150mm} \tag{2}$$

Equating (3) with (4), both from EN 1194, and resolving leads to (5). The agreement between (2) and (5) shows that strength models, depending on the finger joint tensile strength, are also valid for a characteristic finger joint tensile strength determined according to EN 408 with a free span of 200 mm in length (= $f_{t,j,k,\ell=200mm} \rightarrow f_{t,j,k}$).

$$f_{t,j,k,\ell=200} \geq 5 + f_{t,\ell,k} \tag{3}$$

$$f_{m,j,k} \geq 8 + 1,4 \cdot f_{t,\ell,k} \tag{4}$$

$$f_{m,j,k} = 1 + 1,4 \cdot f_{t,j,k,\ell=200} \approx 1,4 \cdot f_{t,j,k,\ell=200} \tag{5}$$

An important finding in Blaß et al [2] is that a universal strength model, covering all the grading methods, does not describe the lamination effect as accurately as possible. As a consequence, two strength models were specified considered to be suitable to cover two grading

methods each with a similar lamination effect: Visual grading and mechanical grading. The assignment of the grading methods to the reference numbers of the corresponding regression equations (→ strength models) is given in Table 3. The strength models are plotted in Fig. 3 followed by the regression equations (6) and (7) for visual as well as (9) and (10) for mechanical grading.

The portion of finger joint failure (= $\eta_{j,crack}$) is an important dependent variable to determine a balanced relation between the board tensile strength and the finger joint bending strength. Therefore, corresponding regression equations (8) and (11) were additionally derived to estimate the portion of finger joint failure.

Table 3 Number of triples (=N) used in the regression analysis, coefficient of determination ($=r^2$) and standard deviation of the residuals ($=s_R$)

Grading method	Regression equation	N	r^2	s_R
Explanatory variable: characteristic glulam bending strength				
VIS I, II, III	(6) (7)	80 *	0.900	.979 N/mm²
DENS I, II, EDYN I, II, III, IV	(9) (10)	252	0.904	1.57 N/mm²
Explanatory variable: portion of finger joint failure				
VIS I, II, III	(8)	81	0.940	5.77 %
DENS I, II, EDYN I, II, III, IV	(11)	252	0.931	6.01 %
* one triple (=statistical anomaly) disregarded in the regression analysis				

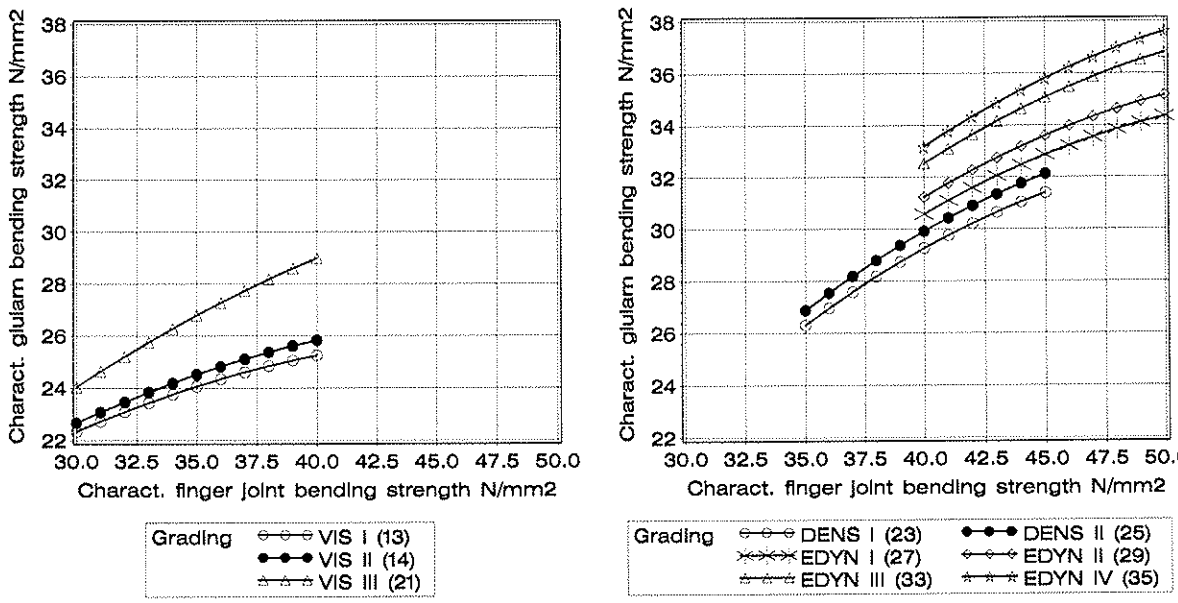

Fig. 3 Strength models: characteristic glulam bending strength over characteristic finger joint bending strength; curves comply with grading methods or characteristic board tensile strength (values in brackets); equation (7) (left-hand side) and (10) (right-hand side)

- Visual grading:

$$f_{m,g,k} = 3,454 + 0,9975 \cdot f_{t,j,k} - 0,02113 \cdot f_{t,j,k}^{\ 2} - 0,01632 \cdot f_{t,\ell,k}^{\ 2} + 0,03582 \cdot f_{t,j,k} \cdot f_{t,\ell,k} \quad (6)$$

$$f_{m,g,k} = 3,454 + 0,7125 \cdot f_{m,j,k} - 0,01078 \cdot f_{m,j,k}^{\ 2} - 0,01632 \cdot f_{t,l,k}^{\ 2} + 0,02558 \cdot f_{m,j,k} \cdot f_{t,l,k} \quad (7)$$

$$\eta_{j,crack} \approx 93,5 - 2,35 \cdot f_{m,j,k} + 2,29 \cdot f_{t,\ell,k} \quad (8)$$

- Mechanical grading:

$$f_{m,g,k} = -17,39 + 2,290 \cdot f_{t,j,k} - 0,03223 \cdot f_{t,j,k}^{\ 2} + 0,01144 \cdot f_{t,j,k} \cdot f_{t,\ell,k} \quad (9)$$

$$f_{m,g,k} = -17{,}39 + 1{,}636 \cdot f_{m,j,k} - 0{,}01644 \cdot f_{m,j,k}^{\ 2} + 0{,}008169 \cdot f_{m,j,k} \cdot f_{t,l,k} \quad (10)$$

$$\eta_{j,crack} \approx 131 - 2{,}40 \cdot f_{m,j,k} + 0{,}873 \cdot f_{t,\ell,k} \quad (11)$$

Strength values in N/mm², $\eta_{j,crack}$ in %, reference depth 600 mm, homogeneous lay-up

To simplify matters with regard to putting into practice the two models the equations (6) and (7) should be valid up to a characteristic board tensile strength of 21 N/mm². For values exceeding 21 N/mm² the equations (9) and (10) apply. With that the relation between the models and the grading method, visual or mechanical, caused by the development, disappears.

- Area of application of the models:

  (6) and (7) for 13 N/mm² ≤ $f_{t,\ell,k}$ ≤ 21 N/mm²

  (9) and (10) for 22 N/mm² ≤ $f_{t,\ell,k}$ ≤ 35 N/mm²

3.2 Effect of beam depth and beam span on the bending strength

It is well known that a beam depth of less than 600 mm leads to higher strength values and a depth greater than 600 mm to lower ones. That is partly considered eg in EN 1995-1-1 and DIN 1052 for a depth less than 600 mm which leads up to a 10% higher bending strength. In contrast to this there is no conversion for depths exceeding 600 mm. In that case the security factor γ_M has to compensate for the decreasing bending strength.
To newly examine the effect of depth on the characteristic bending strength a total of 7200 simulations were performed with the computer model in order to determine the limit depth at which the depth effect wears off. The result is shown in Fig. 4: The course of the k_h-factor is based on six simulation studies represented by six dots over the stepwise increased beam depth at a time. The quadratic regression curve matches equation (12). With that the characteristic glulam bending strength decreases down to 85% of the reference value referring to beams 600 mm in depth. k_h for 300 mm (=1.09) is as expected, compare EN 1995-1-1, DIN 1052 and test results of Aasheim and Solli [9]. The good correspondence with values from the literature valid between 300 and 600 mm increases the reliability of k_h for depths exceeding 600 mm.

$$\begin{aligned} k_h &= 1.19 - 3.73 \cdot 10^{-4} \cdot h + 1.04 \cdot 10^{-7} \cdot h^2 && 300\,mm < h < 1800\,mm \\ k_h &= 1.09 && h \le 300\,mm \\ k_h &= 0.85 && 1800\,mm \le h \end{aligned} \quad (12)$$

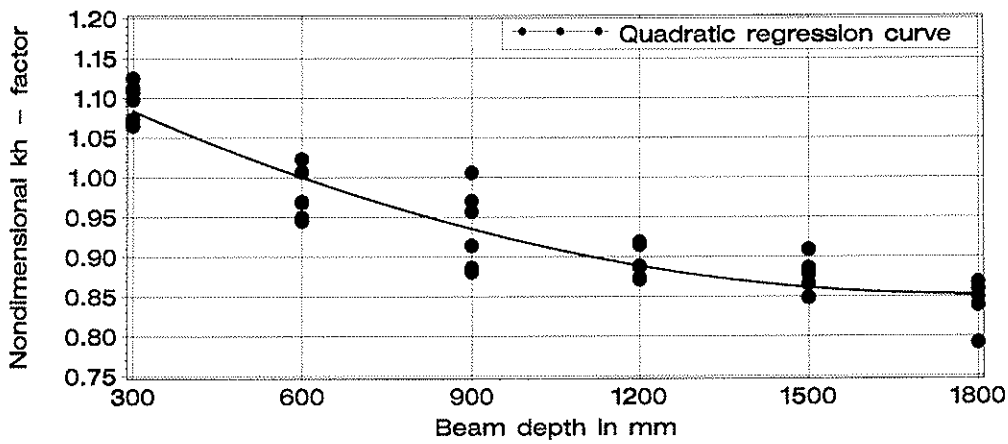

Fig. 4 k_h – factor plotted over variable beam depth; dots gained from simulations

3.3 Verification

The strength models are verified by comparable values from chapter 1.1 and the literature as well as by Colling's model. Ratios of predicted values (according to the strength models) to the published ones are displayed in brackets in the following tables.
The theoretical 5th percentile of the 19 bending strength values for GL32c is 27.1 N/mm². Due to the effective mechanical grading the assumption is justified that board and finger joint strength at least meet the requirements 22 N/mm² and 40 N/mm², respectively. With that the characteristic value according to equation (10) amounts to 28.9 N/mm². With the denominator 1.04, compensating for a combined lay-up, follows:

$$f_{m,g,k} = \frac{28.9}{1.04} = 27.8\,N/mm^2 \rightarrow \frac{27.8}{27.1} = 1.03$$

The predicted value of 27.8 N/mm² not only lies in between the 95% confidence limits [23.8, 29.1] but also meets the theoretical 5th percentile of 27.1 N/mm² quite well. It applies analogously to the 19 bending strength values of GL36c: theoretical 5th percentile 27.6 N/mm², board and finger joint strength at least meet the requirements 26 N/mm² and 45 N/mm², respectively.

$$f_{m,g,k} = \frac{32.5}{1.04} = 31.3\,N/mm^2 \rightarrow \frac{31.3}{27.6} = 1.13$$

The predicted value of 31.3 N/mm² marginally exceeds the upper threshold of the 95% confidence limits [22.7, 30.7] and is even 13% higher than the theoretical 5th percentile of 27.6 N/mm². In this case the prediction is better than the observed value.
The equations (7) and (10) are compared with Colling's model in Table 4 by means of the requirements in EN 1194 for board and in DIN 1052 for finger joint strength. The agreement is surprisingly good although the strength models have a different technical and development background.

Table 4 Agreement with Colling's model

Colling's Model				Strength models
Strength class	$f_{t,f,k}$ EN 1194 N/mm²	$f_{m,j,k}$ DIN 1052 N/mm²	$f_{m,g,k}$ Colling's curves N/mm²	$f_{m,g,k}$ equation (7) N/mm²
C24	14.5	30	21.8	22.8 (1.05)
C30	18	35	25.7	26.0 (1.01)
				equation (10)
C35	22	40	29.3	28.9 (0.99)
C40	26	45	32.9	32.5 (0.99)

Results of 101 bending tests on glulam beams, divided into five different test series, as well as corresponding results of tension tests on boards and finger joints were selected from the publication of Schickhofer [10]. The bending tests were performed on homogeneous glulam. The boards came from Austrian sawmills and were mechanically strength graded. The comparison between the test results, theoretical 5th percentile values, and the predicted values according to equation (6) and (9), both depending on the finger joint tensile strength, is summarized in Table 5. The comparison shows a tendency of overpredicting the test values. Theoretical 5th percentile values, published by Schickhofer, were preferred for the comparison due to the small sample sizes of 23, 30, 20, 10 and 18 in the five series of the test beams.
Furthermore, results of 312 bending tests on glulam beams, divided into three different test series, as well as corresponding results of tension tests on boards and bending tests on finger

joints were selected from the publication of Falk et al [11]. The selected bending tests were performed on homogeneous and combined glulam. The boards came from Norwegian sawmills and were mechanically strength graded. The comparison in Table 6 on average shows good agreement.

The four comparisons above verify that the prediction of the characteristic bending strength with the strength models (6) or (7) and (9) or (10) is in good agreement with Colling's model as well as with the test results published. The all-over ratio of predicted values to test results amounts to 1.02. In this ratio all the relevant bending strength values (19+19+101+312=451) are proportionally taken into account. With that the ratio covers different growth areas of softwood, mechanical grading methods, glulam manufacturers, dates of manufacture and scientists at a time. Against the background of level of knowledge it is justified to assume that the proposed strength models rather accurately describe the reality.

Table 5 Agreement with test results of Schickhofer [10]

Theoretical 5th percentile				Strength models
Strength class	$f_{t,l,k}$ N/mm² (b = 160 mm)	$f_{t,j,k}$ N/mm² (b = 160 mm)	$f_{m,g,k}$ N/mm² (h = 600 mm)	$f_{m,g,k}$ N/mm² equation (6)
MS10	11.6[1]	24.7[2]	20.6[3]	23.3 (1.13)
MS13	17.5[1]	24[2]	24[3]	25.3 (1.05)
				equation (9)
MS17	21.9[1]	34.8[2]	29.8[3]	32.0 (1.07)
			(h = 594 mm)	equation (6)
MS10	11.6[1]	24.7[2]	21.5[4]	23.3 (1.08)
				equation (9)
MS17	21.9[1]	34.8[2]	31.2[4]	32.0 (1.03)

[1] from „Table 6“,
[2] from „Table 9“
[3] from „Table 12“, series 1, 2 and 3 converted with k_h=1.09 from 297 to 600 mm
[4] from „Table 12“, series 6 and 7

Table 6 Agreement with test results of Falk et al [11]

Empirical 5th percentile				Strength model
Strength class	$f_{t,l,k}$ N/mm² (b = 90 mm)	$f_{m,j,k}$ N/mm² (b = 90 mm)	$f_{m,g,k}$ N/mm² (h = 600 mm)	$f_{m,g,k}$ N/mm² equation (10)
C30	22[1]	49.5[2]	30.1[3]	32.2 (1.07)
C37	26.5[1]	52.2[2]	36.1[3]	34.5 (0.96)
C37/C30	26.5[1]	52.2[2]	35.8[4]	34.5 (0.96)

[1] from empirical distribution in „Figure 21“
[2] from „Table 10“
[3] from „Table 12“, with k_h=1.09 converted from 300 to 600 mm
[4] from „Table 12“, with k_h=1.09 converted from 300 to 600 mm and with 1.03 from combined to homogeneous lay-up

3.4 Simplified models for standardization

An indirect conversion of the two strength models into a basic proposal for standardization is given in Table 7. The glulam strength classes are ordered in steps of 2 N/mm². The requirements for boards and finger joints for this basic proposal were determined by means of the equations (7) and (10) which are based on the characteristic finger joint bending strength.

Equation (7) applies up to a characteristic board tensile strength of 21 N/mm² and above that Equation (10). The relation between the board tensile strength and the finger joint bending strength was determined so that the portion of finger joint failure approximately meets a target of 50%. The exact values calculated with the equations (8) and (11), respectively, are shown in column six. Equation (13) continuously describes the relation between the nominal strength values in column one and the board tensile strength in column two. The differentiation in visual and mechanical grading and the area of application are covered implicitely in this equation. Equation (14) continuously represents the pairs of values in the columns three and two.

$$f_{m,g,k} = 16,8 + 0,450 \cdot f_{t,\ell,k} + 0,00408 \cdot f_{t,\ell,k}^{\ 2} \tag{13}$$

$$f_{m,j,k} = 40,1 - 1,85 \cdot f_{t,\ell,k} + 0,1196 \cdot f_{t,\ell,k}^{\ 2} - 0,001737 \cdot f_{t,\ell,k}^{\ 3} \tag{14}$$

(or linear alternative: $f_{m,j,k} = 21,9 + 0,769 \cdot f_{t,\ell,k}$)

Both equations are illustrated in Fig. 5. They comply with the current format in EN 1194: glulam bending strength depending on board tensile strength and additional requirements for finger joints depending on board tensile strength. Annex A 2 contains an elaborated proposal for prEN 14080 for the chapter "Strength and stiffness properties of glued laminated timber". Furthermore, this proposal stipulates requirements for boards and finger joints for combined glulam.

Table 7 Requirements for boards and finger joints for homogeneous glulam

1	2	3	4	5	6	7
Strength class	$f_{t,\ell,k}$ N/mm²	$f_{m,j,k}$ N/mm²	$f_{m,g,k}$ N/mm²	Values in column 4 with	$\eta_{j,crack}$ %	Values in column 6 with
GL24h	14	33	23.8	equation (7)	47	equation (8)
GL26h	18	35	26.0		50	
GL28h	21	38	28.2		48	
GL30h	24	41	30.1	equation (10)	54	equation (11)
GL32h	27	43	32.0		48	
GL34h	30	45	34.0		46	
GL36h	33	47	35.9		46	

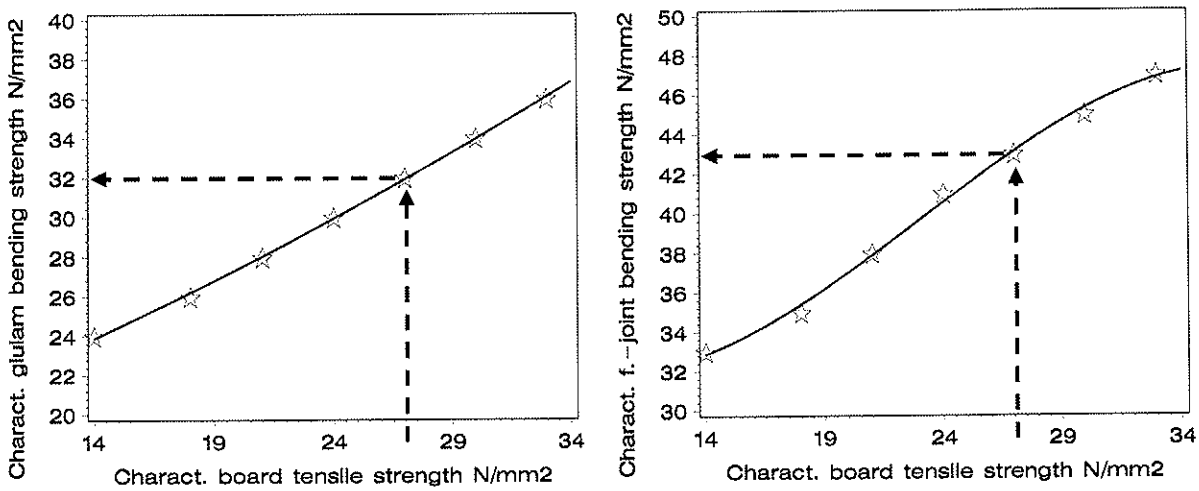

Fig. 5 Basic proposal for further glulam standardization: Characteristic glulam bending strength (left-hand side) and characteristic finger joint bending strength (right-hand side) depending on characteristic board tensile strength; equations (13) and (14), respectively; dashed arrows exemplifying requirements for GL32h

4 Conclusions

38 bending tests on full size spruce glulam beams were performed. Since the strength values were obviously too low compared with EN 1194, this investigation was motivated. It was the aim to explain the low bending strength values by developing new strength models for the characteristic glulam bending strength.

By means of a computer model, suitable to simulate different strength grading methods, the mechanical properties of glulam beams were calculated and bending tests on those beams were numerically performed. The simulation results and the board tensile strength, belonging to the grading methods, form a database which was used to perform a regression analysis in order to derive new strength models. Two models, being of importance to calculate the characteristic glulam bending strength, were determined. They are particularly suitable to predict the bending strength of glulam manufactured from visually and mechanically graded boards, respectively.

There is good agreement between the strength models and Colling's results from the 1990s. They can also be verified by bending tests published in the literature. The all-over ratio of predicted values to test results in the literature on average amounts to 1.02. In this ratio 451 bending strength values of glulam are considered.

One can infer from the strength models, that the current requirements for board tensile and/or finger joint strength are not sufficient to ensure the characteristic glulam bending strength values assigned to the strength classes GL24 to GL36. This finding is to be explained for homogeneous GL32: Whereas the current standard EN 1194 stipulates 22 N/mm² and 38.8 N/mm² for characteristic values of board tensile and finger joint bending strength, respectively, the new strength models lead to demands of about 27 N/mm² and 43 N/mm². For combined beams even higher values are required. Against the background of knowledge the poor characteristic bending strength values of the 38 test beams were caused by too low requirements for boards and finger joints.

For further standardization, the paper contains a basic proposal for the characteristic glulam bending strength in the well known format of EN 1194. In addition, it contains an elaborated proposal for prEN 14080 for the chapter "Strength and stiffness properties of glued laminated timber".

5 References

[1] Frese M, Blaß HJ (2005). Beech Glulam Strength Classes. CIB-W18/38-6-2, Karlsruhe, Germany

[2] Blaß HJ, Frese M, Glos P, Denzler JK, Linsenmann P, Ranta-Maunus A (2008). Zuverlässigkeit von Fichten-Brettschichtholz mit modifiziertem Aufbau – Reliability of spruce glulam – Modelling the characteristic bending strength. Karlsruher Berichte zum Ingenieurholzbau. In preparation for publication in Universitätsverlag Karlsruhe: Karlsruhe

[3] Colling F (1995). Brettschichtholz unter Biegebeanspruchung – Glulam with regard to bending stress (only available in German). Step 3. Fachverlag Holz der Arbeitsgemeinschaft Holz e.V.: Düsseldorf 1995

[4] Ehlbeck J, Colling F, Görlacher R (1985). Einfluss keilgezinkter Lamellen auf die Biegefestigkeit von Brettschichtholzträgern – The effect of finger jointed lamellas on the glulam bending strength (in German). Holz als Roh- und Werkstoff 43: 333-337, 369-373, 439-442

[5] Colling F (1990). Tragfähigkeit von Biegeträgern aus Brettschichtholz in Abhängigkeit von den festigkeitsrelevanten Einflussgrößen – The load bearing capacity depending on parameters influencing the strength (only available in German). Karlsruhe, Universität (TH). Dissertation

[6] Görlacher R (1990). Klassifizierung von Brettschichtholzlamellen durch Messung von Longitudinalschwingungen – Classification of glulam lamellas by means of longitudinal vibrations (only available in German). Karlsruhe, Universität (TH). Dissertation

[7] Colling F, Ehlbeck J, Görlacher R (1991). Glued laminated timber – Contribution to the determination of the bending strength of glulam beams. CIB-W18A/24-12-1, Oxford, United Kingdom

[8] Frese M (2006). Die Biegefestigkeit von Brettschichtholz aus Buche - Experimentelle und numerische Untersuchungen zum Laminierungseffekt – The bending strength of beech glulam – Experimental and numerical investigations (only available in German). Band 5. Karlsruher Berichte zum Ingenieurholzbau. Universitätsverlag Karlsruhe: Karlsruhe 2006. Dissertation

[9] Aasheim E, Solli KH (1995). Size factor of Norwegian glued laminated beams. CIB-W18/28-12-2, Copenhagen, Denmark

[10] Schickhofer G (1996). Development of Efficient Glued Laminated Timber. CIB-W18/29-12-1, Bordeaux, France

[11] Falk R, Solli K, Aasheim E (1992). The performance of glued laminated beams manufactured from machine stress graded Norwegian spruce. Norsk Treteknist Institutt. Meddelelse 77

DIN 1052:2004-08. Entwurf, Berechnung und Bemessung von Holzbauwerken – Allgemeine Bemessungsregeln und Bemessungsregeln für den Hochbau – Design of timber structures – General rules and rules for buildings (only available in German)

DIN 4074-1:2003-06. Sortierung von Holz nach der Tragfähigkeit, Teil 1: Nadelschnittholz – Strength grading of wood - Part 1: Coniferous sawn timber (only available in German)

EN 408:1995. Bauholz für tragende Zwecke und Brettschichtholz – Bestimmung einiger physikalischer und mechanischer Eigenschaften – Structural timber and glued laminated timber – Determination of some physical and mechanical properties

EN 1194:1999. Brettschichtholz – Festigkeitsklassen und Bestimmung charakteristischer Werte – Glued laminated timber – Strength classes and determination of characteristic values

EN 1995-1-1:2004. Eurocode 5: Design of timber structures – Part 1-1: General – Common rules and rules for buildings

A 1 Simulation results

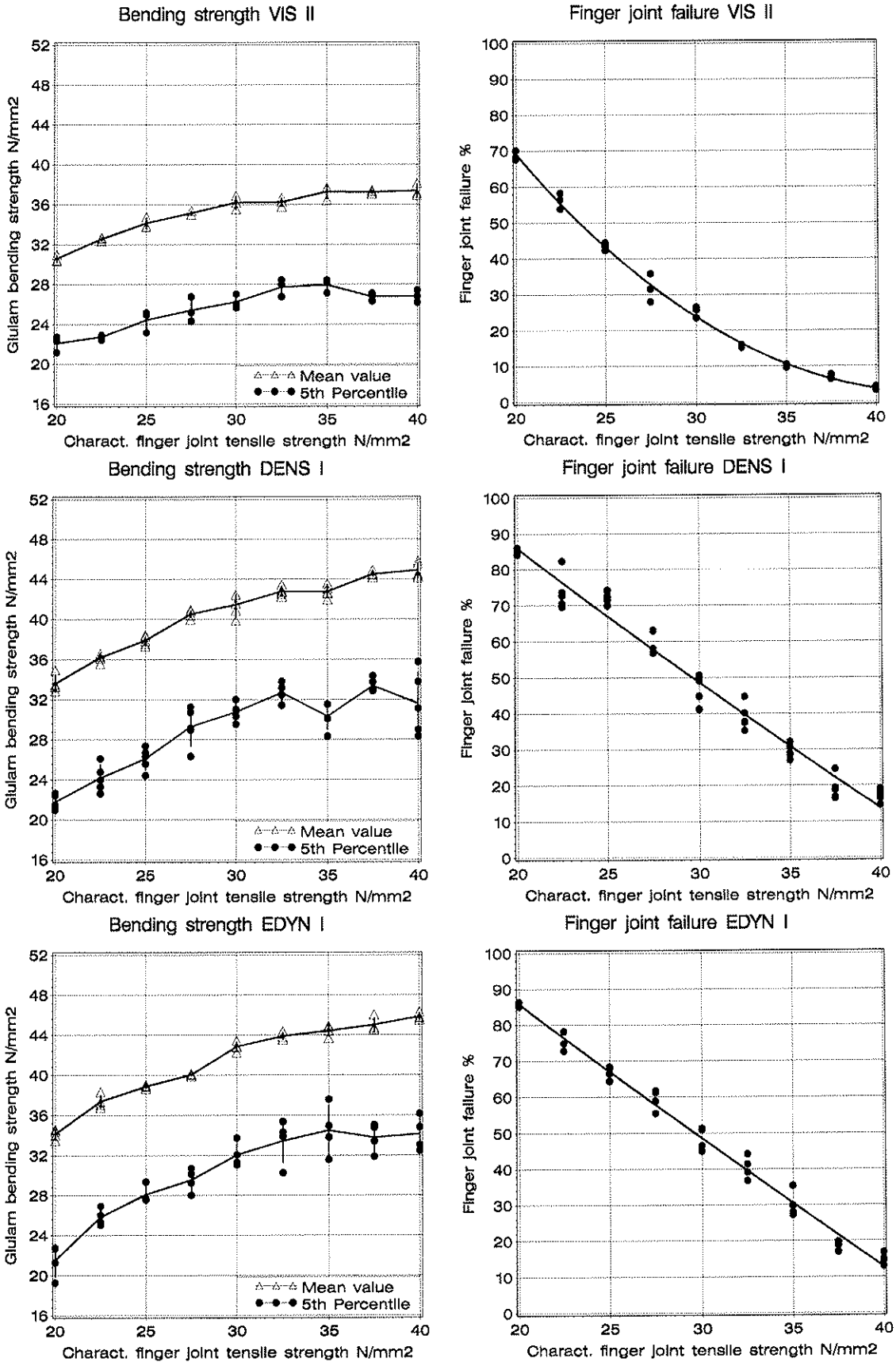

Fig. 6 Simulated glulam bending strength (left-hand side) and portion of finger joint failure (right-hand side) plotted over characteristic finger joint bending strength at a time

A 2 Proposal for prEN 14080

5.5 Strength and stiffness properties of glued laminated timber

5.5.1 General

The strength- and stiffness-properties of the glued laminated timber can be verified from tests with glued laminated timber, from calculations and documented properties of the laminations or from classifications from lamination properties.

The characteristic strength and stiffness properties are based on tests in accordance with EN 408. The characteristic bending strength is related to elements with a depth of 600 mm.
The characteristic tensile strength parallel to the grain is related to elements with a depth of 600 mm h or a width b of 600 mm.
The characteristic tensile strength perpendicular to the grain is related to elements with a stressed volume of 0,01 m^3.
The characteristic shear strength is related to elements with homogeneously stressed volume of 0,0005 m^3.
The compression strength perpendicular to the grain given in this European standard are approximately half of those used in some design codes for the strength verification of supports.
The 5%-percentile of a shear modulus or a modulus of elasticity can be estimated from the mean value taken into account a ratio of $G_{05}/G_{50} = 5/6$ respectively $E_{05}/E_{50} = 5/6$.
NOTE: According to EN 1995-1-1 the characteristic value for the bending strength can be enlarged by a factor k for glulam members subjected to flatwise-bending.
For the verification of the lateral torsional stability of glued laminated timber members made of at least ten lamellas ($E_{0,g,05} \cdot G_{g,05}$) may be enlarged by a factor $k = 1{,}40$.
The requirements for the strength and stiffness properties of the lamellas given in 5.5 shall be fulfilled.
If the grading procedures reliably ensure that all parts of the split member meet the declared properties, members are allowed to be split lengthwise. Splitting is also allowed for glued laminated timber whose outer lamellas have a characteristic tensile strength of not less than 18 N/mm^2 if the characteristic bending and tensile strength of the split members is reduced by 4 N/mm^2 compared with the non-split member.

5.5.2 Verification from classification of standardised beam lay ups and lamella properties which can be classified into a strength class

5.5.2.1 Properties of the lamellas

The lamellas shall comply to a strength class given in table 3.

Table 3 – Characteristic strength and stiffness properties in N/mm^2 and densities in kg/m^3 for lamellas for glued laminated timber

Lamella strength class	$f_{t,0,l,k}$	$E_{t,0,l,k}$	$\rho_{l,k}$
	[N/mm^2]	[N/mm^2]	[kg/m^3]
T11 E9	11	9.000	320
T14 E11	14	11.000	350
T18 E12	18	12.000	380
T21 E13	21	13.000	400
T24 E14	24	14.000	420
T27 E14.8	27	14.800	430
T30 E15.6	30	15.600	440
T33 E16.4	33	16.400	450
T36 E17.2	36	17.200	460

NOTE: The first five classes given in table 3 comply with C-Classes given in EN 338: 2005.

5.5.2.2 Strength of finger joints

The requirements for finger joints in lamellas can be taken from table 4 or have to be calculated according to 5.5.3.2.

Table 4 – Required characteristic values for tensile strength or bending strength of finger joints in lamellas in N/mm^2 for lamella strength classes given in table 3

Lamella strength class	$f_{t,j,k}$	$f_{m,j,k}$
	[N/mm2]	[N/mm2]
T11 E9	22	31
T14 E11	24	33
T18 E12	25	35
T21 E13	27	38
T24 E14	29	41
T27 E14.8	31	43
T30 E15.6	32	45
T33 E16.4	34	47
T36 E17.2	35	49

5.5.2.3 Beam lay up and strength class

It can be assumed that glued laminated timber fulfils the requirements of a strength class given in table 6 or table 7 if the beam lay-up is in accordance with table 5.

Table 5 – Beam lay-up of glued laminated timber

Homogeneous glued laminated timber		Combined glued laminated timber		
Strength class		Strength class		
lamellas	glued laminated timber	outer lamellas	inner lamellas	glued laminated timber
T14 E11	GL 24h	T18 E12	T11 E9	GL 24c
T18 E12	GL 26h	T21 E13	T14 E11	GL 26c
T21 E13	GL 28h	T24 E14	T18 E12	GL 28c
T24 E14	GL 30h	T27 E14.8	T18 E12	GL 30c
T27 E14.8	GL 32h	T30 E15.6	T21 E13	GL 32c
T30 E15.6	GL 34h	T33 E16.4	T24 E14	GL 34c
T33 E16.4	GL 36h	T36 E17.2	T27 E14.8	GL 36c

Homogeneous glued laminated timber consists of lamellas of the same strength class or strength profile.
For combined glued laminated timber it is assumed that zones of different lamella grades amount to at least 1/6 of the beam depth or two lamellas, whichever is the greater.
The outer lamellas are of a higher strength class or strength profile, the inner part of the cross-section comprises lamellas of a lower strength class or strength profile, see table 5.

Table 6 - Characteristic strength and stiffness properties in N/mm^2 and densities in kg/m^3 (for homogeneous glulam)

Glulam strength class		GL24h	GL26h	GL28h	GL30h	GL32h	GL34h	GL36h
Bending strength	$f_{m,g,k}$	24	26	28	30	32	34	36
Tensile strength	$f_{t,0,g,k}$	20	22	24	26	27	29	30
	$f_{t,90,g,k}$	0,4						
Compression strength	$f_{c,0,g,k}$	20	22	24	26	27	29	30
	$f_{c,90,g,k}$	2,5						
Shear strength (shear and torsion)	$f_{v,g,k}$	3,0						
Rolling shear strength	$f_{r,g,k}$	1,5						
Modulus of elasticity	$E_{0,g,mean}$	11.000	12.000	13.000	14.000	14.800	15.600	16.400
	$E_{90,g,mean}$	300						
Shear-Modulus	$G_{g,mean}$	650						
Rolling shear modulus	$G_{r,g,mean}$	65						
Density	$\rho_{g,k}$	380	420	440	460	470	480	490

Table 7 - Characteristic strength and stiffness properties in N/mm^2 and densities in kg/m^3 (for combined glulam)

Glulam strength class		GL24c	GL26c	GL28c	GL30c	GL32c	GL34c	GL36c
Bending strength	$f_{m,g,k}$	24	26	28	30	32	34	36
Tensile strength	$f_{t,0,g,k}$	22	24	24	26	27	29	30
	$f_{t,90,g,k}$	0,4						
Compression strength	$f_{c,0,g,k}$	22	24	24	26	27	29	30
	$f_{c,90,g,k}$	2,5						
Shear strength (shear and torsion)	$f_{v,g,k}$	3,0						
Rolling shear strength	$f_{r,g,k}$	1,5						
Modulus of elasticity	$E_{0,g,mean}$	11.000	12.000	13.000	14.000	14.800	15.600	16.400
	$E_{90,g,mean}$	300						
Shear-Modulus	$G_{g,mean}$	650						
Rolling shear modulus	$G_{r,g,mean}$	65						
Density	$\rho_{g,k}$	350	380	420	420	440	460	470

5.5.3 Verifications from calculations based on the properties of the lamellas

5.5.3.1 Properties of the lamellas

If the lamellas comply with one of the relevant grading rules the strength and stiffness properties may be taken from table 3.

If lamellas are used, which do not comply with table 3 of this European standard, the characteristic values of the tensile strength parallel to the grain $f_{t,0,l,k}$, the modulus of elasticity parallel to the grain $E_{0,l,mean}$ and the density $\rho_{l,k}$ shall be derived from tests according to EN 408 and calculated according to the principles given in EN 384.

5.5.3.2 Strength of finger joints

If the lamellas comply with one of the relevant grading rules the strength of the finger joints may be taken from table 4 or have to be calculated according to 5.5.3.2.

If lamellas are used which do not comply with table 3 of this European standard, the declared strength of finger joints shall be verified by tests in accordance with Annex F. The finger joints of each lamellas shall fulfil the requirements either given in equation (3) or (4).

$$f_{t,j,k} \geq 16 + 0{,}53\, f_{t,0,l,k} \quad (3)$$

Where:

$f_{t,j,k}$ is the characteristic tensile strength of the finger joint in N/mm^2;
$f_{t,0,l,k}$ is the characteristic tensile strength of the lamella in N/mm^2.

$$f_{m,j,k} \geq 22{,}5 + 0{,}75\, f_{t,0,l,k} \quad (4)$$

Where:

$f_{m,j,k}$ is the characteristic bending strength of the finger joint in N/mm^2;
$f_{t,0,l,k}$ is the characteristic tensile strength of the lamella in N/mm^2;

5.5.3.3 Calculation of characteristic values for glued laminated timber

The strength and stiffness properties of glued laminated timber shall be calculated from the strength and stiffness properties of the lamellas using the equations given in table 8.

The stress analysis may be carried out by linear elastic beam theory.
The strength verification shall be made at all relevant points of the cross-section.
It is assumed that zones of different lamination grades amount to at least two lamellas.

Table 8 – Characteristic strength and stiffness properties in N/mm^2 and densities in kg/m^3 of glued laminated timber

Property		
Bending strength	$f_{m,g,k}$	$17 + 0{,}45\, f_{t,0,l,k} + 0{,}004\, f^2_{t,0,l,k}$
Tensile strength	$f_{t,0,g,k}$	$0{,}85\, f_{m,g,k}$
	$f_{t,90,g,k}$	0,40 N/mm^2
Compression strength	$f_{c,0,g,k}$	$0{,}85\, f_{m,g,k}$
	$f_{c,90,g,k}$	2,5 N/mm^2
Shear strength	$f_{v,g,k}$	3,0 N/mm^2
	$f_{r,g,k}$	1,5 N/mm^2
Modulus of elasticity	$E_{0,g,mean}$	$330 + 450\, f_{m,g,k}$
	$E_{90,g,mean}$	300 N/mm^2
Shear modulus	$G_{g,mean}$	650 N/mm^2
	$G_{r,g,mean}$	65 N/mm^2
Density	$\rho_{g,k}$	$1{,}1\ \rho_{l,k}$ [1)]
[1)] Where $\rho_{l,k}$ is the density of the lamella having the lowest characteristic value of tensile strength.		

5.5.4 Verifications from tests with glued laminated timber

5.5.4.1 Properties of the lamellas

Section 5.5.3.1 applies.

5.5.4.2 Strength of finger joints

Section 5.5.3.2 applies with the following exception. If lamellas are used, which do not comply with table 3 of this European standard, the declared strength of the finger joints shall be verified by tests in accordance with Annex F.

5.5.4.3 Testing of glued laminated timber

A homogenous glued laminated member can be assigned to one of the strength classes given in tables 6 or table 7 or to any other strength profile if its characteristic bending strength par-

allel to the grain, its modulus of elasticity parallel to the grain and density derived from tests according to Annex G are not less than the declared values.

The other strength and stiffness properties may be assessed using the equations given in table 9.

Table 9 – Assessment of the strength and stiffness properties in N/mm^2 and the densities in kg/m^3 for glued laminated timber which have not been derived from tests

Modulus of elasticity	$E_{90,g,mean}$	$= 300\ N/mm^2$
Shear modulus	$G_{g,mean}$	$= 650\ N/mm^2$
Tensile strength	$f_{t,0,g,k}$	$= 0{,}85\ f_{m,g,k}$
	$f_{t,90,g,k}$	$= 0{,}40$
Compression strength	$f_{c,0,g,k}$	$= 0{,}85\ f_{m,g,k}$
	$f_{c,90,g,k}$	$= 2{,}5\ N/mm^2$
Shear strength	$f_{v,g,k}$	$= 3{,}0\ N/mm^2$
	$f_{r,g,k}$	$= 1{,}5\ N/mm^2$
	$G_{r,g,mean}$	$= 65\ N/mm^2$
Density	$\rho_{g,k}$	$= 1{,}1\ \rho_{l,k}$ [1)]
[1)] Where $\rho_{l,k}$ is the density of the lamella having the lowest characteristic value of tensile strength.		

INTERNATIONAL COUNCIL FOR RESEARCH AND INNOVATION
IN BUILDING AND CONSTRUCTION

WORKING COMMISSION W18 - TIMBER STRUCTURES

IN-PLANE SHEAR STRENGTH OF CROSS LAMINATED TIMBER

R A Joebstl
Th Bogensperger
G Schickhofer

Institute for Timber Engineering and Wood Technology
Graz University of Technology

AUSTRIA

Presented by R. A. Joebstl

H. Blass asked if the 10 MPa value is proposed for the code. R.A. Joebstl said that it is too early as only 20 specimens with uncommon sizes were studied. A. Salenikovich asked if this is a real shear failure mode and not perpendicular to grain failure. R.A. Joebstl responded that this is really a shear failure mode as observed in the specimen and drop of load in the load deformation curve. H. Blass asked if the test was stopped or the load reduced at 4 mm deformation. R.A. Joebstl responded that the test was stopped at this point so the specimen did not completely fail. A. Asiz asked if data of 7 or 9 layer material were available. R.A. Joebstl said no the 7 or 9 layer material was not tested.

IN-PLANE SHEAR STRENGTH OF CROSS LAMINATED TIMBER

R.A. Jöbstl, Th. Bogenperger, G. Schickhofer
Institute for Timber Engineering and Wood Technology
Graz University of Technology, Austria

1 Introduction

The mass product Cross Laminated Timber (CLT) – general of spruce (picea Abies karst.) – is build up of an uneven number of layers of boards. Each layer is oriented 90° to the two adjacent ones. All layers are connected stiff by adhesive. The boards of each layer can be positioned with or without gaps. If gaps are used, their clearance is up to $w_{gap} = 6$ mm. In case of no gaps, lateral adhesive at the narrow sides of the boards can afford additional stiffness.

CLT is a large-sized derived timber product. Due to transportation issues each element has a length of approx. 13 m and a width of approx. 3 m. Thickness of a CLT plate depends on the number of layers (3, 5, 7 or 9 but up to 21 layers for bridge decks) and the range of application. When dealing with CLT for wall elements, it starts usually with 60 mm and ends up with an overall thickness of 400 mm, when used as a CLT-slab element e.g. with 21 layer for a timber bridge.

Fig. 1 Example for residential building made of clt-elements as wall and ceilings.

Regardless the main focus of applications lies in building constructions, which can easily also be recognized by the typical size of a CLT plate, which has been already mentioned above. CLT plates act as wall, slab and roof elements, carrying loads in and out of plane (e.g.: shear walls).

2 Motivation

CLT elements are characterised by high dimensional stability in case of climate changes. Swelling and shrinking in regard to humidity changes induce internal stresses which cause lengthwise splitting of the boards, preferable within the top layers, and leads to 'residual

board widths'. For safety reasons the ability of shear transfer between the boards within each layer has to be disregarded.

In the last years several investigations due to the shear carrying behaviour have been carried out [1] [2] [3] [4] [5] [6]. Results have also been partially taken into account in various approvals on the one hand and in diverse national codes on the other hand. When using European codes (Eurocodes), European technical approvals provide the framework in conjunction to the EC 5 for the engaged engineer.

For CLT shear verifications in plane, two different possibilities have been developed in respect to the available shear strength values of the boards regarding the shear carrying capacity:

- Verification of the shear stresses regarding mechanism I (acc. to [6], chap. 7) of the boards with the general shear strength values for timber acc. to EN 338. It should be noticed, that only the actual net sections for both main directions of the particular CLT plate can be taken into account. As no particular advice can be found, the general shear strength of timber $f_{v,k}$ acc. to EN 338 has to be used [7]. Additionally the second torsional mechanism (mechanism II, see [6]) has also to be checked.
- Verification of the shear stresses regarding mechanism I under use of the net sections, but with shear strength values, deduced from tests acc. to [8]. Actually shear strength values can be stated with a value of $f_{v,k} = 5{,}2$ N/mm² on basis of this CUAP test. This shear strength value is significantly higher [9] than the value, which can be found in EN 338. Mechanism II is not asked.

The actual work should give a contribution to an improved shear strength value of mechanism I and allow a unification of the verification process of CLT elements under shear in plane.

3 Shear carrying mechanisms of CLT in plane

3.1 Example

The shear strength of CLT, when only small gaps are assembled between the narrow sides of the boards, is remarkable high, as it has already been demonstrated in [6]. The following example should demonstrate that at least with the actual verification procedures acc. to [7] and [9] the shear verification (mechanism I or mechanism II) can also be the dominant one.

The regarded section is part of a CLT wall above an open area of a window. Additionally the wall above the window acts as an upstand beam for the loads from the adjacent ceiling. As shear forces are regarded, the considered section lies near the support of the beam. In detail, a three-layered CLT wall element with two outer vertically oriented layers and a middle horizontally oriented layer with a thickness of 30 mm for each layer should be taken into account for the following verification process.

The controlling net section $A_{V,net}$ is the middle layer of the CLT plate and therefore the thickness t_V is 30 mm and the width of the boards can be considered with a=300 mm.

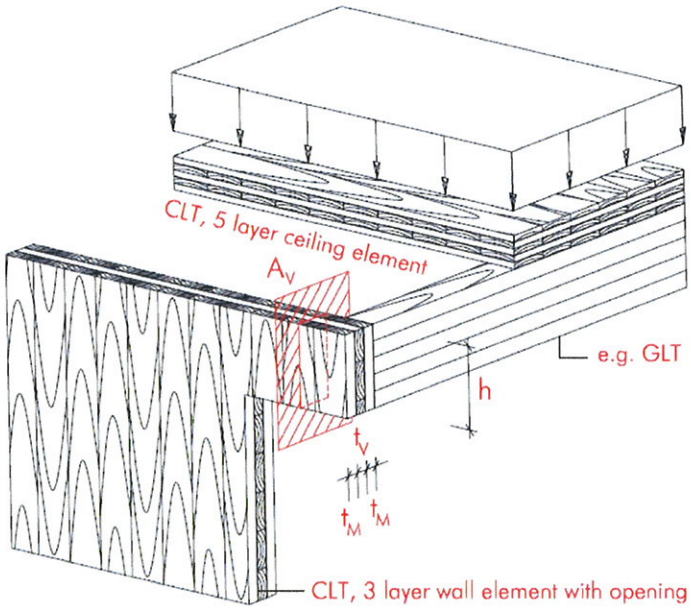

Fig. 2 Drawing of example's base

The loads from the attached slab result from the dead load of the slab with a characteristic value of g_k = 2,0 kN/m² and a characteristic life load of q_k = 3,0 kN/m². By applying the partial safety factors γ_g = 1,3 and γ_q = 1,5 a total design load of 7,1 kN/m² can be evaluated. Self weight of the CLT wall is neglected in this illustrating example.

Two additional further needed factors for the static analysis are k_{mod} and γ_M, which are assumed to be k_{mod} = 0,8 and γ_M = 1,3. The influence surface for the maximal shear force near the bearing of the CLT upstand beam can be calculated for the uniformly distributed loads, acting on the slab, and is illustrated in Tab. 1. Practically the span of the CLT upstand should be significantly small for this example, in order to ensure, that shear stresses are dominant in comparison to the bending stresses of the upstand beam.

$$F_d = A_{\max} \cdot \left(g_k \cdot \gamma_g + q_k \cdot \gamma_q\right) = f_{V,090,d} \cdot A_{V,net}$$

$$A_{\max} = \frac{f_{V,090,k} \frac{k_{\mathrm{mod}}}{\gamma_M} \cdot A_{V,net}}{\left(g_k \cdot \gamma_g + q_k \cdot \gamma_q\right)} \qquad (1)$$

Tab. 1 *Influence surface for the maximal shear force in the upstand beam of the CLT wall*

$f_{V,090,k}$	k_{mod} / γ_M	$A_{V,net} = h \cdot t_{V,net}$	$g_k \cdot \gamma_g + q_k \cdot \gamma_q$	A_{max}
[N/mm²]	[-]	[mm²]	[kN/m²]	[m²]
2,5 (acc. to [7])	0,8 / 1,3	300 · 30	2,0·1,3+3,0·1,5	1,95
5,2 (acc. to [9])	0,8 / 1,3	300 · 30	2,0·1,3+3,0·1,5	4,06

As it can easily be seen in Tab. 1, the influence surface for loads acting on the slab and thereby the load, which has to be taken over from the slab, is not extra big. If shear strength acc. to EN 338 with $f_{v,090,k}$ = 2,5 is chosen, the influence surface reaches less than 2 m². With other words the shear strength of the CLT upstand beam above the window is the limiting bearing capacity in this system and therefore the controlling verification in the static analysis.

3.2 Shear bearing mechanisms

As described in [6, chapter 2] it is assumed, that the boards are not glued together at their narrow sides. If they are glued regardless, cracks due to swelling and shrinking decomposite the CLT element in a similar structure in comparison to CLT elements without adhesive at their narrow sides of the single boards. When a CLT wall acts under shear in plane, two different mechanisms (shear bearing mechanism I in the boards and torsion-like mechanism II in the gluing interfaces) are awakened as described previous and in chapter 2.3 of [6].

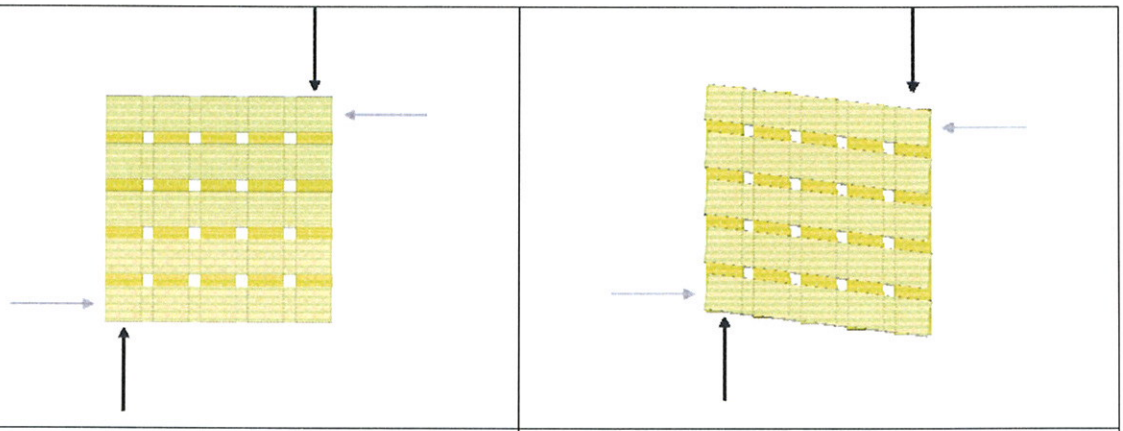

CLT element as shear field	deformed shear field

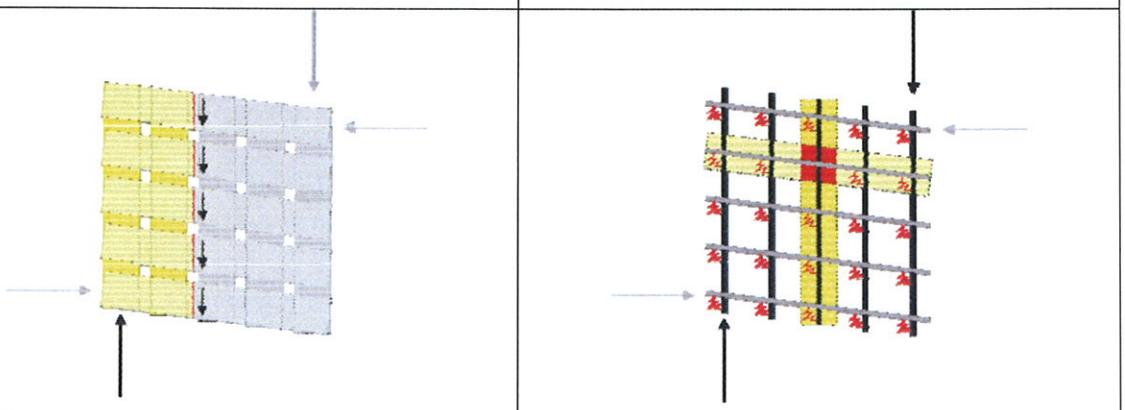

shear bearing mechanism (mechanism 1): shear bearing capacity caused by net cross section within gap of two lamellas which are not glued together	torsion-like mechanism in the gluing interfaces (mechanism 2): Vierendeel girder mechanism due to glue-surfaces (torsionfield)

Fig. 3 Cross laminated timber CLT as shear wall and it's two shear bearing mechanism

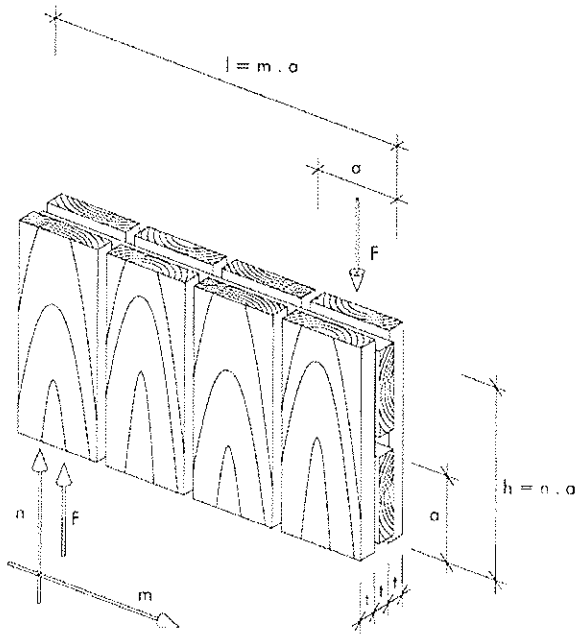

Fig. 4 Cross laminated timber element as shear field

3.3 Theoretical considerations

In the following considerations, it is assumed, that all layers of the CLT element are built up with the same sizes of boards. Therefore the geometry of the gluing interfaces between two adjacent boards is quadratic with the width a. The dominant thickness of all layer is the minimal one and described with the symbol t_v:

Mechanism I: shear bearing capacity with relevant net-area section:

$$\frac{a}{t_V} \geq 4$$

$$\tau_{V,\max} = \frac{F}{A} = \frac{F}{(k-1)\cdot t_V \cdot h} = \frac{F}{(k-1)\cdot t_V \cdot n \cdot a} = \frac{4 \cdot F}{(k-1)\cdot n \cdot a^2}$$

The shear stress distribution can be assumed to be approximately constant, if the gaps between the boards are relatively small, which is usually the normal case.

Mechanism II: torsion-like behaviour in the gluing interfaces acc. to Blaß/Görlacher [4]

$$I_p = \frac{b \cdot a^3 + a \cdot b^3}{12} = \frac{a^4}{6}$$

$$M_{total} = F \cdot l$$

$l = m \cdot a$ with m … number of glue surfaces above length

$h = n \cdot a$ with n … number of glue surfaces above height

$$M_{one} = \frac{M_{total}}{k \cdot m \cdot n} = \frac{F \cdot l}{k \cdot m \cdot n} = \frac{F \cdot m \cdot a}{k \cdot m \cdot n} = \frac{F \cdot a}{k \cdot n}$$ with k … number of gluelines above thickness

$$\tau_{M,\max} = \frac{M_{one}}{I_p} \cdot \frac{a}{2} = \frac{F \cdot a \cdot 6}{k \cdot n \cdot a^4} \cdot \frac{a}{2} = \frac{F \cdot 3}{k \cdot n \cdot a^2}$$

Subsumption

By comparison of the stresses of both mechanisms, the influence of the parameter ‚k', the geometric parameters ‚a' and ‚t_V' on the controlling mechanism and the decision, which mechanism is the limiting one, can be derived and shown.

$$\frac{\tau_{M,\max}}{\tau_{V,\max}} = \frac{\frac{F \cdot 3}{k \cdot n \cdot a^2}}{\frac{F}{(k-1) \cdot t_V \cdot n \cdot a}} = \frac{t_V}{a} \cdot \frac{3 \cdot (k-1)}{k}$$

In Fig. 5 the shear stress in the net section (mechanism I) is summarized under the assumption that the torsion-like mechanism II is fully utilized. The characteristic value of the strength for the torsion-like mechanism $f_{M,k}$ is supposed to be $f_{M,k}$ = 2,5 N/mm² [7].

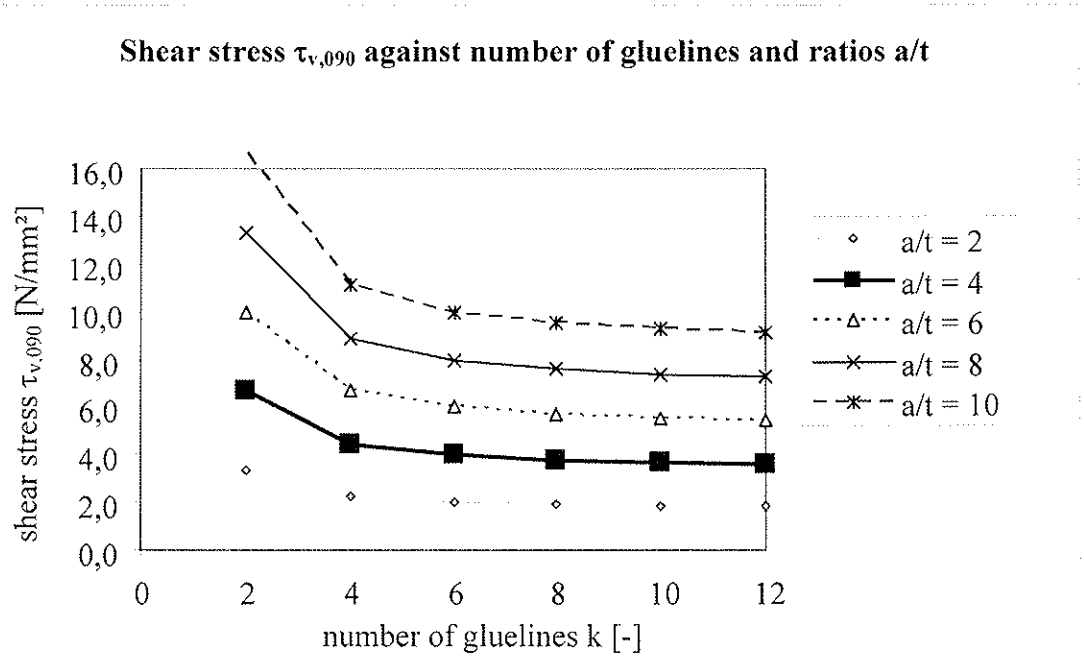

Fig. 5 Shear stress $\tau_{v,90}$ against number of gluelines k and ratios a/t

The shear stress in the net section already exceeds the shear strength $f_{V,090,k}$ = 2,5 N/mm² (C24 acc. to EN 338) for the minimal relation of board width to thickness a/t_v = 4, as it is demanded in the approvals [7] und [9]. This means, that the mechanism I is the dominating one, independently from the numbers of gluing interfaces k. When the relation a/t is steadily increased, the dominance of mechanism I is also increasing. If the shear strength $f_{V,090,k}$ is been replaced by the higher value of $f_{V,090,k}$ = 5,2 N/mm², acc. to the CUAP test configuration [8, 9], the dominant mechanism is also always the shear mechanism I for 3-

layered plates. If the CLT plate is built up with more layers, mechanism I dominates, starting from $a/t_v \geq 6$

4 Testing methods

4.1 CUAP procedure

A four-point bending test configuration acc. to EN 408 is assessed in [8] for determination of the shear strength characteristic values. All boards, oriented in direction of the beam axis, must feature a clear gap, in order to activate shear failure in the orthogonally oriented boards.

Relation of shear stress $\tau_{v,090}$ to bending stress σ_m can be detected by geometric properties of the test configuration and the cross section size.

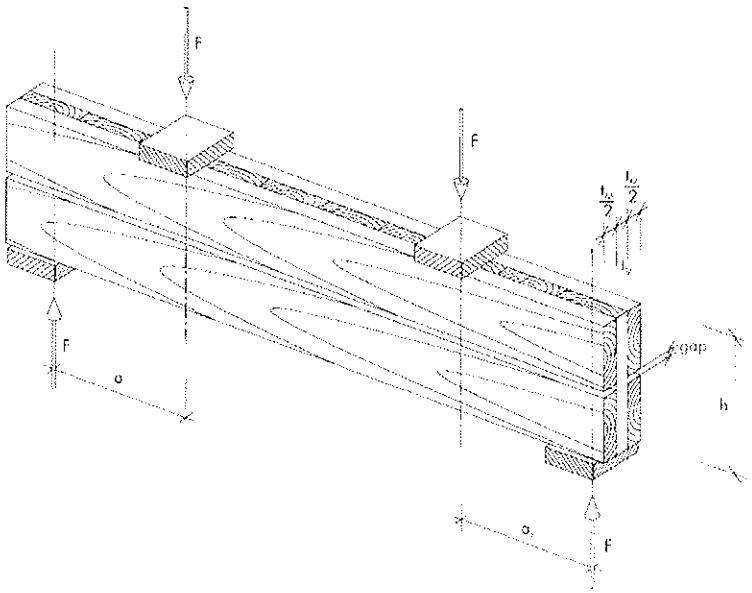

$$t = t_m + t_V$$

$$\sigma_m = \frac{M}{W_m} = \frac{a_1 \cdot F}{\frac{t_m \cdot h^2}{6}}$$

$$\tau_{V,090} = \frac{3}{2} \cdot \frac{F}{A_V} = \frac{3}{2} \cdot \frac{F}{t_V \cdot h}$$

$$\frac{\sigma_m}{\tau_V} = 4 \cdot \frac{a_1}{h} \cdot \frac{t_V}{t_m}$$

Fig. 6 *Test configuration according to [8] for getting shear values of cross laminated timber in plane*

4.2 Shear tests on symmetric test configurations

It can be realized, that the CUAP test configuration does not lead in most cases to failure due to shear fracture in those layers, oriented orthogonally to the beam axis. For this reason a alternative test configuration was developed, which should allow to determine a reliable shear strength value.

A symmetric test configuration was chosen. Therefore two relevant shear sections A_v exist. The developed test configuration is rather simple, the support conditions are also easy to realize, especially in comparison to the propagated test configuration found in EN 789. The disadvantage can be found in the fact that only one of the two shear sections can fail. This results in a underestimation of the statistical distribution function of the shear strength values.

Both shear areas are situated in a horizontal middle board. In the middle of the span of the central horizontal board two vertical boards are situated on both sides for transferring the supporting forces. Further vertical boards are located outside with a clearance of 5 mm for take-over of the external load. In order to prevent tension perpendicular to grain normal to the plain of the test configuration all vertical boards have little cuts over and under the main central horizontal board. The core of the test configuration agrees completely with the test configuration, which is used in the CUAP tests.

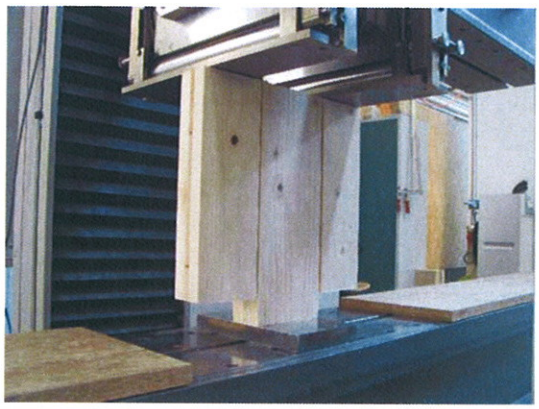

Fig. 7 Test configuration on optimized specimen

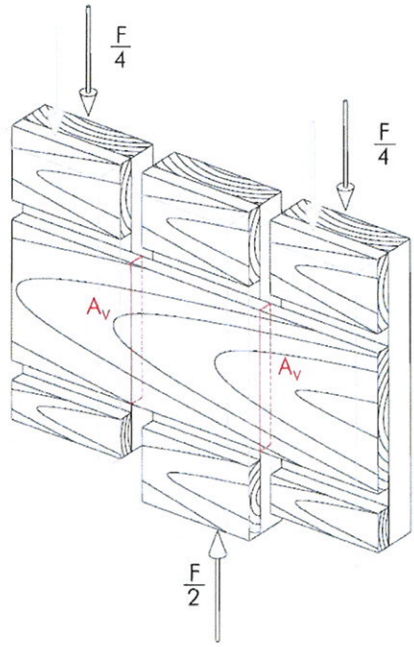

Fig. 8 Drawing of half of the optimized test specimen

5 Test results

5.1 CUAP tests

Eight series in sum 90 tests were conducted at the Graz University of Technology with the CUAP test configuration. Results are summarized in Tab. 2. The shear strength values, which can be found in this table, are actual shear stresses at the moment, when tests have failed due to bending stresses in the middle span zone, which is free of any shear stresses. None of the 90 tests has failed due to shear. In some cases secondary shear fracture has been detected as a consequence of the primary bending failure. In a few exceptions failure due to rolling shear has been detected. For these reasons, the present test procedure can be addressed as a coupled bending-shear test configuration.

Tab. 2 Results of the coupled bending-shear test configuration according to [8]

Series	1	2	3	4	5	6	7
#	16	14	10	10	10	15	15
n layers	5	3	5	5	3	3	3
$t_{i,lengthwise}$	25-25-25	50-50	32-32-32	40-40-40	40-40	37-37	32,4-32,4
$t_{i,cross}$	25-25	25	19,2-19,2	19,2-19,2	19,2	40	33,2
t_V / t_M	0,67	0,25	0,40	0,32	0,24	0,54	0,51
height h	260	300	293	293	293	400	400
a1 / h	2,5	3	3	3	3	3	3
$\sigma_{m,mean}$	59,2	34,9	37,3	34,3	31,0	35,5	39,9
$\tau_{v,090,mean}$	8,88	11,5	7,77	8,93	10,8	5,43	6,50
COV	13,0%	3,6%	14,3%	11,4%	11,7%	15,0%	15,7%

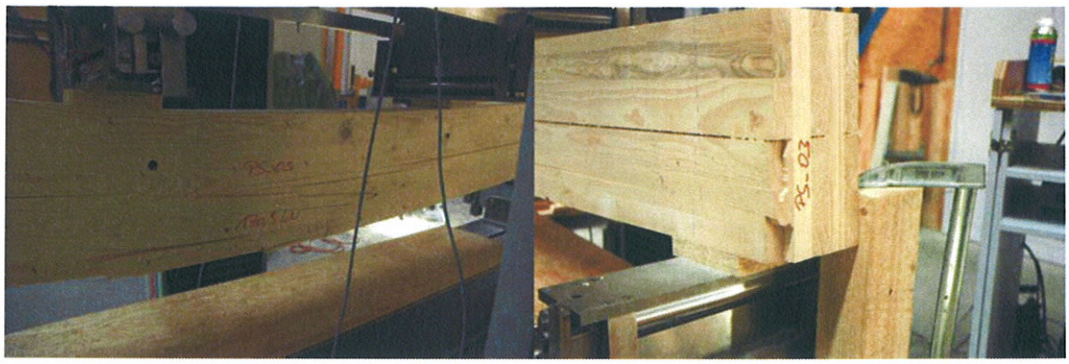

Fig. 9 Tensile failure in bending zone with local shear failure in tensile lamella in area of glue line.

5.2 Shear tests on symmetric shear block

20 shear tests were carried out at the Graz University of Technology with a symmetric test configuration and two shear areas, as already mentioned in 4.2, in order to get a reliable shear strength value for CLT under shear in plane.

The observed load – displacement curves are illustrated in Fig. 10. When reaching the distinct maximum, all test samples failed due to shear failure in one of the both shear areas A_V. Afterwards large deformations can be detected. After some loss of the bearable shear force, an almost horizontal plateau is adjusted due to the activated tension field of the fibres under large deformations.

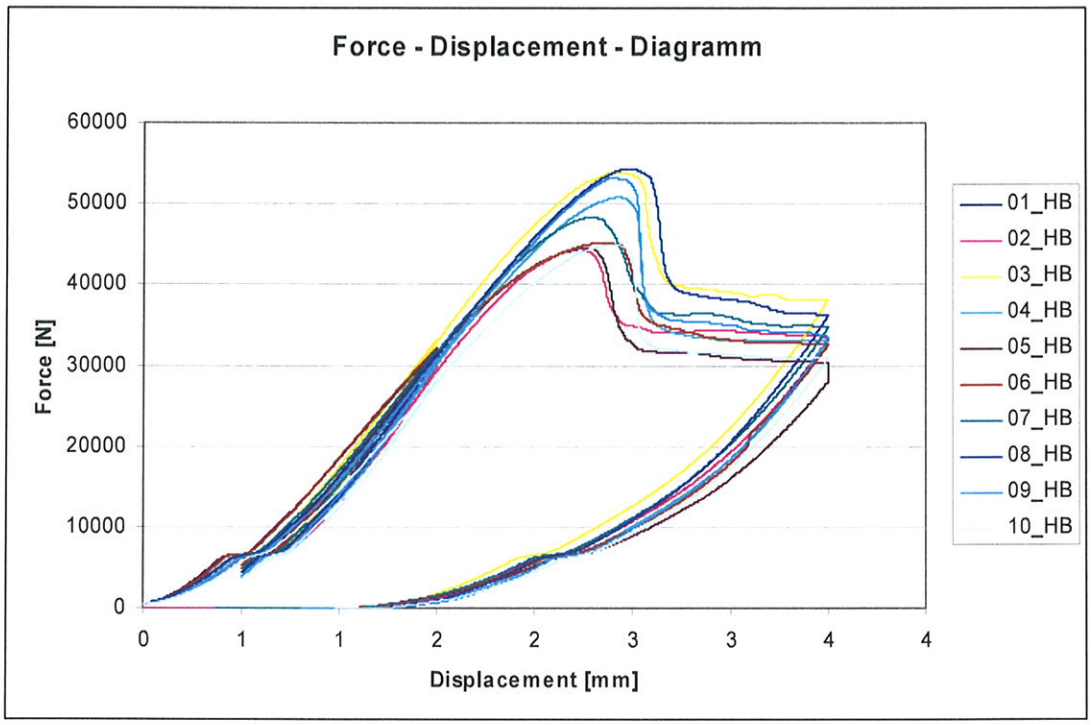

Fig. 10 Force – Displacement – Diagram of shear field-tests ‚TUG'

Fig. 11 Shear failure at the new developed symmetric shear block – serie 'TUG'

The shear stresses are assumed to be constant over the shear area A_V. All 20 tests deliver a mean value of 12,8 N/mm² and a coefficient of variation (COV) of 11,3 %. With these two values a 5%-Quantile value of 10,3 N/mm² up to 10,6 N/mm² can be determined, depending on the chosen statistical distribution function. All results are summarized in Tab. 3.

Tab. 3 Results of series ‚TUG'

Series	TUG
#	20
Height h [mm]	200
Thickness t [mm]	10
Mean value [N/mm²]	12,8
Standard deviation [N/mm²]	1,45
COV [%]	11,3%
5% - Quantile normal distribution [N/mm²]	10,4
5% - Quantile log normal distribution [N/mm²]	10,6
k_s	1,926
5% - Quantile EN 14358 [N/mm²]	10,3

6 Discussion of results

Comparison to the CUAP procedure

It was not possible, to establish a shear strength value with the test configuration according to [8], because bending failures are observed in almost all tests. Sporadically shear failure can also be detected, but only on the lamellas, which are oriented parallel to the beam axis, but not in the shear area, which should be taken for the scheduled shear verification. Numerical shear strength values, which are lower than the real shear strength values at the moment of bending failure can be established with a mean value of up to 11,6 N/mm² and a COV value of about 11 % to 16 % , which leads to significantly higher 5% quantile values than those of EN 338 (e.g. $f_{v,090,k} = 2,5$ for C24).

Shear failure was detectable at 20 tests with an optimized test configuration ‚TUG'. Due to the symmetry of the test configuration, failure occurred only in the weaker shear area A_v. Mean value of 12,8 N/mm² is only little higher than the analogous value of the CUAP procedure.

Comparison to plywood plate strength values

As already pointed out in [6] a higher shear strength value can be argued with the "strain-locking-effect" of the present structure. A comparison can be set up to the softwood-plywood plate with shear strength values of $f_{v,090,k} = 5$ N/mm² for a three layered plate and $f_{v,090,k} = 8$ N/mm² for five and more layers. Starting the argumentation in a similar way with ideal width of the single layers, the same mechanical model can be applied to the softwood-plywood plate. The shear verification should be carried out with appropriate net areas and adapted shear strength values to the net area concept. Shear strength values of $f_{v,090,k} = 5 \cdot 3 = 15$ N/mm² for a three layered plywood plate and $f_{v,090,k} = 8 \cdot 2 = 16$ N/mm² for a multi layered plywood plate can be derived on this concept. The shear strength value

is about 50% higher than the comparable value on basis on the here introduced test configuration 'TUG'. If the comparison is even acceptable, has still to be checked in further investigations.

Mechanically improved stress evaluation

The theoretical consideration in 3.3, regarding the shear stresses of mechanism I, has the drawback, that the duality of shear stresses and the boundary effect is not meet with this formula. An alternative, mechanically more consistent formulation could be the verification of stresses, acting on a Representative Sub-Volume Element (RVSE), as presented in [6] and [10].

Further research to be done

Still open questions are summarized in the following:

- The limits of the relations a/t should be checked; within the previous assumptions are still valid.
- Investigation about increased width of the gaps: What is the influence on the "strain-locking-effect" due to the orthogonality of the structure.
- Comparison of verification, presented in chap. 3 with an alternative one, introduced in [6] and [10]. Exploration of the limits of both procedures in respect to strong different thicknesses of the single layers.

7 Summary

The determination of the shear strength for CLT in plane is not possible with the procedure acc. to [8]. The technical shear strength values (term see chap.7 of [6]) supply significantly higher values than established in EN 338 and in [9]. A shear failure was detected in all 20 tests with an optimized test configuration. The mean value has been identified with 12,8 N/mm² and the COV value with 11,3 %. Depending on the statistical distribution function, a 5% quantile value between $f_{v,090,CLT,k}$ = 10,3 N/mm² and 10,6 N/mm² can de derived. Comparable shear strength values of softwood plywood plates are about 50% higher than the strength value on basis of these 20 tests. Geometric parameters like the a/t relation or the gap between two boards in one layer have to be further studied in future research.

Acknowledgement

The research work within the project COMET 1.1.2 is financed by the competence centre holz.bau forschungs gmbh and performed in collaboration with the Institute for Timber Engineering and Wood Technology of the Graz University of Technology and the partners from industry HMS Bausysteme and HAAS Fertigbau.
The project is fostered through the funds of the Federal Ministry of Economics and Labour, the Federal Ministry of Transport, Innovation and Technology, the Styrian Business Promotion Agency Association and the province of Styria.

References

[1] Bosl R.: Zum Nachweis des Trag- und Verformungsverhaltens von Wandscheiben aus Brettsperrholz, Institut for structural engineering, Military University Munich, January 2002.

[2] Jeitler G.: Versuchstechnische Ermittlung der Verdrehungskenngrößen von orthogonal verklebten Brettlamellen, Institute for Steel, Timber and Shell Structure, Graz University of Technology, January 2004.

[3] Wallner G.: Versuchstechnische Ermittlung der Verschiebungskenngr¨oßen von orthogonal verklebten Brettlamellen, Institute for Steel, Timber and Shell Structure, Graz University of Technology, January 2004.

[4] Görlacher R., Blaß H. J.: Bauen mit Holz, Edition 12/2002.

[5] Dujic,B.; Klobcar,S.; Zarnic,R.; Influence of openings on shear capacity of wooden walls, Proceedings of CIB W18/40-15-6, Bled, Slovenia, 2007

[6] Bogensperger, Th., Moosbrugger, Th., Schickhofer, G.: New test configuration for CLT-wall-elements under shear load, Proceedings of CIB W18/40-21-2, Bled, Slovenia, 2007

[7] EOTA: ETA-06/0009, Binder Brettsperrholz BBS, Multilayered timberelements for walls, ceilings and special construction components, 2006

[8] CUAP Common Understanding of Assessment Procedure: Solid wood slab element to be used as a structural element in buildings, ETA request No 03.04/06, prepared by "OIB Österreichisches Institut für Bautechnik", Schenkenstraße 4, 1010 Wien, Austria, June 2005.

[9] EOTA: ETA-06/0138, KLH solid wood slabs, Solid wood slab element to be used as structural elements in buildings, 2006

[10] Bogensperger, Th.: A contribution to the characteristic shear strength of a CLT wall under shear, Presentation at 3nd Workshop of COST E55 action in Espoo/Finland, 2008.

INTERNATIONAL COUNCIL FOR RESEARCH AND INNOVATION
IN BUILDING AND CONSTRUCTION

WORKING COMMISSION W18 - TIMBER STRUCTURES

STRENGTH OF GLULAM BEAMS WITH HOLES – TESTS OF QUADRATIC HOLES AND LITERATURE TEST RESULTS COMPILATION

H Danielsson
P J Gustafsson
Division of Structural Mechanics, Lund University

SWEDEN

Presented by H. Danielsson

H. Blass received confirmation that the definition of failure was the occurrence of crack propagation. He asked why maximum load out of the test was not used. H Danielsson said that when crack propagation occurred in general the load was close to maximum and later on bending failure occurred. T. Williamson said that this is a common problem in N. America. Test just completed in APA with circular hole put in high shear area near end of the beam. H Danielsson explained that test set up No.2 took this into consideration although the crack propagation stopped as the hole was further from the end. R. Steiger asked what was the characteristic value of shear strength used in the analysis. H Danielsson said it was 3.8 MPa according to 1990 reference. R. Steiger stated that the 3.8 MPa has been reduced in recent code change and revise the paper to clarify the information. J. Köhler said that code results come from model and comparison with the model in the paper may not be totally appropriate. A. Buchanan received further clarification about whether load increase was observed when crack propagation stopped. H. Danielsson said that a small increase of 5 to 20% in general was observed. A. Buchanan and H. Danielsson further discussed the geometry of the hole with rounded corner and comparison with circular hole and relative comparison in terms of radius of the hole and the rounded corner. F. Lam commented the drying during service can cause cracks in beams in service which can further influence results. B.J. Yeh stated that the location of hole has a strong influence on the results and asked whether this aspect has been studied. H. Danielsson said that this has not been studied in detail. S. Aicher stated that when moving the hole to the end, compression stress may be introduced which could reinforce the beam in shear mode thus increasing capacity. B.J. Yeh stated that this is different from US observations.

Strength of Glulam Beams with Holes – Tests of Quadratic Holes and Literature Test Result Compilation

Henrik Danielsson and Per Johan Gustafsson

Division of Structural Mechanics, Lund University, Sweden

1 Background

Looking at design recommendations for glulam beams with holes in European timber engineering codes over the last decades, it can be seen that the strength design has been treated in many different ways. The theoretical backgrounds on which the recommendations are based shows fundamental differences and there are major discrepancies between the strength estimations according to the different codes as well as between tests and estimations according to codes [5]. The contemporary version of Eurocode 5 [7] does not state any equations concerning design of glulam beams with holes and the recommendations in the German code DIN 1052 [3] concerning rectangular holes were withdrawn during the fall of 2007. The absence of design recommendations indicates a need for further investigations of the subject. There are, however, several tests found in the literature concerning the strength of glulam beams with holes. Two of the most recent and more comprehensive studies were presented by Höfflin in 2005 [10] and by Aicher and Höfflin in 2006 [1]. These studies dealt exclusively with beams with circular holes. Although the test results found in literature all in all represent much work, important parameters such as mode of loading, beam size and hole placement have often been varied only within a very limit range. Among other limitations, it seems that all available test results relate to glulam beams with holes that are centrically placed with respect to the beam height [5].

2 Strength tests of glulam beams with quadratic holes

2.1 Test series and test setups

Experimental tests of the strength of glulam beams with quadratic holes have been carried out at the Division of Structural Mechanics at Lund University and they are in detail reported in [6]. The study comprised investigations of four design variables: *bending moment to shear force ratio at hole center*, *material strength class*, *beam size effect* and the previously overlooked design variable of *hole placement with respect to beam height*. Two different test setups were used to investigate the influence of bending moment to shear force ratio. Three different hole placements were used for one of the test setups to investigate the influence of hole placement with respect to beam height. The size effect was investigated for each combination of test setup and hole placement by using two test series with a scale factor of 3.5 for the length and height dimensions while the width was kept constant. All holes had rounded corners and a side length equal to 1/3 of the beam height. Altogether, the study consists of nine separate test series with four nominally equal tests in each series according to Table 1 and Figure 1.

Table 1: *Description of test series.*

Test series	Number of tests	Test setup	Hole placement	Strength class type	Beam size $T \times H$ [mm]	Hole size $a \times b$ [mm]	r [mm]
AMh	4	1	Middle	homogeneous	115 × 630	210 × 210	25
AMc	4	1	Middle	combined	115 × 630	210 × 210	25
AUh	4	1	Upper	homogeneous	115 × 630	210 × 210	25
ALh	4	1	Lower	homogeneous	115 × 630	210 × 210	25
BMh	4	2	Middle	homogeneous	115 × 630	210 × 210	25
CMh	4	1	Middle	homogeneous	115 × 180	60 × 60	7
CUh	4	1	Upper	homogeneous	115 × 180	60 × 60	7
CLh	4	1	Lower	homogeneous	115 × 180	60 × 60	7
DMh	4	2	Middle	homogeneous	115 × 180	60 × 60	7

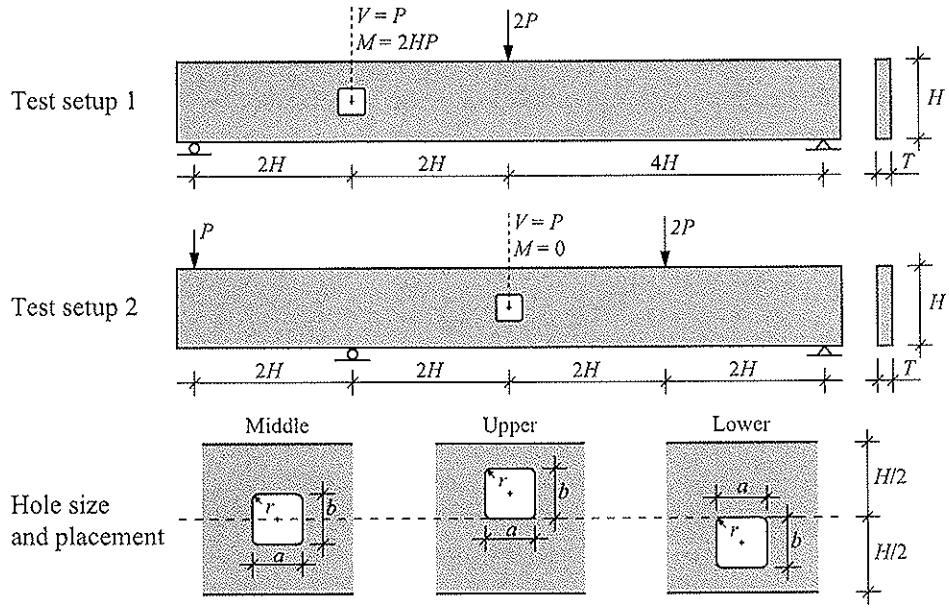

Figure 1: *Test setups and hole placements.*

2.2 Materials

The beams were all made of spruce (Lat. *Picea Abies*) and glued with melamine-urea-formaldehyde (MUF) resin. The lamella thickness was consistently 45 mm. All beams except the beams of test series AMc were of strength class homogeneous glulam. The strength class combined beams of test series AMc were composed of lamination strength class LS22 in the three outmost lamellae on each side and of lamination strength class LS15 in the remaining eight lamellae. The strength class homogeneous glulam beams were composed of lamination strength class LS22 throughout the entire beam height. The requirements on the two lamination strength classes are stated in [15] as: characteristic tensile strength, 14.5 and 22 MPa; mean tensile Young's modulus, 11 000 and 13 000 MPa and density (5^{th} percentile), 350 and 390 kg/m^3 for LS15 and LS22, respectively. The homogeneous beams correspond to the requirements in SS-EN 1194 [16] for glulam strength class GL 32h. The strength class combined beams correspond to the Swedish strength class L40. The mean value of the moisture content at the time of testing was measured to 11.7 % and the mean densities for the two different lamination strength classes was measured to 444 kg/m^3 and 469 kg/m^3 for LS15 and LS22, respectively.

2.3 Test Results

Three different load levels are used to present and compare the test results according to the definitions in Figure 2. The test results are presented in Figure 3 and in Table 2. The crack initiation shear force V_{c0} is only given in the cases when there was a visually observable crack in the cross section before there was a crack spreading across the entire beam width at the given corner. The crack shear force V_c is given for both corner B and corner T for all tests. The maximum shear force V_f is not given for test series BMh and DMh since the test setup for these test series is such that this load level is irrelevant.

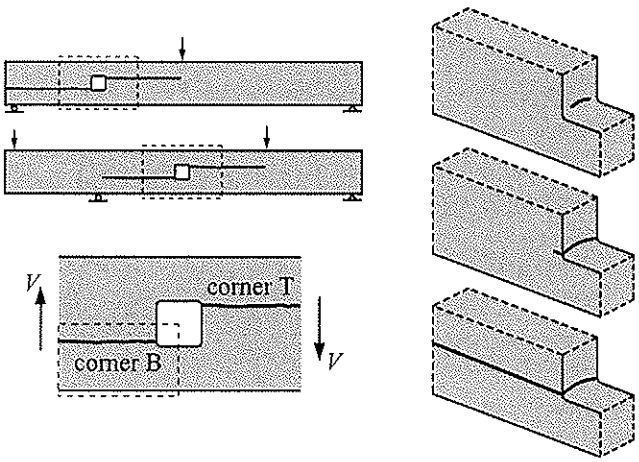

Crack initiation shear force V_{c0}
Shear force at first crack development visually observable by the naked eye.

Crack shear force V_c
Shear force at the instant of crack development across the entire beam width.

Maximum shear force V_f
Shear force at instant of either a sudden crack propagation or a step-wise stable/unstable crack growth to the end of the beam.

Figure 2: *Definitions and illustrations of load levels.*

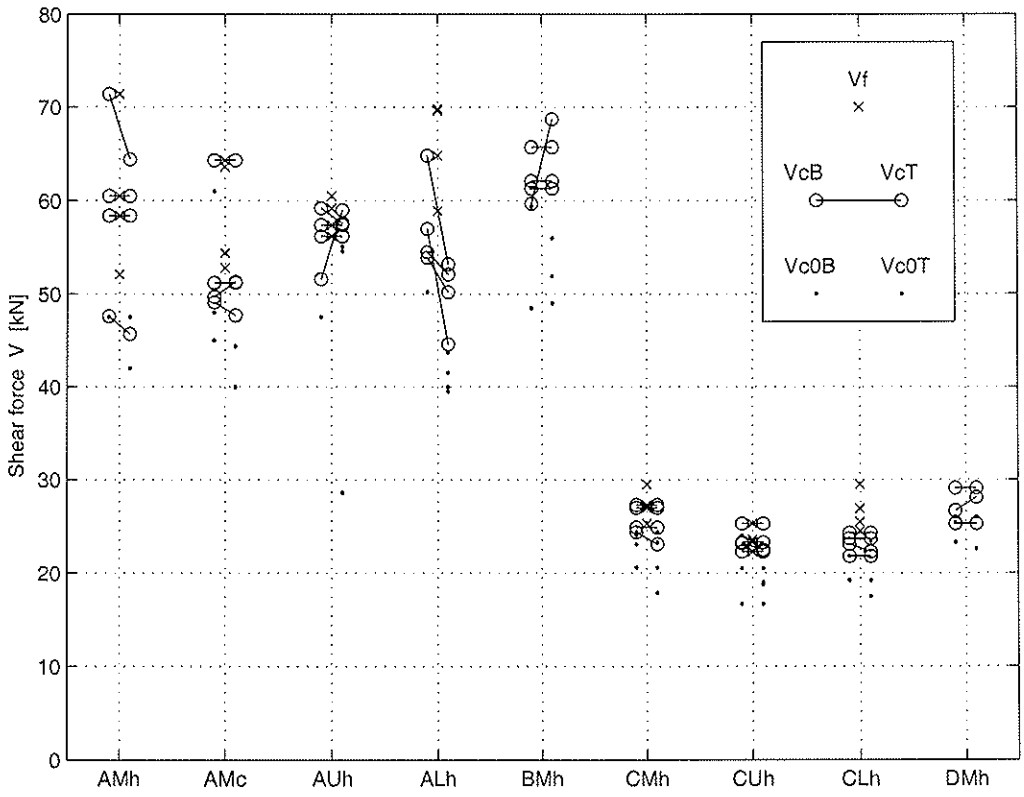

Figure 3: *Shear forces V for the three load levels and all tests in all nine test series.*

Table 2: *Beam cross section, hole size, hole placement, bending moment to shear force ratio and test results for the three defined load levels for all tests in all nine test series.*

Test series	$T \times H$ [mm]	$a \times b$ [mm]	r [mm]	hole placement	$\frac{M}{VH}$ [-]		V_{c0} V_{c0B} [kN]	V_{c0T} [kN]	min [kN]	V_c V_{cB} [kN]	V_{cT} [kN]	min [kN]	V_f [kN]
AMh	115 × 630	210 × 210	25	middle	2.0	1				47.6	45.7	45.7	52.1
						2	47.5	47.5	47.5	71.4	64.4	64.4	71.4
						3		42.0	42.0	58.4	58.4	58.4	58.4
						4				60.5	60.5	60.5	60.5
						mean			44.8			57.3	60.6
						(std)			(3.9)			(8.1)	(8.0)
AMc	115 × 630	210 × 210	25	middle	2.0	1	61.0		61.0	64.3	64.3	64.3	64.3
						2	48.0	44.4	44.4	49.7	51.3	49.7	63.6
						3	45.0	40.0	40.0	51.2	51.2	51.2	52.8
						4				49.1	47.7	47.7	54.4
						mean			48.5			53.2	58.8
						(std)			(11.1)			(7.5)	(6.0)
AUh	115 × 630	210 × 210	25	upper	2.0	1		28.6	28.6	59.2	57.6	57.6	59.2
						2				51.6	59.0	51.6	60.5
						3		55.1	55.1	56.2	56.2	56.2	56.2
						4	47.5	54.6	47.5	57.4	57.4	57.4	57.4
						mean			43.7			55.7	58.3
						(std)			(13.6)			(2.8)	(1.9)
ALh	115 × 630	210 × 210	25	lower	2.0	1	50.2	41.5	41.5	53.9	50.2	50.2	58.9
						2		43.7	43.7	54.5	52.1	52.1	69.6
						3		40.0	40.0	64.8	53.2	53.2	64.8
						4		39.5	39.5	57.0	44.6	44.6	69.8
						mean			41.2			50.0	65.8
						(std)			(1.9)			(3.8)	(5.1)
BMh	115 × 630	210 × 210	25	middle	0.0	1		51.9	51.9	61.3	61.3	61.3	-
						2	59.4	49.0	49.0	65.7	65.7	65.7	-
						3	61.4	56.0	56.0	62.1	62.1	62.1	-
						4	48.5		48.5	59.7	68.7	59.7	-
						mean			51.4			62.2	
						(std)			(3.4)			(2.5)	
CMh	115 × 180	60 × 60	7	middle	2.0	1	20.6	20.6	20.6	27.3	27.3	27.3	27.3
						2	24.1	23.3	23.3	24.9	24.9	24.9	29.5
						3	23.1	17.9	17.9	24.4	23.1	23.1	25.3
						4	24.4	24.4	24.4	27.0	27.0	27.0	27.0
						mean			21.6			25.6	27.3
						(std)			(2.9)			(2.0)	(1.7)
CUh	115 × 180	60 × 60	7	upper	2.0	1	24.0	18.8	18.8	25.3	25.3	25.3	25.3
						2		19.0	19.0	23.2	22.5	22.5	25.3
						3	20.5	20.5	20.5	23.3	23.3	23.3	23.3
						4	16.7	16.7	16.7	22.3	22.3	22.3	22.3
						mean			18.8			23.4	23.6
						(std)			(1.6)			(1.4)	(2.2)
CLh	115 × 180	60 × 60	7	lower	2.0	1		17.5	17.5	23.1	22.3	22.3	26.9
						2	19.2	19.2	19.2	23.7	23.7	23.7	29.5
						3	21.8	23.4	21.8	24.3	24.3	24.3	25.5
						4				21.8	21.8	21.8	24.5
						mean			19.5			23.0	26.6
						(std)			(2.2)			(1.2)	(2.2)
DMh	115 × 180	60 × 60	7	middle	0.0	1	26.0	26.0	26.0	29.1	29.1	29.1	-
						2				25.3	25.3	25.3	-
						3	23.3		23.3	25.3	25.3	25.3	-
						4	25.4	22.6	22.6	26.7	28.1	26.7	-
						mean			24.0			26.6	
						(std)			(1.8)			(1.8)	

2.4 Comments concerning test results

The scatter in the strength between nominally equal tests within a test series is not very large, the coefficient of variation of $V_{c,min}$ being from 4 % to 14 % with an average of 8 %. The test results furthermore show that it was more frequent with crack development across the entire beam width at the upper corner T before the lower corner B than the other way around. The most frequent scenario was, however, that cracks developed simultaneously at both corners. The most common place for crack initiation was in the middle of the beam width although some tests showed a crack initiation all the way to one side of the beam width. Some further comments on the test results concerning the influence of the four investigated design parameters are listed below. When nothing else is stated, the crack shear force V_c refers to the minimum of V_{cB} and V_{cT}.

Bending moment to shear force ratio: For beams with centrically placed holes, two different bending moment to shear force ratios were investigated. The beams with holes placed in a position of zero bending moment (test series BMh and DMh) shows on average slightly higher (approximately 5-10 % considering mean values) crack shear forces V_c compared to the beams with holes placed in a position of combined bending moment and shear force (test series AMh and CMh).

Material Strength Class: There was no significant difference in the behavior between the material strength class homogeneous beams of test series AMh and the strength class combined beams of test series AMc. The results of these two test series are, however, comparatively scattered.

Beam size: The test results indicate a strong beam size effect on the strength. Increasing the beam size by a factor 3.5 gave about 30-35 % reduction in nominal shear stress V_c/A_{net}.

Hole placement with respect to beam height: Slightly lower (approximately 5-15 % considering mean values) crack shear forces V_c were found for the beams with eccentrically placed holes compared to the beams with centrically placed holes. There is furthermore another interesting difference concerning the beams with eccentrically placed holes. Both among the large and the small beams the tests generally showed a more sudden crack propagation all the way to the end of beam for the beams with the hole placed in the upper part of the beam (test series AUh and CUh) compared to the beams with the hole placed in the lower part of the beam (test series ALh and CLh).

3 Previous tests of glulam beams with holes

3.1 Compilation of test results in literature

A compilation of previously performed tests of glulam beams with holes from various sources is presented in Table 3. The tests are described concerning beam cross section, hole design, bending moment to shear force ratio, number of tests and results corresponding to the three load levels defined in Figure 2. All holes were centrically placed with respect to beam height. Load levels V_{c0} and V_c refers to the minimum of the values for the two corners, if values for both corners are given in the original source. A more comprehensive compilation including further details such as material strength class, moisture content, how well the definition of load levels correspond with the ones found in the original sources, etc. is found in [5].

Table 3: *Compilation of test results of glulam beams with holes. n = number of tests.*

Reference	$T \times H$	□ : $a \times b$ ○ : ϕ	r	$\frac{M}{VH}$	n	V_{c0} mean	V_{c0} (std)	V_c mean	V_c (std)	V_f mean	V_f (std)
	[mm]	[mm]		[-]	[-]	[kN]	[kN]	[kN]	[kN]	[kN]	[kN]
Bengtsson & Dahl [2]	90 × 500	300 × 150	0	1.20	2					39.0	(0.3)
	90 × 500	200 × 100	0	1.20	2					49.6	(1.1)
Kolb & Frech [12]	80 × 550	250 × 250	?	0.91	2					32.7	(2.1)
	80 × 550	250 × 150	?	0.91	2					44.0	(2.8)
	80 × 550	250 × 250	?	1.82	2					33.8	(1.1)
	80 × 550	250 × 150	?	1.82	2					35.4	(4.0)
Penttala [13]	90 × 500	200 × 200	?	1.60	1					33.8	
	90 × 500	400 × 200	?	1.60	1	25.0				31.3	
	90 × 500	600 × 200	?	1.60	1	20.8				30.0	
	115 × 800	400 × 200	?	1.25	1					69.1	
	115 × 800	200 × 200	?	1.25	1	52.5				84.4	
Johannesson [11]	90 × 500	250 × 250	25	1.30	2			26.8	(0.5)	28.5	(2.8)
	90 × 500	250 × 250	25	2.80	2			22.2	(2.3)	25.6	(0.6)
	140 × 400	600 × 200	25	2.25	1			30.0		37.0	
	88 × 495	125 × 125	25	2.53	4			40.4	(11.1)		
	88 × 495	375 × 125	25	2.53	4			37.7	(6.4)		
	88 × 495	370 × 370	25	2.53	4			9.1	(2.1)		
	88 × 495	735 × 245	25	2.53	4			12.8	(1.1)		
	88 × 495	1100 × 370	25	2.53	4			4.2	(0.3)		
Pizio [14]	120 × 400	180 × 180	0	1.05	2	24.1	(12.4)	30.6	(3.1)	63.7	(4.6)
	120 × 400	180 × 90	0	1.05	2	37.2	(15.4)	54.9	(3.4)	75.5	(1.6)
	120 × 400	180 × 10	0	1.05	2	92.5	(26.3)	103.3	(14.8)	103.3	(14.8)
	120 × 400	180 × 90	0	1.05	1	56.6		71.0		84.5	
	120 × 400	180 × 10	0	1.05	1	110.1		110.1		110.1	
	120 × 400	360 × 180	0	1.75	2	21.7	(2.3)	23.3	(0.0)	24.8	(2.1)
	120 × 400	10 × 180	0	1.75	1	34.0		34.0		34.0	
	120 × 400	360 × 180	0	1.75	1	19.2		21.1		28.8	
	120 × 400	10 × 180	0	1.75	2	30.0	(1.1)	33.8	(0.0)	33.8	(0.0)
	120 × 400	180 × 90	0	1.75	3	45.8	(11.2)	54.2	(7.0)	54.2	(0.7)
	120 × 400	180 × 180	0	1.05	2	20.6	(4.9)	26.8	(3.8)	70.0	(11.2)
Hallström [9]	90 × 315	400 × 150	25	2.78	5			11.9	(1.5)		
	90 × 315	400 × 150	0	2.78	5			12.2	(1.1)		
	90 × 315	400 × 150	25	2.78	5			12.2	(0.5)		
	90 × 315	400 × 150	25	?	1			12.2			
	165 × 585	600 × 295	25	?	4			27.1	(1.9)		
Bengtsson & Dahl [2]	90 × 500	ϕ250		1.20	2					38.4	(1.2)
	90 × 500	ϕ150		1.20	1					52.5	
Penttala [13]	90 × 500	ϕ255		1.20	1					33.8	
	90 × 500	ϕ250		2.10	1					31.6	
	90 × 500	ϕ150		1.20	1					51.3	
	115 × 800	ϕ400		1.03	1	57.1				65.9	
	115 × 800	ϕ300		2.00	1					89.5	
Johannesson [11]	90 × 500	ϕ250		1.30	2			29.6	(5.4)	36.5	(4.3)
	90 × 500	ϕ250		2.80	2			33.2	(2.6)	37.5	(3.5)
	90 × 500	ϕ250		0.60	2			33.8	(7.1)	41.7	(4.1)
	90 × 500	ϕ125		0.60	2			-		40.1	(0.1)
	88 × 495	ϕ125		2.53	4			51.9	(4.6)		
	88 × 495	ϕ396		2.53	4			16.1	(1.5)		
Hallström [9]	90 × 315	ϕ150		2.78	5			24.5	(3.5)		
Höfflin H1	120 × 900	ϕ180		1.50	5	69.2	(23.2)	106.4	(27.8)	128.1	(19.2)
[10] H2	120 × 900	ϕ270		1.50	6	65.3	(22.1)	96.4	(11.7)	108.7	(6.7)
H3	120 × 900	ϕ360		1.50	5	48.0	(8.4)	69.2	(9.0)	88.6	(15.6)
H4	120 × 900	ϕ270		5.00	5	43.1	(8.3)	55.1	(8.6)	84.2	(18.0)
H5	120 × 450	ϕ90		1.50	5	62.8	(15.6)	76.8	(13.8)	82.1	(7.6)
H6	120 × 450	ϕ135		1.50	6	38.8	(6.0)	65.5	(7.6)	67.9	(7.0)
H7	120 × 450	ϕ180		1.50	4	34.6	(7.4)	47.6	(8.5)	51.8	(5.9)
H8	120 × 450	ϕ135		5.00	5	34.7	(18.2)	58.0	(7.1)	63.4	(6.5)
Aicher & Höfflin A1	120 × 900	ϕ180		5.00	4	66.4	(21.5)	106.4	(15.0)	111.6	(13.1)
[1] A2	120 × 900	ϕ360		5.00	5	46.7	(15.3)	61.6	(15.0)	79.9	(3.2)
A3	120 × 450	ϕ180		5.00	6	42.4	(9.6)	48.8	(7.7)	53.7	(8.0)
	120 × 450*	ϕ180		5.00	3	15.4	(3.1)	37.9	(6.8)	44.8	(2.5)
	120 × 900*	ϕ360		5.00	3	33.5	(13.6)	49.6	(17.4)	66.6	(6.9)

* = curved beam, radius of curvature = $H/0.03$

3.2 Influence of bending moment to shear force ratio

Figure 4 illustrates the influence of the bending moment to shear force ratio on the strength. The results indicate a only a small influence of the bending moment on the crack shear force V_c. There is however one exception: The test series with $T \times H = 120 \times 900$ mm^2 and $\phi = 270$ mm shows a 43 % reduction in the crack shear force V_c for $M/(VH) = 5.0$ compared to $M/(VH) = 1.5$. It is worth pointing out that the mean value of the crack shear force is lower for the test series with $T \times H = 120 \times 900$ mm^2, $M/(VH) = 5.0$ and $\phi = 270$ mm than it is for the test series with equal cross section and bending moment to shear force ratio but with a larger hole, $\phi = 360$ mm, as can be seen in Figure 4 and in Table 3.

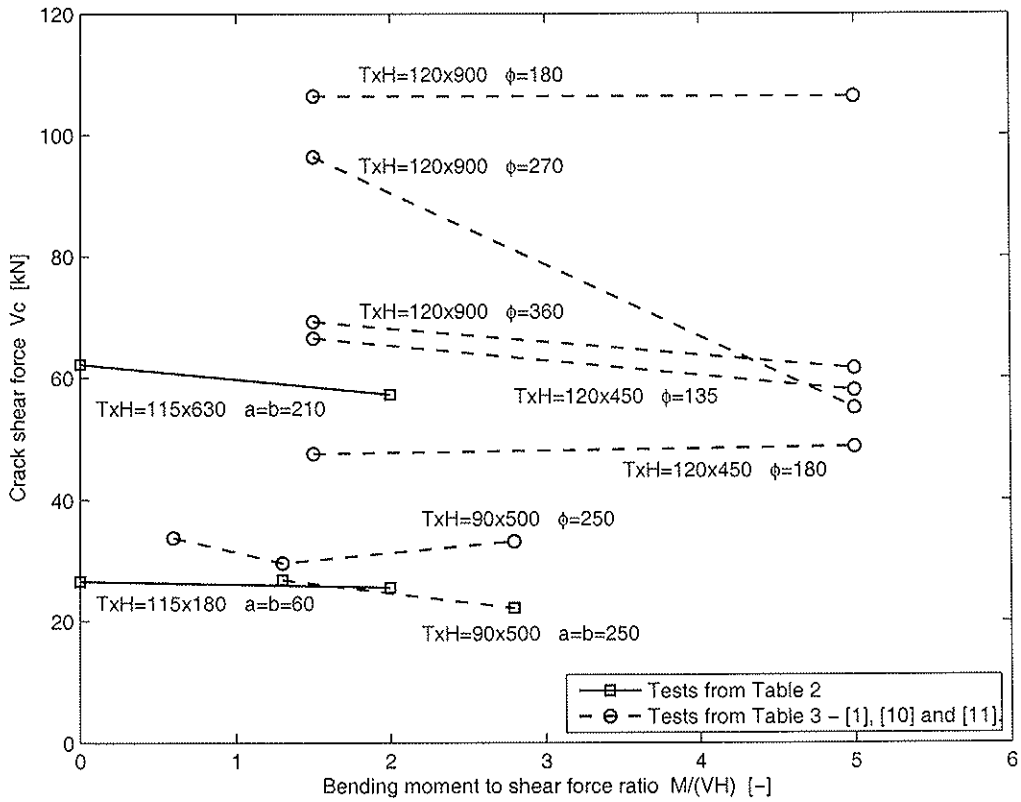

Figure 4: *Influence on strength of bending moment to shear force ratio for nominally equal tests concerning beam cross section, material strength class, hole size and hole placement.*

3.3 Influence of beam size

The present tests of glulam beams with quadratic holes indicated a strong beam size effect. Figure 5 shows the test series mean of the nominal shear stress V_c/A_{net} vs. beam height H for these tests and tests presented in [1] and [10]. Test results connected with lines represent test series which are equal concerning bending moment to shear force ratio, material strength class, beam width and hole size to beam height ratio but with different beam height H. The beam size effect can be expressed according to $V_c/A_{net} \sim H^{-m}$ where the parameter m describing the beam size effect can be determined from two test series of different size scale. The values of m are for the nine pair of test series given in Figure 5. It can be seen that the tests from [1] and [10] and relating to circular holes indicate a stronger beam size effect than the tests relating to quadratic holes presented in Section 2. The value of the parameter

$m = 1.07$ for test series with $M/(VH) = 5.0$ and $\phi = 0.3H$ is substantially higher than the value for the other eight pair of test series. This deviating result is due to the test series with $T \times H = 120 \times 900$ mm^2, $M/(VH) = 5.0$ and $\phi = 270$ mm. The result of that series gave also the deviating result with respect to influence of bending moment according to Figure 4 and showed lower strength than the corresponding beam with a larger hole, $\phi = 360$ mm.

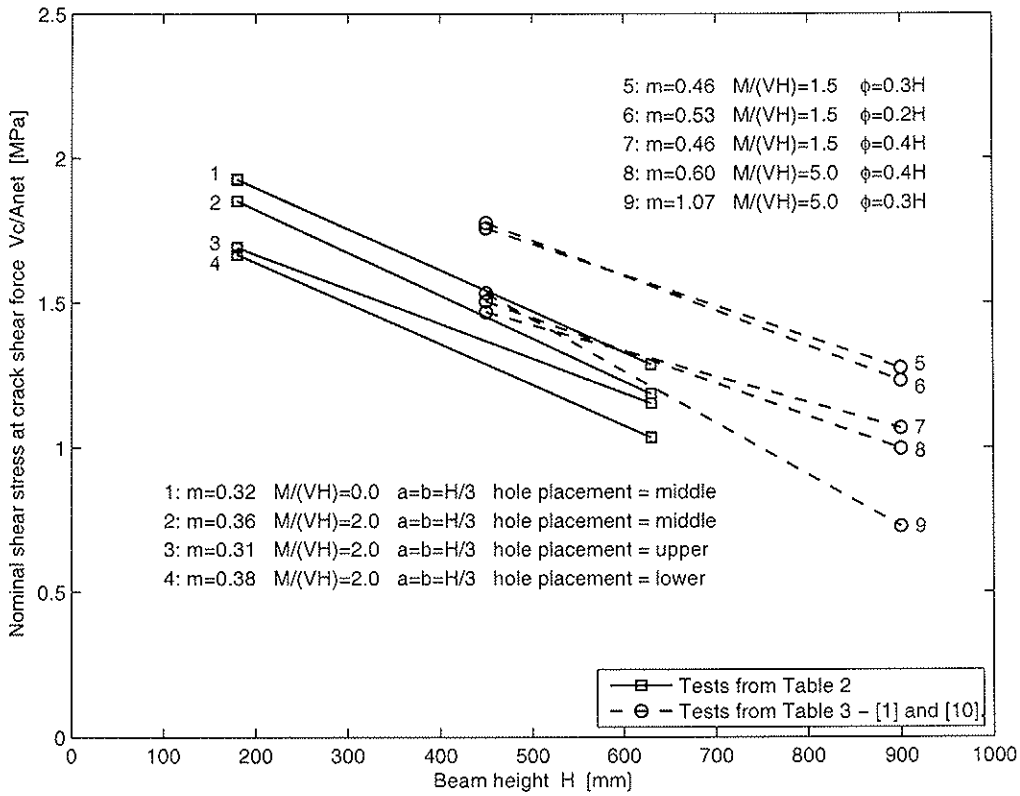

Figure 5: *Influence on strength of beam size (beam height, beam length and hole size uniformly scaled) for otherwise nominally equal tests.*

4 Comparison of design codes and test results

In order to make a simple evaluation of some of the proposed design recommendations, a comparison between test results and the shear force capacities according to codes is presented. The characteristic shear force capacities according to the following three methods are used in the comparison; (1) the empirically based method found in Swedish code of practise *Limträhandbok* [4], (2) The "end-notched beam analogy"-method found in a previous version of Eurocode 5 (prEN 1995-1-1 [8]) and also found in *Limträhandbok* and (3) the design method found in the German code DIN 1052 [3] (recently withdrawn for rectangular holes). The present results of beams with quadratic holes and test results of straight beams with circular holes presented in [1] and [10] are used in the comparison. The beams of test series AMc are considered to correspond to strength class GL 32c while the material strength class of all other beams is GL 32h. The following strength values (taken from SS-EN 1194 [16]) are used when determining characteristic capacities according to codes; $f_{v,k} = 3.8$ MPa and $f_{t,90,k} = 0.5$ MPa for GL 32h and $f_{v,k} = 3.2$ MPa and $f_{t,90,k} = 0.45$ MPa for GL 32c. Characteristic values for the beam test results $V_{i,k}$ and the coefficient of variation *cov* are determined according to Equations (1) and (2)

$$V_{i,k} = \bar{V}_i \cdot (1 - 1.645 \cdot cov) \quad (1)$$

$$cov = \sqrt{\frac{1}{n_{tot} - 1} \sum_{i=1}^{n_i} \sum_{j=1}^{n_j} \left(\frac{\bar{V}_i - V_{ij}}{\bar{V}_i} \right)^2} \quad (2)$$

where n_{tot} is the total number of individual tests, n_i is the number of test series, n_j is the number of individual tests within the test series, $\bar{V}_i$ is the mean value of the crack shear force V_c for test series i and V_{ij} is the individual value of the crack shear force V_c for test j in test series i. For the beams with quadratic holes, the minimum crack shear force $V_c = \min(V_{cB}, V_{cT})$ of the test results according to Table 2 and the overall coefficient of variation $cov = 7.55$ % based on these 36 test is used to determine the characteristic values $V_{i,k}$. For the beams with circular holes, the crack shear force V_c according to Table 3 and the overall coefficient of variation $cov = 15.3$ % based on these 56 tests is used to determine the characteristic values $V_{i,k}$. The comparison between tests and codes is presented in Table 4 and in Figure 6 for the quadratic holes and in Figure 7 for the circular holes. The test series notations for circular holes (H1-H8 and A1-A3) refer to notations in Table 3.

Comparing the characteristic values $V_{i,k}$ based on the test results and the characteristic strength values V_{code} according to codes, some observations are worth pointing out. *Limträhandbok* and DIN 1052 underestimates the capacity of all test series with quadratic holes. This underestimation is more severe for the test series with small beams since the beam size effect is not taken into account in any way in these two codes. The test results of beams with quadratic holes do however not indicate the strong size effect suggested by Eurocode 5. This code is on the unsafe side for all test series with quadratic and circular holes, but shows a fairly good ability to predict relative influence of the various parameters.

Table 4: *Test results and characteristic shear force capacities according to codes in kN.*

Test series	Test results		Characteristic shear force capacities V_{code} according to codes		
	mean $\bar{V}_i$	characteristic $V_{i,k}$	*Limträhandbok* empirical method	Eurocode 5 prEN 1995-1-1	DIN 1052
AMh	57.3	50.1	36.6	60.1	41.8
AMc	53.2	46.6	30.8	50.6	37.6
AUh	55.7	48.8	36.6	53.3*	35.9*
ALh	50.0	43.8	36.6	53.3*	35.9*
BMh	62.2	54.5	36.6	60.1	50.2
CMh	25.6	22.4	10.5	32.1	11.9
CUh	23.4	20.5	10.5	28.5*	10.2*
CLh	23.0	20.2	10.5	28.5*	10.2*
DMh	26.6	23.3	10.5	32.1	14.3
H1	106.4	79.6	83.7	176.4	116.5
H2	96.4	72.2	66.4	134.7	88.2
H3	69.2	51.8	51.9	108.0	72.8
A1	106.4	79.6	83.7	176.4	78.1
H4	55.1	41.3	66.4	134.7	63.8
A2	61.6	46.1	51.9	108.0	54.9
H5	76.8	57.5	41.8	109.4	58.3
H6	65.5	49.0	33.2	95.8	44.1
H7	47.6	35.6	25.9	77.9	36.4
H8	58.0	43.4	33.2	95.8	31.9
A3	48.8	36.5	25.9	77.9	27.4

* = Hole placement with respect to beam height not according to regulations in code.

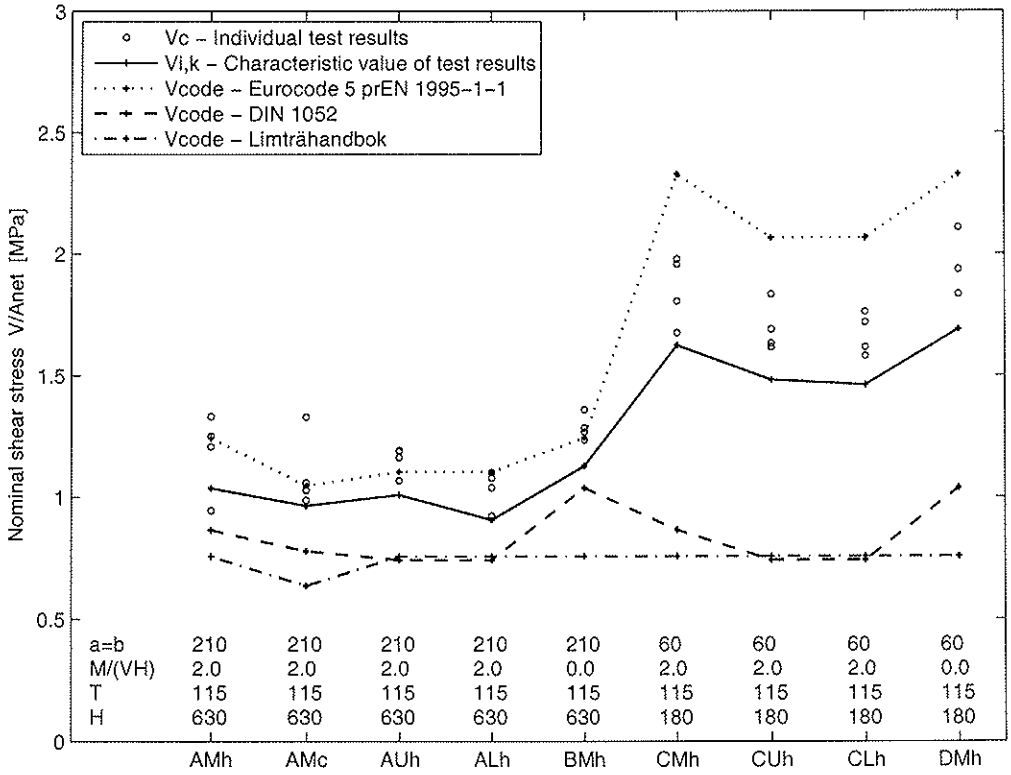

Figure 6: *Comparison of codes and test results for quadratic holes.*

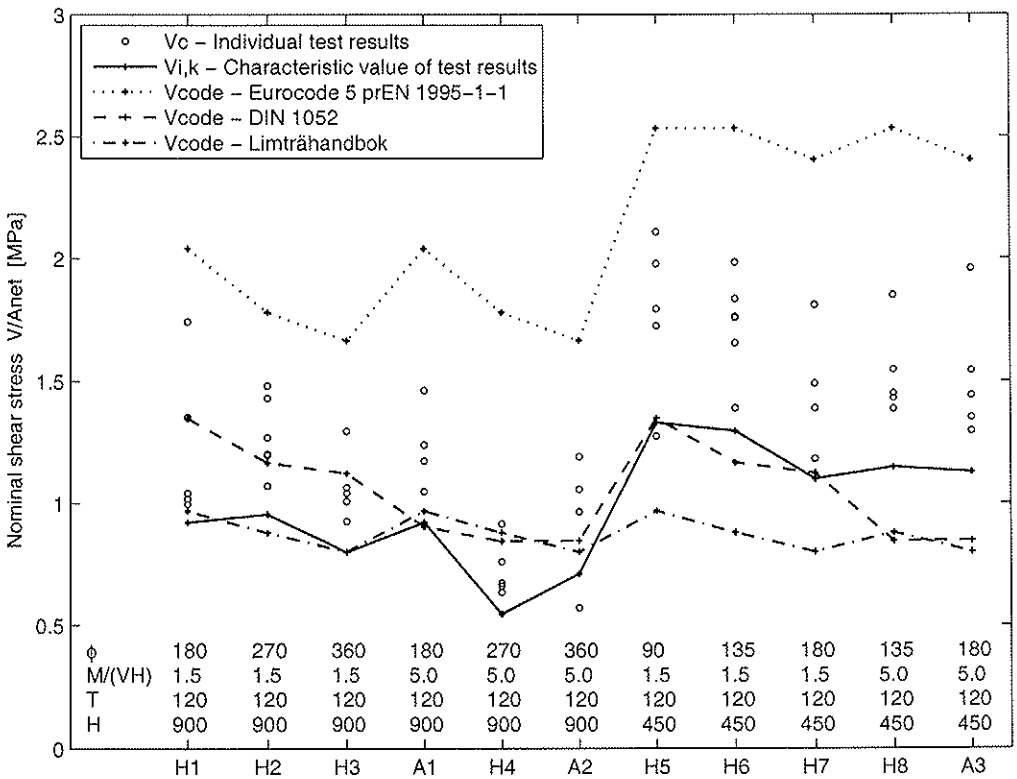

Figure 7: *Comparison of codes and test results for circular holes.*

References

[1] Aicher S., Höfflin L.
Tragfähigkeit und Bemessung von Brettschichtholzträgern mit runden Durchbrüchen – Sicherheitsrelevante Modifikationen der Bemessungsverfahren nach Eurocode 5 und DIN 1052
MPA Otto-Graf-Institute, University of Stuttgart, 2006.

[2] Bengtsson S., Dahl G.
Inverkan av hål nära upplag på hållfastheten hos limträbalkar
Master's Thesis, Byggnadsteknik II, Lund University, 1971.

[3] Blaß H.J., Ehlbeck J., Kreuzinger H., Steck G.
Erläuterungen zu DIN 1052:2004-08 – Entwurf, Berechnung und Bemessung von Holzbauwerken
2nd Edition including original text. DGfH innovations- und Service GmbH, München, 2005.

[4] Carling O.
Limträhandbok
Svenskt Limträ AB, Print & Media Center i Sundsvall AB, 2001.

[5] Danielsson H.
The Strength of Glulam Beams with Holes – A Survey of Tests and Calculation Methods
Report TVSM-3068, Division of Structural Mechanics, Lund University, 2007.
(available for download at: www.byggmek.lth.se/english/publications/)

[6] Danielsson H.
Strength Tests of Glulam Beams with Quadratic Holes – Test Report
Report TVSM-7153, Division of Structural Mechanics, Lund University, 2008.
(available for download at: www.byggmek.lth.se/english/publications/)

[7] *Eurocode 5: Design of timber structures - Part 1-1: General - Common rules and rules for buildings*
EN 1995-1-1:2004 (E).

[8] *Eurocode 5: Design of timber structures - Part 1-1: General Rules-General rules and rules for buildings*
prEN 1995-1-1: Final Draft 2002-10-09.

[9] Hallström S.
Glass fibre reinforcemed laminated timber beams with holes
Report 95-12, Department of Lightweight Structures, Royal Institute of Technology, Stockholm, 1995.

[10] Höfflin L.
Runde Durchbrüche in Brettschichtholzträger – Experimentelle und theoretische Untersuchungen
Dissertation, MPA Otto-Graf-Institute, University of Stuttgart, 2005.

[11] Johannesson B.
Design problems for glulam beams with holes
Dissertation, Div. of Steel and Timber structures, Chalmers University of Technology, Göteborg, 1983.

[12] Kolb H., Frech P.
Untersuchungen an durchbrochenen Bindern aus Brettschichtholz
Holz als Roh- und Werkstoff 35, p. 125-134, 1977.

[13] Penttala V.
Reiällinen liimapuupalkki
Publication 33, Division of Structural Engineering, Helsinki Univeristy of Technology, Otaniemi, 1980.

[14] Pizio S.
Die Anwendung der Bruchmechanik zur Bemessung von Holzbauteilen, untersucht am durchbrochen und am ausgeklinkten Träger
Publication 91:1, Dissertation, Baustatik und Stahlbau, ETH, Zürich, 1991.

[15] SP – Sveriges Provnings- och Forskningsinstitut
Lamination strength classes for glued laminated timber according to EN 1194
PM, 2002-06-14.

[16] SS-EN 1194:1999
Träkonstruktioner – Limträ – Hållfasthetsklasser och bestämning av karakteristiska värden
SIS Förlag, Stockholm, 2000.

INTERNATIONAL COUNCIL FOR RESEARCH AND INNOVATION
IN BUILDING AND CONSTRUCTION

WORKING COMMISSION W18 - TIMBER STRUCTURES

NEED FOR A HARMONIZED APPROACH FOR CALCULATIONS OF DUCTILITY OF TIMBER ASSEMBLIES

W Muñoz

M Mohammad

Building Systems, FPInnovations – Forintek Division, Québec (QC)

CANADA

A Salenikovich

Department of Wood and Forest Sciences, Université Laval, Québec (QC)

CANADA

P Quenneville

University of Auckland, Auckland

NEW ZEALAND

Presented by W. Muñoz

B.J. Yeh received clarification as shown in Figure 4 that glued connections with screws have the highest ductility. He stated in the US adhesive in connection is not considered as ductility. F. Lam stated that it may be dangerous to use bolted connection test results loaded parallel to grain to quantify the ductility behaviour of assembly or system where there is no guarantee that moments may not be introduced which could cause different failure mode. W. Muñoz agreed that more work is needed. B. Dujic stated that this paper intends to discuss the meaning of ductility for seismic design, however the cyclic test protocol information is missing. This information can be used by looking at the load /capacity drop from cycle to cycle based on the work at UC Berkeley. A. Salenikovich stated that this was tried before. U. Kuhlmann stated that redistribution with a system is also important. System ductility should be examined as well where information on absolute deformation rather than ratios of deformation is needed. A. Ceccotti stated that timber structures copied from steel structures in the approach to consider ductility. It is a concept important in standard for comparison purposes. We should overpass this. In EC8 Q factor takes into account the system behaviour. I. Smith commented that he had forgotten why we had such a task group in Canada. He agreed that behaviour of connection does not map into the behaviour of system. F. Lam agreed that absolute displacement is important but the definition of limit state is also important for different building system. A. Ceccotti said that here engineering judgment is needed.

Need for a Harmonised Approach for Calculations of Ductility of Timber Assemblies

Williams Muñoz[1], Mohammad Mohammad[2], Alexander Salenikovich[3], Pierre Quenneville[4]

[1] Research Scientist, Building Systems, FPInnovations – Forintek Division, Québec (QC) Canada.

[2] Group Leader, Building Systems, FPInnovations – Forintek Division, Québec (QC) Canada.

[3] Associate professor, Department of Wood and Forest Sciences, Université Laval, Québec (QC) Canada.

[4] Professor of Timber Design, University of Auckland, Auckland, New Zealand.

ABSTRACT

Knowledge of the ductility of timber structures is important in seismic design. The ductility of an assembly can be determined from the analysis of the load-displacement curve resulting from a destructive test. Although several methods have been utilised around the world to determine this value for timber structures, there is no agreement among researchers on a standardised approach. Particularly, there are differences in the methods adopted for estimation of the yield point which is used as basis for the calculations of the ductility ratio. In Europe, the CEN bilinear elastic-plastic approach is put forward, whereas in the USA the ASTM standards, the 5% diameter offset for connections and the equivalent elastic-plastic curve for shear walls approaches are commonly used. Alternative methods have been proposed in Japan, Australia and Canada. Moreover, the choice between the use of the displacement at maximum load and that at the failure load for the calculation of the ductility ratio has been disputed. This is another parameter that could significantly affect the final ductility value.

This paper provides some background information on the ductility calculations for connections and bolted connections in particular. Included in the discussion are comparisons between the current methods for estimation of the yield points in North America, Europe, Australia and Japan. Highlghted are some of the key issues associated with the need to adopt a consistent approach/methodology for the estimation of the yield point and ductility from available data base on timber connections. Preliminary results indicate the differences in the calculations of the ductility among the various methods. This work has been launched in support of the new Section on "Lateral Load Resisting Systems" in the Canadian timber design standard (CSA O86) and a new design approach for fastenings.

1. INTRODUCTION

It has been recognised by designers and codes and standards committees that connections should not only be designed to resist the design loads of the members and the elements that they join, but also to absorb energy and maintain the integrity of the structural system in the events of overloading. This has been triggered by the fact that the behaviour of timber structures under lateral loads generated by seismic and wind actions is mainly controlled by the response of the connections under high and low cycle loads, respectively. It has been demonstrated by previous studies (Ceccotti 1995) that a structure with plastic and dissipative connections, if appropriately designed, can resist higher seismic motions than the same structure with rigid and non-dissipative type of connections. In seismic design,

the term "ductility" is defined as the ability of an assembly or a structure to undergo large deformations in the inelastic range without substantial reduction in strength. Most collapses and damages that occur during extreme wind and seismic events are attributed to inadequate or inappropriate connections.

To estimate ductility, one needs to determine when the assembly begins to yield. Around the world, different methods exist for the determination of the yield point for timber structures but none has been adopted in Canadian standards yet. In Europe, the CEN bilinear elastic-plastic approach is proposed, whereas in the USA the ASTM standards use the 5% diameter offset for connections and the equivalent energy elastic-plastic (EEEP) curve for shear walls. Other methods have been proposed in Japan, Australia and Canada. The absence of a universal approach for yield point and ductility calculations does not help the harmonisation of standard testing and analysis procedures needed for seismic design of timber systems. In Europe, three ductility classes for timber connections have been proposed, which depend on the type of fastener (e.g., nails, screws, dowel-type fasteners), loading conditions and failure mode (Racher 1995). Ductility categories were also put forward under a proposed design approach for the Fastenings Section in the CSA Standard O86 (see Table 1), where connections or components could be classified by the failure mode as "brittle", or with "low ductility", "moderate ductility" or "high ductility" (Smith *et.al.* 2006a). Yet more advanced classification system for connections in Canada was proposed by Smith *et al.* (2006b) that associates the connection classification with a specific failure mode (i.e., fastener yielding, row tear out, block shear or net tension). The underlying assumption is that failure mechanisms individually or in combination control the global system failure mode. One of the main objectives of such proposed classification system is to link connection behaviour to that of the overall system. However, little information is available to support the proposed classes.

There is a need for the development of ductility categories based on analysis of the available test data, especially for bolted connections. It is expected that this work will generate important technical information that will be used to verify some of the proposed ductility categories and will provide a better understanding of the ductility of bolted connections in particular. Efforts will be made later on to verify if the same approach could be generalised and adopted for connections made with other types of fasteners (e.g., glulam rivets, lag bolts, etc.) and for structural systems (portal frames, shear walls and diaphragms).

Table 1. Proposed ductility classes for connections or components (Smith et. al. 2006a)

Classification	Average ductility ratio
Brittle	$\mu \leq 2$
Low ductility	$2 < \mu < 4$
Moderate ductility	$4 < \mu \leq 6$
High ductility	$\mu > 6$

1.1. How to Evaluate Ductility in Timber Connections?

The ductility of connections or assemblies is usually expressed as the "ductility ratio (μ)", which is defined as the ratio of the displacement at the ultimate or failure load to that at the yield load as follows:

$$\mu = \Delta_{failure} / \Delta_y \quad \text{or} \quad \mu = \Delta_{max} / \Delta_y \qquad [1]$$

Where, $\Delta_{failure}$ = displacement at failure load; Δ_{max} = displacement at maximum load (P_{max}), and Δ_y = displacement at yield load.

The yield point of an assembly is typically defined as the load (or stress) at which a material or an assembly begins to plastically deform (i.e irreversible deformation). This is usually detectable under monotonic loading tests as divergence from a linear-elastic response (Figure 1). Prior to yield point, the connection or assembly deforms elastically and will return to its original shape when the applied stress is removed.

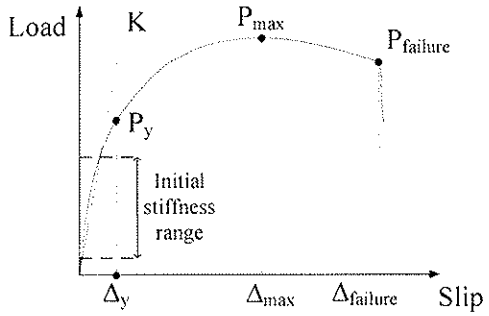

Figure 1. Typical load-displacement curve showing the characteristic points.

Obviously, the estimate of the yield point and the choice between the maximum and failure loads determine the numerical value of the ductility ratio. In most structural timber connections, the load-displacement relationship is nonlinear and there is no distinct transition between the elastic and plastic behaviour and unambiguous definition of yield point is difficult. As discussed below, different analysis methods produce different yield point estimates, which could ultimately lead to over- or under-estimation of the ductility ratio, hence assigning the same connection to a different ductility category. In many types of connections, extensive post-yield inelastic deformation and, sometimes, apparent hardening occurs (Smith et. al. 2006a). In such cases, the test usually is terminated before reaching the ultimate load. To estimate the ultimate load and corresponding displacement, some acceptable conservative approaches have been proposed. Furthermore, the basis for the calculation of the ductility ratio (i.e., use of $\Delta_{failure}$ vs. Δ_{max}) may also result in a different ductility category. The following sections highlight differences between the various analysis methods and assumptions adopted in the calculations of the yield points and ductility ratio and their range of applicability.

1.2. Determination of Yield Loads and Displacements

The following provides details of the analysis methods that are commonly used in North America, Europe, Japan and Australia for the estimation of the yield point from typical load-displacement curves generated from laboratory tests on timber connections or assemblies.

(a) Karacabeyli and Ceccotti (K&C)

The yield point is determined at the point on the load-displacement curve corresponding to 50% of P_{max} as shown in Figure 2a (Karacabeyli and Ceccotti, 1998).

(b) European Committee for Standardisation (CEN)

The yield point is determined as the intersection of two lines on the load-displacement curve as shown in Figure 2b (Ceccotti 1995). The first line represents the initial stiffness (K_α), which is usually calculated in the range from 10% to 40% of P_{max}. This secant line forms an angle α with the horizontal axis, while the second tangent line (K_β) is drawn at a slope equal to one sixth of the initial.

(c) Equivalent Energy Elastic-Plastic (EEEP) Curve

This bilinear curve, originally proposed for concrete and steel structures (Foliente 1996), approximates perfectly elastic-plastic behaviour of an assembly (Figure 2c). The initial slope of the EEEP curve, drawn through 40% of P_{max} on the observed curve, determines the elastic stiffness (K) of the assembly. Displacement at failure is found on the descending part of the load-displacement curve at 80% of P_{max}. The yield load (P_y) is calculated by equating the areas under the observed and EEEP curves using the following equation:

$$P_y = \left[\Delta_{failure} - \sqrt{\Delta^2_{failure} - \frac{2w_{failure}}{K}}\right] * K \qquad [2]$$

Where, $w_{failure}$: area under the load-displacement curve until failure.

The intersection of the line representing the initial stiffness and a horizontal line fixed at P_y defines the yield point, where the corresponding yield displacement is determined.

(d) Yasumura and Kawai (Y&K)

Yasumura and Kawai (1998) proposed a method to determine the yield point based on the intersection of two lines located on the load-displacement curve. Similar to the CEN method, the initial stiffness is calculated as a slope of a line passing through the points corresponding to 10% and 40% of P_{max}. The second line is drawn tangent to the load–displacement curve and parallel to a secant line passing through the points corresponding to 40% and 90% of P_{max}. The point of intersection between the two lines is projected horizontally towards the load–displacement curve to obtain the corresponding yield point (see Figure 2d).

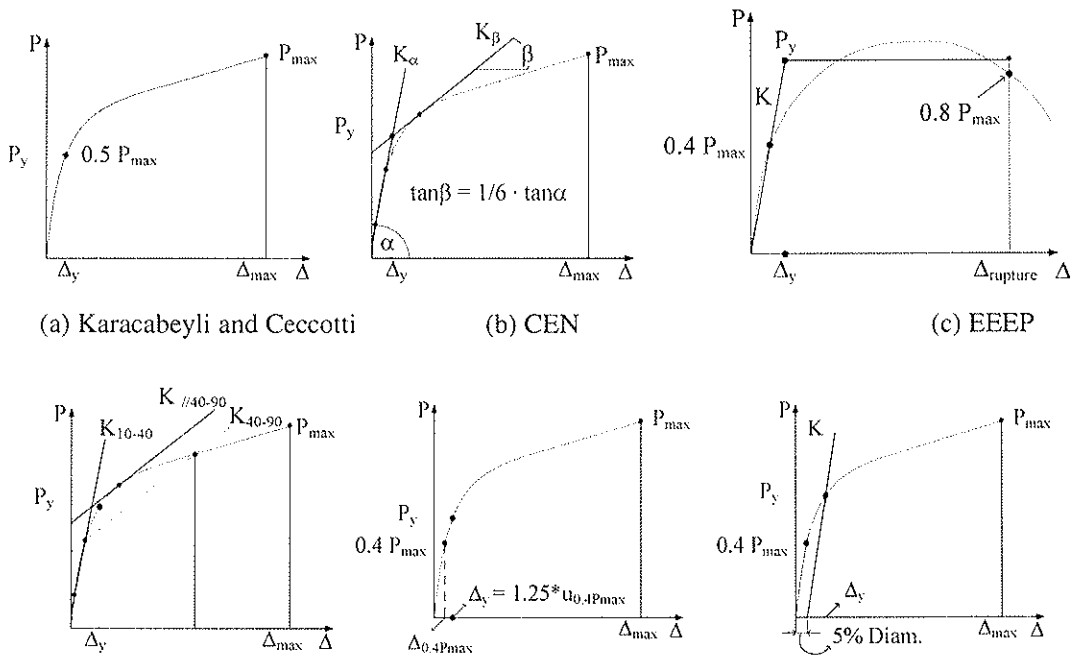

(a) Karacabeyli and Ceccotti (b) CEN (c) EEEP

(d) Yasumura and Kawai (e) CSIRO (f) 5% diameter

Figure 2. Methods commonly used for estimation of the yield point.

(e) Commonwealth Scientific and Industrial Research Organisation (CSIRO)

The yield point is the point on the load-displacement curve corresponding to the displacement at 40% of P_{max} multiplied by a factor of 1.25 (Figure 2e).

(f) 5% diameter offset (5% d)

This method is used to determine the dowel-bearing strength and the lateral resistance of fasteners in wood for the National Design Specification (AF&PA 2006). The yield point is found at the intersection of the load-displacement curve with a straight line which is drawn parallel to the initial stiffness (slope between 0% and 40% of P_{max}) with an offset on the horizontal axis equal to 5% of the fastener diameter (Figure 2f).

2. APPROACH / CASE STUDY

To examine differences between the various calculation methods, existing test data on several types of wood connections were analysed, including; nailed, screwed and bolted connections (Table 2). For nailed connections with multiple fasteners, the load was divided by the number of fasteners.

Table 2: Connections configurations used in the analysis.

Assembly	Fastener type	Number of fasteners	Type of test	Number of specimens
Wood-to-wood	Nail Ø4.1 x 89-mm	2	static	10
	Screw SDS Ø6.4 x 76.2 mm	1	static	10
	Screw SDS Ø6.4 x 76.2 mm and glue*	1	static	10
OSB-to-wood	Nail Ø2.9 x 63.5-mm	1	static	15
	Nail Ø2.9 x 63.5-mm	3	static	15
Wood-steel-wood (Glulam)	(1)** Bolt Ø19 mm	1	static	10
	(2)** Bolt Ø19 mm	4	static	10
	(3)** Bolt Ø19 mm	2	static	10
Steel-wood-steel (Glulam)	(4)** Bolt Ø19 mm	2	static	10
	(5)** Bolt Ø19 mm	4	static	10
	(6)** Bolt Ø13 mm	1	static	10

* Non-structural glue. ** The number in parentheses identifies the connection configuration.

3. RESULTS AND DISCUSSION

3.1. Nailed and screwed connections

The average yield load per fastener, the corresponding displacement, and the ductility ratio ($\Delta_{failure}/\Delta_y = \mu_f$) values for each series of wood connections are presented in Table 3.

Graphically, the EEEP yield loads were always located off the curve, giving unrealistic values (Figure 3a, b and c). The other methods were found to be close to each other in terms of load and displacement, except for connections with a low initial stiffness, where CEN gives load values located off the curve while K&C provided values that were clearly in the plastic zone (Figure 3c). The yield loads determined with the EEEP method were always higher while those calculated using CSIRO method were lower than the other methods. The differences between other methods were less significant.

Table 3: Yield points and ductility ratios for nailed and screwed connections*.

Method	Property	Type of connection				
		Nail *	Screw	Sc. & Glue	OSB-wood S	OSB-wood M*
EEEP	P_y (kN)	1.56 (8%)	4.16 (14%)	3.91 (7%)	1.21 (13%)	1.09 (10%)
	Δ_y (mm)	1.19 (78%)	1.29 (52%)	1.45 (22%)	1.29 (50%)	1.59 (34%)
	μ	30 (53%)	30 (58%)	22 (29%)	21 (73%)	14 (36%)
CEN	P_y (kN)	0.95 (12%)	2.26 (13%)	2.25 (11%)	0.70 (21%)	0.65 (20%)
	Δ_y (mm)	0.61 (63%)	0.68 (66%)	0.88 (25%)	0.87 (70%)	1.06 (52%)
	μ	52 (48%)	55 (65%)	38 (36%)	38 (85%)	23 (47%)
Y&K	P_y (kN)	1.02 (11%)	2.61 (9%)	2.53 (5%)	0.63 (11%)	0.58 (5%)
	Δ_y (mm)	0.95 (48%)	1.41 (27%)	1.57 (17%)	0.98 (31%)	1.11 (23%)
	μ	31 (56%)	22 (26%)	21 (16%)	22 (54%)	19 (22%)
K&C	P_y (kN)	0.86 (9%)	2.38 (13%)	2.22 (6%)	0.71 (13%)	0.62 (10%)
	Δ_y (mm)	0.75 (59%)	1.15 (59%)	1.09 (20%)	1.48 (44)	1.50 (41)
	μ	43 (54%)	36 (62%)	30 (18%)	17 (68%)	15 (37%)
CSIRO	P_y (kN)	0.75 (10%)	1.99 (15%)	1.90 (6%)	0.59 (12%)	0.54 (9%)
	Δ_y (mm)	0.65 (76%)	0.75 (57%)	0.82 (23%)	0.76 (51%)	0.92 (35%)
	μ	54 (53%)	53 (60%)	40 (29%)	36 (74%)	24 (36%)
5% Diam.	P_y (kN)	0.93 (7%)	2.35 (8%)	2.27 (7%)	0.62 (11%)	0.55 (7%)
	Δ_y (mm)	0.75 (40%)	1.04 (34%)	1.17 (16%)	0.82 (38%)	0.97 (26%)
	μ	36 (32%)	32 (35%)	27 (19%)	28 (55%)	22 (27%)

*Values of load per fastener. Numbers in parentheses represent the coefficient of variation.

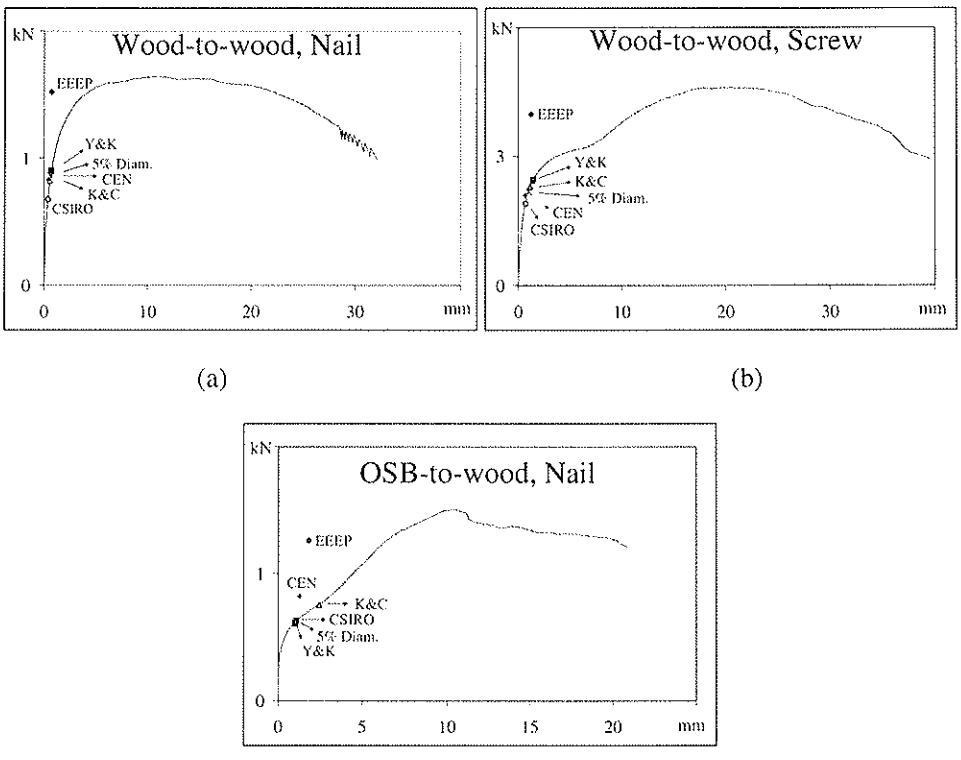

(a) (b)

(c)

Figure 3: Location of yield points on the load-displacement curves.

Figure 4a illustrates differences among the various methods using the 5% diameter offset as a reference. It can be noticed again that the EEEP and CSIRO methods tend to produce the highest and lowest yield displacements among the methods considered. The variation of Δ_y between the six methods was evident, reaching in some cases up to 80% for the same

connection. The significant variations in Δ_y affect the estimates of the ductility ratio but, due to their high values, the variation becomes insignificant as all of connections are classified as highly ductile, regardless of the yield point method utilised.

To analyse the difference when using $\Delta_{failure}/\Delta_y$ (μ_f) or Δ_{max}/Δ_y (μ_m) for ductility ratio calculations, a ratio of ductilities (μ_f / μ_m) is shown in Figure 4b. The little variation within the connections for all the yield point methods used, allowed grouping the ratio values per type of connection. The value obtained for these ratios, ranges from 0.45 to 0.58, which indicates that the type of reference for ultimate displacement influences the value of ductility ratio. For these connections, either μ_f or μ_m give ductility ratios that allow for classifying these assemblies as highly ductile.

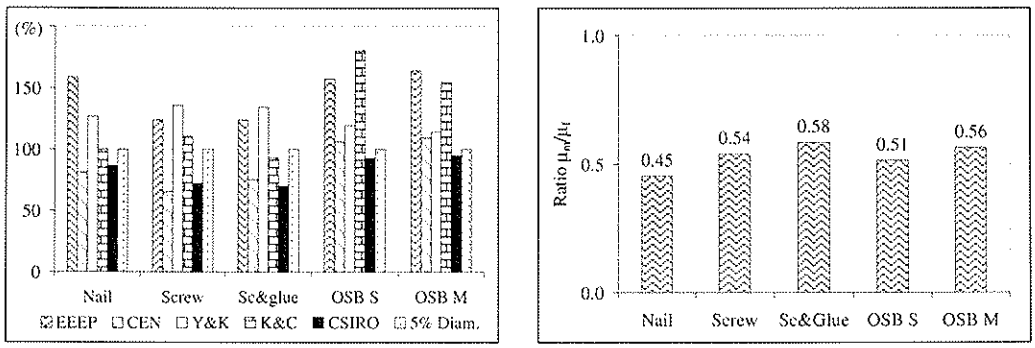

(a) (b)

Figure 4: Yield displacements expressed as a percentage of 5% diam. - Δ_y, and (b) Ratio of ductilities.

3.2. Bolted Connections

In this type of connections, irregularities in the shape of the load-displacement curves are typical which mainly depend on the connection configuration (e.g., number of bolts or rows, geometry, etc.). This was observed in the large test data base of bolted connections that was generated in previous studies (Quenneville and Mohammad 2000). It was decided not to apply the EEEP method to bolted connections as they usually do not have a well defined non-linear behaviour. Similarly, the 5% diameter approach was also eliminated from the analysis due to the fact that it applies to connections with a single fastener.

A preliminary analysis of available data base on bolted timber connections was carried out and results of yield point values and ductility ratios are given in Table 4. It was noticed that the obtained values of yield loads were always higher when using the CEN method, whereas the CSIRO method underestimated such loads. Low variability was observed in all types of connection configurations analysed for all methods. In the case of yield displacements, the CEN method gave the highest displacements, while K&C and CSIRO methods provided the lowest ones. This is quite important as different yield point methods result in different ductility categories for a same connection (see Table 4). This divergence could lead to misclassification of the connections in terms of ductility classes. Therefore, it is necessary to adopt a standardised methodology for the determination of yield loads and displacements applicable to bolted connections.

Further analysis of available data base on bolted timber connections have indicated that using either Δ_{max} or $\Delta_{failure}$ (defined as 80% of P_{max}) as a numerator significantly affect the ductility ratio values. Although for some connections the maximum load was found to

correspond to failure load (Figure 5a), the majority of test specimens showed distinct differences. Sometimes, connections that exhibited highly ductile behaviour (Figure 5b) would be considered of low ductility if the ductility ratio is calculated on the basis of Δ_{max}.

Table 4: Yield points and ductility ratios for bolted connections.

Method	Property	Configuration					
		WSW 1	WSW 2	WSW 3	SWS 4	SWS 5	SWS 6
CEN	P_y (kN)	32.5 (10%)	93.2 (4%)	88.3 (8%)	105.8 (16%)	169.8 (8%)	28.7 (10%)
	Δ_y (mm)	1.4 (24%)	1.8 (20%)	2.3 (19%)	1.8 (52%)	1.3 (39%)	2.0 (78%)
	μ	5.3 (40%)	2.4 (26%)	2.8 (28%)	3.6 (53%)	5.3 (42%)	5.4 (70%)
Y&K	P_y (kN)	27.3 (12%)	73.2 (10%)	71.5 (9%)	73.4 (10%)	130.8 (12%)	21.3 (14%)
	Δ_y (mm)	1.2 (15%)	1.4 (24%)	1.9 (17%)	1.2 (37%)	1.0 (29%)	1.6 (51%)
	μ	5.6 (29%)	3.0 (25%)	3.3 (28%)	4.0 (30%)	5.8 (38%)	5.6 (54%)
K&C	P_y (kN)	21.2 (9%)	55.6 (6%)	53.2 (6%)	69.7 (8%)	116.6 (9%)	20.3 (10%)
	Δ_y (mm)	0.9 (18%)	1.0 (18%)	1.3 (16%)	1.2 (26%)	0.9 (29%)	1.5 (58%)
	μ	7.8 (31%)	4.1 (24%)	4.5 (28%)	4.1 (24%)	6.7 (41%)	6.2 (50%)
CSIRO	Py (kN)	20.3 (11%)	54.6 (8%)	52.6 (7%)	65.4 (7%)	108.4 (12%)	18.6 (15%)
	Δy (mm)	0.9 (18%)	1.0 (17%)	1.3 (17%)	1.1 (31%)	0.9 (32%)	1.3 (66%)
	μ	8.2 (33%)	4.1 (21%)	4.5 (27%)	4.5 (28%)	7.1 (40%)	7.1 (53%)

Numbers in parentheses represent the coefficient of variation.

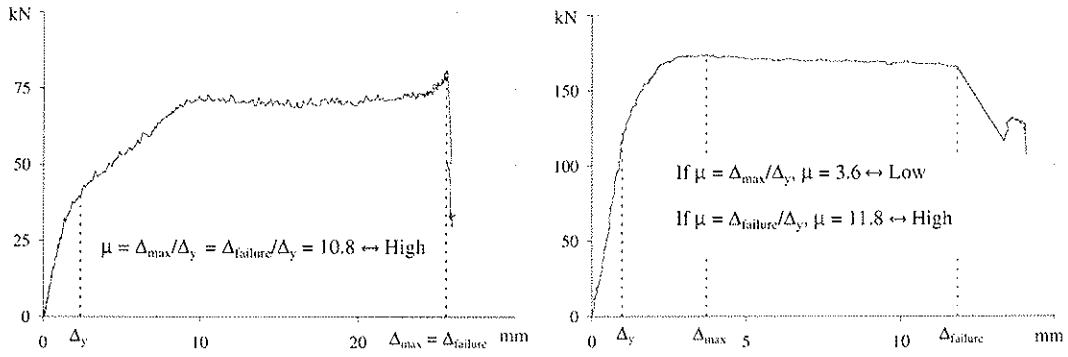

(a) (b)

Figure 5. Impact of the selection of either Δ_{max} or $\Delta_{failure}$ for the ductility calculations.

Currently proposed design procedures for bolted connections in Canada are focused on predicting actual failure modes and corresponding capacities. Designers need a tool to estimate not only the capacity of connections and how they fail, but also how ductile they are. This is quite important for lateral load design systems in high seismic and wind zones.

One of the possible scenarios is to express the ductility of the bolted connections as a function of connection stiffness, slenderness ratio, failure modes and any other parameter that could affect the ductility. The designer will be able to estimate the ductility of any connection configuration by simply substituting these parameters in a given expression and be able to know how ductile the designed connections are. The proposed expression for the estimation of ductility ratio of bolted connections could have the following form:

$\mu = f(K, \lambda)$ Where: K: Initial stiffness; λ: Reserved capacity between ductile and brittle failure modes.

While K represents how stiff the connection system is, λ provides a measure of the connection ductility. To better understand this, it is important to think of the way a connection with low-to-moderate ductility behaves. For cases where bearing failure mode

controls the design for strength, connections will deform plastically until failure ultimately occurs due to fracture of wood in row shear-out or group tear out. The difference between the ductile (i.e., bearing) and brittle (e.g., row shear-out) could be used as an estimation of the reserved capacity of the connection. This reserved capacity could be used to determine the residual deformation in the connection which is a good indicator for ductility.

This approach will, ultimately, enable designers to have better control over the connections behaviour at the very early stages of design and will help to optimise the connection design as well. More work is needed to investigate closely the relative influence of each parameter on the ductility ratio and what type of mechano-based or empirical model than be used to estimate ductility ratio based on existing data base on bolted connections.

3.3. Connection Ductility vs. System Ductility

Current Canadian design codes, including CSA O86, are based on the design of individual structural members and fastenings with the assumption that the structural system will behave under loading in a way that is similar to the behaviour of its individual components. This approach may lead to designs and solutions that are considered to be conservative and uneconomical with some major uncertainties associated with the system behaviour, especially at failure (Asiz and Smith 2005). Although the design of connections subjected to seismic load combinations could be supplemented by the assessment of their assigned ductility classes, there are no guaranties that the system will have the same ductility level/class. For such load combinations, it is important to design the connections to yield first and to avoid brittle failure in the members and that, even when failure in some connections occurs, some alternative load path(s) are developed to continue carrying the load. According to Asiz and Smith (2005), general design provisions should require attainment of a certain level of ductility by whole systems and critical connections, which should be developed and be consistent with proposed provisions by the CSA O86 Lateral Load Design Task Group (Popovski and Karacabeyli 2005).

Adoption of the "capacity design" principles for wood structures will be almost impossible without providing a clear answer as to how one can relate the ductility classes of connections to those of the whole structural systems. Such approach will provide the necessary tools to design structures in such a way that ductile failure would most likely occur in the connections and not in the main members.

4. Conclusions

Several existing methods for the determination of yield loads and displacements and for ductility calculations were examined. Analysis of existing data on nailed, screwed and bolted connections was carried out to compare the various methods and to verify its influence on the ductility calculations. The following conclusions can be made:

- Significant differences were found between the various methods used for the determination of yield loads and displacements.
- Assemblies that showed highly ductile behaviour, as nailed and screwed connections, were less affected by the method adopted for ductility calculation.
- For bolted connections, where all the types of failure modes can be observed, the selected yield point method produced different ductility categories, which could yield to misclassification of connections.

- Ductility ratio of bolted connections depends significantly on whether Δ_{max}, or $\Delta_{failure}$ being used as basis for the calculations.
- Ductility could be expressed as a function of certain connection configurations parameters such as initial stiffness, slenderness ratio, failure mode, etc.
- It is important to derive procedure as to how to link ductility of connections to that of the lateral load resisting systems? This is crucial for implementation of "Capacity Design" principles in timber design.

5. References

AF&PA. 2006. National Design Specification (NDS) for Wood Construction Commentary 2005 Edition. American Forest & Paper Association. Washington, DC.

Asiz, A. and I. Smith. 2005. New Generation of Timber Design Practices and Code Provisions Linking System and Connection Design. Proceedings of the International Council for Research and Innovation in Building and Construction, Working Commission W18 - Timber Structures. Karlsruhe, Germany.

Ceccotti, A. 1995. Timber Connections under Seismic Actions. In: Timber Engineering – STEP 1. 1st Edition. STEP/EUROFORTECH. STEP Lecture C17. The Netherlands, ISBN 90-5645-001-08.

Foliente, G.C. 1996. Issues in Seismic Performance Testing and Evaluation of Timber Structural Systems. Proceedings of the 1996 International Timber Engineering Conference, Vol. 1, New Orleans, LA, pp. 1.29-1.36.

Karacabeyli, E. and A. Ceccotti. 1998. Nailed Wood-frame Shear Walls for Seismic Loads: Test Results and Design Considerations. Structural Engineering World Wide 1998, ISBN: 0-08-042845-2. Paper reference: T207-6. 1998.

Popovski, M. and Karacabeyli, E. 2005. Framework for Lateral Load Design Provisions for Engineered Wood Structures in Canada. Proceedings of the International Council for Research and Innovation in Building and Construction, Working Commission W18 - Timber Structures. Karlsruhe, Germany.

Quenneville, J.H.P., and Mohammad, M. 2000. "On the Failure Modes of Steel-Wood-Steel Bolted Timber Connections Loaded Parallel-to-Grain". Canadian Journal of Civil Engineering (CJCE) 27: 761-773.

Racher, P. 1995. Mechanical Timber Joints. In: Timber Engineering – STEP 1. 1st Edition. STEP/EUROFORTECH. STEP Lecture C1. The Netherlands, ISBN 90-5645-001-08.

Smith, I., A. Asiz, M. Snow and Y.H. Chui. 2006a. Possible Canadian / ISO Approach to Deriving Design Values from Test Data. Proceedings of the International Council for Research and Innovation in Building and Construction, Working Commission W18 - Timber Structures. Florence, Italy, August 2006.

Smith, I., Y.H. Chui, P. Quenneville. 2006b. Overview of a New Approach to Handling System Effects in Timber Structures. Proceedings of the International Council for Research and Innovation in Building and Construction, Working Commission W18 - Timber Structures. Florence, Italy, August 2006.

Yasumura, M. and N. Kawai. 1998. Estimating Seismic Performance of Wood-framed Structures. Proceedings of 1998 I.W.E.C. Switzerland. Vol.2. pp. 564-571.

INTERNATIONAL COUNCIL FOR RESEARCH AND INNOVATION
IN BUILDING AND CONSTRUCTION

WORKING COMMISSION W18 - TIMBER STRUCTURES

PLASTIC DESIGN OF WOOD FRAME WALL DIAPHRAGMS IN LOW AND MEDIUM RISE BUILDINGS

B Källsner
School of Technology and Design, Växjö University
SP, Technical Research Institute of Sweden, Stockholm

U A Girhammar
Department of TFE – Civil Engineering, Faculty of Science and Technology
Umeå University

SWEDEN

Presented by B. Källsner

Tom Williamson asked if there is any information on the details of transfer connections. B. Källsner responded that this information is available. A Salenikovich asked whether experimental work is available. B. Källsner answered yes much data is available and more than one story wall tests will also be available. B. Dujic asked if this model can be used to calculate the performance of the 3 story CLT building tested in Japan. B. Källsner responded that he is not sure but thinks it is possible. A. Ceccotti received confirmation from B. Källsner that the book will be published in English.

Plastic design of wood frame wall diaphragms in low and medium rise buildings

Bo Källsner
School of Technology and Design, Växjö University, Sweden
SP, Technical Research Institute of Sweden, Stockholm, Sweden
Ulf Arne Girhammar
Department of TFE – Civil Engineering, Faculty of Science and Technology,
Umeå University, Sweden

Abstract

Design of wall diaphragms has been a topic of major discussions during the development of the European timber design code, Eurocode 5. The main problem has been that wall diaphragms are fastened to the substrate in different ways in different countries and that this fact must be reflected in the code.

A plastic method for design of wood frame wall diaphragms is presented which can be used in case of partially or fully anchored studs and fully anchored bottom rail. In this paper the method is applied to walls that are more than one storey high. The principles of the method are demonstrated for walls with and without openings. The possibility of using transverse walls for anchoring with respect to vertical uplift is illustrated.

1 Introduction

Since 2001 the authors have presented a number of papers dealing with plastic design of sheathed wood-framed wall diaphragms. The most important of these papers are [1] dealing with walls without openings, [2] dealing with walls including openings and [3] and [4] dealing with transverse walls. The plastic design method has successively been improved and soon a Swedish handbook based on the principles will be published.

The purpose of this paper is to demonstrate how the plastic design method can be applied to buildings that are more than one storey high. In this paper the general principles of the design method will be applied to wall diaphragms with and without openings. The influence of transverse walls will also be incorporated in the design method.

2 Design method

The design is carried out using the principles of a so called plastic lower bound method [5]. In this method a force distribution is chosen that fulfils the conditions of force and moment equilibrium for all parts of the structure studied.

The plastic design method can only be applied to wall diaphragms where the sheet material is fixed by mechanical fasteners to the timber members and where these sheathing-to-timber joints show plastic behaviour.

The design method only covers static loads and can not be used for determination of deformations in the serviceability limit state.

The proposed plastic method is flexible with respect to load configurations and boundary conditions and can for example be applied to walls where the leading stud on the windward side is fully or partially anchored with respect to vertical uplift and where the bottom rail is fully anchored to the substrate.

In case of buildings more than one storey high, the principle of superposition is used for horizontal loads acting at different storeys according to Figure 1.

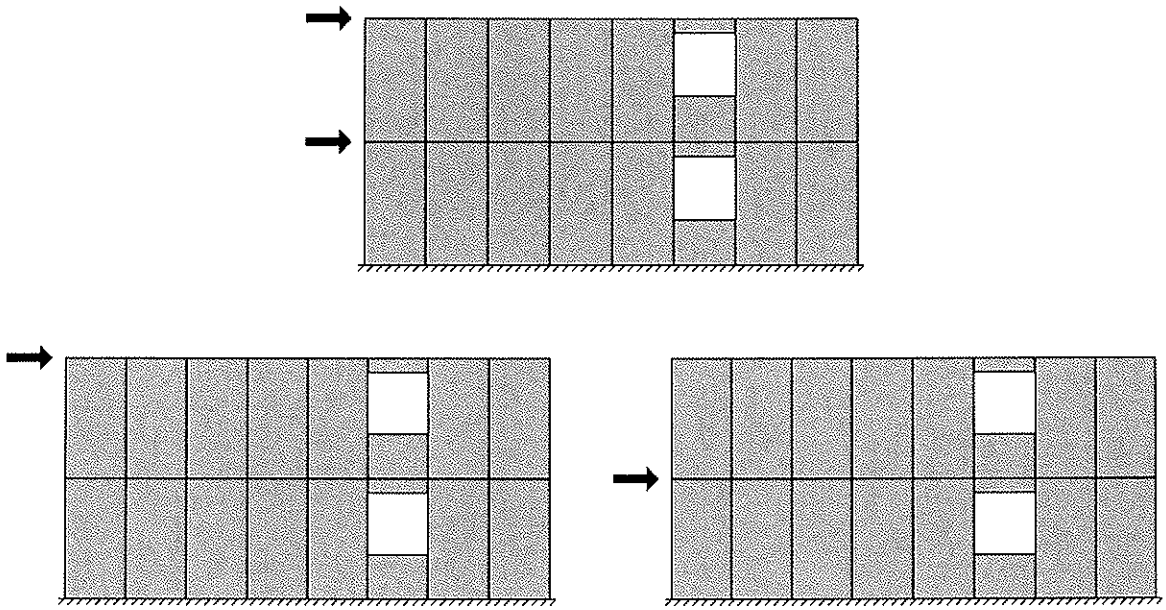

Figure 1. The principle of superposition is used for horizontal loads.

3 Walls without openings

The general principles of the plastic design method will be presented for a wall configuration of a two storey building subjected to a horizontal load H along the top rail and vertical loads V_i along the studs according to Figure 2. The length of the wall is denoted by l and the total height by h_{tot}. The width and height of the full format sheets are denoted by b and h, respectively. The bottom rail is assumed to be fully anchored to the substrate by screws or other mechanical fasteners. The studs are not assumed to have any tie-downs. The influence of tie-downs can be taken into account considering them as external point loads acting on top of the studs. In the lower part of Figure 2 the assumed internal force distribution of the wall is shown in one horizontal and one vertical section through the wall. The forces acting along the bottom of the wall are shown in a section immediately above the bottom rail and represent the forces in the sheathing-to-timber joints and the stud-to-rail (framing) joints. These forces are assumed to act either perpendicular or parallel to the bottom rail. The plastic capacity per unit length of the sheathing-to-timber joints is denoted by f_p and it is assumed that this plastic value has been attained along the entire bottom rail. Along the left part of the bottom rail a distributed force f is shown originating from the stud-to-rail joints. A more thorough discussion of this force contribution will be presented later.

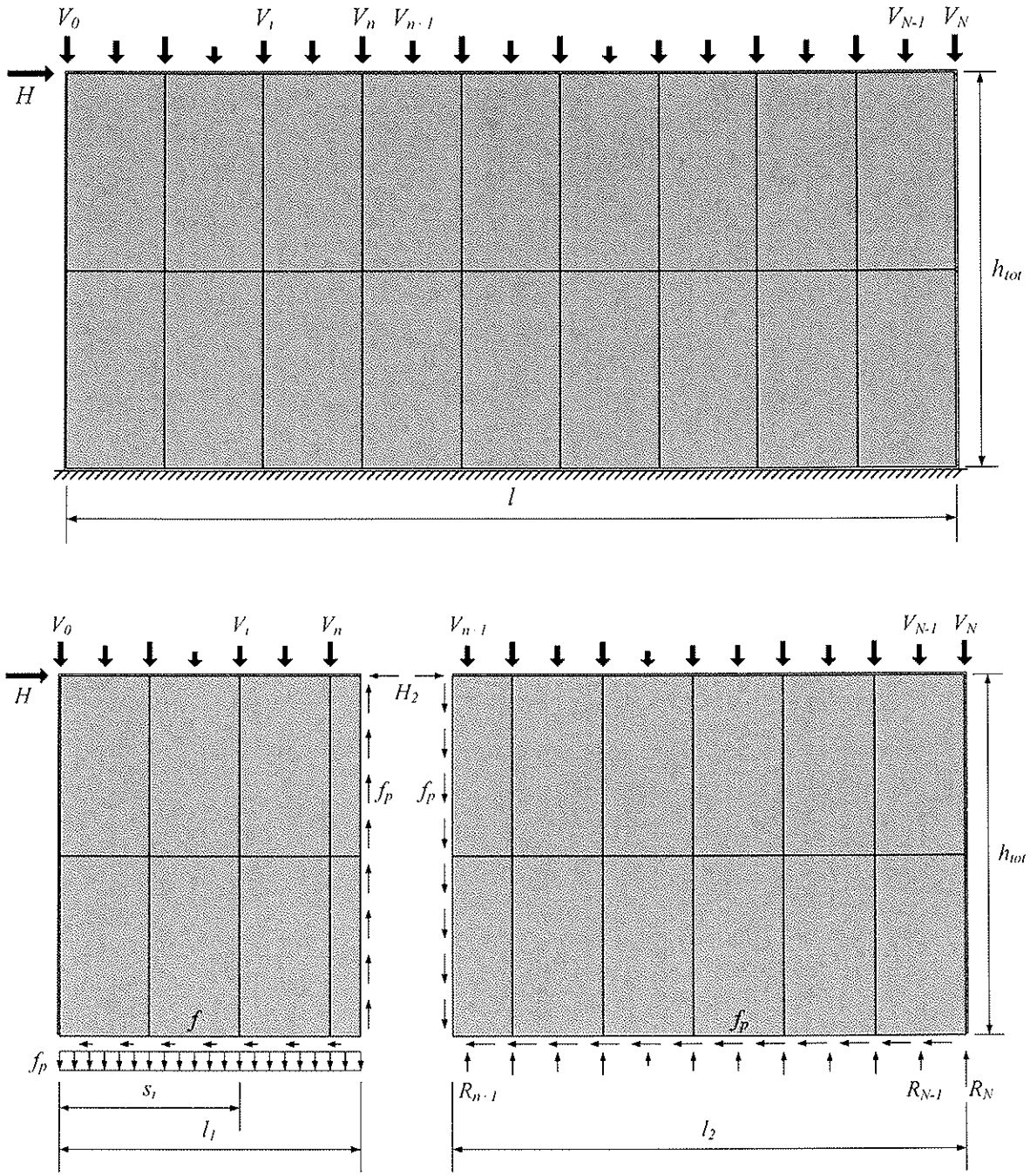

Figure 2. Forces acting on a wall diaphragm with fully anchored bottom rail. The plastic capacity has been attained in the vertical section l_1 from the leading stud. The distance from the leading stud to the vertical load V_i is denoted s_i.

The wall is separated into two fictitious elements 1 and 2 of length l_1 and l_2, respectively. The length l_1 is determined from the condition that the plastic shear capacity $f_p h_{tot}$ is assumed to be attained in this vertical section of the wall, i.e.

$$\sum_{i=0}^{n} V_i + f_p l_1 = f_p h_{tot} \tag{1}$$

This means that all the sheets within wall element 2 will be subjected to a pure shear flow equal to f_p and that the vertical forces V_{n+1} to V_N will be transferred directly to the bottom

rail via the vertical studs. Wall element 1 will behave like a rigid body since the shear flow in the vertical sheathing-to-timber joints will always be smaller than the plastic one. The length l_1 is obtained from Eq. (1) as

$$l_1 = h_{tot}\,(1-\sum_{i=0}^{n}\frac{V_i}{f_p h_{tot}}) \tag{2}$$

There are two occasions when Eq. (1) cannot be fulfilled. The first one occurs when the vertical load on the leading stud $V_0 > f_p h_{tot}$, corresponding to the conditions of a fully anchored wall. In this case the wall is fully effective with respect to shear transfer and l_1 becomes equal to zero. The second case occurs when the wall length l is too short in order to attain the vertical plastic shear capacity within the wall. In this case $l_1 = l$.

Denoting the horizontal forces transferred to wall element 1 by H_1 and to wall element 2 by H_2, a moment equation with respect to wall element 1 around its lower right corner gives

$$H_1 h_{tot} - f_p l_1 \frac{l_1}{2} - \sum_{i=0}^{n} V_i (l_1 - s_i) = 0 \tag{3}$$

We introduce the notation

$$V_{eq} = \sum_{i=0}^{n} V_i \frac{l_1 - s_i}{l_1} \tag{4}$$

for the equivalent vertical force acting on the leading stud, considering wall element 1 as a simply supported beam on two supports. The horizontal force H_1 is obtained from Eq. (3) as

$$H_1 = f l_1 = (\frac{1}{2}\frac{l_1}{h_{tot}} + \frac{V_{eq}}{f_p h_{tot}}) f_p l_1 \tag{5}$$

Adding the force contribution H_2 from wall element 2, corresponding to a pure plastic shear flow f_p, the resulting capacity of the two fictitious wall elements is obtained as

$$H = H_1 + H_2 = (\frac{1}{2}\frac{l_1}{h_{tot}} + \frac{V_{eq}}{f_p h_{tot}}) f_p l_1 + f_p l_2 \tag{6}$$

In the analysis given above the equilibrium of both storeys was considered at the same time. In the case of different wall configurations on different storeys it is easier to consider each storey separately. This is for example the case when there in a wall are vertical sheathing strips without openings mixed with vertical sheathing strips including openings. The principle is shown in Figure 3 for the wall configuration previously studied, where the internal forces also are shown in a horizontal section just above the rail of the intermediate floor. In order to obtain an even force distribution within wall element 1 we assume that the external forces V_0 to V_n and the distributed force f_p are transferred to each storey in proportion to the height of the storey. This means that the distributed vertical anchorage force in wall element 1 varies linearly between the value f_p at the bottom rail and the value zero at the top rail. This means also that the external vertical forces V_i acting on wall element 1 generate compression forces in the studs varying linearly from the value V_i at the top rail to the value zero at the bottom rail.

A dimensionless load factor η_j is introduced as

$$\eta_j = \frac{h_j}{h_{tot}} \tag{7}$$

where the height of storey no. j is denoted by h_j. The load factor η_j specifies the share of the vertical loads V_0 to V_n and the distributed anchorage force f_p that is taken up by storey no. j.

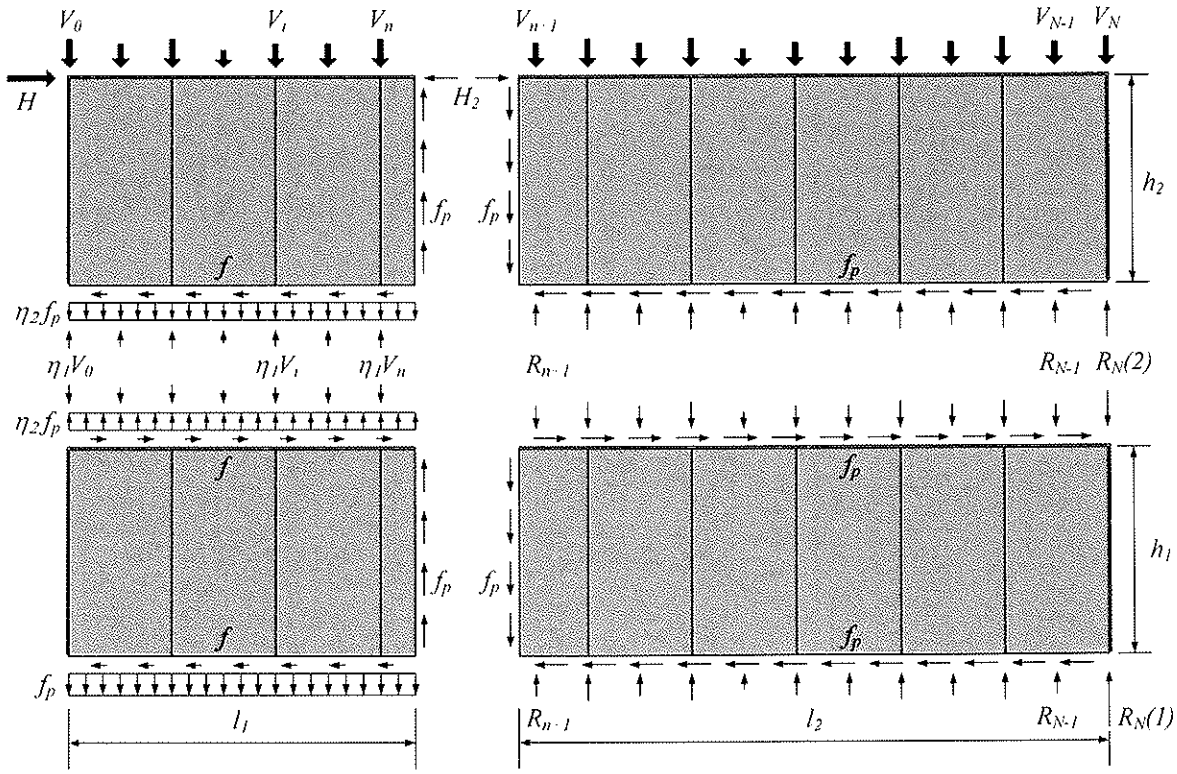

Figure 3. Assumed external and internal forces acting on a wall diaphragm with fully anchored bottom rail. The plastic capacity has been attained in the vertical section l_1 from the leading stud.

The length l_1 can, as an example, be determined by studying the equilibrium of the left part of storey no. 2 assuming that the plastic shear capacity $f_p h_2$ is attained in the vertical section of the wall shown in Figure 3, i.e.

$$\eta_2 \sum_{i=0}^{n} V_i + \eta_2 f_p l_1 = f_p h_2 \tag{8}$$

Note here that $(1-\eta_1) = \eta_2$. The difference between Eq. (1) and Eq. (8) is just that all terms in Eq. (8) have been multiplied by η_2. Eqs. (3), (5) and (6) can be derived in the same way.

In the beginning of this section it was mentioned that the stud-to-rail joints were used for taking up the distributed horizontal force f acting along the bottom rail of the left part of the wall. Two questions are relevant: Which capacity f of the framing joints is required in relation to the plastic capacity f_p of the sheathing-to-timber joints in order to ensure that we have a plastic lower bound method? What do we do if the capacity f is too low?

Some calculations have been carried out considering the influence of the framing joints and also that the distributed force of the sheathing-to-timber joints can be slightly inclined without losing any essential anchorage capacity. These calculations show that for $f = 0.3\, f_p$

no reduction of the wall capacity H needs to be done for normal wall configurations. For $f = 0$ a reduction of about 5 % is reasonable.

4 Walls with openings

The capacity of walls including openings will be studied considering the wall configuration shown in Figure 4 where the openings are placed in the same vertical sheathing strip. The principle will be demonstrated for the upper storey. First, the part of the wall left of the opening will be studied. In order to obtain a simple representation of the force distribution we divide the load case into the two separate load cases (a) and (b) according to Figure 5. Note that the vertical loads have been given new indices in comparison with Figure 4. Note also that only a fraction $\eta_j = h_j/h_{tot}$ of the external vertical loads and the distributed anchorage force f_p can be used as stabilising forces for each storey. For a two-storey building with the same wall height of each storey $\eta_1 = \eta_2 = 0.5$. Like in Chapter 3, the wall is divided into two fictitious elements of length l_1 and l_2 where element 1 is used for anchoring and element 2 is only used for shear transfer. The horizontal forces H_1 and H_2 from load case (a) are calculated considering that only a fraction η_2 of the vertical loads and the distributed anchorage force are acting on the wall.

In load case (b) a contact force H_w is assumed to be transferred from the low wall element to the left part of the wall. By studying the moment equilibrium of the low wall element, assuming that the plastic shear flow f_p has been attained, this contact force is determined as

$$H_w = f_p l_w \tag{9}$$

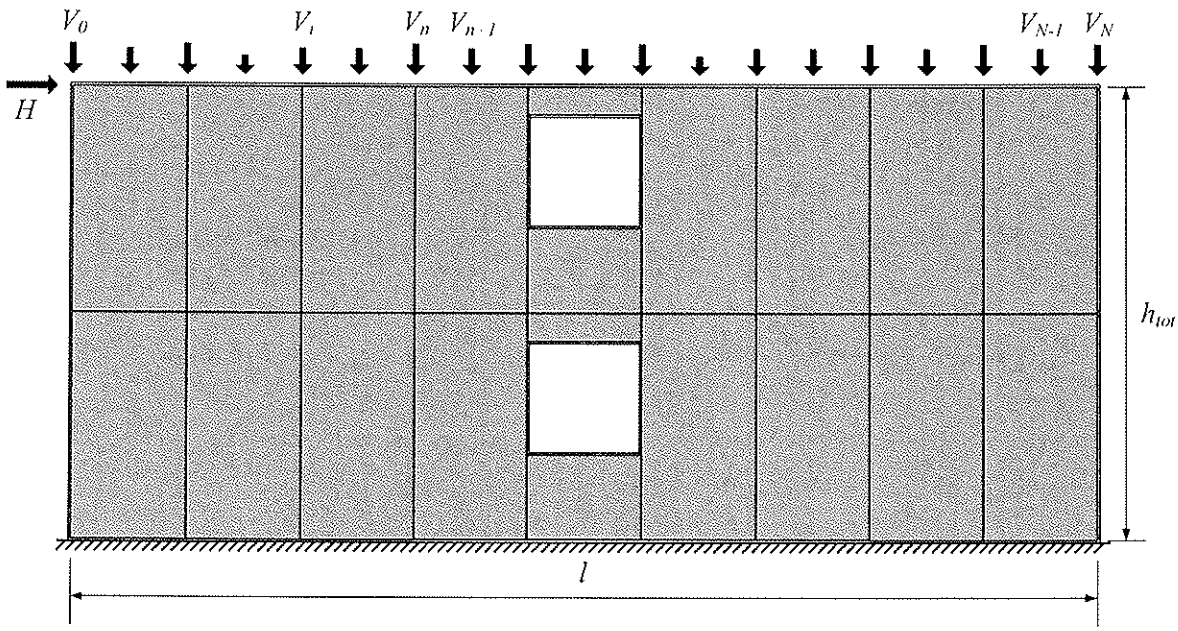

Figure 4. Forces acting on a two-storey wall diaphragm with openings and fully anchored bottom rail.

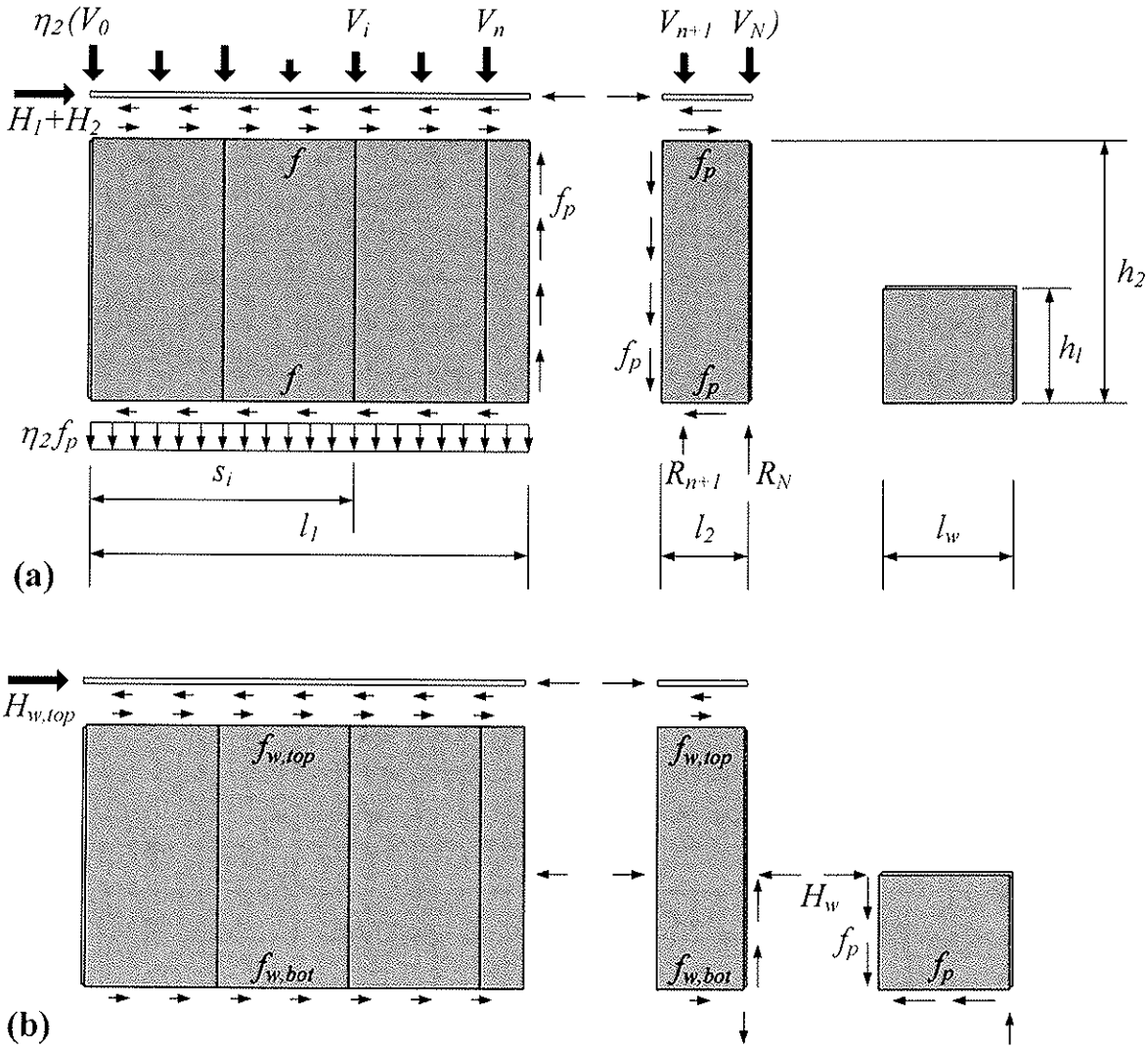

Figure 5. Assumed external and internal forces acting on the wall part left of the opening on the second storey. (a) Forces due to wall element 1 and 2. (b) Forces due to wall element below window opening.

The contact force H_w give rise to the forces $H_{w,top}$ and $H_{w,bot}$ acting along the top and bottom rail, respectively. The corresponding shear flows, denoted by $f_{w,top}$ and $f_{w,bot}$ in Figure 5, need not to be uniformly distributed. We note that $f_{w,top}$ act in the same direction as the distributed forces f and f_p along the top rail while $f_{w,bot}$ act in the opposite direction as f and f_p along the bottom rail. This means that the shear flow within wall element 1 and 2 is increased along the top rail while it is decreased along the bottom rail. Considering the equilibrium of the wall, the forces $H_{w,top}$ and $H_{w,bot}$ are obtained as

$$H_{w,top} = \frac{h_1}{h_2} f_p l_w \tag{10}$$

$$H_{w,bot} = \frac{h_2 - h_1}{h_2} f_p l_w \tag{11}$$

Adding the forces H_1, H_2 and $H_{w,top}$ we obtain the total capacity of the wall left of the opening as

$$H = H_1 + H_2 + H_{w,top} = \eta_2 (\frac{l_1}{2h_2} + \frac{V_{eq}}{f_p h_2}) f_p l_1 + f_p l_2 + \frac{h_l}{h_2} f_p l_w \tag{12}$$

So far we have not checked that the shear flow from the force H can be transferred from the top rail to the wall elements 1 and 2. Utilising both the sheathing-to-timber and the stud-to-rail joints the condition can be formulated as

$$H \le (l_1 + l_2) f_p + n_{joint} F_{joint} \tag{13}$$

where n_{joint} denotes the number of stud-to-rail joints that can be used for shear transfer and F_{joint} denotes the capacity of such a joint. Here it seems reasonable to assume that only the centre stud of each sheet can be used for such shear transfer.

Up to now only the force distribution within the second storey has been analysed. Within the first storey it is obvious that the shear flow is identical to the one within the second storey. The distributed anchorage forces, however, are higher within the first storey than within the second storey. Considering that the distributed anchorage force along the top rail of wall element 1 together with the distributed horizontal force give rise to an inclined force, we find that for the first storey the condition given by Eq. (13) should be modified to

$$H \le (\sqrt{1 - (1 - \frac{1}{n_{storey}})^2}\, l_1 + l_2) f_p + n_{joint} F_{joint} \tag{14}$$

where n_{storey} denotes the number of storeys in the wall studied. The capacity of the wall part left of the opening consequently can be expressed as

$$H = \min \begin{cases} \eta_2 (\frac{l_1}{2h_2} + \frac{V_{eq}}{f_p h_2}) f_p l_1 + f_p l_2 + \frac{h_l}{h_2} f_p l_w \\ (\sqrt{1 - (1 - \frac{1}{n_{storey}})^2}\, l_1 + l_2) f_p + n_{joint} F_{joint} \end{cases} \tag{15}$$

If the length of the wall to the left of the opening is small there is a possibility that the vertical plastic shear flow f_p is not attained until within the low wall element. The solution for this load case is not presented here.

The capacity of the wall part to the right of the opening, see Figure 6, can be derived in a similar manner considering the influence of the η-factor and the cantilever.

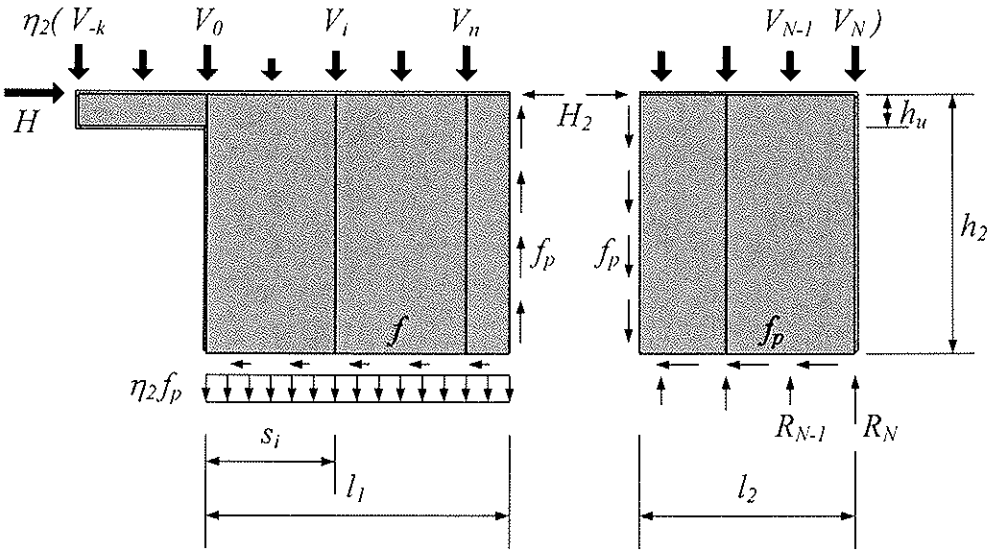

Figure 5. Assumed external and internal forces acting on the upper wall part right of the opening.

5 Anchoring by transverse walls

Transverse walls are often very effective for anchoring of wall diaphragms in shear. In Figure 7 such a situation is illustrated for a two-storey building where the bottom rail is assumed to be fully anchored. The transverse wall is in this case assumed to be subjected to a vertical uplift force resulting in the internal force distribution shown in the figure. It is noted that the vertical forces in the transverse wall must be balanced by horizontal forces in order to fulfil moment equilibrium. The horizontal forces acting on top of the transverse wall must be transferred to the floor/ceiling structure or to other parts of the transverse wall.

A theoretical background and some test results are given by the authors in [3], and [4] for one-storey transverse walls. In this paper a simple method suitable to design purposes is proposed giving results close to the previous ones reported. The simple method is based on the assumption that the sheathing-to-timber joints along the vertical studs also can transfer some tensile stresses between the adjacent sheets in contrast to the method recommended in [3] and [4].

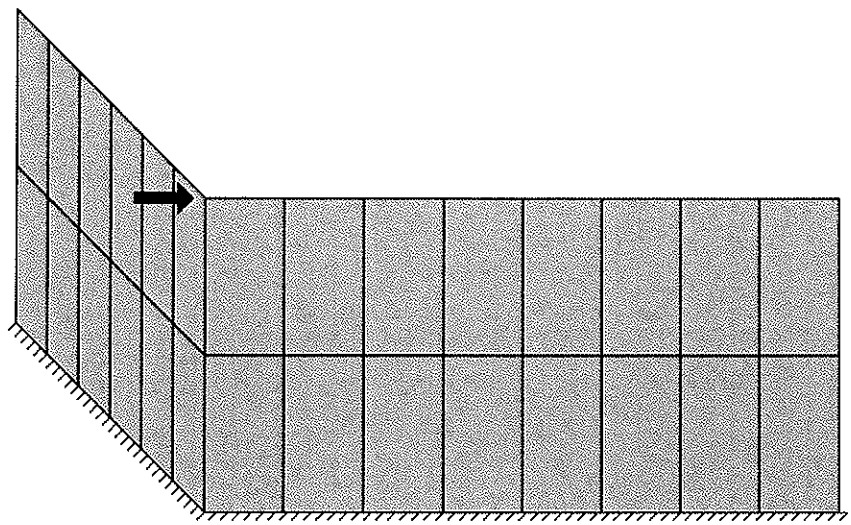

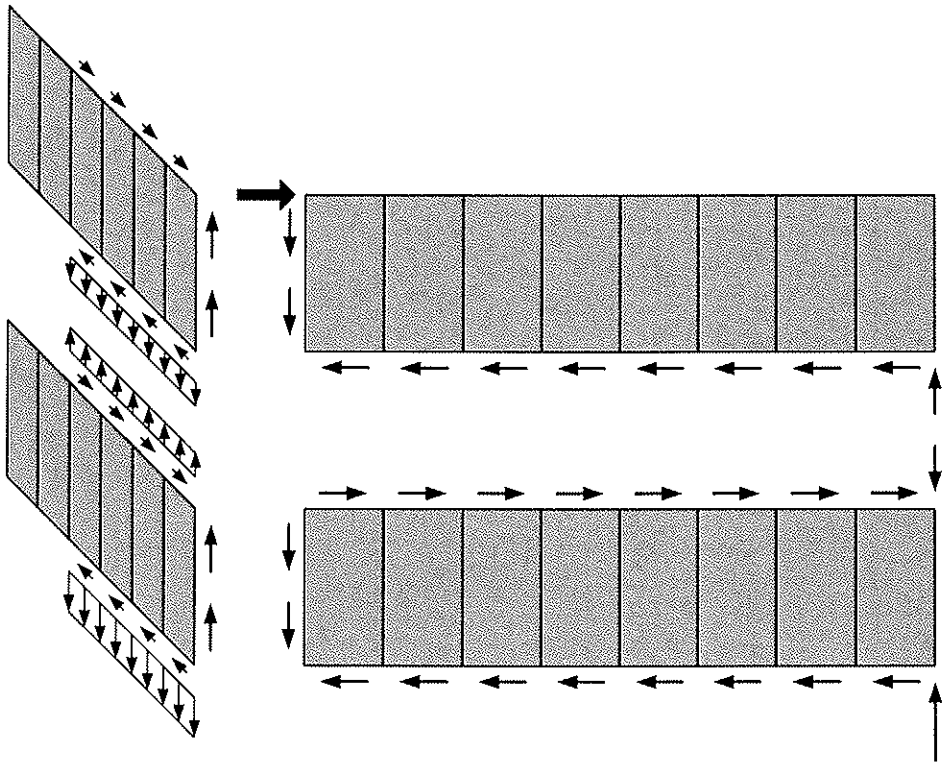

Figure 7. Assumed external and internal forces acting on a two-storey wall diaphragm connected to a transverse wall with fully anchored bottom rail.

In Figure 8 a part of a transverse wall subjected to a vertical uplift force V is shown. The top rail is assumed to be prevented from displacing horizontally, giving rise to a reaction force R. For a given distance l, the angle φ can be calculated as

$$\varphi = \arctan(\frac{l}{2h}) \tag{16}$$

Vertical force equilibrium gives

$$V = f_p l \cos\varphi \tag{17}$$

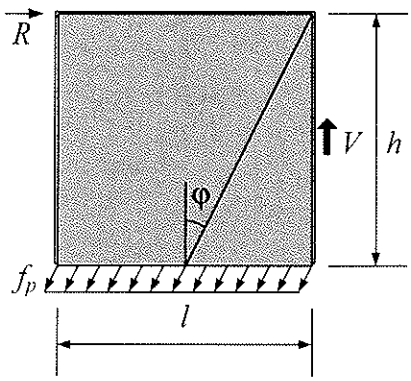

Figure 8. Assumed force distribution in transverse wall.

Insertion of Eq. (16) into Eq. (17) and considering that V must be less than $f_p h$ gives

$$V = \min \begin{cases} f_p l \cos[\arctan(\frac{l}{2h})] \\ f_p h \end{cases} \quad (18)$$

The reaction force R is obtained from horizontal force equilibrium as

$$R = f_p l \sin\varphi = f_p l \sin[\arctan(\frac{l}{2h})] \quad (19)$$

The equations above can be used for transverse walls that are more than one storey high. This means that for the load case shown in Figure 7, h is defined as the total height of the two storeys. Note also that a portion of the vertical component of the distributed anchorage force f_p must be transferred between the two storeys.

If the reaction force R only can be balanced within the transverse wall itself, then l must always be less than or equal to half the total length of the transverse wall.

6 Conclusions

A plastic method for design of wood frame wall diaphragms is presented which can be used in case of partially or fully anchored studs and fully anchored bottom rail. In this paper the method is applied to walls that are more than one storey high. The principles of the method are demonstrated for walls with and without openings. The possibility of using transverse walls for anchoring with respect to vertical uplift is illustrated.

Acknowledgements

The authors express sincere appreciation for the financial support from The Development Fund of the Swedish Construction Industry (SBUF), The Swedish Research Council for Environment, Agricultural Sciences and Spatial Planning (FORMAS), Umeå University, SP Wood Technology – Technical Research Institute of Sweden, Växjö University, The County Administrative Board of Västerbotten and The European Union's Structural Funds – The Regional Fund, together with the timber and building industry.

References

[1] Källsner, B., Girhammar, U. A.: Influence of framing joints on plastic capacity of partially anchored wood-framed shear walls. *Proceedings CIB/W18 Meeting*, Edinburgh, United Kingdom, August 31 – September 3, 2004.

[2] Källsner, B., Girhammar, U. A.: Plastic design of partially anchored wood-framed wall diaphragms with and without openings. *Proceedings CIB/W18 Meeting*, Karlsruhe, Germany, August 29-31, 2005.

[3] Girhammar U.A., Källsner B., "Effect of transverse walls on capacity of wood-framed wall diaphragms", *Proceedings CIB-W18 Meeting*, Florence, Italy, August 28-31, 2006.

[4] Girhammar U.A., Källsner B., "Effect of transverse walls on capacity of wood-framed wall diaphragms without tie-downs" *Proceedings 10th World Conference on Timber Engineering*, Miyazaki, Japan, June 2-5, 2008.

[5] Neal B.G., *Plastic methods of structural analysis*, 2nd edition, London, 1978.

INTERNATIONAL COUNCIL FOR RESEARCH AND INNOVATION
IN BUILDING AND CONSTRUCTION

WORKING COMMISSION W18 - TIMBER STRUCTURES

FAILURE ANALYSIS OF LIGHT WOOD FRAME STRUCTURES UNDER WIND LOAD

A Asiz
M Noory
Y H Chui
I Smith

University of New Brunswick, Fredericton

CANADA

Presented by A. Asiz

Tom Williamson said that high wind area requires hurricane anchors. He received clarification of the details of the connections for concrete slab end with raised floor foundation (toe nailed first and anchors will be tied at University of Western Ontario tests). As such this also depends on the detailing of the raised wall. A. Buchanan asked about the contribution of gypsum and interior lining which is important. A. Asiz answered that this is not considered in the model and will look into this as part of the model. A. Asiz said that the contribution from gypsum is approximately 25% to the system of the system but older gypsum boards may not be very durable. A. Buchanan said this in such case better quality gypsum board would be needed. A Salenikovich questioned and Y.H. Chiu confirmed that system factor will depend on geometry and energy absorption mechanism.

Failure Analysis of Light Wood Frame Structures Under Wind Load

Andi Asiz, Ying Hei Chui and Ian Smith
University of New Brunswick, Canada

1. Introduction

North American style light wood frame buildings are known to have excellent ability to withstand short-term extreme loads, such as those caused by earthquakes and strong wind. This is due to its highly redundant structural form and the use of slender fasteners in connecting components together. Structural redundancy offers alternative load paths and redistribute applied loads when one member or connection fails. Slender fasteners such as nails fail by plastic yielding and therefore are a major source of energy absorption under extreme loads. These factors allow light frame wood structures (LFWS) to exhibit some level of damage and undergo large deformation without collapse.

The current generation of material design codes generally have only one level of limit state i.e. failure. In recent years, there has been interest to offer design engineers the option of selecting various levels of limit state at the design stage, in accordance with the severity of the anticipated damage when 'failure' occurs. As an example, one limit state differentiation system that has been proposed for steel structures consists of five levels of structural damage; light damage, moderate damage, serious damage, complete damage without loss of life and complete damage with loss of life. Due to their highly redundant structural form and energy absorbing capability, light wood frame buildings are an ideal candidate for the timber engineering community to explore the feasibility of adopting this new design methodology in timber design codes.

Researchers at the University of New Brunswick (UNB), in conjunction with colleagues from a number of Canadian universities, industrial and research organizations, are conducting a research project to investigate the system behaviour of light wood frame structures. The ultimate goal of this project is to generate design code provisions that recognize the benefits brought about by structural redundancy and the presence of ductile elements in a structure. This project dovetails previous and other current projects in Canada, also involving UNB researchers, that investigate how wind loads are transmitted through a light wood frame structure.

One of the key activities of the system design project is to investigate the failure process of three-dimensional light wood frame structures, using finite element program. To that end, a typical one-storey North American wood frame house is analysed using the finite element program. The focus of this exercise is on response of the structure to wind loads. As failure in light wood frame structures is likely to occur in connections between sub-systems, such as wall, roof and floor, an extensive connection test program is being conducted to obtain the complete load-deformation response, including strength and stiffness degradation, of these connections, which is used as input into the finite element program.

The objective of the research discussed in this paper is to identify location of first failure in these structures and how the applied loads will be distributed after progressive failure of structural elements or connections. This project will allow researchers to study how the structures will continue to resist applied loads after progressive level of structural damage, leading to possible definitions of various levels of limit state, as was discussed above.

To understand load distributions and internal force flows and failure mechanisms of LFWS it is necessary to study complete three-dimensional building systems, with finite element models being a convenient theoretical tool. Several finite element (FE) models of light-frame buildings have already been created. Early models were quite simplistic, limited to static linear-elastic analyses, and implemented through specially developed FE programs (Gupta and Kuo 1987; Nateghi 1988). Efforts have been made recently to develop models capable of predicting nonlinear and dynamic behaviours using either extensive FE programming (application-specific coding), advanced commercially available software, or a combination of both involving user-defined elements (Collins et al. 2005). All models to date focus on prediction of global responses like movements at key locations rather than prediction of localized damage.

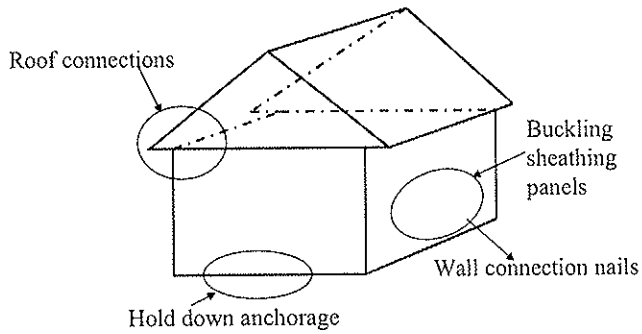

Figure 1: Possible failure locations of LFWS building under lateral loads

Numerical LFWS models should be equipped with solution algorithms that can predict failure mechanisms and the associated failure load at any response scale. Experimental and field observations of failure mechanisms in light-frame buildings (subjected to simulated or real natural hazards, respectively) indicate that the type of damage depends on the type of external load applied and the construction details (Foliente 1998). Lateral loads produced from wind storms and earthquakes produce different failure mechanisms. The magnitude of wind loads is dependent on the exposed surface areas of the building, whereas earthquake force depends significantly on the mass and stiffness of the structural system. However, the typical failure mechanisms in LFWS buildings subjected to lateral loads can still be broadly categorised as involving damage at: wall stud-to-sheathing connections, hold-down and other anchorage points, and buckling of sheathing (Liska and Bohannan 1973; Patton-Mallory et al. 1985) as shown in Fig. 1. With respect to the wind load regardless of the type of construction, buildings are subjected to two basic types of loads. Uplift loads result from air flowing over the roof causing a suction force. Lateral loads result from wind blowing on the windward wall as well as wind blowing past the leeward wall. These two lateral forces act in the same direction and combine together to create a force that tries to push the building over or slide it in the direction of the wind.

The remainder of the paper is focussed on non-linear and failure analysis of a single-storey LFWS building subjected to wind load using a finite element model to elucidate system effect in the structural performance.

2. Three-dimensional structural model

A 9 m x 12.6 m one-storey residential wood building was modelled using commercial FE software SAP2000 version 11 (CSI 2007) as shown in Figure 2. The height of the structure up to the roof ridge is 3.53 m, and the exterior wall height is 2.66 m. The arrangement followed the so-called platform frame construction method wherein a floor platform is constructed to extend fully beneath all walls and above a perimeter supporting foundation wall. Selection of the structural members and other components was based on construction guidelines from the Canada Mortgage and Housing Corporation (CMHC 2003). Linear-elastic orthotropic shell elements were used to model the sheathing panels in the walls, roof and floor plate. Those elements

had four nodes with six degrees of freedom at each node. Wall studs, floor joists, and roof truss framing members were modelled using two-node linear frame elements with six degrees of freedom at each node. Roof rafter and tie members were made continuous within their length with hinge joints at apex and heel connections. Interior truss members were hinge connected to rafters and the tie. Internal wall partitions were connected to the floor frame and exterior wall frames, but they were not connected to the roof frames. Mechanical properties and element types used are given in Table 1, with mechanical properties taken from previous thesis projects at the University of New Brunswick (Mi 2004; Winkel 2006).

All nailed sheathing-to-framing and framing-to-framing connections were modelled using non-linear link elements composed of internal springs with axial, shear and rotational degrees of freedom. Figure 2c shows typical modelling of connections at a corner junction where walls and the roof meet. 3mm gaps were included between wall sheathing panels to simulate discontinuities existing in practice, Figure 2d. Properties of the link elements for each degree of freedom were derived from experimental load-deformation responses and are summarised in Table 2.

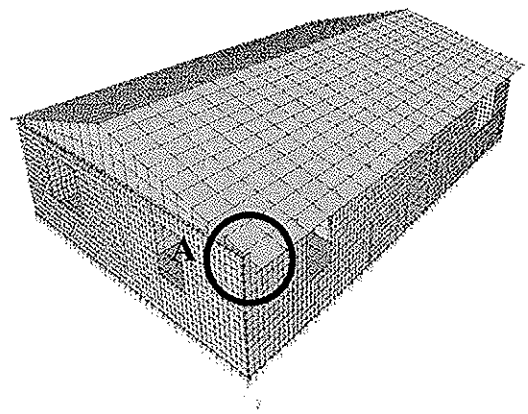

(a) whole building

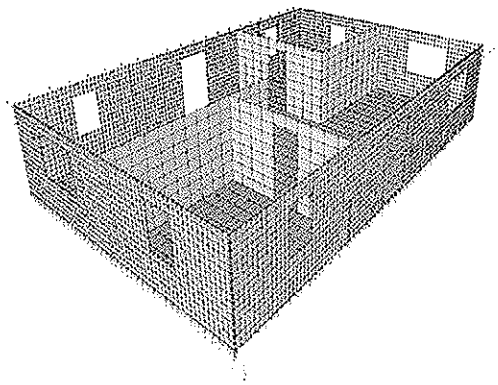

(b) external and internal walls

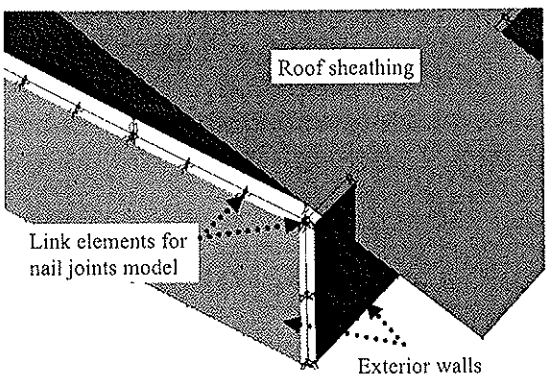

(c) corner details (detail A)

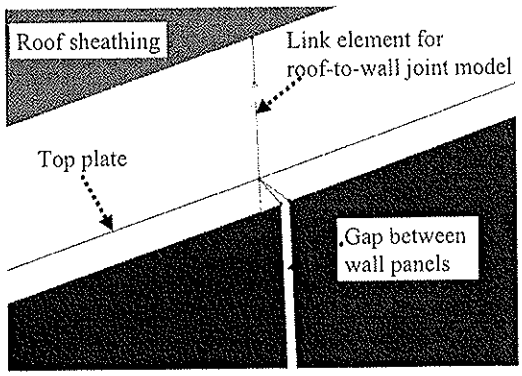

(d) wall panel-to-wall panel and wall-to-roof model

Figure 2: Three-dimensional FE model

Table 1: Mechanical properties used in the analysis (Mi 2004; Winkel 2006)

Element (mm)	Element type & thickness (mm)	Modulus of elasticity (MPa)			Poisson's ratio			Shear modulus (MPa)		
		E_x (Dir 1)	E_y (Dir 2)	E_z (Dir 3)	Dir 1-2	Dir 1-3	Dir 2-3	Dir 1-2	Dir 1-3	Dir 2-3
38x140 wall studs	Frame (38)	12000	900	500	0.3	0.3	0.3	900	700	50
OSB wall sheathing	Shell (11.1)	3000	5000	3000	0.3	0.3	0.15	1200	1700	1200
OSB roof sheathing	Shell (11.1)	3000	5000	3000	0.3	0.3	0.15	1200	1700	1200
OSB floor sheathing	Shell (15.9)	3000	5000	3000	0.3	0.3	0.15	1200	1700	1200
38x235 floor joists	Frame (38)	12000	900	500	0.3	0.3	0.3	900	700	50
38X89 truss framing	Frame (38)	12000	900	500	0.3	0.3	0.3	900	700	50

Boundary conditions at the base of exterior walls were modelled using non-linear contact-link elements with zero lengths in combination with spring elements, spaced at 2.44 m (8 ft), to represent anchor bolts connecting to the foundation. Only the outside face of exterior walls was sheathed with OSB. Modelling of door and window openings included framing modifications that are typical of building practice (CMHC 2003), but no attempt was made to model doors, windows, or their frames and glazing. So far no plasterboard wall or ceiling linings have been incorporated into the model. In total the finite element mesh generated to analyse the one-storey building comprises 11,539 nodes, 5,348 frame elements, 6,218 shell elements, and 4,294 link elements.

Table 2: Link element properties used in the analysis

Link element	Direction	Assigned stiffness (load-deformation response)
Sheathing-to-framing nails	Horizontal	Non-linear shear stiffness from connection tests by Mi (2004)
	Vertical	Non-linear shear stiffness from connection tests by Mi (2004)
Framing-to-framing nails	Horizontal	Non-linear shear stiffness from connection tests by Mi (2004)
	Vertical	Compressive mode, linear stiffness = 106.8 kN/mm (Winkel 2006)
	Rotation	Non-linear moment-rotation stiffness from connection tests by Mi (2004)
Anchor bolts	Horizontal	Linear stiffness = 2.292 kN/mm (Winkel 2006)
	Vertical	Linear stiffness, tensile mode= 53,590 N/mm Linear stiffness, compressive mode = 1 GN/mm
Roof truss-to-external wall	Horizontal	Non-linear shear stiffness from connection tests by Asiz et al (2008)
	Vertical	Non-linear withdrawal stiffness from connection tests (Asiz et al., 2008) Compressive mode, Linear stiffness = 106.8 kN/mm (Winkel 2006)

The applied uniformly distributed loads simulate code-specified wind loads and neglect the self-weight of the structure. The assumed wind direction is perpendicular to the plan of the windward wall of the building, Figure 3. A wind speed of 144 kph

(90 mph) was considered, which corresponds to a reference velocity pressure of 1000 Pa (Nateghi 1988). The wind load pressure p exerted on the building surfaces was calculated based on the following equation:

[1] $$p = qC_eC_gC_p$$

where:

q = reference wind velocity pressure (Pa),
C_e = exposure coefficient, and
C_gC_p = combined gust and pressure coefficient.

In this analysis, C_e was taken as 1.0 and C_gC_p as given in Figure 3a. No wind pressure was applied on the end walls oriented parallel with the wind direction (NRC 2005).

3. Failure analysis

To analyze post-yield (overload) behaviour of structures subject to wind loads, non-linear static analysis must be performed using load or displacement control to define the failure mechanism. The load control method was used because that is most appropriate for wind effects. All loads on elements were applied incrementally from zero to a user-specified target value. Zero initial damage conditions were assumed, i.e. no pre-stressed elements, no prior loading beyond the elastic range at the beginning of incremental analysis. Ten increments of wind speed were used with 10 iterations per step to ensure equilibrium achieved throughout the analysis satisfied a relative iteration convergence tolerance of 0.01 % of the actual force acting on the structure at the end of each load increment.

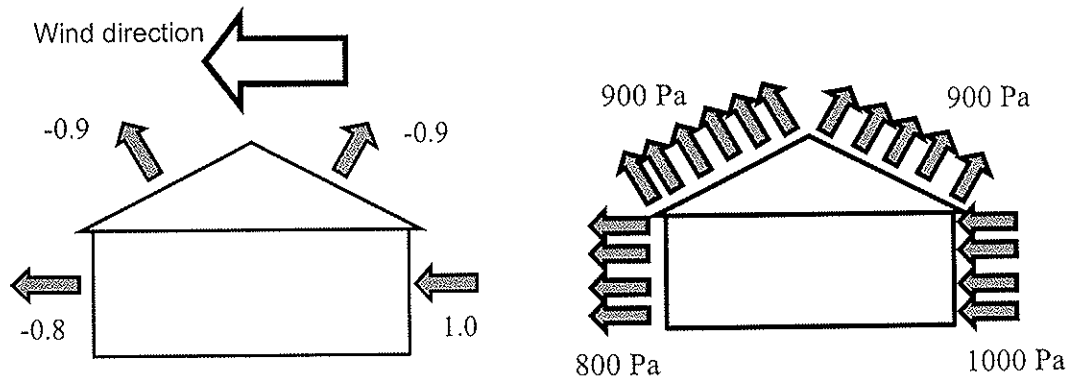

(a) Values of wind pressure coefficient C_qC_p (b) wind pressure

Figure 3: Wind pressure coefficients and associated wind pressures

The non-linear scheme in the FE software adopts the 'implicit method' to define the failure mechanisms in the structural elements. The analysis for each increment of load checks all elements that already reached post-linear (post-yield) response. However, since only nailed connections were defined as having non-linear load-deformation response, attention was focused on checking link elements such as those in the walls and roof-to-wall anchorage. When individual elements yielded, load re-distributions to adjacent elements were automatically applied within the solution algorithm. This was accomplished by applying a localized self-equilibrating condition near any element that sustained loading beyond its peak force capacity. The solution algorithm became unstable when more than one element became overloaded in a particular region where the self-equilibrating condition had previously been applied. It was assumed that progressive failure of the complete LFWS building would ensue. This

may not necessarily reflect actual behaviour but as yet alternative assumptions have not been investigated.

4. Results

Two structural models were analyzed using the same wind speed 144 kmh (90mph), one complete structure with internal wall partitions included (Model A) and another one without inclusion of all internal wall partitions (Model B). Using 2 GB-computer memory, the run time for Model A was approximately 20 minutes, while for Model B was about 3 hours. After checking the load-deformation response for all link elements, the critical elements were found to be the roof-to-wall roof truss connections where the trusses were toe-nailed to the top plates of the windward and leeward walls. Figure 4 shows the load-deformation response along the axial direction of selected link elements superimposed on the uplift response for the toe-nail connection to the top wall plate. It can be seen that the link element of the middle roof trusses for both models have reached the peak resistance of the connection, which is 2.41 kN (Asiz et al, 2008), while other link elements are still below this load. However, the numerical solution obtained in Model A was stable. After checking internal axial forces for all link elements in Model A, it was found that only one link element has reached this peak load. While for Model B the numerical solution obtained was unstable, and it was found that four link elements have reached the peak resistance of the connection. This could indicate that progressive failure has been initiated in Model B. In term of computer running time, the unstable solution needed more time to run compared to the stable solution. It can be concluded from this analysis that internal wall partition contributed significantly to the overall structural response.

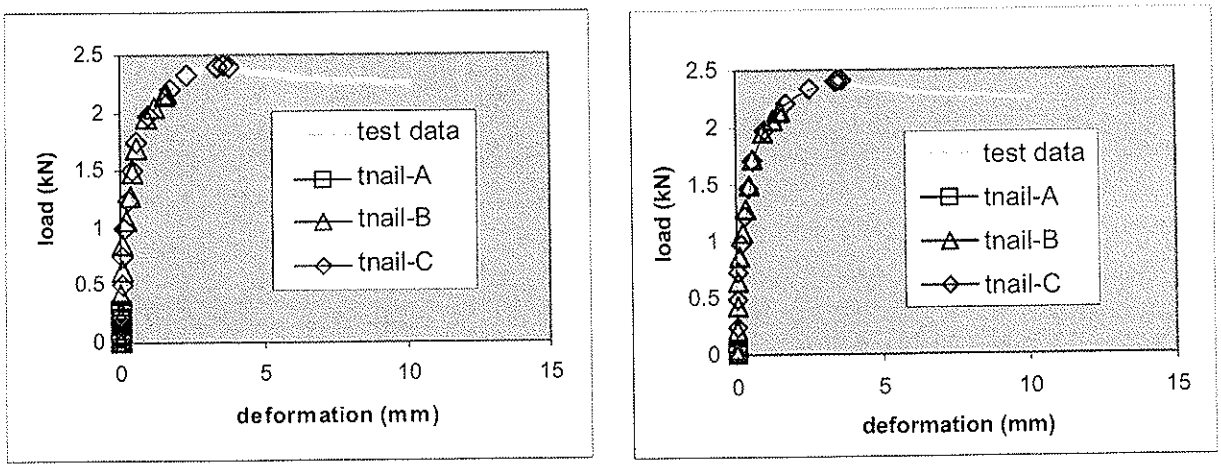

(a) Model A (b) Model B

Notes: - tnail-A=heel joint (toe-nail) at building corner, between gable frame (bottom chord) and exterior wall

- tnail-B=heel joint (toe-nail) at between the mid roof truss (bottom chord) and the top wall plate
- tnail-C= heel joint (toe-nail) at the mid roof truss
- test signifies resistance of an isolated connection tested in the laboratory(Asiz et al, 2008)

Figure 4: Load-deformation response for selected wall-to-roof toe-nail connections

Figure 5 shows contours of resultant displacement at the final increment for each model. By comparing the contour patterns, it is clear that in Model A a significant force concentration developed around the intersection of one internal wall and the external wall. The tendency towards force concentration at roof-to-wall link elements (i.e., the toe-nailed connections) was suppressed by the elimination of the internal partition walls as shown in Model B. However, since there were no internal wall supports in Model B larger lateral forces were carried by the leeward wall side causing more roof-to-wall link elements that have reached their peak resistance In general it can be concluded that openings in walls and wall junctions cause irregularities in force transfers between roofs and walls. Although it is probably premature to draw broad conclusions from the single situation analysed, the results do suggest that it is highly feasible to create quite simple construction practice 'rules' for placement of reinforcements in roof anchoring systems. However, as is often the case, reinforcement introduced at one location of a structure will shift failure location and change failure mode. It is useful to have a tool, such as the model being presented here, to evaluate these impacts before physically introducing the reinforcement.

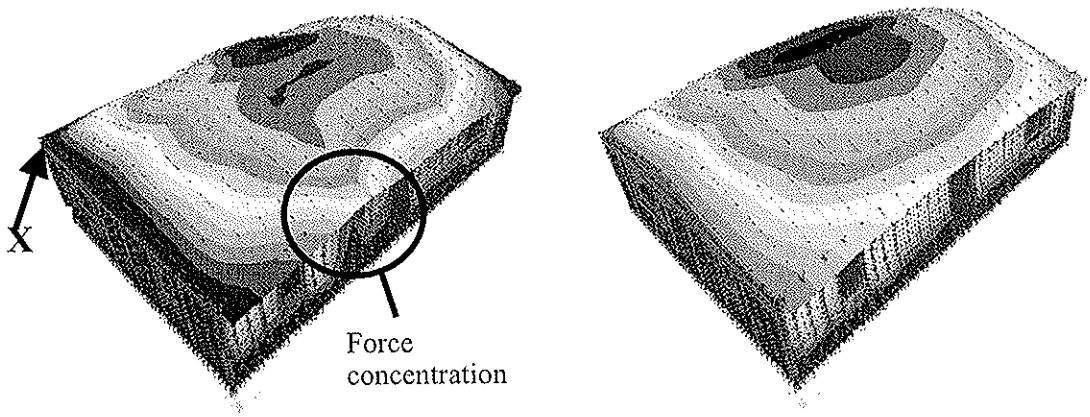

(a) Model A *(b) Model B*

Figure 5: Resultant displacement contours for the building internal walls

Figure 6 shows the displacement responses at point X (as illustrated in Figure 5a) increase as a function of the loading step. The displacement responded linearly as the load was increased when internal walls were present but not when those walls were absent. At the end of the loading step, the displacement response for Model A is about twice of that Model B. Again this is a strong indication of the systemic effects in LFWS.

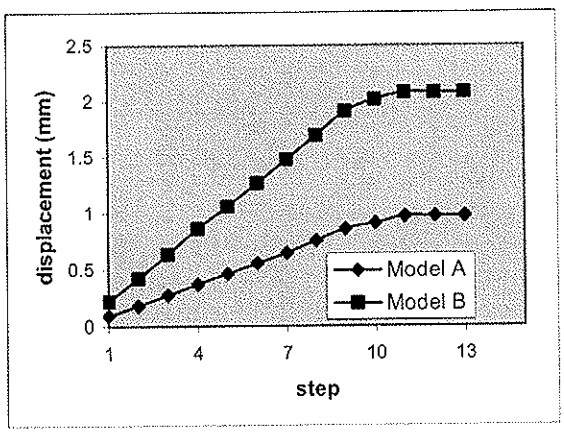

Figure 6: Displacement responses

The analysis was extended to simulate progressive failure in a manner closer to actual physical conditions. This was conducted by removing one or more link elements in the roof-wall connections that have reached the peak resistance of the connection and replacing them with the internal forces equal to their corresponding peak capacities, then re-analysing the structure. In this study, only one

stage removal was conducted, i.e. no further analysis performed after the first removal stage. For Model A, although the numerical solution obtained was stable, one link element in the roof-truss joint located in the leeward wall was removed to further check whether failure would propagate. For Model B, four link elements were removed from the roof-truss joints located on the leeward wall. The results showed that for Model A the numerical solution obtained was still stable, while for Model B the solution was unstable. Further checking of the internal axial forces in Model B indicated that several link elements adjacent to the removed link elements produced much larger deformation than those before removal of these elements. This finding reinforced the previous analysis result that progressive failure occurred in Model B. Figure 7 shows the deformed shape comparison between Models A and B before and after removal of some of the link elements. Force redistributions in these elements before and after elements removal are discussed in the following section.

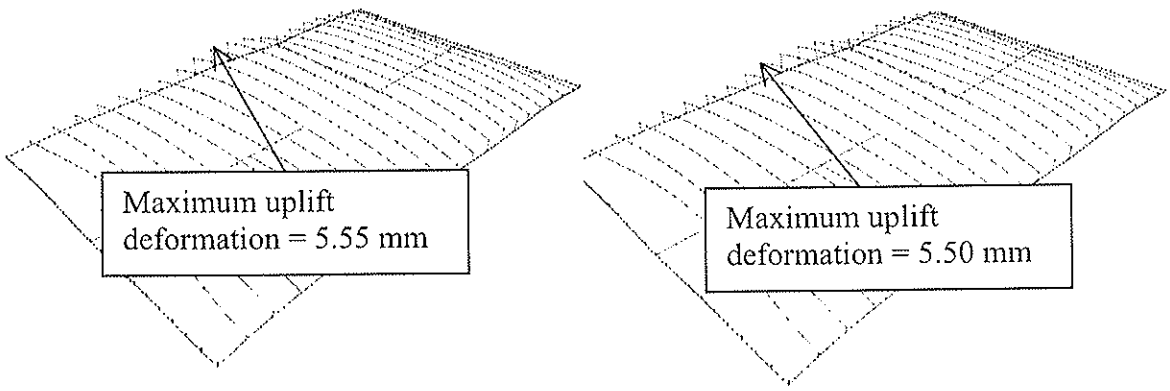

(a) Model A, intact structure

(b) Model A, after removing one link element

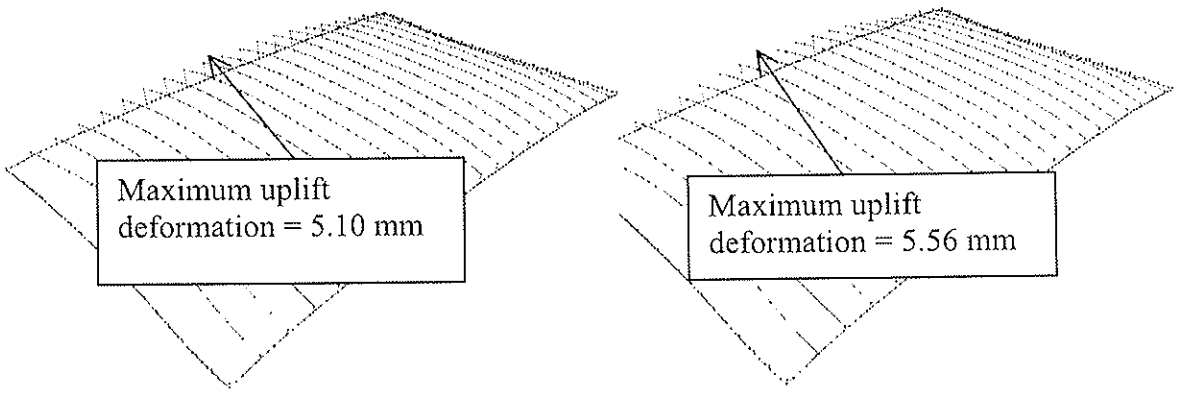

(c) Model B, intact structure

(d) Model B, after removing four link elements

Figure 7: Deformed shapes at the roof-to-wall junction

5. Load distribution

This section describes how the applied wind load is redistributed to other structural components when the internal axial (uplift) forces in the link element(s) have reached the peak resistance of the toe-nail connection. To find the force redistribution, internal shear and axial forces in the link elements between the roof and exterior wall frames, including the toe nail joints between the roof truss-top wall plate and in the joints between the gable frame-top wall plates, were extracted from the load-deformation responses.

Uplift design load (un-factored) distribution in the roof-to-wall joint can be determined by simply calculating the reaction force of simply supported roof sub-system subjected to wind suction force shown in Figure 3 (Figure 8). This reflects common calculations performed by design engineers. Figure 9 shows the axial force predicted by the FE program in each wall-to-roof joint located on the leeward wall before removing some of the link elements in Models A and B. In general it can be seen that the uplift forces based on simple mechanics calculation performed by engineers agrees very well with those predicted by the 3-D FE program. Some of the axial forces in the connections slightly exceeded the uplift design load calculated by simple mechanics for Models A and B. However, as described previously, roof-wall joint failure was considered to occur in Model B due to unstable numerical solutions obtained before and after removal of four link elements. Comparing to the design load (un-factored), significant force reduction was observed at the corner of the roof-wall anchorage due to corner and gable frame effects. Load redistribution was observed in the link elements for Models A and B adjacent to the removed link elements that have reached the peak resistance (Figures 10 and 11).

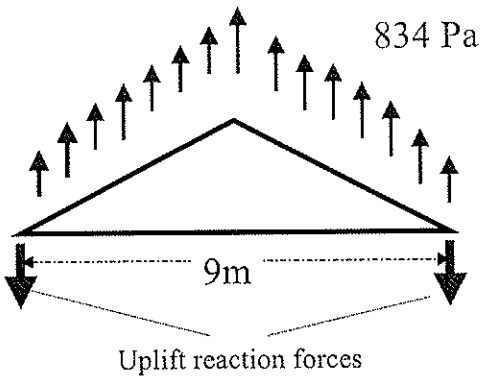

Figure 8: Uplift force distribution

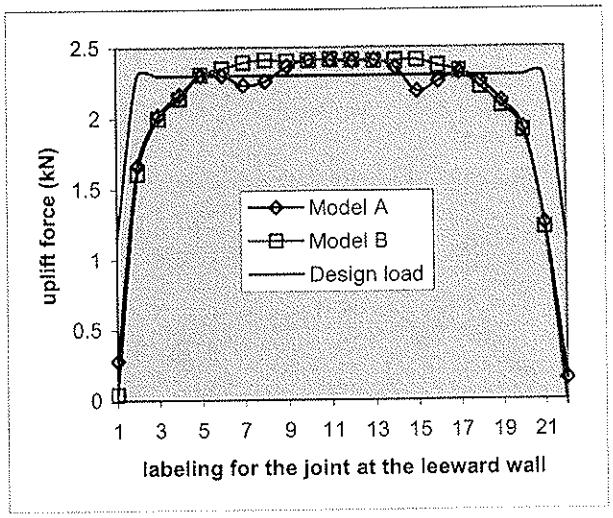

Figure 9: Uplift force distribution before removal of link elements

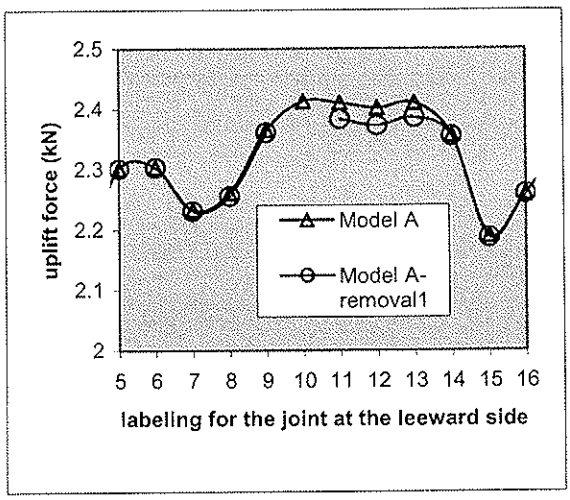

Figure 10: Uplift force redistribution after removal of one link element in Model A

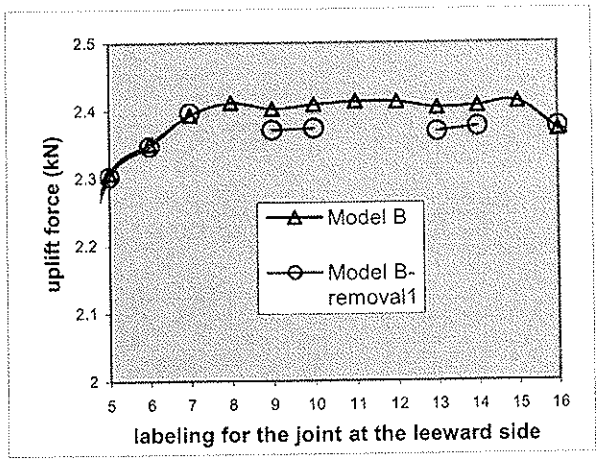

Figure 11: Uplift force redistribution after removal of four link elements in Model B

Figure 12 shows the lateral load distribution in LFWS due to wind pressure (p) commonly used in design practice, considering rigid roof diaphragm behaviour relative to the wall components and ignoring stiffness contribution of the internal wall partitions (CWC, 2001). In this figure, no wind pressure was considered on the roof because the lateral components of the wind suction pressure acting perpendicular to the roof envelope cancelled each other out (Figure 3). The wall receiving the wind pressure distributes the top half of its horizontal wind load to the roof and the bottom half to the foundation. The portion of the load going to the roof tends to cause the roof to move laterally, and this lateral movement is resisted by the end walls.

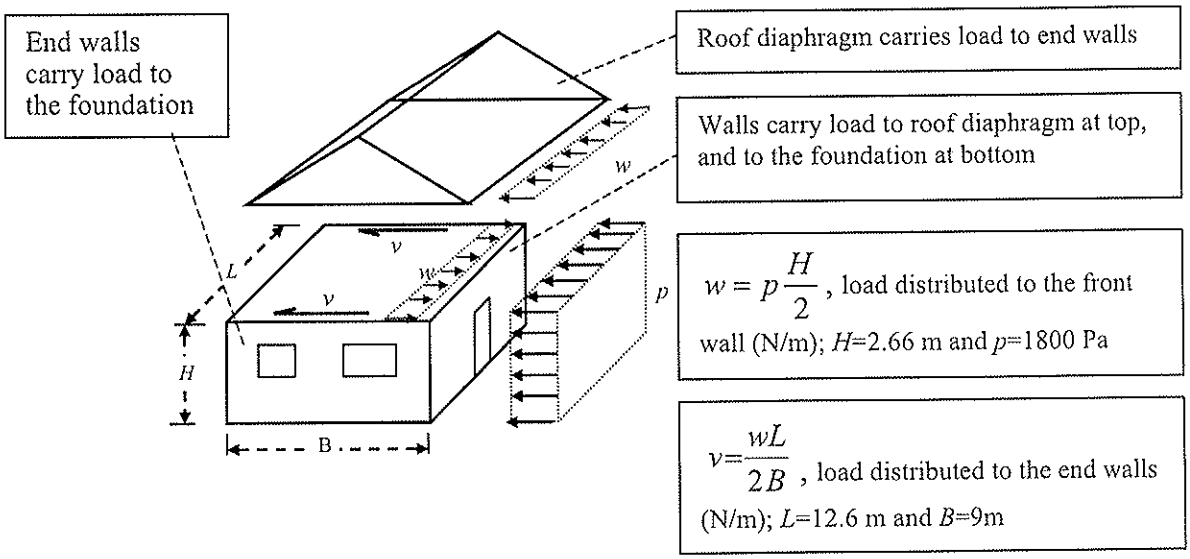

Figure 12: Lateral load distribution due to wind load

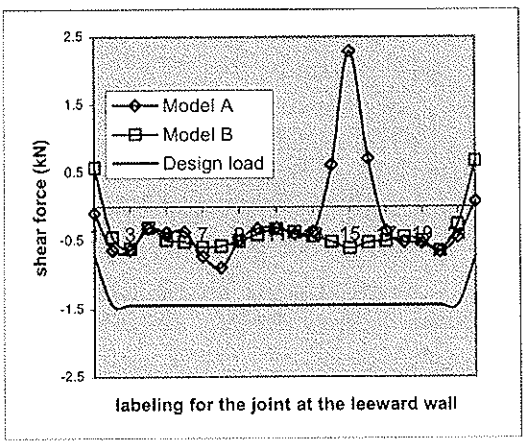

Figure 13: Shear load distribution

Table 3: Lateral load distributions (kN)

	Loaded wall
Model A	6.20
Model B	13.48
Design practice (Figure 13)	15.08

Figure 13 shows the shear force distribution in the roof-to-wall joints perpendicular to the roof ridge. Since there are no lateral loads applied in the direction parallel to the roof ridge, no shear forces were generated in this direction. In general it can be noted that there is a significant difference between Model A and Model B in distributing load to the roof-wall joint from the loaded wall. This is because the presence of internal wall partitions in Model A that changes the direction of the shear force response in the roof-to-wall joints near the junction of internal and external walls.

Table 3 shows summary of the lateral load distributions for Models A and B, which included the total shear force contribution in the gable frame-to-end wall joints. It also included the lateral design load calculated using diagram shown in Figure 3, which ignored the gable-ends effect. It can be seen that the lateral load distribution for Model B is close to those of the design practice, because the load is distributed almost equally to the end walls. Small difference in the value could be due to unsymmetrical arrangement of the openings. Furthermore, for particular structural models studied here, ignoring the internal walls contribution to the overall structural response leads to over-conservative design. This is in accordance with previous analytical study conducted by Kasal et al (2004) and Paevere et al (2003) that shear wall force (v) could be over-predicted by more than 100%, in which load distribution in building is idealized such as shown in Figure 3.

The shear forces developed in these joints were also checked after a few elements were removed from the structure. It was found that no apparent load re-distribution was observed for both models. This is because the shear responses in the link elements are far below the peak resistance of the connection, i.e. still in the linear range. (Note: The ultimate shear resistance for the toe-nail connection is around 6.6 kN for the perpendicular to the roof-ridge direction and 9.3 kN for the parallel to the roof-ridge (Asiz, et al., 2008)).

6. Discussion

The finding that a 144 kph wind causes failure of typical toe-nailed roof-to-wall connections for LFWS without internal wall partitions (Model B) is consistent with practical experience that most such connections fail when the wind speed exceeds 144 kph (Cheng 2004). However, so far only one wind direction and one pressure distribution have been considered for a single-storey LFWS building. In reality turbulence in wind creates temporally and spatially varying pressures on building surfaces rather than a uniformly distributed pressure as specified in design codes. This topic deserves further investigation. To supplement the numerical modelling work reported here, a full-size experiment is being planned to investigate the influence of temporal and spatial variation on failure behaviour of the roof-wall connections.

7. Concluding remarks

Although rather limited in scope to date, the numerical simulations reported here clearly demonstrate the importance of systemic thinking in structural design of light-frame wood buildings. What is reported is part of consortium research in Canada aimed at creating a new generation wood engineering design methods and design code provisions.

Acknowledgements

The authors gratefully acknowledge the financial support provided by Natural Resources Canada under the Value to Wood Project 'Development of Advanced System Design Procedures for the Canadian Wood Design Standard (2007-09). This project is being performed under a Steering Committee which consists of members from the industry, those being Ms. Peggy Lepper of Canadian Wood Council, Mr Dominique Janssens, formerly of Structural Board Association, Mr Ken Koo of Jager Building Systems and Dr. Marjan Popovski of FPInnovations – Forintek Division. Dr. Frank Lam from the University of British Columbia is an academic partner in the project.

References

Asiz, A. Chui, Y.H. Smith, I. 2008. Development of Advanced System Design Procedures for the Canadian Wood Design Standard, *UNB01 Progress Report-Year 1*, Natural Resources Canada under the Value-to-Wood Program, Ottawa, ON, p 84.

Canada Mortgage and Housing Corporation (CMHC). 2003. *Canadian wood-frame house construction.* Canada Mortgage and Housing Corporation, Ottawa, ON.

Canadian Wood Council. 2001. *Engineering Guide for Wood Frame Construction*, Ottawa, ON.

Cheng, J. 2004. Testing and analysis of the toe-nailed connection in the residential roof-to-wall system. *Forest Products Journal*, 54(4): 58-65.

Collins, M., Kasal, B., Paevere, P., Foliente, G.C., 2005. Three-dimensional model of light frame wood building. I: Model description. *ASCE Journal of Structural Engineering*, 131(4): 676-683.

Conner, H.W., Gromala, D.S., Burgess, D.W., 1987. Roof connections in houses: Key to wind resistance. *ASCE Journal of Structural Engineering*, 113 (12): 2459-2474.

Computers and Structures Inc. (CSI). 2007. *Structural Analysis Program SAP2000-NonLinear version 11-User Guide.* Computer and Structures, Inc., Berkeley, CA.

Foliente, G. 1998. Design of timber structures subjected to extreme loads. *Progress in Structural Engineering and Materials*, 1(3): 236-244.

Gupta, A. K. and Kuo, G.P. 1987. Modeling of a wood-framed house. *ASCE Journal of Structural Engineering*, 113(2): 260-278.

Kasal, B., Collins, M.S., Paevere, P., Foliente. G.C. 2004. Design Models of Light Frame Wood Buildings under Lateral Load, *Journal of Structural Engineering*, 130 (8): 1263-1271.

Liska, A. J. and Bohannan, B. 1973. Performance of wood construction in disaster areas. *ASCE Journal of the Structural Division*, 99(ST12): 2345-2354.

Mi, H. 2004. *Behaviour of unblocked wood shearwalls*. MScFE Thesis, University of New Brunswick, Fredericton, NB, 220p.

Nateghi, F. 1988. Analysis of wind forces on light-frame timber structures. *Doctoral Dissertation*, Dept. of Civil Engineering, University of Missouri, Columbia, MO. 194p.

National Research Council (NRC). 2005. *National Building Code of Canada.* National Research Council, Ottawa, ON.

Paevere, P., Foliente. G.C., Kasal, B. 2003. Load-Sharing and Redistribution in a One-Story Woodframe Building, *Journal of Structural Engineering*, 129 (9): 1275-1284.

Patton-Mallory, M., Wolfe, R., Soltis, L., and Gutkowski, R. 1985. Light-frame shear wall length and opening. *ASCE Journal of Structural Engineering*, 111(10): 2227-2239.

Winkel, M. 2006. *Behaviour of light-frame walls subject to combined in-plane and out of plane loads*. MScFE Thesis, University of New Brunswick, Fredericton, NB, 191p.

INTERNATIONAL COUNCIL FOR RESEARCH AND INNOVATION
IN BUILDING AND CONSTRUCTION

WORKING COMMISSION W18 - TIMBER STRUCTURES

COMBINED SHEAR AND WIND UPLIFT RESISTANCE OF WOOD STRUCTURAL PANEL SHEARWALLS

B Yeh

T G Williamson

APA – The Engineered Wood Association

USA

Presented by B. Yeh

Y.H. Chiu received confirmation about the one of the failure modes as cross grain bending. A. Asiz asked about combined uplift and shear in 3 dimensions. T. Williamson said that this is not considered as the test is one of the most complicated set up at APA already. I. Smith said that the out of plane motion does not have interaction with the in plane motion. S. Winter asked why through anchor from top was not used. B.J. Yeh responded that a lot of cases this is not used in practice as it is too expensive. F. Lam asked about the dead load and its possible influence with the shear. B.J. Yeh answered that this is not yet done but will consider it in the future.

Combined Shear and Wind Uplift Resistance of Wood Structural Panel Shearwalls

Borjen Yeh, Ph.D., P.E. and Thomas G. Williamson, P.E.
APA – The Engineered Wood Association, U.S.A.

Abstract

Shearwalls constructed with wood structural panels, such as plywood and oriented strand board (OSB), have been used to resist combined shear and wind uplift forces for many years in the U.S. For example, the Southern Building Code Congress International (SBCCI) published SSTD 10, *Standard for Hurricane Resistant Residential Construction*, in 1999, which provided the shear resistance table for wood structural panels. When wood structural panels are used in combined shear and wind uplift, SSTD 10-99 also tabulated the wind uplift resistance of wood structural panels with a minimum thickness of 12 mm (15/32 in.) when used in conjunction with the shear resistance table.

Working with researchers at the National Home Builders Association Research Center (NAHB RC), Norbord Industries sponsored full-scale combined shear and uplift tests, showing that the cross-grain bending of the bottom plate, which is a brittle failure mode, could be avoided by using 5.8 x 76 x 76 mm (0.229 x 3 x 3 in.) plate washers with anchor bolts. The NAHB RC tests were conducted in lateral shear and tension (uplift) separately, and the effect of combined shear and uplift was evaluated based on an engineering analysis.

After reviewing the NAHB RC study, APA and Norbord jointly conducted full-scale combined shear and wind uplift tests at Clemson University to gather more data on this subject. The test setup at Clemson University was capable of increasing the shear and wind uplift forces simultaneously until failure was reached by using a pulley system controlling the bi-axial forces in both lateral and vertical directions. Results of the Clemson study were used to support the development of engineering standards and changes to the national building code in the U.S., and are reported in this paper.

In 2007, APA constructed new combined shear and wind uplift test equipment that is capable of bi-axial loading in both lateral and vertical directions with independent but synchronized loading mechanisms. The vertical load can be applied as either an uplift force or a downward gravity load. Research results using this new equipment are utilized to enhance the understanding of the design on the bi-axial combined shear and wind uplift. This paper describes the latest finding from this research.

1. Introduction

Wood structural panels, by definition of the U.S. International Building Code (IBC) [1] and International Residential Code (IRC) [2], include plywood manufactured in accordance with Voluntary Product Standard PS1, *Structural Plywood* [3], and oriented strand boards (OSB) and plywood manufactured in accordance with Voluntary Product Standard PS2, *Performance Standard for Wood-Based Structural-Use Panels* [4]. While most wood structural panels are specified based on their span rating, the mechanical properties of wood structural panels are published by APA – The Engineered Wood Association in the *Panel Design Specification* [5]. When used as a lateral force resisting element, wood

structural panels can be designed in accordance with the shearwall design values established by APA and published in the IBC.

Most buildings subjected to lateral forces from wind are usually subjected to simultaneous wind uplift forces. Shearwalls constructed with wood structural panels have been used to resist combined shear and wind uplift forces for years in the U.S. For example, the Southern Building Code Congress International (SBCCI) published SSTD 10, *Standard for Hurricane Resistant Residential Construction* [6], in 1999, which provided not only the shear resistance, but also the wind uplift resistance of wood structural panels. When wood structural panels are designed to resist combined shear and wind uplift forces, SSTD 10-99 tabulated the wind uplift resistance of wood structural panels with a minimum thickness of 12 mm (15/32 inch) when used in conjunction with the shear resistance table.

The SSTD 10 wind uplift table was developed based on the principle of engineering mechanics. It assumes that the nails installed in the shearwall assembly are used primarily to resist the lateral shear forces. If there are extra nails that are beyond the demand for the lateral shear resistance, they can be used to resist wind uplift forces. The through-the-thickness shear and tensile strength of the sheathing are checked, but they do not govern the capacity of the wall. While this principle seems straightforward, a major concern in this application is the possible cross-grain bending of the bottom wall plate due to the non-concentric uplift forces acting on one face of the wall. This cross-grain bending can split the bottom plate, usually 2x4 lumber, and the design value for this property is unavailable in the code. Therefore, a practical solution to avoid this failure mode is to specify anchor bolts at a tight spacing with plate washers that are thick and wide enough to hold the bottom plate in place without inducing splitting.

Due to the merge of three regional U.S. model building codes into the IBC in 2000, SBCCI was no longer in existence as an organization and SSTD 10 has not been maintained. In 2005, the Institute for Business & Home Safety (IBHS) published the *Guidelines for Hurricane Resistant Residential Construction* [7] based on SSTD 10. In the meantime, the International Code Council (ICC) is developing ICC 600, *Standards for Residential Construction in High Wind Regions* [8] and the American Forest & Paper Association (AF&PA) is also revising the 2005 ANSI/AF&PA *Special Design Provisions for Wind and Seismic* (SDPWS) [9]. All of the referenced standards mentioned above contain provisions for combined shear and wind uplift using wood structural panels. The SDPWS revisions include the re-calculation of the mechanics-based uplift resistance using the nail yield model, as given in the 2005 *National Design Specification for Wood Construction* (NDS) [10].

In support of these code and standard development activities, APA and its members, specifically Norbord Industries, conducted full-scale combined shear and uplift tests at Clemson University in 2006. An additional series of tests were conducted at the APA Research Center, Tacoma, Washington, in 2008. This paper provides results and analyses from those tests.

2. Materials and Test Methods

2.1 Material Description

The full-scale tests conducted at Clemson University in 2006 were largely designed to address the concern of cross-grain bending of the bottom wall plate. In a previous pilot study conducted by the National Home Builders Association Research Center (NAHB RC) [12] in 2005, it was shown that the cross-grain bending of the bottom plate could be

avoided by using 5.8 x 76 x 76-mm (0.229 x 3 x 3-in.) plate washers with 15.9-mm (5/8-in.) diameter anchor bolts spaced at 406 mm (16 in.) on center. However, the NAHB RC study was conducted in lateral shear and tension (pure uplift) separately, and the effect of combined shear and uplift was evaluated based on an engineering analysis. The Clemson study was conducted in full-scale to apply the shear and uplift forces simultaneously so that the ultimate shear and uplift forces could be reached approximately at the same time.

A total of seven full-scale walls were tested at Clemson University using 11-mm (7/16-in.) commodity OSB sheathing (rated Wall 24) supplied by Norbord Industries. Due to the length limitation of this paper, only one typical framing detail (for Walls 4a and 4b) is shown in Appendix A. The framing materials (2x4 No. 2 spruce-pine-fir) were purchased from a local lumber yard by Clemson University with an estimated moisture content of 16% or higher. The holdowns were ordered from Simpson Strong-Tie. Most test assemblies were constructed by Clemson's students with very limited wall framing experience and therefore the workmanship was expected to represent the lower end of construction practice. Other test details are summarized in Table 1 and below.

Table 1. Summary of test assemblies conducted at Clemson University [a]

Wall ID	Nail spacing [b]	Holddown	Plate washer	Uplift	Shear
1a	152&305 mm (6&12 in.)	Yes	3.2 x 76 x 76 mm (0.125 x 3 x 3 in.)	x	NA
1b	152&305 mm (6&12 in.)	No	5.8 x 76 x 76 mm (0.229 x 3 x 3 in.)	x	NA
2	152&305 mm (6&12 in.)	Yes	3.2 x 76 x 76 mm (0.125 x 3 x 3 in.)	NA	x
3a	152&305 mm (6&12 in.)	Yes	3.2 x 76 x 76 mm (0.125 x 3 x 3 in.)	x	x
3b	152&305 mm (6&12 in.)	Yes	5.8 x 76 x 76 mm (0.229 x 3 x 3 in.)	x	x
4a	102&305 mm (4&12 in.)	Yes	5.8 x 76 x 76 mm (0.229 x 3 x 3 in.)	x	x
4b	102&305 mm (4&12 in.)	Yes	5.8 x 76 x 76 mm (0.229 x 3 x 3 in.)	x	x

[a] See below for more detailed information.
[b] 8d common nails (3.3 x 64 mm or 0.131 x 2-1/2 in.).

- Framing – 2 x 4 No. 2 spruce-pine-fir studs at 406 mm (16 in.) o.c. with a single 2x4 center stud.
- Sheathing – Two 11-mm (7/16-in.) Wall-24 OSB panels 1219 x 2438 mm (4 x 8 ft) applied vertically.
- Fasteners – 8d common nails (3.3 x 64 mm or 0.131 x 2-1/2 in.).
- Nailing Pattern – A single row of 8d nails at 152 mm (6 in.) or 102 mm (4 in.) o.c. on panel sides (vertical edges) with a 9.5 mm (3/8 in.) edge distance and double rows of 8d nails at 76 mm (3 in.) o.c. along top and bottom plates (horizontal edges) with a 13 mm (1/2 in.) edge distance. A 305 mm (12 in.) o.c. nailing in the field of panel.
- Holddown (when used) – Holddown has a 17.4 kN (3,920 lbf) design capacity and is attached with 6.4 x 76 mm (1/4 x 3 in.) SDS screws. The holddown bolts were installed wrench-tight.

- Anchor Bolts – 16-mm (5/8-in.) -dia. bolts with 3.2 x 76 x 76 mm (0.125 x 3 x 3 in.) or 5.8 x 76 x 76 mm (0.229 x 3 x 3 in.) plate washers at 406 mm (16 in.) o.c. The anchor bolts were installed wrench-tight.

For the full-scale tests conducted at APA in 2008, the objective was to confirm the design values with 10d common (3.8 x 76 mm or 0.148 x 3 in.) nails using 12-mm (15/32-in.) commodity OSB Structural I sheathing (rated 32/16), which were not previously tested at Clemson University and represent the highest design capacities proposed for the adoption into SDPWS. A total of six full-scale walls were tested at APA using OSB sheathing purchased from a local lumber yard along with framing materials (2x4 No. 2 Douglas-fir) with an estimated moisture content of 16% or higher. The holdowns were manufactured by Simpson Strong-Tie. Other test details are summarized in Table 2 and below.

Table 2. Summary of test assemblies conducted at APA [a]

Wall ID	Nail spacing [b]	Holddown	Plate washer	Uplift	Shear
A1	152&305 mm (6&12 in.)	Yes	5.8 x 76 x 76 mm (0.229 x 3 x 3 in.)	x	–
A2				x	–
A3				–	x
A4				x	x
A5				x	x
A6				x	X

[a] See below for more detailed information.
[b] 10d common nails (3.8 x 76 mm or 0.148 x 3 in.).

- Framing – 2 x 4 No. 2 Douglas-fir at 406 mm (16 in.) o.c. with a single 2x4 center stud.
- Sheathing – Two 12-mm (15/32-in.) 32/16 OSB panels 1219 x 2438 mm (4 x 8 ft) applied vertically.
- Fasteners – 10d common nails (3.8 x 76 mm or 0.148 x 3 in.).
- Nailing Pattern – A single row of 10d nails at 152 mm (6 in.) o.c. on panel sides (vertical edges) with a 9.5 mm (3/8 in.) edge distance and double rows of 10d nails at 76 mm (3 in.) o.c. along top and bottom plates (horizontal edges) with a 13 mm (1/2 in.) edge distance. A 305 mm (12 in.) o.c. nailing in the field of panel.
- Holddown – Holddown has a 21.4 kN (4,800 lbf) design capacity and is attached with 6.4 x 76 mm (1/4 x 3 in.) SDS screws. The holddown bolts were installed finger-tight + 1/8 turn except for Wall A6, which was wrench-tight.
- Anchor Bolts – 12.7-mm (1/2-in.) -dia. bolts with 5.8 x 76 x 76 mm (0.229 x 3 x 3 in.) plate washers at 406 mm (16 in.) o.c. The anchor bolts were installed finger-tight + 1/8 turn except for Wall A6, which was wrench-tight.

2.2 Test Methods

The Clemson test setup, as shown in Figure 1, was capable of increasing the shear and wind uplift forces simultaneously until failure was reached by using a pulley system controlling the bi-axial forces in both lateral and vertical directions. The APA setup, as shown in Figure 2, is also capable of bi-axial loading, but using independent, synchronized loading systems to reach the ultimate shear and uplift loads at approximately the same time. The vertical load can be applied as either an uplift force or a downward gravity load. All tests were conducted monotonically at indoor environmental conditions.

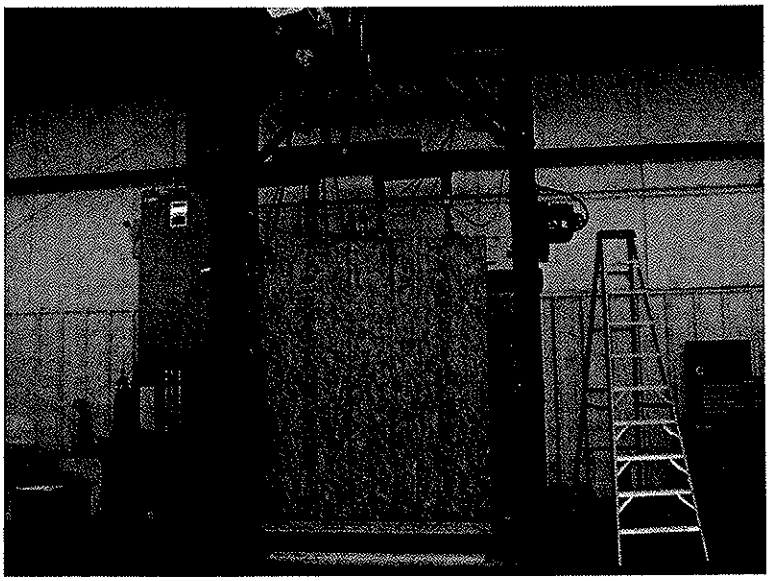

Figure 1. Test setup at Clemson University

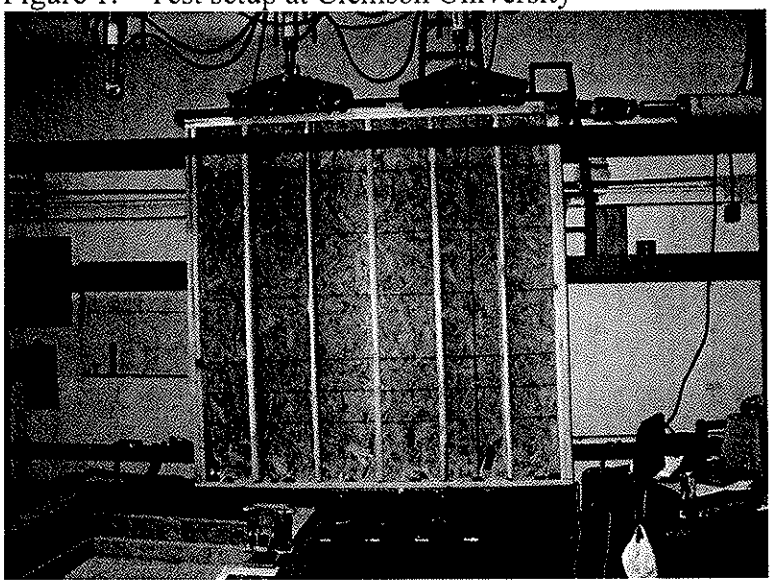

Figure 2. Test setup at APA

It should be noted that the Clemson tests were not necessarily conducted in the sequence shown in Table 1. For example, Walls 1a (uplift only) and 2 (shear only) were conducted first, followed by Wall 3a (combined shear and uplift with 3.2 x 76 x 76 mm or 0.125 x 3 x 3 in. plate washers). Due to an observed bending of the 3.2-mm (0.125-in.) plate washers on Wall 3a, which led to a cross-grain bending failure on the bottom wall plate, Walls 3b, 4a, and 4b were tested with 5.8 x 76 x 76-mm (0.229 x 3 x 3-in.) plate washers. Note that Wall 4b was a replicate of Wall 4a so as to gain more confidence in the test results for such a wall configuration. Wall 1b was conducted last to study the effect of holddown on the uplift-only capacity of the wall by comparing the results with Wall 1a. Both Walls 1a and 1b failed due to the nail withdrawal from the top plates and panel tear-out. The washer plates did not bend in either wall.

3. Results and Discussions

Based on the principle of mechanics, the capacities (allowable stress design) of walls for the combined shear and uplift can be calculated in accordance with NDS, as shown in Table 3.

Table 3. Wood Structural Panels for Combined Shear and Wind Uplift [a,b,c]

	Nail Spacing Required for Shearwall Design [d]											
	6d @ 152 & 305 mm			8d @ 152 & 305 mm			8d @ 102 & 305 mm			10d @ 152 & 305 mm		
	Alternate Nail Spacing at Top and Bottom Plate Edges (mm)											
	152	102	76	152	102	76	152	102	76	152	102	76
	Allowable Uplift Capacity (kN/m) [c]											
Nails-Single Row [e]	0.0	1.2	2.5	0.0	1.6	3.2	NP	0.0	1.6	0.0	1.9	3.8
Nails-Double Row [f]	2.5	4.9	7.4	3.2	6.3	**9.5**	1.6	4.7	**7.9**	3.8	7.6	**11.5**

[a] Minimum 11-mm (7/16-inch) OSB supported by vertical framing at 406 mm (16 in.) on center or less. The framing species shall have a published specific gravity of 0.42 (spruce-pine-fir) or greater.

[b] Anchor bolts shall be installed at 406 mm (16 in.) on center.

[c] For framing with a specific gravity of 0.49 or greater, divide uplift values listed in above table by 0.92.

[d] Where nail size is 6d or 8d, the tabulated uplift values are applicable to 11 mm (7/16 in.) minimum OSB panels. Where nail size is 10d, the tabulated uplift values are applicable to 12 mm (15/32 in.) minimum OSB.

[e] OSB panels shall overlap the top member of the double top plate and bottom plate by 38 mm (1-1/2 in.) and a single row of fasteners shall be placed 19 mm (3/4 in.) from the panel edge.

[f] OSB panels shall overlap the top member of the double top plate and bottom plate by 38 mm (1-1/2 in.). Rows of fasteners shall be 13 mm (1/2 in.) apart with a minimum edge distance of 13 mm (1/2 in.). Each row shall have nails at the specified spacing.

Results from Clemson and APA tests are shown in Tables 4 and 5, respectively. The tables also include the ratio of applied uplift and shear loads, which was intended to cover a range of ratios based on Table 3. It should be noted that since the APA tests were conducted using Douglas-fir framing, the tabulated uplift design value shown in Table 5 for the assembly configuration (10d @ 152 & 305 mm with double row of nails at 76 mm) was calculated by dividing the tabulated value of 11.5 kN/m (786 plf) by 0.92 (see Footnote c to Table 3), which yields 12.5 kN/m (854 plf).

Table 4. Clemson Test Results.

Wall ID	Test Results (kN/m)		Uplift / Shear	Design Values [a] (kN/m)		Load Factor [b]	
	Uplift	Shear		Uplift	Shear	Uplift	Shear
Uni-axial Tests							
1a	27.8	NA	NA	12.6	NA	2.20	NA
1b	27.5					2.18	
2	NA	11.0	NA	NA	4.9	NA	2.24
Bi-axial Tests							
3a	19.7	8.7	2.3	9.5	4.9	2.08	1.78
3b	20.6	9.4	2.2			2.18	1.93
4a	15.7	13.9	1.1	7.9	7.1	1.99	1.94
4b	16.6	14.4	1.2			2.11	2.02
Average (Walls 4a and 4b)						2.05	1.98

[a] For wind load duration.

[b] Targeted load factor is 2.0.

Table 5. APA Test Results.

Wall [a] ID	Test Results (kN/m)		Uplift / Shear	Design Values [b] (kN/m)		Load Factor [c]	
	Uplift	Shear		Uplift	Shear	Uplift	Shear
Uni-axial Tests							
A1	46.4	NA	NA	16.6	NA	2.78	NA
A2	50.1					3.01	
Average (Walls A1 and A2)						2.90	
A3	NA	19.1	NA	NA	6.9	NA	2.74
Bi-axial Tests							
A4	28.3	16.9	1.68	12.5	6.9	2.27	2.43
A5	25.9	15.5	1.67			2.08	2.23
A6	26.8	16.4	1.64			2.15	2.35
Average (Walls A4, A5, and A6)						2.17	2.34

[a] The anchor/holddown bolts were installed finger-tight with an additional 1/8 turn except for Wall A6, which was wrench-tight.
[b] For wind load duration.
[c] Targeted load factor is 2.0.

3.1 Failure Modes

Among all uni-axial tests, Walls 1a, 1b, A1, and A2 (uplift only) failed due to nail withdrawal from the top plates and panel tear-out. Walls 2 and A3 (shear only) failed by a combination of nail withdrawal and nail-head pull through. Among all bi-axial tests, Wall 3a failed as a result of cross-bending failure on the bottom plate of the wall due to the use of thin 3.2 mm (0.125 in.) plate washers. When the thicker 5.8 mm (0.229 in.) plate washers were used, the plate washers did not bend and there was no cross-grain bending failure on the wall bottom plate. Figures 3 through 5 show the typical failure modes.

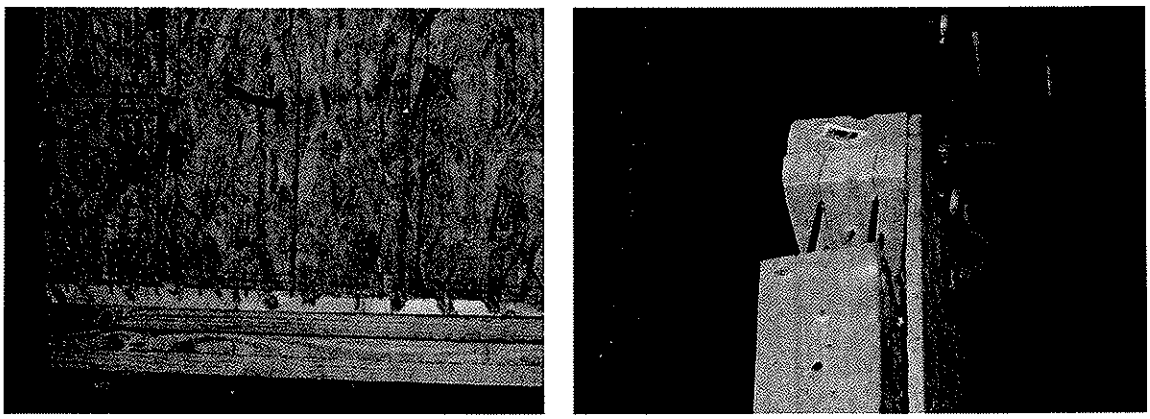

Figure 3. Panel tear-out and withdrawal of top plates (Wall 3b)

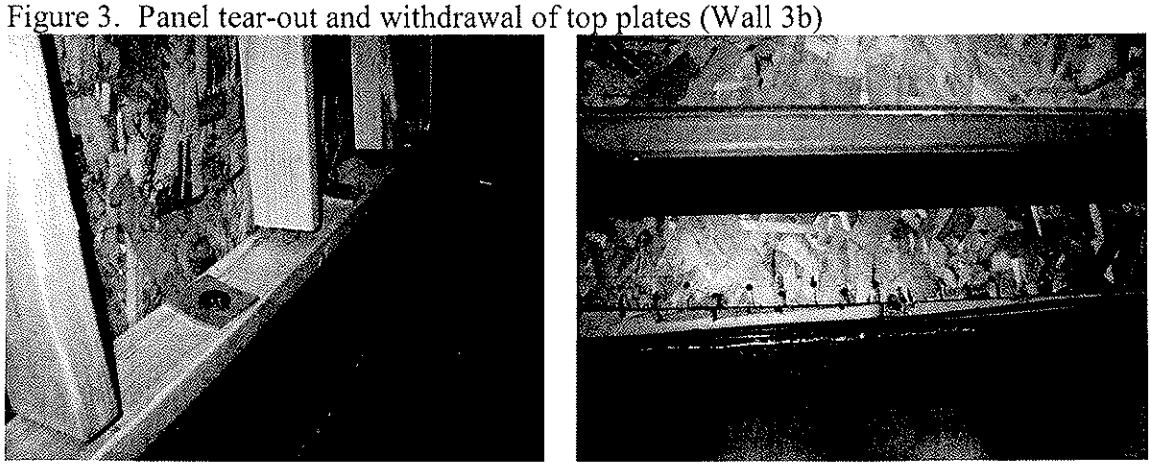

Figure 4. Typical failure mode from combined shear and uplift tests (Wall A5)

Figure 5. Typical failure mode from uplift only tests (Wall A2)

3.2 Load and Real Time Plots

Typical load and real time plots are shown in Figures 6 through 8.

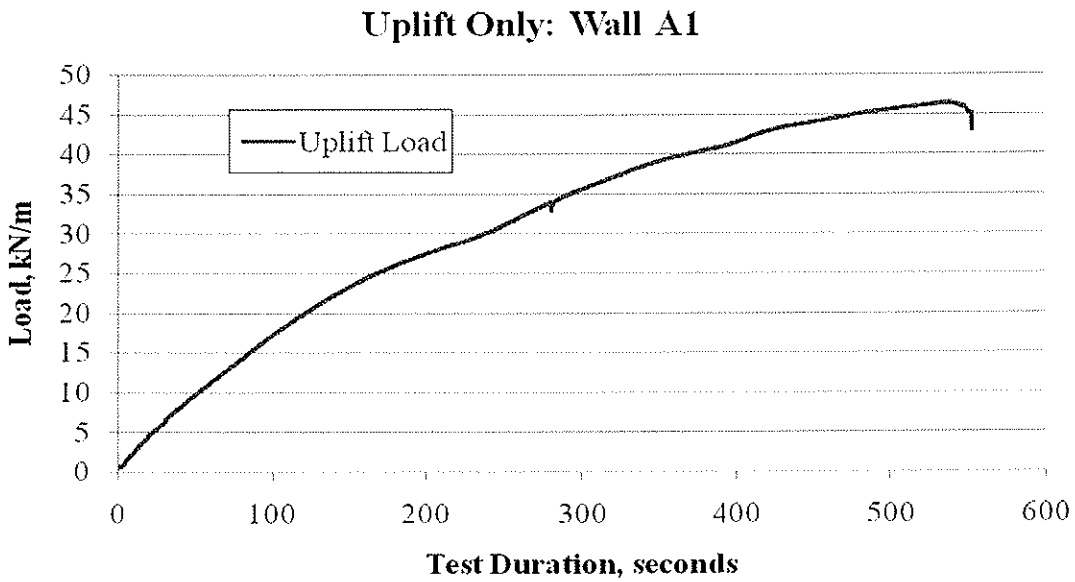

Figure 6. Test results from Wall A1 (uplift only)

3.3 Discussion

Results obtained from these studies confirm that the load factors for combined shear and uplift of walls constructed with 11 mm (7/16 in.) and 12 mm (15/32 in.) OSB panels are approximately 2.0, which is deemed adequate for wind design. This validates the uplift values calculated in accordance with the engineering mechanics analysis (i.e., NDS-05) and the shear values published in SDPWS provided that 5.8 x 76 x 76 mm (0.229 x 3 x 3 in.) plate washers are installed with anchor bolts spaced at 406 mm (16 in.) or less on center so that the cross-grain bending of the bottom wall plate can be avoided.

Test results obtained from these studies also support the conclusion that the holdowns do not affect the uplift resistance of walls constructed with wood structural panels (see results from Walls 1a with holdowns and 1b without holdowns). While this is not unexpected

since holdowns are designed primarily to resist the overturning moment due to lateral loads, the test results confirm this general expectation.

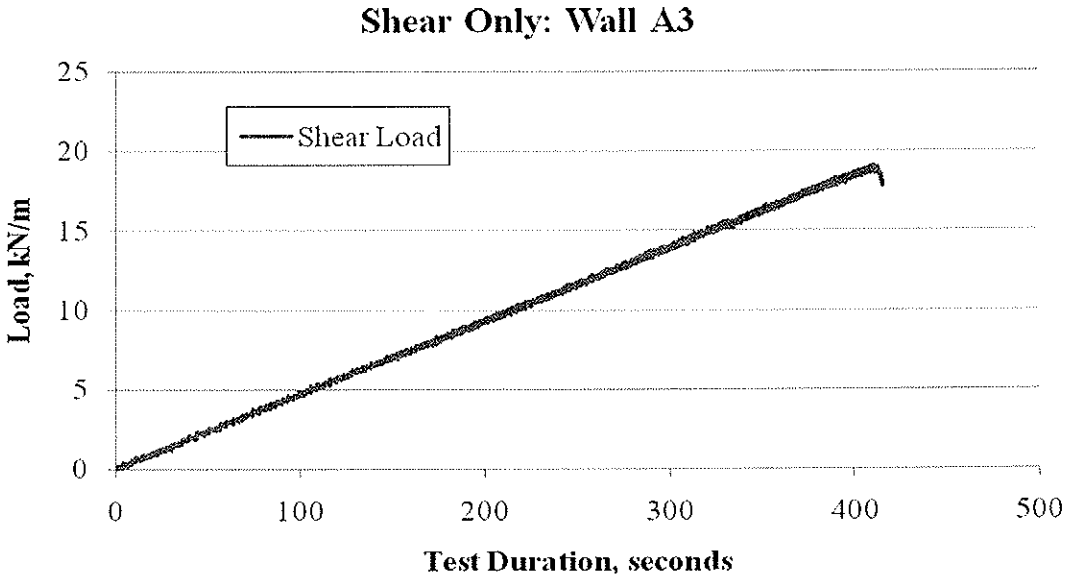

Figure 7. Test results from Wall A3 (shear only)

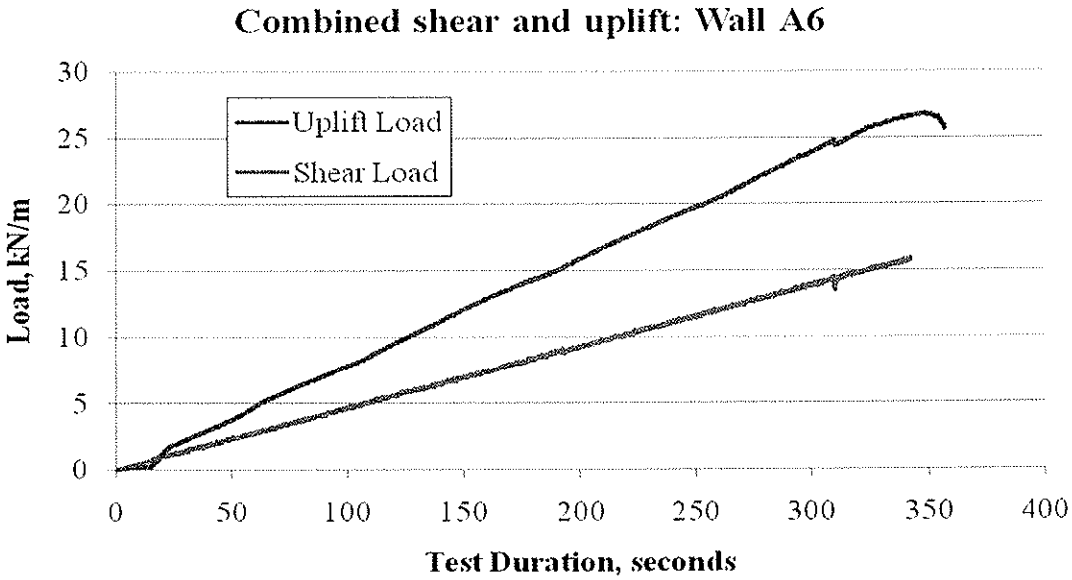

Figure 8. Test results from Wall A6 (combined shear and uplift)

4. Conclusions and Recommendations

Results obtained from these studies confirm the adequacy of using an engineering mechanics analysis to evaluate the resistance of shearwalls when subjected to combined shear and wind uplift provided that that 5.8 x 76 x 76 mm (0.229 x 3 x 3 in.) plate washers are installed with anchor bolts spaced at 406 mm (16 in.) or less on center so that the cross-grain bending of the bottom wall plate can be avoided. In the future, the anchor bolt spacing may be further optimized and the design values provided in Table 3 of this paper expanded to include other shearwall configurations.

5. References

1. International Code Council. 2006. *International Building Code*. Country Club Hills, IL.
2. International Code Council. 2006. *International Residential Code*. Country Club Hills, IL.
3. National Institute of Standards and Technology. 2007. Voluntary Product Standard PS1-07, *Structural Plywood*. Gaithersburg, MD.
4. National Institute of Standards and Technology. 2004. Voluntary Product Standard PS2-04, *Performance Standard for Wood-Based Structural-Use Panels*. Gaithersburg, MD.
5. APA – The Engineered Wood Association. 2008. *Panel Design Specification*. Tacoma, WA.
6. Southern Building Code Congress International. 1999. *Standard for Hurricane Resistant Residential Construction*. Birmingham, AL.
7. Institute for Business & Home Safety. 2005. *Guidelines for Hurricane Resistant Residential Construction*. Tampa, FL.
8. International Code Council. 2008 (In print). *Standards for Residential Construction in High Wind Regions*, ICC-600. Country Club Hills, IL.
9. American Forest & Paper Association. 2005. *Special Design Provisions for Wind and Seismic*. Washington, D.C.
10. American Forest & Paper Association. 2005. *National Design Specification for Wood Construction*. Washington, D.C.
11. NAHB Research Center. 2005. Full-Scale Tensile and Shear Wall Performance Testing of Light-Frame Wall Assemblies Sheathed with Windstorm OSB Panels. Upper Marlboro, MD.

Appendix A. Example details for tested assemblies

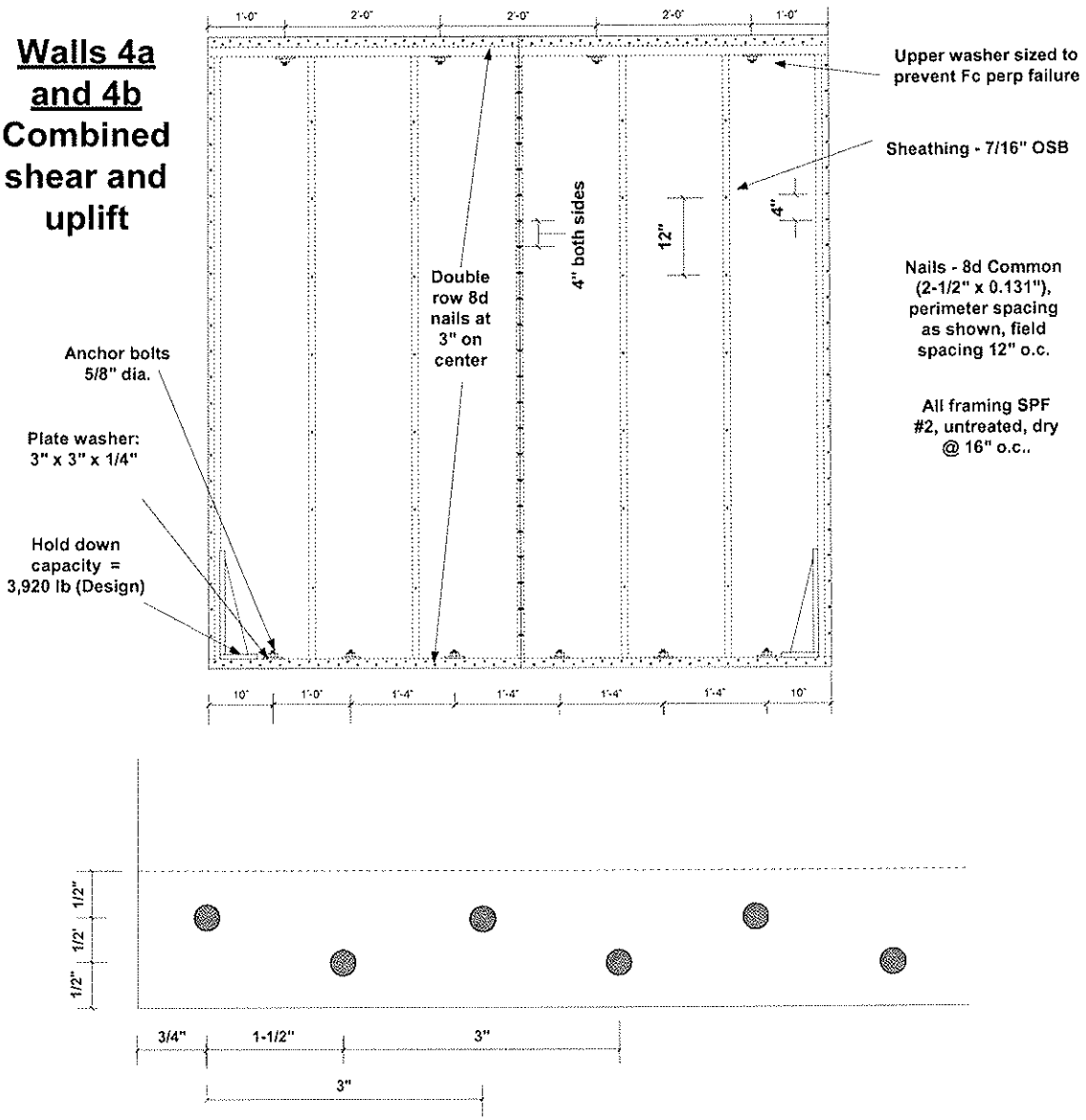

Nailing pattern on the bottom plate (1 in. = 25.4 mm)

INTERNATIONAL COUNCIL FOR RESEARCH AND INNOVATION
IN BUILDING AND CONSTRUCTION

WORKING COMMISSION W18 - TIMBER STRUCTURES

BEHAVIOUR OF PREFABRICATED TIMBER WALL ELEMENTS UNDER STATIC AND CYCLIC LOADING

P Schädle

H J Blass

Universität Karlsruhe

GERMANY

Presented by P. Schädle

B Dujic discussed contact issue related to shear wall resistance. A. Buchanan asked about the geometry of the system and why bigger sections were not used. P. Schädle the size was designed so that it can be easily handled by few workers and can be built with few friends. A. Buchanan received clarification that downward load goes through the stud in compression and no glue is used. I. Smith asked about the detail of the intercept with floor. P Schädle said that the floor would be installed be on top of the plates. F. Lam commented that this is an interesting system. He suggested that dynamic behaviour be considered as the damping increase comes from increased vertical dead load. Here the vertical dead load will have an influence on the natural frequency of the system. Also the damping generated by the stones is very interesting. T. Williamson asked about the openings and the analysis of the walls with openings. Y.H. Chiu received confirmation that the system is approved for 3 storey buildings in Germany. He asked whether it is approved as bricks or system. P Schädle said that it is approved for both as bricks and as system. J. M. Andersen stated that the gravels will move after shaking. P Schädle said that after cyclic test the gravels may come out of the blocks. B.J. Yeh asked about fire protection and insulation. H. Blass said that in 160 mm wall thickness additional insulation may be needed. 240 – 300 mm wall thicknesses are also available. For fire protection gypsum boards will handle it and mineral rock fibre can also be used.

Behaviour of Prefabricated Timber Wall Elements Under Static and Cyclic Loading

Patrick Schädle, Hans Joachim Blaß
Lehrstuhl für Ingenieurholzbau und Baukonstruktionen
Universität Karlsruhe, Germany

1 Introduction

Prefabricated Timber Wall Elements (PFTE) represent a simple, easy to handle and sustainable construction system. In a current research project at Universität Karlsruhe the PFTE building system is tested under both vertical and horizontal loading to determine its shear wall capacities. For this purpose a new testing assembly for vertical and horizontal loads able to produce various boundary conditions was installed at Universität Karlsruhe. The shear walls were tested following ISO/CD 21581 [3] while assuming boundary conditions reflecting the intended construction details. In this paper the test results are presented and are compared with test results of conventional timber frame walls.

2 Idea of the PFTE building system

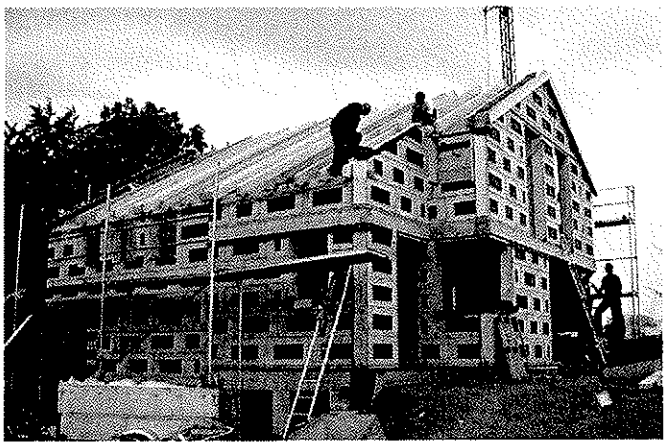

Fig. 1 Building made of Prefabricated Timber Wall Elements

The main feature of PFTE is prefabricating wooden "brick" elements primarily out of the residues of a sawmill. The brick-like elements can be easily transported to the building site and are easy to handle even for beginners under the guidance of a site foreman. The mass of a single element is less than 25 kg, it can be moved by hand and walls can be built without a crane. Thus the system can be cost-saving. In Germany a technical approval for up to three - storey buildings was issued in Sept. 2007.

The basic element (as shown in Fig. 2 and Fig. 3) consists of four solid wood columns and two OSB–like chipboards as an inner sheathing layer on both sides. The wood columns are connected by dove tails to the chipboard layers. On the one hand this means a simple and close connection between the inner sheathing layer and the columns, on the other hand it allows the columns of the lower element to slide into the sheathing of the element on top. Quite similar to the Lego brick system the single elements are stuck together by these overlapping/shortened columns with dove tail geometry at the top/bottom of the element. The

overlapping/shortening of the columns gives the wall initial stability. On both sides a second sheathing layer is fixed to the inner sheathing layer. The second (outer) layer consists of chipboard on the subsequent inner side of the building and of timber boards on the subsequent outer side of the building. The second sheathing layer is fixed with an offset of 30 mm horizontally and vertically. When setting up the wall the offset of the outer layers of lower and upper elements slide into the next one, so that the outer layer overlaps from one element to another. After finishing erection the overlapping parts of the sheathing are connected on the inner side of the building by staples to create a continuous shear wall.

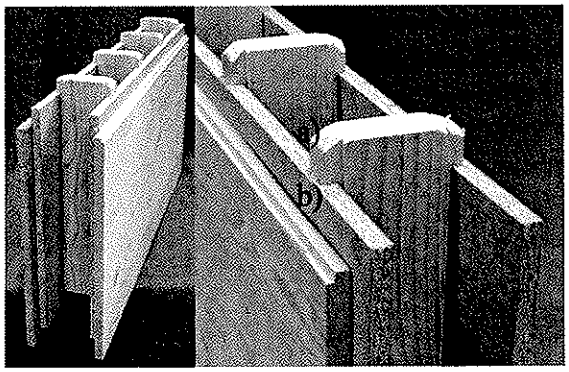

Fig. 2 Prefabricated Timber Wall Element (left); Offset of columns (a) offset of layers (b) (right)

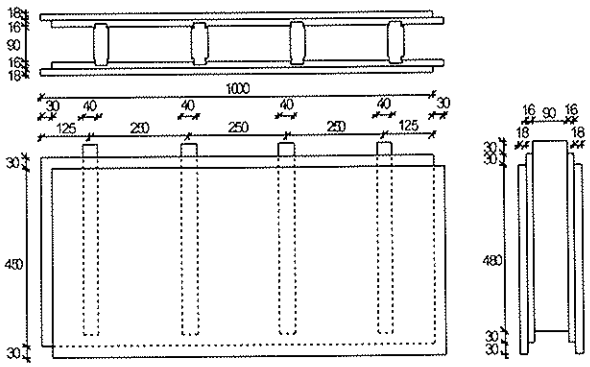

Fig. 3 Scheme of Prefabricated Timber Wall Element, dimensions in mm

The basic element with a length of ℓ = 1,0 m and a depth of h = 0,5 m is available in wall thicknesses of b = 160 mm, b = 240 mm or b = 300 mm. The columns are spaced 250 mm, the hollow space between the colums can be used for insulation and installation. For the acceptance of the technical approval in 2007, tests with loads perpendicular to the surface were successfully carried out. Also some tests with in-plane shear forces were performed. The manufacturer and Universität Karlsruhe decided to study more extensively the shear wall behaviour of the system particularly with regard to exporting the system to regions with seismic activity and high wind loads. Because the wall sheathing is not continous but is composed of several smaller areas, the main attention was focussed on the connection between the single elements. When ere-cting a wall with PFTE, first a wall plate is fixed to the foundation. The first row of the elements is installed by fixing each element to the wall plate via one BMF 90 x 90 mm angle connector. When the wall

Top rail on top element, fixed with:
-vertical screw 6 x 140 mm every 2nd column
-Horizontal screw 5 x 60 mm – spaced 250 mm solely on chipboard side
-Horizontal staples 64 mm – dist. 50 mm solely on chipboard side

Basic elements, overlap connected with staples 32 mm – spaced 50 mm solely on chipboard side

-Douglas fir wall plate with spruce element, connected via screws 6 x 160 mm spaced 250 mm
-First line connected to spruce element via 1 BMF-Angle per wall element
-First-Line elements connected with staples 64 mm – spaced 50 mm solely on chipboard side

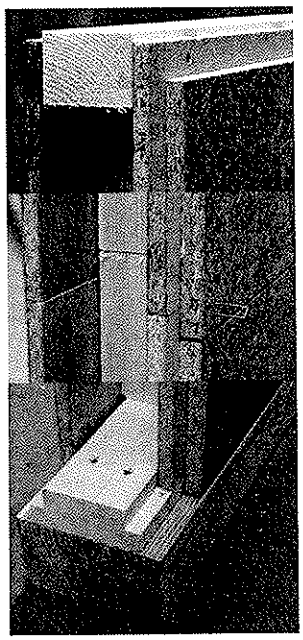

Fig. 4 Details of Prefabricated Timber Wall Element System

height is reached, a continuous vertical stud is inserted from the top at least every 3 m of wall length. The vertical studs transfer the in-plane uplift forces to the foundation, and they provide bending stiffness for loads perpendicular to the wall plane, e.g. wind loads. At the top of the wall the top rail is put into position and the vertical studs as well as the top rail are connected to the elements via self-drilling screws. Normally the spaces between the vertical columns are filled with insulation. The tests, however, were performed without insulation. All the connections described in Fig. 4 are of prime importance for the behaviour of the wall under the different loading conditions.

3 Test Setup at Universität Karlsruhe

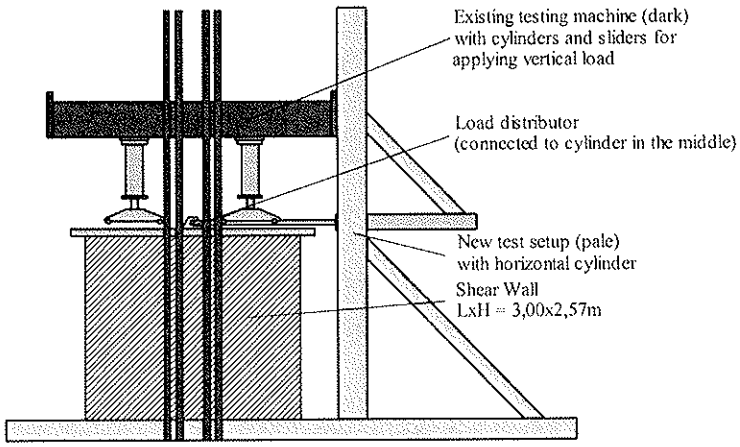

Fig. 5 Scheme of new test equipment at Universität Karlsruhe

A new test equipment for shear wall tests was part of the research project. In the past years it was discussed [1], [2] how to apply realistic boundary conditions in shear wall tests. An existing testing machine for applying vertical loads was incorporated into the new wall testing facility. The new test setup should enable different boundary conditions for the test specimens. The two hydraulic jacks for the vertical loads are either force or displacement controlled, so that the three different boundary conditions "Shear Wall Mechanism", "Restricted Rocking Mechanism" and "Shear Cantilever Mechanism" (see Fig. 6) can be applied.

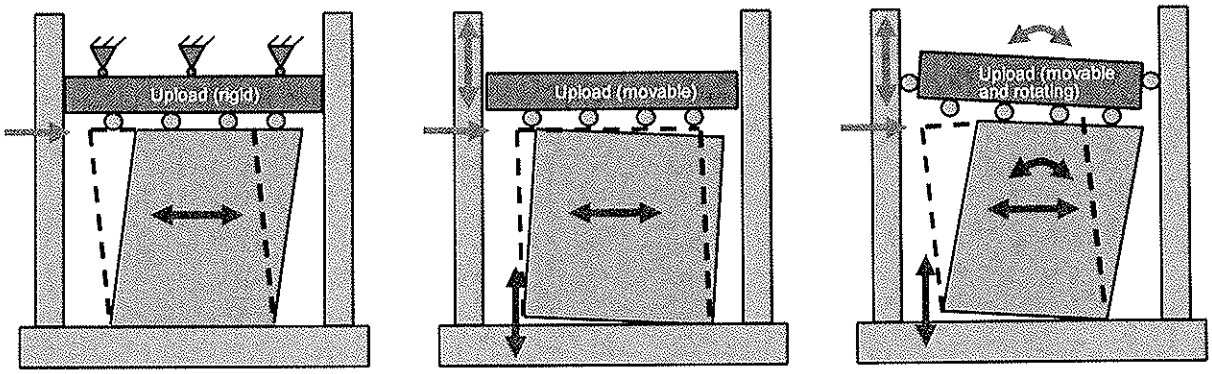

Fig. 6 Boundary conditions as described in [1], a) Shear Wall Mechanism, b) Restricted Rocking Mechanism, c) Shear Cantilever Mechnism

The centre of the load distributor is connected to the horizontal hydraulic jack. A powerful 400 kN hydraulic jack with a displacement range of +/- 300 mm was chosen to enable tests with cross-laminated timber wall elements with very high lateral resistance. By attaching the centre of the load distributor to the horizontal hydraulic jack it is assured that all three boundary conditions are possible while always keeping the hydraulic jack nearly horizontal. The vertical load is applied to the test setup via two slides on the load distributor.

4 Shear Wall Tests

4.1 Shear Wall Tests with PFTE

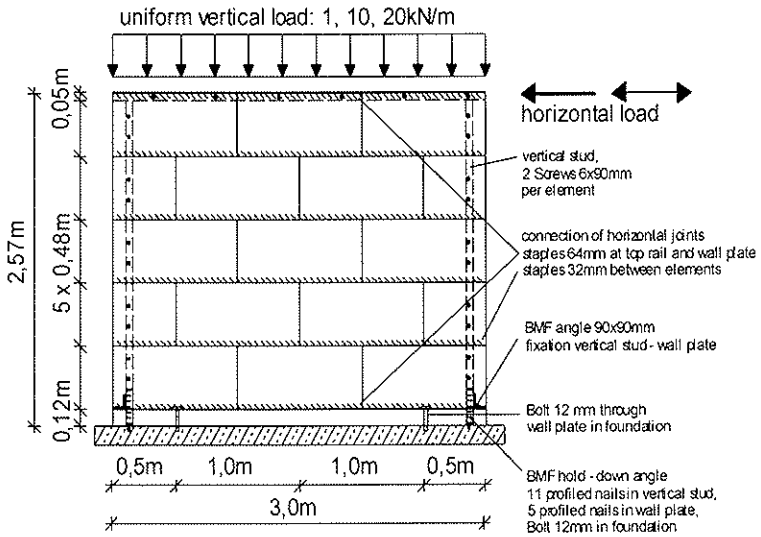

Fig. 7 PFTE Test Wall Specimen

The test setup for the PFTE shear wall tests is shown in Fig. 7. Similar to the approach in practice, first of all the wall plate is fixed to the foundation of the test setup via two 12 mm bolts (one bolt in each outer element). The first layer of elements is put on the wall plate and fixed via one BMF 90 x 90 mm angle per element. The next four layers are simply laid by putting the wooden "bricks" together. Afterwards the vertical studs and the top rail are put into position and the load distributor is attached to the top rail by multiple inclined screws. The inclined screws perform very well as they exhibit a very stiff behaviour even at high loads. After the weight of the load distributor is applied on the wall, the fasteners between the wall elements are driven in. All tests were performed using a PFTE wall thickness of 160 mm.

4.1.1 Monotonic Tests with PFTE

The monotonic tests with PFTE were performed using the ISO/CD 21581 [3] load protocol which corresponds to the load protocol given in EN 594 [5]. A total of 11 monotonic tests was performed with PFTE.

Three tests were carried out without additional vertical load on top (only the weight of load distributor itself being 1,33 kN/m, in the following denoted as 1 kN/m). The tests with a vertical load of 1 kN/m were carried out using a test setup according to Fig. 7. On the outer wall side a steel nailing plate was additionally fixed as a connection between wall plate and the first line of elements. The nails were driven through the plate into the vertical studs to relieve the hold-down on the chipboard side. The first two tests with a load of 1 kN/m achieved maximum horizontal loads of about 48 kN, however with different failure mechanisms. In the first test, the stapled connection loaded in shear between top rail and the upper wall elements failed in a ductile manner, while the wall itself showed minimal displacements. In the second test the hold-down of the vertical tensile stud failed. At a certain displacement, additionally the first horizontal joint began to open because the staples were pulled out. The third test was performed with additional staples in the vertical joints to increase maximum load as well as stiffness. This test showed a very sudden failure because the hold-down failed and simultaneously the nails in the horizontal part of the inner BMF angle were suddenly pulled out.

Five tests with an additional vertical load of 10 kN/m were conducted: three with additional screws in the overlap of the vertical columns and two without those screws.

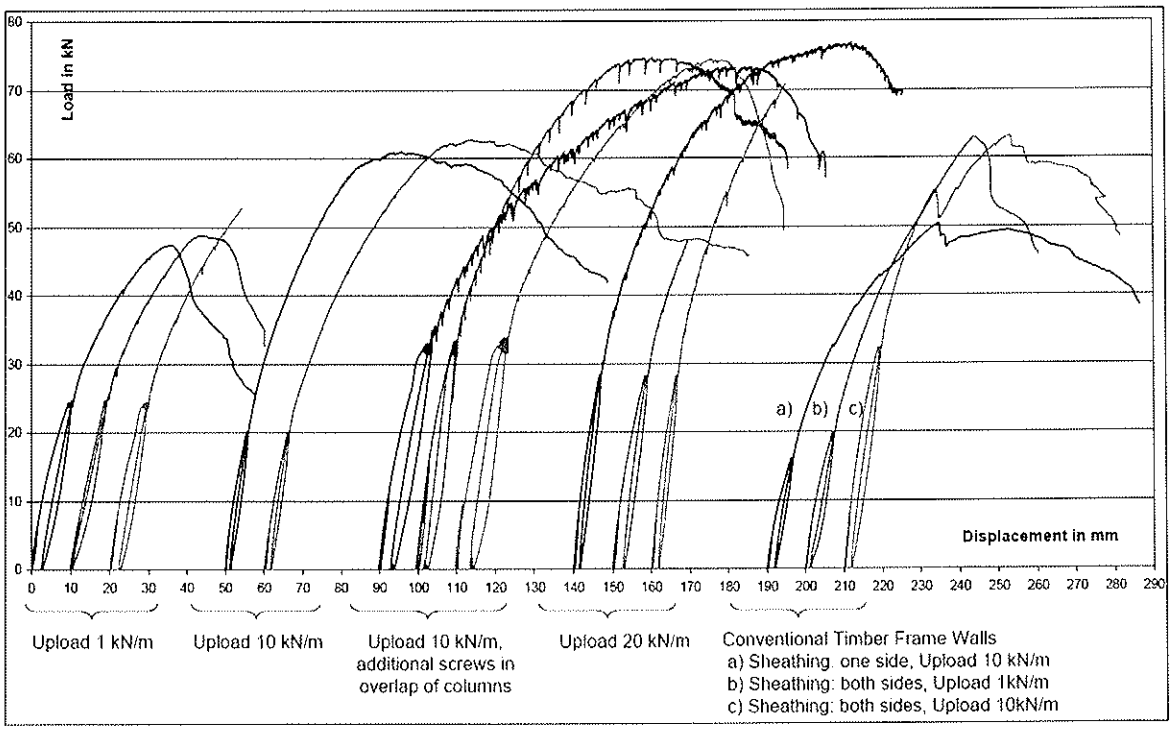

Fig. 8 Load-displacement curves of monotonic (Push-Over) Tests

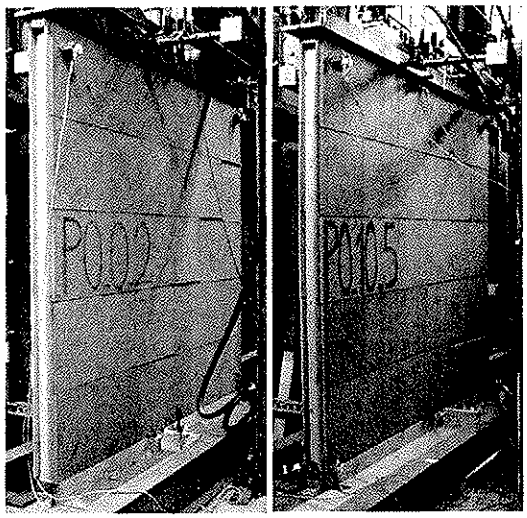

Fig. 9 Test Wall Specimen after test

The test results with vertical load 10 kN/m using no additional screws (PO_10_4 and PO_10_5) are shown at position 50 and 60 mm in Fig. 8. The test configuration was nearly the same as in the tests with no vertical load, only the steel plate as an additional connection between the lower elements and the wall plate was left out. Compared to the tests with no additional vertical load, the horizontal load capacity increased to about 62 kN while the stiffness only slightly increased. Ductility of the wall raised, as can be seen from the displacements at 80% of F_{max}: while being about 44 mm in the case with no additional vertical load, it rose to about 93 mm with a vertical load of 10 kN/m. This is a result of changed boundary conditions between the two cases. While the wall without additional vertical load shows restricted rocking behaviour [1], the shear deformations of the wall turn out to be rocking behaviour [1] until failure of the test specimen was reached by the staples in the horizontal joints being pulled (see Fig. 9 on the right).

The screws provide additional shear resistance, however, placing the screws means a lot of extra work: for the test wall with 2,5 x 3,0 m about 50 screws have to be placed. The load bearing capacity increased due to the additional screws to about 74 kN compared to the 62 kN in the tests without screws.

Finally, three tests with an additional vertical load of 20 kN/m were carried out. In the first test a horizontal load of nearly 77 kN was reached with a ductile failure mode. Failure of this specimen was quite similar to the failure with lower vertical loads. Beginning from the

vertical stud on the tensile side, the horizontal joints started to open because the staples were pulled out. In the second test, similarly to PO_0_3 the top rail connection failed in shear due to a very low timber density. The third test with a vertical load of 20 kN/m showed a brittle failure at a maximum load of about 71 kN. Suddenly the first horizontal joint and the connection between the vertical stud and the wall plate failed simultaneously.

Table 1: Overview and Results of monotonic (Push – Over) Tests

	F_{max} in kN	u_{max} in mm	$u_{80\%Fmax}$ in mm	F at disp. u = 5mm	Stiffness K [1)]	Comment
PO_0_1	47,4	35,2	42,7	16,0	2693,1	top rail connection failed (ductile)
PO_0_2	48,9	32,8	45,1	14,4	2757,2	
PO_0_3	52,7	35,5	-	16,2	2875,8	Staples in vertical joints too, brittle failure of specimen
Mean Value	49,7	34,5	43,9	15,5	2775,4	
PO_10_1	73,4	87,7	110	18,9	2715,4	Additonal screws in overlap of vertical columns
PO_10_2	74,6	65,8	101,1	22,9	3127,4	
PO_10_3	74,4	51,8	64,9	20,0	3500,5	
Mean Value	74,1	68,4	58,7	20,6	3114,4	
PO_10_4	61,0	47,8	86,1	18,8	2892,0	
PO_10_5	62,8	52,3	100,2	17,6	2773,7	
Mean Value	61,9	50,0	93,2	18,2	2832,9	
PO_20_1	76,8	70,9	106,6	23,3	3390,0	
PO_20_2	47,4	19,4	-	19,8	3625,1	top rail connection failed (brittle)
PO_20_3	70,8	34,6	-	23,5	3603,8	Failure of vertical stud and first horizontal joint, brittle behaviour of specimen
Mean Value	65,0	41,6	-	22,2	3539,6	
TF_one_10 [2)]	50,3	50,6	107,7	13,2	1915,7	
TF_two_1	63,1	45,8	54,3	16,3	2400,2	
TF_two_10	63	49,1	78,6	21,6	3651,0	

[1] Stiffness $K = \frac{0,3 \cdot F_{max}}{\upsilon_{40\% Fmax} - \upsilon_{10\% Fmax}}$ where e.g. $\upsilon_{40\% Fmax}$ is the displacement at 40% of F_{max}

[2] Timber Frame_Sheathing one/two sides_Vertical load 1/10 kN/m

4.1.2 Cyclic Tests with PFTE

The cyclic tests were performed using the same test setup as for the monotonic tests (see Fig. 7). All cyclic tests were carried out using the cyclic displacement schedule given in ISO/CD 21581 [3] which corresponds to the displacement schedule given in ISO 16670 [6]. Before cyclic testing, the ultimate displacement v_u was determined from the monotonic tests. The ultimate displacement is defined a) as the displacement at failure or b) the displacement at 80% of F_{max} in the descending portion of the load-displacement curve or c) the displacement reaching H/15 (PFTE: 2570/15 = 171 mm) whichever occurs first. Having three tests each, v_u was taken to be the average of the three tests.

The multiple element connections with a large number of mechanical fasteners and the friction between the elements should lead to a favourable behaviour under cyclic loading. The staples used for the connections are very slender fasteners which bend easily. The subsequent plasticity of the staples as well as the timber under embedding lead to a ductile behaviour and a large energy dissipation during the repeated cycles. The friction between the elements cause additional energy dissipation. In ISO/CD 21581 [3] there is no approach to determine the energy dissipation of the wall, but it is noted that in future there may be a need to determine such additional properties. To gain some information about the energy dissipation of the tested walls, the equivalent hysteretic damping v_{ed} according to

EN 12512 [4] is used. In Table 2 and Table 4, selected tests and the energy dissipation are tabulated.

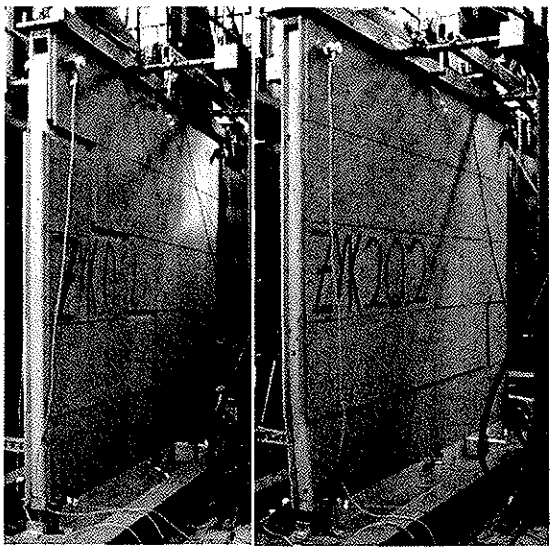

Fig. 10 Typical failure in cyclic tests. Vertical load 1 kN/m (left) 20 kN/m (right)

All tests were carried out using boundary condition "Shear Cantilever Mechanism" [1]. This boundary condition was chosen because it is the boundary condition assumed to appear in most PFTE buildings. Because of the light-weight structures of such buildings, rotation of the wall is possible. Again, while conducting the tests with a vertical load of 1 kN/m, a steel plate was affixed as a connection between wall plate and the first line of the elements on the timber board side. The tests without additional vertical load showed a higher ductility than expected from the monotonic tests (See Fig. 11 a) compared to Fig. 8). This is caused by the various connections between the elements and the connection between the vertical studs and the elements. Having no additional vertical load in combination with cyclic loading the connections very soon become loose. However the maximum load is similar to the one in the monotonic tests.

The tests with vertical load 10 kN/m and 20 kN/m showed higher maximum loads and higher energy dissipation values v_{ed} due to the friction activated by the vertical load. As can be seen in Fig. 11 b) and c) the hysteretic curves become more voluminous. Also the uneven course of the curve shows friction effects between the columns as well as between sheathing panels of the single elements.

Two tests with gravel infill were carried out. Filling the wall with gravel improves the acoustic and the temperature storage capacity of the wall. The higher dead load of the wall itself especially in low-rise buildings also leads to a better performance in the case of high wind loads. The friction between the pebbles causes an additional energy dissipation in cyclic loading. Finally in case of tornados the additional mass of the wall increases the safety for residents in a building by preventing parts flying around to penetrate the wall. As can be seen in Fig. 11 d), its equivalent hysteretic damping compared to the wall without gravel infill is exellent. However it must be said that the maximum loads and also the ductility of the wall is reduced by pepples locking the joints between the elements once the gap is open.

Table 2 Tabulated Values of Cyclic Test with PFTE, Vertical load 10 kN/m

ZYK_10_1, Cyclic, Upload 10 kN/m, No. 1																		
ultimate displacement obtained in static test vu = 70mm							*) length of wall = 3,0m						equivalent hysteretic damping v_{ed} = Ed/(2*pi*Epot)					
displacement rate for cyclic test dr = 40mm/min																		
total duration of test 1h 40min																		
	First envelope curve						Second envelope curve						Third envelope curve					
	Positive			Negative			Positive			Negative			Positive			Negative		
% of vu	mm	kN *)	ved in %	mm	kN *)	ved in %	mm	kN *)	ved in %	mm	kN *)	ved in %	mm	kN *)	ved in %	mm	kN *)	ved in %
1,25	0,83	3,75		-0,82	-5,74													
2,50	1,61	5,40		-1,54	-9,13													
5,00	2,99	10,49		-3,49	-15,45													
7,50	4,97	15,48		-5,22	-19,64													
10,00	6,59	18,15		-6,96	-24,13													
20,00	13,93	30,41	13,1	-13,64	-35,80	13,8	13,92	30,28	13,1	-13,60	-34,97	11,7	13,90	29,74	12,3	-13,59	-34,69	11,0
40,00	27,92	45,18	14,6	-27,65	-50,70	13,8	27,96	43,20	12,7	-27,71	-48,65	11,3	27,99	41,70	12,4	-27,79	-47,79	10,9
60,00	41,50	51,58	14,4	-41,24	-56,20	13,2	41,58	48,86	12,3	-41,93	-53,24	10,8	41,63	47,26	12,4	-41,99	-51,29	10,6
80,00	55,08	54,22	13,6	-55,52	-56,66	12,7	55,88	50,04	12,9	-55,61	-53,01	11,2	55,91	47,90	12,2	-55,59	-51,52	10,6
100,00	69,26	52,84	13,9	-69,57	-48,98	15,7	69,89	44,80	14,5	-69,59	-44,49	14,4	69,90	41,83	14,8	-69,53	-42,23	14,1
120,00	83,84	46,49	15,0	-82,86	-45,54	15,3	83,85	42,52	14,7	-83,50	-42,53	14,2	83,86	40,75	14,8	-84,03	-40,73	14,1
140,00	97,17	44,29	15,3	-96,86	-43,54	14,8												

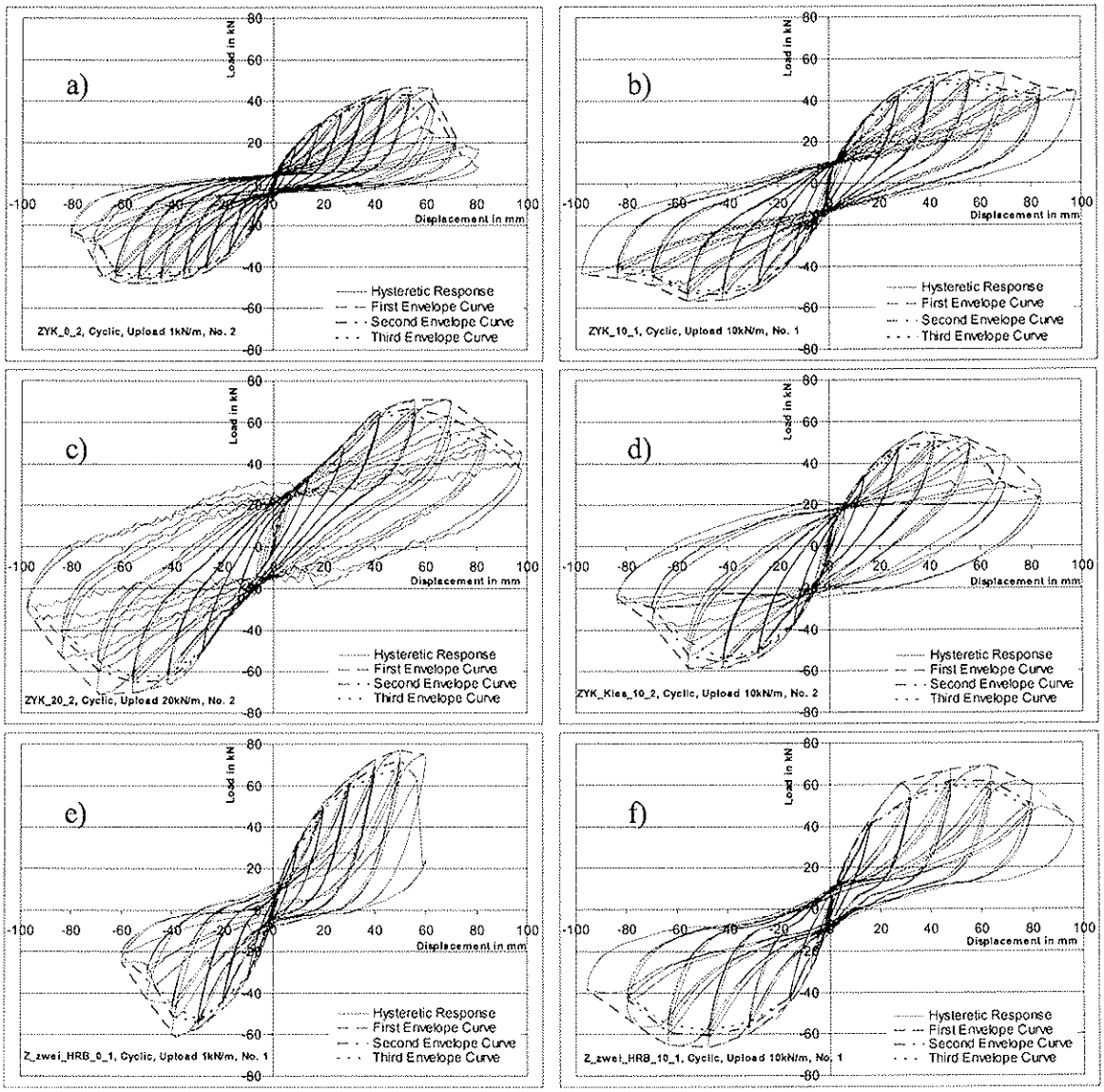

Fig. 11 Hysteretic responses of tested walls

4.2 Shear Wall Tests with conventional Timber Framed Walls

To compare the test results of PFTE with other timber construction methods, six tests with conventional timber framed shear walls were carried out. Fig. 12 shows the test setup for these walls. The walls have the same height as PFTE walls, due to the standard dimension of the sheathing (2,5 x 1,25m), length was shorter. Therefore two panels of sheathing could be used with only one joint in the middle of the wall.

Since PFTE wall elements are connected by staples on the chipboard side only, a continuous sheathing only exists on one side of the wall. The first tests similarly were carried out with timber framed walls sheathed on one side. The results of the monotonic test can be seen in Fig. 8 and Table 1. The load bearing capacity increased due to the additional screws to about 74 kN compared to the 62 kN in the tests withot screws. While the maximum horizontal load for a PFTE wall is about 62 kN, the timber frame wall achieves a maximum load of about 50 kN at a displacement of approx. 50 mm.

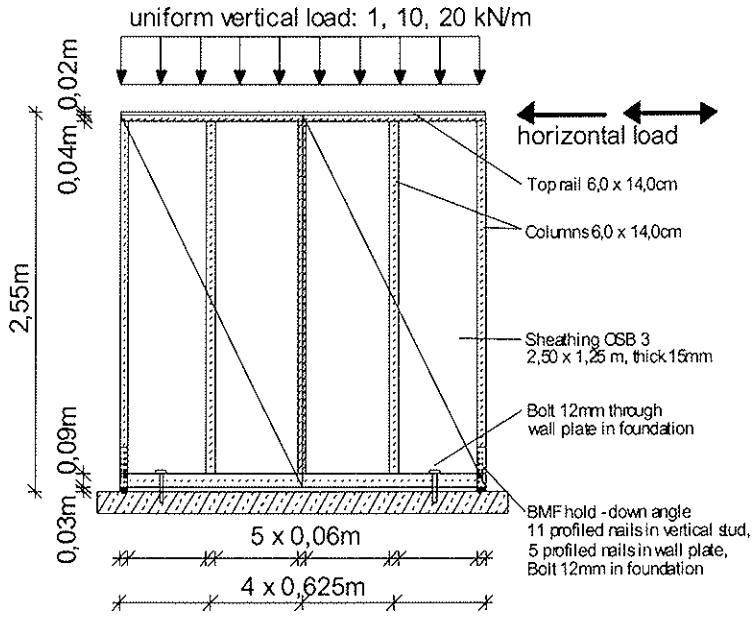

Fig. 12 Test Specimen of Timber Framed Wall

Failure of the test specimen was reached by tensile failure of the OSB sheathing just above the hold-down. The first envelope curve of the cyclic test with the timber frame wall showed nearly the same behaviour as the monotonic one, achieving about the same loads and displacements. The equivalent hysteretic damping v_{ed} for the first cycles is similar to the values achieved by PFTE, v_{ed} for the second and third cycle is significantly lower than the corresponding values of PFTE system.

The next four tests were conducted with the same test setup as shown in Fig. 12, but with the wall being sheathed on both sides. Two tests were carried out with a vertical load of 1 kN/m, two tests with a vertical load of 10 kN/m, each with monotonic and cyclic loading. Beginning with the monotonic test and a vertical load of 10 kN/m, a maximum horizontal load of 63 kN at a displacement of 49 mm was reached, compared to the 3 m long PFTE wall without screws in the overlap of the columns with values of 62 kN at a displacement of 50 mm. Again failure was caused by the OSB sheathing's tensile failure just above the hold-down angle connector.

Table 3 Test Matrix for Timber Framed Walls

	Sheathing	upload	Load
TF_Mon_One_10_1	One side	10 kN/m	Monotonic
TF_Cyc_One_10_1	One side	10 kN/m	Cyclic
TF_Mon_Two_1_1	Two sides	1 kN/m	Monotonic
TF_Cyc_Two_1_1	Two sides	1 kN/m	Cyclic
TF_Mon_Two_10_1	Two sides	10 kN/m	Monotonic
TF_Cyc_Two_10_1	Two sides	10 kN/m	Cyclic

For the first envelope curve a maximum horizontal load of 69 kN at a displacement 63 mm was reached. While energy dissipation for the first cycles achieved values between 10,6% and 15,4%, the dissipation for the second and third cycles ranged from 7,5% – 9,2%. The corresponding values with PFTE walls are 12,7% to 15,3% in the first cycles and 10,6% to 14,8% in the second and third cycles. PFTE hence shows very good performance even when damaged in previous load cycles.

Due to the tensile failure of the OSB sheathing right above the hold-down the angle was elongated for the final tests without vertical load. The total number of nails driven in the vertical stud was doubled by this measure. As can be seen in the results for both the monotonic and cyclic test, performance of the wall was consequently improved. The monotonic test without additional vertical load achieved the same results as the test with vertical load 10 kN/m. The cyclic test with the elongated angle achieved a maximum horizontal load of 77 kN at a displacement of 49 mm. Again the energy dissipation in the first cycles was quite high (from 8,6% to 17,9%) while the energy dissipation for the second and third cycle showed lower values (from 7,7% to 15,0%).

Table 4 Values of Cyclic Test with timber-framed shear wall, Vertical load 10 kN/m

HRB_zwei_ZYK_10_1, Cyclic, Upload 10 kN/m, No. 1																		
ultimate displacement obtained in static test vu = 80mm							*) length of wall = 2,5 m equivalent hysteretic damping v_{ed} = Ed/(2*pi*Epot)											
displacement rate for cyclic test dr = 100mm/min																		
total duration of test 34min																		
	First envelope curve						Second envelope curve						Third envelope curve					
	Positive			Negative			Positive			Negative			Positive			Negative		
% of vu	mm	kN *)	ved in %	mm	kN *)	ved in %	mm	kN *)	ved in %	mm	kN *)	ved in %	mm	kN *)	ved in %	mm	kN *)	ved in %
1,25	0,80	3,41		-0,88	-4,45													
2,50	1,66	8,66		-1,76	-7,85													
5,00	3,94	16,33		-3,88	-16,55													
7,50	5,31	20,98		-5,27	-22,77													
10,00	7,98	27,47		-7,70	-29,27													
20,00	15,28	42,46	10,0	-15,22	-44,48	10,9	15,11	40,02	8,4	-15,88	-42,22	8,7	15,94	40,05	8,0	-15,98	-42,45	8,2
40,00	28,21	60,79	15,4	-31,17	-59,41	14,5	32,00	53,62	8,9	-31,91	-56,80	8,9	31,64	52,31	7,5	-31,22	-54,34	8,7
60,00	47,49	67,26	11,5	-46,75	-66,24	12,9	47,68	62,03	8,5	-46,95	-60,87	8,2	47,80	59,20	7,7	-47,08	-58,24	8,2
80,00	63,00	69,18	10,6	-63,63	-65,35	12,2	63,98	61,68	8,2	-63,09	-59,01	8,8	63,71	58,36	7,6	-64,01	-55,48	8,2
100,00	79,91	59,37	10,9	-75,23	-56,40	12,9	78,79	50,95	8,1	-79,08	-43,91	9,2	79,30	48,08	7,5	-79,53	-41,63	8,5
120,00	96,05	40,74	11,0	-96,06	-37,59	12,1												

5 Discussion and future prospects

All tests were carried out using ISO/CD 21581 [3]. Boundary conditions were assumed to reflect the actual building conditions. At high vertical loads the shear capacities were achieved. The practicability of ISO/CD 21581 [3] is determined, the applicability also for exeptional timber construction systems is proven.

The system with PFTE showed good performance in monotonic and cyclic testing as well. In monotonic tests the results for maximum horizontal load and for stiffness values are quite similar to conventional timber frame systems.

PFTE showed excellent results for the energy dissipation in cyclic loading, enlarging its potential range of application to seismic and windstorm prone areas. Further work is being done to improve the hold-down of the vertical tensile studs. The PFTE system can cover the same application range as conventional timber frame buildings, yet it is easy to handle and therefore cost effective.

Future research work will be developing a finite – element model to simulate the system properties and to give basics to be implemented in codes.

6 References

[1] Dujic, B., Aicher, S., Zarnic, R., 2005. „Investigations on in-plane loaded wooden elements – influence of loading and boundary conditions“ Otto-Graf-Journal Vol. 16, 2005, pp 259 – 272.

[2] Yasumura, M., Karacabeyli, E., 2007. "International Test Standard development for lateral load test method for shear walls" Proceedings CIB-W 18, paper 40-15-5, Bled, Slovenia.

[3] Committee Draft ISO/CD 21581, 2007. Timber Structures – Static and cyclic lateral test method for shear walls

[4] EN 12512, 2001. Timber Structures – Test methods – Cyclic testing of joints made with mechanical fasteners.

[5] EN 594, 1996. Timber Structures – Test methods – Racking strength and stiffness of timber frame wall panels.

[6] ISO Standard 16670, 2003. Timber Structures – Joints made with mechanical fasteners – Quasi-static reversed-cyclic test method.

INTERNATIONAL COUNCIL FOR RESEARCH AND INNOVATION
IN BUILDING AND CONSTRUCTION

WORKING COMMISSION W18 - TIMBER STRUCTURES

EFFECT OF ADHESIVES ON FINGER JOINT PERFORMANCE IN FIRE

J König

J Norén

M Sterley

SP Trätek/Wood Technology

SWEDEN

Presented by J. König

S. Aicher stated that punishing melamine adhesive which is commonly used in glulam with a penalty factor is too harsh. In I joist finger joints in tensile flange melamine adhesive is dangerous. In glulam the random occurrence of finger joints and occurrence of other defects play a role and the influence also depends on timber quality. J. König agrees the reduction may be less and we need information to back it up. The results show that some adhesives are not equivalent to PRF. Only two PUR adhesives and one MUF adhesive were tested as they were originally regarded as equivalent to PRF but the results were surprising. S. Winter asked whether the glue for glulam or glue for finger joints were tested. J. König answered that in some test cases the same glue for both face and finger joint was used. S. Winter asked whether bending moment under code conditions were estimated. Here from test one can see the charring depth so moment resistance of the residual section can be estimated. In real fire situation of larger member size the influence may be less severe compared to the small cross section tested. B.J. Yeh commented that use of PRF as a benchmark was debated in the US since not all PRF are the same. In the US approach comparison with wood was used as a benchmark. J. Köhler received clarification that the mean values were used as comparison.

Effect of adhesives on finger joint performance in fire

Jürgen König, Joakim Norén, Magdalena Sterley
SP Trätek/Wood Technology, Sweden

Abstract

In an experimental investigation, fire tests were performed on small-sized glued laminated timber beams in bending. The beams consisted of three lamellae with the lamella on the tension side being finger jointed in the middle, thus forming a weak link to initiate failure both at ambient temperature and in fire. Four structural adhesives were tested: one phenolic resorcinol formaldehyde adhesive (PRF) as the reference adhesive representing a traditional adhesive with excellent fire performance, one melamine urea formaldehyde adhesive (MUF) and two polyurethane adhesives (PUR), the latter representing novel adhesives, which are today commonly used in Europe in the production of load-bearing engineered wood products.. The resistance of the beams at ambient temperature was determined prior to the fire tests. The applied loads during the fire tests corresponded to load ratios from about 20 to 40 % of ambient resistance. The fire tests showed that the moment resistance of the beams finger-jointed with MUF and PUR adhesives was 70 to 80 % of the moment resistance of the beams finger-jointed with PRF. Since these adhesives offer advantages in terms of increased production capacity, cost-efficiency and environmental aspects, it is important that these adhesives are not banned from the marked place due to too rigorous design rules. It is proposed to modify the design of bonded timber connections, taking into account the thermo-mechanical properties of the bond by introducing modification factors for e.g. finger joint strength, and to create a new classification of structural adhesives with respect to their fire performance.

1 Introduction

In timber structures, bonded connections have been used for more than 100 years, the first patent for glued laminated beams dating back to 1906. While in the beginning mostly casein adhesives were used, in the early forties phenolic formaldehyde adhesives were introduced in structural applications. Later on, in order to achieve lower hardening temperature and to improve bond strength, resorcine was added as an additional component of the adhesive. The phenolic resorcinol formaldehyde adhesives (PRF) thus obtained were successful on the market due to their structural performance, long term performance and insensibility to elevated temperatures, the latter guaranteeing excellent structural performance in fire. During the last decades, new adhesives have entered the market: first melamine urea formaldehyde (MUF) adhesives due to lower costs and shorter hardening times, later on one-component polyurethane (PUR) adhesives, which are fast curing at ambient temperature, offer safe and a broad range of application possibilities (no mixing) and are formaldehyde-free.

In Europe structural adhesives must comply with performance requirements in accordance with EN 301 [1] and EN 15425 [2]. With regard to performance at elevated temperature, the highest temperature in the tests is 70°C, being held over two weeks under constant loading of the specimens.

Due to new requirements in North America with respect to the heat resistance of adhesives, producers of adhesives are facing a new challenge introducing novel adhesive technologies e.g. one-component polyurethanes, for the production of engineered timber products such as I-beams and glued laminated beams. As an alternative to costly full-scale testing for each structural application, a new standard ASTM D 7247 was published in 2006, prescribing a method performing oven tests with pre-heated specimens with lap-shear joints and applying acceptance criteria that include temperatures considerably above 200°C. No link between these tests and the performance in a fire has been presented.

At ETH Zurich a comprehensive research project was carried out on the fire behaviour of timber-concrete composite slabs [3]. The glued laminated timber beams used for the fire tests were bonded with PUR adhesive. Since fire testing of a slab showed an unexpected shear failure of a glued laminated timber beam, a series of oven tests was carried out to study the shear behaviour of different adhesives at high temperatures [4], [5]. The oven tests were performed with small shear specimens bonded with seven different adhesives: five types of PUR adhesives, one PRF adhesive and one epoxy adhesive. The test results clearly showed that the temperature dependent strength of the bond using PUR adhesives was lower than the strength of the bond using PRF. The test results also demonstrated that shear behaviour of the different PUR adhesives tested at high temperature strongly depends on the specific formulation of the adhesive.

This paper deals with an experimental study with focus on the effect of various adhesives on the fire performance of structural timber with finger joints [6]. Contrary to the research reported in [4] and [5] and the test scenario prescribed by ASTM D 7247, all of them applying oven tests with specimens pre-heated to uniform temperature, in this study the test specimens were exposed to ISO 834 standard fire, and consequently, with non-uniform temperature field in the specimen.

2 Specimens and materials

The test specimens designed for this study should exhibit the performance of finger joints in a fire situation as relevant in wooden I-joists or lamellae of glued laminated beams. At ambient temperature failure of engineered wood products is normally initiated due to failure of a finger joint or failure at knots or other defects of the timber. In order to minimize the risk of failure due to the existence of knots or other defects, and to decrease scatter of the test results, fairly defect free and high density timber was selected. For practical reasons with respect to fire testing and evaluation of the test results, glued laminated beams were used as test specimens. The dimensions were chosen in order to

- achieve test loads compatible with the fire testing equipment
- obtain a relative moment resistance of 20 to 40 % at the time of failure (based on average resistance obtained from beams tested at ambient temperature) which is the normal interval of load levels for timber structures in a fire situation
- achieve failure after sufficiently long time of fire exposure, i.e. a stabilized temperature profile should exist, and to
- achieve a temperature profile between 50 and 300°C in the residual part of the finger jointed lamella.

The resulting dimensions of the glued laminated beams were (width × depth) 90 mm × 135 mm, made of three lamellae of size 45 mm × 90 mm. The lower lamella was finger-jointed in the middle of the beam. Two different configurations with respect to partial and complete protection respectively were chosen in order to achieve different temperature gradients which might have an effect on the resistance. The main part of the tests was carried out using a cross-section as shown in Figure 1a. The upper side of the glued laminated beams was protected by one layer of 15,4 mm thick gypsum plasterboard and 45 mm thick rock fibre insulation, while the remaining sides were unprotected, see Figure 2. The goal was to achieve exposure on three sides.

In order to study the influence of a smaller temperature gradient, i.e. larger zones of the residual cross-

section would be heated, some beams were protected with a single layer of 15,4 mm thick plasterboard on the wide and lower narrow side, while the upper narrow side was protected by three layers of gypsum plasterboard, see Figure 1b.

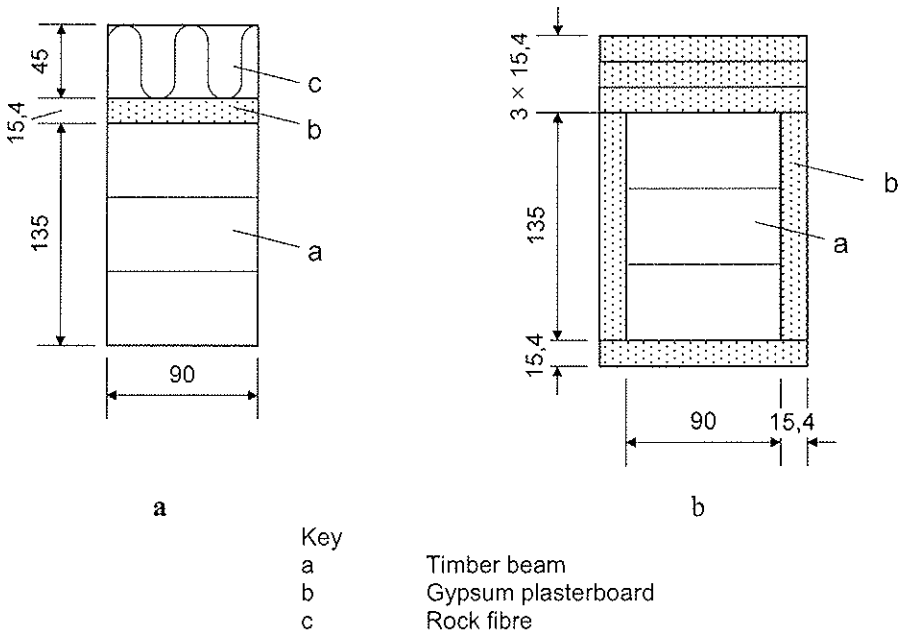

a b

Key

a	Timber beam
b	Gypsum plasterboard
c	Rock fibre

Figure 1 – Cross-section of test specimens

Figure 2 – Example of test specimen for fire testing. Only the central part of the glulam beam with the finger joint in the middle of the bottom lamella is unprotected on three sides.

Performing thermal analyses using SAFIR 2004 [7], it could be seen that these protections would produce fairly constant charring depths on the wide sides of the glued laminated timber beam, see the example shown in Figure 3, and that the finger joint in the lower lamination would be exposed to elevated temperatures between about 50 and 300°C, see Figure 4, showing temperature profiles in the centre line of the cross-section.

The boards (lamellae) were selected at Martinsons Trä AB, Bygdsiljum, Sweden (64°22′ N, 20°29′ E) at two different occasions in February and April 2007. The boards were Norwegian spruce (*picea abies*), taken from the production line of glued laminated beams. The boards were selected after kiln-drying to 12 % moisture content, complying with strength class C30 in accordance with EN 338 [8]. In order to minimise the influence of density on finger joint strength, boards were selected within the density interval from about 440 to 490 kg/m^3.

Five adhesives were chosen for the production of the finger joints, four of which were structural adhesives and one non-structural:

- two polyurethane (PUR) adhesives (structural): test series PUR 1 and PUR 2;
- one melamine urea formaldehyde (MUF) adhesive (structural): test series MUF 1;
- one phenolic resorcinol formaldehyde (PRF) adhesive (structural): test series PRF 1;
- one polyurethane (PUR) adhesive (non-structural): test series PUR 3.

The test beams were produced at two companies in Switzerland under ordinary production conditions, and a company in Sweden (it was not possible to find a workshop that could produce the beams using different adhesives without unduly interfering with regular production).

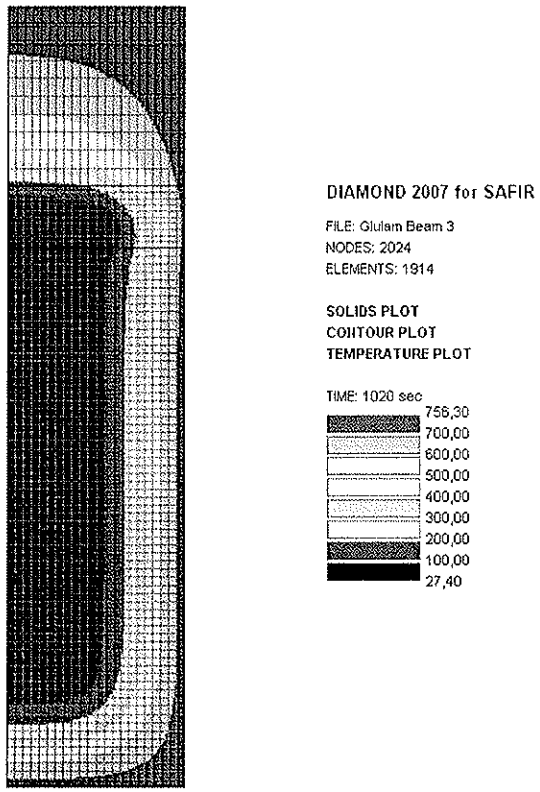

Figure 3 – Results of heat transfer analysis of unprotected beam: Temperature field after 17 minutes of fire exposure. The border of the residual cross-section is represented by the 300°C isotherm.

3 Ambient reference tests

Reference tests at ambient temperature were conducted in accordance with EN 408 [9] of test beams with following adhesives: PUR 1, MUF 1, PRF 1 (all of them structural adhesives), and PUR 3 (non-structural). Each series consisted of 5 specimens. The results are shown in Figure 5. Since two of the test results of series MUF 1 significantly deviated from the others, further examination of the photographs taken of each of the specimens after failure showed that these two specimens exhibited different failure modes, possibly causing premature failure. While all other failures were apparently initiated in the finger joint, failure of one specimen started at a knot at a distance of 450 mm from the finger joint, while, in another specimen, premature failure was caused by a knot very close to the finger joint. Statistical evaluation excluding the two outliers, showed considerably higher mean values and lower standard deviation and coefficient of variation. Therefore, in order to serve as reference values to predict the ambient moment resistance of the beams to be tested under fire exposure, the outliers were not taken into account. The mean values of bending strength of series PUR 1, PRF 1 and MUF 1 are very close together; only series PUR 3 using a non-structural adhesive exhibits a considerably larger variability of results and lower mean bending strength. The bending strength of three out of five test beams is however of the same magnitude as the bending strength of the test beams using structural adhesives. As shown in Figure 5, within the density interval in question, there is no evident effect of density and adhesive type on the strength of the finger joints.

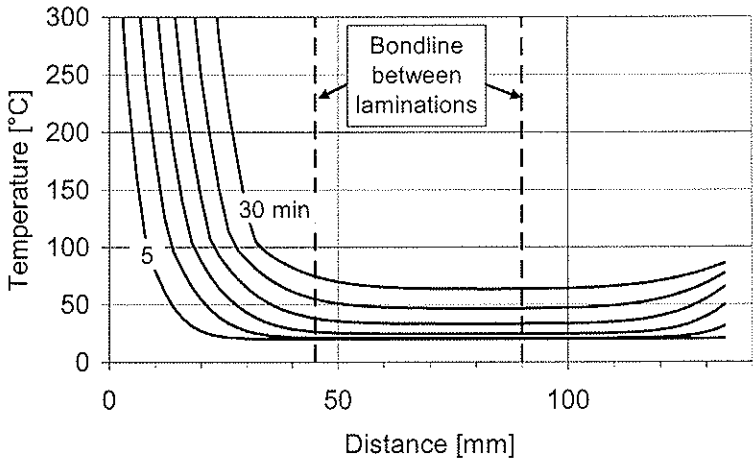

Figure 4 – Calculated temperature profile along the centre line of the unprotected test beam after 5, 10, 15, 20, 25 and 30 minutes of fire exposure. The charring depth in the middle of the bottom lamella is characterized by the distance (x-axis) at temperature of 300°C.

Table 1 – Mean value, standard deviation and coefficient of variation for ambient bending strength values, $f_{m,fi}$, specified for each test series and the combination of series PUR 1 + MUF 1 + PRF 1

	PUR 1	**MUF 1**[1]	**MUF 1**[2]	**PRF 1**	**PUR 3**	**PUR 1 + MUF 1**[2] **+ PRF 1**
Mean value	51,9	43,3	48,7	50,7	43,6	50,7
Standard deviation	5,20	8,04	3,33	3,63	8,35	4,15
COV	0,099	0,186	0,068	0,072	0,191	0,082

[1] All tests
[2] Outliers excluded (knot failure)

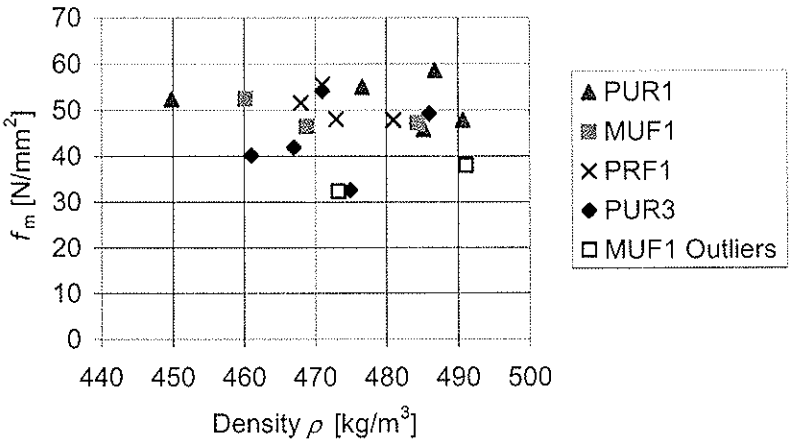

Figure 5 – Test results from reference tests at ambient temperature: Moment resistance vs. density.

4 Fire tests

4.1 Test set-up

A small-scale gas-fired furnace was used, with interior cladding of ceramic fibre and interior dimensions of 1 m × 0,6 m × 0,6 m (length × depth × width). In order to enclose the test specimen, the

depth of the furnace was increased by 320 mm and a cover lock was placed upon the walls, see Figure 6. The furnace temperature was measured by means of a plate thermocouple located in the middle of the furnace 150 mm below the bottom side of the test specimen and used for controlling the furnace temperature. In order to allow visual observation of the specimen during the fire test, an opening was located in the middle of the wide side 300 mm below the specimen.

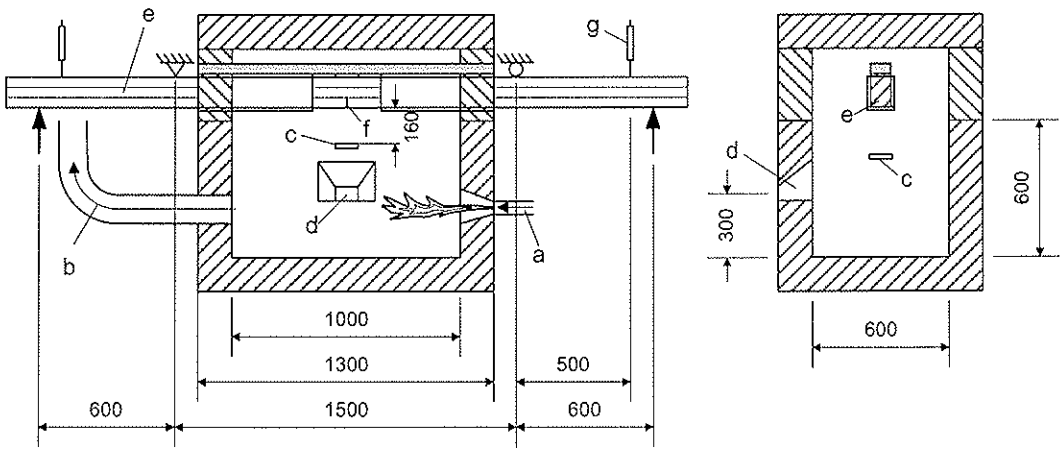

Key:

a	Gas burner	e	test specimen
b	Exhaust	f	position of finger joint
c	Plate thermocouple	g	transducer
d	opening		

Figure 6 – Test set-up: Small-scale furnace and position of supports and load introduction

The supports of the test beams were located outside the furnace with a free span of 1500 mm. The vertical external loads were applied at a distance of 600 mm from the supports by means of hydraulic jacks in such a way that the lower lamella with the finger joint was in tension.

4.2 Fire tests and results

Immediately after application of the load corresponding to 20 to 40 % of resistance at ambient temperature, the fire was started and manually controlled by following the standard fire curve in accordance with ISO 834. After failure of the beam the gas burner was immediately turned off, the lock and one of the upper parts of the furnace wall removed and the fire was extinguished with water, normally within one to maximum two minutes after the burner had been turned off. From each specimen, a slice of the cross-section was cut out close to the finger joint, see e.g. Figure 7, for measuring the charring depth.

An example of the relationship of the bending moment in the fire exposed part of the beam versus time is shown in Figure 8.

The relationship between the relative bending resistance (load ratio) and time of failure is shown in Figure 9. For simplicity, the load ratios of series PUR 3 were related to the mean strength of the combined series PUR 1 + MUF 1 + PRF 1.

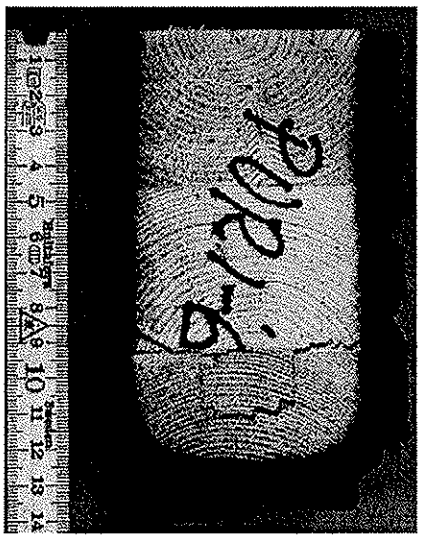

Figure 7 – Example of cross-section after fire test.

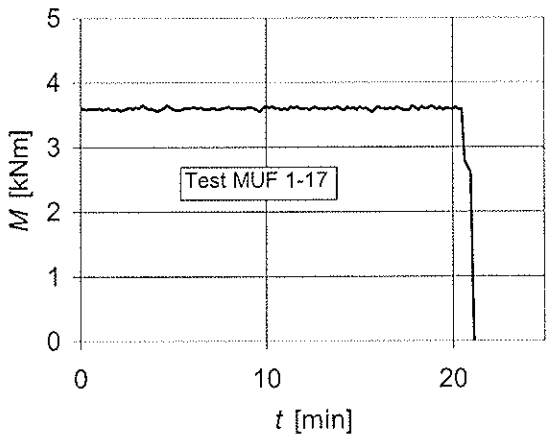

Figure 8 – Example of bending moment vs. time during fire test

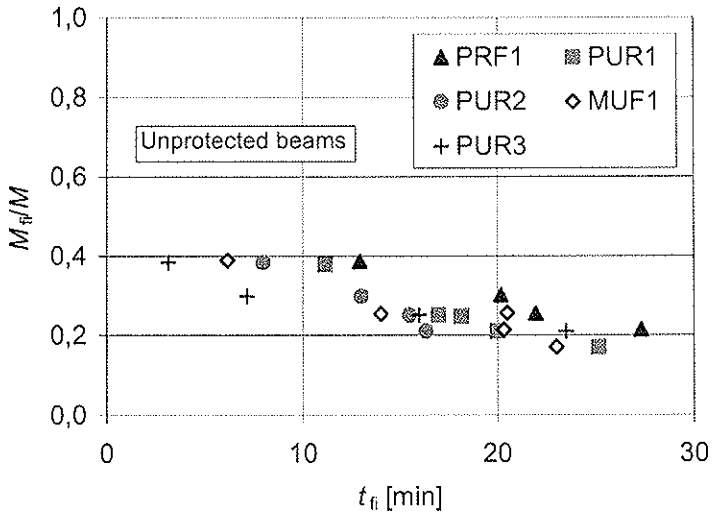

Figure 9 – Relative bending resistance (load ratio) vs. time to failure of unprotected beams

From the results presented can be seen that series PRF 1 exhibits a smaller reduction of moment resistance in the fire situation than all other test series, or with other words, the fire resistance of series PRF 1 is greater than the fire resistance of all other test series. In order to quantify the reduction of moment resistance of test series PUR 1, PUR 2 and MUF 1 in relation to test series PRF 1, as the first step, the results shown in Figure 9 were fitted to regression curves given by

$$\frac{M_{\mathrm{fi}}}{M} = a\, t_{\mathrm{fi}}^{b} \tag{1}$$

see Figure 11. Since each series only consists of four or five test specimens, there exists a considerable scatter of results. Therefore, a regression curve was also determined for the combined results of PUR 1 + PUR 2 and MUF 1, see Figure 12.

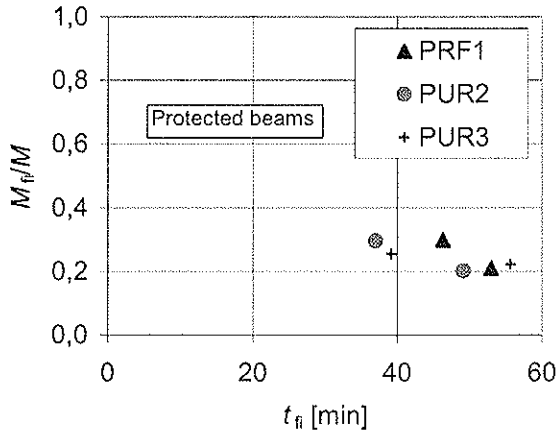

Figure 10 – Relative bending resistance (load ratio) vs. time to failure of protected beams

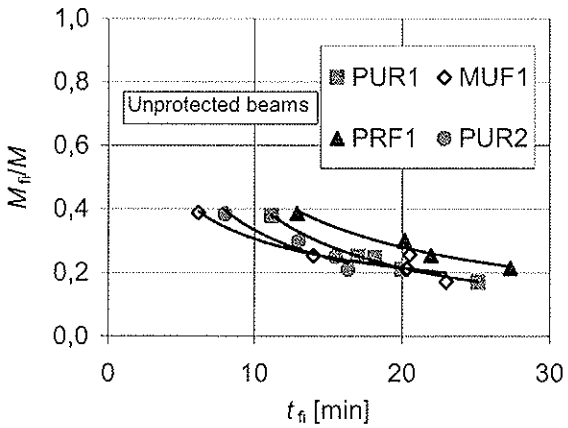

Figure 11 – Fitting of regression curves to test results

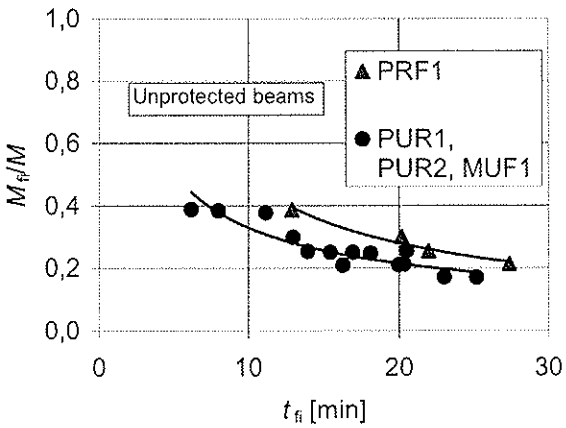

Figure 12 – Fitting of regression curves to test results

For each of the three above mentioned tests series, the ratios of $M_{fi}/M_{fi,PRF1}$ were determined as functions of the failure time, t_{fi}. No extrapolation of the regression curves was applied. The results are shown in Figure 13.

For the same thermal conditions the charring depth and therefore also the residual cross-section are only functions of time. Therefore the bending strength ratio in fire is equal to the moment resistance ratio:

$$\frac{f_{m,fi}}{f_{m,PRF1}} = \frac{M_{fi}}{M_{PRF,fi}} \tag{2}$$

For protected beams only two tests were made in each series. Therefore, for test series PRF 1 and PUR 2 linear expressions were determined for interpolation of test results. The moment resistance ratio of series PUR 1 and PRF 1 is shown in Figure 14.

These results show that the moment resistance – and therefore also the bending strength – of beams of series PUR 1, PUR 2 and MUF 1 is about 70 to 80 % of the corresponding values of series PRF 1.

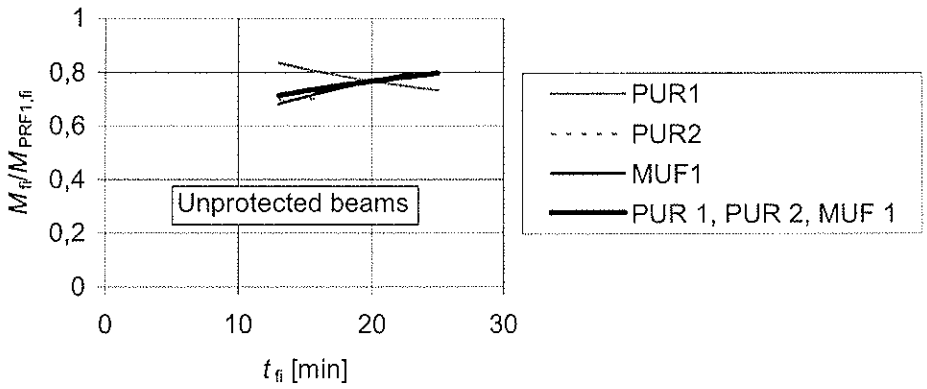

Figure 13 – Relative moment resistance of unprotected beams: Comparison of series PUR 1, PUR 2 and MUF 1 with series PRF 1.

The reduction of strength seems independent of whether the beams are protected or not.

Comparing specimens with the same or almost the same moment resistance shows that protected beams failed when the charring depth was about 50 % of the charring depth of unprotected beams.

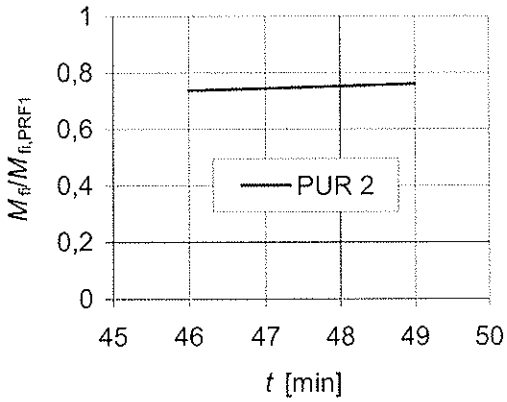

Figure 14 – Relative moment resistance of protected beams: Comparison of series PUR 1 with series PRF 1.

5 Conclusions and further research needs

The fire tests showed that there is a considerable loss of bending resistance of the test beams. Within the interval of time considered in this investigation, for load ratios between 0,2 and 0,4 of the PRF beams, the moment resistance of beams with finger joints bonded with structural PUR and MUF adhesives was between 70 and 80 % of the moment resistance of beams with finger joints bonded with PRF adhesive. There is no apparent influence of the temperature gradient in the timber, i.e. between unprotected and protected beams.

Since the number of tests and adhesives was small, test series should be performed with a larger number of specimens in order to achieve greater statistical reliability. Further, a possible influence of test beam configurations should be investigated, e.g. larger glued laminated beams and composite products such as I-joists should be considered.

These tests reported here were designed with the purpose of obtaining finger joint failure both at ambient temperature and in the fire tests. In commercial grades, however, failure would often be caused by knots or other defects. Since the random occurrence of weak zones – i.e. finger joints, knots or other defects – has an effect on the resistance of the beams, it should be investigated to what extend fire safety is influenced by the performance of various adhesives. In glued laminated beams with lamellae with a large knot area ratio these defects may be the dominating cause of failure, whereas high quality lamellae will cause more finger joint failures.

6 Consequences for the design

The use of some novel adhesives in bonded timber connections may imply reduced safety in fire compared to traditionally used PRF adhesives. The tests showed that beams bonded with some novel adhesives, both MUF and PUR, exhibit smaller fire resistance than those bonded with PRF, although these adhesives are fulfilling current approval criteria in Europe. The North American approach – to exclude all adhesives not satisfying the performance requirements in small-scale tests with specimens pre-heated to a temperature of 225°C – is likely to exclude most novel structural adhesives that would perform well in a fire situation. This would counteract the wish of many countries to eliminate the use of formaldehyde.

A change of the design codes, permitting the *calculation* of bonded connections in fire taking into account the thermo-mechanical material properties, would open the door for the use of novel, formaldehyde-free adhesives, would permit lower costs and reduce production time. Consequently, new classification for structural adhesives should be established with criteria with respect to their performance in fire. A better method would give the designer a tool to take into account the thermo-mechanical properties of the bond by introducing a modification factor for the strength of the bond.

7 Acknowledgement

This investigation was carried out at SP Trätek, Stockholm, Sweden, and commissioned by Purbond AG, Switzerland. The authors wish to express their gratitude to collaborate with Purbond AG, and especially to Stefan Gerber for his deep interest in the work.

8 References

[1] EN 301: Adhesives, phenolic and aminoplastic for load-bearing timber structures – Classification and specifications. European Committee for Standardization, Brussels, 1997.

[2] EN 15425: Adhesives - One component polyurethane for load bearing timber structures - Classification and performance requirements. European Committee for Standardization, Brussels, 2008.

[3] Frangi A, Fontana M, A Design Model for the Fire Resistance of Timber-Concrete Composite Slabs, International Conference on Innovative Wooden Structures and Bridges, Lahti, Finland, August 29-31, 2001, Conference Report edited by IABSE, ETH Zurich.

[4] Frangi A, Fontana M, Mischler A, Shear behaviour of bond lines in glued laminated timber beams at high temperatures, Wood Science and Technology, Volume 38, No. 2, May 2004, pages 119-126, Springer Verlag, Berlin.

[5] Frangi A, Fontana M, Effect of temperature on the structural behaviour of bond lines in glulam, 1th International Symposium on Advanced Timber and Timber-Composite Element for Buildings, Conference Report, COST Action E-29, October 27-29, Florence, 2004.

[6] König J, Norén J, Sterley M, Performance of finger joints in fire exposed glued laminated beams. SP Trätek. Report P700615, Stockholm, 2008.

[7] Franssen, J.M, Kodur, V.K.R., Mason, J., User's manual for SAFIR 2004 – A computer program for analysis of structures subjected to fire. University of Liege, Department Structures du Génie Civil – Service Ponts et Charpentes. Liege, Belgium, 2005.

[8] EN 338: Structural timber – Strength classes. European Standard. European Committee for Standardization, Brussels, 2003.

[9] EN 408: Timber Structures – Structural timber and glued laminated timber – Determination of some physical and mechanical properties. European Committee for Standardization, Brussels, 2003.

INTERNATIONAL COUNCIL FOR RESEARCH AND INNOVATION
IN BUILDING AND CONSTRUCTION

WORKING COMMISSION W18 - TIMBER STRUCTURES

DETERMINATION OF SHEAR MODULUS BY MEANS OF STANDARDIZED FOUR-POINT BENDING TESTS

R Brandner

Competence Center holz.bau forschungs gmbh

B Freytag

Graz University of Technology, Laboratory for Structural Engineering

G Schickhofer

Graz University of Technology, Institute for Timber Engineering and Wood Technology

AUSTRIA

Presented by R. Brandner

H. Blass stated that the last slide shows low COV for G in the test. He asked why 20% was used in the proposal for characteristic values. R. Brandner explained that 20% COV is for single solid members when n (the number timber elements) increased, COV decreased which explained the COV values in the last slide. Since the test data was measured at a distance of h from the support, is there an influence from compression. R. Brandner answered that this was recognized in FEM analysis and already considered this in the study.

Determination of Shear Modulus by means of standardized Four-Point Bending tests

R BRANDNER

Competence Center holz.bau forschungs gmbh
Austria / Europe

B FREYTAG

Graz University of Technology, Laboratory for Structural Engineering
Austria / Europe

G SCHICKHOFER

Graz University of Technology, Institute for Timber Engineering and Wood Technology
Austria / Europe

Abstract

According to EN 408, the shear modulus can be determined by means of two standardized test methods, i.e. the single span method and the variable span method. In the last few years, two further methods, namely torsion tests and 'shear field' tests, have been developed and are now also performed in testing practice. The latter is based on a relatively simple and reproducible measurement of the shear distortion by means of standardized four-point bending tests according to EN 408. The measuring instruments are applied within the areas of constant transverse force. They are arranged symmetrically with respect to the neutral axis, which results in four 'shear fields' under investigation (left-right, front-back).

The practical results, gained from performing standardized test methods, torsion tests as well as the measurement of shear distortion within 'shear fields' on glued laminated timber beams (GLT) of strength classes GL24h (w_g / d_g = 150 / 320 mm), as already published by Brandner et al. (2007), are outlined, discussed and completed by current tests on GL36h and GL36c (w_g / d_g = 160 / 600 mm). Furthermore, the relation of the shear modulus and the GLT-strength class, in comparison with solid timber, is treated.

Torsion tests are simple, robust and do not require expensive equipment, but they only provide the shear modulus $G_{090,tor}$. This method is proposed for the determination of G-values on specimens of small cross sections and for obtaining G-values for solid timber. With the measurement of shear distortion by the application of 'shear fields' on specimens tested in four-point bending according to EN 408 not only the standard values $E_{m,l}$, $E_{m,g}$ and f_m can be determined, but it allows also an easy, affordable and robust determination of the material characteristic G-modulus. The 'shear field' test method is proposed and approved for GLT with $d_g \geq 300$ mm. A proposal for the consideration of both methods within the testing standard EN 408 is presented.

1 Introduction

Wood and timber, in particular, is a heterogenous, natural material with generally high dispering properties. A treatment of wood as orthotropic material in timber engineering and modelling requires nine independent parameters: to link the tensor of strength and elongation, three moduli of elasticity and three shear moduli are necessary. To determine these six material constants, reliable test configurations that also allow practical application are required. This way, robust and reproduceable characteristics can be gained on the one hand and, by means of international standardization, comparability and reduction of costs and resources can be enabled on the other.

When it comes to practical applications, the main focus lies on the modulus of elasticity parallel to the fiber, predominantly in bending, (E_m), e.g. for Nordic spruce (*picea Abies Karst.*) of about $E_{m,l,mean}$ = 12,500 N/mm². The expectable shear modulus in solid timber, by contrast, – due to varying cutting patterns and varying radial positions in the stem a smeared value of G_{12} and G_{13} → G_{090} – lies around $G_{090,mean}$ = 650 N/mm², calculated acc. to the regression function given in Görlacher and Kürth (1994) and in line with Niemz (1993) and Kollmann (1995). This reflects a relationship between $G_{090,mean}$ / $E_{m,0,mean}$ of around 1 / 19 and seems to lead to minor influence and relevance of a correct G-modulus for serviceability in comparison to the E-modulus considering the ratio between bending- and shear deflection. Acc. to EN 338, a constant relationship of $G_{090,mean}$ / $E_{0,mean}$ = 1 / 16 and acc. to EN 1194 a factor of $G_{090,mean}$ / $E_{0,mean}$ = 1 / 15.4 is given. Due to many important reasons (see Harrison (2006), Divos et al. (1998), Görlacher and Kürth (1994), Niemz (1993) and others), the ratio $G_{090,mean}$ / $E_{0,mean}$ can not be treated as constant and varies for example in Nordic spruce in the range of $G_{090,mean}$ / $E_{0,mean}$ = 1 / 11 ÷ 1 / 37, depending on timber quality and applied test methods (see e.g. Brandner et al. (2007)). The importance of a correct G-modulus has already been discussed in several papers. In case of wood modelling and timber engineering, the following question can be rised: how accurate is accurate enough. In case of beams of high span-to-depth ratio (l_{span} / d) under bending, shear deflection plays a minor and even neglectable role compared to bending deflection. Nevertheless, in several constructions G_{090} gains increasing importance, especially in decreasing span-to-depth ratios and in case of lateral torsional buckling (see e.g. Skaggs and Bender (1995), Gehri (2005)).

In this paper, the following two test methods for deriving G-modulus of timber and engineered timber products are discussed: torsion tests and the application of shear fields during standardized 4p.-bending tests. The first method has already been treated in detail in Brandner et al. (2007). Given recommendations for the standardization of torsion tests instead of the two methods regulated in the past in EN 408, the single span method and the variable span method already exist. A draft prEN 408 was worked out and distributed by Leijten (2008). The second method is treated in more detail in this paper as further encouraging experiments have been concluded that reflect and undermine the relatively simple and reliable test method.

2 Materials

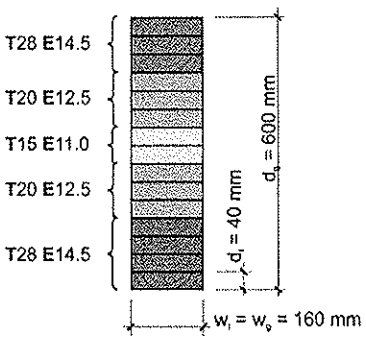

Fig 1: Cross section of GL36c: strength classes of boards

Three independent series of glued laminated timber of Nordic spruce (*picea Abies Karst.*) were tested in four-point bending (4pB) acc. EN 408. The first series – **GLT-I** – was glulam of strength class GL24h acc. EN 1194 of cross section w_g / d_g = 150 / 320 mm. Details are given in Brandner et al. (2007). 25 # glulam beams of the second series **GLT-II** of strength class GL36h acc. to EN 1194 were built up of boards graded to L40 acc. to EN 14081 by means of Golden Eye 706 / Microtec (combination of eigenfrequency and X-ray scanner) to fulfill **T28E**14.5 ($f_{t,0,l,k}$ = 28 N/mm², $E_{t,0,l,mean}$ = 14,500 N/mm²). 5 # GLT-beams of the third series **GLT-III** of GL36c acc. to EN 1194 were built up of three different lamella strength grades – **T28E**14.5, **T20E**12.5 and **T15E**11.0 – graded visually as well as by additional means of density and dynamical E-modulus $E_{dyn,US}$ (see Fig. 1). The cross sections of series **GLT-II** and **GLT-III** were w_g / d_g = 160 / 600 mm, built up of 15 # lamellae of thickness d_l = 40 mm.

3 Methods

All tests were carried out by continuous measurements of time, deflections and forces. Failures were analysed and recorded. The four-point-bending tests were derived by application of hysteresis with peaks of deflections at 50 % of the calculated average maximum stress level. The test configurations for tension tests and 4p.-bending tests were performed acc. to EN 408.

3.1 Tensile tests of boards and finger joints

The tensile tests of boards parallel to the grain were carried out acc. EN 408, with a free testing length of $l_{test} > 9 \cdot w_l = 1{,}420$ mm in series **GLT-I**, $l_{test} > 9 \cdot w_l = 3{,}348$ mm in series **GLT-II**, and $l_{test} > 9 \cdot w_l = 4{,}350$ mm in series **GLT-III**, by measuring the global deflections over adjusted $l_{0,machine}$. Tension tests on finger joints were accomplished with a free testing length of $l_{test} = 200$ mm acc. EN 1194. The tension characteristics $f_{t,0,l}$, $f_{t,j}$ and the modulus of elasticity $E_{t,0,l}$ were calculated acc. to EN 408. The modulus of elasticity $E_{t,0,l}$ was adjusted to a reference moisture content of u = 12 % to $E_{t,0,l,12}$ as given in EN 384.

3.2 Four-point-bending tests on glulam

The standardized 4p.-bending tests on edgewise loaded GLT were conducted acc. to EN 408 with a span of $l_{span} = (18 \pm 3) \cdot d_g$ and with a distance of $l_{load} = 6 \cdot d_g$ between the loading points. During the 4p.-bending tests, measurements of local- (over a length of $l_l = 5 \cdot d_g$) and global bending deflections and forces were recorded (see also Fig. 2). The mechanical characteristics $f_{m,g}$, $E_{m,g,l}$ and $E_{m,g,g}$ were calculated acc. to EN 408 and adjusted to a reference moisture content of u = 12 % to $E_{m,g,l,12}$ and $E_{m,g,g,12}$ as given in EN 384.

3.3 Applied test methods for the determination of shear modulus G_{090} of glulam

In total, four different test methods for deriving the G-modulus of GLT were applied. Firstly, the two methods regulated so far in EN 408 – the 'single span method' and the 'variable span method' – were investigated. Secondly, the shear distortion was measured by means of torsion tests on GL24h beams (series **GLT-I**), as this test method is already established and standardized in the United States (see ASTM D 198). The fourth method, scarce but also already established in practise, measures the shear distortion within shear fields by means of standardized four-point bending tests according to EN 408. The measuring instruments are applied within the areas of constant transverse force. They are arranged symmetrically with respect to the neutral axis, which results in four 'shear fields' under investigation (left-right, front-back). The first three methods have already been discussed in detail in Brandner et al. (2007). The last method – 'measurement of shear distortion within shear fields' – was examined in more detail within the series **GLT-II** and **GLT-III** and is described hereafter.

Measurement of shear distortion within shear fields by means of standardized four-point bending tests acc. to EN 408

Measurements of shear distortion in the area of constant transverse force during shear tests have already been developed in the past e.g. by FMPA (1983) and Gehri (2005). The idea was to adjust this test configuration, generally applied in shear tests, for the standard 4p.-bending test configuration given in EN 408 (see Fig. 2, Fig. 3 and Fig. 4).

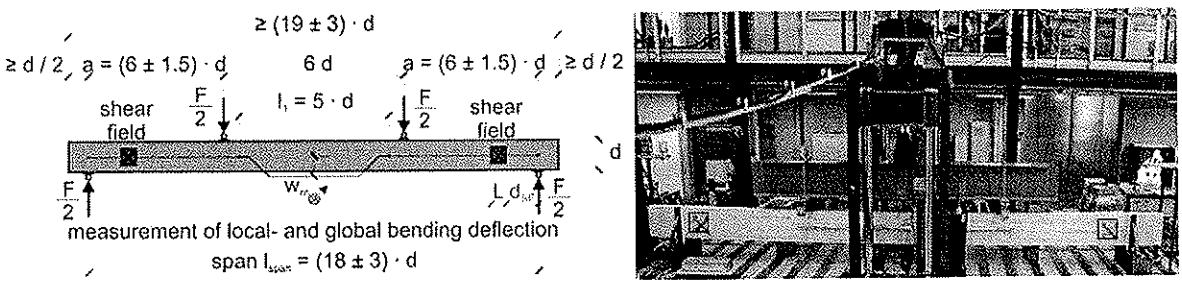

Fig. 2: Test configuration of 4p.-bending tests on GLT acc. to EN 408: measurement of local- and global bending deflection and application of shear fields for measurement of shear deflection (left), image of the 4p.-bending tests of series **GLT-II** and **GLT-III** (right)

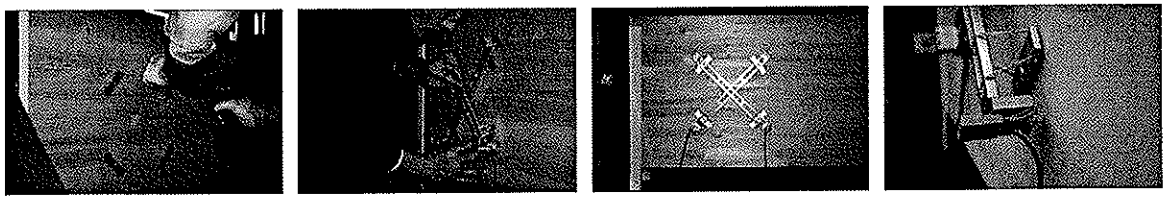

Fig. 3: Application of shear fields of series **GLT-II** and **GLT-III**: fixing of holders for rubber bands (left), mounting of measurement device (left-middle), overview (middle-right), detail of distortion measurement device DD1 with metering needle placed on a nail-head (right)

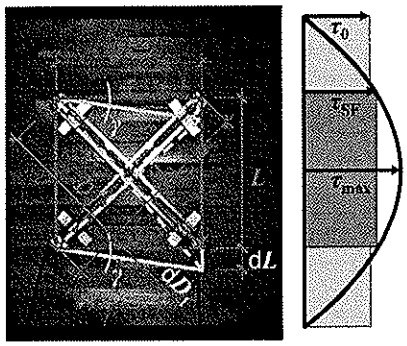

Fig. 4: Shear field and declaration of τ_0, τ_{max} and τ_{SF}

Due to minor induced shear distortion, the precise measurement device DD1 with 1 / 1000 mm accuracy was applied on all of the four shear fields of each GLT-beam, placed on both sides of the constant transverse force and opposite each side of the beam (left-right, front-back) and tested edgewise in 4p.-bending acc. to EN 408. The dimension of the squared shear fields was L / L = 283 / 283 mm with D = 400 mm and d_{SF} = 500 mm. They were arranged symmetrically to the neutral axis. In general a distance between the shear field and the bearing point of $d_{SF} \geq d$ is recommended to reduce the influence of compression stress perpendicular to the grain to a non-relevant level. Due to the squared parabola shape of the shear stress distribution over the cross section and the reduced monitoring field of shear distortion over the depth of the beam, the generally applied shear correction factor κ = 6 / 5 was adjusted and replaced by α acc. to [1], [2] and in reference to Gehri (2005). The calculation of α is a simple relationship of the distribution of shear stress over the whole depth of the beam versus the shear stress distribution within the shear field in relationship to the maximum shear stress in the middle of the beam τ_{max}. The calculation procedure for deriving $G_{090,SF}$ is given in [3] and [4].

$$\alpha = \frac{\tau_{SF}}{\tau_0} + \frac{2}{3} \cdot \left(\frac{\tau_{max}}{\tau_0} - \frac{\tau_{SF}}{\tau_0} \right) = 1 + \frac{1}{3} \cdot \frac{\tau_{SF}}{\tau_0} \qquad [1]$$

$$\tau_0 = G_{090} \cdot \gamma = \frac{Q_z}{w \cdot d}, \quad \tau_{SF} = \tau_{xz}\left(z = \frac{L}{2}\right) = \frac{Q_z \cdot S(z)}{I_y \cdot w}, \quad \frac{\tau_{max}}{\tau_0} = \frac{3}{2} \qquad [2]$$

$$\gamma = \frac{dD_1 - dD_2}{L \cdot \sqrt{2}} \quad \text{.... with} \quad dD_1 > dD_2 \qquad [3]$$

$$G_{090,SF} = \alpha \cdot \frac{\tau_0}{\gamma} = \alpha \cdot \frac{\sqrt{2} \cdot L}{A} \cdot \frac{dQ_z}{dD_1 - dD_2} \qquad [4]$$

4 Results

4.1 $G_{090,SF}$ in connection with the GLT strength class of series GLT-II

4.1.1 Tensile test data of boards and finger joints

The results of the performed static tensile tests ($f_{t,0,l}$, $E_{t,0,l,12}$, $\rho_{l,12}$) of series **GLT-II** are given in Tab. 1. The statistical analysis reflects the expected COV-$f_{t,0,l}$ = (25 ± 5 %) = 26.9 % for the high strength class **T28E**14.5 and also the fulfilment of the requirements for the **T28E**14.5 strength class acc. to Brandner and Schickhofer (2008) with $f_{t,0,l,k}$ = 28.6 N/mm², $E_{t,0,l,mean,12}$ = 14,440 N/mm² and $\rho_{l,k,12}$ = 440 kg/m³. The statistics of the finger joints tensile strength values also corresponds with the expected COV-$f_{t,j}$ = (15 ± 5 %) = 18 %, but shows a bit too low ($\Delta f_{t,j}$ = 2.5 N/mm²) with a characteristic strength of $f_{t,j,k}$ = 31.1 N/mm² instead of required $f_{t,j,k,requ} = 1.2 \cdot f_{t,0,l,k,requ} = 1.2 \cdot 28.0$ = 33.6 N/mm² acc. to the proposed model given in Tab. 3.

Tab. 1: Statistics of tensile tests on boards and finger joints of the base material of series **GLT-II**

GLT-II Base material	**Tension tests – boards**			**Finger joints**
	$\rho_{t,12}$ [kg/m³]	$E_{t,0,l,12}$ [N/mm²]	$f_{t,0,l}$ [N/mm²]	$f_{t,j}$ [N/mm²]
Quantity	102 #	102 #	98 #	30 #
mean	**494**	**14,440**	**45.6**	**52.0**
COV	**6.9 %**	**8.7 %**	**26.9 %**	**18.1 %**
$x_{05,empD}$	439	12,600	26.6	33.3
$x_{05,DM}$	440 (2pLND)	12,620 (3pWD)	26.3 (3pWD)	32.6 (2pWD)
$k_{size,EN\ 1194}$	--	--	1.07	--
$x_{k,DM}$	--	--	**27.2**	**31.1**
$x_{k,EN\ 14358}$	--	--	**28.6**	--

4.1.2 Four-point-bending test data of GL 36h

The 25 # glulam beams were tested acc. Fig. 2-left, with a span of $l_{span} = 15 \cdot d_g = 15 \cdot 600 = 9{,}000$ mm. The predominant failure criteria were analysed by continuously observing each 4p.-bending test and by painstaking examination of the fracture region under consideration of years of practical experience. Consequently, the failure criteria were grouped to 'predominant failures in timber due to bending' – 'wood failure' (WF) (16 #), 'predominant failure in timber due to shear' – 'shear failure' (SF) (3 #) and 'predominant failure in the finger joint' – 'finger joint failure' (FJF) (6 #). For further discussion relevant statistics are given in Tab. 2, including the values of $G_{090,SF}$.

Tab. 2: Statistics of series **GLT-II** – GL36h acc. EN 1194 – tested in 4p.-bending acc. EN 408: test results of all 25 # beams and statistiscs of beams with wood failures in bending (WF)

GLT-II_all	$\rho_{g,12}$ [kg/m³]	$E_{m,g,l,12}$ [N/mm²]	$E_{m,g,g,12}$ [N/mm²]	$G_{090,SF,12}$ [N/mm²]	$f_{m,g}$ [N/mm²]
quantity	25 #	25 #	25 #	25 #	25 #
mean	**498**	**15,880**	**14,650**	**660**	**41.9**
COV	**1.2 %**	**3.8 %**	**3.5 %**	**4.8 %**	**12.2 %**
$x_{05,empD}$	490	15,080	13,950	608	32.7
$x_{05,DM}$	489 (2pLND)	15,090 (3pWD)	13,960 (3pWD)	609 (2pLND)	33.5 (ND)
$x_{k,EN\ 14358}$	--	--	--	--	**33.2**
GLT-II_WF	$\rho_{g,12}$ [kg/m³]	$E_{m,g,l,12}$ [N/mm²]	$E_{m,g,g,12}$ [N/mm²]	$G_{090,SF,12}$ [N/mm²]	$f_{m,g}$ [N/mm²]
quantity	16 #	16 #	16 #	16 #	16 #
mean	**499**	**15,750**	**14,540**	**662**	**42.3**
COV	**1.4 %**	**3.7 %**	**3.5 %**	**5.0 %**	**7.7 %**
$x_{05,DM}$	483 (2pWD)	15,050 (3pWD)	13,930 (3pWD)	609 (2pLND)	37.0 (ND)
$x_{k,EN\ 14358}$	--	--	--	--	**36.7**

4.1.3 Verification of the 'Graz bearing model for GLT in bending'

The 'Graz bearing model for GLT in bending' consists, in accordance to EN 1194, of two sub-models: the first sub-model concerns the requirements for the tensile strength of boards, and the second sub-model regulates the minimum requirements for the tensile strength of finger joints. Furthermore, the sub-models are splitted into two practically relevant ranges of COV-$f_{t,0,l}$ as one of the main parameters which influences the homogenisation effect (laminating effect – k_{lam}) in the system structure GLT on the decisive 5 %-quantile-level. A comparison with other bearing models and further details are given in Brandner (2006) and Brandner and Schickhofer (2007, 2008). The model itself – a proposal for the glulam standard prEN 14080 – is given in Tab. 3.

The verification of the 'Graz bearing model for GLT in bending' acc. to Tab. 3 by utilisation of the test results of series **GLT-II** can easily be carried out by means of two different verification processes: The first verification process only considers the requirements on the tensile strength of the boards, assuming a GLT without finger joints. Acc. to the results given in Tab. 1,

($f_{t,0,l,k}$ = 28.6 N/mm², COV-$f_{t,0,l}$ = 26.9 %) the bearing model for COV-$f_{t,0,l}$ = 25 ± 5 % was applied and led to $f_{m,g,k,calc\text{-}1} = 2.5 \cdot f_{t,0,l,k}^{0.8} \cdot k_{size,g,m} = 2.5 \cdot 28.6^{0.8} \cdot 1.00 = 36.6$ N/mm². The comparison with $f_{m,g,k}$ from performed tests, by only considering failures in timber (WF) (see Tab. 2-below) – as the verification only considers the mechanical requirements on the boards, but not those on the finger joints – , leads to $f_{m,g,k,calc\text{-}1} / f_{m,g,k,WF} = 36.6 / 36.7 =$ **99.7 % compliance**. The second verification process considers both parts of the bearing model – the requirements on the tensile strength of the boards and the minimum requirements on the tensile strength of finger joints. As visible from the statistics in Tab. 2 and Fig. 8-left (chapter 4.2), the finger joints were the limitative parameter of the 5 %-quantile and induced the lowest strength values of tested GL36h. Consequently, the tensile strength of the boards as necessary and economically meaningful for GLT acc. to the potential of the finger joints, can be calculated based on the requirement $f_{t,j,k} \geq 1.2 \cdot f_{t,0,l,k}$ with prefactor 1.2 for COV-$f_{t,0,l,k}$ = 25 ± 5 %. Taking the boarder case of $f_{t,j,k} = 1.2 \cdot f_{t,0,l,k}$ and the test results given in Tab. 1, the result is $f_{t,0,l,k,theor} = f_{t,j,k} / 1.2 = 31.1 / 1.2 = 25.9$ N/mm². The insertion of the tensile strength of the boards in the second relationship to calculate the bending strength potential of GLT on the decisive 5 %-quantile level leads to $f_{m,g,k,calc\text{-}2} = 2.5 \cdot f_{t,0,l,k,theor}^{0.8} = 2.5 \cdot 25.9^{0.8} = 33.8$ N/mm². The comparison of the calculated value with the test results given in Tab. 2, by consideration of the statistics of all tested beams, leads to $f_{m,g,k,calc\text{-}2} / f_{m,g,k,all} = 33.8 / 33.2 =$ **101.8 % compliance**. The test result, in comparison with other proposals and models for prEN 14080 and past models, is given in Fig. 5.

Tab. 3: 'Grazer bearing model for GLT in bending': proposal for the prEN 14080 (Brandner and Schickhofer (2008))

$f_{m,g,k}$	$= 2.5 \cdot f_{t,0,l,k}^{0.8} \cdot k_{size,g,m}$	for COV-$f_{t,0,l}$ = 25 ± 5 %
	$= 2.8 \cdot f_{t,0,l,k}^{0.8} \cdot k_{size,g,m}$	for COV-$f_{t,0,l}$ = 35 ± 5 %
	$k_{size,g,m} = (d_g / 600)^{0.10}$	for $d_g \geq 150$ mm, else d_g = 150 mm
	$f_{t,j,k} \geq 1.2 \cdot f_{t,0,l,k}$	for COV-$f_{t,0,l}$ = 25 ± 5 %
	$f_{t,j,k} \geq 1.4 \cdot f_{t,0,l,k}$	for COV-$f_{t,0,l}$ = 35 ± 5 %

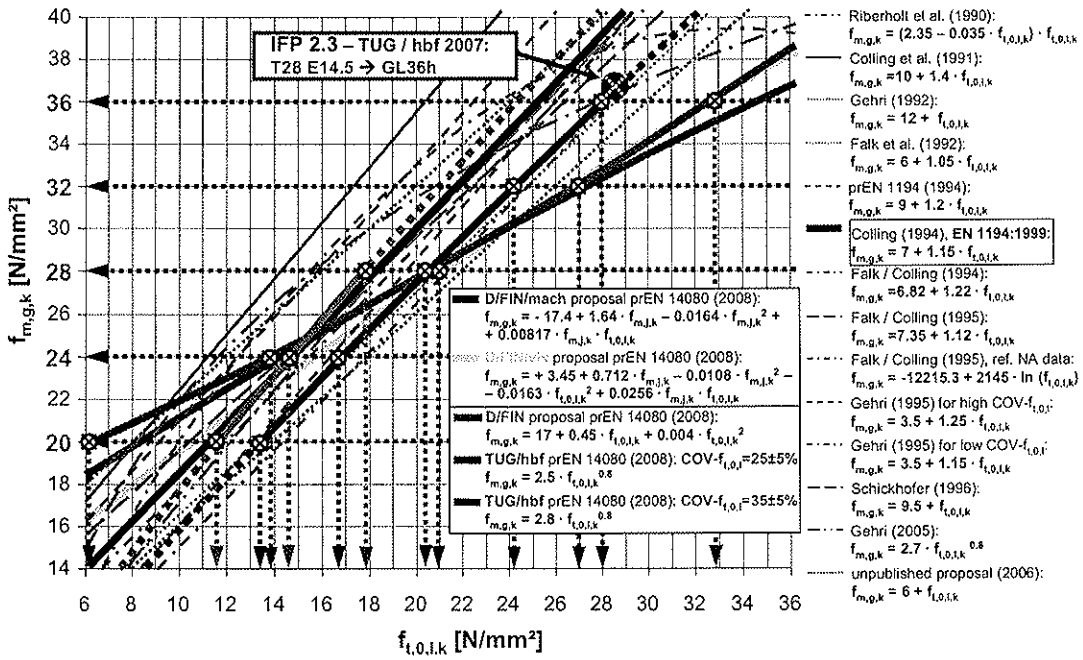

Fig. 5: 'Bearing models for GLT in bending' – sub-model concerning the requirements on boards – relationship $f_{m,g,k}$ vers. $f_{t,0,l,k}$: past models in comparison with current bearing models for prEN 14080 and the test result of series **GLT-II** of GL36h (see Brandner and Schickhofer (2008))

4.2 Further statistics of shear field test data by means of destructive 4-point bending tests acc. to EN 408

The test results and statistics of $G_{090,SF}$ of series **GLT-I** are summarized in Tab. 4. Data of **GLT-II** are included in Tab. 2 in chapter 4.1. Tab. 5 gives the 4p.-bending test results of series **GLT-III**.

Tab. 4: Statistics of series **GLT-I** – GL24h acc. EN 1194 – tested in 4p.-bending acc. EN 408

GLT-I	$\rho_{g,12}$ [kg/m³]	$E_{m,g,l,12}$ [N/mm²]	$E_{m,g,g,12}$ [N/mm²]	$G_{090,SF,12}$ [N/mm²]
quantity	10 #	10 #	10 #	10 #
mean	**436**	**11,170**	**10,190**	**694**
COV	**2.1 %**	**8.8 %**	**6.7 %**	**8.4 %**

Tab. 5: Statistics of series **GLT-III** – GL36c acc. EN 1194 – tested in 4p.-bending acc. EN 408

GLT-III	$\rho_{g,12}$ [kg/m³]	$E_{m,g,l,12}$ [N/mm²]	$E_{m,g,g,12}$ [N/mm²]	$G_{090,SF,12}$ [N/mm²]	$f_{m,g}$ [N/mm²]
quantity	5 #	5 #	5 #	4 #	5 #
mean	**492**	**15,140**	**14,030**	**653**	**42.0**
COV	**1.6 %**	**2.5 %**	**2.2 %**	**1.5 %**	**20.6 %**

5 Discussion

5.1 Test results of shear fields by means of 4p.-bend. tests acc. EN 408

5.1.1 Comparison of tests values of series GLT-I, GLT-II and GLT-III

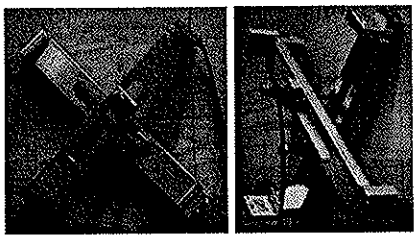

Fig. 6: Shear field test configuration of series **GLT-I** with L = 160 mm

The first tests for the determination of $G_{090,SF}$ within series **GLT-I** on GL24h with a size of L / L = 160 / 160 mm in 2007 (see Tab. 4) lead to $G_{090,SF,12,mean}$ = 694 N/mm² with an unexpected relatively high COV-$G_{090,SF,12}$ = 8.4 %. A possible explanation for the high COV-$G_{090,SF}$ lies in the fuzziness of the measurement of minor shear distortion in comparison to large bending deflection, in combination with instability of the load-distortion-relationship. A possible explanation of the relatively high $G_{090,SF,mean}$ compared to data from torsion tests $G_{090,tor,mean}$ lies in the former applied test configuration which induced a certain 'blocking-effect' due to the fixation of the measurement device by a spring pressing on a support and guided by a screw (see Fig. 6). The 'blocking effect' was visible in discontinuous force-distortion curves which showed partially unreliable and irregular, nonlinear relationships within some shear fields. The current test configuration, which has already been extensively and satisfactorily approved during measurements of deformations on concrete structures by the Laboratory of Structural Engineering of the Graz University of Technology / Austria / Europe, was solely positioned and fixed by rubber bands.

As already discussed in Brandner et al. (2007), the COV-$G_{090,SF}$ can be expected in the range of COV-$E_{m,g}$. The current test results on **GLT-II** and **GLT-III** are in line with this assumption. In general, $G_{090,SF}$ is an averaged value within and between the GLT-lamellae that results from the following three operations: 'balancing' the distortions within each shear field, averaging the $G_{090,SF}$ between both opposite shear fields on each side of the test specimen, and averaging $G_{090,SF}$-values between both ends of the specimen. The E-modules ($E_{m,g,l}$ and $E_{m,g,g}$) are also averaged values that result from the following operations: taking the mean of the bending deflection of opposite measurements, and, thanks to the homogenisation of the dispersion of E_0 through rigid connection, taking the mean within and between the GLT-lamellae.

The G-values $G_{090,SF,mean}$ of GL36h and GL36c, in the range of $G_{090,SF,mean}$ = 650 ÷ 660 N/mm², are more or less in between $G_{090,tor,mean}$ and $G_{090,SF,mean}$ of series **GLT-I** on GL24h. Both COV-$G_{090,SF}$ of **GLT-II** and **GLT-III** are in the range of expectation. Furthermore, the G-values appear unaffected by the strength class of the laminations as given by comparison of G-values of **GLT-II** and **GLT-III**: in series **GLT-II** the shear distortion was only measured over boards of strength class **T28E14.5**, in series **GLT-III**, the shear distortion was examined over a combination of board-strength classes **T15E11.0** and **T20E12.5**. A constant $G_{090,g,mean}$ = 650 N/mm² for all GLT-strength classes GL20 up to GL36 of Norway spruce is proposed.

5.1.2 Stability, reliability and cost effectiveness of the shear field testing method

Standardized test methods and standardized material characteristics have to be reproduceable, reliable, repeatable and consistent. The torsion test method proposed in Brandner et al. (2007) and already standardized in ASTM D 198, has been proved a reliable, consistent and cost efficient test method for the derivation of G_{090}-values and can be applied to solid timber as well as to bar-like timber products e.g. GLT. The first shear field test configuration applied on **GLT-I** produced – in comparison to torsion tests – relatively high dispersing, and due to 'blocking effects' within the test configuration, unreliable data. The shear field test configuration applied on **GLT-II** and **GLT-III** led to reliable, robust and repeatable test values which was proved on four shear fields at least – in a 1st test run with DD1s placed on the nail-head, in a 2nd test run with DD1s placed direct on the timber surface – and led to maximal ± 10 N/mm² nominal difference within each shear field. For further illustration, randomly chosen load-distortion curves are given in Fig. 7.

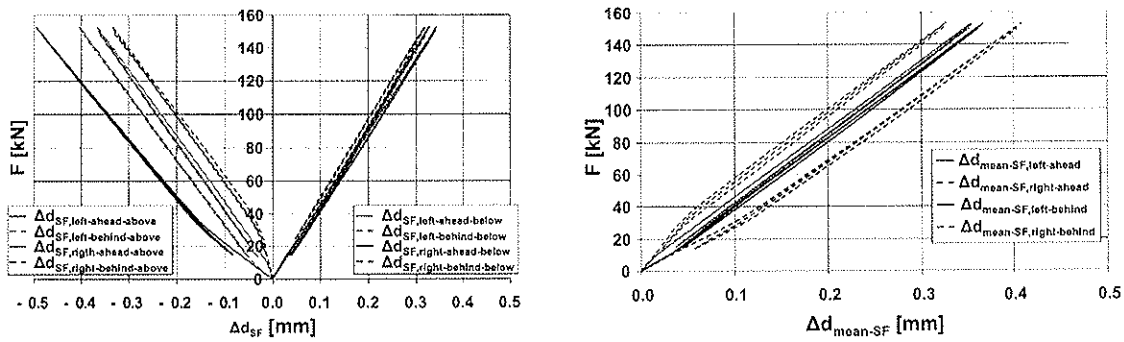

Fig. 7: Bending test diagrams: measurement of extensions of shear-field diagonals in relationship to applied force (applied force corresponds to 50 % of estimated $F_{max,mean,est}$) – elongation of each shear-field diagonal measurement (left), mean elongation of each shear-field diagonal (right)

Tab. 6: Summary of time-and-motion-study on four static test configurations for the determination of G_{090}

TIME-and-MOTION-Study [0]	Single span method acc. to EN 408	Variable span method acc. to EN 408	Torsion test method	Shear field test method by means of 4p.-bending tests acc. to EN 408
Determinable characteristics of interest	f_m, $E_{m,l}$, $E_{m,g}$, $G_{090,app}$, ρ	f_m, $E_{m,l}$, $E_{m,g}$, $G_{090,app}$, ρ	$G_{090,tor}$, ρ	f_m, $E_{m,l}$, $E_{m,g}$, $G_{090,SF}$, ρ
Summary of time-and-motion-study [1] (expectable values)	54'	102' [2]	26' [3]	41'

[0] Time for assembling and disassembling is excluded due to dependency on the specimen's dimensions

[1] Time steps were subdivided into: Preparation of the test specimen, application of the measurement device, test-duration (with hysteresis slope), modification of the test configuration (if necessary), first data examination (see Lackner et al. (2008))

[2] Acc. to EN 408 with a minimum of four variable spans

[3] To obtain the same characteristics as in the other three methods, the combination of torsion- and 4p.-bending test leads to an expectable time need of 23' + 22' = **45'**

The reliability is reflected by the low COV-$G_{090,SF}$ in the range of COV-$E_{m,g}$. For evaluation concerning the cost effectivness, data of time-and-motion-studies of tests on series **GLT-I** (GL24h) of all four applied test methods for the derivation of the G-modulus, updated by the new shear field test configuration, are given and compared in Tab. 6. The time for assembling and disassembling of the specimen has been excluded due to dependency on the specimen's dimensions.

In conclusion, the torsion test method is the best choice when testing timber components if G_{090}-values are derivated only. If bending characteristics like $f_{m,g}$, $E_{m,g}$, and $E_{m,l}$ are also of interest and the depth of the specimen is $d \geq 300$ mm (due to minimum, adviseable size of the shear field with $L \geq 150$ mm), the shear field test method is only recommended as a cost efficient and reliable test method if the accuracy of the measurement device is adjusted to the minor shear distortion. For smaller cross sections, a combination of torsion- and 4p.-bending test is suitable.

5.2 Examinations of potential relationships between G and other mechanical and physical characteristics

The interest in certain relationships between G and other characteristics of timber for modelling and other easy-to-handle values gained by calculations is evident. Fig 8 reflects the empirical distributions of $f_{m,g}$ and $G_{090,SF}$ of series **GLT-II** – the data points are marked acc. to the predominant failure criteria. The empirical distribution (empD) of $f_{m,g}$ can be divided into three nearly homogeneous regions acc. to the class of failure criteria, the empD of $G_{090,SF}$, as it was expected, shows no clear clustering or differentiability of certain regions of preferred failure criteria. All regions are widely overlapping with the field of 'WF' occurring within the whole range. Similar results are given in the box-plots of $f_{m,g}$, $E_{m,g,l,12}$ and $G_{090,SF}$ in Fig 9.

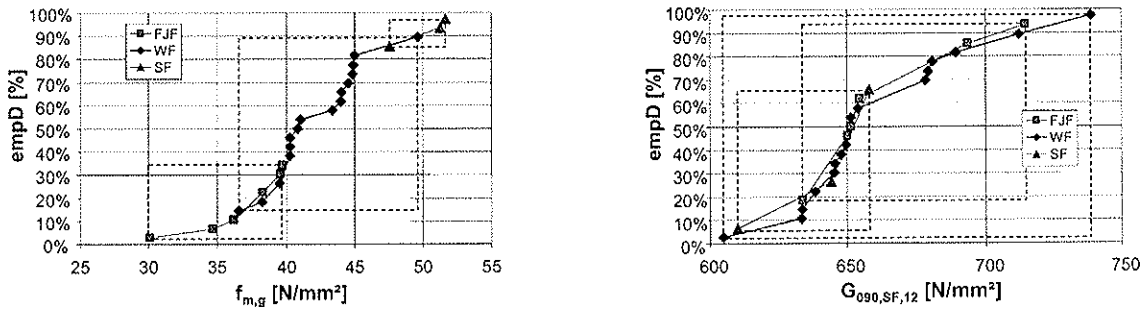

Fig. 8: Empirical distribution of the bending strength $f_{m,g}$ (left) and shear-modulus $G_{090,SF,12}$ (right) of series **GLT-II** – GL36h: classified failure criterias – wood failure in bending (WF), failure in the finger joint (FJF) and wood failure in shear (SF)

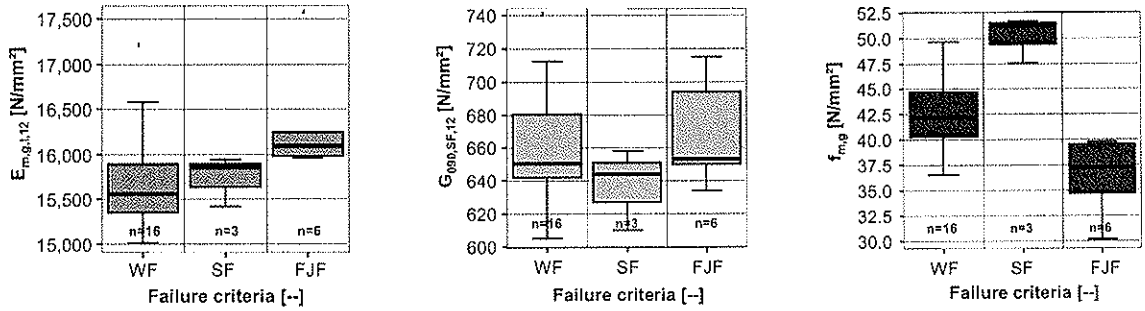

Fig. 9: Box-plots of series **GLT-II** – GL36h: according failure criteria grouped mechanical properties: local bending E-modulus $E_{m,g,l,12}$ (left), shear modulus $G_{090,SF,12}$ (middle) and bending strength $f_{m,g}$ (right)

Scatter-plots with linear regression lines of $G_{090,SF}$ vers. $E_{m,g,l,12}$ and $E_{m,g,g,12}$ in Fig. 10-left-above may appear to reflect a certain positive tendency. By consideration of the negative tendencies for $G_{090,SF}$ vers. $f_{,m,g}$ and $\rho_{g,12}$ in Fig. 10-right-above and -left-below – with a generally positive correlation r ($E_{m,g}$; ($f_{m,g}$, $\rho_{g,12}$)) >> 0 – this can not be confirmed. A residual positive, weak correlation of $G_{090,SF,12}$ vers. $u_{g,middle}$, with r ($G_{090,SF,12}$, $u_{g,middle}$) ≈ 0.45, is given in Fig. 10-right-below and may reflect that the G-modulus is more moisture sensitive than the E-modulus because the G-values were already adjusted to u_{ref} = 12 % acc. the adjustment for E-values as given in EN 384.

In general, a quantifiyable dependency of G on the examined mechanical and physical properties can not be confirmed. This is also in compliance with the G staying constant in all GLT-strength classes by simultaneous variation of E, f and ρ. Furthermore, shear fields of 20 # specimens of series **GLT-II** and all 5 # beams of series **GLT-III** were examined, concerning the influence of knots within the measuring field in the data of shear deflection. All four shear fields of each specimen with / and without knots were separately analysed. The results reflect no significant influence of knots on the recorded shear distortion measurements.

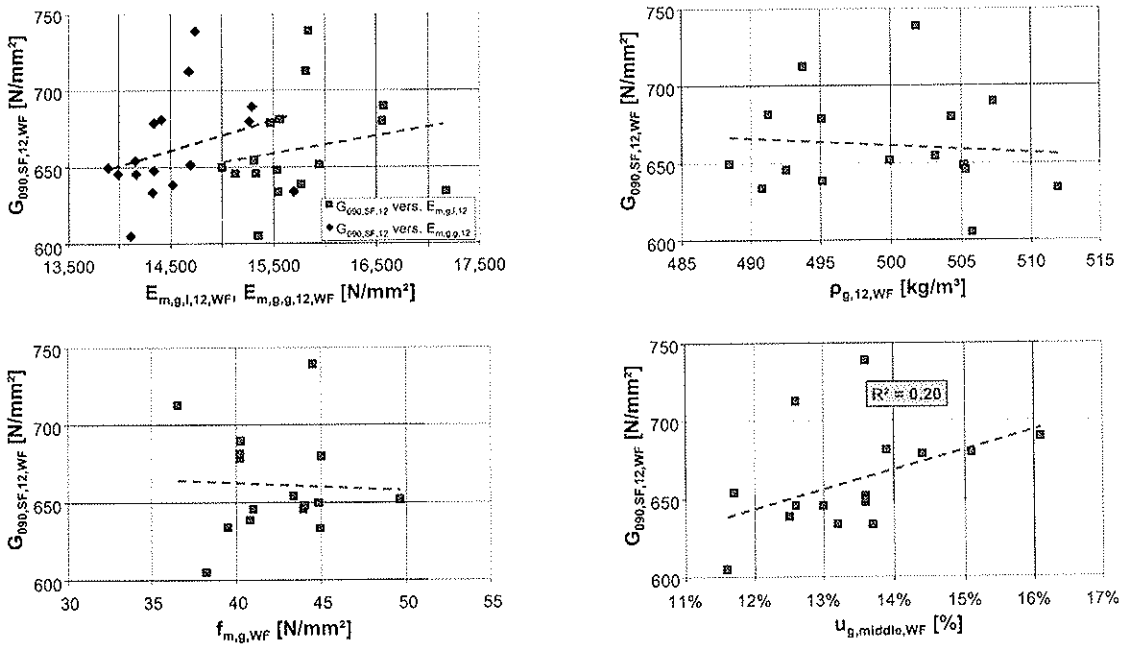

Fig. 10: $G_{090,SF,12,WF}$ vers. $E_{m,g,l,12,WF}$, $E_{m,g,g,12,WF}$ (left-above), vers. $\rho_{g,12,WF}$ (right-above), vers. $f_{m,g,WF}$ (left-below) and vers. moisture in the middle of beam-depth $u_{g,middle,WF}$ (right-below) – series **GLT-II** / WF

5.3 G-modulus of GLT in comparison to G-modulus of solid timber

Acc. to EN 338, a ratio of G / E = 1 / 16 for solid timber is standardized. In EN 1194 a ratio of G / E = 1 / 15.4 is given. Thus, there is one important question to be asked: Is there a difference between the G of GLT and G of solid timber? First of all, the distribution of E and G can be well described by the statistical normal distribution function. Through homogenisation within the system structure of GLT, the mean level of both values – solid timber and GLT – can be treated as being constant, but the COV and the 5 %-quantiles change significantly as given in Brandner et al. (2007) and Blaß (2005). There is no reason why the expectable values of G_{090} in solid timber and GLT should be different, but for stability considerations the reduction of COV-G_{090} provoking an increase of $G_{090,05}$ lead to a quantifiable, well-tempered performance of GLT. The dependency of G_{090} on the strength class in GLT cannot be confirmed by the tests, a constant value of $G_{090,g,mean}$ = 650 N/mm² is proposed based on test results on GL24h, GL36h and GL36c. From this point of view, it does not appear logical why G_{090} in solid timber should behave in a different manner. A certain dependency is published e.g. in Görlacher and Kürth (1994), based on vibration tests. Due to test results and for simplification of design of timber structures of Norway spruce, a constant value of $G_{090,mean}$ = 650 N/mm² also for solid timber is proposed.

6 Conclusion

Further proposals include test results and related considerations. They are only valid for the related standard with regard to solid timber or glued laminated timber of Norway spruce (*picea Abies Karst.*). Because of the equality of numerous mechanical and physical properties of Norway spruce and fir (*abies Alba Mill.*) – when used for engineering purposes – the proposals may also be valid for this wood species.

- For the determination of static G_{090} of solid timber and bar-like timber products with d < 300 mm, an application of the torsion test method is proposed which should be standardized in EN 408.
- For the determination of static G_{090} of solid timber and timber products with d ≥ 300 mm, an application of shear fields by means of shear tests or by means of standardized 4p.-bending tests acc. EN 408 is proposed and enables an aditional examination of $E_{m,l}$, $E_{m,g}$ and f_m.

Tab. 7: Proposed values and models for $E_{m,0,mean}$, $E_{m,0,05}$, $G_{090,mean}$ and $G_{090,05}$ for solid timber (EN 338) and glued laminated timber (EN 1194 and EN 14080)

Shear modulus	$G_{090,mean}$	$= 650$ N/mm²	1)
	$G_{090,05,n}$	$= G_{090,mean} \cdot \min\left\{\frac{1}{60}\cdot(n-1)+0.67;\ 0.90\right\}$	2)
		$= G_{090,mean} \cdot \min\left\{\left[1-1.645\cdot\frac{0.20}{\sqrt{n}}\right];\ 0.90\right\}$	3)
	$G_{090,05}$	$= 0.67 \cdot G_{090,mean} = 435$ N/mm²	4)
Modulus of elasticity	$E_{m,0,05,n}$	$= E_{m,0,mean} \cdot \min\left\{\frac{1}{60}\cdot(n-1)+0.67;\ 0.90\right\}$	2)
		$= E_{m,0,mean} \cdot \min\left\{\left[1-1.645\cdot\frac{0.20}{\sqrt{n}}\right];\ 0.90\right\}$	3)
	$E_{m,0,05}$	$= 0.67 \cdot E_{m,0,mean}$	4)

1)	proposal acc. to presented test results for consideration in EN 1194, EN 14080 and EN 338
2)	proposal for linearized calculation of $X_{05,n}$ in dependency of the quantity of interacting components n with a max. of $X_{05,n} / X_{mean} = 0.9$ at n = 15 representing a GLT of 15 laminations with $d_l = 40$ mm → $d_g = 15 \cdot 40 = 600$ mm = $d_{g,ref}$, acc. to Brandner et al. (2007) for consideration in EN 1194 and EN 14080
3)	proposal for calculation of $X_{05,n}$ in dependency of the quantity of interacting components n and approximation of G- and E-module by the statistical normal distribution with COV-X = 20 %, for consideration in EN 1194 and EN 14080
4)	proposal for calculation of X_{05} for solid timber with COV-X = 20 %, for consideration in EN 338

- The determination of G_{090} by means of shear fields leads to two independent G_{090}-values of each specimen and each applied test. In comparison only one value for E-modulus can be gained in one test.
- The achieved 4p.-bending tests on GL24h, GL36h and GL36c reflect no or minor dependency of G_{090} from the board's strength class. A constant value of $G_{090,mean} = 650$ N/mm² for all strength classes of GLT (GL20 to GL36) in EN 1194 and EN 14080 is proposed. Furthermore, a constant value of $G_{090,mean} = 650$ N/mm² for solid timber for consideration in EN 338 is proposed.
- The statistical normal distribution was found to represent the values of E_0 and $G_{090,SF}$ satisfactorily. Because of the averaging of the E_0 and G_{090}-values of boards within the system structure GLT a reduction of the COV-$G_{090,SF,n}$, in dependency the quantity of interacting boards n, acc. [5] can be assumed. The calculation scheme of the characteristic G- and E-values in dependency of n is given in [6].

$$COV_n = \frac{COV_{n=1}}{\sqrt{n}} \qquad [5]$$

$$X_{05} = X_{mean} \cdot (1 - 1.645 \cdot COV_n) = X_{mean} \cdot \left(1 - 1.645 \cdot \frac{COV_{n=1}}{\sqrt{n}}\right) \qquad [6]$$

- As given in Brandner et al. (2007) a COV-$G_{090,n=1}$ = COV-$E_{m,0,n=1}$ = 20 % can be assumed. Furthermore the proposed level of homogenisation is restricted to n = 15 # interacting lamellae and leads to a maximum of $X_{05,n} = 90$ % of X_{mean}. The calculation procedure for the 5 %-quantile $G_{090,05}$ and $E_{m,05}$ for solid timber (n = 1) and for the system product GLT ($n \geq 2$) are given in Tab 7 and proposed for consideration within EN 1194, EN 14080 and EN 338.

7 Acknowledgements

The research within the projects P05 grading, IFP 2.3 large_dimension_timber, APTM 2.1-2.1.1 mature_wood and MMSM 2.2-2.2.1 stoch_mod is financed by the competence centre holz.bau

forschungs gmbh and performed in collaboration with the Institute of Timber Engineering and Wood Technology of the Graz University of Technology and several partners from industry. The project is sponsored by the Federal Ministry of Economics and Labour and the Styrian Business Promotion Agency Association.

Special thanks go to em. Prof. E. Gehri for his highly valuable discussions and for enabling the testing procedures at n'H-Lungern GmbH / CH which also produced the GLT-beams of series GLT-II and GLT-III Thanks also go to n'H-Lungern GmbH / CH for sponsoring the series GLT-III. Further thanks go to the Laboratory for Structural Engineering at the Graz University of Technology / AT for performing the 4p.-bending tests of series GLT-II and series GLT-III on a very sophisticated level.

8 References

8.1 Papers and reports

Blaß H J (2005) **Ermittlung des 5 %-Quantils des Produktes aus Elastizitätsmodul und Torsionsschubmodul für Brettschichtholz**. Forschungsbericht der Versuchsanstalt für Stahl, Holz und Steine der Universität Karlsruhe, 11 Seiten.

Brandner R (2006) **Darstellung des Festigkeits- und Steifigkeitspotentials von BSH-Lamellen in Hinblick auf das „Trägermodell"**. Präsentation, 2. Grazer Holzbau Workshop (2.GraHWS'06), 23.06.2006

Brandner R, Gehri E, Bogensperger T, Schickhofer G (2007) **Determination of Modulus of Shear and Elasticity of Glued Laminated Timber and related Examinations**. CIB W18/40-12-2, Bled, Slovenia, 14 p.

Brandner R, Schickhofer G (2007) **Bearing model for glued laminated timber in bending – new aspects concerning modelling**. COST E55-Workshop, Graz, Austria, 14.-15.05.2007, 31 p.

Brandner R, Schickhofer G (2008) **Strength models for GLT – Statements in regard to the TUG / hbf proposal concerning prEN 14080**. Presentation at the CEN TC124/WG3-meeting, Vienna, Austria, 3rd April 2008, 25 p.

Brandner R, Schickhofer G (2008) **Glued laminated timber in bending: new aspects concerning modelling**. Wood Science Technology, DOI 10.1007/s00226-008-0189-2, Vol. 42, No. 5, p. 401-425

Colling F, Ehlbeck J, Görlacher R (1991) **Glued laminated timber – Contribution to the determination of the bending strength of glulam beams**. CIB-W18 / 24-12-1, Oxford, United Kingdom, p. 1-17

Colling F (1991) **Design of Glulam beams**. International Timber Engineering Conference, London, p. 1.82–1.88

Colling F (1995) **Brettschichtholz unter Biegebeanspruchung**. Informationsdienst Holz; Holzbauwerke; STEP 3: Holzbauwerke nach Eurocode 5: Grundlagen, Entwicklungen, Ergänzungen, Arbeitsgemeinschaft Holz e.V., Düsseldorf, p. 5/1-5/18

Colling F (1994) **Annexes to new draft of prEN 1194** (Ref. by Gehri 1995)

Divos F, Tanaka T, Nagao H, Kato H (1998) **Determination of shear modulus on construction size timber**. Wood Science and Technology, 32 (1998) 393-402.

Falk R H, Colling F (1994) **Glued-laminated timber: laminating effects**. PTEC 94, Gold Coast Australia, Australia, p. 618-625

Falk RH, Colling F (1995) **Laminating effects in glued-laminated timber beams**. J Struct Eng 121/12, p. 1857-1863

FMPA (1983) **FMPA – Prüfung von Furnierschichtholz „Kertopuu"**. Bericht I.4-34523.

Gehri E (1992) **Determination of characteristic bending values of glued laminated timber – EN-approach and reality**. CIB-W18/25-12-1, Åhus, Sweden, p. 1-10

Gehri E (1995) **Determination of characteristic bending strength of glued laminated timber**. CIB-W18/28-12-1, Copenhagen, Denmark, p. 1-4

Gehri E (2005) **Zur Erfassung des Biegewiderstandes von Brettschichtholz – Gedanken im Hinblick auf die Überarbeitung der EN 1194**. Internes Paper, Rüschlikon, Schweiz, p. 1-9

Gehri E (2005) **Zur Schubfestigkeit von Brettschichtholz aus Fichte und Esche**. Versuchsbericht, Rüschlikon, 9 Seiten.

Gehri E (2005) **Verformung unter Schub – Bestimmung des Schubmoduls**. Theoretische Betrachtungen und Versuchsbericht, Rüschlikon, 10 Seiten.

Gehri E (2005) **Zur Erfassung des Schubmoduls über die Schiebung**. Versuchsbericht, Rüschlikon, 7 Seiten.

Görlacher R, Kürth J (1994) **Determination of shear modulus**. CIB W18/27-10-1, Sidney, 6 pages.

Harrison S K (2006) **Comparison of Shear Modulus Test Methods**. Master thesis, Faculty of Virginia Polytechnic and State University, 106 pages.

Kollmann F (1951) **Technologie des Holzes und der Holzwerkstoffe**. Springer-Verlag – Berlin-Göttingen-Heidelberg, Zweite Auflage, Erster Band.

Lackner H, Brandner R, Schickhofer G (2008) **Betrachtungen zur Robustheit und Ökonomie von statischen Versuchskonfigurationen zur Ermittlung des Schubmoduls an Brettschichtholz**. Forschungsbericht (in Bearbeitung), Kompetenzzentrum holz.bau forschungs gmbh, Graz, Austria, 22 p.

Niemz P (1993) **Physik des Holzes und der Holzwerkstoffe**. DRW-Verlag, ISBN 3-87181-324-9.

Riberholt H (1990) **Glued laminated timber – strength classes and determination of characteristic properties**. CIB-W18/23-12-4, Lisbon, Portugal, p. 1–9

Schickhofer G (1996) **Development of efficient glued laminated timber**. CIB-W18/29-12-1, Bordeaux, France, p. 1-17

Skaggs T D, Bender D A (1995) **Shear deflection of composite wood beams**. Wood and Fiber Science, 27(3), 327-338.

8.2 Standards

ASTM D 198:2003-05 Standard Test Methods of Static Tests of Lumber in Structural Sizes

EN 338:2003-07-01 Structural timber – Strength classes

EN 384:2004-05-01 Structural timber – Determination of characteristic values of mechanical properties and density

EN 408:2005-04-01 Timber structures – Structural timber and glued laminated timber – Determination of some physical and mechanical properties

pr**EN 408**:xxx-xx-xx Timber structures – Structural timber and glued laminated timber – Determination of some physical and mechanical properties (proposal for 'Determination of the shear modulus – Torsion test method', Leijten A J M (2008-05-16)

EN 1194:1999-09-01 Timber structures – Glued laminated timber – Strength classes and determination of characteristic values

pr**EN 14080**:xxxx-xx-xx Timber structures – Glued laminated timber and Glued laminated solid timber - Requirements

EN 14081:2006-02-01 Timber structures – Strength graded structural timber with rectangular cross section

INTERNATIONAL COUNCIL FOR RESEARCH AND INNOVATION
IN BUILDING AND CONSTRUCTION

WORKING COMMISSION W18 - TIMBER STRUCTURES

CONSEQUENCES OF EC 5 FOR DANISH BEST PRACTICE

J Munch-Andersen

Danish Timber Information

DENMARK

Presented by J. Munch-Andersen

I. Smith commented that in Canada design methods are given in the design code and not in a supporting standard. The influence of grade on density is treated differently in Canada. J. Munch-Andersen agreed that two committees are involved but this is not a problem as both are working towards the same safety level/concept. H.J. Larsen stated screw design has had a strange history in EC5 development as it started as very strict and then evolved. He questioned about the scientific basis behind screw design and whether the material was discussed in CIB W18. H. Blass disagreed and stated that there is a wide scientific basis behind the EC5 screw design provisions with discussion in CIB W18 meetings. H. Blass stated that head pull through should be the same for both screws and nails if the shapes of the head are the same; therefore, the values in EC5 are set conservatively. He agreed that restrictions to smooth shank nails are questionable. H. Blass and J. Munch-Andersen clarified the spacing requirement for laterally loaded and axially loaded cases. H. Blass commented that applying group effect to rope effect is incorrect and in 1994 CIB W 18 meeting R. Görlacher presented results showing that the failure modes belonging to thick steel plates were observed with 2 mm thick steel plates and 4 mm diameter nails. A. Leijten asked why these results were not presented earlier. J. Munch-Andersen responded that the work was just completed. J. König commented that EC5 was developed with few comments received outside the committee. It is a general problem that as EC5 is examined more closely inconsistencies are uncovered. He suggests comments should be forwarded to the EC5 secretariat so that the issues can be addressed in the next code cycle as this errors are on the side of too conservative. J. Munch-Andersen mentioned that being too conservative also requires immediate attention as it prevents some connectors from being used. H. Blass commented that EC5 and supporting standard TC124 need to coordinate. I. Smith discussed the issue of safety and the differences with current practice.

Consequences of EC 5 for Danish best practise

Jørgen Munch-Andersen

Danish Timber Information, Denmark

1 Introduction

The Danish structural codes, including the one for timber structures, DS 413, has over the last 10 years approached first the ENV's and later the Eurocode. This means that the practical consequence of swapping to use the Eurocode form 2009 will be limited in most cases. However, the Danish rules for fasteners in timber are still quite different from Eurocode 5.

A study of the load bearing capacity of the most frequently used nails and screws has revealed that the capacity according to Eurocode 5 in almost all cases are smaller than according to DS 413. In some cases the decrease is quite significant. The paper will compare typical capacities for axial and lateral load and discuss the causes for the differences.

For some fasteners initial type testing is expected to be able to prove higher strengths than the equations in Eurocode 5. This can to some extent solve the problems. But there will remain numerous types of connections in typical timber structures that cannot be used any more without increasing the timber dimensions. Examples are given of connections that cannot meet the requirements of Eurocode 5, even though the practical experience is absolutely satisfying.

2 Measured strength parameters for Danish fasteners

The strength of nails according to the Danish code for timber structures is to a large extent based on works from T. Feldborg and M. Johansen, e.g. (Feldborg and Johansen, 1974), (Feldborg, 1982) and (Feldborg and Johansen, 1988).

K. F. Hansen (Hansen, 2002) has by testing determined strength parameters as well as the load capacity for typical nails and screws used for timber joints in Denmark, see Table 1. The wood density is ranging from 350 to 500 kg/m^3. The results will be referred to in the following to support the discussion. The tests are carried out according to the relevant standards, also used for initial type testing.

Table 1. Nails and screws used by Hansen (2002).

	Reference name	Length, mm	Threaded length l_e, mm	Diameter of head, mm	Max. diameter d, mm	Root diameter d_1, mm
Smooth square nail	FS	100	-	9.4	3.8	-
Threaded nail	RS	66	31	8.4	3.5	-
Wood screw	S4	59	40	7.8	4.0	2.4
	S5	79	44	9.9	4.9	2.8
	S6	99	59	11.7	6.0	3.5
Connector screw	B35	38	30	8.3	4.9	2.8
	B40	42	34	8.3	4.9	2.8
	B50	51	43	8.3	4.9	2.8

3 Density

The strength of mechanical joints depends significantly on the density of the timber. The characteristic density given in EN 338 declines rapidly with the strength-class. This is not true for the timber sold in Denmark and in many other countries. It is very hard to find timber with density below 350 kg/m^2, which is the characteristic density given for C24. For C14 the characteristic density is given as 290 kg/m^2. This is not possible to find at all.

The reason for the higher densities might be that the strength-class for Nordic timber in effect is determined by the knots size. The density seems to be the same for all grades up to at least C24. In Denmark all strengths of fasteners are presupposing a characteristic density of 350 kg/m^2. As C18 is the most commonly used class in Denmark the lower density has a significant influence on the load capacity of fasteners.

If the low densities really exist for species from southern Europe provisions must be introduced in EN 338 to take those differences into account in order to obtain fair load bearing capacities for all species.

4 Axially loaded fasteners

4.1 Head pull-through

According to EC5 the pull-through strength for smooth nails can be determined from $f_{head,k} = 70 \cdot 10^{-6} \rho^2$ and $F_{head,k} = f_{head,k}\, d_{head}^{\,2}$.

For screws a quite different approach is chosen in amendment A1:2008 to EC5. For one screw it is stated that $F_{head,k} = f_{head,k}\, d_{head}^{\,2} (\rho_k / \rho_a)^{0.8}$, where $f_{head,k}$ is the characteristic value of the measured pull-through strength for the associated density ρ_a. Besides $f_{head,k}$ meaning different things in the two expressions it is difficult to understand that the pull-through strength for a nail head should depend on the square of the density, whereas it for screws depends on the density raised to 0.8!

The results from Hansen (2002), see Figure 1, give no evidence that there should be any significant difference between nails and screws. A linear relationship appears reasonable. The characteristic value for ρ = 350 kg/m^3 is $f_{head,k}$ = 14,3 MPa whereas the above formula for smooth nails only gives 8,6 MPa. Hansen's value is based on a limited number of tests

with five different screws and nails so the coefficient of variation is quite large, causing a low characteristic value.

Formally nothing is said in Eurocode 5 about threaded nails. In a test report from an approved institute the measured values for the pull-through (and withdrawal) strength are corrected to the reference density 350 kg/m^3 assuming a linear relationship.

Assume that tests with a threaded nail carried out in accordance with EN 1383 has given a mean pull-through load capacity F_{mean} = 1500 N and CoV = 12.5% for a nail with d_{head} = 5.5 mm and timber density 475 kg/m^3. The characteristic value is then about 75% of the mean value giving $F_{k,475} \sim 1100$ N and $f_{k,475} = 1100/5.5^2 = 36.4$ MPa. A linear correction to the reference density gives $f_{k,350} = 36.4 \cdot 350/475 = 26.8$ MPa. Using the EC5 format where the strength is expressed as $f_{ax} = a\rho^2$ the factor is determined as $a = 26.8/350^2 = 219 \cdot 10^{-6}$ for this nail, three times more than the value $70 \cdot 10^{-6}$ given in Eurocode 5.

Using this expression might lead to unsafe results as illustrated by the following example. The pull-through strength for the nail in glulam GL32h with the characteristic density 430 kg/m^3 gives $f_{ax,k}$ = 40.5 MPa. This is more than the original characteristic value determined for the density 475 kg/m^3 (36.4 MPa). This obvious flaw is due to the correction up and down being carried out with different assumptions regarding the dependency on the density.

The obvious procedure to avoid this problem is to calculate the factor for the density used for the tests. Then the factor becomes $a = 36.4/475^2 = 161 \cdot 10^{-6}$. This is in effect the procedure prescribed for screws, except for the different power on the density.

The value for a becomes smaller and is a quite conservative estimate if the true relation between strength and density is linear. But still the factor is 2.3 times the value given in Eurocode 5.

It should also be mentioned that the power 0.8 on the density for screws makes very little difference compared to using a linear relationship. If for example f_{head} is determined for ρ_a = 410 kg/m^3 the load capacity $F_{head,k}$ for ρ_k = 350 kg/m^3 only reduced by 3% if a linear relationship is used in stead of the power 0.8. This small difference can hardly argue for the increased complexity.

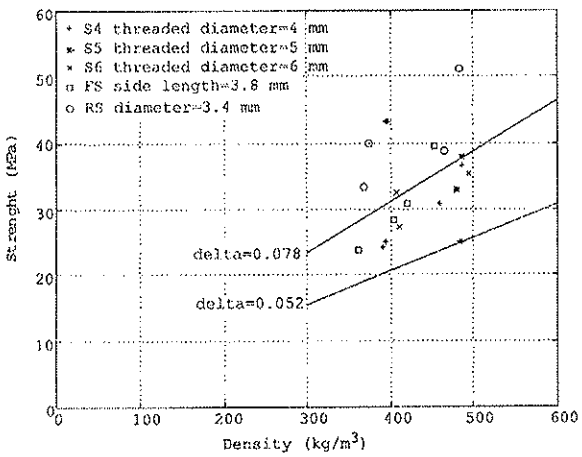

Figure 1. Pull-through strength for nails and screws. $F_{head} = \delta\, d_{head}^2\, \pi/4\, \rho$. The upper line represents the mean value, the lower the characteristic value. (Hansen, 2002).

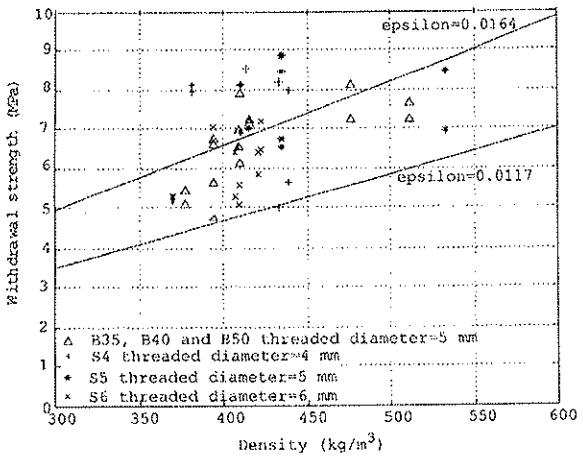

Figure 2. Withdrawal strength for screws. $F_{ax} = \varepsilon\, d\, \pi\, (l_e\text{-}d)\, \rho$. The upper line represents the mean value, the lower the characteristic value. (Hansen, 2002).

The problems regarding pull-through strength can be summarized as follows:

1. The pull-through strength given in EC5 is very low compared to measurements.

2. The relation between density and strength ought to be reconsidered and should be similar for nails and screws.

3. One of the relevant standards, EN 1383 and prEN 14592, should define how the correction for density should be done and which density that should be regarded as reference density.

4.2 Withdrawal

Withdrawal is treated very similar to pull-through in Eurocode 5, including the different power on the density for nails and screws. Below only subjects related to the withdrawal capacity at the reference density is dealt with.

4.2.1 Smooth nails

It is obvious that the withdrawal strength is different for different nails which make it reasonable to require separate determination for each product and therefore understandable that the Eurocode only gives strengths for smooth nails.

Regarding smooth nails Eurocode 5 disregards the difference between round and square nails. In Denmark the strength has effectively been assumed to be proportional to the circumference using a withdrawal parameter 1.0 MPa for square nails and 0.8 MPa for round nails, assuming the density to be 350 kg/m^3 and disregarding the point in the embedment length. The values include allowance for changing moisture content after installing.

For that density the Eurocode estimate a withdrawal strength of 2,45 MPa, which should be reduced by 2/3 if the nails are installed near to the saturation point, reducing the strength to 1,63 MPa, which for round nails is twice the Danish strength. Further, allowing the length of the point to be included in the embedment length will increase the load capacity by some 10%.

The Danish values are based on Feldborg (1982). For a square nail the mean value of the withdrawal strength is found to be 5.0 MPa for nails installed and withdrawn at 15% moisture content in timber with the density 380 kg/m^3. The coefficient of variation is 20% so the characteristic value becomes about 3.0 MPa. Assuming the strength to be proportional to the circumference the characteristic value for round nails is found by multiplying by $\pi/4$, giving 2.4 MPa. Even it is for a slightly higher density the match with the value given by the Eurocode before correcting for changing moisture content is good.

For nails installed at 20% and withdrawn at 7% Feldborg finds that the strength drops to 1/3. The characteristic values therefore drops to 1.0 and 0.8 MPa for square and round nails, as given in the Danish code. Feldborg also demonstrates that the strength can be reduced if the moisture content is increased.

The strength parameters given in the Eurocode ought to be conservative. This is obviously not the case for smooth nails, although the Danish allowance for changing moisture content might be a bit conservative. The quite high values in the Eurocode might undesirably encourage the use of smooth nails for example for fastening of roof battens. Most failures of roof structures during windstorms are due to the use of smooth nails for fastening roof battens – but only when the design load capacity in not sufficient.

The penetration length for full strength is increased from 9,5d (8d + the point) in the Danish code to 12d including the point. EC5 allows smaller penetration lengths, down to 8d, but the prescribed reduction of the strength is so large that the possibility is of almost no practical interest. If for example the penetration length for a smooth nail is reduced from 12d to 10d the load capacity is reduced to 42 %. For 8d the strength becomes 0.

It might be reasonable to be cautious for small penetration lengths, but a less severe reduction would do. A suggestion could be to reduce the load capacity by the ratio between the actual penetration length and the minimum length for full capacity. Then the capacity for a smooth nail with penetration length of 10d in stead of 12d would then be 69 %.

The problems regarding withdrawal strength for smooth nails can be summarized as follows:

1. The withdrawal strength should be given for both square and round nails.

2. The reduction factor 2/3 for nails installed near to the saturation point is unsafe, and reduction is also needed for other changes of moisture content.

3. The reduction of the withdrawal strength for penetration lengths below 12d is extremely conservative.

4.2.2 Threaded nails

Eurocode 5 states that the reduction factor of 2/3 for changing moisture content also should be used for the pull-through strength and – since the paragraph is not restricted to smooth nails – for the withdrawal strength of threaded nails. Feldborg & Johansen (CIB W18, Vancouver, 1988) demonstrates that the moisture content has very little effect on the withdrawal strength of threaded nails, and it is hard to believe that the pull-through strength should be more sensitive to changing moisture content than the withdrawal of threaded nails. This very conservative correction cannot be avoided by type testing of the individual product.

The penetration length is in Eurocode 5 defined as the length of the threaded part in the pointside member. It is unclear if that length includes the point, but it is most reasonably if it is not included. The penetration length for full strength is increased from 5d in the Danish code to 8d. Lengths down to 6d can be used with a severe decrease of the strength, as for smooth nails.

The problems regarding withdrawal strength for threaded nails can be summarized as follows:

1. The reduction factor for changing moisture content should be removed for threaded nails, and for pull-through for both smooth and threaded nails.

2. The minimum penetration length for full strength is quite high.

3. The reduction of the withdrawal strength for penetration lengths below 8d is extremely conservative.

4.2.3 Screws

In amendment A1 to Eurocode 5 – quite complicated – expressions for calculating the withdrawal strength and the load capacity for some geometries of screws is given. The expressions yields for the outer diameter $d \in$ [6 mm; 12 mm] so the most commonly used screws in today's timber structure are not covered. The withdrawal strength must therefore be determined by initial type testing for each type of screw.

In the above mentioned expression for larger screws the withdrawal strength $f_{ax,k}$ depends on the diameter and the penetration length in a quite complicated manner. That might suggest that $f_{ax,k}$ for other screws cannot be given accurately as a single figure. On the other hand, if the given expression for the load capacity $F_{ax,k}$ for larger screws is replaced by the straight forward formula $F_{ax,k} = 0.035\, d\, l_{pen} \rho$ the difference is within about 10% for $d \in [6$ mm; 10 mm]. So it is most likely that a single figure will lead to an accurate expression.

There are separate spacing requirements for axially loaded screws, whereas it for nails must be assumed that the requirements are the same as for lateral load. Since it is about avoiding splitting it is strange and awkward to have separate rules. Further, no spacing rules are given if the timber thickness is less than $12d$, and it is not stated if the thickness requirement yields for the head-side or the point-side member. There is also a group effect, which reduces the load capacity of each screw in a group. These rules make it very complicated to use the rope-effect for laterally loaded connections, se section 5.2 below.

The problems regarding withdrawal strength for screws can be summarized as follows:

1. The expressions given do not cover the most widely used screws.
2. The expressions appear to be much more complex than necessary.
3. The spacing requirements do not cover common member thicknesses.

5 Laterally loaded fasteners

5.1 Embedment strength

Eurocode 5 specifies the embedment strength both with and without pre-drilling and – for bolts and dowels – the dependency on the grain direction. These expressions are well established, including that the embedment strength is assumed to be proportional to the density. It is therefore reasonable that the embedment strength is not a parameter that shall be declared for the individual product.

But for modern screws with little or no smooth shank the rules are insufficient. It is stated that the effective diameter could be taken as 1.1 × root diameter, but not if this diameter should be used for calculating the yield moment M_y as well as in the Johansen-formulas. If it is used in both calculations it is most likely that a very safe value is obtained. M_y can be measured directly and declared in accordance with prEN 14592, but that possibility does not exist for the embedment strength, which is not dealt with in prEN 14592.

Hansen (2002) has, see Figure 3, demonstrated that the embedment strength parallel to the grain for screws are much smaller than for nails and that two types of screws with very similar threads has very different strength, presumably because the surface has different roughness. Perpendicular to the grain the difference between nails and screws and between the screws is smaller as seen from Figure 4. It should be noted that for this particular case the strength is proportional to the square of the density!

It is obvious that a fairly accurate estimate for the lateral load capacity requires that the embedment force is measured for the specific product. It also ought to be stated which diameter that should be used for calculating the embedment strength. The outer diameter seems to be the most appropriate. Alternatively, the effective diameter could be determined using the embedment strength from the Eurocode.

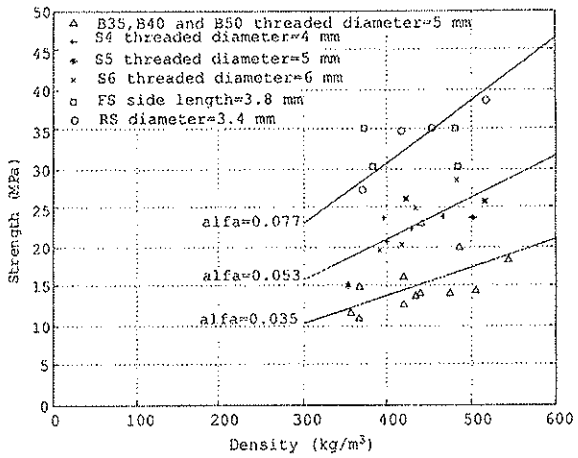

Figure 3. Embedment strength parallel to the grain for nails and screws. $F_e = \alpha\, d\, \rho$. The lines represent the mean values for nails, wooden screws and connector screws. The slopes for the characteristic values are 0.059, 0.042 and 0.024. (Hansen, 2002).

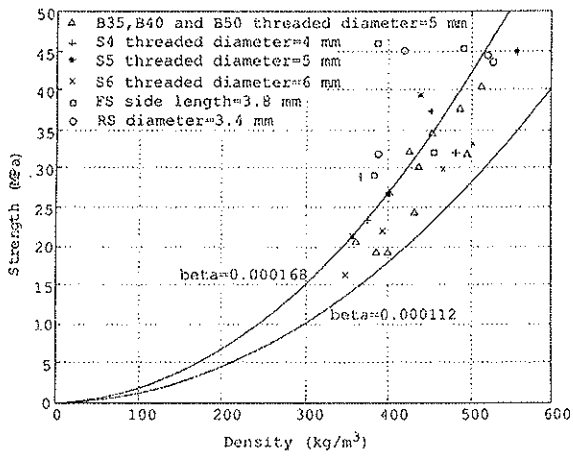

Figure 4. Embedment strength perpendicular to the grain for nails and screws. $F_e = \beta\, d\, \rho^2$. The upper line represents the mean value, the lower the characteristic value for all types. The nails alone could be assigned higher values. (Hansen, 2002).

The problems regarding embedment strength for screws can be summarized as follows:

1. The expressions given do yield for modern screws.

2. Provisions should be made for declaration of either the embedment strength of the threaded part or an effective diameter.

5.2 Lateral strength

Including the rope effect in the expressions for lateral strength of nails and screws is an important achievement. Hansen (2002) found that a friction coefficient of 0.3 between steel and timber was a quite accurate value. The term $F_{ax,Rk}/4$ in the expressions in Eurocode 5 equal a friction coefficient of 0.25. As the friction is likely to depend on the manufacturing of the steel and/or timber it is reasonable to choose a safe value.

5.2.1 Timber to timber

The Danish code has for nails assumed that both ends of the nails are fixed against rotation (failure mode f in Eurocode 5). The rope-effect has been included by a judgmentally increase of the dowel strength.

Table 2 shows that the lateral load capacity is decreasing when using Eurocode 5 for a smooth nail. For t_1 = 45 mm where the failure mode is the same the difference between the Eurocode value (1172 N) and the Danish value (1361 N) must be assigned to a mistake in the Danish code. (A reduction in the relation between the partial coefficients for timber and steel has not been taken into account. The present relation agrees well with the factor 1.15 introduced for failure mode f in Eurocode 5).

For smaller values of t_1 the Eurocode values are likely to be conservative because it does not take the fixing effect of the nail head into account. This fixation will cause the real failure mode to approach mode f, as assumed in the Danish code.

For C18-timber with density 320 kg/m^3 the load capacity according to the Eurocode will be further reduced by 6% to 8%.

Table 2. Lateral load capacity in N *for one square and smooth nail 3.4 × 90 mm for a timber to timber connection and density 350 kg/m³. t_1 is the thickness of the head side member.*

t_1 , mm	Eurocode 5				DS 413
	Mode d/e	Mode f	Rope-effect	$F_{v,Rk}$	
$7d = 23.8$	821	1078	138	958	1361
30	922	1078	125	1047	1361
45	1211	1078	94	1172	1361
60	922	1078	0	922	- *

* DS 413 requires half of the nail length to be in the point side member and 2/3 are recommended for smooth nails.

If screws were used in stead of nails the rope-effect is very difficult to take advantage of. As mentioned in section 5.2.3 it should formally have been taken as 0 for $t_1 < 12d$ because no spacing rules are given for smaller thicknesses. For normal 4 mm screws a thickness of 48 mm is required. This is prohibitive for fastening most members used in Denmark.

The group-effect on the axial load capacity means that the rope-effect depends on the number of screws. This makes is almost impossible to create tables for the lateral load capacity.

5.2.2 Steel to timber

For steel to timber the Danish code has a simple approach, too. The timber to timber strength is increased by 25%. The strength has been used irrespective of the plate thickness.

In the Eurocode is given formulas for thin steel plates ($t \leq 0{,}5d$) and for thick plates ($t \geq d$) where the head can be assumed fixed against rotation.

Table 3. Lateral load capacity in N *for one threaded connector nail with d =4 mm and f_{ax} = 6 MPa for a steel to timber connection and density 350 kg/m³. t is the thickness of the steel plate, l is the length of the nail and l_{thr} is the length of the threaded part excluding the point (6 mm).*

l , mm	l_{thr} , mm	Eurocode 5					DS 413
		Dowel $t = 0{,}5d$	Dowel $t = d$	Rope-effect	$F_{v,Rk}$ $t = 0{,}5d$	$F_{v,Rk}$ $t = d$	
35	19	1000	1262	0	1000	1262	1781
38.5	24	1106	1344	0	1106	1344	1781
48.5	34	1151	1602	204	1355	1806	1781
58.5	44	1151	1628	264	1415	1892	1781

A typical steel plate is 2 mm thick in Denmark and it is usually fastened with the shorter of the nails in Table 3. The load capacity is seen to decreases dramatically when using the Eurocode. One reason is the missing rope-effect which in turn is due to the required penetration length of $8d$ = 32 mm for assessing a withdrawal strength for those nails. Another that the head is assumed to rotate freely. The resulting load capacities do not reflect neither tests nor experience. The problems cannot be met by initial type testing giving more realistic values. A Danish manufacturer will get a European Techincal Approval containing more realistic load capacities, but this is a very costly way to solve the problems caused by introducing the Eurocode in Denmark.

2 mm steel plates are very often used on both sides of 45 mm planned timber and fastened with 4 × 35 mm connector nails. These nails just fulfilled the Danish requirement, which are that the penetration length including the point should be $8d$ and that the distance from

the point to the opposite side of the timber should be $3d$. The latter distance is in Eurocode 5 increased to $4d$. In principle the length of the nail could be reduced by $1d$ as the minimum penetration length in Eurocode 5 is only $6d$, but the load capacity becomes only 818 N, less than half of the Danish value. And again, there are no evidence that problems has occurred.

A further calamity is the row effect, which in the Eurocode has been invoked also for thin fasteners. For timber to timber it can be avoided by staggering the nails as usual, but for steel plates this has not been done and there is no experience that indicates that it should be necessary. The reason might be that the steel plate will ensure some reinforcement that reduces the risk of splitting. Therefore, the row effect should not apply to steel plates. (If the row effect is maintained it is unclear if the spacing for determining the reduction factor can be reduced by 0.7 as all other intermediate spacing for steel plates).

The problems regarding lateral load capacity can be summarized as follows:

1. For timber to timber connections the load capacity of a connector is reduced quite significantly compared to Danish rules for especially thin head-side members.

2. The minimum penetration depth for axially loaded threaded nails and the special requirements for axially loaded screws are prohibitive for taking advantage of the rope-effect.

3. The increased requirement for the distance from the point to the opposite side for two-sided connections rules out a very common type of connections in Denmark.

4. The rule for row-effect appears to be very conservative for steel to timber connections and it is unclear.

6 Conclusions

The replacement of the Danish code for timber structures with Eurocode 5 has quite severe practical implications. Some load capacities are reduced significantly and common type of connections cannot be used according to the Eurocode.

Initial type testing of each type of fastener in accordance with prEN 14592 permits for declaring improved values of some parameters. But the rules for screws are – even they have been changed in amendment A1 – not sufficient.

Very conservative rules like the penetration length for threaded nails calls for methods to bypass the Eurocode. This can be done by the major manufactures by acquiring European Technical Agreements (ETA's), but this expensive mean is prohibitive for the development of new products.

Regarding the fastener strength's dependency on the density the rules for nails and screws must be more similar if they are to be trustworthy.

There is also a need for clear rules for correcting the strength parameter from tests carried out with a density higher than the reference density. This correction could be done with much more confidence if the tests were carried with timber with as different density as possible as done by Hansen (2002), in stead of using timber with the same density for the tests. It takes a slightly more complicated statistical treatment, but the result will be much more representative and possible errors in the models will have much smaller effect.

7 References

EN 338:2003 Structural timber - Strength classes.

EN 383:2007 Timber Structures - Test methods - Determination of embedment strength and foundation values for dowel type fasteners.

EN 409:1993 Timber structures - Determination of the yield moment of dowel type fasteners - Nails.

EN 1382:2000 Timber structures - Test methods - Withdrawal capacity of timber fasteners.

EN 1383:2000 Timber structures - Test methods - Pull through resistance of timber fasteners.

prEN 14592:2007 Timber structures - Dowel-type fasteners - Requirements.

Feldborg, T & M Johansen (1972). Withdrawal resistance of nails (in Danish). SBI-rapport 84. Danish Building Research Institute.

Feldborg, T (1982). Smooth nails withdrawal strength for large wood moisture content variations (in Danish). SBI-meddelelse 23. Danish Building Research Institute.

Feldborg, T & M Johansen (1988). Nails under long-term withdrawal loading. CIB-W18 meeting September 1988, Vancouver.

Hansen, K F (2002). Mechanical properties of self-tapping screws and nails in wood. Can. J. of Civ. Eng. Vol. 29, no. 5, pp 725-733.

INTERNATIONAL COUNCIL FOR RESEARCH AND INNOVATION
IN BUILDING AND CONSTRUCTION

WORKING COMMISSION W18 - TIMBER STRUCTURES

DEVELOPMENT OF NEW SWISS STANDARDS FOR THE ASSESSMENT OF EXISTING LOAD BEARING STRUCTURES

R Steiger

Empa, Swiss Federal Laboratories for Materials Testing and Research, Dübendorf

J Köhler

Institute of Structural Engineering, ETH Zurich

SWITZERLAND

Presented by R. Steiger

T. Williamson mentioned that this is also a problem in the US and complimented the approach. He asked how to deal with the cases of altered members such as drilled holes and decay. He commented that seismic code has also changed in US recently and ASCE has a 400 page document on the issue. R. Steiger agreed with the 1st issue and there are additional standards under development in Switzerland to address them. The 2nd issue is also important in Switzerland as recent changes to seismic load also made it very difficult. There are standards developed to address this issue also. A. Ranta Maunus asked about the setting of target beta values. R. Steiger responded that the type of building is important as well as the cost or consequence of failure. A. Ceccotti stated that this work is especially important to historic structures where it is important to create a design solution not to significantly interfere with the original historic structure. Y.H. Chui received clarification from R. Steiger that ultrasonics and proof loading can be used to update information on stiffness and use the information in the new procedures. R. Steiger also stated that one needs to rely on prior research results in linking scientific work to code. H. Blass asked when measuring the deflection of structure to assess stiffness, how the influence of composite action and non-load bearing support is taken into consideration. R. Steiger stated that the example given is not a real problem but it was posed to illustrate the process.

Development of new Swiss standards for the reassessment of existing load bearing structures

René Steiger

Empa, Swiss Federal Laboratories for Materials Testing and Research
Dübendorf, Switzerland

Jochen Köhler

Institute of Structural Engineering, ETH Zurich, Switzerland

1 Introduction

Structures are planned and designed to fulfil certain requirements in regard to the safety of the users and in regard to the reliability of the fulfilment of the purpose of the structures over the prospected service life. The fulfilment of these requirements is often understood as the performance of the structure. Usually the design follows the relevant codes and standards and in general it is assumed that a structure designed according to these codes is efficient and fulfils the given requirements. Sometimes however, the conditions presumed in the design of the structure, including its exposure to loads and environment during the service life are violated or subject of changes. In these cases the reassessment of the performance of existing structures becomes necessary.

Apart from ISO standard 13822 [1], most available codes (incl. the CEN Structural Eurocodes) have been written for the design of new structures and therefore lack of adequate tools and formulations needed for the reassessment of existing structures. CEN/TC 250 therefore recently has decided to include the reassessment of existing structures in the strategy plan as a possible item for the further development within the Eurocode programme [2].

Recent efforts in Switzerland aim at editing a new series of standards for the maintenance and reassessment of existing structures. A set of codes will be edited, including basic rules (standard SIA 269) and specific adaptive rules for actions on existing structures, for building materials concrete, steel, composite (steel – concrete), timber, masonry, for geotechnical design and earthquake action (standards SIA 269/1 – 269/8). The work is based on already existing Swiss standards [3-5] as well as on international standards [6-9]. In the present paper the rationale which is followed by the new Swiss reassessment code SIA 269 [10] is presented.

2 Reassessment of existing structures

2.1 Motivation and starting point

The reassessment of an existing structure aims at proofing that its associated requirements are fulfilled over a specified residual service life (RSL) [11]. The need for an assessment of an existing structure fundamentally takes basis either in a change of the requirements to the use and/or the requirements to the structure and/or doubts in regard to whether the

assumptions underlying its design are fulfilled or not. Typical situations where the use/purpose of a structure is changed are:

- increased loading (e.g. higher live loads, revised models for snow loads)
- increased service life (The structure is still needed after the planned service life.)
- request of increased reliability (due to the importance of the structure for society)
- modification / strengthening of the structure to accommodate changes in use.

Situations where doubts may be raised in regard to the design assumptions are e.g.:

- The structure has not been inspected for an extended period of time (Damages and unforeseen degradation might have taken place.).
- Adverse results of a periodic investigation of the structure's state took place (Unexpected degradation (rot, decay, increased moisture, corrosion, etc.) has been observed. Deviations from the original project layout are observed. An inadequate serviceability is noticed. Construction or design errors are becoming aware.)
- The structure has been subjected to an accidental or otherwise non-foreseen extreme load (excessive load, earthquake, impact of vehicles, fire, etc.)
- Similar structure(s) exhibit unsatisfactory performance.
- New knowledge and revised design codes are available.

2.2 Procedure

Before starting the assessment, it is essential to take down the aspects of the further use of the structure (purpose) as well as the intended RSL (which might be associated with a certain inspection and maintenance program) together with the owner of the building. The owner's and engineer's agreement on the future use of the building has to address appropriate counteracting safety measures to defined hazard scenarios as well as (possibly) a list of accepted risks.

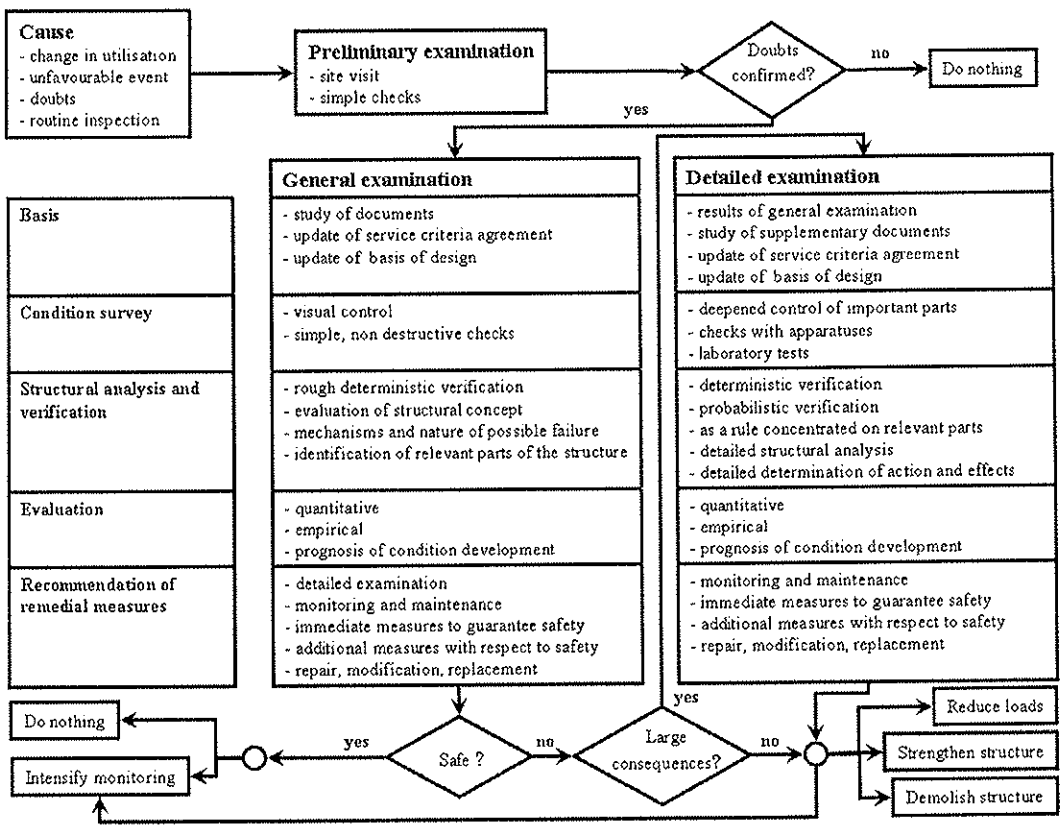

Fig. 1: Stepwise procedure when assessing existing structures [10, 11].

It is suggested to perform the reassessment in different steps with increasing deepening, the degree of deepening thereby depending on the amount and the quality of information being at disposal as well as on the importance of the building. This can be reached by breaking down the assessment into different phases (Fig. 1) [10, 11].

The assessment starts with a *preliminary examination,* including a site visit with simple, mainly visual checks. Special attention in this step is paid to the overall state of the structure and to its critical parts. Typical hazard scenarios, which could endanger the situation, have to be identified and as a result of this, immediate measures eventually are needed.

If doubts are confirmed, reassessment is continued with a *general examination*, in the course of which the whole structure (including non load-bearing parts, if these parts are relevant in terms of safety of individuals, valuables and environment) is examined. The general examination has to be based on a study of existing documents and on an agreement on service criteria or on similar documents like utilisation and safety plans. Then the concept of the existing structure has to be evaluated, paying special attention to the robustness of the system (serial and parallel systems, static redundancy, etc.). Visual and simple, mostly non-destructive examination on site serve at identifying deterioration and deficiencies. Finally a rough limit states (LS) analysis (serviceability and ultimate limit state, SLS, ULS) is performed, in order to recognize zones and members of the structure which are of decisive influence on the structure's integrity.

If the general examination did not confirm the building's adequate state with regard to its intended further use, a single *detailed examination* or perhaps several of them are needed. Key zones and members of the structure are examined in detail (again with increasing deepening) using more sophisticated methods (expert's opinion, proof loading, destructive and non-destructive tests of representative samples, etc.). Causes of deterioration and deficiencies of the key zones and members have to be found. The load-bearing behaviour of the structure is analysed in more detail and in the course of the limit states analysis the actions and the resistances are determined with higher accuracy, using more sophisticated models. Regarding the resistance, possible failure modes (brittle failure, ductile failure with/without strength capacity from strain hardening) of the load-bearing members and connection have to be evaluated, taking into account the deformation development (past) as well as the deformation behaviour/capacity (future).

Compared to the design of new structures, when assessing existing structures the engineer's thinking should be more analytical in terms of for example a differentiation between processes/actions driven by load ($F = m \cdot g$), by force ($F = m \cdot a$) or by deformation (settlement, deviation in temperature, etc.).

2.3 Decision process

If the requirements regarding the present and future use of a structure are specified, the assessment is a *decision process* with the purpose of identifying those measures which lead to the most economical fulfilment of these requirements with regard to the RSL. Hereby a subordinate decision has to be taken in regard to the level of detail of the analysis to be performed. It is believed that a general examination (see above) is a sufficient level of detail for the most cases in practice – however, this has to be verified for each individual case by following the scheme illustrated in Fig. 1. It is essential, that the committed engineer can make his decisions based on codified standards which reflect the present best practices in regard to the assessment of existing structures.

2.4 Codification aspects

Guidelines for the use and the maintenance of existing structures exist in many countries. At least in the USA, Canada, Switzerland [3], UK such guidelines have been prepared at a detailed level [11]. At present however only a few countries (for example the Netherlands [12] and Switzerland [3, 4, 13-16]) have or work out general applicable code-type documents for the assessment of existing structures. In 2001 the first edition of an ISO-standard [1] on the assessment of existing structures has been approved. Codes for the assessment of existing structures have to include [11]:

- area of application (incl. differentiation between assessment of existing parts of a structure and design of new parts or strengthening elements)
- general principles of assessment (incl. stepwise procedure)
- methods for updating
- methods and format for verification
- risk acceptance criteria
- guidelines for decisions and intervention planning.

The code formulation should be such that the committed engineer is able to use his knowledge gathered from the design of new structures. That is why deterministic verification on base of partial safety factor format of limit states design should be the "usual" case (corresponding to the "general examination" phase mentioned above). However, even here with regard e.g. to possible adaption of partial safety factors, it is important to consider the information from the inspected structure in the design equations appropriately. In case of the "detailed examination" a comprehensive risk based assessment of the structural performance might be necessary where issues as the structural reliability and the cost efficiency of possible measures can be assessed explicitly.

3 Draft Swiss Reassessment Code SIA 269

3.1 Structure of the code

The Draft Swiss Code SIA 269 for the assessment and maintenance of existing structures [16] includes the following main parts:

- General (examination, monitoring and maintenance, economic and cultural value)
- Requirements (use, structural safety, serviceability, proportionality/effectiveness of maintenance interventions)
- Updating (actions, properties and condition of construction products and soil/foundation, structural model, geometry, ultimate resistance, deformations)
- Structural analysis and verification (deterministic and probabilistic)
- Examination (procedure, condition survey and evaluation, recommendation of maintenance interventions)
- Maintenance interventions (concept, realisation, monitoring, maintenance, immediate measures, additional measures regarding safety, repair, modification)
- Construction documents (service criteria agreement, service instructions, basis of design, history of the structure, hazard events, monitoring and maintenance plan, inspection reports, result of monitoring, documents resulting from examination and maintenance interventions, record/plans of construction)
- Annex (stepwise procedure in examination, updated examination values, hints for the probabilistic verification).

3.2 Basic principles and kernels of the code

3.2.1 Updating

The main point being different compared to the design of new structures is that the amount and the quality of information are different: For new structures we have more or less general and in some sense imprecise information about the critical characteristics of the structure to be designed. For existing structures there is much more information available and it is important to use this information when assessing existing structures.

At the time when a structure is designed, the only information available are the projected geometrical and material properties (e.g. strength class of glulam) as well as code values of loads derived from the intended location, shape and purpose of the building. On the basis of such general information either deterministic design using the partial safety factor concept or so-called *prior* probabilistic design can be formulated. As soon as the structure has been realised and the building is in use, knowledge about the structure can be updated. The information to be collected can be of very diverse nature e.g. in type of measurement data, subjective information, etc. Some information is purely qualitative (no, minor, severe damage) whereas other is of quantitative type (crack lengths and depths, displacements, etc.). After updating the information a so-called *posterior* probabilistic design or decision analysis can be established. Accordingly there are prior or posterior probability density functions (PDF) to be used for modelling the basic random variables (BRV) [17]. Updating of information can be done in two different ways [11]:

- updating of individual random variables based on measurements and observations using Bayesian techniques
- updating of failure probability by conditioning, e. g. conditional failure probabilities due to measured cracks, or due to arrival of extreme loads, etc.

New information about the structure such as inspection and test results can be defined as:

$$\mathbf{I} = \{\mathbf{x} | h(\mathbf{x}) * 0\} \qquad \text{(Eq. 1)}$$

where * represents $\leq$, $>$ or $=$ depending on the type of information (= for equality type and $\leq$, $>$ for inequality type of information). Information of the equality type means, that for some basic or response variables some realisations have been directly measured. Of course such measurements may suffer from measurement errors, which themselves can be modelled as additional random variables having means, standard deviations and (if necessary) some correlation pattern. Inequality type information refers to observations where it is only known that the observed value is $>$ or $<$ than some limit (threshold). Additionally there always is a degree of correlation between observations at different places and different points in time, which is important but difficult to model. Examples of information, which is available or can be made available at given costs, are [11]:

- the structure has survived certain load conditions
- characteristics of material from a known source
- geometry
- local climate (indoor + outdoor!)
- damages and deterioration
- proof loading
- static and dynamic response to controlled loading.

It is important to notice, that updating can also make use of indirect information, which does not origin from the structure itself, but which is correlated to the structural performance, e.g. common loading, correlated material properties or correlated degradation processes.

Qualitative information ("The structure looks fine.") has to be formalized in order to be able to use it in calculations. Properties, values and terms which had been updated based on new information should be clearly distinguished from those used for the design of new structures, i.e. they are "actual" and should be marked by an additional index "*act*".

The Draft Swiss reassessment code SIA 269 [10] uses the following semi-probabilistic approach to derive updated design values from known (and updated) probability distributions of BRV (effects of actions, ultimate resistance and stiffness properties):

- Effects of permanent actions are modelled Normal distributed. Effects resulting from variable loads or accidental loads are to be modelled with a Gumbel distribution. To model strength and stiffness related material properties LogNormal distributions have to be used. Exceptions are the timber density and the compression strength perpendicular to the grain, which are modelled as Normal distributed random variables and the tension strength perpendicular to the grain which is modelled as a 2p-Weibull distributed random variable. These assumptions follow the recommendations of JCCS Probabilistic Model Code [9, 18].

- The updated examination value of Normal distributed effects of actions E, strength and stiffness properties R can be calculated from:

$$E_{d,act} = E_{\mu,act}\left(1+\alpha_E \beta_0 v_{E,act}\right) \qquad \text{(Eq. 2)} \qquad R_{d,act} = R_{\mu,act}\left(1+\alpha_R \beta_0 v_{R,act}\right) \qquad \text{(Eq. 3)}$$

  $E_{\mu,act}$ and $R_{\mu,act}$ are updated expected values, $v_{E,act}$ and $v_{R,act}$ are updated coefficients of variation and α_E and α_R are factors to account for sensitivity. β_0 is the target reliability index, which can be derived from the target failure probabilities p_f given in Table 2 by using Eq. (14).

- The updated examination value of effects of actions and of strength properties following a LogNormal distribution can be calculated from:

$$E_{d,act} = E_{\mu,act} \cdot e^{\left(\alpha_E \beta_0 \delta_E - 0.5\delta_E^2\right)} \qquad \text{(Eq. 4)} \qquad R_{d,act} = R_{\mu,act} \cdot e^{\left(\alpha_R \beta_0 \delta_R - 0.5\delta_R^2\right)} \qquad \text{(Eq. 5)}$$

  with: $\delta_E^2 = \ln\left(v_{E,act}^2+1\right)$ (Eq. 6) $\delta_R^2 = \ln\left(v_{R,act}^2+1\right)$ (Eq. 7)

  $E_{\mu,act}$ and $R_{\mu,act}$ are updated expected values, $v_{E,act}$ and $v_{R,act}$ are updated coefficients of variation and α_E and α_R are factors to account for sensitivity. δ_E and δ_R are parameters of the LogNormal distribution.

- The updated examination value of action effects following a Gumbel distribution may be calculated as follows:

$$E_{d,act} = E_{\mu,act}\left[1 - v_{E,act}\left(0.45 + 0.78\ln\left\{-\ln\left[\Phi\left(\alpha_E \beta_0\right)\right]\right\}\right)\right] \qquad \text{(Eq. 8)}$$

  $E_{\mu,act}$ is the expected value, $v_{E,act}$ is the updated coefficient of variation and α_E is a factor to account for sensitivity. β_0 is the target reliability index, which can be derived from the target failure probabilities p_f given in Table 2 by using Eq. (14).

- In case of the factors to account for sensitivity not being updated on base of a FORM-analysis (FORM = First Order Reliability Method) [17], the following simplified values can be used:
  $\alpha_E =$ 0.7 for effects of leading actions
  $\alpha_E =$ 0.3 for effects of accompanying actions
  $\alpha_R =$ −0.8 for strength values being of big importance for the structural safety
  $\alpha_R =$ −0.3 for strength values with minor influence on the structural safety.

3.2.2 Verification and decision making

The format of verification depends on the degree of sophistication of the assessment analysis. Either (and this should be the "usual case") a deterministic verification with the partial safety factor format or a semi- or full probabilistic design format may be used [6, 7], the accuracy of verification thereby being improved from one format to the other.

Decisions have to be taken following certain criteria, e.g. target reliability, economical considerations, time constraints, socio-economical and political preferences and codes.

3.2.3 Deterministic verification

The deterministic verification of existing structures in partial safety factor format differs from designing a new structure in terms of available information. As already mentioned, all BRV have to be updated accordingly. Compared to the designing of new structures, where *design situations* are examined using *design values* of action effects and material resistance, in the assessment of existing structures *examination situations* described by *examination values* of action effects and resistances are evaluated. In order to be able to better get aware of immanent deficiencies and reserves, the format of verification is changed

from $E_{d,act} \le R_{d,act}$ (Eq. 9) to $DC = \frac{R_{d,act}}{E_{d,act}} \ge 1$ (Eq. 10)

where DC stands for *degree of compliance*. If $DC < 1$ the structure has to be strengthened or the loads have to be reduced. In cases where the proof of an adequate resistance did just not pass, a semi-probabilistic or a probabilistic verification might be useful before arranging tedious and costly strengthening measures.

3.2.4 Probabilistic verification

A probabilistic design means that a structure is designed/verified so that the probability of failure P_f does not exceed a specified value P_s over some specified period of time:

$$P_f \le P_s \qquad \text{(Eq. 11)}$$

Failure $\mathbf{F}$ is associated with a transition of the limit state function $g(\mathbf{x})$ from the desired state to the undesired one:

$$\mathbf{F} = \{\mathbf{x} | g(\mathbf{x}) \le 0\} \qquad \text{(Eq. 12)}$$

where $\mathbf{x}$ (vector) are the basic variables (actions $\mathbf{s}$, resistances $\mathbf{r}$, etc.) which are relevant for the problem. The limit state function (LSF) $g(\mathbf{x})$ can often be separated into one resistance function $r(.)$ and one loading (or action effect) function $s(.)$:

$$g(\mathbf{x}) = r(\mathbf{x}) - s(\mathbf{x}) \qquad \text{(Eq. 13)}$$

The failure probability P_f may be represented by a reliability index β through the definition:

$\beta \leq -\Phi^{-1}(P_f)$ (Φ^{-1} is the inverse standardized Normal distribution.) (Eq. 14)

The relationship between β and P_f is given in Table 1.

Table 1: Relationship between β and P_f

P_f	10^{-1}	10^{-2}	10^{-3}	10^{-4}	10^{-5}	10^{-6}	10^{-7}
β	1.3	2.3	3.1	3.7	4.2	4.7	5.2

In probabilistic verifications the calculated probabilities of failure or the reliability index β have to be compared to certain acceptable limits or targets. The selection of target reliability levels (TRL) depends on different parameters such as type and importance of the structure, possible failure consequences, socio-economic criteria, etc. When setting TRL the following items have to be taken into account [11]:

- TRL are not necessarily the same for structures to be designed and for structures which already exist, because the situation may have changed (RSL, use and/or importance of the building).
- TRL may differ depending on whether an entire building facility including other than structural failure modes or the structure itself in the narrow sense is considered.
- It is to be distinguished between limits or targets set for facilities including human error in its various forms (design error, failure of quality management, operation failure, ignorance, etc.) and limits or targets where such failures are not included.
- It is important, whether limits or targets are related to individual failure modes or to failure modes of a system / collapse.

In a probabilistic format (code) limits or targets on the failure probability are not independent of the set of probabilistic models used to verify them [19]! It is therefore important that probabilistic assessments of structures are based on a common set of models and procedures. The Probabilistic Model Code of the Joint Committee on Structural Safety (JCSS) [9] is such a basis where probabilistic assessments should be based on. When setting TRL the relative costs of safety measures and the consequences of failure (see Table 2) have to be taken into account. Reasonable TRL for ultimate limit states (ULS) as well as for serviceability limit states (SLS) are given in Tables 2 [9] and 3 [16] respectively.

Table 2: Target reliability indices β (and associated target failure rates P_f) related to one year reference period and ultimate limit state [9]

Relative cost of safety measures	**Minor consequences of failure**	**Moderate consequences of failure**	**Large consequences of failure**
Large	$\beta = 3.1$ ($P_f \approx 10^{-3}$)	$\beta = 3.3$ ($P_f \approx 5 \cdot 10^{-4}$)	$\beta = 3.7$ ($P_f \approx 10^{-4}$)
Normal	$\beta = 3.7$ ($P_f \approx 10^{-4}$)	$\beta = 4.2$ ($P_f \approx 10^{-5}$) [1)]	$\beta = 4.4$ ($P_f \approx 5 \cdot 10^{-6}$)
Small	$\beta = 4.2$ ($P_f \approx 10^{-5}$)	$\beta = 4.4$ ($P_f \approx 5 \cdot 10^{-5}$)	$\beta = 4.7$ ($P_f \approx 10^{-6}$)

[1)] most common design situation

Table 3: Target reliability indices β (and associated target failure rates P_f) related to one year reference period and service limit state [16]

Type of SLS	**Target reliability / failure rate**
Irreversible consequences	$\beta = 2.3$ ($P_f \approx 10^{-2}$)
Reversible consequences	$\beta = 1.3$ ($P_f \approx 10^{-1}$)

In order to be able to properly apply the reliability indices β for ULS (Table 2), the terms "large, normal, small, minor, moderate" have to be quantified. According to the Draft Swiss Reassessment Code SIA 269 [16], the relative cost of safety measures can be assessed by calculating the proportionality/effectiveness of maintenance interventions EF_M (see 3.2.5). EF_M is judged to be small, if $EF_M < 0.5$; normal, if $0.5 \leq EF_M \leq 2{,}0$ and large, if $EF_M > 2.0$. The consequences of failure can be grouped on base of the ratio κ [16]:

$$\kappa = \frac{C_F}{C_W} \qquad \text{(Eq. 15)}$$

where C_F stands for all direct costs upon failure of the structure and C_W are the costs for restoring the structure. Minor consequences are assigned to $\kappa < 2$, moderate consequences to $2 < \kappa < 5$ and large ones to $5 < \kappa < 10$ [11].

3.2.5 Verification of proportionality/effectiveness of maintenance interventions

In the Draft Swiss Reassessment Code SIA 269 the proportionality of maintenance interventions related to safety is assessed [16] on base of their effectiveness and taking into account the following aspects:

- safety requested by individuals and by public
- availability of a building or a facility
- consequences of failure for human beings, valuables and environment
- preservation of cultural values.

The expenses for maintenance interventions can be expressed in costs for granting the requests of structural safety and serviceability of a structure. As a benefit of maintenance interventions, the increase in financial and cultural values, the reduction in costs for inspections/monitoring and maintenance as well as the reduction in risk because of restoring the required structural safety and serviceability can be revealed. Finally the proportionality of maintenance interventions EF_M can be assessed by comparing the costs of safety measures with the efficiency of interventions [16]:

$$EF_M = \frac{\Delta R_M}{SC_M} \qquad \text{(Eq. 16)}$$

(A specific maintenance intervention is proportional/effective if $EF_M \geq 1$ with respect to the RSL.)

ΔR_M stands for the reduction of risk to loss of life and limb by providing safety and maintenance measures. SC_M are the costs of safety measures implemented in the structure. Both ΔR_M and SC_M are formulated as a discounted monetary value per year, over the RSL. The measures taken to save the last human life can be accounted for 10^7 Swiss Francs as a rule [16], which at the time of writing this paper equals 10^7 US Dollars or $6 \cdot 10^6$ Euros. To account for insured or invalid persons, data provided by assurance companies can be used. The discounting has to be based on a specified rate. In [16], a rate of $i = 2\%$ is suggested. The discounting factor DF can be calculated from the rate i and the intended RSL:

$$DF = \frac{i(1+i)^n}{(1+i)^n - 1} \qquad \text{(Eq. 17)}$$

where i = ratio for discounting [-] and n = RSL [a].

4 Example

4.1 Description of the problem

The load-bearing structure to be examined in this (artificial) example consists of a series of parallel simply supported glulam beams of strength class GL24h [20] ($f_{m,g,k}$ = 24 N/mm^2, $f_{v,g,k}$ = 2.7 N/mm^2, $E_{0,g,mean}$ = 11600 N/mm^2, $G_{g,mean}$ = 720 N/mm^2) with a span of 6 m and a distance of 2.5 m between the beams. According to the initial use of the building, a live load of 4 kN/m^2 (q_k = 10 kN/m) had to be taken into account when designing the glulam beams. The input parameters of the example are summarized in Tables 4 and 5. Note that the probabilistic models for the input variable as well as the correlations of the BRV are derived by following the recommendations of the JCSS probabilistic model code [9, 18].

Table 4: Input parameters for the exemplary calculation

BRV	Char. value [N/mm^2]	Percentile	PDF	COV	Mean [N/mm^2]	Standard deviation [N/mm^2]
Bending strength F_m	24	5	LogNormal	0.15	31.0	4.65
Shear strength F_v	2.7	5	LogNormal	0.2	3.81	0.76
MOE	11600	-	LogNormal	0.13	11600	1508
Shear modulus	720	-	LogNormal	0.13	720	93.6
Live load situation 1	1	50	Normal	0.1	1.00	0.10
Live load situation 2	10	98	Gumbel	0.6	3.91	2.35

Table 5: Correlation ρ of BRV

BRV	F_v	E	G
F_m	0.4	0.8	0.4
F_v		0.4	0.6
G		0.6	–

4.2 Initial design of the load-bearing structure (design situation 1)

Assuming a dead load (including self weight) of g_k = 1 kN/m and partial safety factors $\gamma_{f,g}$ = 1.35 for self weight and dead load and $\gamma_{f,q}$ = 1.5 for live loads [5], the maximum bending moment and shear forces result in:

$$M_d = \frac{\left(\gamma_{f,g} \cdot g_k + \gamma_{f,q} \cdot q_k\right) \cdot \ell^2}{8} = 73.6\,\text{kNm} \qquad \text{(Eq. 18)}$$

$$V_d = \frac{\left(\gamma_{f,g} \cdot g_k + \gamma_{f,q} \cdot q_k\right) \cdot \ell}{2} = 49.1\,\text{kN} \qquad \text{(Eq. 19)}$$

The initial design of the beams with a cross-section of 160 mm x 440 mm is done by verifying the bending strength and the shear strength assuming a k_{mod}-value of 0.80 (medium term action) and a partial safety factor of γ_M = 1.25 [21]. Additionally the maximal deflection u at mid-span under live load is calculated:

$$M_{Rd} = \frac{k_{\text{mod}} \cdot f_{m,g,k} \cdot \frac{160 \cdot 440^2}{6}}{\gamma_M} = 79.3\,\text{kNm} > M_d = 73.6\,\text{kNm} \qquad \text{(Eq. 20)}$$

$$V_{Rd} = \frac{k_{\mathrm{mod}} \cdot \frac{2}{3} \cdot f_{v,g,k} \cdot 160 \cdot 440}{\gamma_M} = 81.1\,\mathrm{kN} \; > \; V_d = 49.1\,\mathrm{kN} \qquad \text{(Eq. 21)}$$

$$u = \frac{5 \cdot q_k \cdot \ell^4}{384 \cdot E \cdot \frac{160 \cdot 440^3}{12}} + \frac{q_k \cdot \ell^2}{8 \cdot G \cdot \frac{5}{6} \cdot 160 \cdot 440} = 12.8 + 1.1 = 13.9\,\mathrm{mm} \; < \; \ell/400 = 15\,\mathrm{mm} \qquad \text{(Eq. 22)}$$

4.3 Change in use (design situation 2)

Due to a change in use, the live load will be altered. This leads to a characteristic value to be considered of q_k = 12.5 kN/m. The coefficient of variation of the yearly maximum of the new load is estimated as $v_{Q,act}$ = 0.7. The safety of the glulam beam will now be checked by:

- a deterministic verification (degree of compliance)
- a semi-probabilistic verification by updating the information about the live load
- probabilistic verification (comparing situation 1 and 2)
- probabilistic verification using new information (measurement of deflection)

4.3.1 Deterministic verification

The updated effects of actions $g_{k,act} = g_k$ and $q_{k,act}$ = 12.5 kN/m result in:

$$M_{d,act} = \frac{\left(\gamma_{f,g} \cdot g_{k,act} + \gamma_{f,q.act} \cdot q_{k,act}\right) \cdot \ell^2}{8} = 90.5\ \mathrm{kNm} \qquad \text{(Eq. 23)}$$

$$V_{d,act} = \frac{\left(\gamma_{f,g} \cdot g_{k.act} + \gamma_{f,q} \cdot q_{k.act}\right) \cdot \ell}{2} = 60.3\,\mathrm{kN} \qquad \text{(Eq. 24)}$$

The update of the resistance has to be based on an examination of the glulam beams. Let us for the moment assume, that a preliminary or a general examination has taken place resulting in the information that the glulam beams are likely to be of strength class GL24h and that they are in good shape (i.e. $R_{d,act} = R_d$). The geometrical properties (span, cross-section) have been verified and there is no change in dead load. The degree of compliance DC for bending and shear resistance can then be calculated as:

$$DC_M = \frac{M_{Rd,act}}{M_{d,act}} = \frac{79.3}{90.5} = 0.88 \qquad \text{(Eq. 25)} \qquad DC_V = \frac{V_{Rd,act}}{V_{d,act}} = \frac{81.1}{60.3} = 1.35 \qquad \text{(Eq. 26)}$$

Hence the bending strength is not adequate for design situation 2. The resistance of the beam being nearly sufficient, it will be now tried to prove sufficient reliability by performing a semi-probabilistic verification.

4.3.2 Semi-probabilistic verification

According to Eq. (8) the design value of the live load can be estimated taking into account the target reliability β_0, the mean value ($\mu_{Q,act} = 12.5$ kN/m) and the coefficient of variation of the live load $v_{Q,act} = 0.7$ and the mathematical structure of the limit state equation ($\alpha_E = 0.7$). This gives an updated design value for the live load of $q_{d,act} = 18.6$ kN/m compared to the design value ($q_d = 1.5 \cdot 12.5 = 18.75$ kN/m) considered

above. The degree of compliance DC for bending and shear resistance can then be calculated according to the semi-probabilistic verification as:

$$DC_M = \frac{M_{Rd,act}}{M_{d,act}} = \frac{79.3}{89.7} = 0.88 \quad \text{(Eq. 27)} \qquad DC_V = \frac{V_{Rd,act}}{V_{d,act}} = \frac{81.1}{59.8} = 1.36 \quad \text{(Eq. 28)}$$

Hence the bending strength is still not adequate for design situation 2.

4.3.3 Probabilistic verification

The probability of failure might be directly estimated by using the probabilistic models summarized in Table 4. Two different limit state equations are formulated:

Bending limit state: $$g_{bending}(\mathbf{X}) = \frac{1}{6} X_1 k_{\mathrm{mod}} F_m b h^2 - \frac{1}{8}(G+Q) l^2 \quad \text{(Eq. 29)}$$

Shear limit state: $$g_{shear}(\mathbf{X}) = \frac{2}{3} X_2 k_{\mathrm{mod}} F_v b h - \frac{1}{2}(G+Q) l \quad \text{(Eq. 30)}$$

The failure criterion can be formulated as: $\mathbf{F} = \left\{ \mathbf{x} \middle| g_{bending}(\mathbf{x}) \le 0 \cup g_{shear}(\mathbf{x}) \le 0 \right\}$ (Eq. 31)

The problem is solved by using FORM/SORM see e.g. [17]. For design situation 1 the estimated prior failure probability is $p_f = 2.196 \cdot 10^{-5}$ which corresponds to an equivalent reliability index of $\beta = 4.08$. If we consider Table 2 where target reliabilities are suggested for given consequence and cost of safety measure class, it can be noted that the reliability index is lower than 4.2, the value which is suggested for the most common type of structures, i.e. a structure with moderate cost of failure and normal cost for additional safety measures.

For design situation 2 the estimated failure probability is $p_f = 2.233 \cdot 10^{-4}$ which corresponds to an equivalent reliability index of $\beta = 3.51$. Note that this is a clear violation of the normal target safety index of $\beta_0 = 4.2$. It might be judged that the reliability is not sufficient.

4.3.4 Updating

New information about the structural resistance might become available, e.g. by measuring the deflection of the beam loaded with a given proof load in the course of a detailed verification. Let us assume that $P_{proof} = 20$ kN are applied at mid-span of the beam and the deflection is measured before and after loading. The difference in deflection results in $\Delta u = 6$ mm. The deflection measurement provides information about the stiffness properties of the beam (On base of the MOE ($E_{0,g,mean} = 11600$ N/mm^2) used for the initial design of the beam a difference in deflection of $\Delta u = 6.83$ mm would have been expected). This information can be used to update our knowledge about the load bearing capacity of the beam, since it can be assumed that stiffness and strength are positively correlated with $\rho_{(F_m,E)} = 0.8$ (Table 5).

4.3.4.1 Updating of the random variable

The bending capacity of the beam might be updated directly; i.e. update the random variable "bending strength" F_m based on the information about the bending stiffness and its correlation to the strength $\rho_{(F_m,E)}$. The deflection measurement of $\Delta u = 6$ mm indicates an apparent modulus of elasticity $E_{app} = 16500$ N/mm^2. Note that the shear deflection is

ignored here. The mean value and the standard deviation of the bending strength F_m may be updated as follows:

$$\mu_{F_m|E_{app}} = \mu_{F_m} + \rho_{F_m,E}\sigma_{F_m}\frac{E_{app}-\mu_E}{\sigma_E} = 43.1 \text{ N/mm}^2 \quad \text{(Eq. 32)}$$

$$\sigma_{F_m|E_{app}} = \sigma_{F_m}\sqrt{1-\rho^2_{F_m,E}} = 2.8 \text{ N/mm}^2 \quad \text{(Eq. 33)}$$

- Semi-probabilistic verification
  According to Eq. (5) the design value of the bending strength can be estimated by taking into account the target reliability β_0, the mean value $\mu_{F_m|E_{app}}$ and the coefficient of variation of the bending strength $v_{F_m,act} = 2.8/43.1 = 0.06$ and the mathematical structure of the limit state equation ($\alpha_R = -0.8$). This gives an updated design value for the bending strength of $r_{d,act} = 34.6\,\text{N/mm}^2$ compared to the design value considered above ($24/1.25 = 19.2$ N/mm^2). The degree of compliance DC for the bending resistance can then be calculated according to the semi-probabilistic verification as:

  $$DC_M = \frac{M_{Rd,act}}{M_{d,act}} = \frac{143}{89.7} = 1.59 \quad \text{(Eq. 34)}$$

  Hence the bending strength is adequate for design situation 2.

- Probabilistic Verification
  Redoing the reliability analysis analogue to section 4.3.3 but with an updated bending strength model the updated probability of failure is $p_{f,act} = 4.8\cdot10^{-6}$ which corresponds to an equivalent reliability index of $\beta_{act} = 4.43$.

4.3.4.2 Direct updating

The information of the deflection measurement might be directly used by formulating an artificial limit state function $H(\mathbf{x})$ as

$$H(\mathbf{x}) = 48EIu_{measurment} - P_{proof}l^3 \quad \text{(Eq. 35)}$$

Where I is the modulus of inertia. Note that for $H(\mathbf{x}) = 0$ the realisation of E corresponds to the situation where the deflection is equal to the measurement.

The new information can now be integrated into the failure criterion:

$$\mathbf{F} = \left\{\mathbf{x}\middle|\left(g_{bending}(\mathbf{x}) \le 0 \cup g_{shear}(\mathbf{x}) \le 0\right) \cap H(\mathbf{x}) = 0\right\} \quad \text{(Eq. 36)}$$

The deflection measurement of Δu = 6 mm gives an updated failure probability of $p_{f,act} = 4.8\cdot10^{-6}$ corresponding to β_{act} = 4.43. The estimated reliability index is larger than the suggested target of $\beta_0 = 4.2$.

5 Conclusions and outlook

5.1 Conclusions

It can be concluded that:

- Assessing existing structures is getting more and more important. Whereas ISO standards and some national codes exist, the structural Eurocode program by CEN up to now lacks of adequate tools.
- The assessment of existing structures should be performed on base of a stepwise procedure with increasing deepening (see Fig. 1).
- Assessing the structural safety and serviceability of new structures to be designed differs from reassessing existing structures because the amount and the quality of available information are different. When reassessing existing buildings all available information has to be made use of by updating the design variables. However the detail of the analysis is subject to the stepwise approach illustrated in Figure 1.
- The deterministic verification of existing structures on base of the well-established partial safety factor concept should be the "usual" case. Updating of the basic random variables is of great importance.
- In cases where either the deterministic verification was not successful or where the costs for strengthening a structure are large, a semi-probabilistic or a probabilistic verification can be helpful. Furthermore it has to be mentioned that the probabilistic approach provides a better basis from which system behaviour can be explored and assessed. This might be advantageous especially for the assessment of existing structures where strength reserves due to system effects can alleviate the need for expensive strengthening.

5.2 Outlook

The provision of a codified basis for the assessment of existing structures is an important step towards the efficient management of our built infrastructure. However, for the implementation of the tools and procedures presented in the present paper it is essential that the additional information that is gathered during the reassessment procedure can be related to the basic variables of the limit state function at hand. It is the responsibility of the corresponding research community to develop and deliver models describing these relationships.

6 References

1. International Organization for Standardization I. (2001): ISO 13822: Bases for design of structures - Assessment of existing structures.
2. CEN/TC 250 (2008): Document N 764 of CEN/TC 250: Draft report of thirty-second meeting of CEN/TC 250 held in Limassol, Cyprus on 15th and 16th October 2007.
3. Schweizerischer Ingenieur- und Architektenverein (1994): SIA-Richtlinie 462: Beurteilung der Tragsicherheit bestehender Bauwerke (Guideline SIA 462: Assessment of the structural safety of existing buildings). SIA, Zurich, Switzerland.
4. Schweizerischer Ingenieur- und Architektenverein (1997): SIA-Norm 469: Erhaltung von Bauwerken (Standard SIA 469: Maintenance of buildings). SIA, Zurich, Switzerland.
5. Swiss Society of Engineers and Architects (2003): Standard SIA 260: Basis of Structural Design SIA, Zurich, Switzerland.
6. European Committee for Standardization CEN (2002): EN 1990: Eurocode 0: Basis of structural design CEN, Bruxelles, Belgium.
7. International Organization for Standardization ISO (1998): ISO 2394: General principles on reliability for structures.
8. International Organization for Standardization ISO (2001): ISO 13822: Bases for design of structures - Assessment of existing structures.
9. Joint Committee on Structural Safety J. (2001): Probabilistic Model Code. http://www.jcss.ethz.ch/
10. Schweizerischer Ingenieur- und Architektenverein (2008): Normentwurf SIA 269: Grundlagen der Erhaltung von Tragwerken (Draft Standard SIA 269: Basis of Maintenance of Structures). SIA, Zurich, Switzerland.
11. Diamantidis D. (2001): Probabilistic assessment of existing structures. RILEM publications, Cachan, France.
12. Nederlands Normalisatie-instituut N. (2008): Ontwerp of NEN 8700: Grondslagen van de beoordeling van de constructieve veiligheid van een bestaand bouwwerk - Gebouwen (Draft NEN 8700: Basis of structural assessment of existing structures - Buildings).
13. Schweizerischer Ingenieur- und Architektenverein (1997): SIA-Empfehlung 162/5: Erhaltung von Betontragwerken (Recommendation SIA 162/5: Maintenance of concrete structures). SIA, Zurich, Switzerland.
14. Schweizerischer Ingenieur- und Architektenverein (2000): Merkblatt SIA 2017: Erhaltungswert von Bauwerken (Leaflet SIA 2017: Assessing the value of buildings). SIA, Zurich, Switzerland.
15. Schweizerischer Ingenieur- und Architektenverein (2004): Merkblatt SIA 2018: Überprüfung bestehender Gebäude bezüglich Erdbeben (Leaflet SIA 2018: Assessment of the earthquake resistance of existing buildings). SIA, Zurich, Switzerland.
16. Swiss Society of Engineers and Architects S. (2007): Normentwurf SIA 269: Grundlagen der Erhaltung von Tragwerken (Draft Standard SIA 269: Basis of Maintenance of Structures). SIA, Zürich.
17. Madsen H. O., Krenk S., Lind N. C. (2006): Methods of structural safety. Dover Publications, Mineola, NY.
18. Köhler J., Sørensen J. D., Faber M. H. (2007): Probabilistic modeling of timber structures. Structural Safety 29 (4) 255-267.
19. Faber M. H., Sorensen J. D. (2003): Reliability based code calibration - The JCSS approach. In: Proceedings of the 9th International Conference on Applications of Statistics and Probability in Civil Engineering - ICASP9, Millpress Science Publishers, 1, San Francisco, USA.
20. European Committee for Standardization CEN (1999): EN 1194: Timber structures - Glued laminated timber: Strength classes and determination of characteristic values CEN, Bruxelles, Belgium.
21. European Committee for Standardization CEN (2004): EN 1995-1-1: Eurocode 5: Design of timber structures - Part 1-1: General - Common rules and rules for buildings CEN, Bruxelles, Belgium.

INTERNATIONAL COUNCIL FOR RESEARCH AND INNOVATION
IN BUILDING AND CONSTRUCTION

WORKING COMMISSION W18 - TIMBER STRUCTURES

MEASURING THE CO2 FOOTPRINT OF TIMBER BUILDINGS

A Buchanan

S John

University of Canterbury, Christchurch

NEW ZEALAND

Presented by A. Buchanan

T. Williamson stated that in US this is an important issue because LEEDS is unfriendly to wood. Two ANSI standards are available. LCA makes sense but concrete and steel are negative towards LCA as the results are favourable to wood. J. König stated that in EC stability and fire have been the key issues. The commission is now interested to develop Eurocodes for all essential requirements. Requirement #7 is sustainability of material and will be the future. The exercise is highly relevant and this committee should be involved. S. Winter agreed with J. König and added that health and environmental protection are also important issues. Leeds standard is driven by the concrete industry and tries to hide in the process with strong participation. Lifetime of the building is also important. We need scientific base information to help lobbying. The paper seems to be too favourable to wood as there seems to be some double accounting of CO2. J. Munch-Andersen states that it is very difficult to calculate CO2 footprint. For example the use of nuclear power or hydro power to make Aluminium will make a large difference. In N. America it is very apparent that there is a strong need to reduce energy consumption on heating and cooling of buildings.

CIB-W18 meeting — St. Andrews, New Brunswick, Canada 24 to 28 August 2008

Measuring the CO_2 Footprint of Timber Buildings

Andy Buchanan, Stephen John
University of Canterbury, Christchurch, New Zealand

Abstract

As climate change and sustainability become increasingly important in the built environment, standard methods are needed to asses environmental impacts of buildings. This paper proposes a standard method to measure the CO_2 footprint of timber buildings.

Timber construction can compare extremely well with conventional materials, but this can only be demonstrated by using quantitative data which is collected and presented in a uniform way which considers the whole lifetime of the building. Whatever done needs to be clearly described so that others can check the data, or recalculate for different assumptions.

A full assessment must consider all major structural materials including steel, concrete, wood (in several forms), also non-structural materials such as aluminium, glass, plastic, and even paint, over the full life cycle of the building.

1 Introduction

As used in this paper, the CO_2 footprint of a building is the mass of greenhouse gases (in CO_2 equivalent units) per square metre of floor area, emitted during the construction, use and demolition of the building, considering only the production and use of construction materials.

1.1 Forestry and the Kyoto Protocol

It is well known that trees absorb carbon from the atmosphere, some of which is retained in wood and wood products, and that carbon absorbed by forests can be used to offset CO_2 emissions from burning of fossil fuels [Maclaren, 2000]. Hence some countries are using commercial forestry to help meet their Kyoto Protocol commitments. Carbon retained in timber buildings or other wood products might also be used to offset CO_2 emissions from burning fossil fuels, depending on the Harvested Wood Product (HWP) rules set under the UN's Kyoto protocol. The current HWP assumption is that all carbon in a forest is "instantly oxidised" at harvest – a simplistic and incorrect assumption in the Kyoto accounting system. Many international standards require that wood may only be considered for offsetting greenhouse gas emissions if it is obtained from forests which have certified sustainable forest management [eg BSI 2008].

The annual harvest of plantation wood in New Zealand is currently around 20 million m^3, yielding about 4.5 million m^3 of sawn timber, the balance going to plywood and MDF production, pulp and paper, or being exported as logs [MAF, 2007]. Given that one cubic metre of radiata pine wood contains about 210 kg of elemental carbon, equivalent to 0.77 tonnes of CO_2, the current annual log harvest amounts to around 14.7 million tonnes of CO_2 sequestered from the atmosphere, with a similar amount left behind as harvesting residues on the forest floor or in the ground. The government's wood availability forecasts (based on age class distribution of the existing plantation estate) show the annual harvest increasing to 30 million m^3 per year within the next decade (assuming replanting of the existing estate but no new plantings), equivalent to around 22.7 million tonnes of sequestered CO_2. The Australian situation is different but the same principles apply [FWPRDC 2006].

1.2 CO_2 Emissions and Energy Issues for Building Materials

Considering global CO_2 emissions, the main benefits of using more timber as a building material are:

1. An increase in the pool of carbon in wood and wood products
2. Reduction of fossil fuel use in manufacturing wood rather than more energy intensive materials such as steel, concrete and aluminium (less embodied energy)
3. Displacement of fossil fuel by burning of wood waste materials

1.2.1 Carbon Stored in Materials and Released During Manufacture

The most often quoted reason for building in wood, from a climate change perspective, is the increase in the pool of carbon stored in wood and wood products. The carbon sink for wood and wood products in new New Zealand buildings is roughly half a million tonnes of CO_2 per year [Buchanan & Levine, 1999]. The carbon is only stored for the life of the building and returns to the atmosphere when timber buildings are finally demolished, and the wood decays or is burned, so assumptions about the end-of-life of the building must be made clear.

The manufacturing of some materials results in a chemical release of CO_2 to the atmosphere. This is a particular problem for manufacturing of cement where the process of converting limestone to quick-lime gives CO_2 emissions of about 0.5 tonnes of CO_2 per tonne of cement. This needs to be included in any assessment of the greenhouse gas implications of building materials.

1.2.2 Embodied Energy

"Embodied energy" is the energy required to manufacture building materials. The fossil fuel component of embodied energy results in CO_2 emissions. Estimates of embodied energy are available for building materials in New Zealand [Alcorn, 2003] and Australia [Tucker et al. 2008]. A recent BRANZ report [Page, 2006] shows that embodied energy is up to 9% of lifetime energy use for several New Zealand buildings. This percentage will increase as new buildings are designed to be much more thermally efficient.

The amount of fossil fuel energy used to manufacture individual building materials is steadily decreasing. Modern steel mills, aluminium smelters and cement plants use less energy than earlier ones. Modern cement plants use dry technology which requires much less energy than the traditional wet cake process, and an increasing trend to burn wood waste to provide renewable energy. A complete energy balance and a CO_2 balance considers the lifetime use of different building materials, considering such issues as cement and aggregate production, use of recycled steel, and the transportation of materials [Gustavsson et al., 2006].

Because of the large amount of stored solar energy in wood, it takes less energy to manufacture logs into timber than to manufacture materials like cement and concrete, and much less than most metallic materials such as steel and aluminium, depending on the proportion of recycled product in each material. Many medium sized wood processing plants in New Zealand are close to energy-neutral, operating on-site combined heat and power plants driven by steam boilers fired by wood residues, so that the embodied energy in sawn and processed wood from such plants is not obtained from fossil fuel. The only significant embodied energy derived from fossil fuel is then the component from harvesting and trucking which uses diesel fuel. Data on this energy is increasingly available from Life Cycle Inventory (LCI) databases for most materials. Databases should be prepared using international guidelines [ISO 2006, BSI 2008]. Comparisons of total embodied energy for alternative building designs are available [e.g. Upton et al. 2006, Buchanan & Levine 1999].

2 Components of CO_2 footprint assessment

There are many components of CO_2 emissions. The time frame for material production and use is very important, as shown in the steps below, listing the possible components. The components related to demolition and re-use must be assessed carefully to avoid double-counting.

1. Construction of the building:
a. CO_2 emissions from the fossil fuel component of the energy required to make the building materials (emissions from fossil fuel component of the embodied energy). "Cradle-to-gate" emissions. This is sometimes called "embodied CO_2".
b. Chemical CO_2 emissions from manufacturing the building materials (i.e. cement).
c. Less the carbon (CO_2-equivalent) in the carbon pool which remains stored in the building materials for the life of the building (i.e. in timber elements).
d. CO_2 emissions from the fossil fuel component of the energy required to transport materials to the construction site.
e. CO_2 emissions from the fossil fuel component of all the energy required on site for construction.
f. Less the carbon (CO_2-equivalent) in the carbon pool which remains stored in the area of newly-planted and sustainably-managed forest required for production of wood for the timber elements in this building.
g. Less the CO_2 emissions avoided by burning of wood waste for energy in lieu of fossil fuels (waste wood in forest, sawmill and building site).
2. Operation of the building:
a. CO_2 emissions from the fossil fuel component of the energy required for heating and cooling and lighting over the building life. A standard lifetime is needed for each building.
b. CO_2 emissions from the fossil fuel component of the energy required for routine maintenance.
c. CO_2 -equivalent emissions from manufacturing the materials required for routine maintenance.
3. Demolition and possible re-use of the building:
a. CO_2 emissions from the fossil fuel component of the energy required to demolish the building.
b. CO_2 emissions from the fossil fuel component of the energy required for land-filling.
c. CO_2 -equivalent emissions from decomposition of wood-based building materials in a land-fill.
d. Less the CO_2 stored indefinitely in re-used timber components, or in a land-fill.
e. Less the CO_2 emissions avoided by burning demolition wood for energy in lieu of fossil fuels.

The "CO_2 footprint" of a building, has units of *kg of CO_2 equivalent emissions per square metre of floor area*. The word *equivalent* is used to allow for non-CO_2 emissions such as methane to be included, converted back to CO_2 equivalent units. Total CO_2 equivalent emissions are sometimes called Global Warming Potential (GWP) or Greenhouse Gas (GHG) Emissions. The term "carbon footprint" is sometimes used, but it must be very clear whether the units are carbon or carbon dioxide. For conversion, one tonne of carbon storage offsets 3.67 tonnes of CO_2 emissions (44/12 = 3.67). This paper recommends a simple approach only considering CO_2 because very little methane is emitted during manufacture of building materials. Units used in this paper are CO_2 not Carbon.

Construction and demolition energy

The energy required to construct and demolish a building is small and not very dependant on the building materials. Construction site energy has been estimated to be only 5% to 10% of embodied energy in materials [Gustavsson et al., 2006]. Most studies into comparative building materials assume that the construction energy is the same for all materials, so not needed here.

Operational energy
The energy required to heat and cool an energy-efficient building is not strongly dependant on the building materials if the building is well designed. The important parameters are thermal insulation and thermal mass, both of which can be provided in timber buildings. Operational energy is the largest component of CO_2 lifetime CO_2 emissions, but will not be considered further in this paper.

Transport energy
The energy required to transport the building materials is a small number, only important for materials which are imported or moved long distances [John et al. 2008]. Transport energy will not be considered further in this paper.

2.1 End of life assumption – permanent storage

A full LCA analysis covers the full life cycle of the buildings – often referred to as a 'cradle-to-grave' assessment. All life cycle assessments require assumptions about the end-of-life of the building. These scenarios are difficult to predict because many things may change in 60 years time (or longer) when the buildings reach the end of their useful lives.

The assumption in this proposal is an end-of-life scenario where there is no net increase in greenhouse gas emissions after the building is demolished. This assumption is consistent with the carbon sequestered in the wood products being retained permanently in perpetuity, in one of the following ways:

- Landfill of all wood products with no subsequent release of GWP emissions.
- Landfill, with any decomposition to methane being collected for energy production.
- Re-use of all wood products in re-located buildings or other new buildings.
- Replacement of all buildings with new buildings containing at least the same amount of wood.

The underlying consideration is that as long as the products 'exist', they are storing carbon. This approach does not assume any particular end-of-life scenario; it simply says that timber products, that are real and being utilised, store carbon, and there are mechanisms for retaining this storage over the very long term. BSI [2008] allows wood products in a building with a life of 100 years or more to be considered "permanent removal" of greenhouse gases.

The Kyoto Protocol does not recognise this approach. It considers all the carbon in wood is 100% volatilised at the time of harvesting – which it clearly is not – and has let to much debate about how to account for carbon storage in timber products.

2.2 Calculation steps for CO_2 footprint:

1. Obtain a schedule of all construction materials (by mass).
2. Multiply the mass of each material by a coefficient (or number of coefficients) to estimate the CO_2 emissions related to each aspect of material use.
3. Sum the emissions to get a building total.

Wood based materials require a much larger number of coefficients than other materials if all the benefits of wood construction are to be considered. Indicative coefficients are shown in Table 1, most obtained from the roughly estimated numbers in the following tables.

Material	CO_2 emission	Mass	Coefficient	Total
Units		kg	kg CO_2 / kg	kg CO_2
Wood products	• CO_2 emissions from embodied energy	-	0.2*	=
	• Carbon storage in building materials	-	-1.7*	=
	• New forest sequestration (from Table 3)	-	-6.2	=
	• Avoided CO_2 emissions, waste energy (Table 4)	-	-0.63	=
Concrete	• CO_2 emissions from embodied energy	-	0.1*	=
	• Chemical CO_2 emissions	-		=
Steel	• CO_2 emissions from embodied energy	-	1.6*	=
Others	• CO_2 emissions from embodied energy	-	-	=
TOTAL				==

* from Table 2

Table 1 Calculation table. The coefficients have units of kg CO_2 emissions per kg of material.

2.2.1 Coefficients for CO_2 emissions from embodied energy and for carbon storage

Coefficients for CO_2 emissions from embodied energy are available from Life Cycle Inventory (LCI) databases for many materials. They can also be obtained from Life Cycle Assessment (LCA) studies using comprehensive LCA software which contains data for manufacturing of many materials.

Material	Embodied energy	Embodied CO_2	Carbon storage	Total
	MJ / kg	kg CO_2 / kg	kg $_{CO2}$ / kg	kg CO_2 / kg
Concrete	0.7	0.1	0	0.1
Structural steel	21.5	1.6	0	1.6
Stainless steel	60.6	5.0	0	5.0
Reinforcing steel	9.5	0.7	0	0.7
Glass	14.0	1.4	0	1.4
NZ timber	1.1	0.1	-1.7	-1.6*
Canadian timber	7.2	0.7	-1.7	-1.0*
Glulam	7.8	1.0	-1.7	-0.7*
Plywood	7.2	0.9	-1.7	-0.8*
MDF	14.3	1.2	-1.7	-0.5*
Aluminium, virgin, anodized	254	18.5	0	18.5
Aluminium, virgin	168	12.9	0	12.9
Plasterboard (gypsum)	3.2	0.2	0	0.2
Paint	56.6	2.5	0	2.5
Fibre glass insulation	40.4	2.6	0	2.6
Polystyrene insulation	81.0	2.6	0	2.6
Fibre cement	16.6	1.3	0	1.3

Table 2: Embodied energy and CO_2 coefficients

The embodied energy and CO_2 coefficients in Table 2 have been obtained from John et al. [2008], derived from European data using the Gabi software package. The right hand column and the embodied energy figures are directly from that document. The embodied energy figures are only given for information as they are not used in this paper. The embodied energy emissions have been calculated from the total emissions by subtracting the carbon storage figure of 1.7 kg CO_2 / kg of wood product, obtained from 210kgC/m^3 of dry wood with density of 450kg/m^3 giving 0.47kgC/kg x44/12 = 1.70kg CO_2 /kg. The carbon storage has been calculated assuming full sequestration, not including any potential decomposition at a land-fill stage so this should be taken into account when combining with other figures. The figures in Table 2 are only indicative. More accurate figures from a reliable source for each country should be obtained before making calculations. New figures for New Zealand are in preparation.

2.2.2 Coefficients for new forest sequestration

Coefficients for new forest sequestration are more controversial. All the previous figures is this paper assume that all forests that are felled will be replanted. This section looks at the additional benefits which can be accrued if new forests are planted on previously un-forested land to supply wood and wood-products sufficient to construct the building. This benefit is limited in place and time (not sustainable indefinitely) because it requires more and more un-forested land to be planted in forest. The coefficients can be obtained by a calculation such as shown in Table 3. The numbers in Table 3 are only examples of possible numbers which may be very dependent on growing sites and conditions, and different for other wood products.

	Units	**Sawn wood**	**LVL**	**MDF**
Sawmill conversion factor (m^3 wood product / m^3 of log)		50%*	-	-
Log volume (per m^3 wood product)	m^3	2.0	=	=
Forest wood factor (volume of branches and roots etc, per cubic metre of logs extracted from forest)		0.8*	-	-
Volume of branches roots etc in forest (per m^3 wood product)	m^3	1.6	=	=
Total volume of wood in logs, branches, roots etc in forest (per m^3 wood product)	m^3	3.6	=	=
Carbon sequestered per m^3 of wood	t C / m^3	0.21**	-	-
Total carbon sequestered in forest (per m^3 of wood product)	t C	0.756	=	=
Equivalent CO_2 sequestered (per m^3 of wood product) (x44/12)	t CO_2	2.77	=	=
Density of dry wood product	kg / m^3	450*	-	-
Equivalent CO_2 sequestered (per kg of wood product)	kg CO_2	6.2	=	=

* Input factor (numbers for example only). **Input from page 1. – input value = calculated

Table 3. Calculation of coefficients for carbon sequestration in new planted forest

2.2.3 Coefficients for avoided CO_2 emissions due to energy from waste wood

It is necessary to make many different assumptions about end-of-life if the avoided CO_2 emissions due to energy from waste wood are to be included. This assumes for a start that infrastructure is available for combusting wood waste. Many countries do not have such infrastructure in place. Assumptions are also necessary about re-use or land-filling options

The best way to use plantation forestry to reduce fossil fuel CO_2 emissions is to burn wood or wood waste for energy, as a significant by-product from greater use of wood as a construction material. The CO_2 emissions from burning of wood are not a greenhouse gas problem like burning of fossil fuel because the energy from wood is simply renewable solar energy which has been stored in the wood for a few decades, and the release of CO_2 is part of a natural cycle which will occur anyway. Alternatively, increased availability of wood as a building material may be seen as a significant by-product of woody biomass fuel production. The resulting energy is solar energy which has been stored in the wood for a few decades. As shown in Figure 1, the wood or wood waste may come from many different parts of the wood chain, including

- Forest harvesting
- Wood processing
- Waste on the construction site
- Demolition of the building

The benefits of these energy sources have been demonstrated in recent European studies, considering many different options. Energy recovery from wood waste has been investigated for alternative forestry scenarios, with and without timber buildings as part of the cascade chain [Gustavsson et al., 2006]. There will be continuing debate as to how much of the logging site waste can be recovered as fuel. Wood residues at sawmills and processing plants have been used in this way for many years. One issue which needs consideration in New Zealand is the relatively high proportion of construction timber which has been chemically treated with wood preservatives.

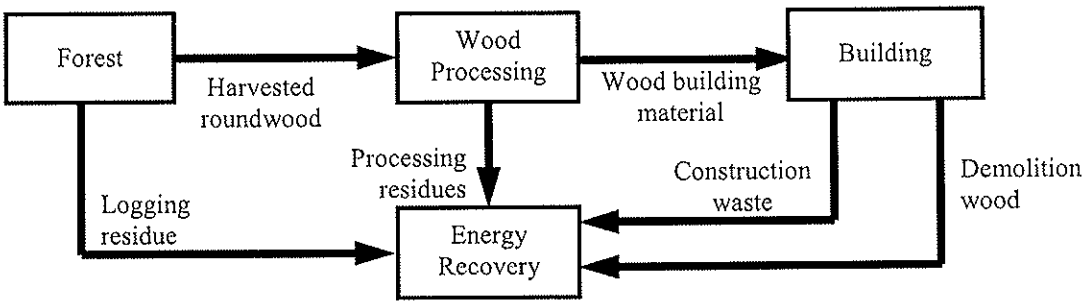

Figure 1. Schematic flow of wood materials during building lifecycle [Gustavsson et al., 2006].

The easiest way to use energy from wood waste is as a heating fuel, but conversion of wood waste into liquid or gaseous fuels for transport and other uses is being seriously investigated. The energy available from wood waste needs to be assessed at all steps in the forestry, construction and demolition industries, along with the resulting reductions in fossil fuel use and carbon emissions.

Wood product ->	Units	**Sawn wood**	**LVL**	**MDF**
Volume of **waste wood in forest** (per m^3 of wood product) From Table 3.	m^3	1.6	-	-
Percentage of the forest waste wood burned for energy.		50%*	-	-
Volume of forest waste wood burned for energy (per m^3 of wood used on site)	m^3	0.8	=	=
Volume of **sawmill wood waste** (per m^3 of wood used on site)	m^3	0.9*	-	-
Percentage of sawmill waste burned for energy.	%	80%*	-	-
Volume of sawmill waste wood burned for energy (per m^3 of wood used on site)	m^3	0.72	=	=
Volume of **construction site wood waste** burned for energy (per m^3 of wood used on site)	m^3	0.05*	-	-
Volume of **demolition wood waste** burned for energy, offcuts etc. (per m^3 of wood used on site)	m^3	0.9*	-	-
Total volume of wood burned for energy (per m^3 of wood used on site)	**m^3**	**2.47**	=	=
Density of dry wood	kg/m^3	450	-	-
Total mass of waste wood burned for energy (per m^3 of wood used on site)	kg	1.11	=	=
CO_2 emissions avoided by burning one tonne of wood waste (coefficient obtained from NZ energy analysis, Johns et al 2008)	t CO_2	0.57	-	-
Coefficient for total CO_2 emissions avoided by burning wood waste (per m^3 of wood used on site)	**t CO_2**	**0.63**	=	=

* Possible numbers for example only. – input value = calculated

Table 4. Calculation of coefficients for CO_2 emissions avoided by burning wood waste.

The coefficients can be obtained by a calculation such as shown in Table 4. The numbers in Table 4 are only examples of possible numbers which may be very dependent on growing sites and conditions, sawmilling and processing, and may be very different for other wood products.

3 Case study building

This case study is based on an actual six-storey 4,250 m^2 floor area building, with of four similar designs using different materials. These are called the Concrete, Steel, Timber and TimberPlus designs which have been made to investigate the influence of construction materials on life cycle energy use and global warming potential (GWP) as reported by Johns et al. [2008].

All four buildings were designed for very similar low operational energy consumption and a lifetime of 60 years. The Concrete and Steel buildings employed conventional design and construction methods; the Timber buildings proposed innovative post-tensioning structural designs using engineered LVL components [Buchanan et al., 2008]. The TimberPlus design additionally increased the use of timber in architectural features such as exterior cladding, windows and ceilings. Construction time and cost of all the buildings are similar.

A summary of the CO_2 emissions from the materials is given in Table 5, calculated according to the method outlined above, considering only CO_2 emissions from embodied energy and carbon storage in building materials. Full details are given in the original document [Johns et al. 2008]. New forest sequestration and avoided CO_2 emissions through energy from waste wood are not included at this stage, but are covered later in the paper.

		Concrete	Steel	Timber	TimberPlus
Concrete	tonnes CO_2	388	233	137	137
Steel	tonnes CO_2	145	591	29	29
Aluminium	tonnes CO_2	630	630	630	18
Other	tonnes CO_2	136	159	194	68
Wood	tonnes CO_2	-23	-22	-383	-561
Total	**tonnes CO_2**	**1275**	**1591**	**607**	**-308**
Total per m^2	*kg CO_2/ m^2*	*300*	*374*	*143*	*-72*

Table 5. Aggregated CO_2 emissions for groups of materials in the four buildings

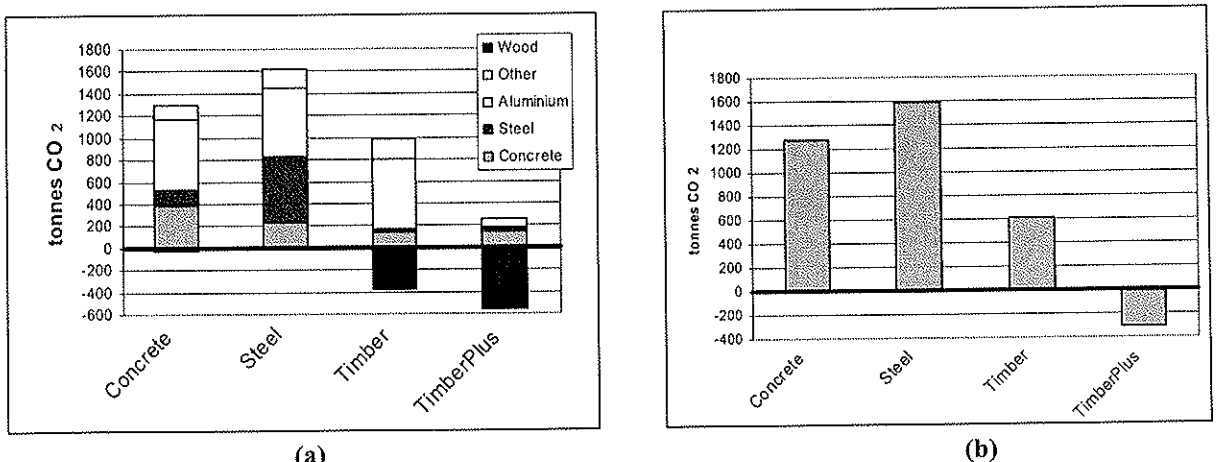

Figure 2. CO_2 emissions for materials in the four buildings, assuming permanent storage of carbon in wood products (a) Major materials (b) Net figures [John et al., 2008].

The values from Table 5 are plotted in Figure 2. It can be seen that the net CO_2 emissions for the Timber building are less than half of those for the Concrete building and less than 40% of those for the Steel building. This is because the carbon stored in the wood-based building materials balances out much of the greenhouse gases emitted in the manufacturing of all the other materials in the building, with the long-term storage of 383 tonnes of CO_2-equivalent carbon.

The net total CO_2 emissions for the TimberPlus building are negative because the carbon stored in the wood-based building materials more than cancels out the greenhouse gases emissions from the manufacturing of all the other materials in the building. The net negative figure is over 300 tonnes of CO_2 equivalent. This study demonstrates that replacing high embodied energy components, such as aluminium windows and louvres with timber, can have a significant effect on environmental impacts.

3.1 Additional benefits

Additional benefits can be achieved if allowance is made for new forest plantings and for combustion of wood waste for energy in lieu of fossil fuel. Table 6 shows how the calculations change if these two additional benefits are added to the four case study buildings. By far the largest benefits accrue from new forest planting for each new building, which will only be possible for a small number of situations.

		Concrete	Steel	Timber	TimberPlus
Wood materials in the building	tonnes	18	17	462	634
Coefficient - new forest planting	t CO_2-e / t	6.2	6.2	6.2	6.2
Carbon sequestered in new forest	tonnes CO_2	112	105	2864	3931
Coefficient - emissions avoided	t CO_2-e / t	0.63	0.63	0.63	0.63
Emissions avoided by burning wood waste	tonnes CO_2	11	11	291	399
Original total from Table 5	tonnes CO_2	1275	1591	607	-308
New total	**tonnes CO_2**	**1152**	**1475**	**-2548**	**-4638**
New total per m^2	*kg CO_2/ m^2*	*271*	*347*	*-600*	*-1091*

Table 6. Modified CO_2 emissions for the four buildings, allowing for new forests and wood waste energy

4 Conclusions

- A procedure has been suggested for standardising CO_2 footprint calculations for buildings.
- It is essential to be very clear about system boundaries and end-of-life scenarios.
- It is sufficiently accurate to use only CO_2 emissions, not considering other greenhouse gases.
- The most simple and recommended analysis is to consider CO_2 emissions from the manufacture of all building materials and carbon stored in the wood components of the building.
- Data should be obtained from a reputable LCI or LCA database of material coefficients.
- Buildings with a large volume of wood and wood products score well (have a small CO_2 footprint) because of the low emissions from manufacturing wood and due to the carbon stored in the wood components for the life of the building and beyond.
- Additional benefits can be achieved if wood waste is burned of for solar energy in lieu of fossil fuel, but only if the infrastructure exists. Calculations require a large number of assumptions.
- Even greater benefits occur if allowance is made for new forest to be planted on non-forested land to provide wood for new timber buildings, but this is not often achievable. The conceptual calculations in this paper show the calculation methods which can be used.

References

Alcorn, A. (2003).Embodied Energy Coefficients of Building Materials. Centre for Building Performance Research, Victoria University of Wellington. www.vuw.ac.nz/cbpr/documents/pdfs/ee-finalreport-vol2.pdf.

BSI (2008). Specification for the Assessment of the Life Cycle Greenhouse Gas Emissions of Goods and Services. PAS 200:2008. British Standards, UK.

Buchanan, A.H. and Levine, S.B. (1999). Wood-Based Building Materials and Atmospheric Carbon Emissions. *Environmental Science and Policy*, **2**, 427-437. www.civil.canterbury.ac.nz/pubs/woodbasedbuildingLevine.pdf

Buchanan, A.H., Deam, B.L., Fragiacomo, M., Pampanin, S. and Palermo, A. (2008). Multi-Storey Prestressed Timber Buildings in New Zealand. *Structural Engineering International.* Journal of IABSE. Vol. 18, No. 2. pp166-173. May 2008.

FWPRDC (2006). *Forests, Wood and Australia's Carbon Balance.* Forest and Wood Products Research and Development Corporation. ISBN 0-9579597-5-3. www.fwprdc.org.au

Gustavsson, L. Pingoud, K. and Sathre, R. (2006).Carbon Dioxide Balance of Wood Substitution: Comparing Concrete and Wood Frames Buildings. *Mitigation and Adaptation Strategies for Global Change,* **11**: 667-691.

ISO (2006). International Standard ISO 14040. Environmental Management - Life Cycle Assessment – Principles and Framework. International Standards Organisation, Geneva.

John, S., Nebel, B., Perez, N. and Buchanan, A.H. (2008). Environmental Impacts of Multi-Storey Buildings Using Different Construction Materials. Research Report 2008-02. Department of Civil and Natural Resources Engineering, University of Canterbury, New Zealand.

Maclaren, P. (2000).Trees in the Greenhouse. *FRI Bulletin No 219.* Forest Research Institute, Rotorua, New Zealand.

MAF (2007). *NZ Forest Industry Facts and Figures, 2005/06.* Ministry of Agriculture and Forestry www.mag.govt.nz

Page, I. (2006). Timber in government buildings - cost and environmental impact analysis. *BRANZ Report E408.* www.maf.govt.nz/forestry/publications/branz-report/branz-report-timber-in-govt-buildings.pdf.

Tucker, S., Syme, M. and Foliente, G. (2008). Life Cycle Assessment of Forest and Wood Products in Australia. Proceedings, 2008 World Conference on Timber Engineering, Japan.